Fundamentals of Hernia Radiology

Salvatore Docimo Jr.
Jeffrey A. Blatnik
Eric M. Pauli
Editors

MOREMEDIA
Springer

Fundamentals of Hernia Radiology

Salvatore Docimo Jr.
Jeffrey A. Blatnik • Eric M. Pauli
Editors

Fundamentals of Hernia Radiology

Springer

Editors
Salvatore Docimo Jr.
Division of Gastrointestinal Surgery
University of South Florida
Tampa, FL, USA

Eric M. Pauli
Division of Minimally Invasive and
Bariatric Surgery
Penn State Health Milton S. Hershey
Medical Center
Hershey, PA, USA

Jeffrey A. Blatnik
Section of Minimally Invasive Surgery
Washington University School of
Medicine in St. Louis
St. Louis, MO, USA

ISBN 978-3-031-21335-9 ISBN 978-3-031-21336-6 (eBook)
https://doi.org/10.1007/978-3-031-21336-6

This Springer imprint is published by the registered company Springer Nature Switzerland AG
The registered company address is: Gewerbestrasse 11, 6330 Cham, Switzerland

I would like to thank my wife Aisa, for her patience and support (whether I deserve it or not) which allows me to find the time to get these extra projects done. To Massimo and Luna, though you are too young to understand the content of this book right now, hopefully one day you look at this dedication and proudly think, "Dad did alright." To my parents, this book is also dedicated to you, though you will probably never read it. Thank you to all the contributing authors for your dedication to this project. Finally, I thank my co-editors, Eric and Jeff—how a small conversation at a meeting among friends led to this book.

— Salvatore Docimo, Jr., DO, MBA, FACS, FASMBS

I would first and foremost like to thank Eric and Sal for all their hard work and commitment to get this project across the finish line. Also, thank you to the many authors who took time out of their already busy schedules to put together some fantastic content for us all to learn from. To my mentors who have all taught me something, whether a small fact or a critical piece of information that has allowed me to become a successful surgeon. Finally, to my wife Terra, and our three kids who make sacrifices every day that allow me to do the things I want to do. Without their support none of this would be possible.

— Jeff A. Blatnik, MD

As a college student, I worked as a file clerk at Mercy Hospital in Scranton, Pennsylvania. Knowing that I wanted to pursue a career in medicine, the radiologists took me under their wing and taught me human anatomy and pathophysiology on a

variety of imaging types. Their dedication to educating me set me apart from my peers in anatomy lab and really made me fall in love with surgery (a field where I could visualize the disease on imaging and then intervene with my hands). I would like to dedicate this book to those amazing community radiologists who recognized something in me that made them want to teach. I should also thank my mom for helping me get the job at the hospital where she worked as a clinical research coordinator. Thanks Mom!!

— Eric M. Pauli, MD

Preface

Fundamentals of Hernia Radiology was an endeavor that began before the world was brought to the brink of catastrophe due to the COVID-19 pandemic. The textbook was placed on the backburner as the medical community battled an unforeseen opponent. Quite often, complex, elective hernia repairs were also put on hold in order to deal with more pressing medical needs. One silver lining in the COVID-19 pandemic was the use of social medial and virtual lectures among the surgical community aimed at improving learning. One important aspect of online postings was the need for radiographic evaluation of hernia pathology in order to develop a roadmap for operative planning. These online requests for radiographic evaluations of hernia pathology further solidified the need for a radiology-based hernia text written for surgeons.

Abdominal wall reconstruction is a constantly evolving field of surgery. The growing complexity of both hernia pathology and surgical repair warrants substantial preoperative preparation. Paramount to a successful surgical repair is understanding in great detail the anatomy of the hernia pathology. An awareness of anatomical landmarks and disruption of tissue plains in the setting of a hernia is the first step in a surgeon's preparation of their surgical intervention. Radiology is a great tool that provides a glimpse of what a surgeon can expect to find in the operative suite. In many cases, a lack of radiographic evaluation would ensure surgical surprises the day of surgery. In some situations, radiographic evaluation of previous hernia repairs provides a more detail glimpse into the patient's previous surgical interventions that the operative report fails to provide.

This textbook was developed with a clear aim: provide a more standardized language and approach to the radiographic evaluation of hernia pathology. Each chapter aims to provide a thorough understanding of how radiology can assist the surgeon in their operative preparation or evaluation of the postoperative patient for surgical complications. Each chapter is written with one goal in mind: leverage radiographic evaluations and understanding to improve surgical outcomes. We also hope our textbook provides a solid foundation and professional language upon which surgeon can better communicate with radiologists. Our goal is to improve collaboration with radiologists which will ensure improved surgical outcomes of all our hernia patients.

Lastly, the editors would like to thank all the authors who made this textbook possible. Their surgical knowledge, patience, and dedicated contributions during a time of great upheaval and fear in our medical community is

inspiring. Let this textbook stand as a marker for perseverance and proof that our close-knit surgical community can overcome adversity, such as the COVID-19 pandemic, and create a resource we hope will serve the surgical community for many years to come.

Tampa, USA — Salvatore Docimo Jr.
St. Louis, USA — Jeffrey A. Blatnik
Hershey, USA — Eric M. Pauli

Contents

Contributors

Diya Alaedeen Department of General Surgery, Cleveland Clinic, Cleveland, OH, USA

Andrus Alian Department of Emergency Medicine, Stony Brook University Medical Center, Stony Brook, NY, USA

Maria S. Altieri Department of Surgery, University of Pennsylvania, Philadelphia, PA, USA

Vedra A. Augenstein General Surgery, Atrium Healthcare, Charlotte, NC, USA

Jesse Bandle Department of General Surgery, Naval Medical Center San Diego, San Diego, CA, USA

Andrew T. Bates Department of Surgery, South Shore University Hospital, Northwell Health, Bay Shore, NY, USA

Roel Beckers Department of Radiology, AZ Maria Middelares, Ghent, Oost-Vlaanderen, Belgium

Jordan A. Bilezikian Department of Surgery, New Hanover Regional Medical Center, Wilmington, NC, USA

Michael J. Bilezikian Department of Surgery, New Hanover Regional Medical Center, Wilmington, NC, USA

James H. Birkholz Department of Radiology, Penn State Milton S. Hershey Medical Center, Hershey, PA, USA

Alfredo M. Carbonell Department of Surgery, Prisma Health-Upstate, Greenville, SC, USA

University of South Carolina School of Medicine-Greenville, Greenville, SC, USA

David C. Chen Department of Surgery, Lichtenstein Amid Hernia Clinic at UCLA, Santa Monica, CA, USA

Verghese T. Cherian Department of Anesthesiology and Perioperative Medicine, Penn State Health Milton S Hershey Medical Center, Hershey, PA, USA

John Childress III Atrium Health CMC, Radiology (Charlotte Radiology), Charlotte, NC, USA

Alisa M. Coker Department of Surgery, Johns Hopkins University School of Medicine, Baltimore, MD, USA

Kimberly R. Coughlin Department of Surgery, Columbia University Medical Center, New York, NY, USA

Colin G. DeLong Department of Surgery, Penn State Health Milton S. Hershey Medical Center, Hershey, PA, USA

Salvatore Docimo Jr., DO, MBA, FACS, FASMBS Division of Gastrointestinal Surgery, University of South Florida, Tampa, FL, USA

Sabrina Drexel Department of General Surgery, University Hospitals Cleveland Medical Center, Cleveland, OH, USA

Christopher DuCoin Department of Surgery, University of South Florida at Tampa General Hospital, Tampa, FL, USA

Frederic E. Eckhauser Department of Surgery, New Hanover Regional Medical Center, Wilmington, NC, USA

Aldo Fafaj Department of General Surgery, Cleveland Clinic, Cleveland, OH, USA

Justin D. Faulkner Department of Surgery, New Hanover Regional Medical Center, Wilmington, NC, USA

John P. Fischer, MD, MPH Division of Plastic Surgery, University of Pennsylvania Health System, Philadelphia, PA, USA

Laura E. Fischer Department of Surgery, University of Oklahoma, Oklahoma City, OK, USA

Michael C. Forney Section of Musculoskeletal Imaging, Cleveland Clinic Foundation, Imaging Institute, Cleveland, OH, USA

Jacob A. Gardner Department of Radiology, Penn State Hershey Medical Center, Hershey, PA, USA

Michael Genz Department of General Surgery, Atrium Health—Carolinas Medical Center, Charlotte, NC, USA

Omar M. Ghanem Department of Surgery, Mayo Clinic, Rochester, MN, USA

Iliya Goldberg Division of Upper GI and General Surgery, Department of Surgery, Keck Medicine of USC, Los Angeles, CA, USA

Jacob A. Greenberg Department of Surgery, University of Cincinnati College of Medicine, Cincinnati, OH, USA

Sara E. Holden Department of Surgery, Washington University in St. Louis, St. Louis, MO, USA

William W. Hope Department of Surgery, New Hanover Regional Medical Center, Wilmington, NC, USA

Charlotte Horne Department of Minimally Invasive Surgery, PennState Health, Milton S. Hershey Medical Center, Hershey, PA, USA

Desmond Huynh Department of Surgery, Cedars-Sinai Medical Center, Los Angeles, CA, USA

Joseph R. Imbus Division of Minimally Invasive Surgery, Department of Surgery, Duke University, Durham, NC, USA

Mazen Iskandar Department of General Surgery, Baylor Scott and White Center for Hernia Surgery, Waxahachie, TX, USA

Brian P. Jacob Department of Surgery, Laparoscopic Surgical Center of New York, New York, NY, USA

Jeffrey E. Janis Department of Plastic and Reconstructive Surgery, The Ohio State University Wexner Medical Center, Columbus, OH, USA

Ryan Michael Juza Department of Surgery, University Hospitals Cleveland Medical Center, Cleveland, OH, USA

David M. Krpata Department of Surgery, Cleveland Clinic, Cleveland, OH, USA

MacKenzie Landin Minimally Invasive/Bariatric Surgery (Division)/ Department of Surgery, University of Arizona-Phoenix, Phoenix, AZ, USA

Alexander T. Liu Department of Surgery, Penn State Milton S. Hershey Medical Center, Hershey, PA, USA

David J. Lourié Department of Surgery, Huntington Hospital, Pasadena, CA, USA

Yang Lu Department of Surgery, David Geffen School of Medicine at UCLA, Los Angeles, CA, USA

Ian T. MacQueen Department of Surgery, Lichtenstein Amid Hernia Clinic at UCLA, Santa Monica, CA, USA

Jaclyn T. Mauch, MD, MBE Division of Plastic Surgery, University of Pennsylvania Health System, Philadelphia, PA, USA

Division of Plastic Surgery, University of Michigan Health System, Ann Arbor, MI, USA

Joseph A. Mellia, MD Division of Plastic Surgery, University of Pennsylvania Health System, Philadelphia, PA, USA

Division of Plastic Surgery, Mount Sinai Health System, New York, NY, USA

Bianca J. Molina Department of Plastic and Reconstructive Surgery, The Ohio State University Wexner Medical Center, Columbus, OH, USA

Filip Muysoms Departement of Surgery, AZ Maria Middelares, Ghent, Oost-Vlaanderen, Belgium

Vahagn C. Nikolian Department of Surgery, Oregon Health & Science University, Portland, OR, USA

Yuri W. Novitsky Department of Surgery, Columbia University Medical Center, New York, NY, USA

Sean C. O'Connor Mission Subspecialty Surgery, Mission Hospital, Asheville, NC, USA

University of North Carolina College of Medicine, Chapel Hill, NC, USA

Sean B. Orenstein, MD Department of Surgery, Division of Gastrointestinal and General Surgery, Oregon Health & Science University, Portland, OR, USA

Eric M. Pauli, MD Division of Minimally Invasive and Bariatric Surgery, Department of Surgery, Penn State Health Milton S. Hershey Medical Center, Hershey, PA, USA

Matthew Peacock Department of General Surgery, Mount Sinai Hospital, New York, NY, USA

Pete Peterson Department of Surgery, University of South Florida at Tampa General Hospital, Tampa, FL, USA

Clayton C. Petro Department of General Surgery—Center for Abdominal Core Health, Cleveland Clinic, Cleveland, OH, USA

Dina Podolsky Department of Surgery, Columbia University Medical Center, New York, NY, USA

Benjamin K. Poulose Center for Abdominal Core Health, Department of Surgery, Division of General and Gastrointestinal Surgery, The Ohio State University Wexner Medical Center, Columbus, OH, USA

Ajita S. Prabhu Department of General Surgery, Cleveland Clinic Foundation, Cleveland, OH, USA

Alaa Sada Department of Surgery, Mayo Clinic, Rochester, MN, USA

Nabeel E. Sarwani Department of Radiology, Penn State Hershey Medical Center, Hershey, PA, USA

Allie E. Steinberger Department of Surgery, Washington University in St. Louis, St. Louis, MO, USA

Joseph Adam Sujka GI Surgery, University of South Florida, Tampa, FL, USA

Shirin Towfigh Beverly Hills Hernia Center, Beverly Hills, CA, USA

Kelly Tunder Department of Surgery, Columbia University Medical Center, New York, NY, USA

Maaike Vierstraete Departement of Surgery, AZ Maria Middelares, Ghent, Oost-Vlaanderen, Belgium

Jason M. Wagner Department of Radiological Sciences, University of Oklahoma, Oklahoma City, OK, USA

Kayla M. Watkins Department of Surgery, University of Oklahoma, Oklahoma City, OK, USA

Ashley Wercholuk Department of General Surgery, Vidant Medical Center, Greenville, NC, USA

Jin Yoo Department of General Surgery, Duke University Health System, Durham, NC, USA

Oscar Gonzalo Talledo Zevallos Department of MIS and Bariatric Surgery, UIHC, Iowa City, IA, USA

Samuel J. Zolin Cleveland Clinic Foundation, Digestive Disease and Surgery Institute, Cleveland, OH, USA

1 Computed Tomography (CT) Scan Basics

Nabeel E. Sarwani and Jacob A. Gardner

Why CT Imaging?

Hernia evaluation requires an accurate assessment of anatomical spaces and hernia contents. This includes being able to assess the abdominal wall musculature and its associated fascia, congenital, physiologic and posttraumatic diaphragmatic openings, and mesenteric defects [1, 2]. Computer tomography is preferred as the first-line imaging modality and forms the mainstay of most hernia evaluations [3]. It is widely available, relatively cheap, and is able to accommodate a wide spectrum of body habitus. CT has excellent anatomical delineation for the purposes of evaluating the myriad of hernias that can occur in the abdomen and pelvis. It also allows accurate measurements to be incorporated into the imaging of hernias. In addition, it permits visualization of the whole abdomen which is especially important when considering mesenteric structures or a large hernia, both to determine the approach to repair and assess the ability to return hernia contents to the abdominal cavity (i.e., "loss of domain [3]," to be addressed elsewhere in this book).

Spatial resolution is the ability to discriminate between two adjacent structures [4]. CT has an excellent spatial resolution which often makes it a first-line modality in the evaluation of hernias. CT also offers superior temporal resolution which, simply put, means that a scan can be completed much more quickly with CT than with MRI. The latest generation CT scanners have the ability to acquire images in seconds, while MRI typically takes up to 30–60 min to acquire. Rapid acquisition mitigates the issue of image degradation due to motion, which is addressed later in this chapter [4, 5].

Ultrasound allows for real-time evaluation of hernias. It is useful in the assessment of superficial hernia such as inguinal or paraumbilical hernias. Ultrasound facilitates visualization of the contents of a hernia, both at rest as well as in response to certain maneuvers such as Valsalva or standing. Pressure can be applied to the hernia with the transducer in real time to determine if the contents are reducible. Limitations of the modality include operator variability, only being able to assess a small part of anatomy at a time, and suboptimal assessment in larger patients. Ultrasound cannot accurately assess large or complex hernias, which are far better assessed on CT [2, 3].

CT allows the accurate evaluation of both superficial and deep soft tissues, defines the fascial planes and defects therein, and evaluates the contents of a hernia with a single rapid exam [1, 3].

N. E. Sarwani (✉) · J. A. Gardner
Department of Radiology, Penn State Hershey Medical Center, Hershey, PA, USA
e-mail: nsarwani@pennstatehealth.psu.edu; jgardner1@pennstatehealth.psu.edu

S. Docimo Jr. et al. (eds.), *Fundamentals of Hernia Radiology*,
https://doi.org/10.1007/978-3-031-21336-6_1

How Do We Get CT Images?

The CT scanner physically can be thought of as a freestanding vertical "donut." The analogy is a bit obvious but it is accurate. The body of the donut or gantry houses a spinning X-ray source in addition to the X-ray detector. The aperture through which the patient passes or "bore" is the donut hole. As the patient is scanned, they are passed through the aperture on a moving table.

CT imaging is an X-ray-based imaging technique therefore it uses ionizing radiation [4, 6]. The principle of X-ray imaging is the differential absorption of X-rays beams in the tissues. From a point source, X-rays spread out in the direction of the patient. As the beam passes through the body, some X-rays penetrate unobstruced, while others interact and get absorbed in the tissues, and hence the "differential absorption." Once the X-rays exit the body, they interact with a detector which assists with image creation and construction.

Historically, this technique was called CAT scanning—Computed Axial Tomography, but over time, the "axial" component has become redundant and removed from the abbreviation, as most, if not all, modern imaging is done using a spiral or helical technique. This refers to the continually spinning X-ray tube around the patient lying on a continually moving table—creating a spiral pattern. This creates a "volume" of data in 3D and is the basis for all the images a clinician sees.

In the case of CT scanners, the X-ray source spins around the patient as the patient lies down on the CT table, with a centrifugal force that can reach up to 14Gs. The opposing X-ray detectors can either also spin around the patient, or are fixed surrounding the hole in the CT scanner, depending on the generation and manufacturer of the machine. As the X-ray tube is spinning, the CT table moves into the opening of the scanner, all the while, data points are being recorded. Then, by applying a mathematical algorithm to the recorded data points and using complex geometry, multiple images of the patient are created, this last step is referred to as "image reconstruction."

Slice Thickness and Multiplanar Reconstruction (MPR)

The volumetric acquisition of data during CT scanning allows for the data to be used and manipulated in several ways to get the information needed to make a clinical diagnosis, to better visualize anatomy for presurgical planning, or assess postsurgical complications and outcomes [7]. To present the images for interpretation, the data is broken down into "slices." Slice thickness is determined taking into consideration the number of images created, the diagnostic yield, storage requirements, and the need for further advanced image processing such as 3D volume renderings. Most radiology services use a slice thickness between 3 and 5 mm, contiguously—meaning there is no gap between one slice and the next. Thinner does not mean better and often leads to poorer image quality. With decreased slice thickness, the amount of useful information (signal) vs the amount of useless information (noise) decreases, as the volume of tissue used to create thin images is less [4, 5]. Images in the 3–5 mm range for CT scans are the happy balance between the useful and useless sides of the equation. Thinner slices are helpful when there is a need for advanced image processing, such as creating images in different planes. These thinner slices are often not archived to long-term storage due to the large file size and associated cost of storing it.

CT images are typically presented in an axial format, but can also be presented in other orthogonal or non-orthogonal planes, depending on the need. The presentation of images in several planes is the definition of a multiplanar reconstruction or "MPR" [7]. In clinical practice, CT images are often presented in both the coronal and sagittal planes in addition to the axial plane and form part of the image interpretation. In hernia imaging, being able to see and evaluate hernias in multiple planes is an especially useful tool.

An advantage of digital imaging is the ability to create pictures that can be used by surgeons to plan a procedure or to explain the procedure to the patient. These pictures are created with

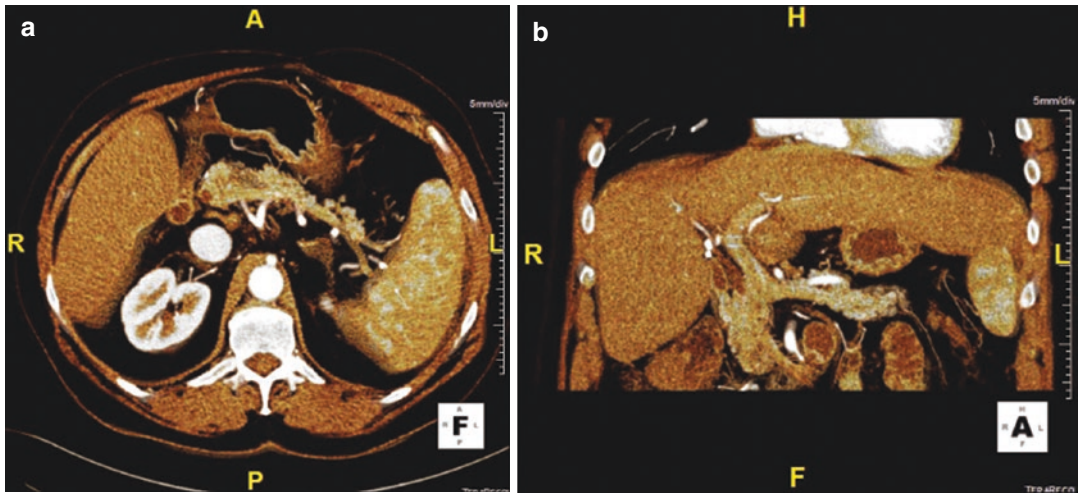

Fig. 1.1 Using an independent advanced imaging workstation, 3D images can be created from CT data. Axial (**a**) and coronal (**b**) thick slab 3D reconstructions show the vascular structures with greater definition

advanced image processing techniques, some of which function as independent programs, while others are built into the imaging viewing application called the Picture Archive and Communication System, or PACS. As an example, Volume Rendered (VR) images use virtual light sources to create 3D models [7]. These 3D models can be combined with another technique creating a thicker "slab" of tissue as opposed to the usual thin image slices, which are especially helpful in vascular assessment (Fig. 1.1).

Window Width and Window Level

The computer is able to "see" far more shades of gray than the human eye can. This is because once you calculate the possible shades of gray for each bit of information the computer can store, it ends up being over 4000 shades of gray per pixel. The human eye can differentiate far less. As such, physicians need to focus on what exactly they are interested in seeing when looking at CT images and adjust the range of grays as appropriate [8]. For example, when evaluating the CT scan for soft tissue components, things like muscles, fat, solid, and hollow visceral, a certain spectrum of grays are selected; however, these settings show nothing of the lung bases or can obscure free air. If air is to be assessed, then a different set of grays need to be chosen.

Table 1.1 Window width and window levels commonly used when reviewing CT images

Tissue of Interest	Window Width	Window Level
Soft tissues	400	40
Lung/Air	1800	−350
Bone	2000	300

The visualized shades are gray when viewing images are determined by what is referred to the Window settings, composed of 2 variables: Window Width and Window Level. Window Width determines the number of shades of gray, and window level determines where the window is to be centered [4]. Think of it this way—when looking at a tall skyscraper, you can choose how many floors you want to see at a time (10 floors, 20 floors, etc.), this is the window width. Then one needs to specify where this range is to be centered (on the 15th floor, 35th floor, etc.), this is the window level. Typical values for the window width and window level for different structure evaluation are shown in Table 1.1.

The three main structures of interest in the pre- and postsurgical evaluation for hernia surgery are soft tissues, lungs/air, and bones.

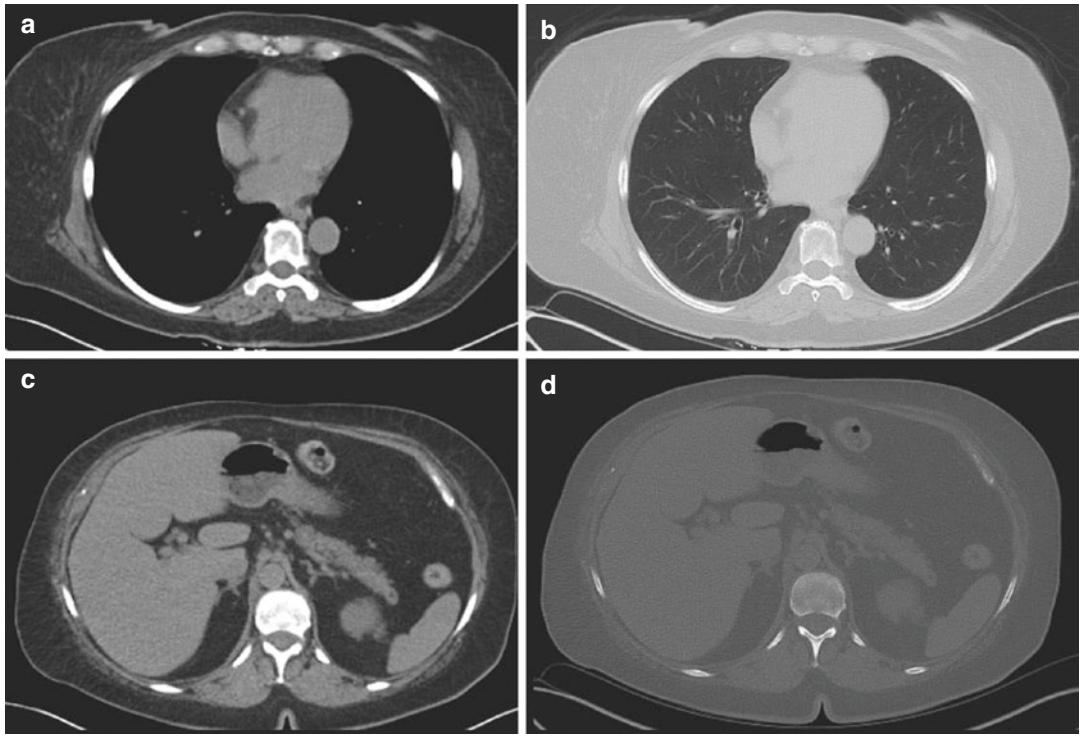

Fig. 1.2 Figure (**a**) shows an axial slice of the abdomen in a "soft tissue" window. In this setting, the heart, descending thoracic aorta, subcutaneous fat, and chest wall musculature are well seen. Changing the window width and levels of the same picture to the "lung" window (**b**) now allows assessment of the lungs which were previously black on the soft tissue window. Figure (**c**) is an axial soft tissue window slice through the upper abdomen that shows a clear assessment of the liver, pancreatic tail, and abdominal musculature on this non-contrast scan, which is due to *inherent contrast*. Again, by changing to the "bone" window at the same slice (**d**) shows the osseous structures to better advantage

Oftentimes, these values are established as "presets" on image viewers, meaning values are registered to more meaningful names such as "soft tissue," "bone," and "lung" facilitating standard viewing of images and rapid switching between the values depending on the tissue of interest (Fig. 1.2).

Contrast

The ability to differentiate one shade of gray from another is termed "contrast." Different structures in the body have different shades of gray, or in CT speak—"density." Bones are white or dense, soft tissues such as muscles, solid viscera, blood, and blood vessels are a medium shade of gray, fat a little darker, with air being the lowest of all densities, black. Shades of gray are measured in Hounsfield Units (HU), with typical values shown in Table 1.2. These different densities provide "inherent contrast" in CT images, which is how one structure is identifiable from the other [4]. It is this contrast that allows visualization of the abdominal and pelvic structures on a non-contrast CT.

For the assessment of the presence or absence of a hernia, non-contrast studies are oftentimes adequate [1, 9]. Defects in the abdominal wall, inguinal and femoral canals, or contents extending through the esophageal hiatus can be adequately assessed without the use of intravenous or oral contrast on CT.

At certain times, there may be a need to assess the solid and hollow viscera with intravenous contrast. This is especially helpful when evaluat-

Table 1.2 Typical HU of CT structures

Structure	Hounsfield Units (HU)
Air	−1000
Fat	−150 to −50
Soft tissue	+40 to +80
Bone	+1000 to +2000

ing for ischemia or to opacify mesenteric vascular structures during assessment for internal hernias. Iodinated-based contrast agents are injected intravenously prior to the CT scan. The interaction of the X-ray beam with the iodine molecules results in an increased density of the vascular structures and viscera on the images. The pause following the administration of contrast and starting of the scan is termed the "delay" and determines the phase of the enhancement. If a vascular map is needed, or there is a concern for arterial-related issues then the scan is started approximately 15–20 s after the start of the injection and is termed the "arterial phase." Whereas if there is a need to assess the solid viscera or venous structures, a delay of 70–90 s is used to allow the contrast agent to percolate through the vascular and extravascular spaces and is termed the "portovenous" or "venous phase" and is commonly referred to as a "routine post-contrast CT." Further phases can be obtained if they would add value to the clinical reason for the study, such as assessing for blood pooling in suspected active extravasation.

The dose of contrast administered varies between 75 and 150 cc, dependent largely upon the local practice of the imaging center, and is also affected by the CT technology available. Newer machines with dual energy capabilities can obtain diagnostic quality images with as little as 20 cc of contrast. Intravenous contrast is not routinely indicated for the presurgical evaluation of common hernia types but is extremely useful in the postoperative patient looking for complications of surgery, such as bleeding, or abscess formation [1, 3]. Venous phase imaging is particularly useful for assessing bowel viability, either prior to or following surgical repair. It is not of value in suspected cases of bowel obstruction but is mandatory to assess for bowel ischemia.

Table 1.3 Indications for use of IV contrast

Indication/ Concern	Non-Contrast CT	Arterial Phase CT	Venous Phase CT
Presurgical evaluation of hernia	X		
Active Bleeding		X	X
Abscess			X
Bowel ischemia			X

Follow-up assessment of the adequacy or integrity of a hernia repair, if needed, can be done without the use of intravenous contrast. Contraindications to the use of iodinated contrast do vary between imaging centers, but generally, contrast should be used with caution in patients who have had a prior reaction, or those with renal failure (eGFR < 30 mL/min/1.73 m^2) [10–12]. In patients who have had a prior anaphylactoid reaction, contrast should not be used [12] (Table 1.3).

Luminal contrast refers to contrast that is either given orally, rectally, or via an ostomy [12]. Oral contrast, as its name implies, refers to the administration of either a barium-based or iodine-based contrast agent via the mouth. It is used to opacify the stomach and small bowel to make them appear bright or dense on the CT image. This is useful to assess for the presence of bowel when the hernia sac contents are in doubt presurgically. In the postoperative patient oral contrast can differentiate between partial or complete bowel obstruction or can be used to assess for a bowel leak when there is suspicion for bowel perforation [13]. Rectal or per ostomy contrast is useful to assess the large bowel anatomy, leaks, or to delineate the contents of a parastomal hernia.

It is important to bear in mind that simultaneous administration of luminal contrast from multiple routes can present challenges to image interpretations. For example, it may be difficult or impossible to determine the origin of extravasation if a patient with a bowel leak receives both oral and rectal contrast. Similarly, it would be difficult to evaluate for the presence of a fistula between bowel loops. As physicians who order these exams, having a clear understanding of the clinical question that imaging needs to answer

can help limit the number of phases and routes of contrast administration. Imaging should aim to answer the clinical questions using the least amount of radiation possible.

CT Dose and Exposure Mitigation

As providers interact with patients, it is prudent for physicians to have a working knowledge and understanding of radiation dose exposure from CT scanning. The first and most important consideration one must always address is the risk-benefit ratio of performing the study, just as with any other test or procedure that a patient may undergo. The basic determination that all physicians who order a CT scan to evaluate for the possibility of a hernia or to plan its surgical correction, or to assess for a complication, is that the benefit of information obtained from the scan outweighs the risks of exposure to radiation [14]. After medical necessity is established, steps should be taken to minimize radiation exposure to patients. This is the central tenet of the ALARA principle which is an acronym for the phrase As Low As Reasonably Achievable [4].

Ionizing radiation transfers energy to electrons in the body and has sufficient energy to break chemical bonds. This generates free radicals which can damage DNA leading to gene mutations. When mutations accumulate, cell death or carcinogenesis may occur. The amount of damage that can occur depends on what is termed absorbed dose, which is the total amount of energy deposited into the tissues. If the absorbed dose is large, which is unlikely to occur in a diagnostic setting, reactions such as erythema, temporary hair loss, or skin burns may occur. These are called "deterministic effects," and only occur after a specific threshold dose is reached. Carcinogenesis is not a deterministic effect but is termed a "stochastic effect" meaning that it can occur independent of radiation dose. Stochastic effects can occur following a cell's exposure to any amount of radiation, possibly resulting in deleterious gene mutation of its DNA. Over time, if enough mutations occur in the same cell, this may cause the cell to become cancerous. Historical studies have shown that increased cancer rates for solid tumors were directly correlated with radiation dose. Simply put, with increased exposure there is an increased risk of acquiring a mutation that could lead to cancer. This is a cumulative phenomenon, with increasing exposure to radiation leading to an increased chance of developing a radiation-induced cancer.

Patient age at exposure is also important as it is the single most important factor in determining lifetime attributable risk of cancer induction and mortality from radiation exposure [6]. In part, this is due to the increased radiosensitivity of cells in the younger population. It is also due to increased sensitivity of rapidly proliferating cells in the young compared to slowly proliferating or nonproliferating cells in older patients. This results in a child, for example, being orders of magnitude more sensitive to the effects of radiation than a 65-year-old adult. Another factor to consider is latency. Radiation-induced cancers may not manifest or become clinically relevant for years after the inciting event, with this delay termed latency. A radiation-induced cancer may not present for decades with elderly patients succumbing to old age or other comorbidities before manifesting a clinically significant radiation-induced cancer. Younger patients on the other hand, as they are expected to live longer after being exposed, could survive long enough to incur morbidity or mortality from radiation-induced cancer.

Hence, patients should be exposed to radiation only when the benefits outweigh the risks, and in most clinical scenarios, the benefits do outweigh the risks. The likelihood of developing a medical radiation-induced cancer is far less than that of spontaneous cancer.

Radiation dose is dependent on several factors, such as the kV of the X-ray beam (how fast the X-rays are passing through the body), the mAs (how many of those X-rays are being used to gather information), the table speed moving per unit time (referred to as table pitch), and the size of the patient [6]. Some of these variables are fixed for the entire exam type, while others are adjusted on the fly automatically by the scanner. An example is increasing the mAs and hence dose in thicker parts of the body, such as scan-

ning through the hips, and lowering the mAs and hence radiation dose when scanning through thinner parts of the body, as in the lung bases. Such automation in newer machines has resulted in significant radiation dose reduction compared to older technology. Exams should only be ordered in the area of interest, as this too can help reduce radiation exposure. Additionally, there are newer reconstruction algorithms using advanced math, and now artificial intelligence, to squeeze out every ounce of useful information obtained during a scan. This allows diagnostic images to be acquired with even less radiation dose. These are referred to as iterative reconstruction techniques and are common on modern scanners.

Measurement of radiation exposure in every CT study is recorded in the "dose sheet" and usually is part of the permanent image archive (Fig. 1.3). There are 2 dose measurements typically given: Computed Tomography Dose Index (CTDI) vol and Dose-Length Product (DLP) [6, 15]. As expected, the lower the value of CTDI and DLP, the better. CTDI vol is a measure of the total radiation exposure to the patient as part of the scan; however, this is an incomplete picture of dose. To add relevance to this number, it is important to consider the area over which this dose was distributed. This is represented in the DLP value [16]. Governing and societal bodies on both sides of the Atlantic have provided reference dose values for typical imaging studies, and imaging centers try to maintain their dose values within these ranges [6, 17]. Many North American centers automatically submit their CT dose sheets to national registries as part of a joint quality assurance program. Occasionally, dose may be higher for certain patients especially with large habitus [18, 19], as the fundamental consideration of any study is to obtain useful diagnostic information to answer the clinical questions using the lowest radiation dose possible, discussed in detail later.

Challenges of Imaging Large Patients

Larger patients require special consideration when being imaged with CT. The CT scanner must be able to accommodate their weight, girth,

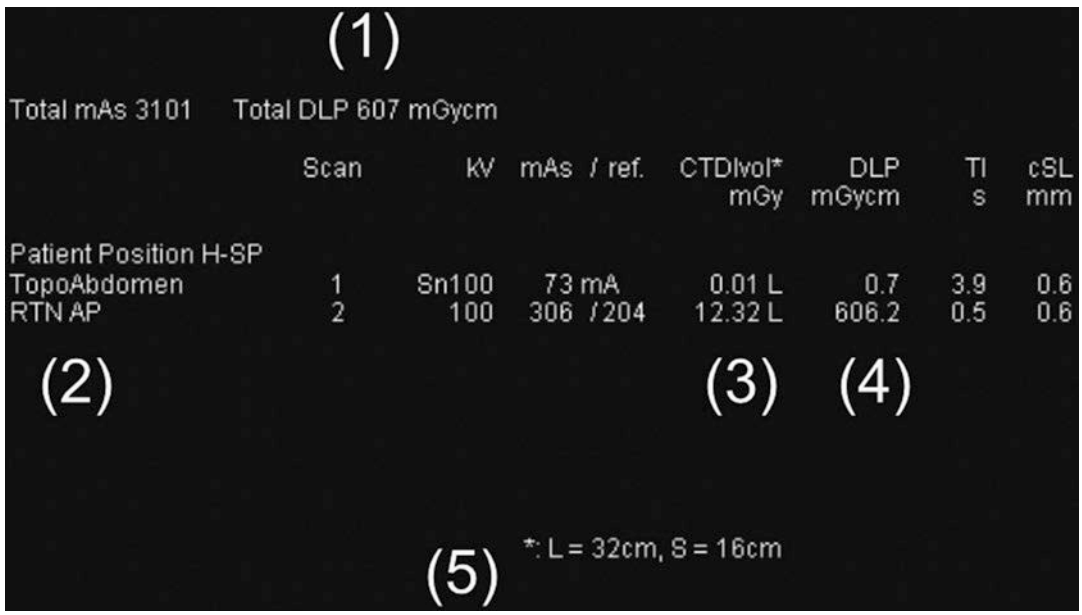

Fig. 1.3 Dose sheet from a CT scan. (1) Total DLP represents the total radiation exposure for the study distributed over the area scanned, (2) the number of scans performed, (3) CTDI vol is the radiation exposure calculated using a standard size phantom (5), and (4) is a breakdown of the DLP by each scan performed

and obtain images without exceeding the X-ray tube capacity [18–20].

Like any machine with moving parts, the CT table has a finite weight limit, determined by the manufacturer. Modern scanners have increased the table weight capacity to scan patients over 300 kg or 670 lbs. There may still be patients who cannot be scanned, as they exceed the table weight limit.

Patients need to be able to move freely through the aperture as they are being scanned. If a patient with a large body habitus is physically in contact with the walls of the gantry, artifacts may obscure the region of interest and degrade image quality. The diameter of the bore on modern CT scanners ranges between 70 and 80 cm, depending upon the manufacturer and specification of the machine. It is not uncommon to encounter patients who are unable to be accommodated in the bore [3].

Dose, as mentioned earlier, is dependent on kV (how fast the X-rays are moving through the patient) and mAs (how many X-rays are moving through the patient). Larger patients receive a greater dose at comparable machine settings. As the X-ray beam passes through larger patients, more radiation is absorbed resulting in an increased dose. Consequently, fewer X-rays make it through to the detector, termed photon starvation, leading to images with excessive noise and graininess. To preserve image quality, the CT scanner may automatically increase the number and energy of the X-rays to compensate, resulting in further increases in dose. Just as there are patients who cannot be scanned because of the physical limitations of the scanner, there are patients who cannot be effectively scanned because their biomass exceeds the X-ray tube's capacity.

Imaging Artifacts on CT

Artifacts are errors in medical imaging that occur as a result of complex physical interactions or flaws in data acquisition and image reconstruction. They are ubiquitous in diagnostic imaging, though there is variance based on modality. While in many cases, artifacts can be beneficial, in CT, artifacts generally result in image degradation. A cursory awareness of common CT artifacts is important to understand the limitations of the modality, with the exact physical basis beyond the scope of this book or of practical use [4, 5].

One of the most commonly encountered artifacts occurs when patients move during the acquisition of the CT images, referred to as "*motion artifact*." This results in blurred images with suboptimal evaluation of muscle planes and the solid viscera (Fig. 1.4).

Partial volume averaging occurs when a structure is partially included on two adjacent slices [8]. The thinner the slice of the CT image, the less the chance for this artifact developing and vice versa. This artifact can lead to an incorrect assessment of the margins or density of an organ, muscle, or fascial boundary (Fig. 1.5). Experienced image interpreters can often accurately identify this artifact and avoid misinterpretations.

Beam hardening artifacts occurs as a result of metal hardware within the body, either iatrogenic or traumatic. Common medical causes include the presence of hip arthroplasties, spinal fusion hardware, or scoliosis correction rods, with traumatic causes being bullet fragments or shot pellets. Due to the presence of the metal, the X-rays are unable to penetrate all the way through the body and hence failed to get detected. This results in alternating black and white bands across the image, appropriately referred to as streak artifacts (Fig. 1.6).

Out of field artifact occurs in larger patients whose body habitus extends outside the field of view of the scanner. This is a particular problem if the body is in contact with the sidewall of the bore, as seen in obese patients or those with large lateral abdominal hernias. It can also commonly be seen in patients whose arms cannot be raised out of the scan field. The scanner, unable to compensate for anatomy outside of the field of view, reconstructs images with bright and dark areas obscuring the outer margins (Fig. 1.7). Proper positioning of the patient on the table and in the bore is therefore essential to obtain diagnostic images.

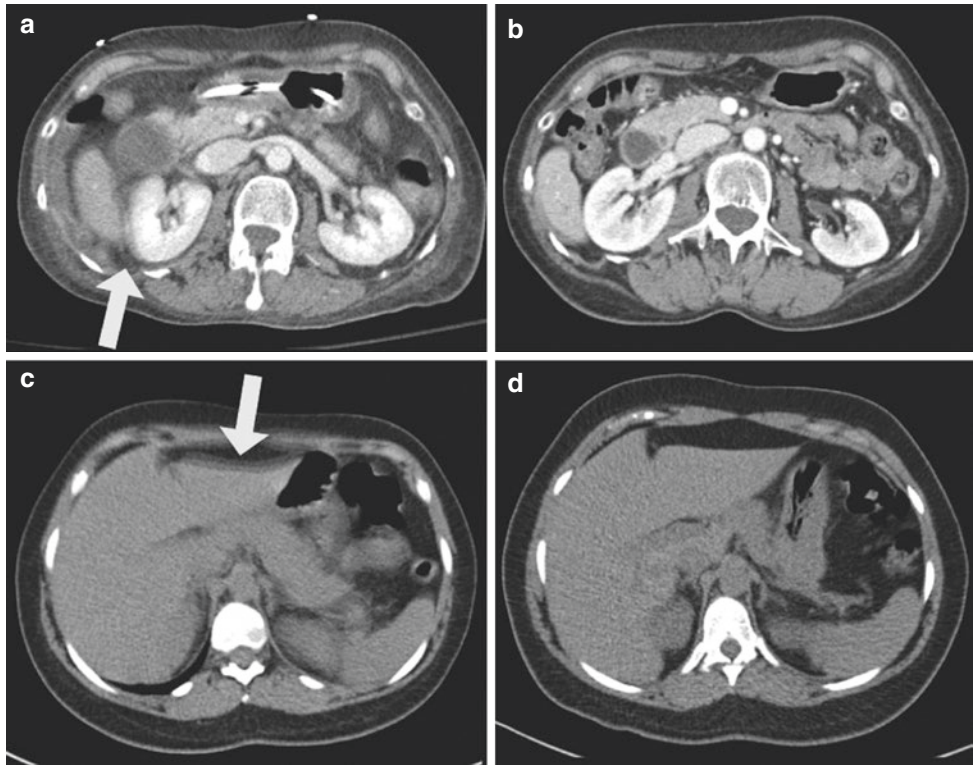

Fig. 1.4 *Motion artifact* obscures details within an image. The margins of the right kidney are blurred (**a**, arrow) compared to a picture where the anatomy is still during the scan (**b**). Similarly, the blurred margins at the anterior left liver lobe (**c**, arrow) becomes sharper with no motion artifact (**d**)

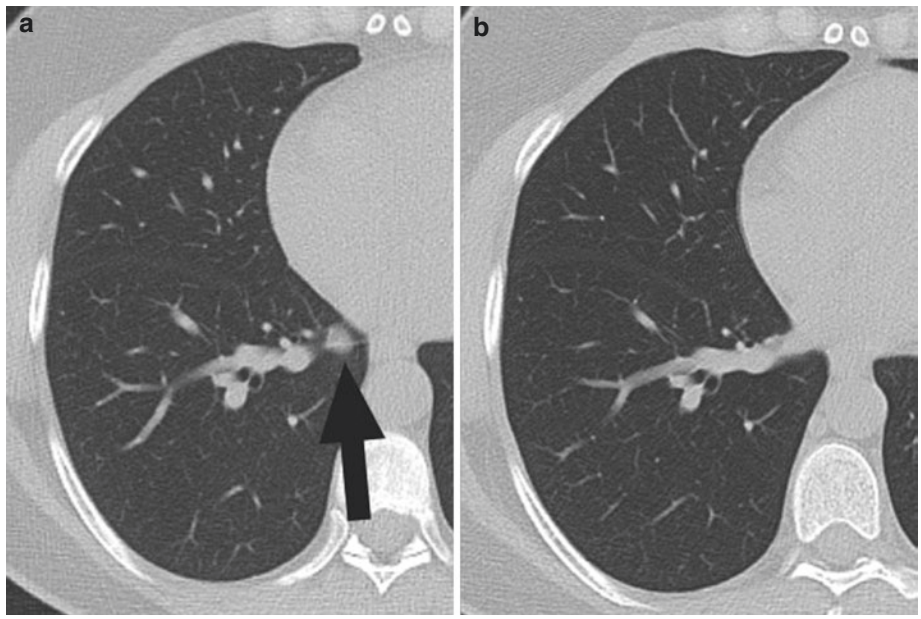

Fig. 1.5 A structure partially included in one slice can give the false impression of a finding. The density in the right lower lung (**a**, arrow) may be misinterpreted as a nodule. A formal evaluation of the chest (**b**) shows a normal right lower lobe. This is an example of "*partial volume averaging*"

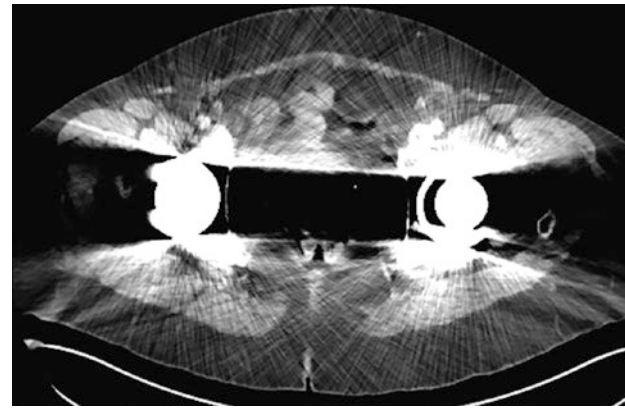

Fig. 1.6 The presence of bilateral hip arthroplasties creates black and white streaks across the image, referred to as "*beam hardening artifact*." In this particular case, the contents of the inner pelvis cannot be resolved

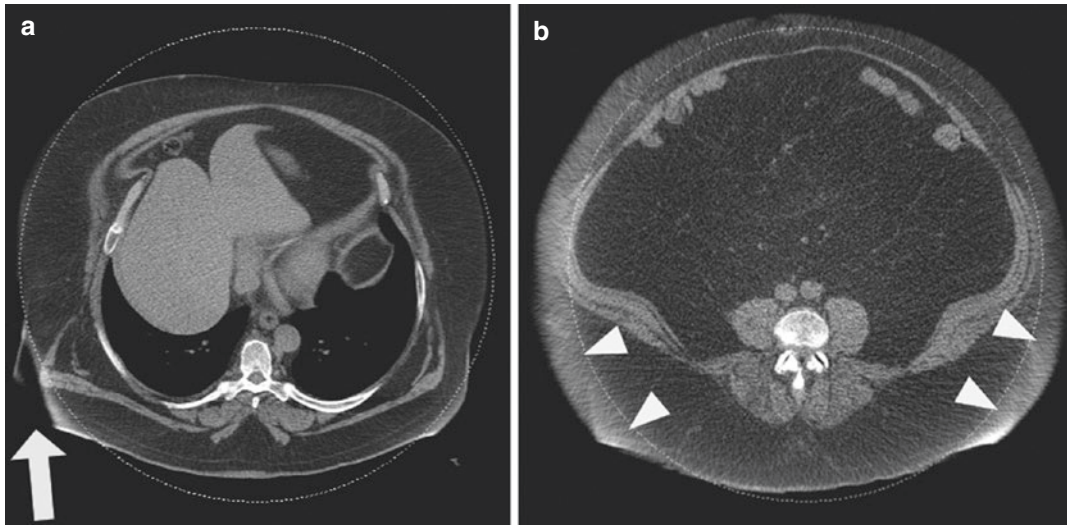

Fig. 1.7 As the body touches the opening of the CT scanner, there are artifactual black bands (**a**, white arrow) and white areas (**b**, arrowheads) at the periphery of the image due to the anatomy being "*out of field.*" Also, the graininess of image (**b**) represents "*noise*" and is due to the paucity of X-rays being detected, as they are absorbed in the body

Large body habitus, faulty X-ray sources, and inappropriately low acquisition settings (kV and mAs values) can lead to a paucity of photons penetrating and hitting the detector, leading to mottled images, referred to technically as "*noise*." Noise degrades imaging quality, which can create difficulty in image interpretation. Oftentimes, large body habitus is the cause of this artifact, and hence it is difficult to correct or overcome. Only rarely are inappropriate settings the cause of noise due to modern scanners being automated.

References

1. Aguirre DA, Santosa AC, Casola G, Sirlin CB. Abdominal wall hernias: imaging features, complications, and diagnostic pitfalls at multi-detector row CT. RadioGraphics. 2005;25(6):1501–20.
2. Lassandro F. Abdominal hernias: radiological features. World J Gastrointest Endosc. 2011;3(6):110.
3. Halligan S, Parker SG, Plumb AA, Windsor ACJ. Imaging complex ventral hernias, their surgical repair, and their complications, vol. 28. European Radiology. Springer Verlag; 2018. p. 3560–9.
4. Huda W. Review of radiologic physics: 3rd ed.; 2012.

5. Barrett JF, Keat N. Artifacts in CT: recognition and avoidance. RadioGraphics. 2004;24(6):1679–91.
6. McNitt-Gray MF. AAPM/RSNA physics tutorial for residents: topics in CT. RadioGraphics. 2002;22(6):1541–53.
7. Cody DD. AAPM/RSNA physics tutorial for residents: topics in CT. RadioGraphics. 2002;22(5):1255–68.
8. Shirkhoda A. Diagnostic pitfalls in abdominal CT. Radiographics. 1991;11(6):969–1002.
9. Kammerer S, Höink AJ, Wessling J, Heinzow H, Koch R, Schuelke C, et al. Abdominal and pelvic CT: is positive enteric contrast still necessary? Results of a retrospective observational study. Eur Radiol. 2015;25(3):669–78.
10. McDonald JS, McDonald RJ, Carter RE, Katzberg RW, Kallmes DF, Williamson EE. Risk of intravenous contrast material–mediated acute kidney injury: a propensity score–matched study stratified by baseline-estimated glomerular filtration rate. Radiology. 2014;271(1):65–73.
11. Beckett KR, Moriarity AK, Langer JM. Safe use of contrast media: what the radiologist needs to know. RadioGraphics. 2015;35(6):1738–50.
12. Davenport MS, Asch D CJ et al. ACR Committee on Drugs and Contrast Media. ACR manual on contrast media: version 10.3 [Internet]. American College of Radiology website; 2020 [Accessed 2020 Mar 31]. Available from: https://www.acr.org/Clinical-Resources/Contrast-Manual
13. Chang KJ, Marin D KD et al. ACR Appropriateness Criteria® Suspected Small-Bowel Obstruction [Internet]. American College of Radiology website; 2019 [Accessed 2020 Mar 31]. Available from: https://acsearch.acr.org/list?_ga=2.206610199.541458916.1585687084-1005367801.1584533907
14. Shah S, Khosa F, Nicolaou S. Radiation dose reduction strategies for acute abdominal and pelvic CT. In: MDCT and MR imaging of acute abdomen: new technologies and emerging issues. Springer International Publishing; 2018. p. 11–21.
15. MacGregor K, Li I, Dowdell T, Gray BG. Identifying institutional diagnostic reference levels for CT with radiation dose index monitoring software. Radiology. 2015;276(2):507–17.
16. Huda W, Mettler FA. Volume CT dose index and dose-length product displayed during CT: what good are they? Radiology. 2011;258(1):236–42.
17. American College of Radiology. ACR-AAPM practice parameter for diagnostic reference levels and achievable doses in medical X-ray imaging [Internet]; 2018 [Accessed 2020 Mar 31]. Available from: https://www.acr.org/-/media/ACR/Files/Practice-Parameters/Diag-Ref-Levels.pdf
18. Huda W, Scalzetti EM, Levin G. Technique factors and image quality as functions of patient weight at abdominal CT. Radiology. 2000;217(2):430–5.
19. Yanch JC, Behrman RH, Hendricks MJ, McCall JH. Increased radiation dose to overweight and obese patients from radiographic examinations. Radiology. 2009;252(1):128–39.
20. Modica MJ, Kanal KM, Gunn ML. The obese emergency patient: imaging challenges and solutions. RadioGraphics. 2011;31(3):811–23.

Magnetic Resonance Imaging (MRI) Basics

2

Kelly Tunder and Kimberly R. Coughlin

Introduction

Hernia repair remains one of the most common surgical procedures performed today. Therefore, there are several imaging modalities used to diagnose hernias. Imaging, particularly ultrasound (US) and computed tomography (CT) have been the imaging study of choice to evaluate for hernias. The long-known benefits of magnetic resonance imaging (MRI) are no radiation and the high specificity for soft tissue and musculoskeletal complaints. However, MRI has been shown to have benefit in both detection of occult hernias as well as for workup of patients with groin pain. A study by Miller et al of 322 patients with occult hernias demonstrated the greatest sensitivity, specificity, and negative predictive value for diagnosing the hernia in patients undergoing a MRI as compared to patients who underwent an ultrasound or CT scan. MRI had a sensitivity of 91% as compared to US (33%) and CT (54%). Ten of the 11 patients that had an occult hernia detected on MRI, that were not otherwise seen on CT scan or US, had confirmation of the hernia at the time of surgery. One patient with a false positive MRI had a surgically correctable fascial tear of the external oblique, but no true hernia. MRI also plays a valuable role in patients with significant groin pain but an otherwise negative workup as it can elucidate other causes of groin pain, such as osteitis pubis, rectus abdominis strain, and rectus abdominis/adductor aponeurosis injury. The value of MRI for athletic pubalgia has been validated due to the recognition of injury patterns in the anatomic structures surrounding the pubic symphysis not otherwise seen on CT or US. As the pathophysiology and anatomy of the pelvic region come to be better understood, so too does the MRI and surgeon's ability to detect pathology in the groin.

Basic MRI Principles

The underlying principles of MRI are complex; however, it is important that surgeons have a general understanding of these basics in order to view and interpret patient's imaging. Along with their clinical presentation, MRI review is imperative for diagnosing and creating a treatment plan for patients. MRI relies on the abundance of hydrogen-rich tissues such as water, fat, and proteins in the human body. When a strong magnetic field acts upon hydrogen protons, a majority of protons align. To obtain an image, a radiofrequency (RF) pulse is applied perpendicular to the region of interest. Following the absorption of the RF pulse, the protons eventually return to their normal low-energy state. In this process, RF sig-

K. Tunder (✉) · K. R. Coughlin
Department of Surgery, Columbia University Medical Center, New York, NY, USA
e-mail: krc2171@cumc.columbia.edu

S. Docimo Jr. et al. (eds.), *Fundamentals of Hernia Radiology*,
https://doi.org/10.1007/978-3-031-21336-6_2

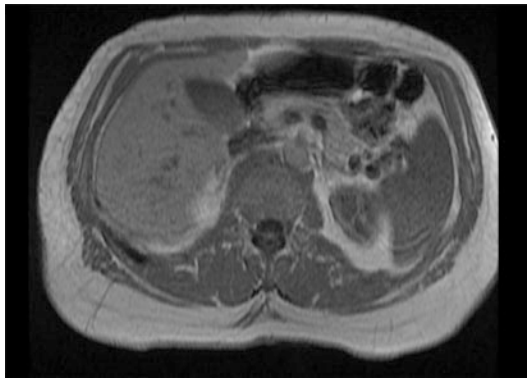

Fig. 2.1 T2-weighted abdominal magnetic resonance imaging

nals are emitted and detected electronically in order to construct the image. The emitted signal provides the information to form the magnetic resonance image. The signal has two components, T1 and T2. T1-weighted images are broken into T1W1 (pre-contrast), in-phase, out-of-phase, and post-contrast. T1W1 demonstrates a low signal for water molecules, i.e, dark. Hyperintense material includes fat, melanin, proteinaceous fluid, and gadolinium contrast. T1W1 images are excellent for the delineation of abdominal anatomy (Fig. 2.1). In-phase can help delineate the boundaries between fat and water which is helpful in identifying fat, for example, within the liver versus a liver lesion. Out-of-phase images are helpful to identify fat within a lesion, for example, delineate a hepatocellular adenoma versus adenocarcinomas. On T2-weighted images, fluid, edema, fat, and some hemorrhagic products are bright by nulling the fat signal.

Normal Pelvic Anatomy on MRI

The pelvis is an anatomically and functionally complex region that has a significant impact on a patient's everyday life. Understanding the anatomy of imaging, particularly MRI, aids in the diagnosis and treatment of patients with groin pain and occult hernias.

The most important attachments to the pubic symphysis are the rectus abdominis and the adductor longus. The rectus abdominis inserts caudally at the anterior and anterior-inferior regions of the pubic symphysis (Fig. 2.2). The lateral rectus abdominis attachment is in close proximity to the external inguinal ring, which may explain the association with inguinal hernia symptoms. The interconnected tendinous attachments play a vital role in pubic symphysis stability. With rotation and extension, the rectus abdominis and adductor longus work against each other. Injury to one tendon results in a tendency toward injury of the opposing tendon, and therefore causing the pubic symphysis to become unstable. This instability leads to osteitis pubis and chronic groin pain in many athletes. This combination of rectus abdominis and adduc-

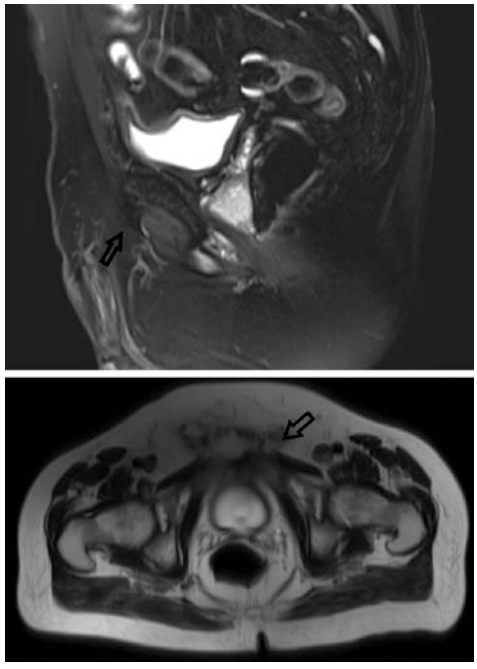

Fig. 2.2 Normal anatomy

Fig. 2.3 Axial oblique T1-weighted image shows normal muscles around the pubic symphysis (PS). *AB/AM* Adductor brevis/adductor magnus, *AL* Adductor longus, *O* Obturator

tor fibers along with the pubic symphysis capsule, arcuate ligament, and anterior pubic periosteum form a large midline aponeurotic plate (Fig. 2.3). This aponeurotic plate is subject to the same range of pathology as other fibrous joints leading to inflammation and instability of the anterior pelvis. Understanding normal anatomy on MRI is extremely important in order to identify abnormal anatomy.

MRI Protocol for Groin Pain

MRI plays a valuable role in patients with significant groin pain but an otherwise negative workup as it can elucidate other causes of groin pain such as osteitis pubis, rectus abdominis strain, and rectus abdominis/adductor aponeurosis injury. Groin pain is a frequent manifestation of athletic injury that is seen in athletes that twist at the waist, perform sudden acute directional change and sideways movements such as soccer, ice hockey, and football. Clinical differentiation of athletic groin pain is challenging due to the multitude of potential etiologies. Typically, patients will present with insidious

onset of pain in the region of the inguinal region, but in other cases, the pain will occur immediately after a twisting/hyperextension injury. At physical exam, pain to palpation is present at the external inguinal ring without a palpable hernia. Groin injuries will often respond to conservative therapy; however, a significant portion will not resolve completely or recur with resuming athletic activities. The large number of terms used to describe athletic groin pain: sports hernia, sportsman hernia, athletic pubalgia, Gilmore groin, osteitis pubis, adductor syndromes, and hockey goalie syndrome reflect the complicated pathophysiology and anatomy of the region. This confusion demonstrates the need for high-quality, reproducible imaging of this area in order to guide effective therapy.

MRI is the current standard for the evaluation of musculoskeletal pelvic pain. A dedicated athletic pubalgia protocol is recommended to delineate the etiology of the groin pain. A MRI of the pelvis with musculoskeletal protocol is ordered, non-contrasted with Valsalva. The patient is positioned supine with an empty bladder. A non-fat-suppressed T1-weighted spin echo is done to evaluate for an infiltrative bone marrow process such as metastases, myeloma, or infection. Axial T2-weighted fast spin echo (FSE) fat-suppressed image is performed to assess the symmetry of muscles, tendons, bursae, and osseous structures. Axial oblique images are then performed paralleling the arcuate line of the pelvis. These images highlight the caudal rectus abdominis attachments and open up the adductor tendon origins. A T2-weighted fat sagittal image is obtained centered at the pubic symphysis. This sequence evaluates the rectus abdominis/adductor aponeurosis with its periosteal attachments on the anterior and anterior-inferior pubic ramus (Fig. 2.4). The advantage of a specific protocol is that it provides specific evaluation for common musculoskeletal causes of groin pain. Furthermore, it allows evaluation for inguinal hernias and non-musculoskeletal groin pain and if not conclusive can guide further evaluation of these conditions.

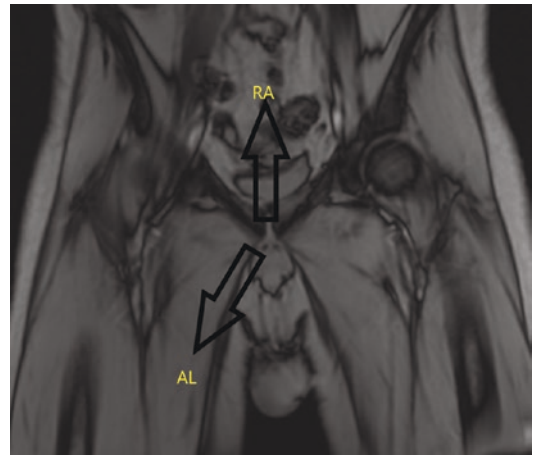

Fig. 2.4 The opposing vectors of force between the aponeurotic insertion of the caudal rectus abdominis (RA) and the adductor longus (AL) muscles on the anterior pubic symphysis

MRI Pathology

Reproducible patterns of pathology have been described using the athletic pubalgia protocol to evaluate musculoskeletal groin pain. A review should be done by a musculoskeletal specialty-trained radiologist as well as the ordering surgeon in a systematic fashion in order to classify injuries based on MRI findings.

Osteitis Pubis

Osteitis pubis is a degenerative process of the pubic symphysis and occurs secondary to repetitive stresses. Subchondral bone marrow edema in a pattern reminiscent of osteoarthritis is the hallmark MRI finding of osteitis pubis (Fig. 2.5). The edema may be bilateral, though it can be, and often is, asymmetric with the side of pain demonstrating more extensive or intense edema. The bone marrow edema should span the subchondral region of the symphysis from anterior to posterior.

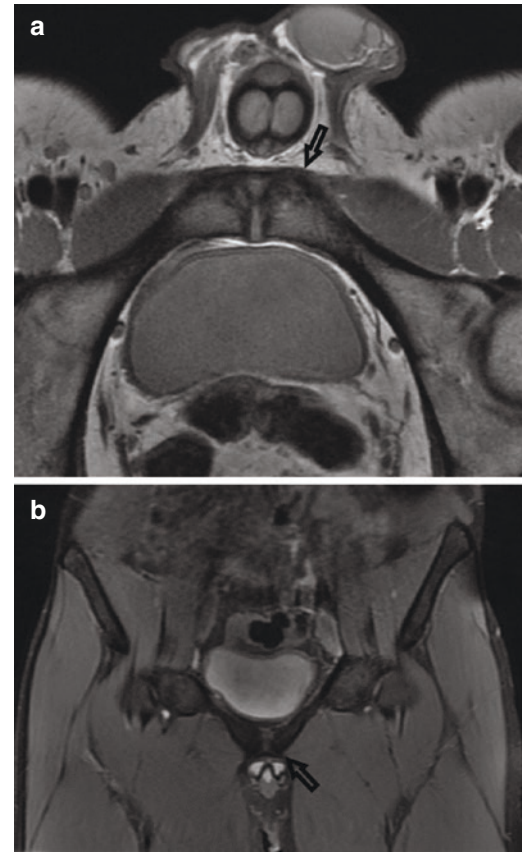

Fig. 2.5 MRI of osteitis pubis. Axial image of a 21-year-old soccer player shows (**a**) left osteitis pubis with the widening of the pubic symphysis and (**b**) shows subchondral edema of the left pubic bone

Rectus Abdominis Strain

Evaluation of signal and morphology of the caudal rectus abdominis is used to differentiate between acute and chronic injury. A tear in the tenoperiosteal caudal rectus abdominis attachment is commonly a source of pain and instability at the pubic symphysis. Commonly the rectus abdominis pathology will extend into the adductor longus origin or the contralateral rectus abdominis attachment.

Adductor Tendon Syndromes

Tendinopathies at the proximal adductor show enlargement and signal abnormalities as hallmark findings. Adductor tendon syndromes range from strains, acute avulsions at the tendon origins, or more chronic findings. MRI has demonstrated accuracy in identifying the numerous adductor injury variants (Figs. 2.6 and 2.7). Rarely, an adductor tendon will avulse and retract without

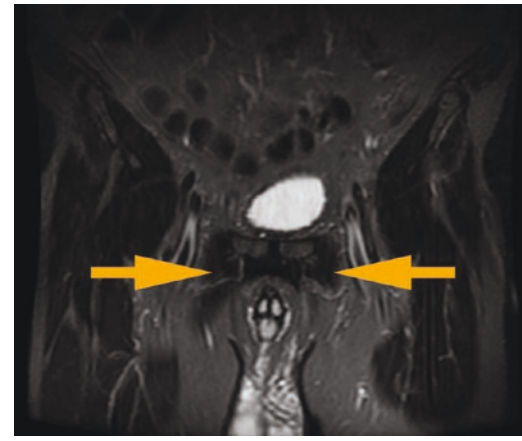

Fig. 2.6 MRI imaging of severe bilateral adductor longus tendinosis

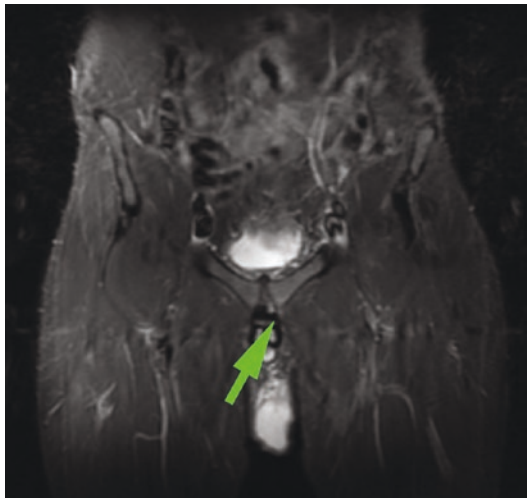

Fig. 2.7 MRI Imaging of left osteitis pubis with adductor tendinosis

osseous fragment, which is almost always seen with ipsilateral rectus abdominis injury.

Rectus Abdominis/Adductor Aponeurosis Injury

The combination of a distal rectus abdominis detachment or tearing from the pubic ramus with a partial or complete adductor longus origin tear can be described as an ipsilateral rectus abdominis/adductor detachment. This pattern of injury is the most frequently encountered lesion for athletic pubalgia on MRI (Fig. 2.8). The lesion can be ipsilateral or bilateral and there is a high association with osteitis pubis. Athletes with this injury are more likely to benefit from an adductor tenotomy than those with isolated rectus or adductor injuries. Atrophy of the rectus muscle is commonly seen with this injury and may represent chronic tendinous lesion, previous rectus abdominis strain, or denervation injury.

Rectus Abdominis/Adductor Aponeurotic Plate Disruption

This injury pattern involves a bilateral caudal rectus attachment-detachment which spans

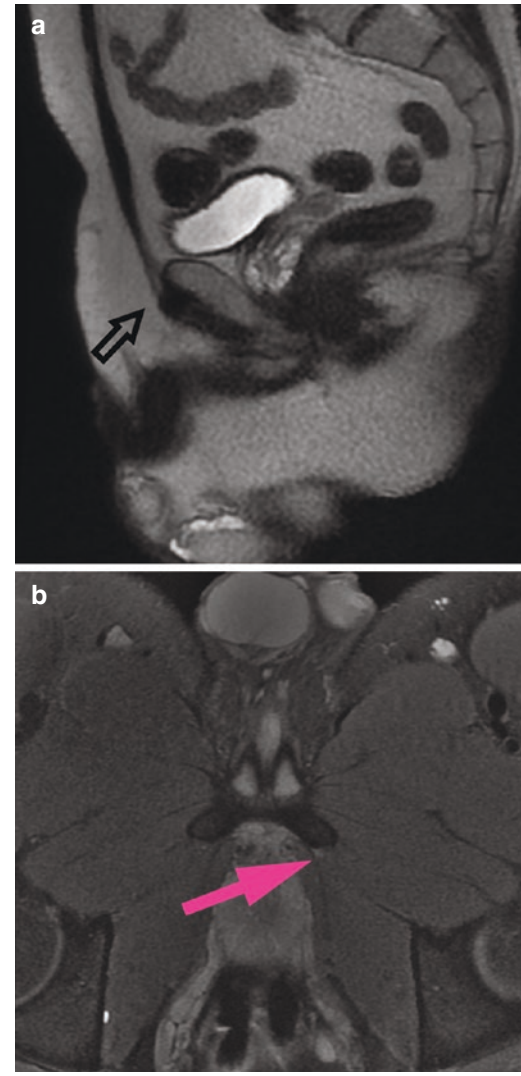

Fig. 2.8 MRI of (**a**) rectus abdominis injury (arrow) and (**b**) adductor aponeurosis injury (arrow)

midline. Osteitis pubis is commonly seen with these lesions. Athletes with this lesion rarely return to optimal performance without surgical intervention.

Inguinal Hernias

The inguinal canals are best evaluated on the coronal oblique images where they will be viewed in the long axis. The hernia is seen as an abnormal widening, beyond the diameter of the spermatic

Fig. 2.9 MRI T2 axial imaging of a left inguinal hernia

cord or round ligament, of the anteroposterior diameter of the inguinal canal and/or simultaneous protrusion of abnormal contents (fat and/or bowel) within the inguinal canal. MRI can be performed dynamically and can aid in the detection of occult hernias. Fluid within the hernia will show hyperintense on T2 and hypointense on T1 and can detect the hernia sac in hernias not otherwise seen on US or CT (Fig. 2.9).

Confounding Pathologies

Given the myriad of adjacent structures, it is not surprising that multiple other pathologic processes are often detected on athletic pubalgia protocol MRI. Muscle strains, stress fractures, hip pathology, lumbar spine and sacroiliac joint pathology, visceral pathology (ovarian follicles, endometriosis, adenomyosis, and uterine fibroids) can present with similar symptoms to athletic pubalgia.

Conclusion

Over the years the imaging modalities for hernias have improved significantly. Imaging, particularly ultrasound (US) and computed tomography (CT) have been the imaging study of choice to evaluate for hernias. MRI has now been proven to have benefit in both detection of occult hernias as well as for workup with patients for groin pain. It is important for surgeons to have a general understanding of the basics of MRI principles and anatomy and pathology to properly guide their treatment plan for patients.

Normal MRI of the rectus abdominis/adductor aponeurotic plate and aponeurosis

Bibliography

1. Currie S, Hoggard N, Craven IJ, et al. Understanding MRI: basic MR physics for physicians. Postgrad Med J. 2013;89:209–23.
2. Jacob BP, Chen DC, Ramshaw B. The SAGES manual of groin pain. Springer; 2016.
3. Miller J, Cho J, Michael MJ, Saouaf R, Towfigh S. Role of imaging in the diagnosis of occult hernias. JAMA Surg. 2014;149(10):1077–80.
4. Mullens FE, Zoga AC, Morrison WB, et al. Review of MRI technique and imaging findings in athletic pubalgia and the "sports hernia". Eur J Radiol. 2012;81:3780–92.
5. Novitsky, et al. Hernia surgery. Springer; 2016.
6. Omar IM, Zoga AC, Kavanagh EC, et al. Athletic pubalgia and "sports hernia": Optimal MR imaging technique and findings. Radiographics. 2008;28:1415–38.
7. Van den Berg JC. Inguinal hernias: MRI and ultrasound. Semin Ultrasound CT MRI. 2002;23:156–73.

Ultrasonography Basics

3

Benjamin K. Poulose

Introduction

Ultrasound may be one of the most underutilized modalities in evaluating hernia and diseases of the abdominal core musculature. The reasoning for this is multifactorial and includes the learning curve necessary to successfully perform in-office ultrasound, the general lack of reliable ultrasound for hernia diagnostics from our radiology colleagues, and the universal ease and familiarity with computed tomography. A major distinction should be made between ultrasound ordered by the surgeon and performed by a radiology department versus surgeon-performed ultrasound. The former often varies in quality and usability given the ultrasonographer's experience in evaluating the abdominal wall, the radiologist's familiarity evaluating complex abdominal wall structures (i.e., inguinal anatomy), and the lack of real-time evaluation by the original surgeon ordering the study. The latter takes advantage of one of the most useful aspects of ultrasound: real-time evaluation of pathology by the treating clinician. A relatively small investment in time and money can pay back rewards of near-instant diagnosis, less exposure to radiation, and time savings from a patient perspective.

Patient Selection

In general, ultrasound is more effective and easier to perform in patients with less subcutaneous fatty tissue. The adipose distribution may vary widely in patients of similar body mass index (BMI). Patients with a high BMI may actually have a large distribution of visceral fat compared to subcutaneous fat, making the evaluation of the anterior abdominal wall relatively easy. Conversely, patients with a similarly high BMI may have extensive depth to the subcutaneous tissue making evaluation of the anterior abdominal wall fairly difficult. Ultrasound should generally be avoided in patients with open wounds and uncovered stomas unless the procedure can be performed while protecting the probe from cross-contamination. Placing the ultrasound probe in a sterile bag can often facilitate this process. Minimizing cross contamination should also be considered when evaluating patients on contact precautions per institutional policies and procedures. Abdominal wall ultrasound can be useful in many contexts including the clinic, inpatient floors, emergency room, and operating room.

One of the keys to performing successful abdominal wall ultrasound is knowing when to refer a patient for ultrasound performed by

B. K. Poulose (✉)
Center for Abdominal Core Health, Department of Surgery, Division of General and Gastrointestinal Surgery, The Ohio State University Wexner Medical Center, Columbus, OH, USA
e-mail: benjamin.poulose@osumc.edu

S. Docimo Jr. et al. (eds.), *Fundamentals of Hernia Radiology*,
https://doi.org/10.1007/978-3-031-21336-6_3

radiology teams. The diagnosis of intra-abdominal or vascular pathology should generally be referred to radiology or vascular centers where capabilities and experience can best serve patients. However, focused ultrasound of the anterior abdominal wall and core musculature can be effectively performed by surgeons.

Evaluation of the linea alba, rectus complex, linea semilunaris, and oblique musculature are readily accomplished by ultrasound. As such, evaluation of ventral hernia lends itself well to surgeon-performed ultrasound. One notable exception to this is the evaluation of the umbilicus due to the inherent air interface that often accompanies the evaluation of this structure. In contrast, evaluation of the inguinal region can be quite challenging given the underlying anatomy, difficulty in obtaining acoustic coupling, and challenge in interpreting images. Some of these shortcomings can be overcome by the dynamic nature of ultrasound where it can be coupled with physical examination and accentuating maneuvers (i.e., Valsalva) in real time.

Ultrasound Scanning

General Overview

The underlying principle of ultrasound utilizes the oscillation of mechanical pressure waves transmitted through a medium. The propagation velocity of sound waves varies through different types of biological tissue and varies with tissue density and compressibility (Table 3.1). The frequency of the sound wave is inversely related to the depth of penetration. Generally speaking, ultrasound probes of higher frequency (e.g., 12 MHz) cannot penetrate as deeply as lower frequency ultrasound probes (e.g., 5 MHz). High frequency however provides higher resolution and fidelity of images, making these probes ideal for the evaluation of the abdominal wall. The key physical principles of ultrasound-based imaging are shown in Fig. 3.1. As an ultrasound transducer emits sound waves, energy is emitted and reflected back toward the probe. This results in the creation of an ultrasound image. In addition to reflection, sound waves are absorbed, scattered, transmitted, and refracted. These actions contribute to "attenuation" of the ultrasound waves. Heterogeneous tissues have increased amounts of attenuation which allows for discernment of the tissues and structures while homogenous tissue (i.e., simple fluid) has minimal attenuation.

Table 3.1 Propagation velocity of sound waves through various biologic media (adapted from Hagopian and Machi)

Medium	Speed of sound wave (m/s)
Air	330
Fat	1460
Water	1480
Brain	1540
Kidney	1560
Liver	1580
Blood	1580
Muscle	1580
Eye lens	1640
Bone	3000–4500

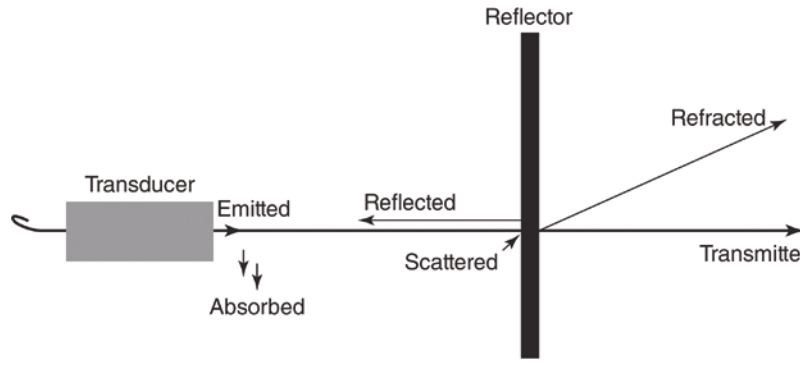

Fig. 3.1 Behavior of an acoustic wave traveling through a medium (adapted from Hagopain and Machi)

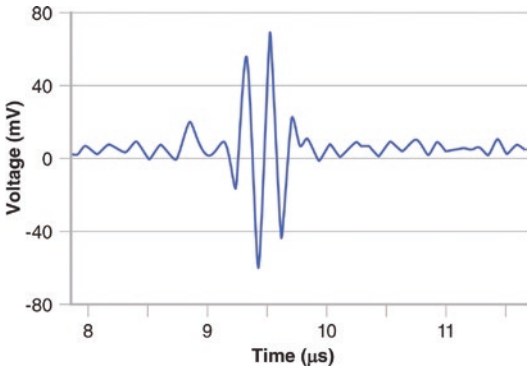

Fig. 3.2 A mode, amplitude modulation (adapted from Hagopian and Machi)

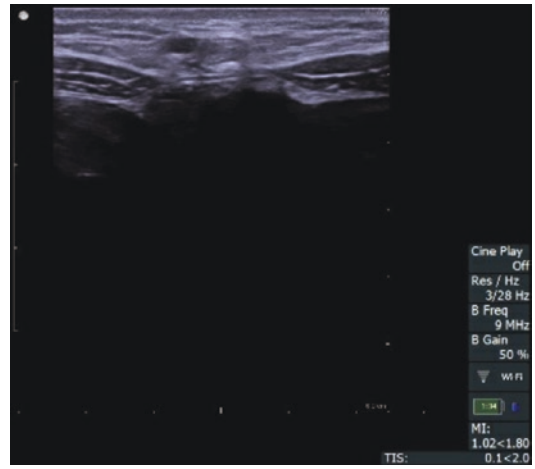

Fig. 3.3 B mode, brightness modulation

Several imaging modes are available for diagnostic ultrasound. A mode (amplitude modulation) is the simplest visualization and reflects the echo from a single transmitted pulse (Fig. 3.2). B mode (brightness modulation) represents a two-dimensional reconstruction of A mode information where the amplitude shown in A mode is converted to a pixel of proportional brightness (Fig. 3.3). B mode represents the most common type of image used in medical ultrasound. M mode shows motion over time; this is commonly used in echocardiography and vascular pathology and allows analysis of velocities and abnormalities in structural motion. Doppler modes allow for the quantification of flow velocities and are also commonly utilized in Cardiology and Vascular applications. Doppler modes can be combined with B mode images to identify vascular structures that can be of interest in the setting of traditional B mode visualization. This type of combined imaging is known as duplex ultrasound.

Ultrasound Probe Options

The ultrasound transducer (i.e., probe) is the most familiar component of an ultrasound diagnostic system to the surgeon. The main function of the transducer is to convert electrical energy into ultrasound energy and also sense the reflected ultrasound energy and convert this back to electrical energy for analysis. Modern piezoelectric transducers come in an array of shapes and sizes to accommodate different clinical approaches and applications (Fig. 3.4). The most common transducer used for the evaluation of abdominal wall pathology is the high frequency linear array (Fig. 3.5). Like most transducers, this has an orientation mark that corresponds to a digital marker seen on the output screen. In addition, most transducers have a multi-use button that commonly is used to freeze and unfreeze scanning for image capture.

Console Basics

The two most common controls utilized for adjusting the ultrasound image are gain and depth. Gain controls amplification of the electrical signal produced by the transducer which is then reflected in brightness on the ultrasound B mode image. Often a single overall gain control is present (Fig. 3.6) along with a more nuanced time gain compensation control. The latter allows selective amplification of signal at selectable depth; the control mechanism itself is reflective of the depth and is fairly intuitive (Fig. 3.7). The depth control (Fig. 3.8) allows changes in frequency and visualization distance from the transducer producing images and different distances from the transducer. The maximal depth is limited by the frequency of the transducer selected.

Fig. 3.4 Different types of ultrasound probes (adapted from Hagopian and Machi)

Fig. 3.5 High-frequency linear transducer used for abdominal wall evaluation

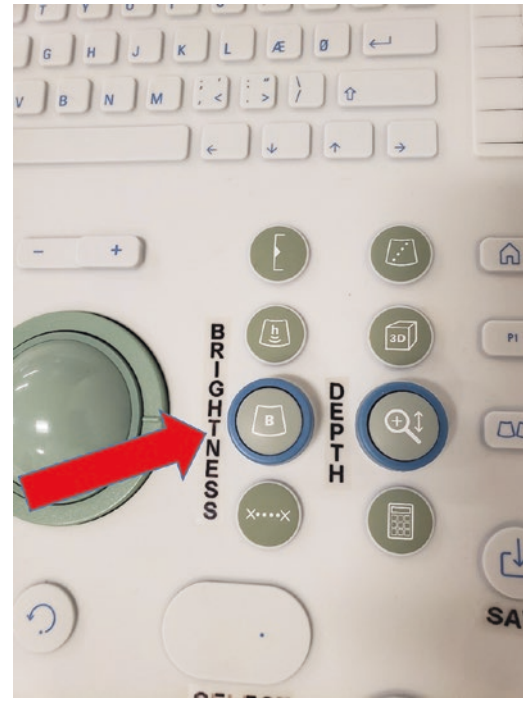

Fig. 3.6 Gain control changes amplification of the electrical signal and alters brightness in B mode

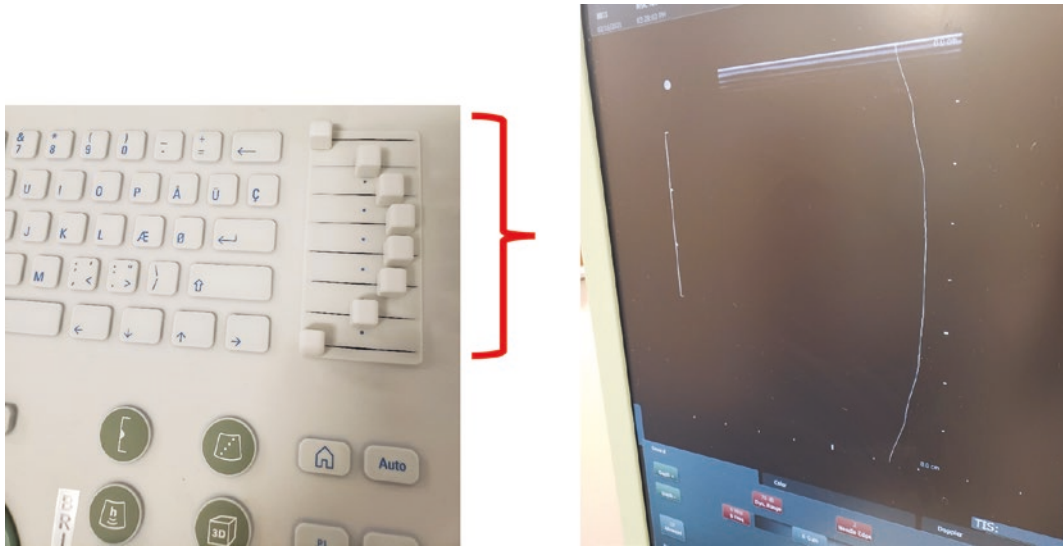

Fig. 3.7 Time gain compensation control

Fig. 3.8 Depth control changes frequency and allows deeper or more superficial evaluation

Ultrasound Procedure

General Considerations—Surgeon-Performed Ultrasound

For diagnostic ultrasonography, the general consent to treat for medical care should suffice for performance of the study. For ultrasonography requiring an interventional component (e.g., ultrasound-guided drainage) specific informed consent documentation is required. It is strongly advisable to check with facility and provider requirements before introducing a new type of procedure (diagnostic or otherwise) into your practice. The minimum documentation necessary in most situations includes an ultrasound procedure note which includes indications, findings, impression(s), and any representative images saved into the electronic medical record. The latter images should conform to local and national standards for documentation of medi-

cal imaging. Most ultrasound systems have the ability to interface directly with radiographic imaging systems greatly facilitating image documentation. Should the surgeon have the appropriate credentials for ultrasound billing, the focused ultrasound code (Current Procedural Terminology (CPT) 76705—abdominal ultrasound, limited) can be used. In the outpatient clinic setting, a separate note must be completed documenting the procedure (with image documentation) and a CPT modifier -25 is used in addition to the Evaluation and Management component CPT code. Before billing for these services, each surgeon should check with local practices and compliance personnel to ensure proper coding and billing.

An outpatient order is placed which should trigger the input of patient information into the ultrasound machine and generate the necessary administrative requirements for successful performance and billing. The ultrasound procedure should be performed in a dimly lit room and the patient prepped by exposing the area of interest. The procedure can be performed from either side of the patient in the supine position. Appropriate infection control practices should be employed to ensure the safe performance of procedures from patient to patient. This is of particular consideration in patients with stomas and open wounds. Generally speaking, stoma appliances are left in place and open wounds are covered with transparent plastic dressings. Liberal use of transducer gel is key to creating high-fidelity images. Specific techniques are outlined below:

Abdominal Wall Evaluation (Dynamic Abdominal Sonography for Hernia)

(a) The linea alba is evaluated first from xiphoid to pubis creating transverse plane images (Fig. 3.9).
(b) Successive images are taken adjacent to this in a similar fashion moving to the left of the patient ensuring overlapping images to ensure the entire anterior abdominal wall is evaluated. At this stage, structures including the subcutaneous tissues, rectus musculature, linea semilunaris, and oblique muscles are carefully evaluated to the left anterior axillary line.
(c) Once this is completed, the right rectus muscle, linea semilunaris, and oblique muscles are evaluated similarly moving to the right anterior axillary line.

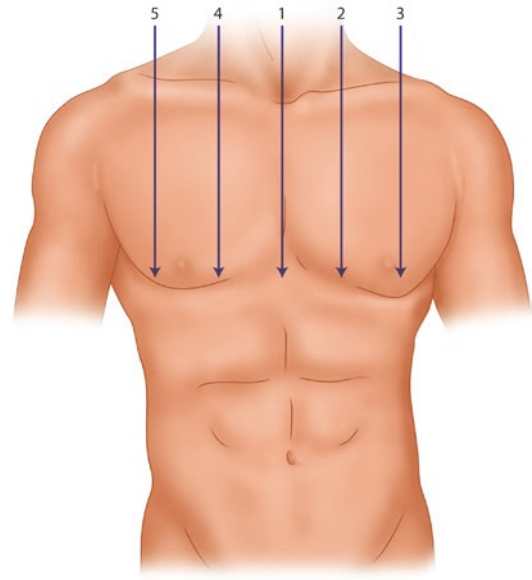

Fig. 3.9 Performance of Dynamic Abdominal Sonography for Hernia (modified from Beck et al)

Inguinal Canal Evaluation

(a) Transverse images are obtained just above the pubic tubercle and the spermatic cord is identified. The cord is tracked cephalad until it is no longer visible.
(b) The cord is tracked proximally until it is no longer visible then identified again and followed caudally.
(c) Identification of the spermatic cord will signify the inguinal canal which can be followed from deep to the superficial ring and into the scrotal sac.
(d) Sagittal images are very helpful in identifying the spermatic cord, alternating with transverse images.
(e) Valsalva can be utilized to visualize a hernia sac that protrudes through the floor or through the inguinal canal.

Clinical Pearls

For both ventral and inguinal hernia, having patients perform a Valsalva maneuver greatly facilitates the identification and characterization of hernia. This is a significant advantage of using ultrasound in the diagnosis of hernia compared to computed tomography and even magnetic resonance imaging. Rapidly transitioning from transverse to sagittal views can give the examiner a three-dimensional construct of the pathology evaluated. The umbilicus can be one of the most difficult structures to evaluate via ultrasound. The linea alba immediately beneath the umbilicus is often obscured by artifact due to the air interface and physical depression of the umbilicus. Oblique views and "filling" the umbilicus with transducer gel can assist with visualization. One of the most important adjuncts to surgeon-performed ultrasound is physical examination which can be used in conjunction with ultrasound to identify and characterize pathology. This is also one of the key benefits to clinicians performing ultrasound.

Bibliography

1. Beck WC, Holzman MD, Sharp KW, Nealon WH, Dupont WD, Poulose BK. Comparative effectiveness of dynamic abdominal sonography for hernia vs computed tomography in the diagnosis of incisional hernia. J Am Coll Surg. 2013;216(3):447–53. https://doi.org/10.1016/j.jamcollsurg.2012.11.012.
2. Jansen CJ, Yielder PC. Evaluation of hernia of the male inguinal canal: sonographic method. J Med Radiat Sci. 2018;65(2):163–8. https://doi.org/10.1002/jmrs.275.

Suggested Readings

Hagopian EJ, Machi J, editors. Abdominal ultrasound for surgeons. New York: Springer; 2014. https://doi.org/10.1007/978-1-4614-9599-4.

4 Standardizing the Approach to Hernia Radiology

Colin G. DeLong and Eric M. Pauli

Introduction

The intersection of surgery and radiology is perhaps nowhere more important than in the care of patients with abdominal wall defects. Radiographic studies are increasingly used in all phases of comprehensive hernia care. Properly conducted abdominal-core surgery therefore requires skillful interpretation of patient imaging by radiologists and hernia surgeons alike. Given this important and increasing interplay between surgeons and radiologists, standardized reporting of the abdominal wall is of utmost importance to ensure efficient, accurate communication between providers. Standardized language is also important on international levels to ensure consistent reporting of research outcomes and novel techniques.

Given these clear advantages, efforts have been made within the community of hernia surgeons to standardize the language used to describe abdominal wall pathology. In a prospective study of surgeons and radiologists interpreting CT scans, Holihan et al. noted that the majority of disagreement between reviewers identifying ventral hernias stemmed from a lack of standardized definitions, not from errors in interpreting the scans [1]. This issue was magnified when attempting to determine the recurrence of hernias after repair. National surveys and consensus meetings have been used to establish definitions for terms such as "giant" and "complex" ventral hernias [2, 3]. The Ventral Hernia Working Group (VHWG) used expert opinion to develop a grading scale to stratify hernia patients based on patient and wound characteristics [4]. This scale was then validated and modified, based on its ability to predict risk for surgical site occurrences (SSOs) [5]. Finally, the European Hernia Society (EHS) has been a leader in publishing classification systems for the description of ventral and inguinal hernias [6].

Even with these modest improvements, the lofty goal of standardized reporting of the abdominal wall is far from achieved. As the field of abdominal-core surgery has become a subspecialty of its own, the collective knowledge of how imaging can be used to plan surgical care and to predict outcomes has grown exponentially. Ultimately, standardization of radiologic hernia language requires global effort and acceptance by both surgeons and radiologists. The goal of this chapter is to describe the current intersection between radiology and hernia surgery and to emphasize the importance of a standardized approach to hernia radiology.

C. G. DeLong
Department of Surgery, Penn State Health Milton S. Hershey Medical Center, Hershey, PA, USA
e-mail: cdelong@pennstatehealth.psu.edu

E. M. Pauli (✉)
Division of Minimally Invasive and Bariatric Surgery, Department of Surgery, Penn State Health Milton S. Hershey Medical Center, Hershey, PA, USA
e-mail: epauli@pennstatehealth.psu.edu

S. Docimo Jr. et al. (eds.), *Fundamentals of Hernia Radiology*,
https://doi.org/10.1007/978-3-031-21336-6_4

This chapter contains three main sections: 1) the use of standard imaging modalities in the care of hernia patients; 2) the use of advanced image processing techniques to predict and improve hernia patient outcomes; and 3) standardized reporting of the abdominal wall.

Standard Imaging Techniques

The comprehensive care of patients with abdominal wall hernias spans five unique phases: (1) diagnosis of hernia; (2) preoperative evaluation and surgical planning; (3) intraoperative care; (4) postoperative management and assessment for complications; and (5) long-term follow-up and evaluation for recurrence. This section details the current uses of standard imaging techniques to assist the hernia surgeon during each phase.

Diagnosis of Hernia

Establishment of a hernia diagnosis, the initial step in the care of hernia patients, is often initiated by primary care physicians prior to a surgical referral. As such, consistent reporting of abdominal wall defects by radiologists is essential so that proper surgical consultation can be established. Though some hernias can be easily diagnosed through physical examination, many require some form of imaging to establish or confirm a diagnosis. Physical examination by surgeons, once considered the standard for hernia diagnosis, is fraught with error. In a prospective study by Baucom et al, surgeon physical examination had a sensitivity of 77% and negative predictive value (NPV) of 77% for the diagnosis of incisional hernia. For obese patients, the sensitivity and NPV dropped to 73% and 69%, respectively [7]. Physical examination to detect ventral hernia recurrence has false negative rates as high as 33% [1].

Even after imaging studies have been obtained, the detection and description of abdominal wall defects are often incorrect. A retrospective study of addenda to radiology reports found that the second most common anatomic site for missed diagnoses was the abdominal wall (in 8.3% of addenda), with ventral hernia being the most commonly missed abnormality at this site [8]. When compared to blinded, surgeon-interpreted CT scans, radiology reports detected incisional hernias with a sensitivity of 79% and specificity of 94% [9]. Even among surgeons, the diagnosis of a ventral hernia is not consistent. A prospective study by Holihan et al. demonstrated disagreement between 9 reviewers (surgeons and radiologists) on the diagnosis of ventral hernia in 73% of cases; this disagreement persisted in 10% of cases, even after discussion [1].

Additional imaging modalities including ultrasound have been proposed as alternatives to CT scans for diagnosis of ventral hernias. Surgeon-performed Dynamic Abdominal Sonography for Hernia (DASH) is a technique in which a 12-MHz linear ultrasound probe is used in the transverse and craniocaudal planes to identify abdominal wall anatomy and full-thickness defects in the fascia. DASH was compared with CT scans for the diagnosis of incisional hernias and found to have sensitivity of 98% and specificity of 88%, with high inter-rater reliability [10]. Of note, patients with stomas and fistulas were excluded from this analysis. DASH was then further tested to assess its ability to characterize incisional hernias [11]. The mean surface area of the hernia was calculated similarly by both CT and ultrasound.

Multiple imaging techniques are also available to assist in the accurate diagnosis of groin hernias. Similar to ventral hernias, physical examination is not reliable for the diagnosis and has a sensitivity of less than 75% [12]. High-resolution multidetector CT scans are able to differentiate direct from indirect inguinal herinas [13], and can also detect femoral hernias [14] and obturator hernias [15]. In cases of occult inguinal hernias, prone-position CT scans have been compared to standard supine position. Numerous studies have demonstrated a higher sensitivity of prone versus supine CT scans, both for the diagnosis of groin hernia and for the classification of hernia type [16, 17].

Other imaging modalities such as ultrasound and herniography also play a role in the diagnosis

of groin hernias. Dynamic groin ultrasonography has been successfully demonstrated in the evaluation of athletes with groin pain with a sensitivity of 100% and PPV of 93% [18]. Herniography, in which radio-opaque contrast is injected into the peritoneal cavity and radiographs of the groin are obtained during provocative maneuvers, has been extensively studied for the diagnosis of occult groin hernias. Long considered the most sensitive diagnostic tool for occult hernias, the role of herniography has recently been questioned. Ward et al. demonstrated that greater than one-third of patients with groin pain, no palpable lump, and a positive herniogram had resolution of their symptoms with watchful waiting [19]. A systematic review by Ng et al. found reported rates of major complications less than 1%, but minor complications ranging from 0 to 80% following herniography [20].

Robinson et al. performed a meta-analysis of radiographic techniques for the diagnosis of occult inguinal hernias [21]. The sensitivity and specificity (sensitivity/specificity) for the techniques included CT scan (80%/65%), ultrasound (86%/77%), and herniography (91%/83%). Finally, the role of MRI in groin hernia diagnosis has been studied. Studies have estimated that the sensitivity of MRI ranges from 85% to 95% [12, 22]. Leander et al. demonstrated that MRI following herniography did not detect additional groin hernias, but was useful in detecting other causes of groin pain including inflammatory changes in the symphysis region [23]. The European Hernia Society and the HerniaSurge Group have both recommended MRI with Valsalva maneuver prior to considering herniography given its noninvasive nature and ability to detect other diagnoses [24, 25].

Preoperative Evaluation and Surgical Planning

Once a hernia diagnosis has been established, the next phase of hernia care involves preoperative evaluation and surgical planning. An "anatomical" preoperative evaluation should be performed on all hernia patients, which includes physical examination, review of prior operative notes (particularly prior hernia repair reports to evaluate for the location of previously implanted mesh), and review of abdominal imaging. As mentioned previously, physical examination alone misses up to one-third of ventral hernias and provides little information regarding underlying anatomy [1]. Unfortunately, the completeness and accuracy of operative notes has also been challenged in numerous surgical settings, including hernia repair [26, 27]. Therefore, skilled interpretation of patient imaging often provides the most objective and comprehensive information to aid the surgeon in preoperative planning.

The number of accepted surgical techniques for the repair of abdominal wall defects is vast and continues to evolve and grow. Careful preoperative planning is crucial to ensure that patients receive the type of operation most suited to their unique condition. Decisions to be made include the operative approach (open, laparoscopic, or robotic), the consideration of mesh use and type, the type of repair and mesh position, and the need for complex reconstructive techniques including component separation. Blair et al. demonstrated that data from preoperative CT scans, including defect width, length, and abdominal wall thickness at various points can successfully predict the need for component separation and concomitant panniculectomy [28]. Franklin et al. also showed that abdominal wall defect ratios and hernia defect area on preoperative CT scans predict the ability to achieve primary abdominal closure versus bridged repair following component separation [29].

More recently, Love et al. developed a novel method to predict the need for myofascial release (versus posterior rectus sheath release alone) by utilizing CT scans to measure the rectus width to hernia width ratio [30]. When this so-called Carbonell ratio is >2 (the combined width of the rectus muscle body is more than twice as wide as the hernia gap between the rectus muscles themselves), only 10.8% of patients required an additional myofascial release to achieve fascial closure and the remaining 89.2% of patients were able to undergo a retro-rectus operation alone (Fig. 4.1).

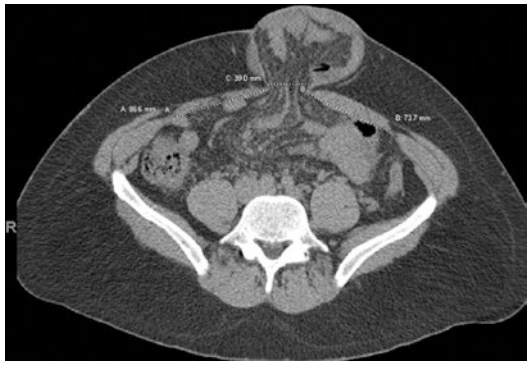

Fig. 4.1 Patient with a Carbonell Ratio of 4.08 (>2) which suggests there is a 90% chance that the recurrent incisional hernia will be able to be repaired with a retrorectus operation alone without the need for an additional myofascial release (TAR or EO release)

Intraoperative Care

Imaging that has been obtained preoperatively should always be available for viewing by the surgeon during the operation. Particularly during complex abdominal wall reconstructions, cross-sectional imaging can serve as a road map to guide the surgeon during difficult portions of the case. In particular, familiarity with the contents of the hernia sac, presence of prior mesh, and assessment of adhesions can aid in a safer entry into the abdomen and can alert the surgeon of areas where particularly cautious dissection must be utilized. Case reports have demonstrated many unique ventral and inguinal hernia sac contents including tumor, persistent Mullerian duct, diverticular abscess, transplant kidney ureter, pancreas in a patient with intestinal malrotation, vesical diverticulum, and duplicated ureter [31–38]. Knowledge of the location of these critical structures can be obtained from imaging prior to or during the operation itself, allowing them to be safely identified and preserved during the conduct of the case.

Postoperative Management and Assessment for Complications

Following operative repair of abdominal wall hernias, patients must be closely monitored for the development of complications. Often, this can be performed on a purely clinical basis without the need for routine postoperative imaging studies. However, some surgeons—particularly after complex abdominal wall reconstructions—do elect to include routine imaging studies in the postoperative care of their patients. CT scans are the most commonly used imaging modality to assess suspected postoperative complications, and can detect occurrences such as seroma, hematoma, abscess, small bowel obstruction, mesh infection/migration, and fistulas [39]. Ultrasound and MRI can be useful when evaluating the patient for the presence of adhesions. Zinther et al. demonstrated that both MRI and ultrasound can be used to detect intra-abdominal adhesions with comparable sensitivity (21.5% and 24%, respectively) and are particularly useful in identifying areas without adhesions when additional entry into the abdomen is needed [40]. Later studies have indicated that MRI is the preferred modality to identify adhesions and that these findings correlated with otherwise unexplained postoperative abdominal pain [41, 42]. Additionally, MRI is able to detect adhesions to mesh after ventral hernia repair but this finding has not been correlated with abdominal pain [43].

Less commonly used for routine follow-up after groin hernia repair, standard imaging modalities are able to reliably detect complications when utilized. CT scans can identify seromas, abscesses, hematoma, mesh infections, bowel complications, and urogenital injuries [44]. MRI is able to detect mesh migration, shrinkage, and folding following laparoscopic hernia repair [45]. Further, MRI is useful in the evaluation of chronic groin pain following laparoscopic inguinal hernia repair, particularly to confirm correct mesh position. However, MRI only identifies treatable causes of groin pain in 15% of cases [46]. Also important to consider when evaluating postoperative imaging are normal surgical findings that can be misdiagnosed as a complication. “Meshoma” or “plugoma” (often reported as a focal pelvic lesion), refers to the postoperative CT appearance of a prosthetic plug used for inguinal hernia repair and should not be misdiagnosed as a soft tissue mass or fluid collection [47, 48].

Long-term Follow-up and Evaluation for Recurrence

The final phase of care for hernia patients involves surveillance for recurrence of the hernia. It is well established that the vast majority of other surgical complications occur within a 90-day timeframe following surgery. Though some providers obtain scheduled routine imaging studies to assess for surveillance at 6 or 12 months, most providers do not—citing cost and radiation exposure. In a systematic review of all published studies on ventral hernia, Halligan et al. noted that only 29% of the included studies employed postoperative imaging, and only 3% of the studies consistently applied the same imaging technique to each subject [49]. Therefore, interpretation of any study's description of recurrence rates requires consideration of the follow-up method.

To reduce radiation and cost, some centers have evaluated the use of other modalities to survey for recurrence. The developers of Dynamic Abdominal Sonography for Hernia (DASH) posit that this method can greatly facilitate long-term follow-up after ventral hernia repair [10]. Ultrasound has proven useful to monitor recurrence of inguinal hernias as well. A prospective study by van Hessen et al. found that prior to surgery for recurrent hernia, physical examination matched surgical findings in 75.2% of cases, while ultrasound findings matched operative findings in 87.0% [50]. Several groups have proposed MRI as a follow-up method after ventral hernia repair as it identifies recurrence, but also intra-abdominal adhesions, mesh positioning, and muscular atrophy [51, 52].

Imaging following hernia repair can also provide information regarding changes to the abdominal wall musculature. Not performed for individual patients, this information is typically obtained in research settings to evaluate physiologic and mechanical response to new abdominal wall reconstruction techniques. Lisiecki et al. demonstrated that following component separation, total body area and total body circumference decreased, while fascia area and circumference did not decrease significantly [53]. De Silva et al. demonstrated changes in the abdominal wall musculature following component separation and transversus abdominis release including hypertrophy of the rectus abdominis and internal and external obliques [54]. In a similar evaluation of abdominal wall changes after component separation hernia repair, Daes et al. evaluated 15 patients who had undergone endoscopic external oblique (EO) release and determined that the EO was laterally displaced a mean of 2.1 cm with no associated changes in the combined lateral muscle thickness [55]. In a follow-up evaluation, the same investigators found lateral displacement of the transverses abdominis (TA) muscle by 1.00 cm following TA release hernia surgery [56]. Together, these studies suggest greater lateral muscle displacement following EO release than after TA release operations.

Advanced Image Processing Techniques and Radiomics

Recent advances in image processing capabilities and understanding of human physiology have opened the door for great advances in the role of radiology in hernia care. Physicians and scientists have just begun tapping into the vast amounts of hidden data contained within radiographic studies and are using this data to learn more about patients undergoing hernia repair. Radiomics, the name given to this emerging field, has been described as the "bridge between medical imaging and personalized medicine" [57]. A translational field of research, radiomics extracts qualitative and quantitative data from clinical images with the goal of enhancing clinical decision support systems and outcome prediction [57, 58]. Notably, these analyses are performed on standard imaging platforms such as CT scans but are "mined with sophisticated bioinformatics tools" to yield complex datasets compatible with high-order statistical analyses [59]. This section describes the use of radiomics and other similar techniques to predict outcomes in hernia patients with data from imaging studies.

Sarcopenia, the loss of muscle tissue during aging, has been extensively studied in its relation

to surgical outcomes and is considered a marker of frailty. For hernia surgery specifically, the results are mixed regarding its predictive value. Barnes et al. demonstrated that preoperative sarcopenia was associated with an increased risk of postoperative complications with an odds ratio of 5.3 [60]. Specifically, the significant differences were in hernia recurrence and renal failure, without significant differences in other postoperative complications. Rinaldi et al. demonstrated that sarcopenia was associated with increased length of stay but not with surgical site occurences [61]. Other studies have not identified such associations. In a retrospective review of 135 patients undergoing ventral hernia repair by Siegal et al., sarcopenia was not associated with an increase in postoperative complications or hernia recurrence [62]. Finally, in a study of 1178 patients, Schlosser et al. found no increases in wound infection, readmission, reoperation, hernia recurrence, or major complications in patients who had sarcopenia or osteopenia [63].

Measures of hepatic fat, or steatosis, have also been studied in relation to hernia outcomes. It has been shown that CT and MRI techniques are capable of quantifying visceral and hepatic fat and can assist in the diagnosis of metabolic syndrome and nonalcoholic fatty liver disease [64]. Ssentongo et al. identified steatosis on preoperative CT scans of patients undergoing ventral hernia repair [65]. In this study, postoperative hyperglycemia was associated with both hepatic steatosis and increased waist circumference-to-height ratio. Further, steatosis was associated with surgical site occurrences, with an odds ratio of 3.31.

Beyond measures of sarcopenia and steatosis, targeted measurements of the abdominal wall have also shown predictive capabilities for hernia patients. Schlosser et al. used three-dimensional volumetric software to measure subcutaneous, intra-abdominal, and hernia volumes [66]. Using these measurements, the group created new component variables (hernia dimension, extra-abdominal volume, and intra-abdominal volume) which correlated with wound complications, readmission, and reoperation and also predicted the need for panniculectomy and component separation. Similarly, Winters et al. demonstrated visceral fat volume as a predictor for rehernia-tion, and hernia sac volume and subcutaneous fat volume as predictors for surgical site infections [67]. Blair et al. demonstrated abdominal wall thickness and hernia size as independent predictors of wound complication [28]. Finally, Mommers et al. demonstrated that hernia volume was predictive of postoperative pulmonary complications, even more so than smoking [68].

Additional techniques have been employed to further understand the capacity of imaging data to determine abdominal wall mechanics. Todros et al. developed a virtual model of the abdominal wall from MRI scans of healthy individuals [69]. Using this model, they were able to analyze the mechanical response of the abdomen to mesh placement including changes in abdominal wall stiffness, displacement, and intra-abdominal pressures. A study by Strigard et al. compared both clinical and CT scan measurements of hernia size with abdominal wall strength measured with a BioDex system [70]. Interestingly, clinical measures of hernia size correlated well with abdominal wall strength, while CT measurements did not. The authors posited that clinical examination differentiates between functional muscles (those that contract on demand) versus those that are denervated, weakened, or replaced with fibrous tissue whereas CT scan identifies all fibers. This study exposes a possible limitation in imaging analysis of the abdominal wall.

In addition to predicting operative and postoperative occurrences, imaging data has also been used to predict the natural history and progression of hernias. In a study of umbilical hernias, hernia size, hernia neck size, and the hernia-neck-ratio (HNR) were used to predict progression from an uncomplicated hernia to complicated, meaning incarceration, intestinal obstruction, or intestinal necrosis [71]. The study found that an HNR >2.5 was associated with a 53-fold increased risk of progression to a complicated hernia and suggested that any patients with this ratio should undergo repair (Fig. 4.2). Mueck et al. evaluated radiographic factors associated with the need for emergent ventral hernia repair. These factors, which include BMI, ascites, height

of the hernia sac, and the angle between the fascial plane and hernia sac, were used to develop a logistic model [72]. In the model, patients with greater than 10 points have 2.5 greater odds of needing emergent hernia repair (Fig. 4.3). Finally, for patients undergoing radical prostatectomy—where the incidence of postoperative radical prostatectomy-related inguinal hernia (RPRIH) is 15–20%—Fukuta et al. investigated preoperative CT findings which would predict the development of RPRIH [73, 74]. Subclinical inguinal hernia was the only predictive factor identified.

More recently, Elhage et al. compared the ability of artificial intelligence to predict the outcomes of hernia surgery with that of expert surgeons [75]. The investigators first selected 9303 images from the CT scans of 369 patients who had undergone open complex hernia repairs. The images were subsequently evaluated by expert surgeons and by a deep learning neural network which was asked to predict three herniorrhaphy-related events; the need for a component separation (a surrogate predictor of complexity), the development of a surgical site infection, and postoperative pulmonary failure. The image-based deep learning model was successful in predicting surgical complexity and the development of surgical site infections and was more accurate than expert surgeon judgment.

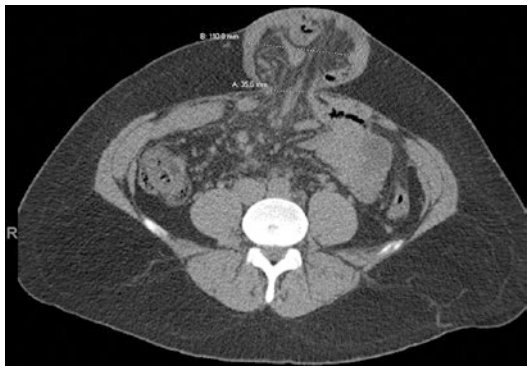

Fig. 4.2 Patient with an umbilical hernia with a Hernia-Neck-Ratio of 3.09 (>2.5) which suggest that the patient is at a substantial risk of progression to a complication. This ratio lends data to favor an elective repair rather than expectant observation even in an asymptomatic patient

Standardized Reporting of the Abdominal Wall

As detailed in the prior sections of this chapter, there is a substantial overlap between abdomen-core health and abdominal wall imaging. There is clearly a bright future in hernia care that can be achieved through the collaboration of radiologists and hernia surgeons. However, a concerted effort by both parties to achieve standardized reporting of the abdominal wall will be required to continue to drive the field forward efficiently and accurately. This section describes the efforts that have been made to accomplish standardization and highlight areas where more work is to be done.

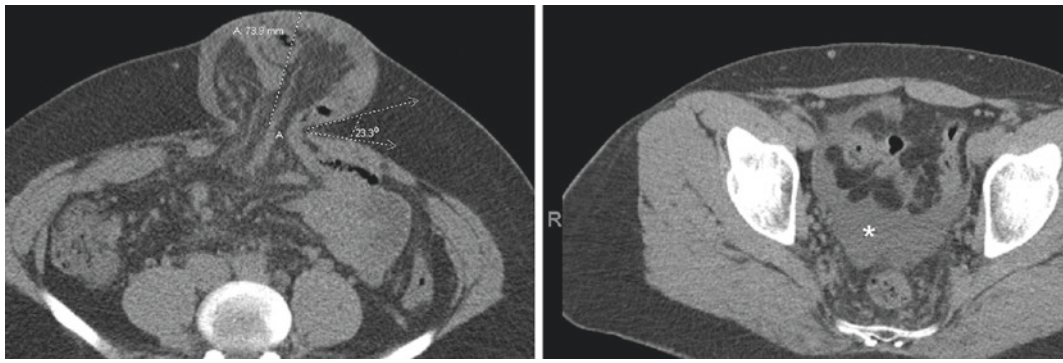

Fig. 4.3 Patient with an Odds Ratio of Emergency Repair Score of 15. A score of >10 suggests a great than 2.5 times likelihood of needing an emergency hernia repair. The score was calculated as follows: 0 (BMI less than 40 kg/m^2) + 7 (ascites present (* in Figure 3B)) + 5 (angle of hernia <30°) + 0.4 × 7.39 cm hernia sac height = 15

Presently, there is no standardized template for the reporting of the abdominal wall within radiological reports. Some authors have proposed options for reporting schemes [76]. Any basic description of the abdominal wall should feature (1) the presence or absence of hernia; (2) hernia size; (3) hernia location; (4) contents of the hernia sac; (5) evidence of previous hernia repairs; (6) evidence of rectus abdominis diastasis; and (7) evaluation for loss of domain.

As previously noted, the lack of a standardized definition for ventral hernia often leads to disagreement between those reviewing images. As Holihan et al. note, the generally accepted definition of a ventral hernia (an abnormal protrusion of tissue through the abdominal wall fascia) "does not differentiate the more subtle differences between recurrence, eventration, and an unclosed fascia defect bridged with mesh." Therefore, without clearer consensus guidelines, establishing the diagnosis of hernia will vary between providers. Importantly, once one hernia has been identified, one must be very careful to identify additional sites of hernia, particularly those away from the midline which is more commonly missed [1]. Additionally, Henriksen et al. detailed the association between development of inguinal hernias and ventral hernias, supporting a broader theory of "herniogenesis" [77]. Therefore, the presence of groin hernias should not be overlooked.

Once identified, the size of the hernia should be objectively described. A prospective study by Cherla et al. demonstrated that there are numerous methods for measuring hernia defect size including radiographic, intraoperative (under varying degrees of insufflation), and clinical, and that these measures are only weakly correlated [78]. Further, differences in these measurements affected mesh selection in 56% of cases. Within radiographic methods alone, there are numerous methods for quantification including length, width, area, and composite hernia size. The European Hernia Society guidelines propose the simple reporting of the length and width of the defect. In cases where multiple hernia defects exist, the measurement is made from the furthest edge of the hernia in each direction [6].

Next, the location of the hernia should be reported. Again, numerous classification schemes have been proposed over time including Chevrel and Rath (2000), Schumpelick (2000), Korenkov (2001), Ammaturo and Bassi (2005), Dietz (2007), and the Swedish Abdominal Wall Hernia Registry (2008) [79–82]. The focus of each methodology varied greatly and none gained widespread use, possibly given their complexity. The simplicity of the European Hernia Society's model has gained more popularity. Midline ventral hernias are divided into five zones (subxyphoidal, epigastric, umbilical, infraumbilical, and suprapubic) classified as M1 (superior) to M5 (inferior). Likewise, lateral hernias are divided into subcostal (L1), flank (L2), iliac (L3), and lumbar (L4). This classification can easily be learned by review of a simple schematic. The EHS also offers a classification for groin hernias which describes the location (lateral, medial, femoral) and grades the size of the hernia orifice as <1 (1), 1–2 (2), and ≥3 (3) finger widths across [83]. One final location parameter that can be useful for a hernia surgeon is the relation of the hernia to the nearest bony landmark, including xiphoid process, anterior superior iliac spine (ASIS), costal margin, pelvis, spine, or pubic symphysis.

Knowledge of the contents of the hernia sac can be very important for operative planning and should be discussed in reports on the abdominal wall. As discussed previously, numerous organs can be involved in a hernia sac including bowel, bladder, liver, ureters, and many more. Additionally, any obstructive findings related to the hernia should be mentioned, including bowel obstruction and hydronephrosis. Finally, Loftus et al. demonstrated that radiographic evidence of fluid in the hernia sac was associated with a significant increase in surgical site infection, with an odds ratio of 8.3, and would be important to include in a CT report [84].

Prior evidence of hernia repair, including the presence of mesh and tacks, is a commonly neglected aspect of abdominal wall reporting that can have significant clinical implications. Numerous types of surgical mesh are used for hernia repair, each with its own unique radiographic appearance [85]. Radiologists and sur-

geons should be familiar with the normal appearance of mesh, common mesh complications including seromas and infections, and mesh failures including shrinkage, detachment, and migration [86]. Also, the position of the mesh is important to describe and, until recently, did not have a standardized format. In 2017, Parker et al. described the highly variable methods of reporting mesh positioning and called for an international expert consensus [87]. In 2020, the British Journal of Surgery published the International Classification of Abdominal Wall Planes (ICAP) which was the result of a Delphi study involving 20 internationally recognized abdominal wall surgeons [88]. Consensus was achieved on 11 possible mesh positions: onlay, anterectus, inlay, interoblique, retro-oblique, retrorectus, retromuscular, transversalis fascial, preperitoneal, and intraperitoneal. It remains to be seen how this classification will be accepted, but it will likely be endorsed by the major international hernia societies. Finally, the presence and degree of intra-abdominal adhesions, including adhesions to the mesh, can be reported. Commonly cited as more distinguishable on MRI, evidence of adhesions can be detected on CT scan as well. There is currently no standardized method to report on the presence or degree of intra-abdominal adhesions.

Rectus abdominis diastasis (diastasis recti) refers to the thinning and widening of the linea alba, without a true fascial defect, and its presence should be noted on a standardized report of the abdominal wall [89]. In a study of patients undergoing suture repair of umbilical and epigastric hernias <2cm, diastasis recti was significantly correlated with hernia recurrence [90]. Therefore, concomitant repair of both diastasis recti and ventral hernias is recommended and has been successfully demonstrated [91]. Until recently, there was not a standardized method to describe diastasis recti. In 2018, a working group of the German Hernia Society and the International Endohernia Society developed a classification system with purposeful similarities to the EHS ventral hernia classification [92]. The method records the length of the diastasis using the identical EHS M1–M5 classification of midline ventral hernias and records the width in a similar fashion where W1 is <3 cm, W2 is 3–5 cm, and W3 is >5 cm.

Finally, standardized reporting of the abdominal wall should include a description of the loss of domain. Assessment for loss of domain, in general, compares the volume of intra-abdominal content to the volume of the hernia. In 2019, a systematic review of 77 articles published on the topic found that only 36% of articles used a written definition for loss of domain, and the definitions were widely varied [93]. The majority of definitions were descriptive, while 26% of definitions used were volumetric definitions. In April 2020, the World Journal of Surgery published a Delphi study involving 20 internationally recognized abdominal wall reconstruction surgeons which reached a consensus on written and volumetric definitions of loss of domain [94]. The consensus written definition is as follows: "A ventral hernia large enough such that simple reduction in its contents and primary fascial closure either cannot be achieved without additional reconstructive techniques or cannot be achieved without significant risk of complications due to the raised intra-abdominal pressure." The previously described Sabbagh method, where the loss of domain occurs when hernia sac volume divided by total peritoneal volume is greater than 20%, was chosen as the consensus volumetric definition.

Perhaps the most widely cited definition of loss of domain was put forth by Tanaka et al. in 2010 [95]. They utilized CT scan imaging to calculate the hernia sac volume and the abdominal cavity volume and managed patients for loss of domain if the volume ratio was >25% (hernia contents represented at least one-fourth of the total abdominal volume). While useful as a definition, this so-called Tanaka Ratio was subsequently studied by Fafaj et al. for its ability to predict fascial closure [96]. Below 25%, the ratio reliably predicted fascial closure. Above 25%, the ratio only had a sensitivity of 76% and specificity of 64% to predict fascial closure.

With the intent of more standardized reporting of the abdominal wall, some groups have proposed advanced image labeling protocols to segment and label the abdominal wall. Allen et al. demonstrated a quantitative anatomic labeling

protocol for the anterior abdominal wall that was employed with encouraging intra- and inter-rater reliability, even by nonphysicians [97]. From this labeling, the group was able to derive quantitative parameters describing the shape, location, and surrounding environment of the ventral hernia and, ultimately, show a clinical correlation between those parameters and technical characteristics of the hernia surgery [98]. One drawback of the protocol was a mean labeling time between 60 and 90 min per scan when performed by humans. In successive pilot studies, the group went on to demonstrate computerized segmentation of the abdominal wall using level-set image processing methods, further improved using texture analysis [99, 100]. Another group has demonstrated the application of computerized image analysis for the automated identification of hernia mesh type [101].

Though these computerized protocols may represent the pathway to a more standardized future of hernia radiology, this fully automated radiographic technology is early in its development and its implementation would take immense effort. Even so, as long as surgeons (not robots) are operating on hernias, the human capacity to interpret hernia radiology studies and effectively convey these findings in a standardized fashion will remain essential. This capacity to standardize the approach to hernia radiology has been demonstrated in prior studies. Holihan et al. demonstrated that 1 year after receiving standardized recommendations for interpreting CT scans of ventral hernias, inter-rater reliability among radiologists was improved from kappa (κ) = 0.21 to κ = 0.50 [102]. In an additional study, inter-rater reliability between surgeons and radiologists improved (κ = 0.21 to κ = 0.34) after reviewing consensus group recommendations of ventral hernia CT scans [1].

Conclusion

The pathway to more standardized hernia radiology is evident. International experts need to reach consensus guidelines on standardized definitions and then surgeons and radiologists globally must commit to learning and following these guidelines. This chapter presents evidence that both of these steps can be accomplished with applied effort. The role of radiology in the comprehensive care of hernia patients—through both standard and advanced techniques—is likely to continue to grow. Global and individual efforts by surgeons and radiologists will ensure a standardized, patient-centered future.

References

1. Holihan JL, Karanjawala B, Ko A, et al. Use of computed tomography in diagnosing ventral hernia recurrence: A blinded, prospective, multispecialty evaluation. JAMA Surg. 2016;151(1):7–13. https://doi.org/10.1001/jamasurg.2015.2580.
2. Passot G, Villeneuve L, Sabbagh C, et al. Definition of giant ventral hernias: Development of standardization through a practice survey. Int J Surg. 2016;28:136–40. https://doi.org/10.1016/j.ijsu.2016.01.097.
3. Slater NJ, Montgomery A, Berrevoet F, et al. Criteria for definition of a complex abdominal wall hernia. Hernia. 2014;18(1):7–17. https://doi.org/10.1007/s10029-013-1168-6.
4. Breuing K, Butler CE, Ferzoco S, et al. Incisional ventral hernias: Review of the literature and recommendations regarding the grading and technique of repair. Surgery. 2010;148(3):544–58. https://doi.org/10.1016/j.surg.2010.01.008.
5. Kanters AE, Krpata DM, Blatnik JA, Novitsky YM, Rosen MJ. Modified hernia grading scale to stratify surgical site occurrence after open ventral hernia repairs. J Am Coll Surg. 2012;215(6):787–93. https://doi.org/10.1016/j.jamcollsurg.2012.08.012.
6. Muysoms FE, Miserez M, Berrevoet F, et al. Classification of primary and incisional abdominal wall hernias. Hernia. 2009;13(4):407–14. https://doi.org/10.1007/s10029-009-0518-x.
7. Baucom RB, Beck WC, Holzman MD, Sharp KW, Nealon WH, Poulose BK. Prospective evaluation of surgeon physical examination for detection of incisional hernias. J Am Coll Surg. 2014;218(3):363–6. https://doi.org/10.1016/j.jamcollsurg.2013.12.007.
8. Rosenkrantz AB, Bansal NK. Diagnostic errors in abdominopelvic CT interpretation: characterization based on report addenda. Abdom Radiol. 2016;41(9):1793–9. https://doi.org/10.1007/s00261-016-0741-8.
9. Baucom RB, Beck WC, Holzman MD, et al. The importance of surgeon-reviewed computed tomography for incisional hernia detection: a prospective study. Am Surg. 2014;80(7):720–2. Accessed March 17, 2020. http://www.embase.com/search/

results?subaction=viewrecord&from=export&id=L604555244
10. Beck WC, Holzman MD, Sharp KW, Nealon WH, Dupont WD, Poulose BK. Comparative effectiveness of dynamic abdominal Sonography for hernia vs computed tomography in the diagnosis of incisional hernia. J Am Coll Surg. 2013;216(3):447–53. https://doi.org/10.1016/j.jamcollsurg.2012.11.012.
11. Baucom RB, Beck WC, Phillips SE, et al. Comparative evaluation of dynamic abdominal sonography for hernia and computed tomography for characterization of incisional hernia. JAMA Surg. 2014;149(6):591–6. https://doi.org/10.1001/jamasurg.2014.36.
12. Van Den Berg JC, De Valois JC, Go PMNYH, Rosenbusch G. Detection of groin hernia with physical examination, ultrasound, and MRI compared with laparoscopic findings. Invest Radiol. 1999;34(12):739–43. https://doi.org/10.1097/00004424-199912000-00002.
13. Burkhardt JH, Arshanskiy Y, Munson JL, Scholz FJ. Diagnosis of inguinal region hernias with axial CT: The lateral crescent sign and other key findings. Radiographics. 2011;31(2):1–12. https://doi.org/10.1148/rg.312105129.
14. Suzuki S, Furui S, Okinaga K, et al. Differentiation of femoral versus inguinal hernia: CT findings. AJR Am J Roentgenol. 2007;189(2):W78–83. https://doi.org/10.2214/AJR.07.2085.
15. Light D, Razi K, Horgan L. Computed tomography in the investigation and management of obturator hernia. Scott Med J. 2016;61(2):103–5. https://doi.org/10.1177/0036933016638974.
16. Miyaki A, Yamaguchi K, Kishibe S, Ida A, Miyauchi T, Naritaka Y. Diagnosis of inguinal hernia by prone- vs. supine-position computed tomography. Hernia. 2017;21(5):705–13. https://doi.org/10.1007/s10029-017-1640-9.
17. Kamei N, Otsubo T, Koizumi S, Morimoto T, Nakajima Y. Prone "computed tomography hernia study" for the diagnosis of inguinal hernia. Surg Today 2019;49(11):936-941. https://doi.org/10.1007/s00595-019-01837-2
18. Vasileff WK, Nekhline M, Kolowich PA, Talpos GB, Eyler WR, van Holsbeeck M. Inguinal hernia in athletes: role of dynamic ultrasound. Sports Health. 2017;9(5):414–21. https://doi.org/10.1177/1941738117717009.
19. Ward ST, Carter JV, Robertson CS. Herniography influences the management of patients with suspected occult herniae and patient factors can predict outcome. Hernia. 2011;15(5):547–51. https://doi.org/10.1007/s10029-011-0825-x.
20. Ng TT, Hamlin JA, Kahn AM. Herniography: analysis of its role and limitations. Hernia. 2009;13(1):7–11. https://doi.org/10.1007/s10029-008-0423-8.
21. Robinson A, Light D, Kasim A, Nice C. A systematic review and meta-analysis of the role of radiology in the diagnosis of occult inguinal hernia. Surg Endosc. 2013;27(1):11–8. https://doi.org/10.1007/s00464-012-2412-3.
22. Van Den Berg JC, De Valois JC, Go PMNYH, Rosenbusch G. Dynamic magnetic resonance imaging in the diagnosis of groin hernia. Invest Radiol. 1997;32(10):644–7. https://doi.org/10.1097/00004424-199710000-00010.
23. Leander P, Ekberg O, Sjoberg S, Kesek P. MR imaging following herniography in patients with unclear groin pain. Eur Radiol. 2000;10(11):1691–6. https://doi.org/10.1007/s003300000555.
24. Simons MP, Aufenacker T, Bay-Nielsen M, et al. European Hernia Society guidelines on the treatment of inguinal hernia in adult patients. Hernia. 2009;13(4):343–403. https://doi.org/10.1007/s10029-009-0529-7.
25. Simons MP, Smietanski M, Bonjer HJ, et al. International guidelines for groin hernia management. Hernia. 2018;22(1) https://doi.org/10.1007/s10029-017-1668-x.
26. Thomson DR, Baldwin MJ, Bellini MI, Silva MA. Improving the quality of operative notes for laparoscopic cholecystectomy: assessing the impact of a standardized operation note proforma. Int J Surg. 2016;27:17–20. https://doi.org/10.1016/j.ijsu.2016.01.037.
27. Ma GW, Pooni A, Forbes SS, et al. Quality of inguinal hernia operative reports: room for improvement. Can J Surg. 2013;56(6):393–7. https://doi.org/10.1503/cjs.017412.
28. Blair LJ, Ross SW, Huntington CR, et al. Computed tomographic measurements predict component separation in ventral hernia repair. J Surg Res. 2015;199(2):420–7. https://doi.org/10.1016/j.jss.2015.06.033.
29. Franklin BR, Patel KM, Nahabedian MY, Baldassari LE, Cohen EI, Bhanot P. Predicting abdominal closure after component separation for complex ventral hernias: Maximizing the use of preoperative computed tomography. Ann Plast Surg. 2013;71:261–5. https://doi.org/10.1097/SAP.0b013e3182773915.
30. Love MW, Warren JA, Davis S, et al. Computed tomography imaging in ventral hernia repair: can we predict the need for myofascial release? Hernia. 2021;25(2):471–7. https://doi.org/10.1007/s10029-020-02181-y.
31. Oruç MT, Akbulut Z, Özozan Ö, Coşkun F. Urological findings in inguinal hernias: a case report and review of the literature. Hernia. 2004;8(1):76–9. https://doi.org/10.1007/s10029-003-0157-6.
32. Ağca B, İşcan Y, Aydın T, Şahin A, Memişoğlu K. Strangulated inguinal hernia accompanied by paratesticular leiomyosarcoma. Ulus Travma ve Acil Cerrahi Derg. 2019;25(3):307–10. https://doi.org/10.5505/tjtes.2018.68709.
33. Alharbi KN, Khushaim AO, Alrasheed M, Akhtar M, Neimatallah M. Radiological findings in persistent Müllerian duct syndrome: case report and review of literature. J Radiol Case Rep. 2017;11(3):7–14. https://doi.org/10.3941/jrcr.v11i3.3027.

34. Andrabi SIH, Pitale A, El-Hakeem AAS. Diverticular abscess presenting as a strangulated inguinal hernia: case report and review of the literature. Ulster Med J. 2007;76(2):107–8. Accessed March 24, 2020. http://www.ncbi.nlm.nih.gov/pubmed/17476826
35. Areda MA, Bailey CR, O'Mara D, Weiss CR. Transplant uretero-inguinal hernia resulting in urosepsis. Radiol Case Reports. 2019;14(1):14–7. https://doi.org/10.1016/j.radcr.2018.09.002.
36. Ballard DH, Sangster GP. Pancreas-containing inguinal hernia in an adult with intestinal malrotation. Surg (United States). 2017;162(5):1185–6. https://doi.org/10.1016/j.surg.2016.12.025.
37. Bolton DM, Joyce G. Vesical diverticulum extending into an inguinal hernia. Br J Urol. 1994;73(3):323–4. https://doi.org/10.1111/j.1464-410x.1994.tb07532.x.
38. Alvarez Mugica M, Bulnes Vazquez V, Jalon Monzon A, et al. Asymptomatic left ureter inguinal hernia during valsalva maneuver in a patient with complete left pyelo ureteral system duplication. Arch Esp Urol. 2013;66(4):389–90.
39. Patil AR, Nandikoor S, Mohanty HS, Godhi S, Bhat R. Mind the gap: imaging spectrum of abdominal ventral hernia repair complications. Insights Imaging. 2019;10(1):40. https://doi.org/10.1186/s13244-019-0730-x.
40. Zinther NB, Zeuten A, Marinovskij E, Haislund M, Friis-Andersen H. Detection of abdominal wall adhesions using visceral slide. Surg Endosc. 2010;24(12):3161–6. https://doi.org/10.1007/s00464-010-1110-2.
41. Mussack T, Fischer T, Ladurner R, et al. Cine magnetic resonance imaging vs high-resolution ultrasonography for detection of adhesions after laparoscopic and open incisional hernia repair: a matched pair pilot analysis. Surg Endosc Other Interv Tech. 2005;19(12):1538–43. https://doi.org/10.1007/s00464-005-0092-y.
42. Zinther NB, Wara P, Friis-Andersen H. Functional cine MRI and transabdominal ultrasonography for the assessment of adhesions to implanted synthetic mesh 5-7 years after laparoscopic ventral hernia repair. Hernia. 2010;14(5):499–504. https://doi.org/10.1007/s10029-010-0676-x.
43. Langbach O, Holmedal SH, Grandal OJ, Røkke O. Adhesions to mesh after ventral hernia mesh repair are detected by MRI but are not a cause of long term chronic abdominal pain. Gastroenterol Res Pract. 2016;2016 https://doi.org/10.1155/2016/2631598.
44. Tonolini M. Multidetector CT of expected findings and complications after contemporary inguinal hernia repair surgery. Diagn Interv Radiol. 2016;22(5):422–9. https://doi.org/10.5152/dir.2016.15578.
45. Hansen NL, Ciritsis A, Otto J, Busch D, Kuhl CK, Kraemer NA. Utility of magnetic resonance imaging to monitor surgical meshes: correlating imaging and clinical outcome of patients undergoing inguinal hernia repair. Invest Radiol. 2015;50(7):436–42. https://doi.org/10.1097/RLI.0000000000000148.
46. Burgmans JPJ, Voorbrood CEH, Van Dalen T, et al. Chronic pain after TEP inguinal hernia repair, does MRI reveal a cause? Hernia. 2016;20(1):55–62. https://doi.org/10.1007/s10029-015-1448-4.
47. Aganovic L, Ishioka KM, Hughes Cassidy F, Chu PK, Cosman BC. Plugoma: CT findings after prosthetic plug inguinal hernia repairs. J Am Coll Surg. 2010;211(4):481–4. https://doi.org/10.1016/j.jamcollsurg.2010.06.001.
48. Chernyak V, Rozenblit AM, Patlas M, Kaul B, Milikow D, Ricci Z. Pelvic pseudolesions after inguinal hernioplasty using prosthetic mesh: CT findings. J Comput Assist Tomogr. 2007;31(5):724–7. https://doi.org/10.1097/rct.0b013e3180315db8.
49. Halligan S, Parker SG, Plumb AAO, et al. Use of imaging for pre- and post-operative characterisation of ventral hernia: systematic review. Br J Radiol. 2018;91(1089):20170954. https://doi.org/10.1259/bjr.20170954.
50. van Hessen CV, Roos MM, Sanders FBM, et al. Recurrence after totally extraperitoneal (TEP) inguinal hernia repair: the role of physical examination and ultrasound. Hernia. 2020;24(1):153–7. https://doi.org/10.1007/s10029-019-02029-0.
51. Fischer T, Ladurner R, Gangkofer A, Mussack T, Reiser M, Lienemann A. Functional cine MRI of the abdomen for the assessment of implanted synthetic mesh in patients after incisional hernia repair: initial results. Eur Radiol. 2007;17(12):3123–9. https://doi.org/10.1007/s00330-007-0678-y.
52. Kirchhoff S, Ladurner R, Kirchhoff C, Mussack T, Reiser MF, Lienemann A. Detection of recurrent hernia and intraabdominal adhesions following incisional hernia repair: a functional cine MRI-study. Abdom Imaging. 2010;35(2):224–31. https://doi.org/10.1007/s00261-009-9505-z.
53. Lisiecki J, Kozlow JH, Agarwal S, et al. Abdominal wall dynamics after component separation hernia repair. J Surg Res. 2015;193(1):497–503. https://doi.org/10.1016/j.jss.2014.08.008.
54. De Silva GS, Krpata DM, Hicks CW, et al. Comparative radiographic analysis of changes in the abdominal wall musculature morphology after open posterior component separation or bridging laparoscopic ventral hernia repair. J Am Coll Surg. 2014;218(3):353–7. https://doi.org/10.1016/j.jamcollsurg.2013.11.014.
55. Daes J, Morrell D, Pauli EM. Changes in the lateral abdominal wall following endoscopic subcutaneous anterior component separation. Hernia. 2021;25(1):85–90. https://doi.org/10.1007/s10029-020-02303-6.
56. Daes J, Winder JS, Pauli EM. Concomitant anterior and posterior component separations: absolutely contraindicated? Surg Innov. 2020;27(4):328–32. https://doi.org/10.1177/1553350620914195.
57. Lambin P, Leijenaar RTH, Deist TM, et al. Radiomics: the bridge between medical imaging and personalized medicine. Nat Rev Clin Oncol. 2017;14(12):749–62. https://doi.org/10.1038/nrclinonc.2017.141.

58. Rizzo S, Botta F, Raimondi S, et al. Radiomics: the facts and the challenges of image analysis. Eur Radiol Exp. 2018;2(1) https://doi.org/10.1186/s41747-018-0068-z.
59. Gillies RJ, Kinahan PE, Hricak H. Radiomics: Images are more than pictures, they are data. Radiology. 2016;278(2):563–77. https://doi.org/10.1148/radiol.2015151169.
60. Barnes LA, Li AY, Wan DC, Momeni A. Determining the impact of sarcopenia on postoperative complications after ventral hernia repair. J Plast Reconstr Aesthet Surg. 2018;71(9):1260–8. https://doi.org/10.1016/j.bjps.2018.05.013.
61. Rinaldi JM, Geletzke AK, Phillips BE, Miller J, Dykes TM, Soybel DI. Sarcopenia and sarcopenic obesity in patients with complex abdominal wall hernias. Am J Surg. 2016;212(5):903–11. https://doi.org/10.1016/j.amjsurg.2016.03.003.
62. Siegal SR, Guimaraes AR, Lasarev MR, Martindale RG, Orenstein SB. Sarcopenia and outcomes in ventral hernia repair: a preliminary review. Hernia. 2018;22(4):645–52. https://doi.org/10.1007/s10029-018-1770-8.
63. Schlosser KA, Maloney SR, Thielan ON, et al. Sarcopenia in patients undergoing open ventral hernia repair. Am Surg. 2019;85(9):985–91. Accessed March 17, 2020. http://www.ncbi.nlm.nih.gov/pubmed/31638511
64. Graffy PM, Pickhardt PJ. Quantification of hepatic and visceral fat by CT and MR imaging: relevance to the obesity epidemic, metabolic syndrome and NAFLD. Br J Radiol. 2016;89(1062):20151024. https://doi.org/10.1259/bjr.20151024.
65. Ssentongo P, Ssentongo AE, Dykes T, Pauli EM, Soybel DI. Nonalcoholic fatty liver disease as a high-value predictor of postoperative hyperglycemia and its associated complications in major abdominal surgery. J Am Coll Surg. 2018;227(4):419–429.e6. https://doi.org/10.1016/j.jamcollsurg.2018.07.655.
66. Schlosser KA, Maloney SR, Prasad T, Colavita PD, Augenstein VA, Heniford BT. Three-dimensional hernia analysis: the impact of size on surgical outcomes. Surg Endosc. 2019; https://doi.org/10.1007/s00464-019-06931-7. Published online.
67. Winters H, Knaapen L, Buyne OR, et al. Preoperative CT scan measurements for predicting complications in patients undergoing complex ventral hernia repair using the component separation technique. Hernia. 2019;23(2):347–54. https://doi.org/10.1007/s10029-019-01899-8.
68. Mommers EHH, Wegdam JA, van der Wolk S, Nienhuijs SW, de Vries Reilingh TS. Impact of hernia volume on pulmonary complications following complex hernia repair. J Surg Res. 2017;211:8–13. https://doi.org/10.1016/j.jss.2016.11.051.
69. Todros S, Pachera P, Baldan N, et al. Computational modeling of abdominal hernia laparoscopic repair with a surgical mesh. Int J Comput Assist Radiol Surg. 2018;13(1):73–81. https://doi.org/10.1007/s11548-017-1681-7.
70. Strigård K, Clay L, Stark B, Gunnarsson U, Falk P. Giant ventral hernia - Relationship between abdominal wall muscle strength and hernia area. BMC Surg. 2016;16(1):50. https://doi.org/10.1186/s12893-016-0166-x.
71. Fueter T, Schäfer M, Fournier P, Bize P, Demartines N, Allemann P. The hernia–neck-ratio (HNR), a novel predictive factor for complications of umbilical hernia. World J Surg. 2016;40(9):2084–90. https://doi.org/10.1007/s00268-016-3556-4.
72. Mueck KM, Holihan JL, Mo J, et al. Computed tomography findings associated with the risk for emergency ventral hernia repair. Am J Surg. 2017;214(1):42–6. https://doi.org/10.1016/j.amjsurg.2016.09.035.
73. Fukuta F, Hisasue S, Yanase M, et al. Preoperative computed tomography finding predicts for postoperative inguinal hernia: new perspective for radical prostatectomy-related inguinal hernia. Urology. 2006;68(2):267–71. https://doi.org/10.1016/j.urology.2006.02.023.
74. Stranne J, Lodding P. Inguinal hernia after radical retropubic prostatectomy: risk factors and prevention. Nat Rev Urol. 2011;8(5):267–73. https://doi.org/10.1038/nrurol.2011.40.
75. Elhage SA, Deerenberg EB, Ayuso SA, et al. Development and validation of image-based deep learning models to predict surgical complexity and complications in abdominal wall reconstruction. JAMA Surg. 2021;156(10):933–40. https://doi.org/10.1001/jamasurg.2021.3012.
76. Claus CMP, Cavalieiri M, Malcher F, et al. DECOMP report: answers surgeons expect from an abdominal wall imaging exam. Rev Col Bras Cir. 2022:49. https://doi.org/10.1590/0100-6991e-20223172en.
77. Henriksen NA, Sorensen LT, Bay-Nielsen M, Jorgensen LN. Direct and recurrent inguinal hernias are associated with ventral hernia repair: a database study. World J Surg. 2013;37(2):306–11. https://doi.org/10.1007/s00268-012-1842-3.
78. Cherla DV, Lew DF, Escamilla RJ, et al. Differences of alternative methods of measuring abdominal wall hernia defect size: a prospective observational study. Surg Endosc. 2018;32(3):1228–33. https://doi.org/10.1007/s00464-017-5797-1.
79. Chevrel JP, Rath AM. Classification of incisional hernias of the abdominal wall. Hernia. 2000;4(1):7–11. https://doi.org/10.1007/BF01230581.
80. Korenkov M, Neugebauer E. Classification and surgical treatment of incisional hernia: results of an experts' meeting. Langenbecks Arch Surg. 2001;386(1):65–73. https://doi.org/10.1007/s004230000182.
81. Ammaturo C, Bassi G. The ratio between anterior abdominal wall surface/wall defect surface: a new parameter to classify abdominal incisional hernias. Hernia. 2005;9(4):316–21. https://doi.org/10.1007/s10029-005-0016-8.
82. Dietz UA, Hamelmann W, Winkler MS, et al. An alternative classification of incisional hernias

enlisting morphology, body type and risk factors in the assessment of prognosis and tailoring of surgical technique. J Plast Reconstr Aesthet Surg. 2007;60(4):383–8. https://doi.org/10.1016/j.bjps.2006.10.010.
83. Miserez M, Alexandre JH, Campanelli G, et al. The European hernia society groin hernia classification: simple and easy to remember. Hernia. 2007;11(2):113–6. https://doi.org/10.1007/s10029-007-0198-3.
84. Loftus TJ, Go KL, Jordan JR, et al. Computed tomography evidence of fluid in the hernia sac predicts surgical site infection following mesh repair of acutely incarcerated ventral and groin hernias. J Trauma Acute Care Surg. 2017;83:170–4. https://doi.org/10.1097/TA.0000000000001503.
85. Parra JA, Revuelta S, Gallego T, Bueno J, Berrio JI, Fariñas MC. Prosthetic mesh used for inguinal and ventral hernia repair: normal appearance and complications in ultrasound and CT. Br J Radiol. 2004;77(915):261–5. https://doi.org/10.1259/bjr/63333975.
86. Gavlin A, Kierans AS, Chen J, Song C, Guniganti P, Mazzariol FS. Imaging and treatment of complications of abdominal and pelvic mesh repair. Radiographics. 2020;40(2):432–53. https://doi.org/10.1148/rg.2020190106.
87. Parker SG, Wood CPJ, Sanders DL, Windsor ACJ. Nomenclature in abdominal wall hernias: is it time for consensus? World J Surg. 2017;41(10):2488–91. https://doi.org/10.1007/s00268-017-4037-0.
88. Parker SG, Halligan S, Liang MK, et al. International classification of abdominal wall planes (ICAP) to describe mesh insertion for ventral hernia repair. Br J Surg. 2020;107(3):209–17. https://doi.org/10.1002/bjs.11400.
89. Mommers EHH, Ponten JEH, Al Omar AK, de Vries Reilingh TS, Bouvy ND, Nienhuijs SW. The general surgeon's perspective of rectus diastasis. A systematic review of treatment options. Surg Endosc. 2017;31(12):4934–49. https://doi.org/10.1007/s00464-017-5607-9.
90. Köhler G, Luketina RR, Emmanuel K. Sutured repair of primary small umbilical and epigastric hernias:concomitant rectus diastasis is a significant risk factor for recurrence. World J Surg 2015;39(1):121-126. https://doi.org/10.1007/s00268-014-2765-y
91. Bellido Luque J, Bellido Luque A, Valdivia J, et al. Totally endoscopic surgery on diastasis recti associated with midline hernias. The advantages of a minimally invasive approach. Prospective cohort study. Hernia. 2015;19(3):493–501. https://doi.org/10.1007/s10029-014-1300-2.
92. Reinpold W, Köckerling F, Bittner R, et al. Classification of rectus diastasis: a proposal by the German Hernia Society (DHG) and the International Endohernia Society (IEHS). Front Surg. 2019;6:1. https://doi.org/10.3389/fsurg.2019.00001.
93. Parker SG, Halligan S, Blackburn S, et al. What exactly is meant by "Loss of Domain" for ventral hernia? Systematic review of definitions. World J Surg. 2019;43(2):396–404. https://doi.org/10.1007/s00268-018-4783-7.
94. Parker SG, Halligan S, Liang MK, et al. Definitions for loss of domain: an international delphi consensus of expert surgeons. World J Surg. 2020;44(4):1070–8. https://doi.org/10.1007/s00268-019-05317-z.
95. Tanaka EY, Yoo JH, Rodrigues AJ, Utiyama EM, Birolini D, Rasslan S. A computerized tomography scan method for calculating the hernia sac and abdominal cavity volume in complex large incisional hernia with loss of domain. Hernia. 2010;14(1):63–9. https://doi.org/10.1007/s10029-009-0560-8.
96. Fafaj A, Thomas J, Zolin SJ, et al. Can hernia sac to abdominal cavity volume ratio predict fascial closure rate for large ventral hernia? Reliability of the tanaka score. J Am Coll Surg. 2021;232:948–53. https://doi.org/10.1016/j.jamcollsurg.2021.03.009.
97. Allen WM, Xu Z, Asman AJ, Poulose BK, Landman BA. Quantitative anatomical labeling of the anterior abdominal wall. In: Medical imaging 2013: image perception, observer performance, and technology assessment, Vol. 8673. SPIE; 2013:867312. https://doi.org/10.1117/12.2007071
98. Xu Z, Asman AJ, Baucom RB, Abramson RG, Poulose BK, Landman BA. Quantitative CT imaging of ventral hernias: Preliminary validation of an anatomical labeling protocol. PLoS One. 2015;10(10) https://doi.org/10.1371/journal.pone.0141671.
99. Xu Z, Allen WM, Poulose BK, Landman BA. Automatic segmentation of abdominal wall in ventral hernia CT: a pilot study. In: Medical Imaging 2013: Image Processing, Vol. 8669. SPIE; 2013:86693T. https://doi.org/10.1117/12.2007060
100. Xu Z, Allen WM, Baucom RB, Poulose BK, Landman BA. Texture analysis improves level set segmentation of the anterior abdominal wall. Med Phys. 2013;40(12):121901. https://doi.org/10.1118/1.4828791.
101. Pham TD, Le DTP, Xu J, Nguyen DT, Martindale RG, Deveney CW. Personalized identification of abdominal wall hernia meshes on computed tomography. Comput Methods Programs Biomed. 2014;113(1):153–61. https://doi.org/10.1016/j.cmpb.2013.09.019.
102. Holihan JL, Cherla D, Blair KJ, et al. Computed tomography in ventral hernia diagnosis: have we improved? A quality improvement initiative. J Surg Res. 2018;224:97–101. https://doi.org/10.1016/j.jss.2017.11.055.

Normal Radiographic Anatomy of Anterior Abdominal Wall

5

Iliya Goldberg and Salvatore Docimo Jr.

Introduction:

Anatomy of Anterior Abdominal Wall

Muscle Layers

While it may appear simple at first glance, the abdominal wall is anatomically complex and layered with intertwined layers of innervation and blood supply. The abdominal wall is of mesodermal origin and develops as two sheets migrate toward each other. These sheets both originate in the paravertebral region and envelop what will become the future abdomen. The leading edges of both of these sheaths eventually develop into the rectus abdominis muscles after they meet at the anterior midline. The rectus abdominis is encased by an aponeurotic sheath which allows the two sheets to fuse in the anterior midline, also referred to as the *linea Alba* (Fig. 5.1). The rectus muscles have several insertion points including the pubic bones inferiorly and the 5th, 6th ribs, 7th costal cartilages, and the xiphoid process superior. The lateral border of the rectus abdominis is known as the *linea semilunaris* (Fig. 5.2). The pyramidalis muscle, a highly variable group of muscles comprising the lower midline muscle group, is reported to be present in only 10–70% of the population [1]. The fibers of this inconsistent muscle typically course superomedially with the inferior origin at the pubic symphysis and the superior attachment onto the linea Alba.

The muscle layers that run lateral to the rectus abdominus muscle include the external oblique, internal oblique, and transversus abdominis (Fig. 5.3). These muscle layers are derived from the mesoderm and start to form during the 6th and 7th weeks of fetal development. The external oblique muscle (EOM) runs superficial to the serratus anterior in the superior margins and superficial to the internal oblique and the latissimus dorsi muscles more inferiorly. Its origins include the 5th to 12th ribs and insert unto the linea Alba, pubic tubercle**,** and anteriorly to the iliac crest while coursing in an inferomedial orientation. The inguinal ligament is the inferior edge of the external oblique aponeurosis.

The internal oblique muscle (IOM) runs deep to the external oblique and superficial to the transversus abdominis muscle (TAM). The IOM originates from the thoracolumbar fascia, iliac crest, and inguinal ligament and inserts along the inferior border to ribs 10–12 and the linea Alba. Its fibers course in a superior-medial orientation. The lower medial and inferior portion of the internal oblique fuses with the transversus abdominis aponeurosis to form the conjoint ten-

I. Goldberg
Division of Upper GI and General Surgery, Department of Surgery, Keck Medicine of USC, Los Angeles, CA, USA

S. Docimo Jr. (✉)
Division of Gastrointestinal Surgery, University of South Florida, Tampa, FL, USA
e-mail: Docimo@USF.edu

S. Docimo Jr. et al. (eds.), *Fundamentals of Hernia Radiology*,
https://doi.org/10.1007/978-3-031-21336-6_5

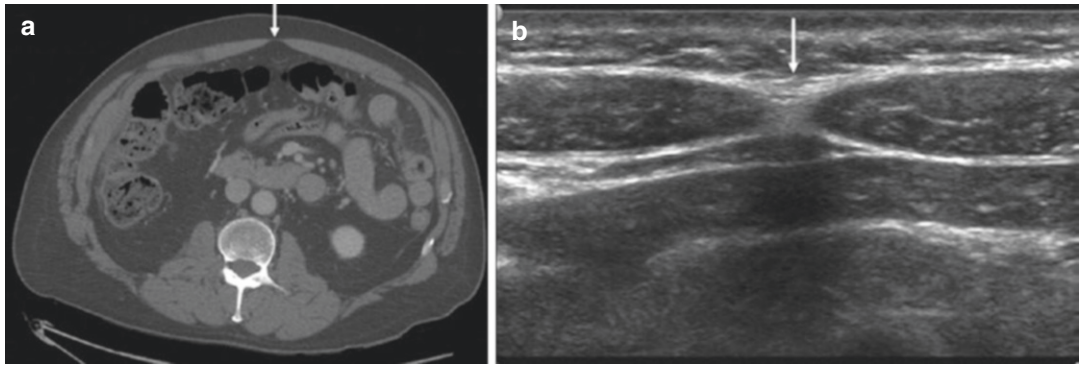

Fig. 5.1 (**a**) Computer tomography cross-sectional (axial) image with white arrow pointing to linea alba. (**b**) Coronal ultrasound of abdomen with white arrow pointing to linea alba

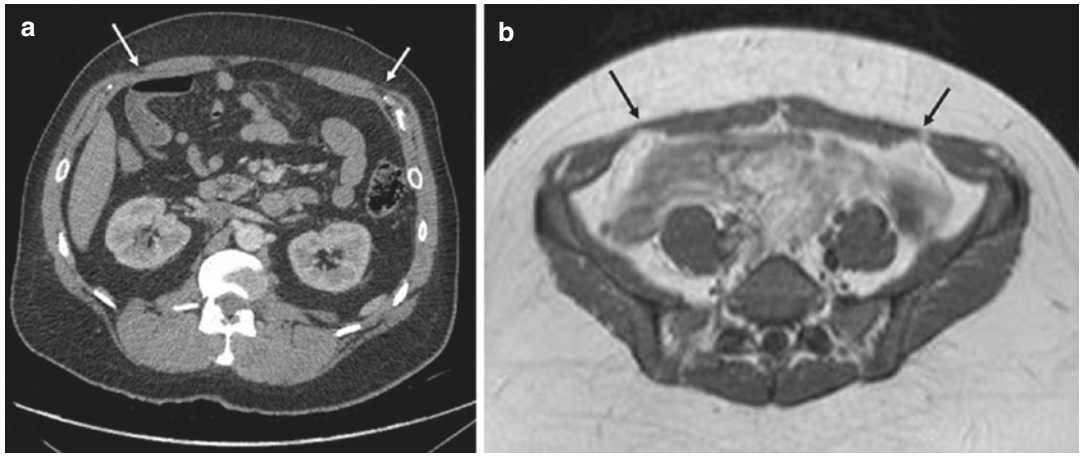

Fig. 5.2 (**a**) Computer tomography cross-sectional (axial) image with white arrow pointing to linea semilunaris on both sides. (**b**) Cross-section MRI image of abdomen with black arrows pointing to the linea semilunaris on both sides

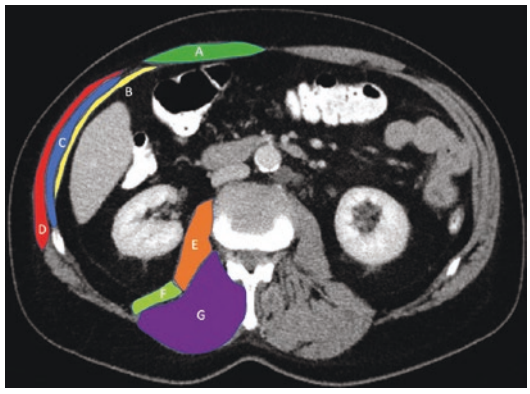

Fig. 5.3 Anatomy of the musculature of the abdominal wall. (A) Rectum abdominis, (B) Transversus abdominis, (C) Internal oblique muscle, (D) External oblique muscle, (E) Psoas major, (F) Quadratus lumborum, (G) Sacrospinalis

don. Furthermore, the internal oblique muscle layers are continuous with the cremasteric muscle fibers of the inguinal canal.

The transversus abdominis muscle is the deepest of the three muscle layers and runs in a horizontal fashion ventral to the transversalis fascia and dorsal to the IOM. The origin of the muscle is from the 7th to 12th costal cartilages, thoracolumbar fascia, iliac crest, and lateral aspect of the inguinal ligament and inserts onto the linea alba, pubic crest, and the pectineal line. The superior aspect of the muscle meets with the diaphragm.

The arcuate line is a key anatomic landmark, typically found at the level of the anterior superior iliac spine (ASIS). Above the arcuate line, the anterior rectus sheath is formed by the aponeurosis of

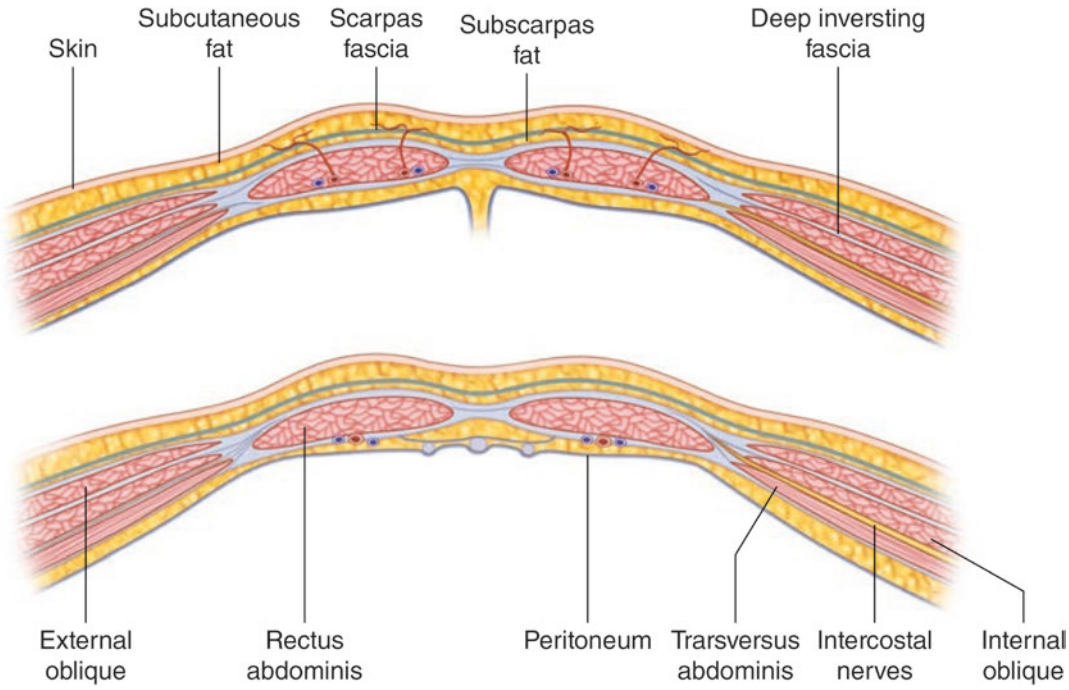

Fig. 5.4 Anatomy of abdominal wall above (top) and below (bottom) arcuate line

Modified from "Hernia Surgery: Current Principles, Yuri Novitsky, Fig. 28.1 page 300"

the external oblique and the internal oblique muscles while the posterior rectus sheath is formed by the aponeurosis of the internal oblique and the transversus abdominis aponeurosis. Below the arcuate line however only the anterior rectus sheath is present, and it is comprised of the aponeurosis of the external oblique, internal oblique, and transversus abdominis muscles. Only the transversalis fascia is present posterior to the rectus abdominus muslce below the arcuate line (Fig. 5.4).

Blood Supply

The two main arteries supplying the anterior abdominal wall include the superior and inferior epigastric arteries. The superior epigastric artery originates from the internal mammary (thoracic) artery while the inferior epigastric artery originates from the external iliac artery. In addition to those two major arteries, the abdominal wall is also supplied by an extensive network of collateral branches of the subcostal and lumbar arteries. The blood supply of the abdominal wall can be divided into three main zones, as was previously described by Huger et al. *Zone 1* is defined as the vascular region of the upper anterior midline region of the abdominal wall which is mainly perfused by the superior epigastric artery and the deep inferior epigastric artery. *Zone 2* is defined as the blood supply to the caudal portion of the anterior abdominal wall which is accomplished by four main arteries including the superficial inferior epigastric, superficial external pudendal, deep inferior epigastric artery, and the deep circumflex iliac artery. Lastly, *Zone 3* is the vascular region of the lateral abdominal wall which is mainly supplied by the lumbar and intercostal arteries which arise directly from the aorta (Fig. 5.5).

Nerves

The innervation of the abdominal wall is segmental and divided into motor and sensory innervation. The motor fibers supplying the rectus abdominis, external oblique, internal oblique, and transversus abdominis originate from the anterior rami of spinal nerves from the T6 to T12 levels. The cutaneous sensory innervation is provided by the afferent fibers from the T4 to L9

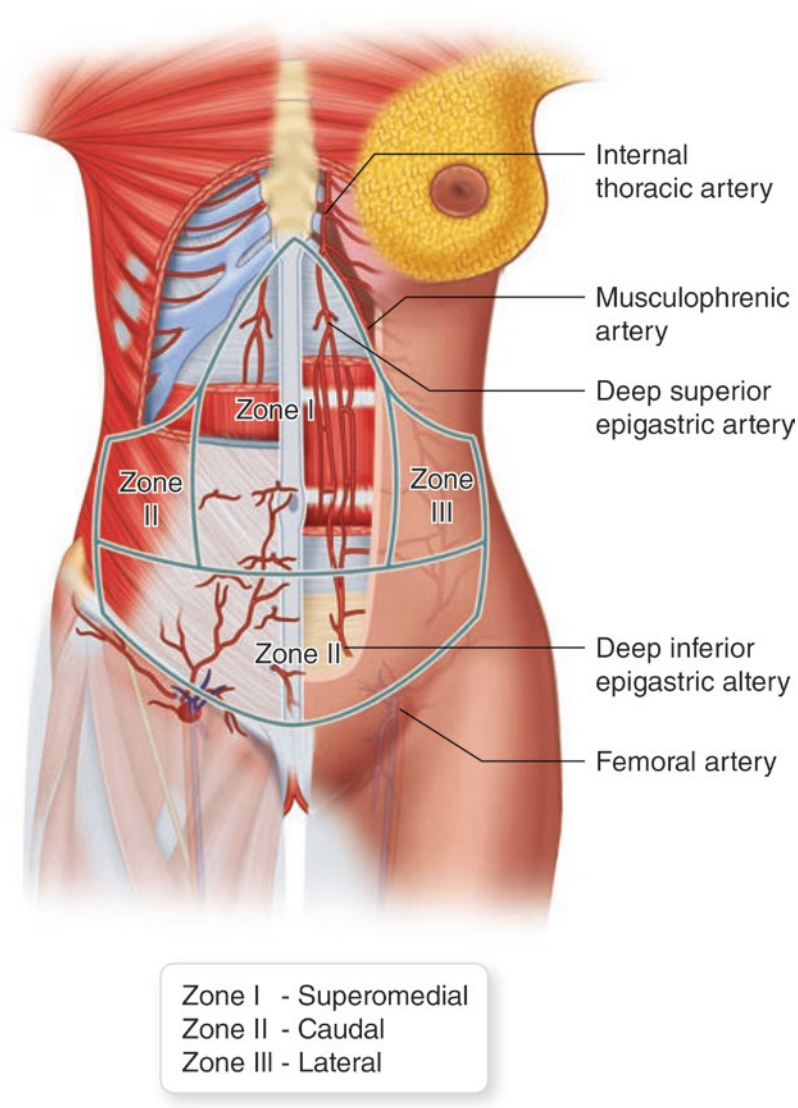

Fig. 5.5 Zones of the vascular supply of the abdominal wall **Modified from "Hernia Surgery: Current Principles, Yuri Novitsky, Fig. 1.7 page 11"**

nerve roots to the levels above the umbilicus. T10 provides sensory periumbilical innervation. The area below the umbilicus is innervated by the T11 to L1 nerve roots. The skin is directly innervated by branches of the intercostal nerves. The lateral neurovascular structures travel between the transversus abdominis muscle and the internal oblique muscle. This is important to consider when performing a transversus abdominis plane (TAP) block (Fig. 5.6).

Lymphatics

The anterior abdominal wall has two major lymphatic drainage systems: the superficial and deep. The superficial system drains the skin and the subcutaneous tissues, and the deep system drains the musculature and bones.

The superficial lymphatic system can essentially be divided by a horizontal line through the umbilicus. Above the umbilicus, the skins and subcutaneous tissue space drain into the pectoral

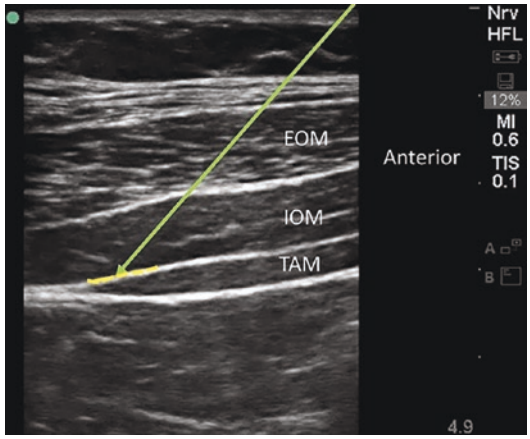

Fig. 5.6 Transversus abdominis plane (TAP) block is performed by injecting analgesic between the transverses abdominis muscle (TAM) and the internal oblique muscle (IOM) muscle layers. EOM—external oblique muscle. Vishal Uppal, Sushil Sancheti & Hari Kalagara. Current Anesthesiology Reports. Current Anesthesiology Reports. Springer Nature. 2019

axillary lymph nodes while some drain into the parasternal lymph nodes. Below the umbilicus, the superficial structures primarily drain into the superficial inguinal lymph nodes.

The deep system, on the other hand, drains into three main lymph node basins. The pathway following the superior epigastric artery drains into the parasternal nodes. The inferior epigastric artery pathway drains into the external iliac lymph nodes. Lastly, the inferior intercostal and subcostal pathways drain into the mediastinal lymph nodes (Fig. 5.7).

Physiology

The muscles of the anterior abdominal wall work as a cohesive unit to provide functionality to the abdominal wall. Anterior and lateral flexion is accomplished by the rectus muscle and the internal and external oblique muscles. Similarly, the

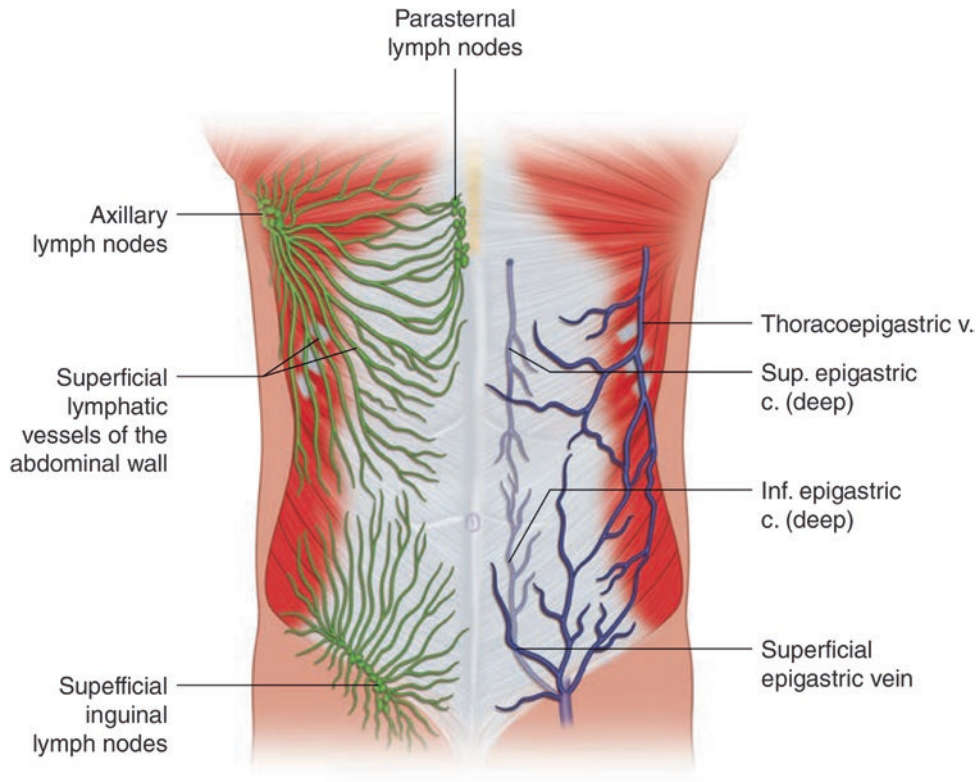

Fig. 5.7 Lymphatic drainage of the anterior abdominal wall. Green color shows the drainage of the superficial lymphatic system and blue color corresponds to the deep lymphatic drainage system

Modified from "Springer Cosmetic Surgery—https://link.springer.com/chapter/10.1007/978-3-642-21837-8_4"

truncal muscles function as a unit to increase intra-abdominal pressure, such as during a Valsalva maneuver or during forced expiration.

The rectus abdominis muscle's primary function is to allow for flexion of the torso. Secondarily, it assists in increasing intra-abdominal pressure. The pyramidalis muscle also has a small role in helping to tense the linea alba; however, its contribution is likely minimal [2]. The lateral muscles function as a unit. The EOM muscle assists in flexion and rotation of the trunk and functions to contract the abdominal wall to support the visceral contents and confine them in the abdominal cavity. Both the IOM and the TAM function in a synergistic fashion to provide circumferential tension on the abdomen and along with the EOM, function to allow rotation and torsion of the abdominal trunk.

Important Anatomical Regions

Space of Bogros and Space of Retzius

The space of Retzius is in the extraperitoneal space between the bladder and the pubic symphysis. The space is enclosed by the transversalis fascia and contains connective tissue and fat. The region may also contain aberrant pudendal and obturator vessels. Furthermore, adequate dissection of this space may be necessary for appropriate placement of mesh in inguinal and ventral hernia repairs. The space of Bogros is another important region that lies lateral to the space of Retzius and is the extraperitoneal space containing structures deep to the inguinal ligament. The space contains several important structures including the femoral vessels and the femoral nerve as well as iliopsoas muscle.

Important Anatomical Triangles and Landmarks

Certain anatomical regions are important to consider during operative interventions as they may lead to complications and comorbidities that can be easily avoided if the anatomy is appreciated. "Hesselbach's Triangle" is located in the lower portion of the posterior abdominal wall. Its boundaries include the lateral border of the rectus abdominis medially, the epigastric vessels superiorly, and the

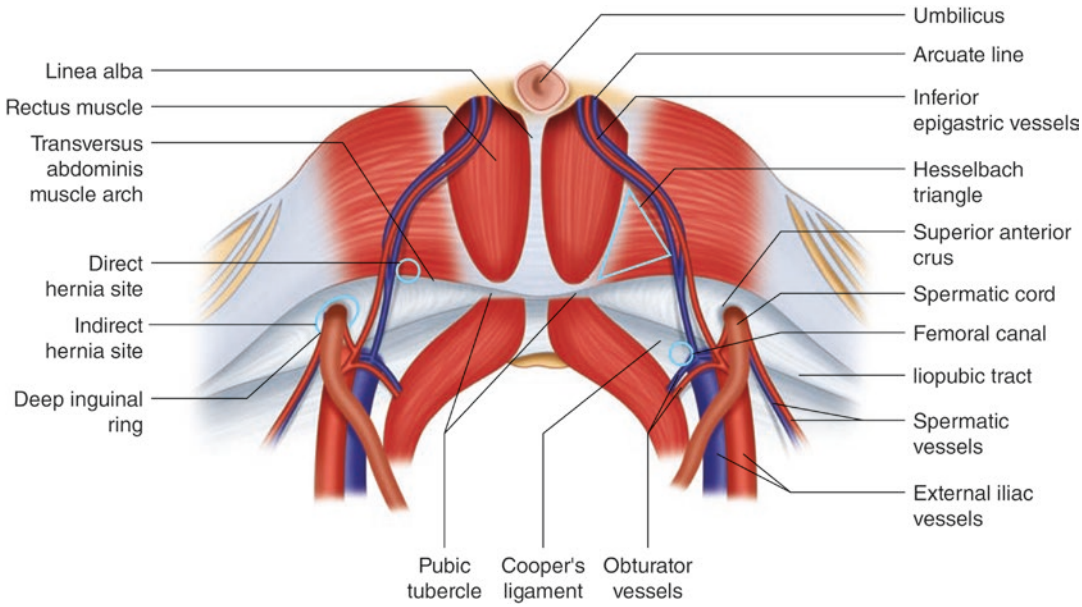

Fig. 5.8 Critical view of the myopectineal orifice Modified from Springer—Betancourt A., Pena A., Lo Menzo E. (2020) Laparoscopic Total Extraperitoneal (TEP) Inguinal Hernia Repair. In: Rosenthal R., Rosales A., Lo Menzo E., Dip F. (eds) Mental Conditioning to Perform Common Operations in General Surgery Training. Springer, Cham. https://doi.org/10.1007/978-3-319-91164-9_38)

inguinal ligament inferiorly. This region is important as it is the region of occurrence of direct inguinal hernias through the external inguinal ring. An indirect hernia, on the other hand, occurs lateral to "Hesselbach's Triangle" (Fig. 5.8).

The "*Triangle of Doom"* is one such region that has crucial vasculature and if tacks or staples are placed in that region, then there is a higher risk for excessive bleeding. The apex of the triangle is the deep inguinal ring. Lateral boundaries are the gonadal vessels and the medial boundary is the vas deferens in a male patient or the round ligament in a female. The two main vascular structures coursing in this triangle include the external iliac artery and vein (Fig. 5.9).

The " *Triangle of Pain"* is another important region to consider during laparoscopic hernia operation given the potential to cause nerve damage. As in the case of the "Triangle of Doom," the deep inguinal ring is the apex of the triangle. Anteriorly, the space is bound by the iliopubic tract and posterior-medially by the testicular vessels. The three crucial nerves that course in this region include the lateral femoral cutaneous nerve (L2-L3), femoral nerve (L2-L4), and the femoral branch of the genitofemoral nerve (L1-L2) (Fig. 5.9).

Critical View of Myopectineal Orifice

The critical view of the myopectineal orifice is defined as the area that must be visualized for the safe placement of a laparoscopic/robotic mesh. The concept has been developed by Daes et al. to standardize the steps of the exposure to minimize complications with laparoscopic inguinal hernia repair consisting of nine critical steps [3]. The first step involves the identification and dissec-

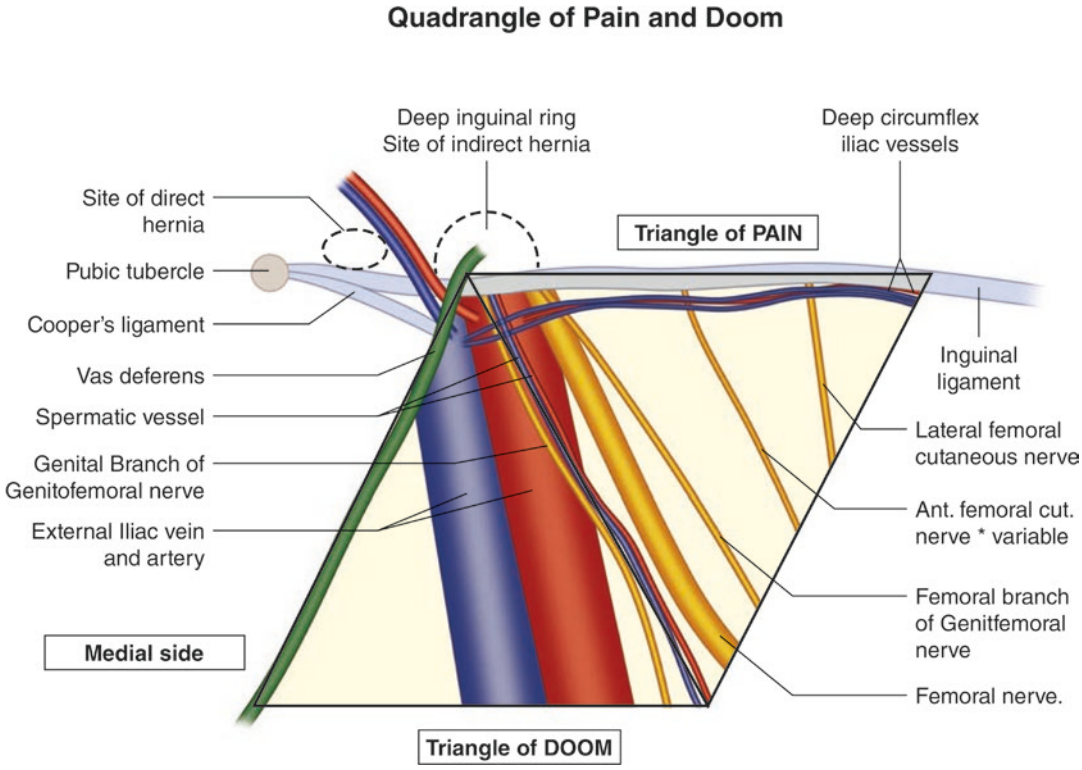

Fig. 5.9 Pre-peritoneal view of the right inguinal space demonstrating "Triangle of Doom" and "Triangle of Pain" Modified from Springer—Maker V.K., Guzman-Arrieta E.D. (2015) Abdominal Wall and Hernias. In: Cognitive Pearls in General Surgery. Springer, New York, NY. https://doi.org/10.1007/978-1-4939-1850-8_8

tion of the pubic tubercle and Cooper ligament. The second step involves dissecting Hesselbach's triangle and removing unusual fat in the area to rule out a direct hernia. The third step involves dissecting at least 2 cm between the Cooper ligament and the bladder to ensure enough medial and inferior space for the mesh to be placed. Next is to dissect the femoral space between the Cooper ligament and the iliac vessels to rule out a femoral hernia. The fifth step is to dissect the indirect sac and peritoneum such that the cord structure lies flat. Step 6 discusses cord lipomas and ensures that they are reduced appropriately and remain outside of the mesh. The seventh step discusses the lateral dissection and ensuring lateral dissection of the peritoneum beyond the cord structures and anterior superior iliac spine (ASIS). The eighth step ensures that the mesh is placed appropriately covering all the defects and that it is fixed above the inter-ASIS line. Lastly, step nine is the final placement of fixation of the mesh after the previous steps have been completed with adequate hemostasis ensuring that the mesh is flat and not rolling up (Fig. 5.8).

Imaging

Overview

Imaging of the abdominal wall is crucial for visualization of both the pathology and the patients' native anatomy, key aspects which need to be considered during surgical planning. Imaging can be as important as a physical exam and patient history and offer vital information regarding previous surgical procedures or mesh placement. The three main modalities that we will focus on include ultrasound, computed tomography, and magnetic resonance imaging in delineating the abdominal wall.

Ultrasound

Background

The quality of ultrasonography has drastically improved with the introduction of high frequency and high-resolution probes allowing it to become an essential tool in the evaluation of abdominal wall hernias. Ultrasonography has several important advantages over CT and MRI in that it is readily available, cheap, and has negligible radiation exposure. On the other hand, the quality of the sonographic imaging is highly dependable on the sonographer which permits significant variability in image quality. Furthermore, an obese body habitus also creates problems in visualizing the relationship between native anatomy and hernia pathology of the abdominal wall [4].

Technique

The best approach to evaluating the layers of the abdominal wall using sonography is using the high-frequency (6–12 MHz) linear probes [5]. The advantage is that no special preparation is necessary, and sterility can be maintained if the probe is covered with a sterile plastic sheath. When visualizing the abdominal wall layers, it is important to ensure that the rectus abdominis muscles are clearly demarcated as an initial reference point. The skin is typically echogenic, the subcutaneous layer is hypoechoic while the muscle layers have variable echogenicity with a lamellar pattern noted on ultrasound (Fig. 5.10). Another approach described by Beck et al. is termed Dynamic Abdominal Sonography for Hernia (DASH), which uses a 12 MHz linear ultrasound probe to look at 5 locations along the abdominal wall to identify small defects [6]. This approach is typically more helpful for the visual-

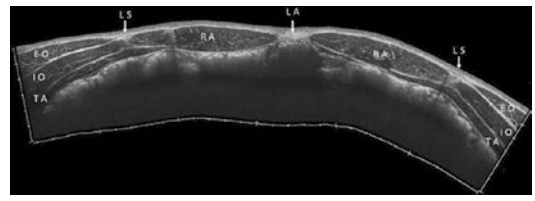

Fig. 5.10 Transverse panoramic scans of the anterior abdominal wall show detailed anatomy. *RA* Rectus abdominis, *EO* External oblique, *IO* Internal oblique, *TA* Transverse abdominis, *LA* Linea Alba, *LS* Linea Semilunaris
With permission from Springer—Draghi, F., Cocco, G., Richelmi, F.M. et al. Abdominal wall sonography: a pictorial review. J Ultrasound 23, 265–278 (2020). https://doi.org/10.1007/s40477-020-00435-0

ization of small abdominal wall defects and less so for larger defects given the size of the probe.

Visualization of Different Types of Hernias

When attempting to visualize various types of hernias, it is crucial to consider certain maneuvers to attempt to elucidate the normal and pathologic anatomy as best as possible. For example, coughing or performing a Valsalva maneuver may help visualize the hernia [7]. Furthermore, a direct vs indirect hernia may be differentiated based on the hernia location relative to the inferior epigastric arteries (Fig. 5.11). Furthermore, bowel wall thickening, that may occur due toincreased vascularity and obstruction, may be visualized with the help of an ultrasound (Fig. 5.12). Ventral hernias can also be recognized with the help of ultrasound by visualizing a defect in the abdominal wall with a "mushroom-like" appearance, which may contain pre-peritoneal fat, omentum, or a loop of bowel (Fig. 5.13). A Spigelian hernia may also be identified if there is a high suspicion of a hernia at the region of the linea semilunaris (Fig. 5.14). Incisional hernias may also be identified if there is a concern for a focal defect at a prior incision (e.g., laparoscopic incision) and will commonly appear as a protru-

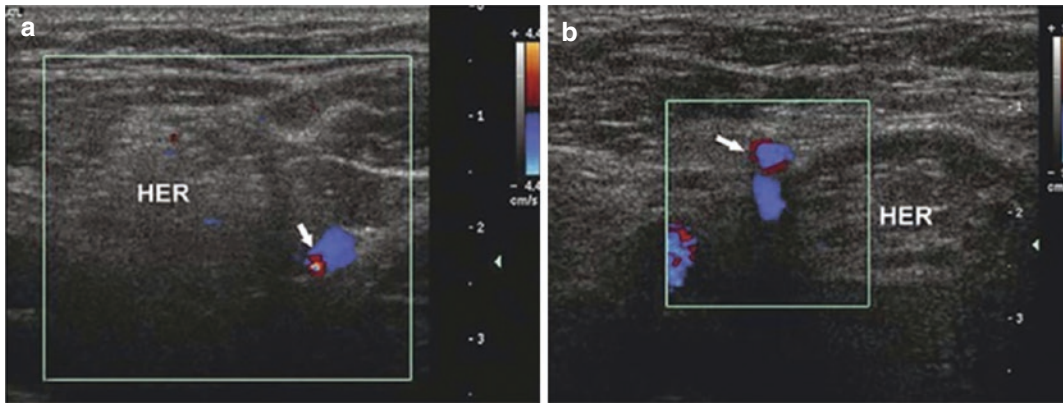

Fig. 5.11 The position of the inferior epigastric artery (arrow), shown in these color Doppler images differentiates an indirect inguinal hernia (**a**) and direct inguinal hernia (**b**)

With permission from Springer—Sutaria R.B. (2017) Inguinal Hernia. In: Kahn S., Xu R. (eds) Musculoskeletal Sports and Spine Disorders. Springer, Cham. https://doi.org/10.1007/978-3-319-50512-139

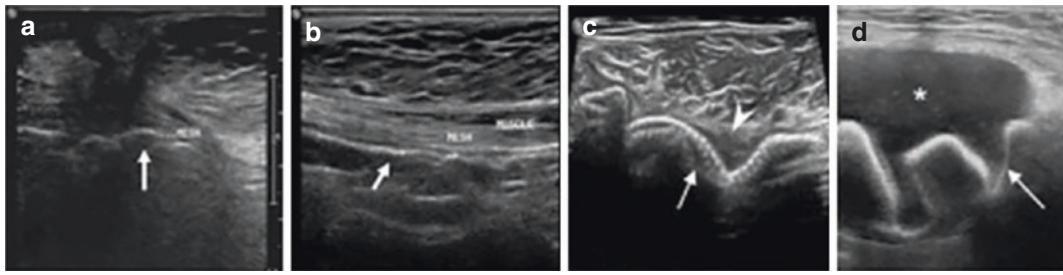

Fig. 5.12 Mesh appearances on ultrasound using high-resolution linear probe. Wavy echogenic appearance of mesh (arrow) in a post umbilical hernia repair (**a**). Inlay placement of mesh appearing echogenic on ultrasound (arrow) (**b**). Early postoperative ultrasound shows wavy echogenic mesh (arrow) made prominent by surrounding thin seroma (arrowhead) (**c**). Mesh migration (arrow) into a collection (*) in a post-inguinal hernia repair (**d**)

With permission from Springer—Patil, A.R., Nandikoor, S., Mohanty, H.S. et al. Mind the gap: imaging spectrum of abdominal ventral hernia repair complications. Insights Imaging 10, 40 (2019). https://doi.org/10.1186/s13244-019-0730-x)

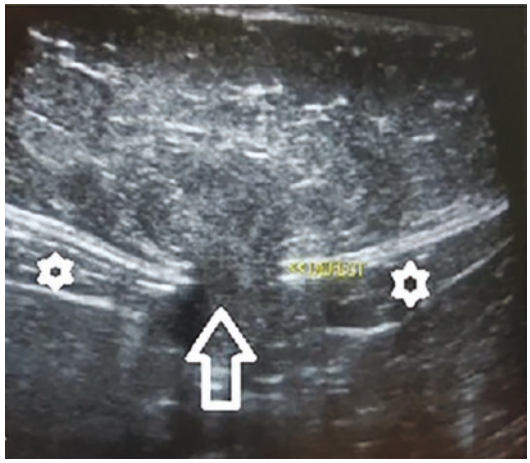

Fig. 5.13 A ventral hernia with a midline defect in the linea alba (white open arrow) between the two recti abdominus muscles (white asterisks) with the abdominal fat being seen protruding through the defect in a mushroom-like configuration
With permission from Ahmed Abdelrahman Mohamed Baz, Hatem Mohamed Said El-Azizi, Mohamed Sayed Qayati Mohamed & Ahmed Yehia Ibrahim Abdeldayem. Egyptian Journal of Radiology and Nuclear Medicine. Egyptian Journal of Radiology and Nuclear Medicine. Springer Nature. 2019

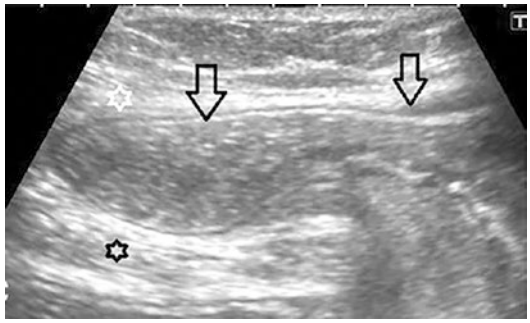

Fig. 5.14 Spigelian hernia with a bowel loop (open black arrows) being seen protruding through an abdominal wall defect to be insinuated between the transverses abdominus (black asterisk) and the internal oblique (white asterisk) muscles
With permission from. Ahmed Abdelrahman Mohamed Baz, Hatem Mohamed Said El-Azizi, Mohamed Sayed Qayati Mohamed & Ahmed Yehia Ibrahim Abdeldayem. Egyptian Journal of Radiology and Nuclear Medicine. Role of high-resolution ultrasound in the assessment of abdominal wall masses and mass-like lesions. Springer Nature. 2019

sion of fat content or bowel through a defect in the abdominal wall.

Computer Tomography (CT)

Background

Computed tomography is an excellent modality for evaluating the abdominal wall and visualizing different types of hernias [8]. The anatomy of the abdominal wall can be clearly appreciated with an axial CT (Fig. 5.15) [9]. The key applicability of CT scans is for preoperative planning to determine access points as well as the ability to close a potential defect. Along the same lines, it is also valuable in recurrent or complex cases where extensive dissection may be necessary to achieve adequate length. One of the main downsides is that it requires the patient to be supine which can cause the hernia to spontaneously reduce. Furthermore, while the radiation doses have been improving, CT is still associated with significantly more radiation exposure than its ultrasound or MRI counterpart. Interestingly, the sensitivity and specificity of CT in detecting occult inguinal hernias have been reported to be 80% and 65%, respectively [10]. While ultrasound has been reported to be the first line for evaluation for an inguinal hernia, if the clinical exam and findings are inconclusive or equivocal, it is reasonable to proceed to a CT scan.

Techniques for Visualization of Different Types of Abdominal Hernias

Multi-detector CT scan enable detailed assessment of various normal and pathological states of the abdominal wall [11]. For example, visualization of inguinal hernias allows differentiation between a direct and indirect inguinal hernia based on the location of the epigastric vessels (Fig. 5.16). An umbilical hernia can also be appreciated and based on the imaging, we can determine if it contains a bowel and whether the bowel is edematous and possibly ischemic

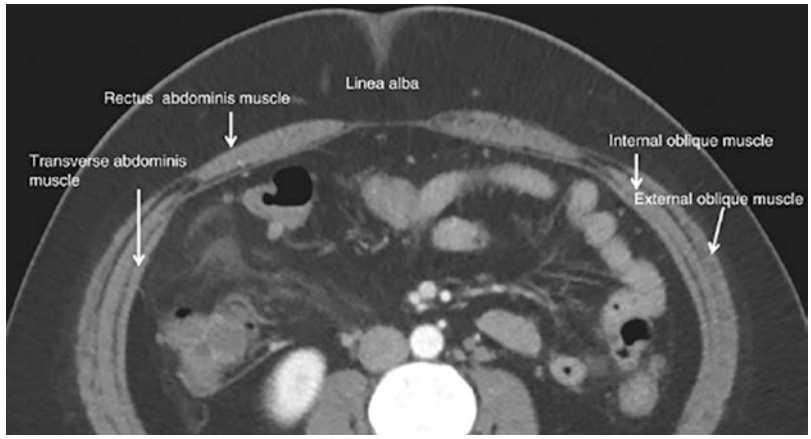

Fig. 5.15 Axial CT demonstrating the anatomy of abdominal wall
With permission from Springer—Mathur R.K., Goyal N. (2020) Imaging of Abdominal Wall Hernias. In: Chowbey P., Lomanto D. (eds) Techniques of Abdominal Wall Hernia Repair. Springer, New Delhi. https://doi.org/10.1007/978-81-322-3944-4_4)

Fig. 5.16 Bilateral direct inguinal hernias located medial to the inferior epigastric vessels (arrow)
With permission from Springer—Sodhi KS, Virmani V, Sandhu MS, Khandelwal N. Multi detector CT Imaging of Abdominal and Diaphragmatic Hernias: Pictorial Essay. The Indian Journal of Surgery. 2015 Apr;77(2):104-110. DOI: 10.1007/s12262-012-0736-9. PMID: 26139963; PMCID: PMC4484534.)

Fig. 5.17 Ventral hernia containing multiple loops of small bowel
With permission from Springer—Hernia, William W. Hope, William S. Cobb, Gina L. Adrales Springer pg278 figure 38.5)

(Fig. 5.17). Given the ability to clearly appreciate the linea semilunaris, a CT scan also enables the diagnosis of Spigelian hernias (Fig. 5.18). In fact, CT is considered first-line imaging modality in patients with concern for femoral or obturator hernias [12]. Several protocols are currently available for evaluation of various hernia defects. One such approach has been described by Xu et al. who developed an anatomical labeling protocol to characterize ventral hernias and predict mesh dimension and the need for mesh bridge closure [13].

Emby et al. describe another approach to visualizing the anterior abdominal wall using fast helical sequence CT imaging. During the scan, the patient is asked to take a full breath (full inspiration) in supine position while CT images are obtained from diaphragm to pubic symphysis. If a bulge is appreciated, it is marked with small metallic skin markers. The patient is then turned onto their side with

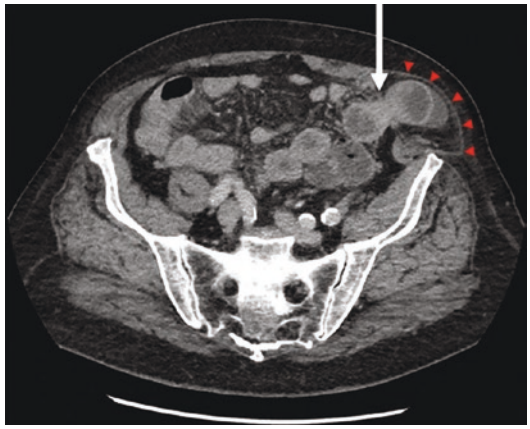

Fig. 5.18 Left-sided Spigelian hernia containing loops of bowel (arrow) through the linea semilunaris with an intact external oblique aponeurosis (red arrowheads)
With permission from Springer—Hanzalova, I., Schäfer, M., Demartines, N. et al. Spigelian hernia: current approaches to surgical treatment—a review. Hernia (2021). https://doi.org/10.1007/s10029-021-02511-8)

the symptomatic side facing downwards toward the table [14]. Another CT is obtained from diaphragm to pubic symphysis with the patient performing a full Valsalva maneuver. Oral and intravenous contrast are optional and are not routinely performed. This technique can help with the visualization of occult defects, especially in the obese population, that could otherwise be missed with a standard supine CT with reconstruction. Furthermore, it can help exclude suspicious areas of abdominal wall thinning that are not true defects.

Magnetic Resonance Imaging (MRI)

Background

Magnetic resonance imaging has several notable advantages including minimal radiation and detailed visualization of various tissues and their subtle planes [15]. Furthermore, the option of having a functional MRI is advantageous as it allows patients to perform certain maneuvers during imaging, including Valsalva. One of the major drawbacks of the modality includes its higher cost and the prolonged duration of the scan making it difficult to perform images in the still supine position. Furthermore, patients who are claustrophobic have a difficult time remaining still for the prolonged period required to obtain adequate MRI images. Though "open air" MRIs are an option, their limited availability makes access difficult. Given the MRI modality level of detail, it may also help eliminate other causes of pain that are unrelated to a hernia. Another key advantage that MRI has over a CT scan is its ability to visualize a prosthetic mesh which can be difficult to visualize on CT [16].

Technique for Abdominal Wall Visualization

While not the first- or even second-line imaging modality for the anterior abdominal wall, MRI imaging of the abdominal wall can provide unique information not appreciated with an ultrasound or a CT scan. MRI may assist in differentiating an inguinal from a femoral hernia with a high positive predictive value [17]. A potentially useful sequence when imaging abdominal wall hernia is to use coronal 3D T1-weighted Volume Interpolated Breath Hold (VIBE) without fat saturation during Valsalva maneuver and at rest [18]. Kielar et al. also recommend adding an axial TSE T2 and Axial short Tau Inversion recovery (STIR) and to include both groin regions for adequate comparison (Fig. 5.19).

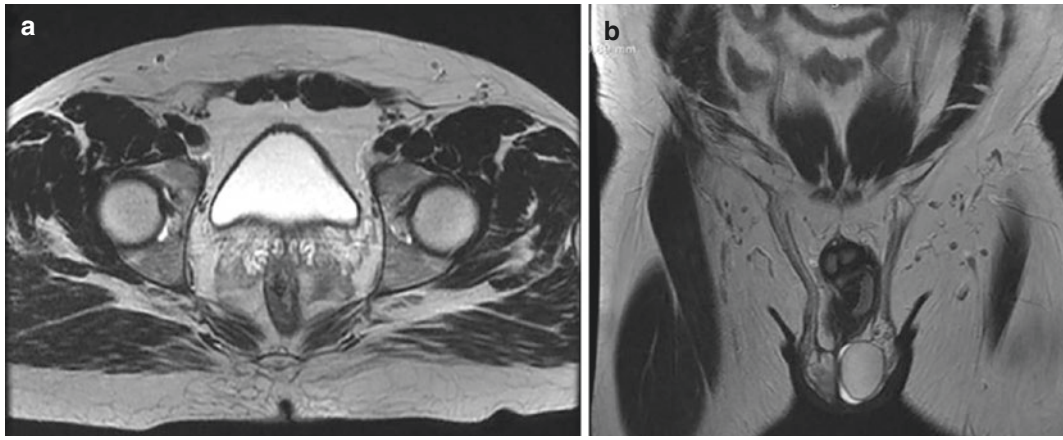

Fig. 5.19 MR image of fat-containing right inguinal hernia in T2 axial (**a**) and coronal (**b**) views. Note the smaller fat-containing left inguinal hernia as well

With permission from Springer—Textbook of Hernia, William W. Hope, William S. Cobb, Gina L. Adrales Springer pg46 figure 6.3

Conclusion

When evaluating the abdominal wall several modalities are available at the surgeon's discretion. While initially an ultrasound is an appropriate first step, it is often not sufficient in cases with obesity and/or complicated abdominal surgery history and distorted planes. CT imaging is an appropriate second modality to evaluate abdominal wall pathology and is often utilized for preoperative evaluation and planning. MRI is essentially a last resort imaging modality often times reserved for cases where a CT is inadequate and a strong clinical suspicion remains for abdominal wall pathology.

References

1. Lovering RM, Anderson LD. Architecture and fiber type of the pyramidalis muscle. Anat Sci Int. 2008;83(4):294–7.
2. Pierce RA, Poulose BK. Preoperative imaging in hernia surgery. In: Novitsky Y, editor. Hernia surgery. Cham: Springer; 2016.
3. Daes J, Felix E. Critical view of the myopectineal orifice. Ann Surg. 2017;266(1):e1–2.
4. Aguirre DA, et al. Abdominal wall hernias: imaging features, complications, and diagnostic pitfalls at multi-detector row CT. Radiographics. 2005;25(6):1501–20.
5. Gokhale S. High resolution ultrasonography of the anterior abdominal wall. Indian J Radiol Imaging. 2017;17
6. Beck WC, et al. Comparative effectiveness of dynamic abdominal sonography for hernia vs computed tomography in the diagnosis of incisional hernia. J Am Coll Surg. 2013;216(3):447–53; quiz 510-1.
7. Davis BS, Dunn DP, Hostetler VC. Beyond hernias: a multimodality review of abdominal wall pathology. Br J Radiol. 2017;90(1069):20160719.
8. Huger WE Jr. The anatomic rationale for abdominal lipectomy. Am Surg. 1979;45(9):612–7.
9. Moore KL, Dalley AF, Agur AMR. Clinically oriented anatomy. 7th ed. Philadelphia, PA: Lippincott Williams & Wilkins; 2014.
10. Robinson A, et al. A systematic review and meta-analysis of the role of radiology in the diagnosis of occult inguinal hernia. Surg Endosc. 2013;27(1):11–8.
11. Sodhi KS, et al. Multi detector CT imaging of abdominal and diaphragmatic hernias: pictorial essay. Indian J Surg. 2015;77(2):104–10.
12. Petrie A, et al. Obturator hernia: anatomy, embryology, diagnosis, and treatment. Clin Anat. 2011;24(5):562–9.
13. Xu Z, et al. Quantitative CT imaging of ventral hernias: preliminary validation of an anatomical labeling protocol. PLoS One. 2015;10(10):e0141671.

14. Emby DJ, Aoun G. CT technique for suspected anterior abdominal wall hernia. AJR Am J Roentgenol. 2003;181(2):431–3.
15. Murphy KP, O'Connor OJ, Maher MM. Adult abdominal hernias. AJR Am J Roentgenol. 2014;202(6):W506–11.
16. Hansen NL, et al. First in-human magnetic resonance visualization of surgical mesh implants for inguinal hernia treatment. Invest Radiol. 2013;48(11):770–8.
17. van den Berg JC, et al. Detection of groin hernia with physical examination, ultrasound, and MRI compared with laparoscopic findings. Invest Radiol. 1999;34(12):739–43.
18. Kielar AZ, Duigenan S, McInnes MD. Muscle beach: abdominal wall musculature and associated hernias. Appl Radiol April 18, 2014.

6 Normal Anatomy: Computed Tomography Scan

Sean B. Orenstein

Introduction

The abdominal wall represents a highly organized conglomeration of varying planes of myofascial tissue that intersect and overlap at specific anatomic locations. Having in-depth anatomic knowledge of the abdominal wall is crucial for successful procedural care and outcomes for hernia repair and abdominal wall reconstruction (AWR). Computed tomography (CT) imaging provides one of the best diagnostic modalities to explore both normal and pathologic features of the abdominal wall, including various types and locations of hernia defects. A robust blood supply along with overlying skin and soft tissue help maintain integrity of the abdominal wall. Specific nuances of the abdominal wall exist that have allowed surgeons to take advantage of differences within each layer, providing a variety of planes for mesh prosthetic placement as well as myofascial release and advancement. This chapter is designed to review basic normal abdominal wall anatomy and such nuances via CT imaging.

S. B. Orenstein (✉)
Department of Surgery, Division of Gastrointestinal and General Surgery, Oregon Health & Science University, Portland, OR, USA
e-mail: orenstei@ohsu.edu

Abdominal Wall Overview

The abdominal wall is primarily composed of multiple layers of fascial tissue and muscle. There are several ways of reviewing abdominal wall imaging, and it can be helpful to organize it within several regions to ensure that the entire abdominal wall is reviewed without missing occult hernias or other pathology. While each region consists of one or multiple distinct myofascial groups, there is an overlap of these regions at certain anatomic landmarks.

Importantly, regardless of which region is being evaluated, there is consistency with the lining of the abdominal wall. Namely, two distinct principal layers exist that line the contours of the abdominal wall—transversalis fascia (not to be confused with transversus abdominis), along with the peritoneum. In between these two layers is a layer of adipose tissue aptly named pre-peritoneal fat. There is ongoing discovery and debate as to these deep layers, with the discussion of two distinct transversalis layers versus one layer plus a more membranous pre-peritoneal fatty layer. The thickness of pre-peritoneal fatty tissue varies from patient to patient, with some patients displaying more obvious thick pre-peritoneal fat (Fig. 6.1). Preoperative CT imaging evaluation of this layer can help determine if a trans-abdominal pre-peritoneal ventral hernia repair (TAPP VHR) is appropriate, though intraoperative examination is the ultimate guide for

S. Docimo Jr. et al. (eds.), *Fundamentals of Hernia Radiology*,
https://doi.org/10.1007/978-3-031-21336-6_6

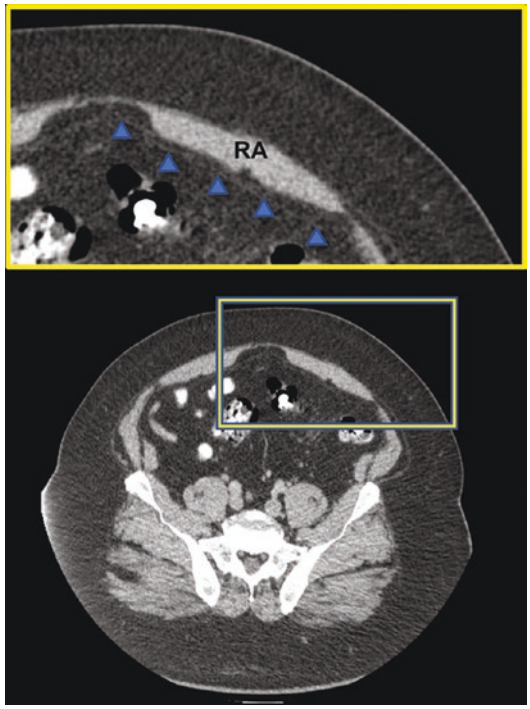

Fig. 6.1 Pre-peritoneal fat. In magnified view, note the separation of the peritoneum (arrowheads) from the rectus abdominis (RA) by fat-dense tissue within this pre-peritoneal plane

use of this tissue plane. Interestingly, pre-peritoneal fat measurements can also be an indicator for coronary and other diseases, though studies have typically focused on ultrasound-based imaging.

Radiographic Regions

Central/Middle Abdominal Wall Region

The central, or middle, region consists of the vertically oriented rectus abdominis muscles, separated by the linea alba in the midline. Each rectus muscle is encased by the anterior and posterior rectus sheaths. As discussed in Chap. 5 (Normal Abdominal Wall Anatomy), the anterior and posterior rectus sheaths are composed of fused layers of fascial tissue, with the anterior rectus sheath comprising layers of the external oblique aponeurosis plus the anterior lamella of the internal oblique aponeurosis. The posterior rectus sheath is comprised of the posterior lamella of the internal oblique aponeurosis plus the transversus abdominis aponeurosis. However, this anatomy holds true only superior to the arcuate line. Inferior to the arcuate line, there is no true posterior rectus sheath, as all rectus sheath layers lie *anterior* to the rectus muscle. Instead, only the transversalis fascia and peritoneal layers exist deep, or posterior, to the rectus muscles inferior to the level of the arcuate line. This anatomy is significant during a variety of hernia repair types including retromuscular repairs as well as pre-peritoneal repairs for both ventral and inguinal hernia repairs.

The contour and size of the rectus muscles vary from person to person. Healthy individuals commonly exhibit thick vascularized rectus muscles when seen in axial cross-sections. Above the arcuate line, the rectus muscle takes on a symmetric fusiform shape (Fig. 6.2a). Whereas, below the arcuate line the rectus muscle is narrower, but thicker, and more cup-shaped with a deep gap between the bilateral muscles as a result of limited containment from lack of a posterior rectus sheath (Fig. 6.2b). Conversely, elderly and deconditioned patients may demonstrate thinner, flatter, and perhaps wider rectus muscles (Fig. 6.3).

As they course throughout the abdominal wall, certain aspects of the vasculature are seen on CT imaging. Principal vessels visualized include the inferior and superior epigastric vessels, as well as periumbilical perforators, if robust enough. Because these vessels may be encased in fatty tissue they can be easily separated from adjacent muscular tissue, showing up as notches within the rectus muscles (Fig. 6.4).

Midline

Linea Alba/Diastasis Recti

The midline consists of a fused composite of fascial tissue from the bilateral anterior and posterior rectus sheaths named the linea alba. This thickened white line of fascial tissue varies in

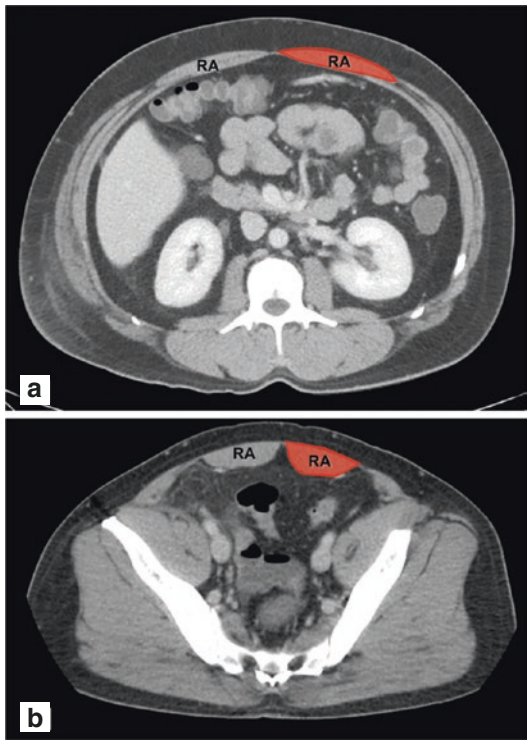

Fig. 6.2 Rectus abdominis muscle contour. (**a**) Above the arcuate line the rectus abdominis muscle is a symmetric fusiform shape. (**b**) Below the arcuate line the rectus abdominis muscle is narrower but thicker, and more cup-shaped as a result of limited containment from the lack of a posterior rectus sheath. (*RA* Rectus abdominis muscle)

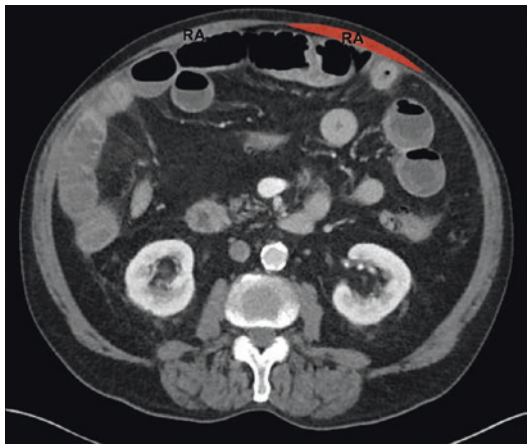

Fig. 6.3 Thinner, flatter, wider rectus muscles are commonly seen in elderly and deconditioned patients. In this patient, the rectus muscles are approximately 10 cm wide × 0.8 cm thick. (*RA* Rectus abdominis muscle)

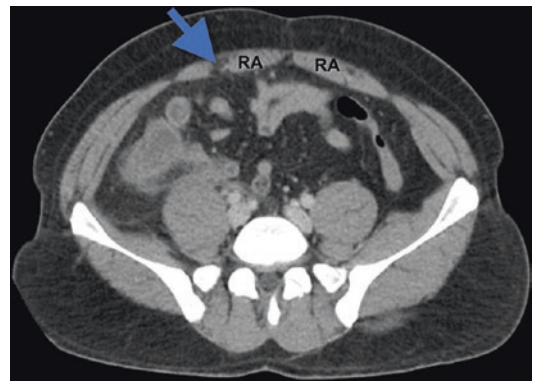

Fig. 6.4 Epigastric vessel "notching" (arrow) with fat wrapping around inferior epigastric vessels. This is not to be confused with atrophy of the muscle. (*RA* Rectus abdominis muscle)

thickness and width from person to person. Additionally, there is natural non-pathogenic width of the linea alba, with a normal space between the medial edges of the rectus abdominis muscles. This gap is more prominent in the upper aspects of the linea alba compared to below the umbilicus. Pathogenic widening of the linea alba, or diastasis recti, can occur de novo (e.g., from pregnancy, obesity, etc.), or following surgical trauma (e.g., laparotomy). Because wide diastasis recti can behave physiologically like a ventral hernia, or immediately adjacent to a true fascial defect, it is helpful to note the characteristics of the diastasis recti when planning elective herniorrhaphy (Fig. 6.5).

Umbilicus and Epigastrium

Primary umbilical and epigastric hernias are quite common, representing approximately 10% or more of all primary fascial defects of the abdominal wall, with up to 25% of the adult population having an umbilical hernia defect and 3–5% of the population having an epigastric hernia defect. And, while these fascial defects are technically pathologic (i.e., true fascial opening secondary to failure of linea alba fusion following involution of the umbilical vessels, or acquired later in life), many of these defects are asymptomatic and go unnoticed. Because of the

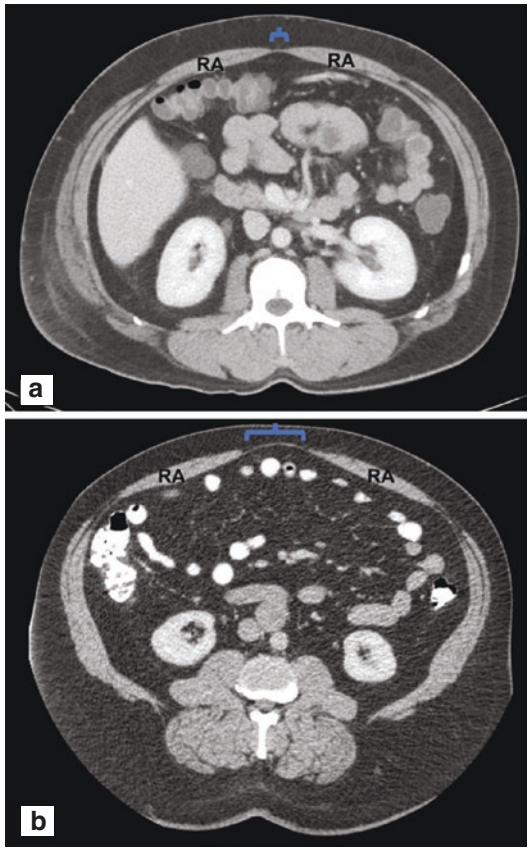

Fig. 6.5 Linea alba. (**a**) Normal linea alba, with a small 1 cm width of fascia between medial edges of the rectus muscles. (**b**) Diastasis recti, with widened 5 cm attenuated fascia between the medial edges of the rectus muscles. (Blue braces = linea alba width; *RA* Rectus abdominis muscle)

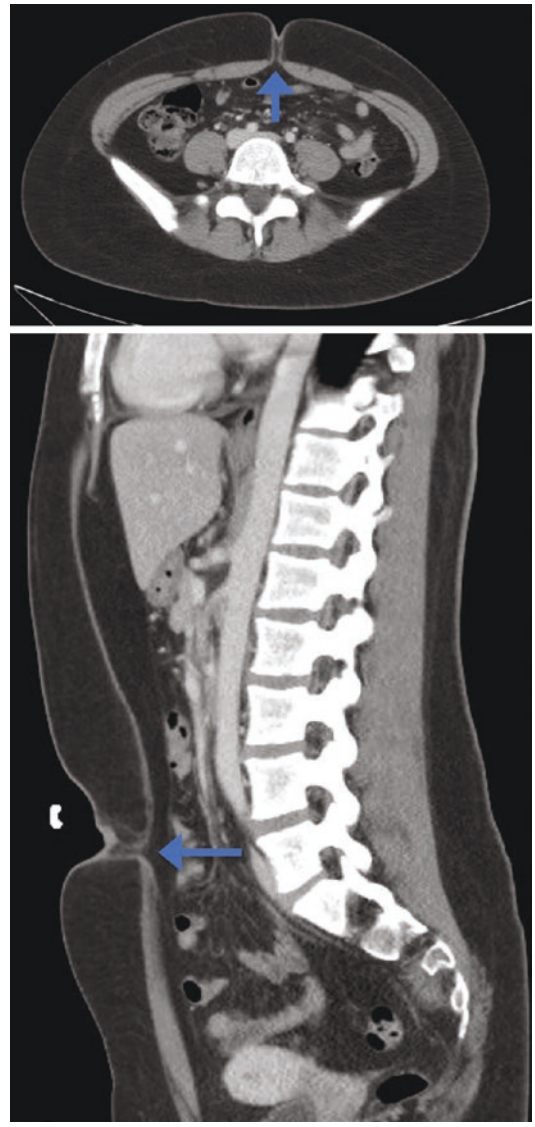

Fig. 6.6 Umbilical defect. While technically abnormal, fat-containing umbilical defects are commonly seen when evaluating the abdominal wall midline. These axial and mid-sagittal images show a 0.5 cm umbilical defect (arrow)

common finding of umbilical defects, as well as potential for involvement of such defects during hernia repair and other surgical procedures, it is beneficial to thoroughly evaluate the midline fascia during routine CT imaging review (Fig. 6.6). Many umbilical defects contain only preperitoneal fatty tissue, while others contain omentum or even bowel, with the latter more likely sources of symptoms that prompt evaluation and repair.

Superior Region

Superiorly, key bony landmarks include the xiphoid process and costal margins. Besides the bony portion of the xiphoid process, cartilaginous extension of the xiphoid process can be present and helpful to note, as this protrusion can obscure dissection planes superiorly during ventral hernia repair (Fig. 6.7).

Costal margin anatomy plays a role in a variety of hernia repairs, especially for incisional hernias following subcostal (e.g., Kocher inci-

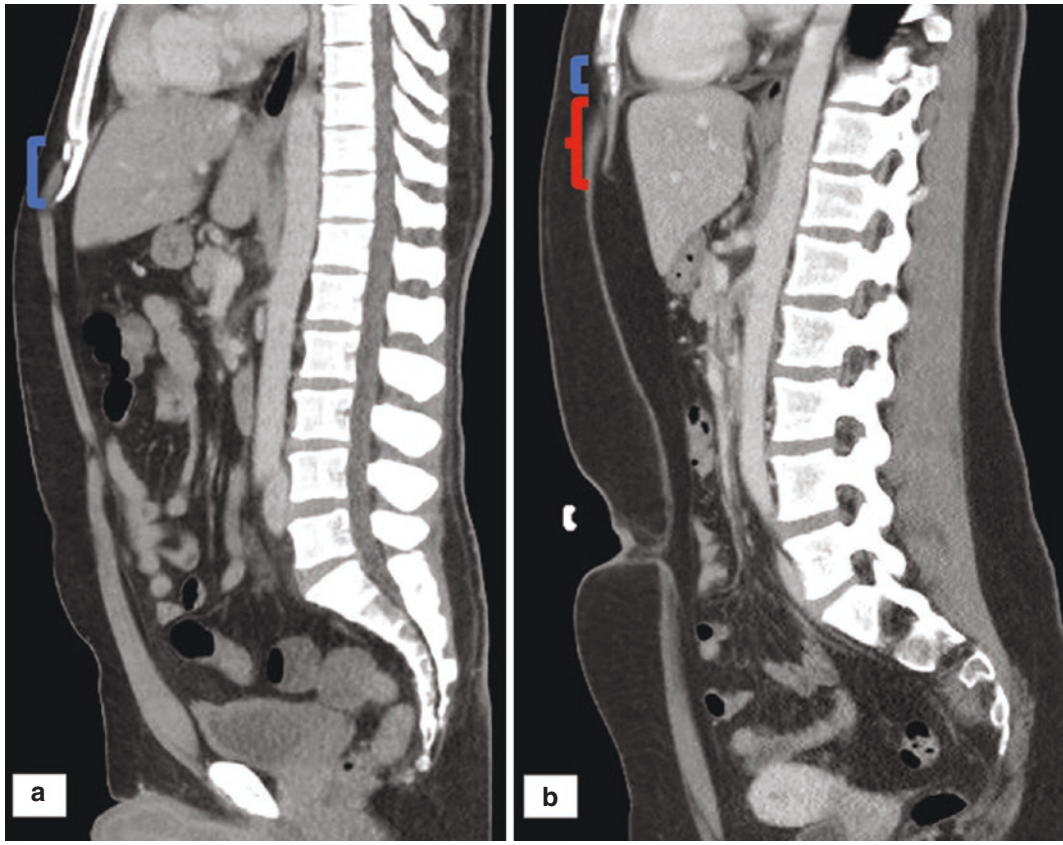

Fig. 6.7 Xiphoid process. (**a**) Bony xiphoid process [blue bracket]. (**b**) Short bony portion [blue bracket] with long cartilaginous extension {red brace} of the xiphoid process

sion for open cholecystectomy), chevron (e.g., liver transplant), or thoraco-abdominal incisions (e.g., trauma, cardiothoracic procedures). Important anatomic aspects include angulation of the costal margins as well as the proximity of a hernia to the costal margin, as this can affect defect closure and/or fixation of the mesh.

Inferior Region

Inferiorly, one should note normal anatomy including relationships of the bladder, uterus, rectum and sigmoid colon to each other. Anteriorly, the retropubic space (i.e., Space of Retzius), located between the pubic bone and bladder, is commonly utilized for inguinal and ventral hernia repairs. The rectus abdominis muscles taper down at their origins to the pubic bone and symphysis. Previous pelvic surgery, traumatic injury, or radiation therapy can alter normal anatomic planes anteriorly or deep in the pelvis and should be noted on CT scan. Normal CT imaging commonly reveals thin fat planes adjacent to the aforementioned structures, as well as lack of superficial scarring (Fig. 6.8).

Detailed groin anatomy is beyond the scope of this chapter. However, it is useful to evaluate for inguinal hernias as well as other obvious groin pathology, as these can impact concomitant procedures during hernia repair. It is common to visualize some degree of fatty tissue within the inguinal canals, especially in males. This fatty tissue represents either cord fat, a cord lipoma (extension of retroperitoneal fat within the testicular canal), or a combination of the two, regardless of obvious fascial defects suggestive of an inguinal hernia (Fig. 6.9).

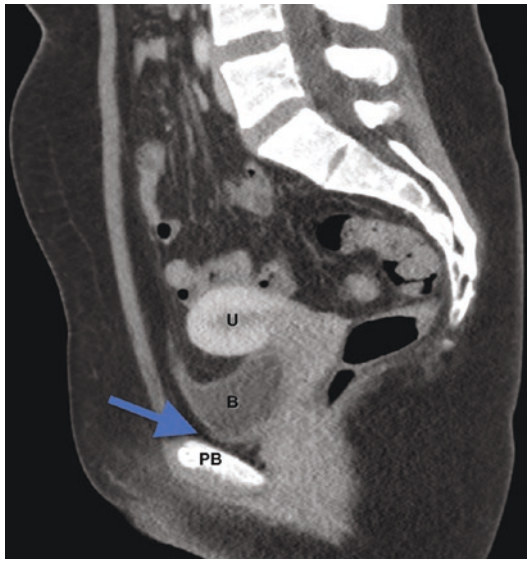

Fig. 6.8 Sagittal view of pelvis. Note clear fat planes in the space of Retzius (arrow) between pubic bone (PB) and bladder (B), and lack of superficial scarring in the region. (*U* Uterus)

Lateral Abdominal Wall Regions

The lateral region is comprised of a tri-muscular complex of muscle layers and their associated aponeuroses. This myofascial complex includes the external oblique, internal oblique, and transversus abdominis, from superficial to deep. These layers are intimately associated with each other as well as with the rectus abdominis complex in the central region. Importantly, while commonly understood more as distinct regions, there is some degree of overlap between the lateral and central regions which carries significance with regard to abdominal wall reconstructive techniques.

Origin and insertion of the lateral muscles is another key aspect, as the layering can be exploited for use in differing hernia repair techniques. For example, the external oblique (EO) muscle originates *anterior* to the lower 5th–12th ribs (Fig. 6.10). Because of its anterior location,

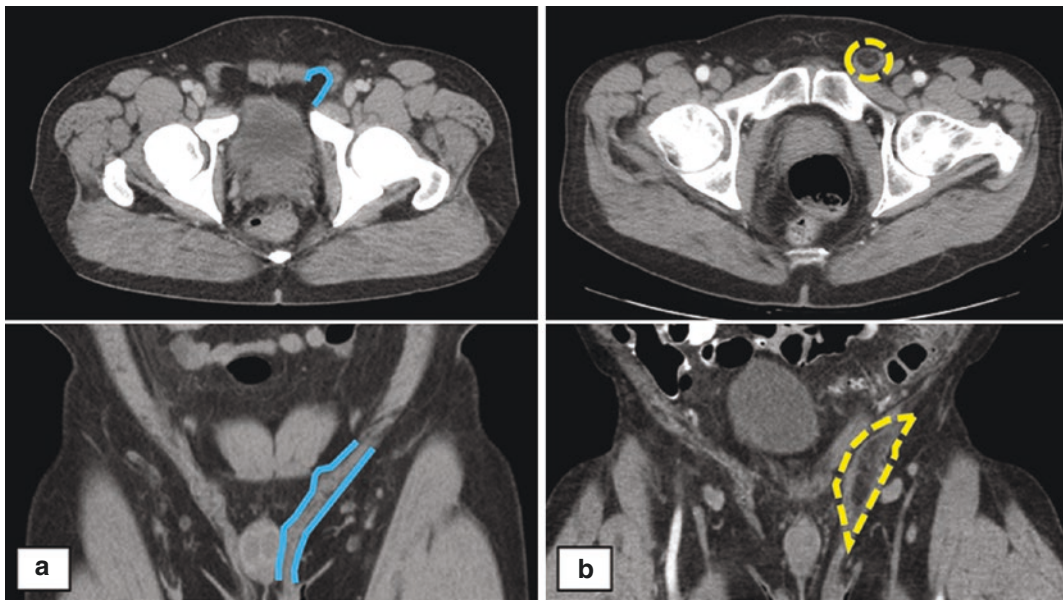

Fig. 6.9 Groin evaluation in axial (top) and coronal views (bottom). (**a**) Normal inguinal anatomy, with relatively smooth contoured tissue planes (blue lines), minimal peri-cord fat, and lack of inguinal hernia defect seen. (**b**) Left-sided cord lipoma seen extending from retroperitoneal fat + testicular cord fat (outlined with dashed yellow lines). Note: no obvious hernia defect(s) seen on CT

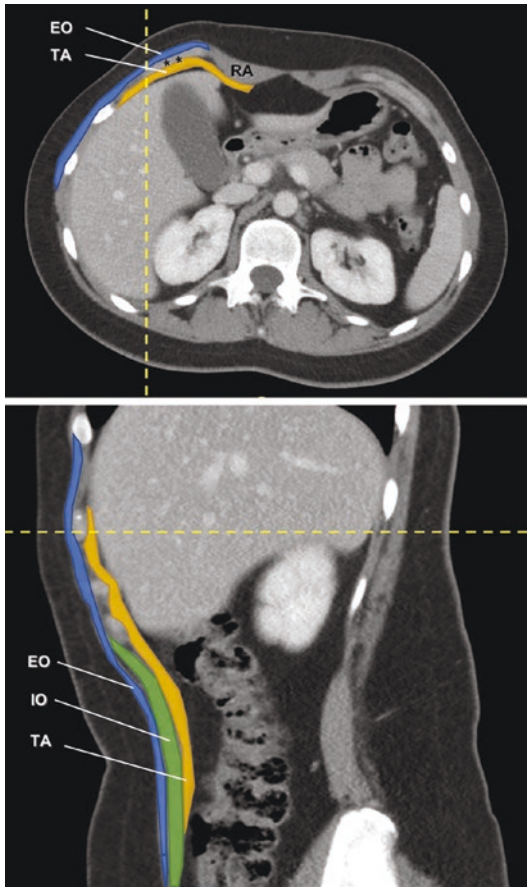

Fig. 6.10 External oblique (EO; blue) and transversus abdominis (TA; orange) and anatomic relationship to the ribcage. Note anterior location of the EO to the 7th and 8th ribs (noted by double asterisks * *), whereas TA lies posterior to the ribs. Dashed yellow lines represent cross-section in other planes (axial vs sagittal). (*RA* Rectus abdominis, *IO* Internal oblique; green)

minimally invasive component separation techniques exist that initiate dissection and external oblique release above the costal margin, cutting down on top of the ribs to reach the external oblique muscle and aponeurosis. Medially, the EO aponeurosis contributes to the anterior rectus sheath.

The internal oblique (IO) muscle and its aponeuroses are interesting, in that they contribute to both the anterior and posterior rectus sheaths. Medially, the IO splits into anterior and posterior lamellae, contributing to the anterior and posterior rectus sheaths, respectively. It is this posterior lamella of the IO that is a crucial dissection layer during transversus abdominis release (TAR) component separation. In this region, neurovascular bundles traverse the abdominal wall between the IO and transversus abdominis (TA) and emanate towards the lateral aspect of the retrorectus space near the semilunar line (aka linea semilunaris). During a TAR procedure division of the posterior lamella of the IO gives access to the TA muscle for division and myofascial release. The aforementioned neurovascular bundles provide a critically important anatomic landmark during TAR, with standard TA division occurring *medial* to the neurovascular bundles. If proper anatomy is not recognized and dissection occurs *laterally* to the neurovascular bundles, injury to the semilunar line layers may occur, creating iatrogenic semilunar line disruption which can be a challenging complication to remedy.

Transversus abdominis (TA) muscle is the deepest of the three lateral myofascial layers. While the EO originates *anterior/superficial* to the ribs, the TA originates *posterior/deep* to the lower ribs (Fig. 6.10). The clinical significance of this lies in the ability to provide wide superior mesh overlap well beyond the costal margin during AWR procedures. This layer is also the most variable with regard to the medial edge of the muscle and its relationship near the semilunar line (Fig. 6.11). Superiorly, the medial edge of the TA muscle extends beyond the semilunar line, lying deep to the rectus abdominis. Essentially, there is underlap of TA muscle to the lateral portion of the rectus abdominis. In the central abdominal wall near the level of the umbilicus, the medial edge of the TA aligns itself with medial edges of EO and IO, with all three layers in alignment near the semilunar line. Inferiorly, the muscular component of the TA lies much more laterally, leaving only the aponeurotic portions present medially.

Knowledge of these anatomic differences can help influence how a TAR is performed. TAR was initially described in a top-down approach, initiating dissection superiorly by incising the posterior lamella of the IO. This maneuver exposes the more medially positioned TA muscle fibers deep to the rectus muscle for division and release. As

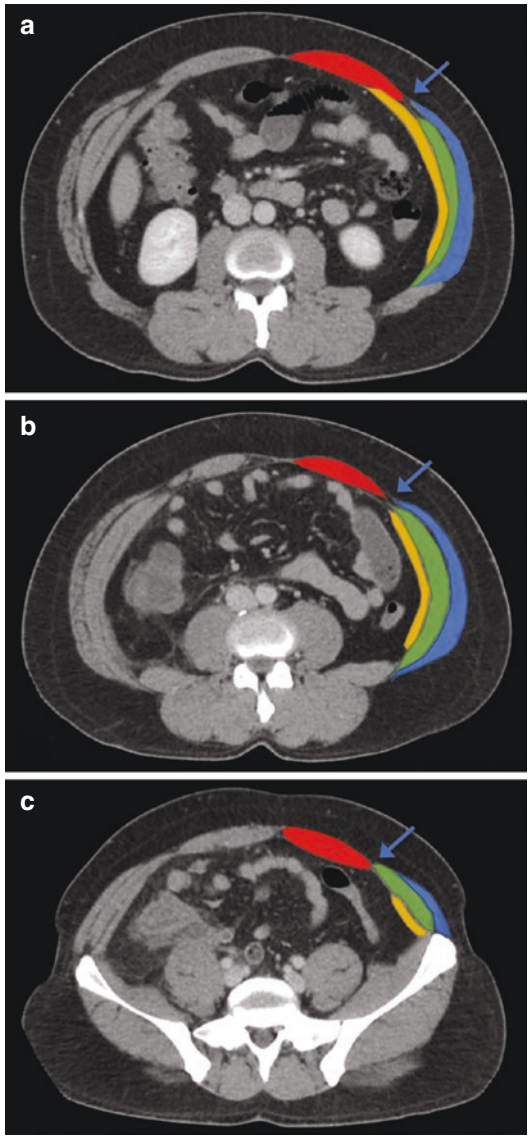

Fig. 6.11 Lateral tri-muscular complex and relationship to rectus abdominis. (**a**) Superiorly, the transversus abdominis muscle extends medially past the semilunar line, lying deep/posterior to the rectus abdominis. (**b**) In the middle of the abdomen, the medial edge of all three myofascial layers (EO, IO, and TA) are aligned near the semilunar line. (**c**) Inferiorly, the medial muscular portion of the TA lies more laterally, with only the TA aponeurosis extending medially towards the semilunar line. (*RA* Rectus abdominis, *EO* External oblique; blue, *IO* Internal oblique; green, *TA* Transversus abdominis; orange, *Arrow*=semilunar line)

TAR proceeds inferiorly, dissection transitions from more muscular division superiorly to strict aponeurotic division in the central and inferior portions, again, as the muscular portion of the TA lies laterally.

Conclusion

CT imaging of the abdominal wall can readily be assessed for preoperative planning for a variety of hernia repairs. Reviewing the abdominal wall region by region can help streamline the evaluation, with care taken to consider the relationships of the various myofascial planes with each other, as there is overlap between the different regions. Knowledge of normal anatomic planes and tissues and differentiating them from pathologic findings, such as hernia defects, with various configurations and sizes, greatly aid in determining an appropriate hernia repair strategy.

Suggested Reading

1. Asakage N. Paradigm shift regarding the transversalis fascia, preperitoneal space, and Retzius' space. Hernia. 2018;22(3):499–506. https://doi.org/10.1007/s10029-018-1746-8.
2. Ansari MM. Transversalis fascia and preperitoneal fascia: a laparoscopic study of live surgical anatomy during TEPP hernioplasty—final report and literature review. Ann Int Med Den Res. 2017;3(6):SG19-SG32.
3. Tadokoro N, Murano S, Nishide T, et al. Preperitoneal fat thickness determined by ultrasonography is correlated with coronary stenosis and lipid disorders in non-obese male subjects. Int J Obes. 2000;24:502–7. https://doi.org/10.1038/sj.ijo.0801187.
4. Hamagawa K, Matsumura Y, Kubo T, et al. Abdominal visceral fat thickness measured by ultrasonography predicts the presence and severity of coronary artery disease. Ultrasound Med Biol. 2010;36(11):1769–75. https://doi.org/10.1016/j.ultrasmedbio.2010.08.004.
5. Rath AM, Attali P, Dumas JL, Goldlust D, Zhang J, Chevrel JP. The abdominal linea alba: an anatomo-radiologic and biomechanical study. Surg Radiol Anat. 1996;18(4):281–8. https://doi.org/10.1007/BF01627606.
6. Beer GM, Schuster A, Seifert B, Manestar M, Mihic-Probst D, Weber SA. The normal width of the linea alba

in nulliparous women. Clin Anat. 2009;22(6):706–11. https://doi.org/10.1002/ca.20836.
7. Cheesborough JE, Dumanian GA. Simultaneous prosthetic mesh abdominal wall reconstruction with abdominoplasty for ventral hernia and severe rectus diastasis repairs. Plast Reconstr Surg. 2015;135(1):268–76. https://doi.org/10.1097/PRS.0000000000000840.
8. Muschaweck U. Umbilical and epigastric hernia repair. Surg Clin North Am. 2003;83(5):1207–21. https://doi.org/10.1016/S0039-6109(03)00119-1.
9. Dabbas N, Adams K, Pearson K, Royle G. Frequency of abdominal wall hernias: is classical teaching out of date? JRSM Short Rep. 2011;2(1):5. Published 2011 Jan 19. https://doi.org/10.1258/shorts.2010.010071.
10. Bedewi MA, El-Sharkawy MS, Al Boukai AA, Al-Nakshabandi N. Prevalence of adult paraumbilical hernia. Assessment by high-resolution sonography: a hospital-based study. Hernia. 2012;16(1):59–62. https://doi.org/10.1007/s10029-011-0863-4.
11. Majumder A. Clinical anatomy and physiology of the abdominal wall. In: Novitsky Y, editor. Hernia Surgery. Cham: Springer; 2016.

7 Normal Anatomy: Ultrasonography

Ashley Wercholuk, Andrus Alian, and Maria S. Altieri

Introduction

The clinical diagnosis of hernias may not always be straightforward and may require additional imaging. Real-time ultrasound can be a potential imaging modality, as it is noninvasive, inexpensive, and readily available. However, it can also be operator dependent, and thus there is variability in terms of sensitivity and specificity. This variability may be mitigated by the use of a standardized method when performing dynamic sonography to aid in the diagnosis of a hernia. In this chapter, we will examine the general approach of ultrasound utilization and review normal anatomy of hernias.

A. Wercholuk
Department of General Surgery, Vidant Medical Center, Greenville, NC, USA
e-mail: wercholuka18@ecu.edu

A. Alian
Department of Emergency Medicine, Stony Brook University Medical Center, Stony Brook, NY, USA
e-mail: andrus.alian@stonybrookmedicine.edu

M. S. Altieri (✉)
Department of Surgery, University of Pennsylvania, Philadelphia, PA, USA
e-mail: altierim19@ecu.edu

General Approach to Using Ultrasound

Ultrasound is a portable, noninvasive, and inexpensive imaging modality that facilitates hernia diagnosis and reduction in real time. The clinician with training in bedside sonography can use ultrasound to streamline the diagnostic work-up of abdominal hernias. While the ability to diagnose an abdominal hernia by ultrasound is greatly influenced by the operator experience, the ability to scan patients in both standing and supine positions as well as during dynamic maneuvers, such as Valsalva, gives ultrasound a clear advantage over other imaging modalities. In select patients, bedside ultrasound has been used in lieu of Computed Tomography (CT) scan to evaluate both inguinal and abdominal wall hernias. In addition, bedside ultrasound has also been used to document hernia reduction in real time.

Ultrasound transducers contain piezoelectric crystals that vibrate when voltage is applied. The crystal vibrations generate sound waves that are then directed at tissue. These waves are emitted as pulses to allow for the same crystals to "listen" for echoes, the reflections of the previously emitted sound waves. These echoes then cause the crystals to vibrate again producing electrical signals that are converted into the images used for clinical interpretation.

Ultrasound wave transmission in the human body is largely dependent on tissue density.

S. Docimo Jr. et al. (eds.), *Fundamentals of Hernia Radiology*,
https://doi.org/10.1007/978-3-031-21336-6_7

Different tissues will vary in their ability to transmit or reflect ultrasound waves. For instance, sound waves travel readily through urine and serous fluid without creating echoes causing them to appear very dark (hypoechoic) on ultrasound images. Dense tissues, such as bone, reflect many of the soundwaves creating echoes that are received by the ultrasound probe and displayed as bright white structures on ultrasound images. Therefore, a sonographer can identify distinct anatomic structures based on the transmission or reflection of ultrasound waves that contact tissues with different densities.

Transducer selection should be based on the location of the area of interest and the patient's body habitus. A high-frequency (≥12 MHz) linear probe may be used to view visualize superficial structures or identify hernias in relatively thin patients. To view deeper structures or identify hernias in obese patients, it might be necessary to use a lower frequency (7–9 MHz) curvilinear probe.

Ultrasound Anatomy: Normal Abdomen

When evaluating the groin with ultrasonography, begin by identifying the inferior epigastric artery. This vessel can be found in the transverse plane behind the rectus abdominis muscle approximately halfway between the umbilicus and pubic symphysis. The inferior epigastric vessels are the primary landmark used to identify Hesselbach's triangle, which is located between the inferior epigastric vessels and the lateral border of the rectus abdominis muscle (Fig. 7.1). Next, visualize the origin on the medial surface of the external iliac artery by tracing the inferior epigastric artery inferiorly and laterally. Once located, the internal inguinal ring can be seen between the medial surface of the internal iliac artery and the lateral side of the inferior epigastric artery (Figs. 7.2 and 7.3). The probe should then be rotated so that it is parallel with the inguinal

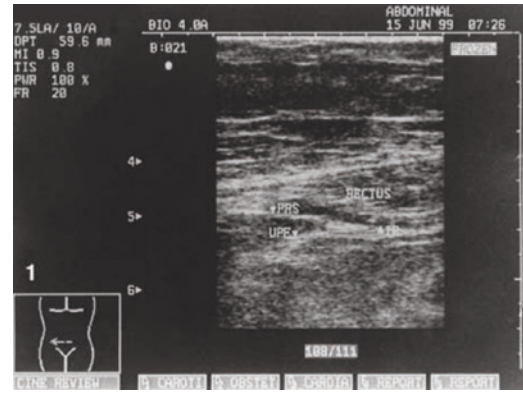

Fig. 7.1 Transverse view of abdominal wall layers and the inferior epigastric vessels (IE) superior to the inguinal canal. PRS posterior rectus sheath; UPF, umbilical prevesicular fascia
With permission from Lilly MC, Arregui ME. Ultrasound of the inguinal floor for evaluation of hernias. Surg Endosc. 2002;16(4):659–662

Fig. 7.2 Transverse view of the right internal ring before Valsalva maneuver. Calipers demonstrate the ring. IE, inferior epigastric vessels
With permission from Lilly MC, Arregui ME. Ultrasound of the inguinal floor for evaluation of hernias. Surg Endosc. 2002;16(4):659–662

ligament, which will appear as a thin hypoechoic band running obliquely from the anterior superior iliac spine to the pubic tubercle. This placement allows for the evaluation of the groin in a long-axis view. To assess the area in a short-axis view, place the probe perpendicular to the inguinal ligament. Placing the probe parallel or perpendicular to the inguinal

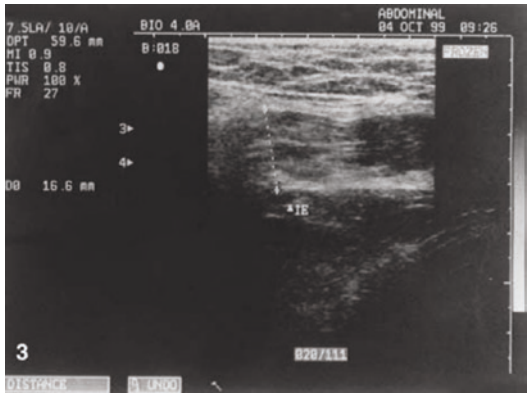

Fig. 7.3 Same internal ring as in Fig. 2, after Valsalva maneuver with large lipoma
With permission from Lilly MC, Arregui ME. Ultrasound of the inguinal floor for evaluation of hernias. Surg Endosc. 2002;16(4):659–662

ligament provides better views compared to scanning longitudinally and transversely.

If the femoral vessels cannot be identified, then the transducer is too lateral and should be moved medially.

Once the cord is identified trace it in a superior lateral orientation so it is in the transverse plane as it travels proximally toward the deep ring. Typically, the spermatic cord has a straight path with no curve to it. At the deep ring, the cord will "disappear" down into the peritoneal cavity, and typically it is lost to view. The canal should be repeatedly panned in the transverse plane from superficial to deep ring, and back again. Straining is not required at this stage. With increasing practice and experience the sonographer will correctly identify any "extra material" in the canal. Dynamic maneuvers can also be used to further assess anatomy (Figs. 7.4 and 7.5).

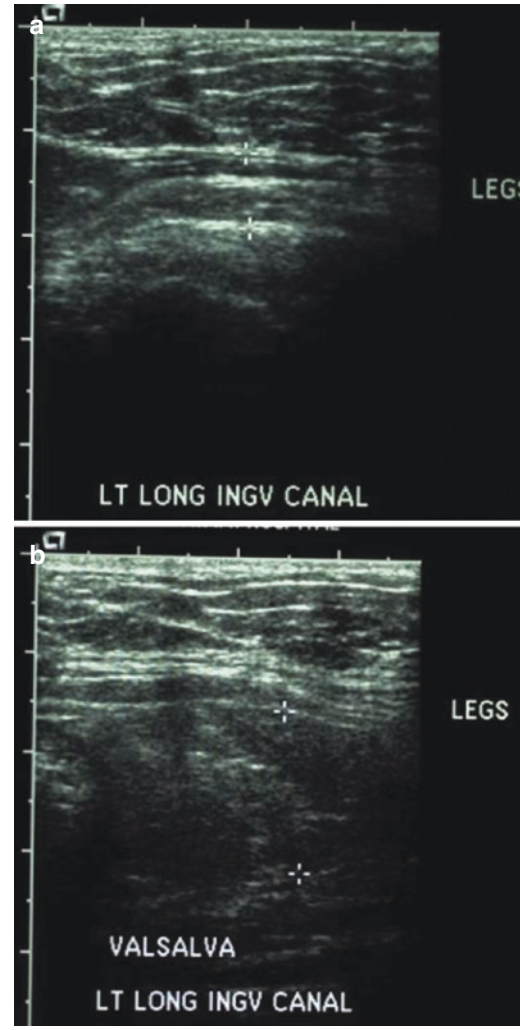

Fig. 7.4 (**a**) Inguinal ultrasound at rest and (**b**) with Valsalva. Note separation of external oblique and floor with Valsalva. With permission from Young J, Gilbert AI, Graham MF. The use of ultrasound in the diagnosis of abdominal wall hernias. Hernia: the journal of hernias and abdominal wall surgery. 2007;11(4):347–351

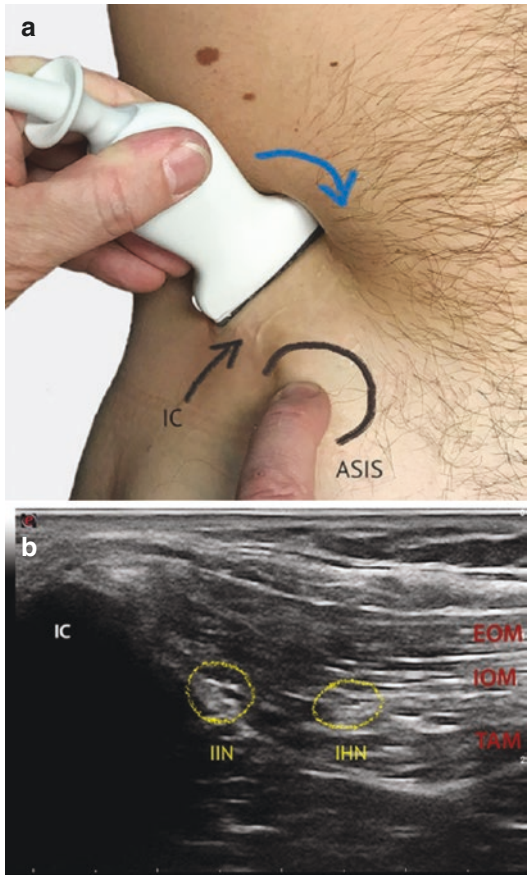

Fig. 7.5 Probe placement for high-resolution ultrasonographic visualization of the iliohypogastric nerve (IHN) and ilioinguinal nerve (IIN). (**a**) The arrow indicates the probe movement. The ASIS (black circle) and iliac crest (IC) as landmarks. (**b**). Ultrasonographic image of IIN and IHN between the internal oblique (IOM) and transversus abdominus (TAM)
With permission from Konschake M, Zwierzina M, Moriggl B, et al. The inguinal region revisited: the surgical point of view: An anatomical–surgical mapping and sonographic approach regarding postoperative chronic groin pain following open hernia repair. Hernia: the journal of hernias and abdominal wall surgery. 2020;24(4):883–894

Ultrasound Anatomy: Indirect Hernia

Indirect inguinal hernias are the most common type of groin hernia and are congenital in nature as they arise from incomplete closure of the processus vaginalis, an outpouching of peritoneum allowing for embryonic testicular descent. A similar process occurs in females, although much less frequently, through the canal of Nuck, an abnormal patent pouch of peritoneum that extends from the round ligament into the labia majora through the inguinal canal. These patent extensions of peritoneum allow intra-abdominal contents to herniate into the inguinal canal through the internal (deep) inguinal ring (Figs. 7.6 and 7.7). The neck of the indirect hernia, which is the portion located within the internal inguinal ring, lies superior and lateral to the inferior epigastric artery. This contrasts with direct inguinal hernias, which lie inferior and medial to the inferior epigastric artery.

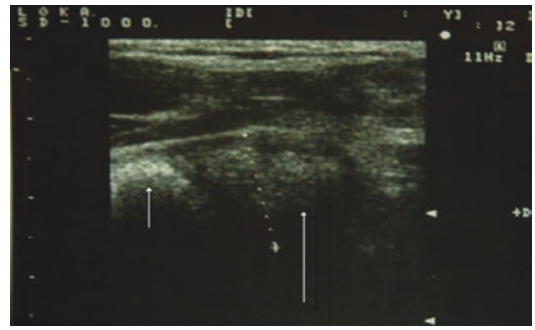

Fig. 7.6 Longitudinal ultrasound image showing an indirect inguinal hernia (white arrow) taken in the resting position. Short white arrow indicates femoral head
With permission from Alam A, Nice C, Uberoi R. The accuracy of ultrasound in the diagnosis of clinically occult groin hernias in adults. Eur Radiol. 2005;15(12):2457–2461

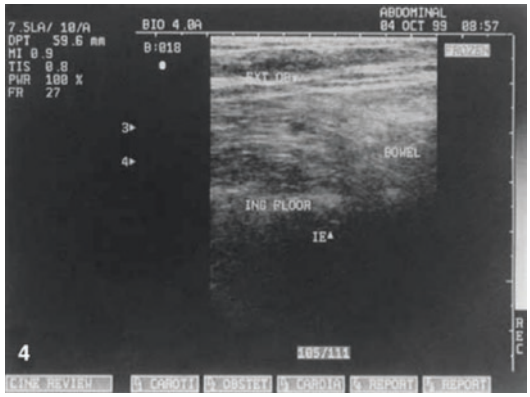

Fig. 7.7 Large left indirect hernia with echogenic bowel entering the inguinal canal
With permission from Lilly MC, Arregui ME. Ultrasound of the inguinal floor for evaluation of hernias. Surg Endosc. 2002;16(4):659–662

Identification of an indirect inguinal hernia using ultrasound begins by locating the origin of the inferior epigastric artery on the medial surface of the external iliac artery. After the vessel has been identified, sweep the ultrasound probe proximally by a few centimeters and the internal inguinal ring should be found lateral to the external iliac vessels. In the short axis, the internal inguinal ring that contains the neck of the indirect hernia is located between the medial surface of the internal iliac artery and the lateral side of the inferior epigastric artery. The probe can then be oriented obliquely along the inguinal canal to look for evidence of herniated contents in the long axis. In this view, indirect hernias can have two distinct appearances, sliding and non-sliding. Sliding hernias have relatively wide necks and loss of the angle between the neck and fundus of the hernia, which makes them more likely to be reducible and contain bowel. In a short-axis view, sliding hernias can be identified at the level of the internal inguinal ring or within the inguinal canal. Non-sliding hernias have relatively narrow necks and possess an approximately 90-degree angle between the neck and fundus. These usually contain only preperitoneal fat and are frequently non-reducible, which makes them much more difficult to diagnose on ultrasound as the fat is almost isoechoic with the other soft tissue and they exhibit little movement with dynamic maneuvers.

Another method to identify indirect inguinal hernias is to locate the spermatic cord within the inguinal canal, which appears as an oval hypoechoic structure in its short axis. Follow the cord proximally until it can be seen crossing over the external iliac vessels and diving down into the deep inguinal ring. The hernia contents can be found anterior and lateral to the spermatic cord in males or the round ligament in females. Identifying this relationship can be helpful in distinguishing indirect from direct inguinal hernias in situations where it is difficult to visualize the position of the hernia neck in relation to the inferior epigastric vessels. Indirect hernias tend to lie anterior and lateral to the spermatic cord. Direct hernias tend to lie posterior and medial to the spermatic cord.

Ultrasound Anatomy: Direct Hernia

Direct inguinal hernias are the second most common type of groin hernia. Unlike indirect inguinal hernias, they are considered to be "acquired" as they occur as a result of abdominal wall weakening and chronically increased intra-abdominal pressure. Direct inguinal hernias enter the inguinal canal directly through a weakened portion of the canal's posterior wall called Hesselbach's triangle. Hasselbach's triangle is delimited by the inferior epigastric arteries laterally, the lateral border of the rectus abdominis muscle medially, and the inguinal ligament inferiorly (Fig. 7.8). The transversalis fascia in this triangle lacks any type of reinforcement which makes the area prone to weakness. The neck of direct inguinal hernias is usually wide, which makes them less prone to incarceration and strangulation.

To identify a direct inguinal hernia using ultrasound, begin by identifying Hesselbach's triangle at the level of the inferior epigastric artery origin. Hesselbach's triangle will appear as a fat-filled region between the inferior epigastric ves-

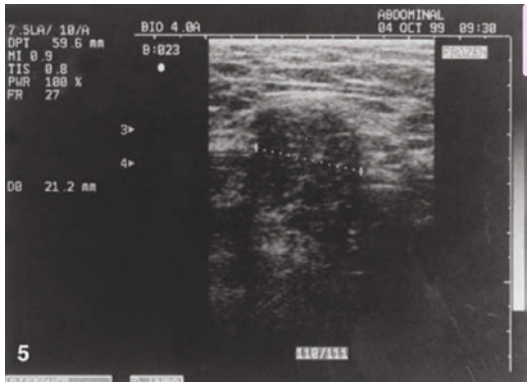

Fig. 7.8 Calipers demonstrate margins of a direct hernia With permission from Lilly MC, Arregui ME. Ultrasound of the inguinal floor for evaluation of hernias. Surg Endosc. 2002;16(4):659–662

sels and the rectus abdominis muscle. Key landmarks to identify this type of hernia include the spermatic cord (in males) and the inferior epigastric artery. Direct inguinal hernias are located inferior and medial to the inferior epigastric artery whereas indirect inguinal hernias lie superior and lateral to the inferior epigastric artery. A direct inguinal hernia will often appear as an anterior protrusion of fatty tissue or bowel within Hasselbach's triangle. Larger direct inguinal hernias may extend inferiorly and medially within the inguinal canal causing compression of the canal contents including the spermatic cord in males, which is echogenic and often found displaced laterally on ultrasound. A significant portion of small direct inguinal hernias will spontaneously reduce in the supine position. Therefore, it is essential to perform ultrasound examination in both standing and supine positions and to utilize dynamic maneuvers, such as Valsalva and compression.

Ultrasound Anatomy: Femoral Hernia

Femoral hernias occur when abdominal contents protrude through the femoral ring into the femoral canal and present as a mass below the inguinal ligament. The femoral canal is housed within the femoral sheath along with the femoral vessels and is located medial to the femoral vein and superior to the saphenofemoral junction. It is bounded by the iliopubic tract superiorly, Cooper's ligament inferiorly, the femoral vein laterally, and the lacunar ligament medially. Most femoral hernias are located medial to the femoral vein. However, some can appear to be located anteriorly after the hernia contents have extended from the medial surface. Femoral hernias that truly arise anteriorly are rare. Femoral hernias account for 3% of all groin hernias and are more common in women, having a female-to-male ratio of 10:1. It is believed that the elevated intra-abdominal pressure and hormone-induced tissue softening experienced during pregnancy leads to the increased incidence in females. Similar to spigelian hernias, femoral hernias usually have narrow necks and wider fundi leading to an increased incidence of strangulation (22% risk over 3 months and 45% risk over 21 months). Femoral hernias can be difficult to diagnose clinically and distinguishing them from an inguinal hernia with physical examination is not always straightforward. Ultrasound has been shown to be highly accurate in distinguishing femoral hernias from inguinal hernias when performed by experienced technicians.

Examination for femoral hernias should begin by aligning the probe in the long axis of the inguinal ligament near the pubic tubercle. Move the probe slightly lateral and caudal to the inguinal ligament to visualize the femoral artery and vein as they pass underneath the ligament and superficial to the pubic ramus. Identify the femoral ring, which is bounded by the inguinal ligament anterosuperiorly, Cooper's ligament posteriorly, and the femoral vein laterally. Be aware that in some cases the femoral vein can be compressed due to direct compression from the hernia contents. It should also be noted that small femoral hernias can reduce completely in the supine position. Therefore, an ultrasound examination should be performed in both supine and upright positions as well as during Valsalva maneuvers to increase the chances of identification.

For specific details on the method for evaluation of the inguinal canal, please see "Evaluation of hernia of the male inguinal canal: sonographic method."

Ultrasound Anatomy: Ventral Hernia

The anterior abdominal wall is comprised of several layers: skin; adipose tissue; myofascial plane, which consists of muscles such as the rectus abdominis, external and internal obliques, and transversus abdominis; transversalis fascia, preperitoneal fat and the parietal peritoneum. Figures 7.9 and 7.10 show normal anterior abdominal wall anatomy.

Umbilical Hernias

Umbilical hernias are the result of a widening umbilical ring and can occur at any age. During infancy, umbilical hernias are caused by failure of the umbilical ring to close. These hernias are typically small and will usually close spontaneously by age 2. Those that persist after age 5 are usually repaired surgically. During adulthood, umbilical hernias develop due to widening of the umbilical ring from connective tissue weakness and/or chronic increased intra-abdominal pressure. The clinical diagnosis of an umbilical hernia is usually more straightforward than that for groin hernias. However, ultrasound remains a valuable diagnostic tool in certain circumstances such as morbidly obese patients with umbilical pain whose body habitus impedes hernia detection through palpation. It should be noted that in obese patients, the location of the umbilical ring is often much more superior than expected as the umbilicus in these patients migrates inferiorly with weight gain. Sonographic evaluation of umbilical hernias is done in a manner similar to what is done for epigastric hernias. The use of dynamic maneuvers should be included in the evaluation as well. Figure 7.11 is an example of an umbilical hernia with fat protruding through the fascia (circle).

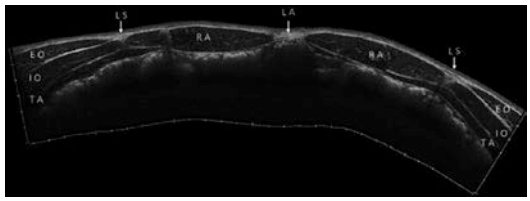

Fig. 7.9 Normal anterior abdominal wall anatomy
Ultrasound panoramic image of the anterior abdominal wall. *RA* Rectus abdominis, *EO* External oblique, *IO* Internal oblique, *TA* Transversus abdominis, *LA* Linea alba, *LS* Semilunar line
With permission from J Ultrasound. 2020 Sep; 23(3): 265–278

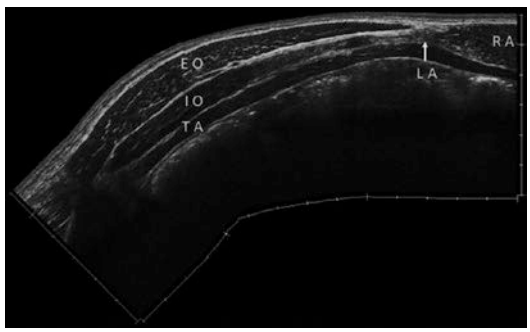

Fig. 7.10 Normal lateral abdominal wall anatomy. The external oblique (EO), internal oblique (IO), and transversus abdominis (TA) muscles extend from the lateral edge of the rectus to the flanks with three overlapping layers

Epigastric and Hypogastric Hernias

Epigastric and hypogastric hernias are anterior abdominal wall hernias that occur through the

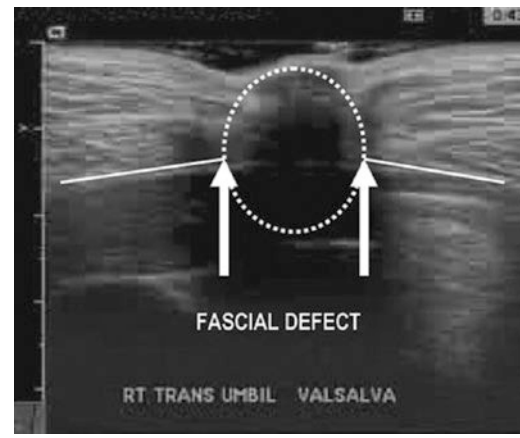

Fig. 7.11 Umbilical hernia. Note far (within circle) protruding through the defect in the fascia
With permission from Young, J., et al. "The Use of Ultrasound in the Diagnosis of Abdominal Wall Hernias." Hernia: The Journal of Hernias and Abdominal Wall Surgery, vol. 11, no. 4, 2007, pp. 347–351. https://doi.org/10.1007/s10029-007-0227-2

linea alba. Epigastric hernias occur superior to the umbilicus and are much more common than hypogastric hernias, which occur below the umbilicus. This is because the linea alba is longer and wider above the umbilicus. As with most other hernias, prolonged increased intra-abdominal pressure contributes to the weakening of the linea alba and development of an epigastric or hypogastric hernia. In most individuals, the linea alba consists of three layers of interwoven fibers from the anterior and posterior sheaths of the rectus muscles. However, some individuals may only have a single layer of interwoven fibers which makes them predisposed to developing diastasis recti or an epigastric hernia. Diastasis recti typically presents as an anterior bulge that extends from the xiphoid process to the umbilicus. This contrasts with epigastric hernias, which will usually present as a more localized midline bulge. Both epigastric and hypogastric hernias tend to be small, contain preperitoneal fat, and have narrow necks, which make them more prone to strangulation. Epigastric and hypogastric hernias that are located very near the umbilicus are sometimes referred to as "paraumbilical" or "periumbilical" hernias. These hernias have a particularly high risk of becoming strangulated.

Epigastric hernias can be best evaluated using a 10–12 MHz linear transducer probe as they are usually quite superficial. Small epigastric hernias and those present in relatively thin patients can be missed if a low-frequency probe is used and focused too deep. The linea alba is identified and appears as a thick, well-defined hyperechoic structure. Most defects within the linea alba occur at the midline and appear hypoechoic or isoechoic compared to the intact linea alba. The entire length of the linea alba should be assessed using the ultrasound as patients with a known epigastric hernia or diastasis recti are at an increased risk for having multiple hernias.

Incisional Hernias

Incisional hernias can occur anywhere on the anterior abdominal wall where an incision has been made. This includes areas where hernias cannot naturally occur, such as through muscles and bellies. Even small surgical scars, like those used for placement of laparoscopy ports, can lead to an incisional hernia. The scar produced by the incision can be stretched or torn, which creates the opportunity for a hernia to develop. Hernias created from stretching of the scar are more likely to possess wide necks and thus be more reducible compared to those made from tearing of the scar. These hernias may be too small for clinical detection, but can be identified using ultrasound evaluation focused on the site of a previous incision. Figure 7.12 represents an incisional hernia with bowel loops protruding through the abdominal wall.

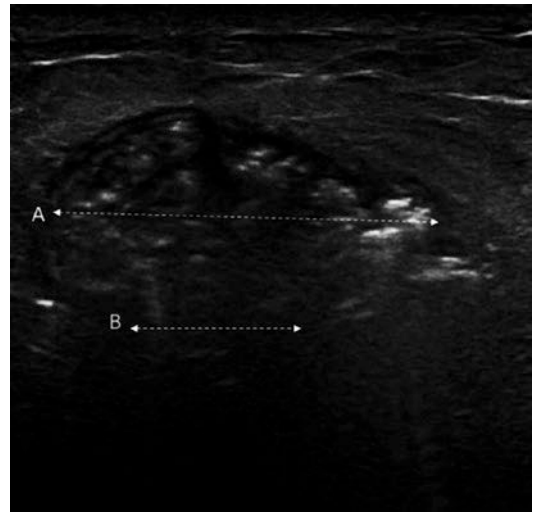

Fig. 7.12 Incisional hernia. Ultrasonography shows bowel loops (A: caliper) through a defect (B: caliper) of the abdominal wall
With permission from J Ultrasound. 2020 Sep; 23(3): 265–278

Ultrasound Anatomy: Obturator Hernia

Obturator hernias are rare hernias that occur within the obturator canal, which is formed by the ischium and pubic bone. The obturator membrane covers the canal and over time becomes weakened leading to enlargement of the canal and the development of a hernia sac. Bowel within the hernia can become incarcerated and

cause compression of the obturator nerve, which can present as anteromedial thigh pain (Howship-Romberg sign). Patients with obturator hernias are usually elderly and frequently present with complete or partial bowel obstructions. Delayed recognition has been related to high morbidity and mortality. These hernias are usually diagnosed using CT scan, which has made it easier to visualize an incarcerated obturator hernia in the pelvis. However, it has been shown that they can also be identified and reduced using ultrasound.

To identify an obturator hernia, place a high-frequency linear transducer in the transverse plane on the medial aspect of the upper thigh caudal to the inguinal ligament to identify the common femoral vessels. Once the vessels have been identified, move the probe medially to locate the pectineus muscle. This muscle courses lateral and caudal from the medial surface of the superior pubic ramus, which can be easily visualized in the sagittal plane. The pectineus muscle is often atrophied in elderly patients making it difficult to identify on ultrasound. The superior pubic ramus, which forms the superior border of the obturator foramen, can serve as a more reliable landmark. An incarcerated hernia can be seen dorsal to the pectineus muscle and caudal to the superior pubic ramus. If identified, reduction can be attempted with graded compression using the ultrasound probe.

Ultrasound Anatomy: Spigelian Hernia

Spigelian hernias occur secondary to a defect in the spigelian fascia, which consists of the internal oblique and transversus abdominis aponeuroses and is bordered by the rectus muscle medially and semilunar line laterally. These hernias can occur at any point along the spigelian fascia but are almost always found at or below the arcuate line where the posterior rectus sheath is absent, and the inferior epigastric vessels pierce the spigelian fascia causing an area of weakness. The internal oblique and transversalis muscle fascia begin to separate into two layers at the level of the arcuate line, which also contributes to the weakness of this area. Spigelian hernias are generally small, measuring 1–2 cm in diameter, anvil/mushroom-shaped with narrow necks and broad fundi. This shape is caused by the configuration of fascial defects that are typically seen with spigelian hernias. The fascia of the transverse abdominis muscle is always torn while the fascia of the external oblique muscle remains intact. The internal oblique fascia is usually torn as well. The intact external oblique fascia causes the herniated contents to extend over the rectus muscle medially or the external oblique laterally. The hernia sac may contain omentum, small bowel, or colon.

Patients typically present with localized pain overlying the hernia which can be accompanied by an intermittently palpable bulge. However, clinical diagnosis of a spigelian hernia is difficult as a mass is not usually felt given that the hernia is present beneath the intact external oblique fascia. Therefore, ultrasound used in combination with clinical examination may aid in diagnosis. To facilitate identification of a spigelian hernia, place the ultrasound probe on the lower one-third of the rectus muscle and identify the inferior epigastric vessels coursing vertically underneath the rectus. Trace the inferior epigastric vessels in their short axis proximally until they pierce the spigelian fascia at the level of the arcuate line. From here, the probe should be moved laterally in the transverse plane to view the aponeuroses of the external oblique, internal obliques, and transversus abdominis. The spigelian fascia can be found between the lateral margin of the rectus and the semilunaris line, which is at the level of the myotendinous junction of the transversus abdominis. The spigelian fascia at the level of the arcuate line should then be thoroughly examined for the presence of a defect. If the suspected hernia is not seen, the entire spigelian fascia should be inspected during the Valsalva maneuver to assist in detection. Compression maneuvers with the ultrasound probe may be performed to evaluate hernia reducibility. If a spigelian hernia is identified, surgical repair is recommended as the presence of a narrow neck predisposes these hernias to incarceration (17–24% of cases).

Conclusion

Real-time dynamic ultrasound has proven to be an invaluable tool in the diagnosis and characterization of groin and abdominal wall hernias. The ability to scan the patient in both supine and upright positions, as well as the use of dynamic maneuvers (Valsalva and compression) give ultrasound the advantage over other popular imaging modalities such as CT and MRI. When a hernia is identified using dynamic ultrasound, the operator should note the type and size of the hernia, its contents, and the ability to reduce the hernia. Furthermore, the sonographic evaluation should be extended to identify any additional hernias as patients with one hernia frequently have multiple hernias. Beyond initial diagnosis, dynamic ultrasound has shown to be useful in the postoperative period when assessing mesh position and hernia recurrences.

Bibliography

1. Alam A, Nice C, Uberoi R. The accuracy of ultrasound in the diagnosis of clinically occult groin hernias in adults. Eur Radiol. 2005;15(12):2457–61.
2. Depasquale R, Lander C, Doyle G. Audit of ultrasound and decision to operate in groin pain of unknown aetiology with ultrasound technique explained. Clinical Radiol. 2008;64(6):608–14.
3. Kwee RM, Kwee TC. Ultrasonography in diagnosing clinically occult groin hernia: systematic review and meta-analysis. Eur Radiol. 2018;28(11):4550–60.
4. Loftus IM, Ubhi SS, Rodgers PM, Watkin DF. A negative herniogram does not exclude the presence of a hernia. Ann R Coll Surg Engl. 1997;79(5):372–5.
5. Niebuhr H, et al. Dynamic inguinal ultrasound (DIUS) in diagnosing groin hernias: technique, examples and results. Int J Abdominal Wall Hernia Surg. 2021;4(2):70–5.
6. Picasso R, et al. High-resolution ultrasound of spigelian and groin hernias: a closer look at fascial architecture and aponeurotic passageways. J Ultrason. 2021;21(84):53–e62.
7. Stavros AT, Rapp C. Dynamic ultrasound of hernias of the groin and anterior abdominal wall. Ultrasound Quart. 2010;26(3):135–69.
8. Townsend CM, et al. Sabiston textbook of surgery: the biological basis of modern surgical practice. Elsevier Saunders; 2017.
9. Young J, Gilbert AI, Graham MF. The use of ultrasound in the diagnosis of abdominal wall hernias. Hernia. 2007;11(4):347–51.
10. Lo CY, Lorentz TG, Lau PW. Obturator hernia presenting as small bowel obstruction. Am J Surg. 1994;167:396–8.
11. Ogata M. Incarcerated obturator hernia: pitfalls in the application of ultrasound. Crit Ultrasound J. 2009;1:59–63.
12. Jansen CJ, Yielder PC. Evaluation of hernia of the male inguinal canal: sonographic method. J of Med Radiat Sci. 2018;65(2):163–8.
13. Lilly MC, Arregui ME. Ultrasound of the inguinal floor for evaluation of hernias. Surg Endosc. 2002;16(4):659–62.
14. Konschake M, Zwierzina M, Moriggl B, et al. The inguinal region revisited: the surgical point of view: an anatomical–surgical mapping and sonographic approach regarding postoperative chronic groin pain following open hernia repair. Hernia. 2020;24(4):883–94.
15. Draghi F, Cocco G, Richelmi FM, Schiavone C. Abdominal wall sonography: a pictorial review. J Ultrasound. 2020;23(3):265–78.

8 Normal Anatomy: Magnetic Resonance Imaging

James H. Birkholz

Why MR Imaging?

While CT and ultrasound remain the mainstays of initial abdominal wall imaging [1, 2], MR has limited, but specific applications. With CT, the patient is interposed between an X-ray tube and several detectors on the opposing side of the tube. When imaging commences, the ionizing X-ray beam energy penetrates the patient, impacts the digital detectors on the opposite side, and the resultant data is then processed into images. Tissue characterization via CT is generally limited to the measurement of density in the form of Hounsfield units (HU). With this method, a specific volume of the image data is selected and the tissue density can be calculated based on X-ray beam penetrance. Lower density regions such as air and fat will have low HU values, while denser structures such as bone and contrast will demonstrate significantly higher HU values. With the assistance of iodinated intravenous contrast, multiphasic (unenhanced, enhanced, delayed phase) CT can also be performed, allowing for additional structural characterization. While CT offers excellent spatial resolution and some tissue characterization, it is dependent upon physical density and X-ray beam attenuation [3]. In contrast, MR imaging relies upon the native proton density and alignment within tissues to create images [4]. Differing structures have varied proton density and orientation. While water and fat are both proton dense, the arrangement and ratio of the protons differ between the two. Different tissues react differently during MR image acquisition and therefore yield a more diverse tissue palette when compared with CT and ultrasound. Therefore, MR allows for a more nuanced delineation of tissue types, an asset upon which specific MR exam types (or "protocols") capitalize in various ways. While muscle may appear "hypointense" or dark, fluid will appear "hyperintense" or bright depending on the sequence (Fig. 8.1).

Some MR imaging protocols seek to maximize conspicuity of water-containing structures, intra- or extra-cellular fat [5] (Figs. 8.2 and 8.3).

Other sequences actively utilize post-processing computing for the specific removal of certain tissue signals from the final image, and still others optimize the visualization of iron, as can be seen in the setting of hemochromatosis (Figs. 8.4, 8.5, 8.6, 8.7, and 8.8).

Collectively, the myriad imaging options allow for greater lesional and tissue characterization when compared with alternate modalities. During imaging of the abdominal wall, this allows for the differentiation of hemorrhage from simple fluid, lesions from muscular derangements, and more [6–10]. An example of this unique ability of MR can be appreciated in Figs. 8.9, 8.10 and 8.11, which demonstrate the presence of an endometriosis implant within the anterior abdominal wall.

J. H. Birkholz (✉)
Department of Radiology, Penn State Milton S. Hershey Medical Center, Hershey, PA, USA
e-mail: jbirkholz@pennstatehealth.psu.edu

S. Docimo Jr. et al. (eds.), *Fundamentals of Hernia Radiology*,
https://doi.org/10.1007/978-3-031-21336-6_8

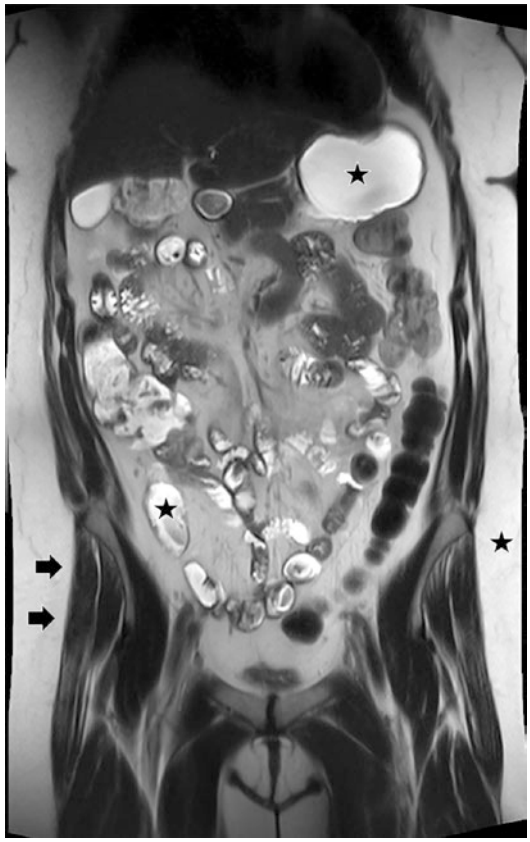

Fig. 8.1 T2-weighted coronal survey view of the abdomen. Note the hyperintense (bright) signal of subcutaneous fat as well as that of fluid within the stomach and bowel (stars). Abdominal wall and lower extremity musculature are relatively hypointense (dark, arrows)

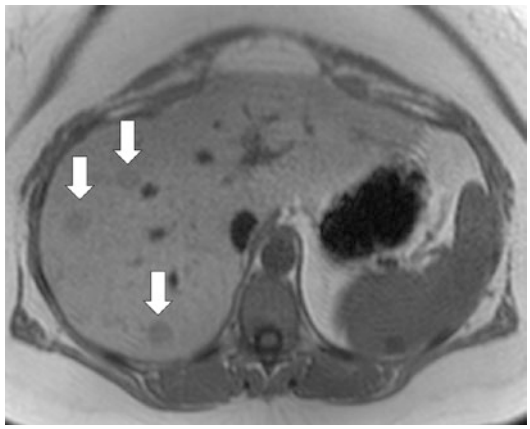

Fig. 8.2 T1-weighted in-phase axial image through the liver demonstrating indeterminate low-signal masses (arrows). In/out-of-phase imaging relies on different resonant frequencies between water and fat in the same voxels

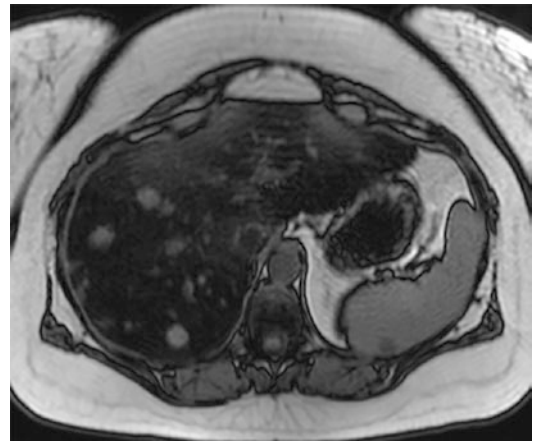

Fig. 8.3 T1-weighted out-of-phase axial image through the liver demonstrating diffuse signal loss compatible with hepatic steatosis. In the presence of microscopic fat, the fat and water signals cancel one another out, yielding hypointense signal

Fig. 8.4 Axial CT image through the level of the liver is unremarkable in this patient

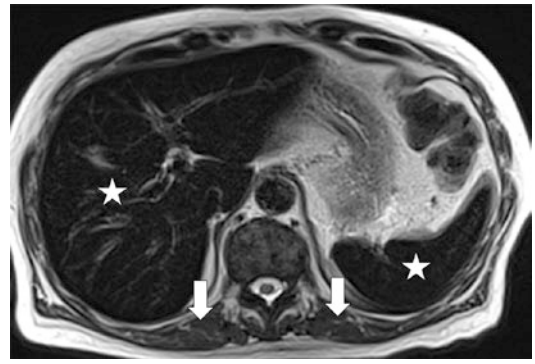

Fig. 8.5 Axial T2 image through the level of the liver demonstrates a markedly low hepatosplenic signal (stars) when compared to the musculature (arrows)

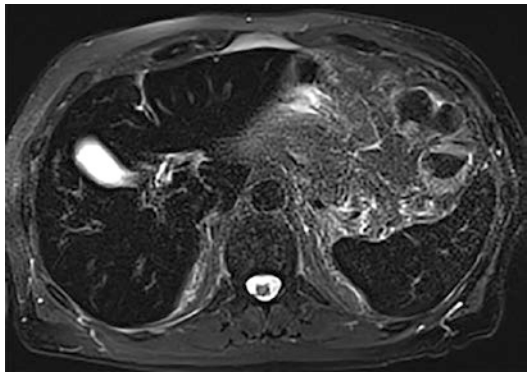

Fig. 8.6 Axial T2 fat-suppressed image through the level of the liver demonstrates the same findings as Fig. 8.5 with the additional benefit of suppression of the fat signal, providing extra information

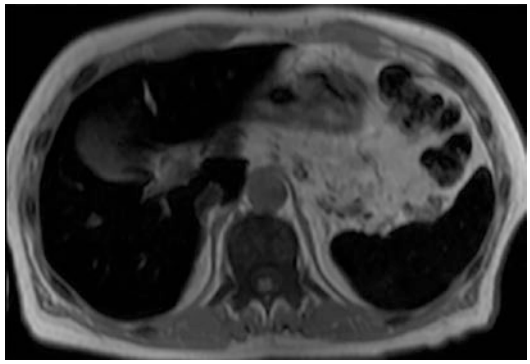

Fig. 8.7 Axial T1-weighted in-phase imaging through the liver demonstrates low hepatosplenic signal

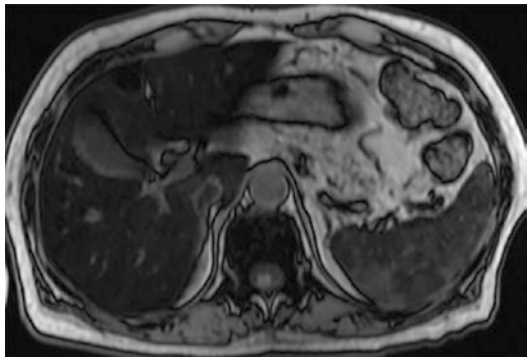

Fig. 8.8 Axial T1-weighted out-of-phase imaging through the liver demonstrates relatively increased signal of the liver and spleen relative to the in-phase imaging in Fig. 8.7

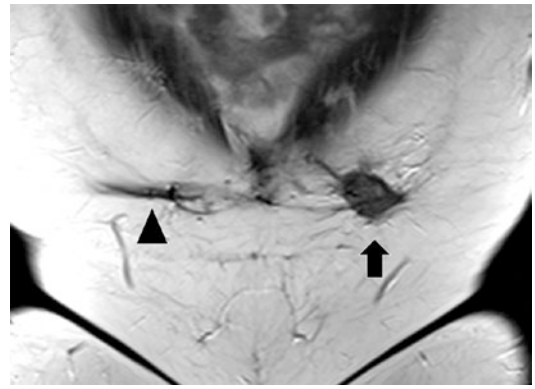

Fig. 8.9 Coronal T2 image of the ventral abdominal wall demonstrates a low-signal focus in the left lower quadrant (arrow) in this patient with a history of prior cesarean section and intermittent abdominal pain. The low-signal transverse postoperative scar can be seen in the right lower quadrant (arrowhead)

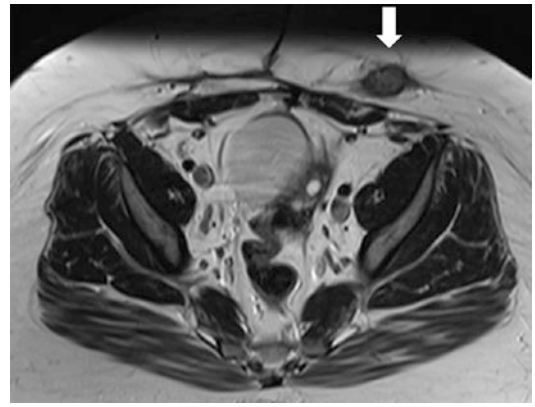

Fig. 8.10 T1-weighted axial image through the same region demonstrates an indeterminate, intermediate signal lesion (arrow) within the subcutaneous operative scar

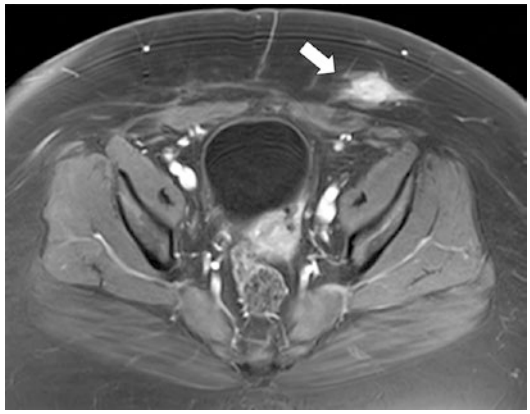

Fig. 8.11 Gadolinium-enhanced T1-weighted, fat-suppressed axial image through the lesion (arrow) demonstrates enhancement. Collectively, the findings are compatible with endometriosis deposition within the operative incision site in the abdominal wall

How Are MR Images Obtained?

While a comprehensive understanding of MR physics is beyond the scope of this chapter, some basic ideas will be explored. With MR, no ionizing radiation is utilized. Therefore, MR serves as a viable alternate modality when ionizing radiation-based imaging (conventional radiography, CT) is clinically undesirable, as may be the case during pregnancy, childhood, or in patients for whom prolonged imaging surveillance is anticipated. With MR, the patient is placed in a large, cylindrical magnetic bore which bidirectionally aligns all of the protons within the patient's tissues. That is to say, the protons do not all align in one common direction, but align along one axis in parallel and anti-parallel directions [4]. The magnet is always on with rare exception for maintenance or emergency (*e.g.,* quenching). In general, unlike CT, each image is formed individually. During each image acquisition, radiofrequency (RF) signals are transmitted from the machine into the patient (transmitter bandwidth), disrupting the protons out of their temporary alignment. The precise frequency necessary to optimally engage the protons can be predicted via the Larmor equation, expressed as $\omega_0=\gamma B_0$, in which ω_0 is the precession frequency (how a proton "spins"), B_0 is the magnetic field strength in Tesla, and γ is the gyromagnetic ratio [4]. As the protons then relax back to their native state, the energy they emit in doing so is detected by the machine (receiver bandwidth) [11]. These signals fill in the "k-space," or raw data matrix. Each point in the k-space has a specific phase (spatial location) and signal intensity (brightness) [5, 12]. Typically, via Fourier transform, the data is then processed into discrete, viewable images. Therefore, with MR, each image "slice" on a workstation represents the result of serially acquired data and the whole target volume then reflects multiple image "slabs" or slices obtained one section at a time. These may be acquired in virtually any pre-planned plane, typically utilizing axial, coronal, and sagittal planes.

A basic understanding of MR also includes recognition of the difference between "T1" and "T2" weighted imaging. The time from when a radio pulse enters the patient and returns to the receiver is called "time to echo" or TE. The time between pulses is referred to as "time to repeat" or TR. Rapid sequences utilizing short TE and TR are referred to as "T1" weighted, as they chiefly capitalize upon the time during which protons return to their baseline alignment in the magnetic field. Sequences utilizing longer TE and TR are referred to as "T2" weighted, and address the time during which protons either equilibrate or go out of phase with one another. For those not formally trained in image production or interpretation, an easy way to remember T1 and T2 sequences is that the former will display water and fat as dark and bright, respectively, and the latter will display both water and fat as bright, or hyperintense (Figs. 8.12 and 8.13).

Other sequences use varying TE and TR to create more complex tissue assessment, such as T2*, gradient sequences, or fluid attenuation inversions recovery (FLAIR).

"Resolution" is the ability to distinguish one structure from another [3, 11]. While CT offers excellent spatial resolution, MR resolution can be tailored to the situation. Decreasing the size of pixels in a generated image will require longer scanning time, but will produce a final image with better resolution, as can be appreciated in Fig. 8.14, which clearly illustrates the extent of disease due to a T4 rectal carcinoma.

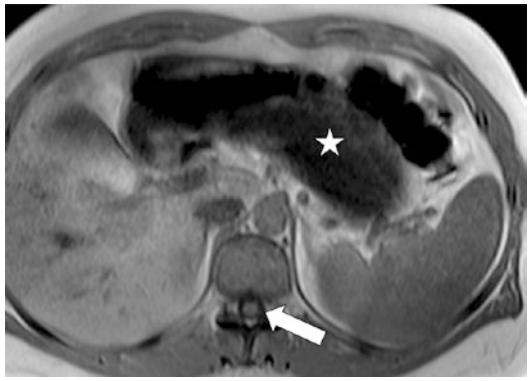

Fig. 8.12 Axial T1 image through the abdomen. Note the hypointense (dark) signal within the cerebrospinal fluid (arrowhead) and gastric contents (star)

Fig. 8.13 Axial T2 image through the abdomen. Note the hyperintense (bright) signal within subcutaneous fat (stars) and within fluid-containing structures such as cerebrospinal fluid and the urinary collecting system (arrows)

In contrast, increasing pixel size will decrease imaging time but result in relative image degradation. In addition, when the number of excitations or instances in which the tissue is sampled by the machine ("NEX") is increased, this results in a higher signal image at the expense of longer scanning time. Therefore, when selecting the means by which MR images are obtained, operators must balance the competing aspects of spatial resolution, scanning time, and reduction of possible motion artifact [13]. MR examinations inherently require more exam time and attention to preexamination planning, the latter of which is frequently referred to as a "protocol." While specific MR protocols may target the presence of water or fat in tissue, others may be designed to

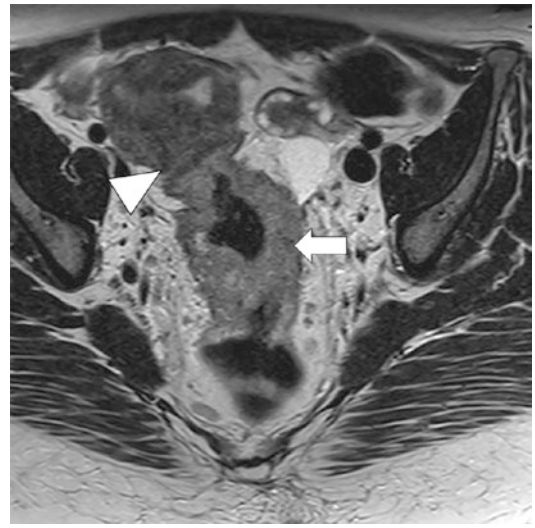

Fig. 8.14 High-resolution, T2-weighted axial image through the pelvis for the purpose of rectal carcinoma staging. The higher resolution allows for precise delineation of disease extent, in this case a T4 rectal carcinoma (arrow) with involvement of the adjacent uterus (arrowhead)

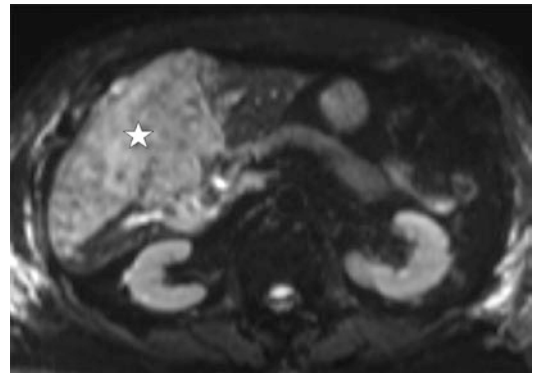

Fig. 8.15 Axial diffusion weighted imaging (DWI) through the level of the liver demonstrating hyperintense (bright) territory within the liver (star)

evaluate for the movement of protons in tissue (diffusion-weighted imaging) as a reflection of underlying Brownian motion, which can help identify highly cellular or edematous tissue [14] (Figs. 8.15 and 8.16).

MR protocol "sequences" utilize specific radio frequencies and patterns to evaluate differing tissue types and to answer various clinical questions. While CT allows for significant image post-processing, the targeted nature of MR image acquisition is less forgiving. As below, some

sequences necessitate specific protocols at the time of imaging, while others allow for post-imaging processing, such as the removal or "saturation" of fat from some images after they are formed (Fig. 8.17).

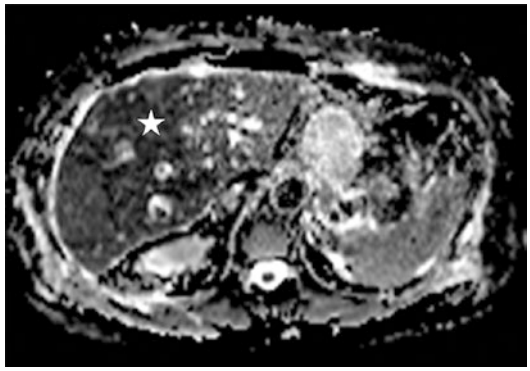

Fig. 8.16 The apparent diffusion coefficient map (ADC) demonstrates a corresponding region of hypointense (dark) signal in the same territory (star) as seen in Fig. 8.15, compatible with restricted diffusion, worrisome for infarction

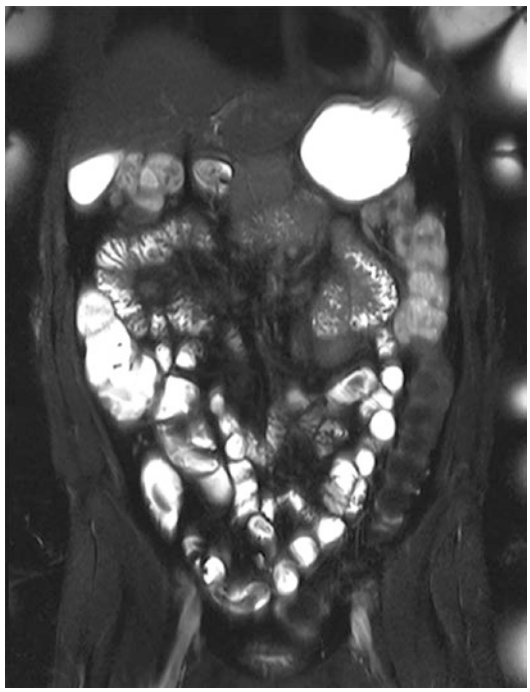

Fig. 8.17 Coronal T2 fat-suppressed image through the abdomen. Note the low signal throughout the intra- and extra-abdominal fat as a result of suppression of the fat signal. This allows for the characterization of fat versus fluid

MR Sequences and Protocols

Given the innumerable clinical indications for MR imaging, there is an expected plethora of protocols available [5]. These vary according to equipment manufacturer, magnet strength, national imaging guidelines, and even local or individual operator preferences. In general, protocols for the evaluation of the abdomen or abdominal wall typically include some common basic sequences. Studies will include several "scout" or limited T1-based orientation images, which assist technologists in the selection of appropriate imaging planes. Following these rapid non-diagnostic images, abdominal imaging exams include a coronal T2 weighted survey view of the abdomen, extending from the lung bases to the pelvis. The coronal images provide a "bird's eye view" of the abdomen and can be useful in the identification of muscular interruption and characterization of hernia contents. These are then followed by axial T1 weighted images, typically "in-phase" and "out of phase," as well as T2 and fat-suppressed T2 axial images. These sequences allow for the assessment of fluid, blood, or fatty processes within hernias. In addition to these baseline images, higher resolution images may be obtained depending on the specific exam protocol, such as targeted examination of the inguinal region (Figs. 8.18 and 8.19).

Fig. 8.18 Axial T2-weighted image through the pelvis indicates the presence of a fat-containing left inguinal hernia (arrow)

Fig. 8.19 Sagittal T2-weighted image through the pelvis indicates the presence of a fat-containing left inguinal hernia (arrow)

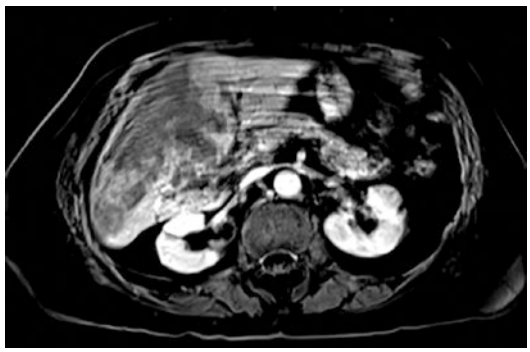

Fig. 8.20 Gadolinium-enhanced, fat-suppressed T1-weighted image through the same liver is shown in Figs. 8.15/8.16. The large region of low (dark) signal within the liver corresponds with the region of restricted diffusion on prior images and is compatible with infarct. Note the diffusely low signal of fatty structures as a result of the fat-suppression technique

Post-enhancement, T1-weighted axial images may then be obtained to evaluate for inflammatory changes, vascular patency, or neural involvement (Fig. 8.20).

These are commonly followed by "subtraction" images, in which a baseline T1 image is subtracted from the enhanced T1 image, leaving only the data that reflects enhancing regions in the field of view. Depending on the specific clinical question, additional sequences may be obtained, bearing in mind that these will prolong exam time. Below are several images reflective of the various common MR sequences one may encounter during assessment of the abdominal wall (Figs. 8.21, 8.22, 8.23, 8.24, 8.25, and 8.26).

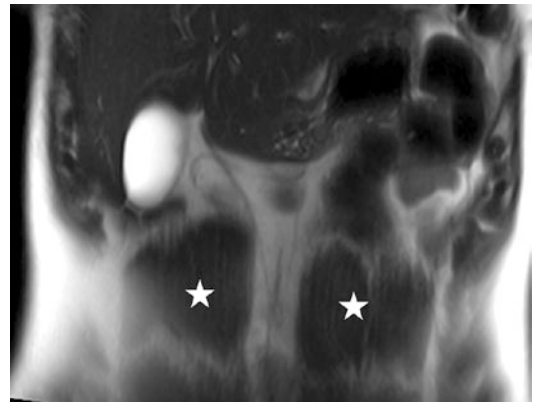

Fig. 8.21 Coronal T2-weighted image through the ventral abdominal wall illustrates the rectus abdominis musculature (stars)

Fig. 8.22 Sagittal T2-weighted image through the ventral abdominal wall illustrates the rectus abdominis musculature (arrow)

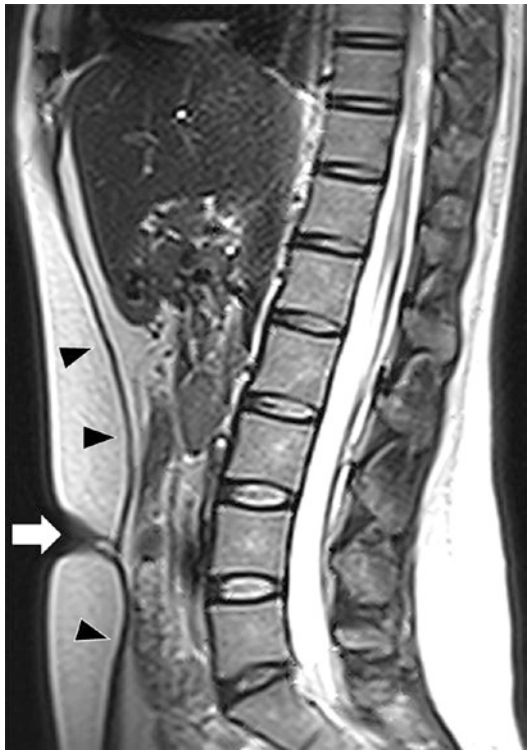

Fig. 8.23 Sagittal T2 image at the midline clearly delineates a normal umbilicus (arrow) and linea alba (arrowheads)

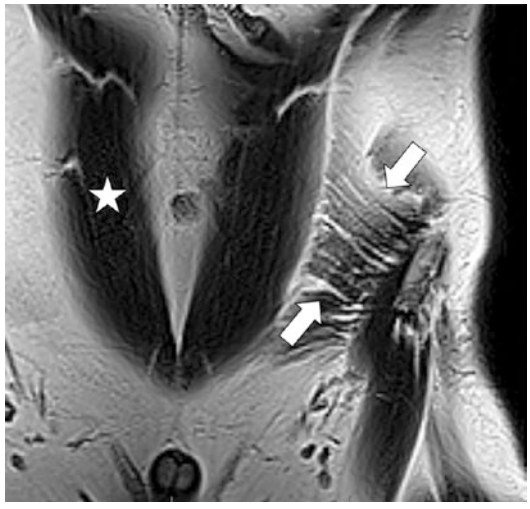

Fig. 8.24 Coronal T2-weighted image through the ventral abdominal wall demonstrates the internal oblique (arrows) and rectus abdominis musculature (star)

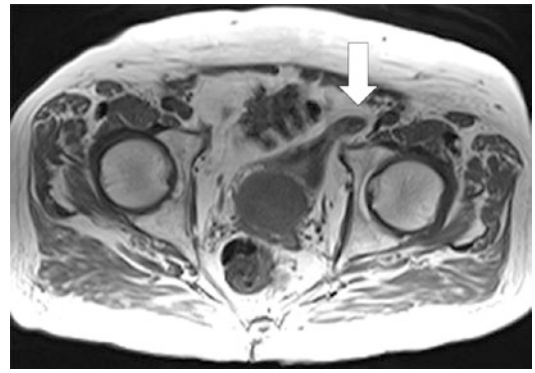

Fig. 8.25 Axial T2-weighted image through the pelvis demonstrates herniation of the urinary bladder into the left inguinal canal (arrow)

Fig. 8.26 Coronal T2 image through the pelvis reveals a fat (star) and sigmoid (arrowhead) colon containing left inguinal hernia

MR Contrast

MR contrast and signal intensity are dependent upon various properties of tissues. As previously discussed, protocols may be tailored to maximize inherent soft tissue contrast. In most instances, unenhanced MR imaging will suffice for the evaluation of abdominal and pelvic hernias. Fat,

fluid, muscle, and bowel can readily be distinguished from one another. However, some situations require additional information regarding vascular patency, lesional characterization (*i.e.,* enhancing endometriosis deposit in the abdominal wall), inflammatory processes (*e.g.,* abscess), or assessment of tissue perfusion [10, 15, 16] (Figs. 8.20 and 8.27).

In those scenarios, intravenous contrast may be administered for improved tissue contrast delineation. While contrast agents can be classified into extra-cellular, hepatobiliary, reticuloendothelial, blood-pool, and mixed types, the most broadly used are gadolinium-derived agents [17]. These are paramagnetic substances that shorten the spin-lattice relaxation time within voxels during imaging, resulting in a "brighter" T1 signal [18, 19]. During the evaluation of hernias, contrast may be of use in establishing patency of involved vasculature, presence or absence of nerve involvement, or viability of bowel. Gadolinium-based agents are typically injected at a dose of 0.1–0.2 mmol/kg [18]. While nearly 6,000,000 gadolinium-enhanced exams are performed annually, the use of contrast is not entirely without risk. While the incidence of allergic reaction to gadolinium-based agents is lower than that of iodinated CT contrast agents at approximately 0.07–2.4% [18]. Specific gadolinium agents carry the rare but potentially debilitating risk of nephrogenic systemic fibrosis (NSF) [20]. With a reported incidence of 0.02–0.4% [20], this is a poorly understood process in which patients with diminished renal function and gadolinium exposure develop diffuse connective tissue fibrosis involving the skin and subcutaneous tissues [21]. This multisystem sclerosis may progress to involve the musculature, pericardium, dura, and pleura, resulting in debilitating harm to patients. Due to new guidelines increased awareness, screening of at-risk populations, and risk stratification of the specific agents, there has been a significant decrease in the occurrence of NSF [22]. Other relative contraindications for contrast include the gravid patient, as the fetal risk has not been clearly elucidated though consideration may be given to emergent use if clinically necessary [17, 18, 22]. Other agents are available, including hepatobiliary-specific agents which are taken up and excreted by hepatocytes, allowing for more detailed evaluation of the biliary tree and of specific liver masses. Contrast selection is based on the clinical question to be answered and, in the setting of abdominal wall hernia evaluation will typically be addressed by the use of gadolinium-based agents, if necessary.

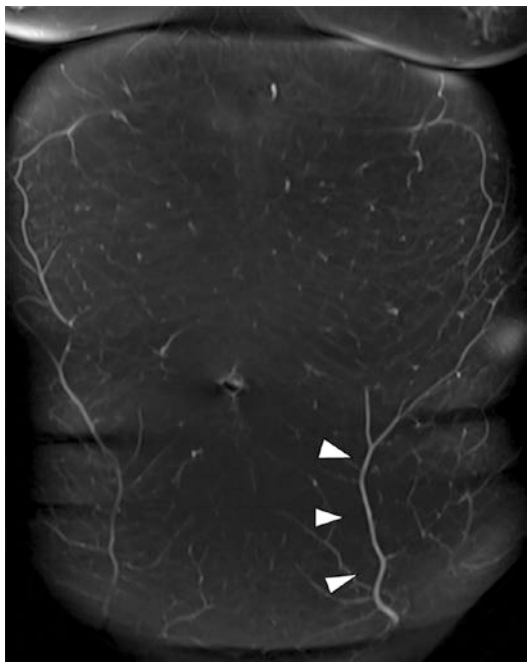

Fig. 8.27 Coronal post-enhancement fat-suppressed T1-weighted image demonstrating the superficial inferior epigastric vessels (arrowheads)

MR Challenges and Limitations

The manner in which MR images are created is inextricably linked with several limitations.

While CT imaging takes seconds for acquisition, MR exams may take 30–90 min to complete, rendering the modality both less accessible and tolerable for patients. Additionally, as MR is more reliant on the sequential and serial production of images, it is more prone to motion artifact, which may occur due to baseline physiologic changes (blood flow, ureteral jets, cerebrospinal fluid shift) or uncontrolled patient

motion (*e.g.,* Parkinson's disease, altered mental status) (Fig. 8.28).

For example, in the time it takes to produce a single axial image through a vascular structure, the intraluminal material has already passed beyond the image plane. Accordingly, there is a signal void on the final image as the intravascular blood has already passed beyond the imaging plane, with a resultant loss of signal to the MR receiver. Consequently, there is no data within this location on the final image. While different MR exam protocols can mitigate or exacerbate the time-sensitive nature of the process, the underlying paradigm remains sensitive to motion. This is of obvious importance during imaging of the abdomen for the evaluation of hernia (Fig. 8.29).

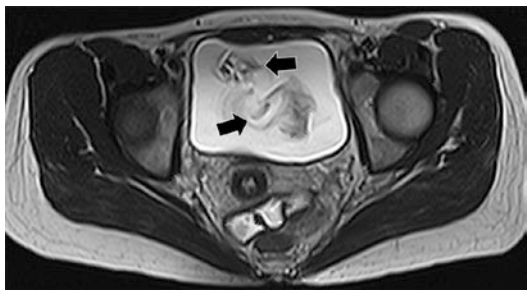

Fig. 8.28 Axial T2-weighted image through the pelvis demonstrates loss of signal (dark) foci within the urinary bladder as a result of fluid shift within, typically related to ureteral jets

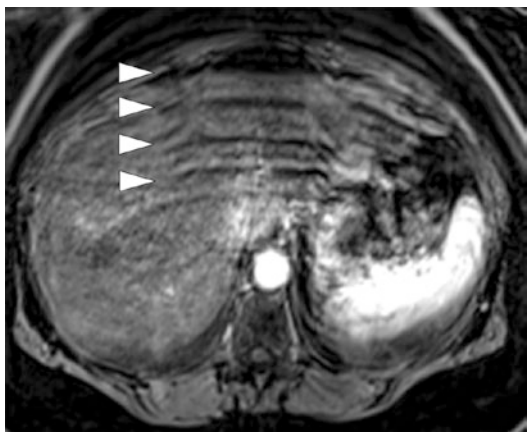

Fig. 8.29 Axial post-enhancement fat-suppressed T1-weighted image demonstrating respiratory motion artifact, as is manifested by the striated appearance in the anteroposterior plane (arrowheads)

The time and motion-sensitive nature of MR is of particular relevance in the obtunded or pediatric populations, at times necessitating associated sedation or anesthesia. Available MR sequences utilize patient breath-holding techniques to maintain smooth images and mitigate motion artifacts. While these rely upon patient cooperation, respiratory-gated imaging utilizes feedback from a sensor about the patient's thorax to time image acquisition relative to their respiratory cycle.

Technical and patient parameters can also limit MR access and utility. Obese patients may not fit within the magnet bore [13, 23]. It is estimated that 2.3% of all MR patients are claustrophobic and that annually 2,000,000 patients worldwide are unable to undergo MR imaging as a result of such [24]. In addition, the vast array of implanted hardware and personal medical devices requires close scrutiny to ensure MR compatibility. Lack of MR compatibility may be on the basis of potential device malfunction (*e.g.,* interrupted cardiac pacing), component migration, or a component heat-sink effect. In some instances, devices may simply malfunction in the magnetic field (*i.e.,* specific cardiac pacemakers/AICDs, cochlear implants). In others, though a device or surgical hardware may retain functionality, the metallic components result in significant "signal loss" and local field distortion, rendering portions of the image uninterpretable (Fig. 8.30).

In the setting of abdominal wall evaluation, this is less common, though surgical clips or

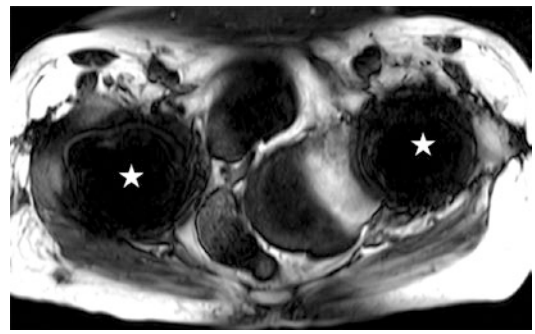

Fig. 8.30 Axial T2 image through the level of the pelvis demonstrates significant signal loss bilaterally due to bilateral hip arthroplasty hardware (stars)

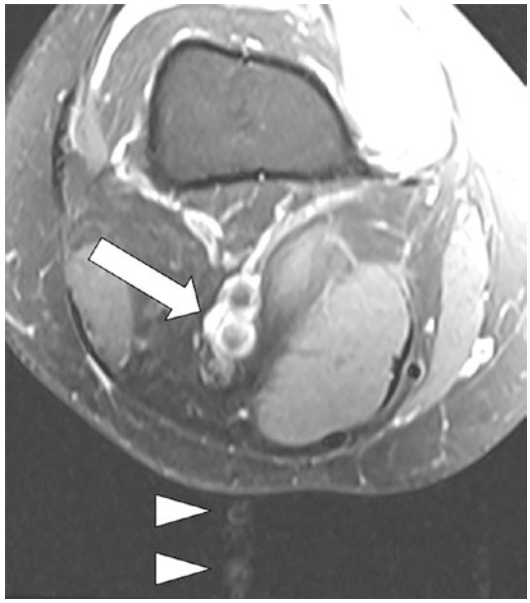

Fig. 8.31 Axial proton density image at the approximate level of the knee demonstrates multiple circular images posteriorly (arrowheads), compatible with pulsation artifacts from adjacent vessels (arrow)

implanted pumps may cause artifacts within the more superficial abdominal structures.

Additional MR artifacts are omnipresent as well, ranging from mild resultant image degradation to completely non-diagnostic imaging. For example, pulsation artifact can be seen when vessels are in the field of view and faded, ghostly duplicates are seen in the phase-encoding direction (Fig. 8.31).

"Zipper" artifacts may similarly interfere with the image. Lastly, MR is limited by the attention directed to appropriate exam protocol selection. While CT data can undergo significant post-processing, inadequate or inaccurate preplanning of MR protocol may result in significant data loss if specific sequences are neglected at the time of image acquisition.

MR Safety and Risks

While CT and ultrasound carry a relatively low risk for the target population other than the inherent ionizing radiation and iodinated contrast risks of the former, MR examinations carry with them

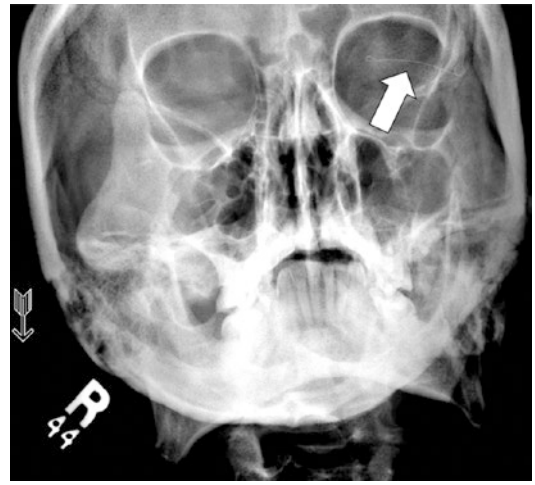

Fig. 8.32 Radiograph of the orbits demonstrating the presence of a metal eyelid spring projecting over the left orbit (arrow)

the need for additional *pre facto* patient screening [25]. The use of intravenous contrast necessitates attention to preexisting patient risk factors such as underlying renal insufficiency, gravid status, or preexisting allergy. Patients must also be prescreened to ensure that any implanted hardware is MR compatible. At-risk patients with a history of prior penetrating traumatic injury (*i.e.,* shrapnel), grinding or welding require conventional radiography of the targeted body region prior to imaging, such as to avoid fragment migration, heat-sink effect, and possible tissue shearing injuries [26] (Fig. 8.32).

Consideration must also be given to the total energy deposited within a patient's body during imaging or specific absorption rate (SAR), as prolonged MR imaging can result in heating of tissues [26]. More focal deposition of energy into the tissue can result in localized burns as a consequence of focused electrical conductivity, whether on the basis of hardware, overlying coiled metallic devices or tattoo ink. There is a significant amount of noise generated during typical MR imaging as the machine sends and receives impulses which can result in hearing loss if patients are not given adequate hearing protection. Compounding these baseline risks are the added risks of unexpected emergent acute care interventions, during which less knowledge-

able personnel may inadvertently enter the room with metallic devices on their person, potentially incurring high-velocity traumatic injuries. Lastly, unresponsive or less communicative patients are at increased risk, as evolving problems may go unnoticed. In sum, the safety aspects of MR are multifaceted and significant but can be addressed with fastidious attention to detail and continuous staff education processes.

Summary

While MR has significant limitations and safety precautions, it can be useful in the tissue characterization and assessment of abdominal wall hernias, particularly when CT and ultrasound are unrevealing.

References

1. Aguirre AD, Santosa AC, Casola G, Sirlin CB. Abdominal wall hernias: imaging features, complications, and diagnostic pitfalls at multi-detector row CT. RadioGraphics. 2005;25:1501–20.
2. Lassandro F. Abdominal hernias: radiological features. World J Gastrointest Endosc. 2011;3(6):110.
3. Huda W. Review of radiologic physics. 4th ed. Philadelphia: Wolters Kluwer; 2016. p. 336.
4. Schild H. MRI made easy (...well almost). Berlin/Bergkamen: Schering AG; 1990. 105 p.
5. Moore MM, Chung T. Review of key concepts in magnetic resonance physics. Pediatr Radiol. 2017;12(47):497–506.
6. Bashir U, Moskovic E, Strauss D, Hayes A, Thway K, Pope R, Messiou C. Soft-tissue masses in the abdominal wall. Clin Radiol. 2014;69:e422–31.
7. Busard MP, Mijatovic V, van Kuijk C, Hompes PG, van Waesberghe JH. Appearance of abdominal wall endometriosis on MR imaging. Eur Radiol. 2010;20:1267–76.
8. Gidwaney R, Badler RL, Yam BL, Hines JJ, Alexeeva V, Donovan V, Katz DS. Endometriosis of abdominal and pelvic wall scars: multimodality imaging findings, pathologic correlation, and radiologic mimics. Radiographics. 2012;32:2031–43.
9. Stein L, Elsayes KM, Wagner-Bartak N. Subcutaneous abdominal wall masses: radiological reasoning. AJR. 2012;198:W146–51.
10. Teo HE, Peh WC, Shek TW. Case 84: desmoid tumor of the abdominal wall. Radiology. 2005;236:81–4.
11. George R, De la Cruz J, Singh R, Ilangovan R, Stewart O. Technique: resolution and image quality. [Internet]. MRIMaster website; 2020. Accessed 2020 April 15. MRIMaster.com.
12. Moratal D, Vallés-Luch A, Martí-Bonmatí L, Brummer ME. *k*-Space tutorial: an MRI educational tool for a better understanding of *k*-space. Biomed Imaging Interv J. 2008;4(1):e15.
13. Modica MJ, Kanal KM, Gunn ML. The obese emergency patient: imaging challenges and solutions. RadioGraphics. 2011;31(3):811–23.
14. Humphries PD, Sebire NJ, Siegel MJ, Olsen OE. Tumors in pediatric patients at diffusion-weighted MR imaging: apparent diffusion coefficient and tumor cellularity. Radiology. 2007;245:848–54.
15. Virmani V, Sethi V, Fasih N, Ryan J, Kielar A. The abdominal wall lumps and bumps: cross-sectional imaging spectrum. Can Assoc Radiol. 2014;65:9–18.
16. Wolf Y, Haddad R, Werbin N, Skornick Y, Kaplan O. Endometriosis in abdominal scars: a diagnostic pitfall. Am Surg. 1996;62:1042–4.
17. Ibrahim MA, Hazhirkarzar B, Dublin AB. Magnetic resonance imaging (MRI) gadolinium. [Updated 2020 Feb 11]. In: StatPearls [Internet]. Treasure Island (FL): StatPearls Publishing; 2020 Jan. Available from: https://www.ncbi.nlm.nih.gov/books/NBK482487/.
18. Sammet S. Magnetic resonance safety. Abdominal Radiol. 2016;41(3):444–51.
19. Seale MK, Onofrio AC, Saini S, Hahn PF, Sahani DV. Hepatobiliary-specific MR contrast agents: role in imaging the liver and biliary tree. RadioGraphics. 2009;29:1725–48.
20. Khawaja AZ, Cassidy DB, Shakarchi JA, McGrogan DG, Inston NG, Jones RG. Revisiting the risks of MRI with Gadolinium based contrast agents—review of literature and guidelines. Insights Imaging. 2015;6:553–8.
21. Wagner B, Drel V, Gorin Y. Pathophysiology of gadolinium-associated systemic fibrosis. Am J Renal Physiology. 2016;311(1):F1–F11.
22. Davenport MS, Asch D CJ et al. ACR Committee on Drugs and Contrast Media. ACR manual on contrast media: version 10.3 [Internet]. American College of Radiology website; 2020. Accessed 2020 Mar 31. Available from: https://www.acr.org/Clinical-Resources/Contrast-Manual.
23. Halligan S, Parker SG, Plumb AA, Windsor ACJ. Imaging complex ventral hernias, their surgical repair, and their complications. Eur Radiol. 2018;28:3560–9; Springer Verlag.
24. Enders J, Zimmerman E, Rief M, Martus P, Klingebiel R, Asbach P, Klessen C, Diederichs G, Bengner T, Teichgräber U, Hamm B, Dewey M. Reduction of claustrophobia during magnetic resonance imaging: methods and design of the "CLAUSTRO" randomized controlled trial. BMC Med Imaging. 2011;11:4.
25. Tsai LL, Grant AK, Mortele KJ, Kung JW, Smith MP. A practical guide to MR imaging safety: what radiologists need to know. RadioGraphics. 2015;35:1722–37.
26. Kanal E, *et al.* ACR Manual on MR Safety: version 1.0 [Internet]. American College of Radiology website. 2020. Accessed 2020 April 17. https://www.acr.org/-/media/ACR/Files/Radiology-Safety/MR-Safety/ACR-Manual-on-MR-Safety.pdf.

9 Hallmarks of Incarcerated and Strangulated Hernias

Andrew T. Bates

Introduction

The strangulated hernia represents a surgical emergency that relies on a combination of thorough physical exams and radiologic findings for prompt and accurate diagnosis. Strangulation, by definition, is the presence of ischemia in the tissue contained within the hernia. Incarceration, in contrast, is defined by the inability of medical professionals to successfully reduce the hernia contents back into the abdominal cavity. Furthermore, long-standing hernias may be "chronically incarcerated" due to adhesions within the hernia sac but show no signs of acute changes or ischemia. Incarceration therefore is a clinical diagnosis of failure of manual reduction, and one that cannot be made by radiologic testing. Strangulation may present with several radiologic signs that suggest visceral ischemia or necrosis.

Any structure within the abdominal cavity can become incarcerated or strangulated within a hernia defect, although the omentum and bowel are most commonly affected. Strangulation occurs when the hernia defect encircles the contained viscera, causing venous stasis and edema that further compromise blood flow [1]. Prolonged ischemia may then lead to tissue necrosis and perforation if the bowel is involved.

Overall, hernia strangulation is a relatively rare event, although the consequences may be catastrophic. Only 3.8% of all inguinal hernia repairs yearly are performed on an emergent basis [1]. Moreover, many of these emergent repairs are not performed for strangulation. A 2012 study by the Mayo Clinic found that the yearly incidence of emergent inguinal hernias has been decreasing over the past 20 years, possibly due to rising rates of elective repairs and greater patient awareness of hernias [2]. Fitzgibbons et al. published in 2012 a 10-year series of men showing only a 2.4% rate of emergent repair during the study period [3]. As a result, the strategy of "watchful waiting" gained in popularity for asymptomatic or minimally symptomatic hernias. Although most of these hernias have been shown to become symptomatic in the following years, the risk of emergent repair remains low.

Although the risk of incarceration for all types of hernias remains relatively low, patients who require emergent repair show significantly worse outcomes [4]. Emergent repairs are associated with higher rates of organ resection, higher 30-day mortality rates, greater 30-day reoperation risk, as well as higher rates of overall complications including mesh infection.

Ventral hernias arise from a wide range of etiologies and represent a broad category of abdom-

A. T. Bates (✉)
Department of Surgery, South Shore University Hospital, Northwell Health, Bay Shore, NY, USA
e-mail: abates@northwell.edu

S. Docimo Jr. et al. (eds.), *Fundamentals of Hernia Radiology*,
https://doi.org/10.1007/978-3-031-21336-6_9

inal wall defects. As such, their risk of incarceration and strangulation is highly dependent on factors such as location and defect size. In a 2019 paper, Sneiders et al. showed that primary defects measuring 3–4 cm were significantly associated with a higher rate of incarceration compared to smaller defects measuring 0–2 cm [5]. For incisional hernias, this comparison remained true. Furthermore, defect location was found to have a significant effect, with defects in the peri- and infra-umbilical region showing a nearly twofold higher risk of incarceration compared to defects in the upper abdomen [5].

For inguinal hernias, multiple patient characteristics have been shown to increase the risk of strangulation, including female sex, recurrent hernias, ASA class >3, overweight, underweight, and the presence of femoral defects. In these cases, higher consideration should be given to prompt elective repair so as to prevent the incidence of incarceration and strangulation [1].

Clinical Presentation

The acute presentation of patients with incarceration can vary depending on the location of the hernia and viscera it contains. It is key to determine the chronicity of the incarceration to determine the appropriate level of surgical emergency [6]. For example, a patient who presents with an incarcerated hernia that has been stable in size and appearance for years does not represent a surgical emergency in the absence of acute changes or other concerning biochemical or radiographic abnormalities. For inguinal hernias, presentation may also differ by the subcategories of indirect, direct, or occult femoral defect. However, most acutely incarcerated groin hernias will present with sudden-onset pain with a palpable, tender mass. If the hernia contains incarcerated bowel, the patient may also present with nausea/vomiting and obstipation indicative of bowel obstruction. On physical exam, the patient may present with a firm, tender mass in the groin that is unable to be reduced. Findings of exquisite tenderness or overlying cutaneous erythema are concerning findings for tissue ischemia and/or necrosis. Biochemical aberrations such as leukocytosis or elevated lactate are also concerning. In this setting, repeated attempts at manual reduction should be avoided due to the risk of perforation or the reduction of necrotic bowel back into the abdominal cavity. Many sources suggest that manual reduction not be attempted if the patient has been symptomatic for more than 4–12 h. However, clinicians should use best judgment after a complete examination and workup, instead of relying on strict temporal cutoffs [6].

Ventral hernias most commonly present at previous incision sites or the umbilicus, although less common hernias such as Spigelian, parastomal, and lumbar hernias may present as well. As in inguinal defects, incarceration or strangulation may present as a palpable, firm, and tender mass with possible overlying erythema. Signs of bowel obstruction may or may not be present. In the case of parastomal hernias, the patient may additionally present with signs of stoma dysfunction.

In the presence of concerning clinical findings, combined with signs of ischemia or necrosis on imaging, the distinction between incarceration and strangulation is often academic—the patient requires emergent exploration and repair. If, upon exploration, the contained viscera is ischemia but viable, prompt diagnosis and treatment have spared the patient an emergent resection.

Radiologic Findings

Most hospitals have CT capabilities in the emergent setting. Ultrasound can be useful for determining the presence of bowel and/or fluid within the hernia sac (Fig. 9.1). However, the modality remains highly user dependent and is not sufficiently sensitive to detect certain concerning characteristics. Even in the case of CT scans, the importance of correlating radiographic findings with the patient's physical exam and overall clinical picture cannot be overstated [7].

In the setting of an incarcerated hernia, the first question to be answered is that of the viscera it contains. Omentum, for example, can be quite

Fig. 9.1 Strangulated inguinal hernia containing small bowel with a large amount of free fluid within hernia sac

Fig. 9.2 Ventral hernia containing strangulated omentum

painful when infarcted but does not represent the same level of emergency as bowel (Fig. 9.2). Any acutely incarcerated hernia that presents containing bowel should be highly scrutinized to determine the need for operative intervention.

Acutely incarcerated bowel within a hernia defect typically shows proximal dilation of the bowel indicative of obstruction. The bowel within the hernia is usually collapsed with a transition point occurring at the neck of the hernia (Fig. 9.3).

Fig. 9.3 Incarcerated ventral hernia causing small bowel obstruction. A transition point in the efferent limb is clearly visualized at the level of the fascia

The use of oral water-soluble contrast is helpful in determining the degree of intestinal obstruction (partial vs. complete/"high-grade") in these cases. While obstruction is typical of acute incarcerations, it does not necessarily indicate strangulation. Moreover, if the bowel lumen remains patient while entering and exiting the hernia, this may help assuage concern for ischemia somewhat as the neck is not constricting the bowel severely enough to cause a transition point, let alone strangulation.

Thickening of the bowel wall that is contained within the hernia is a concerning finding that suggests bowel edema due to venous congestion and/or inflammation (Fig. 9.4). Most sources will cite an upper limit of 2–3 mm for small bowel and 5mm for large bowel. If a substantial amount of bowel has herniated and the mesentery can be visualized, congestion of the mesenteric vessel indicates outflow obstruction. Typically, the vessels will appear prominent and engorged on CT imaging. The adipose tissue of the mesentery may also show signs of "stranding" secondary to edema and decreased lymphatic drainage.

Free extraluminal fluid within the hernia sac is a radiographic finding concerning ischemia or necrosis. While free fluid may be present due to edema rather than ischemia, a more concerning process cannot be excluded.

Fig. 9.4 Strangulated ventral hernia with small bowel wall thickening

Fig. 9.5 Strangulated inguinal hernia with extraluminal free air

Pneumatosis intestinalis and extraluminal air are highly concerning findings that suggest a breakdown in the integrity of the bowel wall, likely secondary to necrosis (Fig. 9.5). Pneumatosis is a radiographic finding rather than a diagnosis itself. However, in the setting of hernia incarceration, it is most likely due to mucosal necrosis and breakdown, allowing intraluminal gas to dissect into the submucosa of the bowel. Extraluminal air implies a full-thickness breakdown and free perforation. Extraluminal air and free fluid are usually seen in concert in the setting of strangulation.

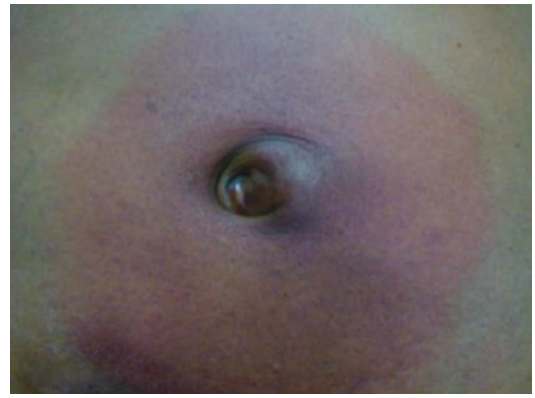

Fig. 9.6 Subcutaneous erythema surrounding strangulated umbilical hernia

Subcutaneous fat stranding surrounding the hernia sac signifies inflammation of the subcutaneous space and is the radiographic correlation of erythema on physical exam (Fig. 9.6). While the simple event of acute herniation and repeated attempts at manual decompression can produce this finding, clinicians should also be highly suspicious of ischemia or necrosis of hernia contents producing a localized inflammatory response.

The use of intravenous contrast during CT scanning also allows the practitioner to assess the relative perfusion of the bowel compared to the surrounding anatomy. In some studies, the lack of contrast enhancement is the leading indicator of ischemia and necrosis [8].

Clinical Pearls/Suggested Algorithm

For patients presenting acutely incarcerated, we would recommend clinicians to assume visceral compromise until proven otherwise. Upon initial evaluation, practitioners should ask the following questions prior to attempting manual reduction:

1. How long has the patient experienced acute symptoms?

   If the patient shows acute changes within the past day, their pathology is more likely to require emergent intervention. Complaints that have been present for weeks to months are likely to warrant observation or elective repair.
2. Does the patient have signs of hemodynamic instability?

   In the setting of acute incarceration, it is very difficult to prove that concerning hemodynamic changes such as tachycardia and hypotension are not the result of compromised viscera. Emergent exploration and repair are recommended for these patients.
3. Does the patient have biochemical aberrations, such as WBC >20k or lactate >2?
4. On examination, does the patient show acute tenderness at the hernia site, peritonitis, or overlying erythema?

In the acute setting, these exam and laboratory findings are concerning for ischemia and possible necrosis. Emergent repair is indicated and attempts at manual decompression should be avoided.

Upon review of the radiologic workup, any of the following findings in the setting of acute bowel incarceration warrant emergent repair (Fig. 9.7).

1. Bowel wall thickening
2. Free abdominal fluid or fluid within hernia sac.
3. Vascular congestion or mesenteric edema
4. Free extraluminal air or pneumatosis intestinalis
5. Fat stranding surrounding bowel or hernia sac
6. Absent IV contrast enhancement of bowel

However, it should be noted that any one of these findings does not definitively predict bowel necrosis or the need for bowel resection. In a recent publication, of the findings listed above, only the lack of contrast enhancement was significantly associated with the need for resection, with an odds ratio of 51.

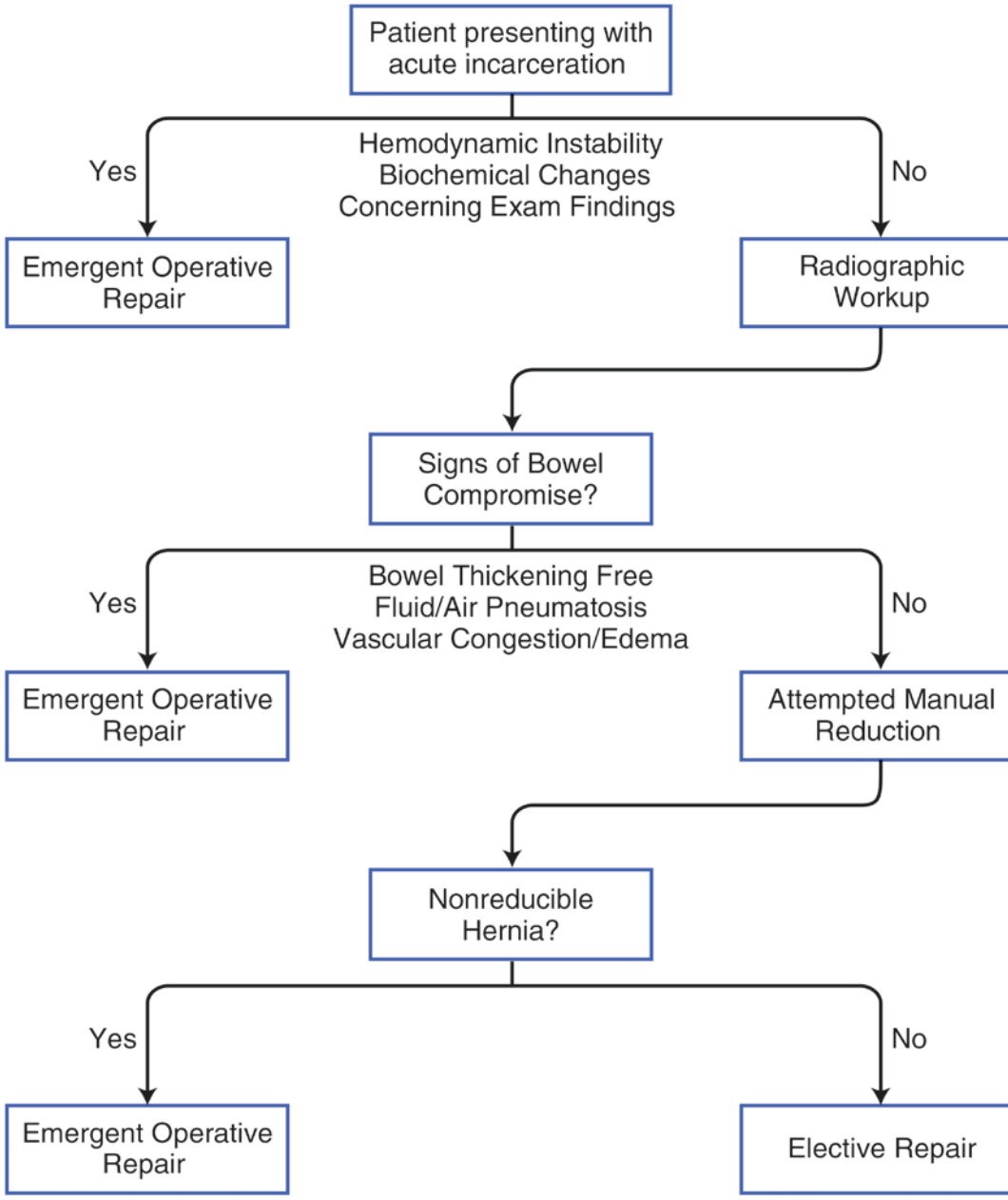

Fig. 9.7 Proposed clinical algorithm for evaluation and treatment of acutely incarcerated hernias

Conclusion

A strangulated hernia represents the most emergent hernia pathology and warrants surgical exploration. Prompt recognition of both clinical and radiographic findings consistent with the strangulated bowl is critical for proper treatment and best surgical outcomes.

References

1. Walle KA, Greenberg JA. Strangulated inguinal hernia: options and strategies. In: The SAGES manual of hernia surgery 2019, pp. 503–514. Springer, Cham.
2. Hernández-Irizarry R, Zendejas B, Ramirez T, Moreno M, Ali SM, Lohse CM, Farley DR. Trends in emergent inguinal hernia surgery in Olmsted County, MN: a population-based study. Hernia. 2012;16(4):397–403.
3. Fitzgibbons RJ Jr, Ramanan B, Arya S, Turner SA, Li X, Gibbs JO, Reda DJ. Long-term results of a randomized controlled trial of a nonoperative strategy (watchful waiting) for men with minimally symptomatic inguinal hernias. Ann Surg. 2013;258(3):508–15.
4. Chung PJ, Lee JS, Tam S, Schwartzman A, Bernstein MO, Dresner L, Alfonso A, Sugiyama G. Predicting 30-day postoperative mortality for emergent anterior abdominal wall hernia repairs using the American College of Surgeons National Surgical Quality Improvement Program database. Hernia. 2017;21(3):323–33.
5. Sneiders D, Yurtkap Y, Kroese LF, Kleinrensink GJ, Lange JF, Gillion JF. Risk factors for incarceration in patients with primary abdominal wall and incisional hernias: a prospective study in 4472 patients. World J Surg. 2019;43(8):1906–13.
6. Doble JA, Pauli EM. Incarcerated and strangulated hernia. In: Clinical algorithms in general surgery 2019 (pp. 805–807). Springer, Cham
7. Cherla DV, Bernardi K, Blair KJ, Chua SS, Hasapes JP, Kao LS, Ko TC, Matta EJ, Moses ML, Shiralkar KG, Surabhi VR. Importance of the physical exam: double-blind randomized controlled trial of radiologic interpretation of ventral hernias after selective clinical information. Hernia. 2019;23(5):987–94.
8. Kohga A, Kawabe A, Yajima K, Okumura T, Yamashita K, Isogaki J, Suzuki K, Muramatsu K, Komiyama A. Does preoperative enhanced CT predict requirement of intestinal resection in the patients with incarcerated myopectineal hernias containing small bowel? Hernia. 2021;25:1279–87.

3D Imaging of the Abdominal Wall

10

Roel Beckers, Maaike Vierstraete, and Filip Muysoms

Introduction

Hernia surgery, by which a protruding, bulging, or sliding part of the abdominal content is put back into its place and the weakened or defective abdominal wall is restored is one of the most frequently performed procedures throughout the world. It comprises a quite large and rather heterogenous group of hernias most frequently of the groin [1, 2], or inguinal type but also primary and secondary ventral hernias according to the 2009 definition of the European Hernia Society [3], and encompasses diaphragmatic hernias and pelvic area hernias, as well. Together they bring the worldwide annual number of surgical interventions well over twenty million [4]. While many hernias are found by coincidence during routine CT exams, the CT scan is a powerful tool that plays a central role in the preoperative workup of elective, complex cases.

There is increasing interest not only in intuitive comprehensive imaging of abdominal wall hernias but also in the physical dimensions of hernias because of the related impact on outcome and surgical approach. It is a challenge to extract maximum clinical and quantitative information from the original scan, which requires in-depth knowledge of the physics of the imaging on the one hand, but especially of the possibilities offered by the different modern software packages on the other hand in order to display images in 3D and to perform quantitative measurements. The resultant information will not only guide the surgeon in their preoperative planning but it gives the opportunity to inform the patient in advance if an increased risk or higher complication rate is present or if more complex surgical strategies should be addressed. It is therefore imperative that radiologists master these techniques to extract maximal information from the CT data [4]. It must be emphasized that an active search for abdominal wall abnormality should be part of a routine investigation. In this chapter, we give a brief overview of the evolution of CT scan as well as the currently available methods for processing the available data with 3D rendering techniques and quantitative morphometrics within the context of abdominal wall imaging. In addition, we provide an overview of the currently available methods to visualize MR-visible abdominal wall grafts. CT images were scanned on a 64 row CT system and reconstructed on a 3D workstation (Somatom Definition Flash and Syngo Via® VB30 Siemens Healthineers Erlangen

Supplementary Information The online version contains supplementary material available at https://doi.org/10.1007/978-3-031-21336-6_10.

R. Beckers (✉)
Department of Radiology, AZ Maria Middelares, Ghent, Oost-Vlaanderen, Belgium

M. Vierstraete · F. Muysoms
Departement of Surgery, AZ Maria Middelares, Ghent, Oost-Vlaanderen, Belgium

S. Docimo Jr. et al. (eds.), *Fundamentals of Hernia Radiology*,
https://doi.org/10.1007/978-3-031-21336-6_10

Germany). MR images were produced on a 1.5 and 3 Tesla scanner (Achieva 1.5 T and Ingenia 3.0 T Philips Medical Systems Best Netherlands) and reconstructed (if not mentioned otherwise) using Syngo Via® software.

3D techniques in CT imaging

Advances in CT Imaging and Computer Capacity

Since the clinical first introduction of CT imaging in 1971 by the hand of Sir Godfrey Hounsfield, enormous advances have been made in CT technology, especially in the last two decades. A revolution in hardware, software, and display technology took place which has led to the widespread use and availability of high-end multidetector-multirow CT systems in combination with advanced 3D workstations.

Slipring technology by the mid-80s enabling cable free transport of energy and data from and to the gantry permitted continuous rotation of the x-ray tube and the oppositely placed detector allowing a rotate-rotate movement of the tube detector unit versus the translate-rotate movement of the older systems. The former paved the way for a new manner of scanning called spiral or helical scan technology by the end of the 80s and gradually replaced the latter sequential scanning in clinical practice [5, 6] at the beginning of the 90s. With the introduction of the single-slice spiral CT in 1990 for the first time, volume data sets were produced [7].

Detector design and technology dramatically changed with the increasing number of detector rows. The introduction of dual-slice spiral CT in 1992 was followed by the introduction of "quad CT" in 1998 and 16 slice CT in 2002 allowing the simultaneous acquisition of 16 data sets derived from the output of a combination of adjacent detector elements in a detector array with equal or unequal-width detector design. Spiral CT became multi-section CT [8] and later multidetector CT (MDCT). Thin millimeter slices in the Z-direction (longitudinal axis of the patient) led to isotropic voxel dimensions.

X-ray tubes with higher power output capacity, operating at variable kilovolt settings and with computerized tube current modulation were introduced. Along with the number of detector rows, the rotation speed of the x-ray tube and detector unit within the gantry increased significantly.

This evolution went on in the coming decades with an increasing number of submillimeter detector rows up to 320 in some systems and with decreasing rotation times as low as 0.23 s for some vendors.

Advances in detector composition and development of digitized data transmission systems were necessary to keep up with the exponentially increased production of data from the scanned volume. This required simultaneous growth both from computing power, and storage capacity. As a result of more powerful computers the reinvented iterative reconstruction (IR) techniques from the early 70s (as a successor to filtered back projection techniques) could finally be applied. Thanks to IR a significant decrease in radiation dose due to noise reduction [9–11] could be achieved and this process is currently still evolving due to the development and implementation of artificial intelligence using deep learning algorithms. Different image reconstruction algorithms also allowed for faster image calculations and increased in-plane resolution. Speed-related reduction of motion artifacts made special applications possible like cardiac imaging [12], imaging of moving vessels, or even more: dynamics within vessels [13].

The final result is that large volumes can be scanned in a few seconds instead of minutes with higher resolution, isotropic voxel dimensions, and better image quality than ever before at an acceptable radiation dose.

Thanks to evolutions in graphics software it became possible to make complex calculations on a data set of hundreds of high-resolution submillimetric overlapping images. Resampling of data into isotropic voxels results in high resolution, artifact-free multiplanar reformatted (MPR) images (Fig. 10.1).

At the beginning of this era investigations were evaluated by looking at images printed on

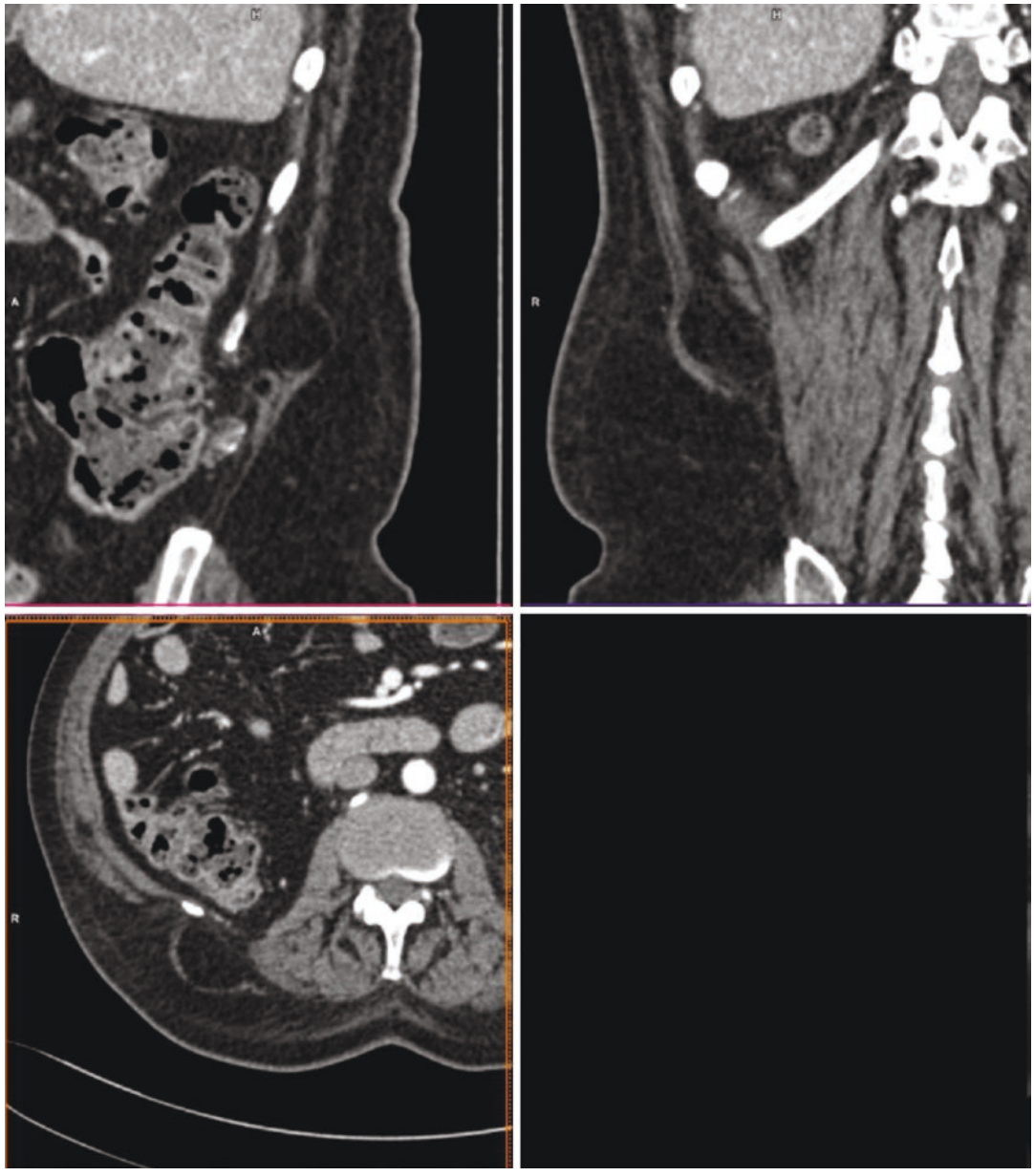

Fig. 10.1 MPR images out of volume scan in three orthogonal directions show motion free reconstructions. Notice a right-sided small lumbar hernia (Grynfeltt-Lesshaft hernia)

films with a reconstructed slice thickness a multiple of the highest possible resolution. With the development of integrated PACS systems and dedicated workstations, it became a new standard to evaluate investigations by scrolling through the native or thin overlapping reconstructed images in an axial plane or in selected multiplanar reconstruction directions, zooming in the region they want to take a closer look at or perform measurements on it. Rendering techniques incorporated into dedicated software became available at the beginning of the millennium for diagnostic or didactic purposes and are now an indispensable tool. This shift from analysis on

plain film to dedicated workstation is a true revolution made possible by the simultaneous developments in technology on all levels discussed and has dramatically changed the workflow of the radiologist.

Classic Rendering Techniques:

With every volume scan, a large amount of mathematical data is generated and transformed in the 3D space into geometrical voxels or volume units that compose the scanned volume. These voxels are converted into two-dimensional pixels when creating an image. The transformation of acquired helical medical CT data into realistic 3D clinical images displayed as an image on a 2D monitor after mathematical calculation based on a suitable computer algorithm is called rendering. It was introduced in the late 80s for CT and MRI [14, 15]. Among several methods, a major distinction is made between thresholding, a binary method, and percentage-based techniques. The former is also known as a surface-based technique and the latter as a volume-based technique. Volume techniques are further divided into maximum intensity projection (MIP) and volume rendering techniques (VRT).

Surface Rendering:

The binary algorithm of surface rendering was developed in the 70s and works on an all-or-nothing principle [16, 17]. Along the path of projection, the voxel that first meets the predefined threshold intensity value that is representable to the chosen organ is recognized as part of the surface of the investigated organ of interest. All the voxels in front that do not meet the criteria are not considered as are all the voxels along the path behind the first voxel that meets the criteria. The resultant pixel intensity is calculated mathematically based on the interaction with a virtual light source and the orientation of the surface gives the aspect of surface shading, and hence the name surface shaded display (SSD). The final 2D image is the result of the viewing orientation and the calculated visible areas from that point of view, edited by further choosing color and opacity. SSD gives information on the surface only, no information along the depth of a structure is given even in transparent models, and overlap with other structures is not recognizable The technique is sensitive to image artifacts. It reduces a volume to a compact surface and consequently limited computer power is needed to generate the images which explains their initial success. However, this technique was abandoned in routine clinical CT practice because of several disadvantages including lack of volume information and more importantly the incompatibility with volume averaging when more than one tissue density is present in one voxel.

MIP Imaging:

The first volume-based technique is MIP. In MIP rendering technique the pixel with the highest density along the path of view or projection throughout the scanned volume is displayed with its corresponding intensity. The result of all these parallel projections make up the image and the image contains information only of the highest density voxel along the path, obscuring the lower density voxels along that path. The thickness of the slice of the volume through which the projection path is calculated can be chosen according to preference. Although MIP imaging has several shortcomings, it is widely used in clinical practice, especially in producing CT or MR angiographic images. 3D sensation with MIP images can be experienced by scrolling through a series of several MIP images or an animation composed of individual images with gradually changing view angles, called a spin. This technique is mainly used in vascular MR images where it was originally introduced.

The most important limitation of MIP imaging is its lack of three-dimensional information in a static image so when, for example, vessels are crossing in the volume it is impossible to see which vessel lies in front. Moreover, high-density structures like calcifications overlying a vascular structure can falsely mimic total occlusion. Image manipulation with adaptation of chosen MIP slab thickness can overcome some of these problems but it remains a common pitfall.

Applied to abdominal wall imaging MIPs are mainly used to depict and localize perforating arteries from the anterior rectus fascia in the setting of preoperative CT angiography with three-dimensional postprocessing for deep inferior epigastric perforator flap breast reconstructive surgery [18]. Subsequently, these points can be located on a VRT image of the skin surface. The use of MIP to visualize abdominal wall hernias is very limited. MinIP is the opposite of MIP where only the darkest voxels in a volume of one or more slices are depicted. It has limited applications but can be used for the imaging of hypointense MRI structures (see below: 3D techniques in MR imaging).

VRT Imaging:

In contrast to MIP imaging, VRT is an imaging technique that uses information from the whole volume to produce an image [19]. Obviously, this requires more computer processing and displaying capacity and although first used in the late 80s it is only since less than two decades that volume rendering is used in clinical practice routinely because the abovementioned required capacity was finally met. VRT holds into account that a voxel is not always filled with solely one material but can be a mixture of several tissue types. As mentioned, VRT is a percentage type of classification being more accurate for voxel content display than the all-or-nothing based approach. With this method, the percentage of each predefined density can be calculated for every single voxel. Along the path of view, all the voxels throughout the scanned volume are analyzed with an algorithm aiming to determine the respective content of each predefined tissue type taking into account the chosen color, predefined color interaction, brightness and opacity (defining transparency), and finally preferential shading setting. The computational load in these processes is a multiple of MIP rendering because in the former each voxel contains more data and the displayed pixel in the image must be a representation of the data within each voxel along the line of projection. It is important to understand that these images contain in-depth volume information which is an essential difference from MIP or SSD images. That is why transparency really increases the information of the image whereas in MIP of SSD it does not.

Based on the voxel density histogram, representing the distribution of grayscale values on the Hounsfield Unit scale, different tissue types are defined using ramps or trapezoids. Upward or downward slopes of the ramp or trapezoid can be shaped creating different effects (Fig. 10.2). Overlap between ramps or trapezoids can exist and alters the result.

Different vendors offer several indications or organ-specific presets in the software packages, for example, vascular, bone, or lung tissue presets. The majority allows the user to adapt existing presets or to design new ones to a varying degree.

Although predefined, simple and sometimes more complex tissue-specific presets are available on commercial software one should keep in mind that finetuning is often needed since a standard density for certain structures in angiographic images or bone imaging is assumed. Hence, understanding the processes by which the image can be altered is important. Most radiologists however experience VRT imaging as difficult and time-consuming although the basic principles are simple and once experienced great results can be obtained in just a few minutes.

Cinematic Rendering

First announced in 2016, cinematic rendering is a recent and innovative 3D rendering technique. In contrast to classic 3D VRT imaging which uses ray-casting, now a new global illumination model was proposed [20, 21].

In ray-casting, a local lightning model, light rays are considered solely as straight lines and the only source of light. Whereas in cinematic rendering, additional reflected light and scattered rays are considered. Much more complex algorithms are utilized based on mathematical calculations which in fact handles thousands of light

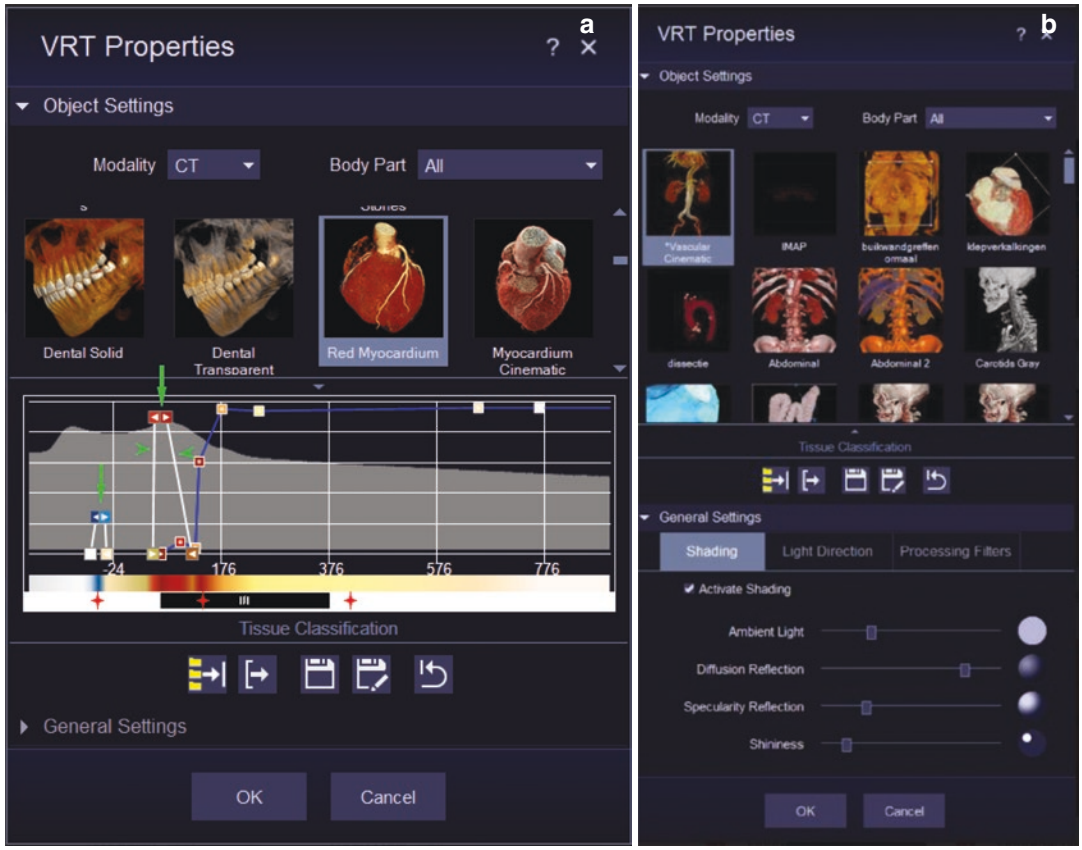

Fig. 10.2 VRT properties as a combination of tissue classification types (**a**) and general light settings (**b**). (**a**) Modern VRT object tissue classification is a body part or tissue designed complex combination of ramps and trapezoids placed on the scan histogram with varying increments of increasing and decreasing intensity (arrowheads), different maximal intensities (arrows), brightness, and different assigned colors (stars). (**b**) Apart from light source direction, shading settings, and extra processing filters can be chosen

rays in a process called path tracing. The resultant is the projection of 3D images in cinematic quality and because of its descent of software from animated film industry, it is called Cinematic Rendering (Fig. 10.3). One of the strong points is the realistic shading that adds extra depth information to the images. In most classic VRT software programs it is not accounted for that one structure can cast a shadow on another. However, in cinematic rendering this obstruction from the light source by overlaying structures is included in the calculation and even the distinction between direct and indirect light is made visible.

Cinematic rendering requires a greatly increased computing power to work smoothly. This problem will be solved with increasing software and hardware capacity in the coming years. Weather to use cinematic rendering or classic VRT is a matter of preference. At this moment the added value of cinematic rendering over classic VRT has yet to be determined in clinical studies.

To conclude, VRT and especially cinematic rendering images lead to a faster and augmented comprehension of complex spatial relations between anatomical structures in comparison to planar imaging in great part due to the human brains capacity for extracting shape and depth information out of subtle shading differences [22].

Fig. 10.3 Cinematic Rendering: example of photorealistic display of the abdominal wall. Notice small bowel loops containing umbilical hernia and left-sided Spigelian hernia

VRT and Segmentation: Editing Step by Step

Although essentially all the information is contained in native axial images in indicated cases, MPR viewing and 3D reconstruction add to the diagnosis and comprehension of clinical cases. In this paragraph, we describe step by step how to produce 3D VRT or cinematic rendered images.

First, the images consisting of a data set of overlapping contiguous slices reconstructed with a noise-reducing soft kernel (convolution algorithm) are loaded into the workstation. If iterative reconstruction is available reconstruct thin slices with a high iterative reconstruction factor. To a certain extent, thicker slices contain less noise than very thin slices (Fig. 10.4); however, one should avoid the slices noted to be too thick because this will show up in the result.

Next, the proper evaluation program within the 3D application is selected and initiated. For analysis, it is preferred to combine three orthogonal MPR images (axial, sagittal, and coronal) with a VRT image. Loading the series of axial overlapping reconstructed slices in the MPR mode initiates a computational process at which the data from the slices are used to create a volume by interpolation. In this volume, non-overlapping slices can be made not only in coronal, axial, or sagittal direction but in any desired orientation. Slices thickness in MPR mode can be chosen from submillimeter to several millimeters.

For example, when a volume is scanned using a 64 times 0.6 mm detector collimated slice, this can subsequently be reconstructed into a series of 1.5 mm thick image slices with an increment of 1.2 mm per slice. Once loaded into the 3D workstation after interpolation a volume is created in the MPR environment and submillimeter continuous slices up to 0.7 mm can be made in every desired direction. This feature gives a smooth VRT appearance without typical "steps" in the images.

Then, in the VRT properties an object setting or preset is chosen. Since specific abdominal wall presets are rare, it is recommended to start with a vascular or soft tissue setting or at least a setting that gives you a natural realistic anatomic-colored appearance of the abdominal wall musculature after window and level adjustments. If possible, use a setting with a predefined active shading. Modifications are basically made on the image histogram. This is, like in photography, the graphical representation of the number of pixels in an image as a function of their intensity. However, for CT imaging we consider voxels instead of pixels and the intensity scale is replaced by the density scale of Hounsfield. Begin with a trapezoid starting from one side of the Hounsfield spectrum and create an object with an opaque skin. This gives an image resembling the clinical situation. This can be done by moving the trapezoid to the left side of the histogram curve and/or changing the window width and level so more pixels with low density are covered under the trapezoid. Start windowing by sliding the ramp to the right side of the histogram curve until abdominal wall musculature becomes visible. Further exaggerating this windowing would show progressively structures with higher density such as

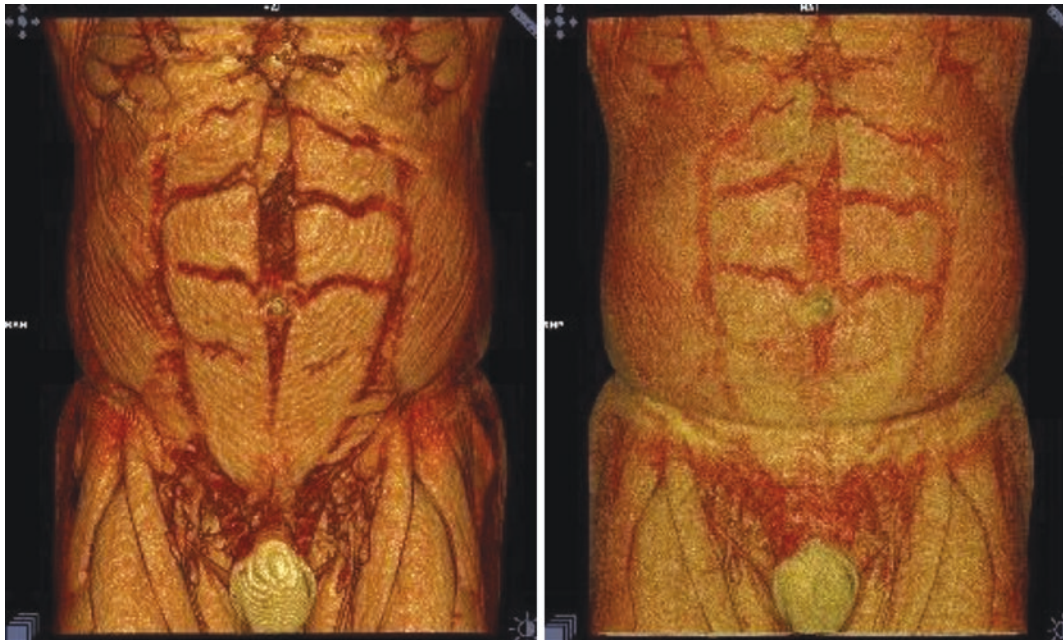

Fig. 10.4 Effect of slice thickness on image noise: VRT reconstructions (corresponding MPR images not shown) out of 2 mm (left) and 1 mm (right) reconstructed slice thickness. Both images with identical window settings. Notice the more clearly anatomical depiction and less noise on the left image

vascular structures in case of intravenous contrast administration (Fig. 10.5a) and eventually skeletal bone independent of contrast application (since bony tissue has the highest density).

To get the abdominal wall view, the window width and level must be changed in such a way that abdominal fat becomes transparent. The left part of the trapezoid must cover a part of the histogram with negative density from 0 to −100 HU. The other part of the ramp must at least cover the density of muscular tissue between 40 and 80 HU, increasing to nearly 100 HU when intravenous contrast is applied.

Assessment of abdominal wall musculature can be now made with rectus abdominis muscle, linea alba, linea semilunaris, and external obliques on both VRT and cinematic rendered images (Fig. 10.5b). This can be even better appreciated when skin is removed with manual cutting or placing of a clip plane. In fact, skin can act as an overlying surface of noise. Although a global overview with opaque skin settings may have some clinical value, often focal selective punching or cutting away the skin is preferred and may improve the result (Fig. 10.6a and b). Trying to window the skin to zero is not advised because it would also degrade residual volume because skin has nearly identical density as muscle. After skin removal, abdominal wall musculature is clearly visible and any diastasis or defect can be appreciated.

At this point herniated content may already have become visible. The visibility of the hernia and its content is function of several factors. For a hernia sac to be visible, the wall of the sac must have a higher CT density than the external surrounding tissue so it must be remarkable on MPR images. As a rule of thumb evaluation of the MPR image must clearly show the wall of the hernia sac, only then it will be visible on the VRT reconstruction to a more or lesser degree. If the wall of the sac is too thin then it can be discernible indirectly only if fluid or intestines in the sac are abutting the border.

Hernia content is often a combination of fatty tissue, vascular structures, fluid and intestinal loops with or without positive oral contrast or air (Fig. 10.7a). the more fat containing the hernia,

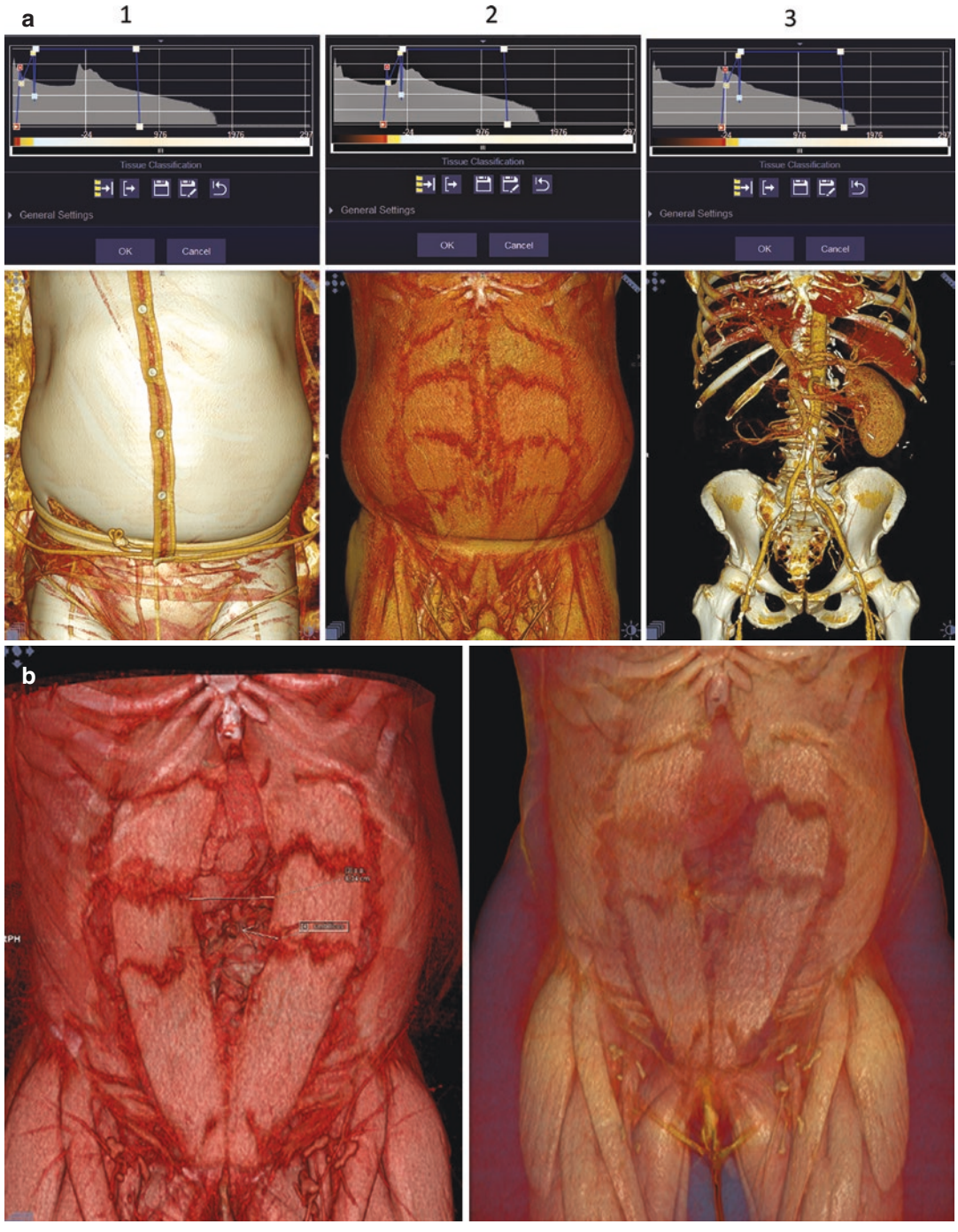

Fig. 10.5 (**a**) Influence of changing window level on the histogram curve (above) on resultant image (below). (1) structure with "skin-tissue" view, (2) "muscular" view, and (3) "vascular" view: the more the trapezoid is placed to the right side of the histogram, the lesser low-density structures are visible and the more bone and contrast containing structures become visible. (**b**) Depiction of abdominal wall anatomy by classic VRT (left) and Cinematic Rendering (right) allowing evaluation of rectal diastasis

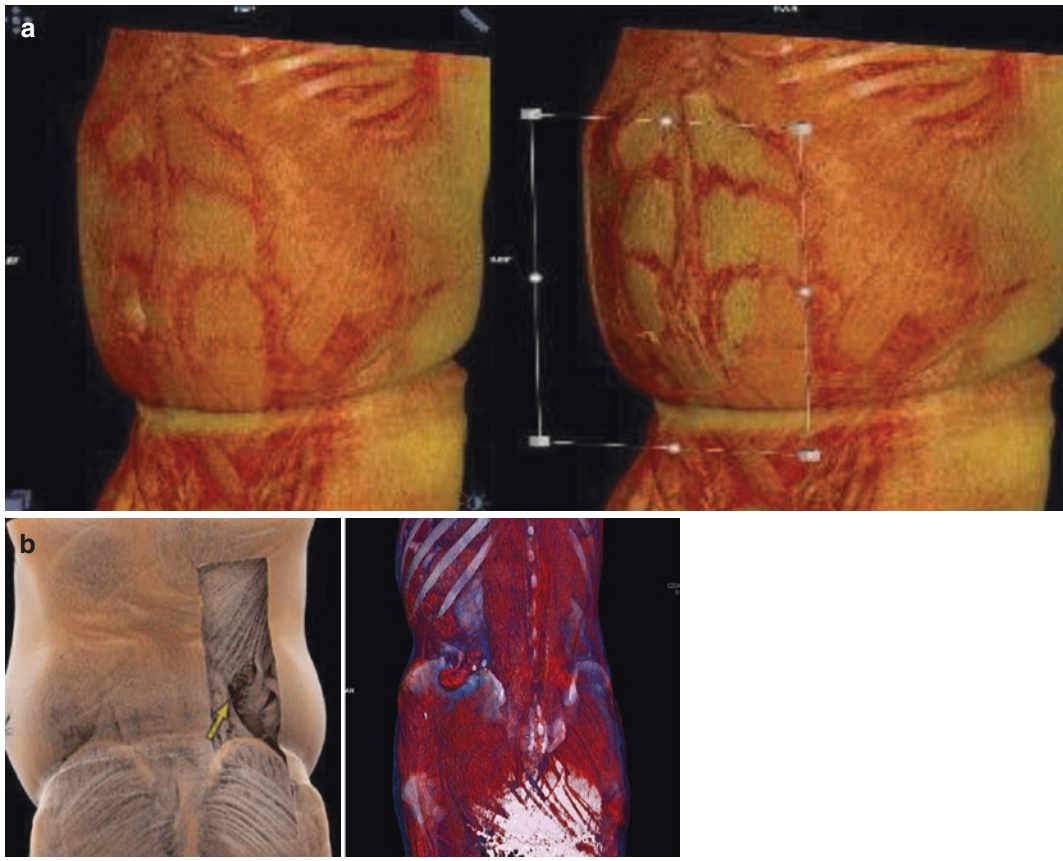

Fig. 10.6 (**a**) Disturbing effect of the overlying skin. Skin can be seen as an overlying layer of noise. Left image: skin not removed, right image: skin removed by anterior placed slab plane. (**b**) Left: Patient with small lumbar Grynfeltt-Leshaft hernia best seen after cutting part of dorsal skin by clip plane. Windowing skin to zero would also eliminate visualization of most of the muscle fibers. Right: VRT reconstruction of left-sided intestinal hernia after crest harvest, skin totally removed

the lesser the visualization of the hernia sac on VRT image will be even if intravenous contrast is administered. Iodinated contrast would enhance the lumen of protruding vessels and enhance the mucosa of any bowel loops however wall enhancement of the thin hernia sac is not generally seen.

The exact composition of the herniating structures will thus determine its visibility on 3D reconstruction. The ideal hernia to visualize with VRT would be a hernia sac with contrast-accentuated vessels and positive contrast-filled bowel loops with nearly no fat.

If the hernia is exclusively or predominantly fat-containing then one should keep in mind that setting the fat tissue transparent on VRT also deletes the lipomatous content of the hernia sac and not setting it transparent would make it indiscernible with subcutaneous fat. In this case manual segmentation with contour editing and automated contour interpolation of the hernia sac may be the only option (Fig. 10.7b,c) (Videos 10.1, 10.2).

One can discuss whether the administration of peroral, retrograde, and/or intravenous contrast is an added value for hernia depiction and evaluation. Each type of administered contrast increases the possibility of a better differentiation between different density structures within the hernia sac, but also from the surrounding tissues including the abdominal wall itself. The more distinct densities, the easier isolation of structures will be

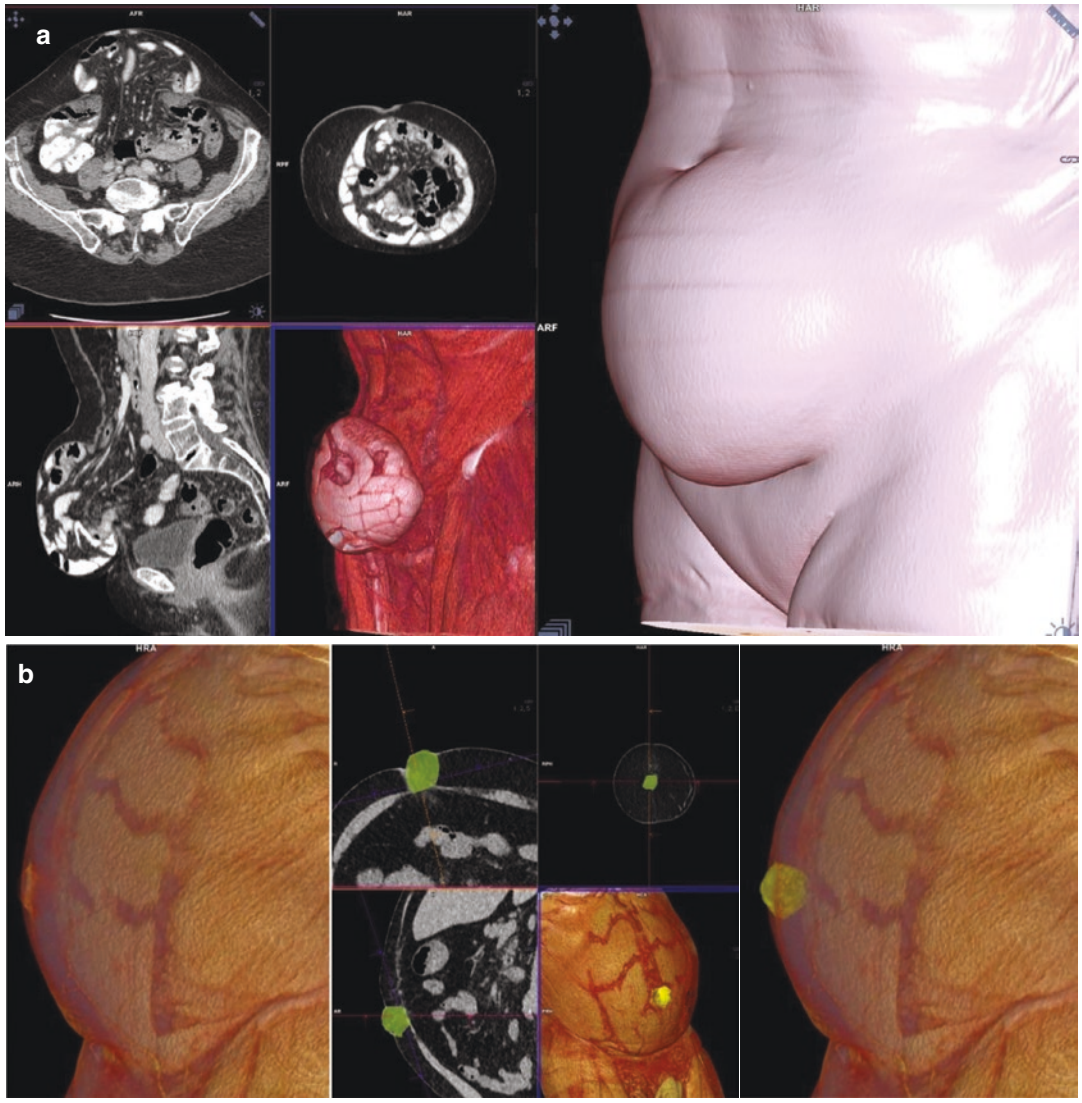

Fig. 10.7 (**a**) Influence of hernia sac content on visualization. Hernia containing bowel loops with significant oral contrast content. Small images: MPR images (axial, coronal, and sagittal) and VRT images Large image right: corresponding "clinical" VRT image. (**b**) Solely fat-containing hernia: cinematic rendering image without and after semiautomated segmentation (see also Video 10.1) Notice invisible hernia without. (**c**) Parastomal hernia with herniation of transverse colon, vessels, and fat adjacent to permanent stoma. Upper row: sagittal MPR image (left), VRT with segmentation of total hernia content (middle), and VRT with segmentation of only intestinal component (right). Below: segmented volume superimposed on 3 orthogonal MPR images

and the more pronounced the tissue contrast in the VRT image. Extensive administration of retrograde or peroral contrast could lead to altered proportions of intra-abdominal content versus hernia content by filling up and distending the herniated bowel loops. However, one can argue that it is merely physiological that the contents of both the herniated sac and intra-abdominal contents change during the day as a result of meals and bowel movements.

Peroral and especially retrograde contrast agent administration in the form of iodinated contrast agents or negative contrast agents such as water requires patient cooperation, a longer

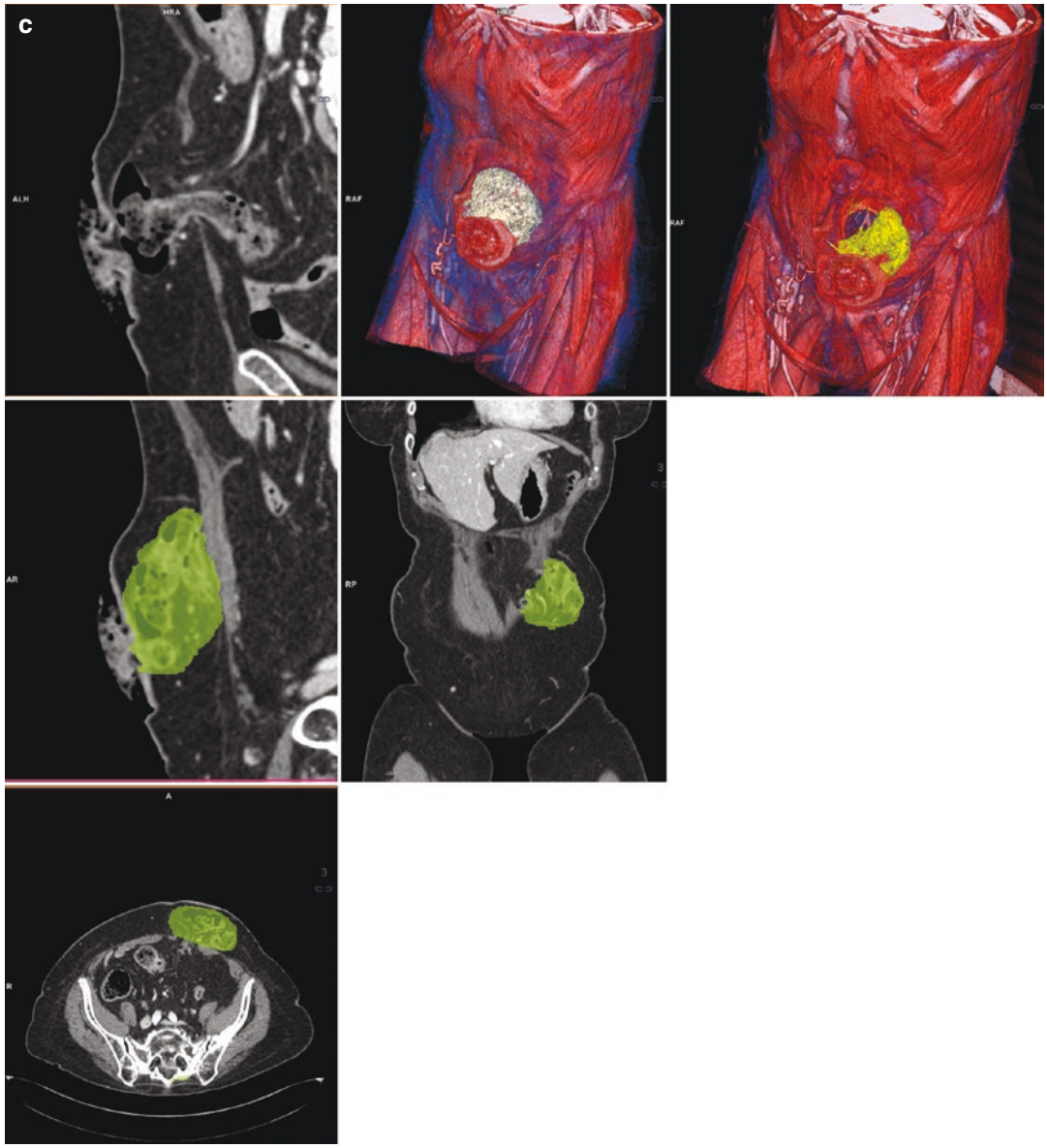

Fig. 10.7 (continued)

preparation time, and makes the investigation more invasive. There is no guarantee that the contrast will be in the herniated bowel loops at the time of the examination. In cases of known or suspected bowel wall protrusion opacification of the herniated loop add in hernia visualization, for example, in pelvic floor hernia (Video 10.3) or Petit hernia (Video 10.4). Intravenous administration of iodinated contrast agents is more invasive and there are several contraindications such as known allergies and impaired kidney function. The difference in the image is limited to the wall and luminal enhancement of the protruding intestinal and vascular structures, respectively. Therefore, no difference can be expected in solely fat-containing hernias. For the musculature of the abdominal wall, no significant differences can be expected (Fig. 10.8).

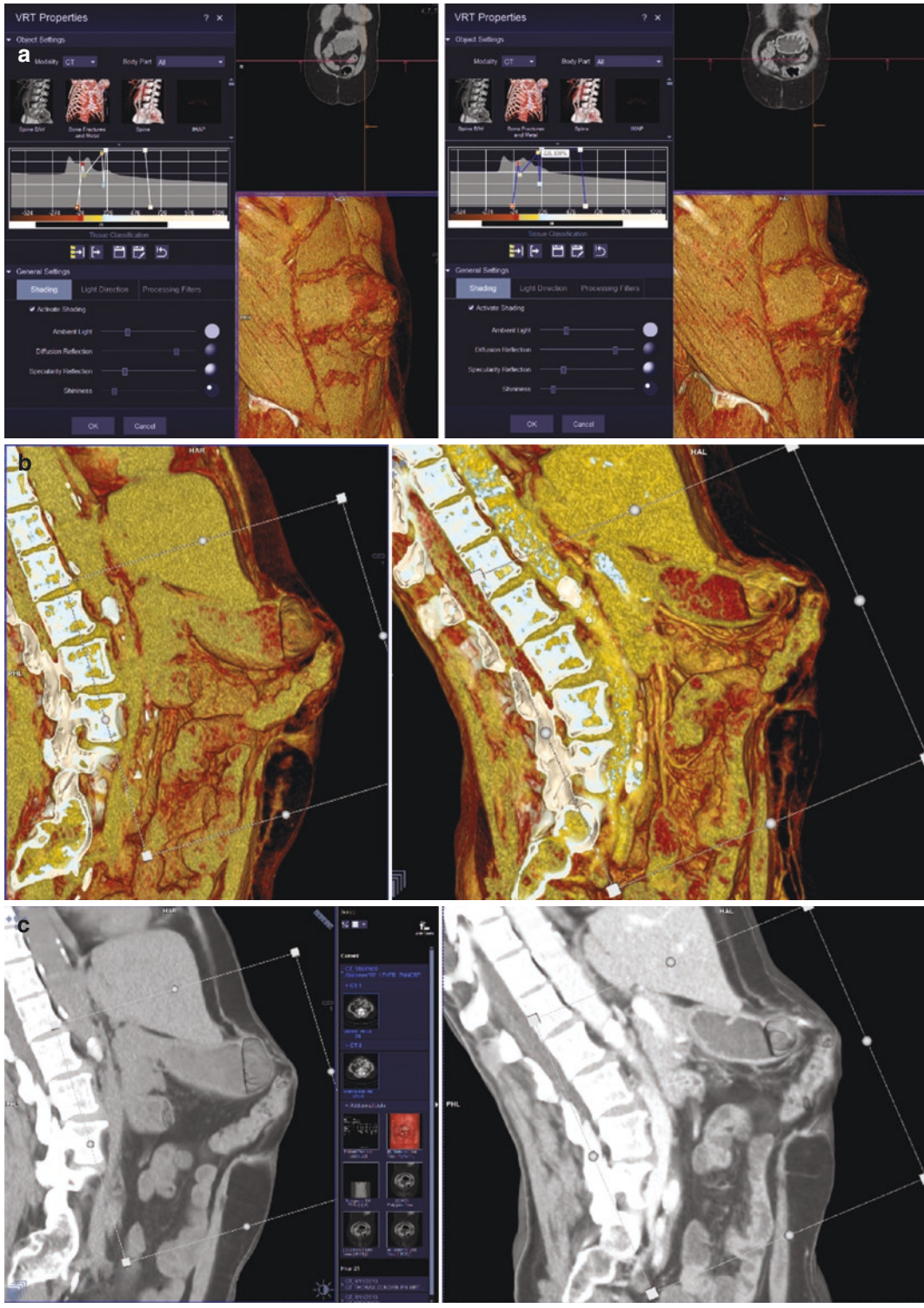

Fig. 10.8 Comparison of abdominal wall hernia pre-contrast (left) and post-contrast (right). (**a**) No significant differences are evident for abdominal wall without and with IV contrast. (**b** and **c**) Better delineation of hernia content on VRT in color mode (**b**) and in grey mode (**c**) showing vasculature and bowel wall enhancement

For ventral abdominal wall hernias sliding with a clip plane or slab through the scanned volume in a perpendicular direction relative to the direction of herniation will allow you to align the slab plane with the plane of the wall defect defined by the hernia ring at the level of the abdominal wall opening (see Videos 10.1, 10.2). Once the correct angulation at the exact depth is achieved various quantitative measurements can be performed, such as the maximum craniocaudal and transverse diameters, the circumference, and especially the surface of the hernia ring (Fig. 10.9). There is a risk of over- or underestimation of these dimensions depending on the

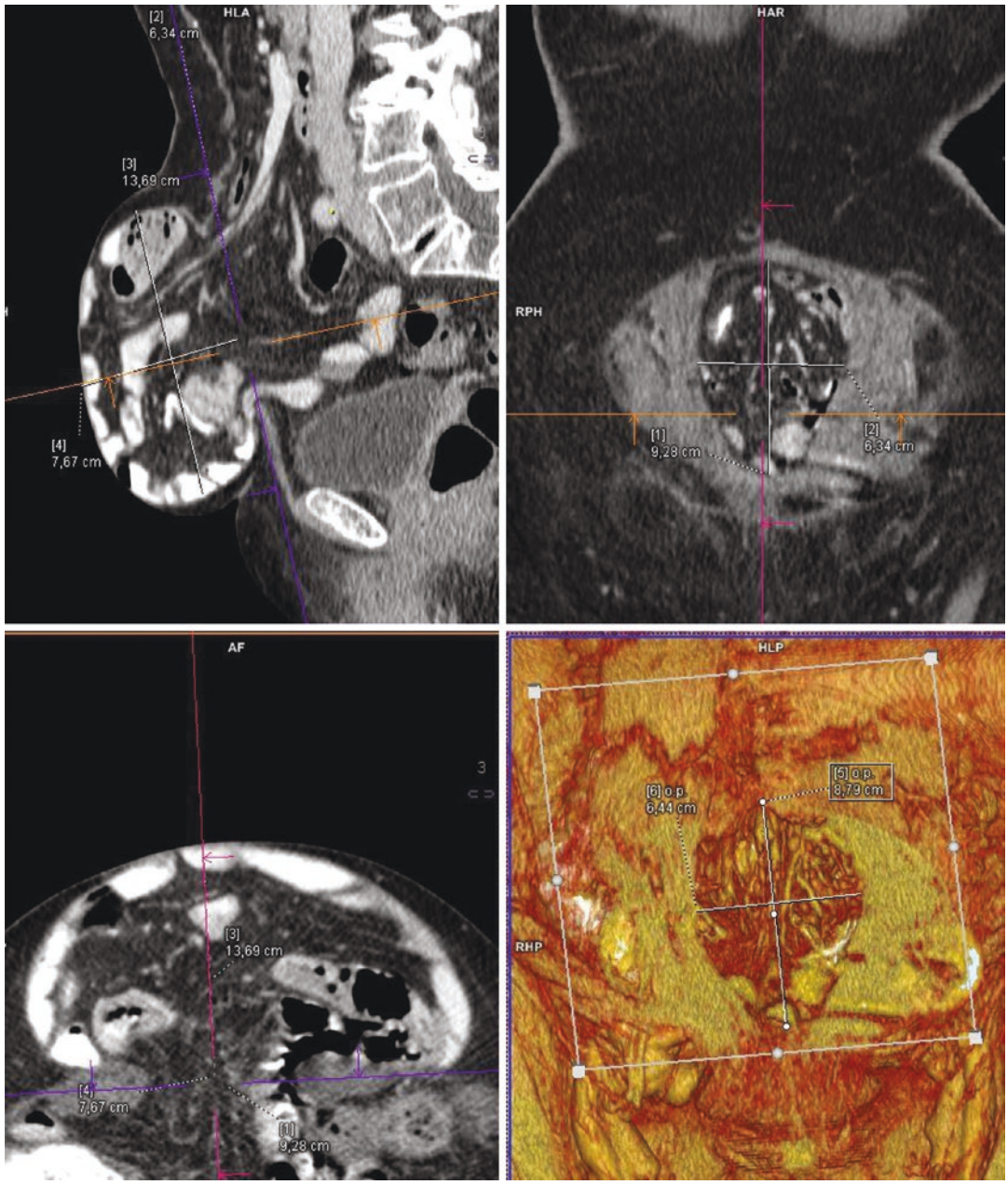

Fig. 10.9 Measurements of hernia ring dimensions and hernia sac dimensions on MPR images and hernia ring on VRT reconstructed image using slab plane

morphology of the hernia with conical hernia type being more challenging than the mushroom type, especially with very thin abdominal musculature. Diameter assessment on correctly orthogonal angled MPR remains the golden standard or should at least be used as a control.

With several computer software packages, it is now possible to step up to more advanced editing allowing to isolate, add, or delete selected structures within the imaged volume. Using thresholding voxels within a given range are selected. Region-growing algorithms will select adjacent voxels near a selected point with similar density. Region on interest selection, manual or semi-automated using automatic contour recognition on individual slices with or without interpolation between edited slices are possible. Although some software programs allow automated organ selection to our knowledge, automated muscular abdominal wall selection is not available.

Each segmented volume can be seen as a separate layer and, certain parameters can be set for each layer like transparency, brightness, color, and even a specific predefined VRT setting. In the final result, one or more layers can be combined to accentuate or erase certain structures (Fig. 10.10a,b). This is a relatively time-consuming technique depending on the level of experience. In many cases, a custom-made solution can be presented in the final result.

Morphometrics and Quantitative 3D CT Imaging

It is well known that hernia repair is much more complex than simply reducing herniated content into the abdominal cavity and closing the defect. Operative strategies change with different types and volumes of hernia with the intent to reduce the risk of complications such as abdominal compartment syndrome, respiratory problems, and re-herniation. Many parameters have to be considered including height, weight, and BMI of the patient. In recent years CT-derived measurements of hernia characteristics have gained importance in preoperative workup. Where initially some of these measurements were performed on basic CT scans, nowadays more and more use is being made of measurements performed on 3D volumetric CT data.

Kavic et al. [23] rendered dynamic three-dimensional computed tomography-based models of hiatal hernias by applying a polygonal mesh surface modeling technique. Their research clearly showed the added value of incorporating sophisticated 3D rendering software in clinical practice not only for advancing and clarifying existing classifications but mostly for the clinical benefit that a comprehensive graphic illustration made in an intuitive fashion would have on the surgeon.

Sabbagh et al. [24] calculated peritoneal volume and compared it to herniated volume by using semiautomated volume calculations offered by specific software programs (Myrian ® Expert) in contrast to Tanaka et al. [25] who used estimation of herniated volume by measuring maximal orthogonal diameters of abdomen and herniated sac and applying these values on volume formulas of ellipsoids.

In 2012, Yao et al. [26] showed in a population of 17 patients with incisional hernia that based on 3D CT reconstructions from submillimeter volume scans abdominal wall hernia area and volume and abdominal cavity volume could be accurately measured using 3D software packages. Like Sabbagh, they also used the calculated ratio of herniary volume to abdominal volume.

Xu et al. [27] investigated a detailed anatomical labeling protocol for description of ventral hernias taking into account 20 derived metrics that could be divided in shape-related, location-related, and body-related metrics. For anatomical labeling MPR measurements were sufficient and auteurs did not find complex 3D rendering an added value while for volumetric measurements interpolation techniques and tri-planar manipulation were needed. Still for the presentation of results, transparent volume rendering techniques with superposition of measurements were used, for example, to demonstrate different hernia types.

Kao et al. [28] found that CT-based volumetric measurements are a valuable tool in preoperative evaluating of the extent and complexity of

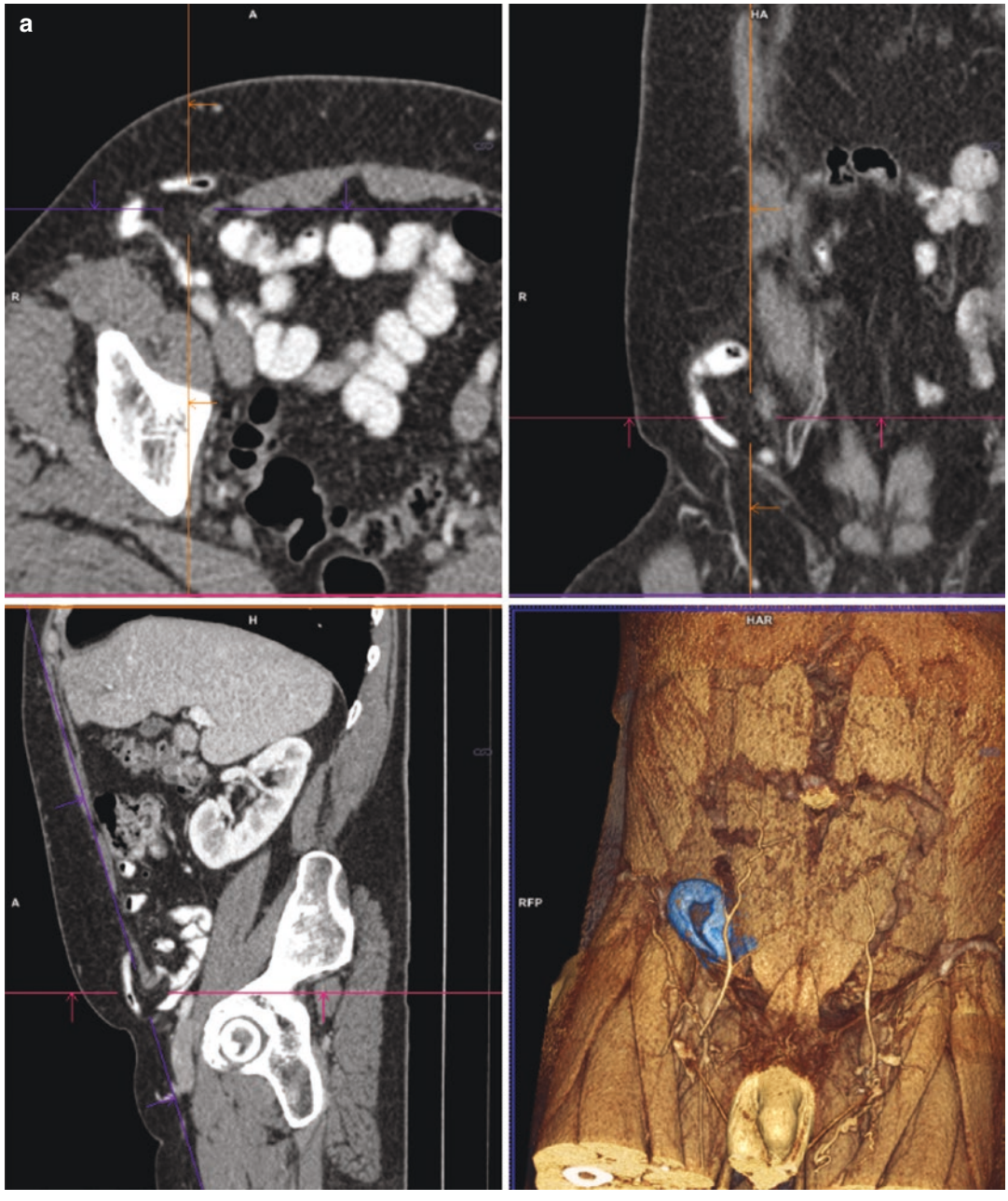

Fig. 10.10 (**a**) Advanced editing—a patient with bulging right-sided intestinal loop containing inguinal hernia: MPR images and Cinematic Rendered image after selective segmenting and editing hernia sac allowing increased visibility of hernia content. (other patient see also Videos 10.3 and 10.4). (**b**) Advanced editing - Left posterior oblique(left) and right posterior oblique (right) internal view on the abdominal wall showing rupture of the left transverse abdominal muscle with forming of a double ridge and hernia sac with bulging and stretching of the oblique abdominal musculature. Editing steps consisted of manual skin removal and semiautomatic removal of the intra-abdominal contents with interpolation. Finally, plane cuts of the volume in craniocaudal direction to reveal the relevant parts and cutting of the spine and surrounding musculature to create an inlet view. Axial MPR image (bottom)

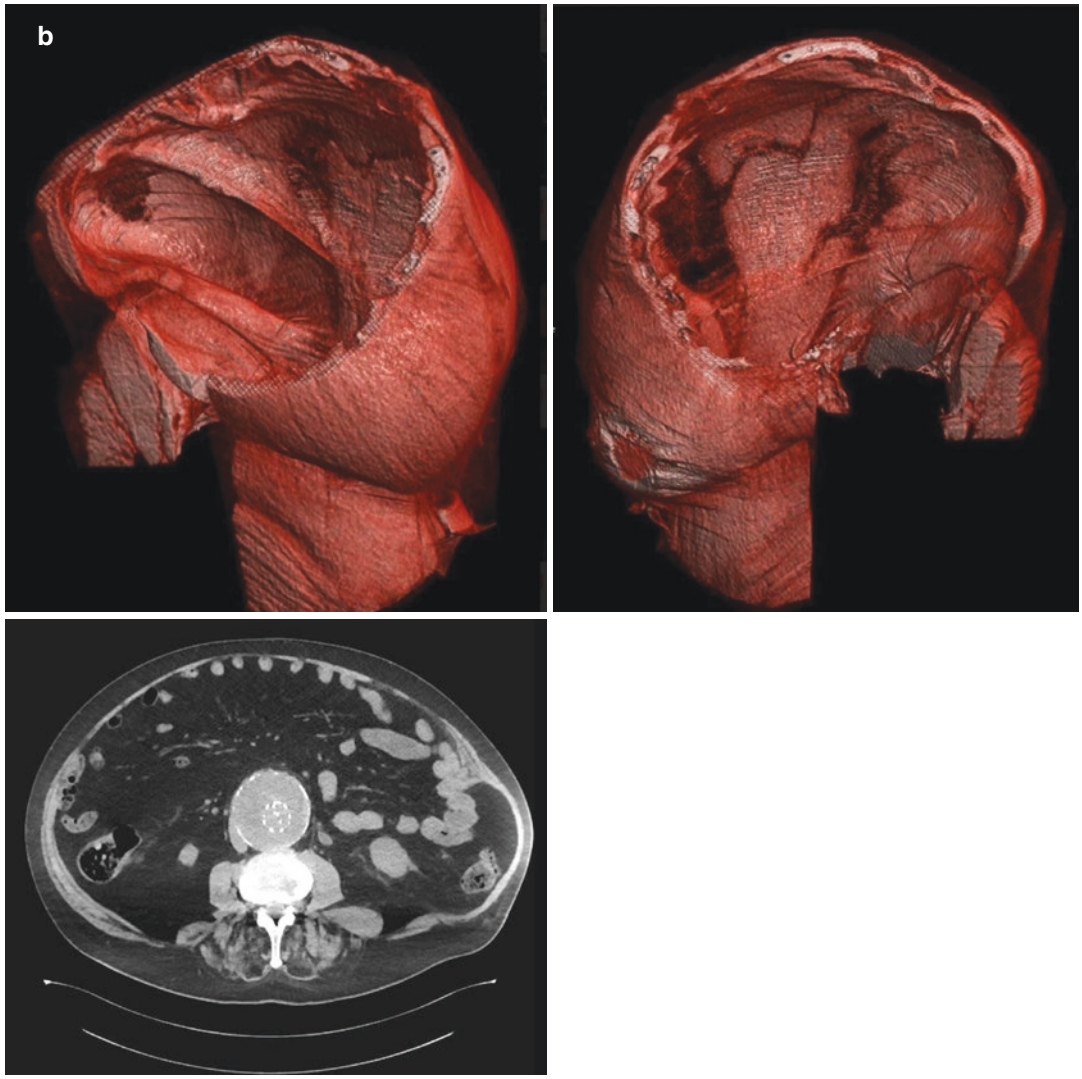

Fig. 10.10 (continued)

para-esophageal hernia that allows the surgeon to decide on an operative approach and to anticipate a difficult crural repair. By using volumetric analysis software hernia defect area or crural defect and hernia sac volume were measured. Not only volume measurements but also multidimensional visualization added in preoperative planning and approach decisions.

Finally, Winters et al. [29] found that the use of extensive CT scan-derived abdominal morphometrics, although time-consuming at this moment, allows a better quantitative risk analysis for the component separation repair technique when performed for solving complex ventral hernias. They determined visceral fat volume, loss of domain, subcutaneous fat volume, total fat volume to predict the recurrence of herniation, and surgical site infection. Analysis was performed on dedicated workstations with semiautomated measurements (Fig. 10.11). This combination of a 3D VRT and quantitative evaluation of morphometric parameters is also recently seen in Elstner's research [30] where the effect of selective botulinum toxin A injection in the

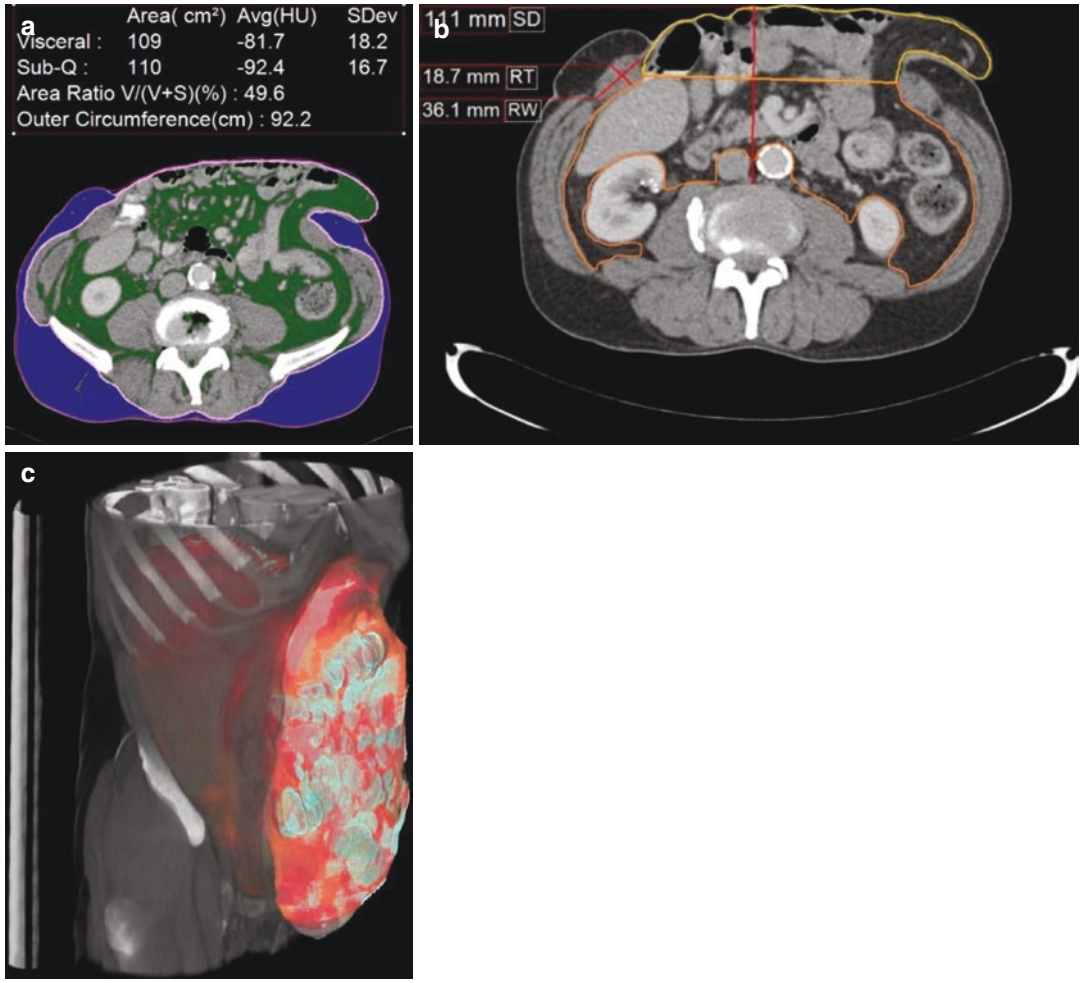

Fig. 10.11 (**a**) Quantification of visceral (green) and subcutaneous (blue) fat. (**b**) Outline of intra-abdominal area (orange line) and hernia sac (yellow line). (**c**) 3D VRT reconstruction of the abdomen: colored parts represent segmented hernia and intra-abdominal content used for volume calculation. From Winters et. al Hernia 2019;23: 347-354 with permission

oblique abdominal muscles is investigated and emphasizes the complementarity of both modalities within the context of a comprehensive preoperative CT examination.

3D Techniques in MR Imaging

Del Olmo et al. [31] found MRI an effective tool for an adequate preoperative depiction of abdominal wall defects and hernia sac content. Moreover, with regards to postoperative follow-up, they concluded that MRI is useful for evaluating mesh integration, diagnosis of hernia recurrence, and evaluation of complications.

Currently, MR is not routinely used for preoperative evaluation of the abdominal wall. The geometric features of respiratory-triggered clinically available 2D sequences are simply not good enough to allow 3D reconstruction with an acceptable resolution or voxel isotropy. Although 3D sequences exist that produce isotropic voxels in MR imaging, these sequences require an absence of motion during acquisition, so breath hold is strictly mandatory. Even then they are relatively slow. Consequently, only limited vol-

umes can be imaged during one breath hold in contrast to a CT scan where whole abdominal imaging in a few seconds is obtained. On the other hand, with MRI the tissue contrast of an abdominal wall defect or herniated content is of no added value compared to this on CT. Visualization of abdominal wall hernias with MR is therefore inferior to CT scan.

It is well known that abdominal wall repair is one of the most frequently performed surgical procedures nowadays. The procedure has evolved towards general use of prosthetic implants for several reasons including lower complication and recurrence rates, lower morbidity, and ease of use. Consequently, mesh implants have undergone a rapid evolution with, among other things, different design and properties. After surgical implantations complications can include shrinkage or deformation, migration with or without erosion, infections, fistulation, and chronic pain or discomfort. Ideally, all mesh types would be clearly visible to rule out mesh-related complications, to avoid unnecessary exploratory surgical laparoscopy or even for preoperative localization and strategy of approach.

Rakic and Leblanc [32] made a literature overview of the radiopaque properties of meshes commonly used in hernia repair. They found that for CT imaging expanded polytetrafluoroethylene (ePTFE) showed a strong difference with the surrounding tissue with a high density (Fig. 10.12). In addition, structure and thickness of the mesh were found to be important factors for visibility. With MRI the contrast between the mesh and the surrounding tissue is weak and generally mesh visibility ranges from not visible at all over faintly visible to always visible (polytetrafluoroethylene Dualmesh® (Gore)). Some of the meshes like polypropylene and polyester composed types are merely visible as a result of the secondary periprosthetic inflammatory response they induce. Consequently, reliable, reproducible mesh dimension or position calculation is not possible.

With the introduction of MRI-visible meshes consisting of a polyvinyliden fluoride base material with integrated iron particles (Dynamesh©FEG Textiltechnik Aachen Germany) direct and clear visualization of mesh became possible [33–35]. Placed in the magnetic field from MRI these iron particles will cause local disturbances in the magnitude of the magnetic field. The consequent susceptibility artifacts are the result of microscopic gradients or variations in the magnetic field strength that occur near the interfaces of substances of different magnetic susceptibility. On an image, they are visible as black spots without signal (signal voids). Consequently, the mechanism of mesh visualization is based on the generation of dark hypointense susceptibility artifacts that form a strong image contrast with the surrounding tissue, the hyperintense abdominal fat, isointense overlying muscles, adjacent hyperintense fluid or fluid-containing intestinal loops (Fig. 10.13).

Most protocols consist of a combination of gradient echo sequences and T2 TSE sequences, the former for mesh visualization and the latter for anatomical assessment. Otto et al. [36] reconstructed a 3D model out of MRI data of an intra-peritoneal placed pre-shaped 3D parastomal mesh implant in a porcine model. Sindhwani et al. [37] performed a complex 3D analysis of MRI-visible meshes implanted to resolve severe anterior vaginal wall prolapse. Brocker et al. [38] were in search for the development of a 3D technique to evaluate postoperative dimensions and location of MR-visible pelvic Fe3O4-polypropylene implant.

Muysoms et al. [39] used MRI of oxide-loaded PVDF mesh in vivo to measure mesh shrinkage over time. They found less than expected mesh shrinkage over a 12-month interval and low inter-reader variability for quantitative mesh evaluation. Sagittal 2D FFE sequences were used to make thick coronal MinIP projections used for geometric analysis (Fig. 10.14a). This measurement can be performed on most clinical PACS workstations within a few seconds. Slab thickness should be as low as possible but minimal equals anterior posterior diameter of the mesh. Even volume reconstructions can be made from these non-isotropic 5mm thick images because of relatively high image contrast with both surrounding fat and overlying muscles (Fig. 10.14b). The use of this multiparametric free breathing MRI protocol performed in the

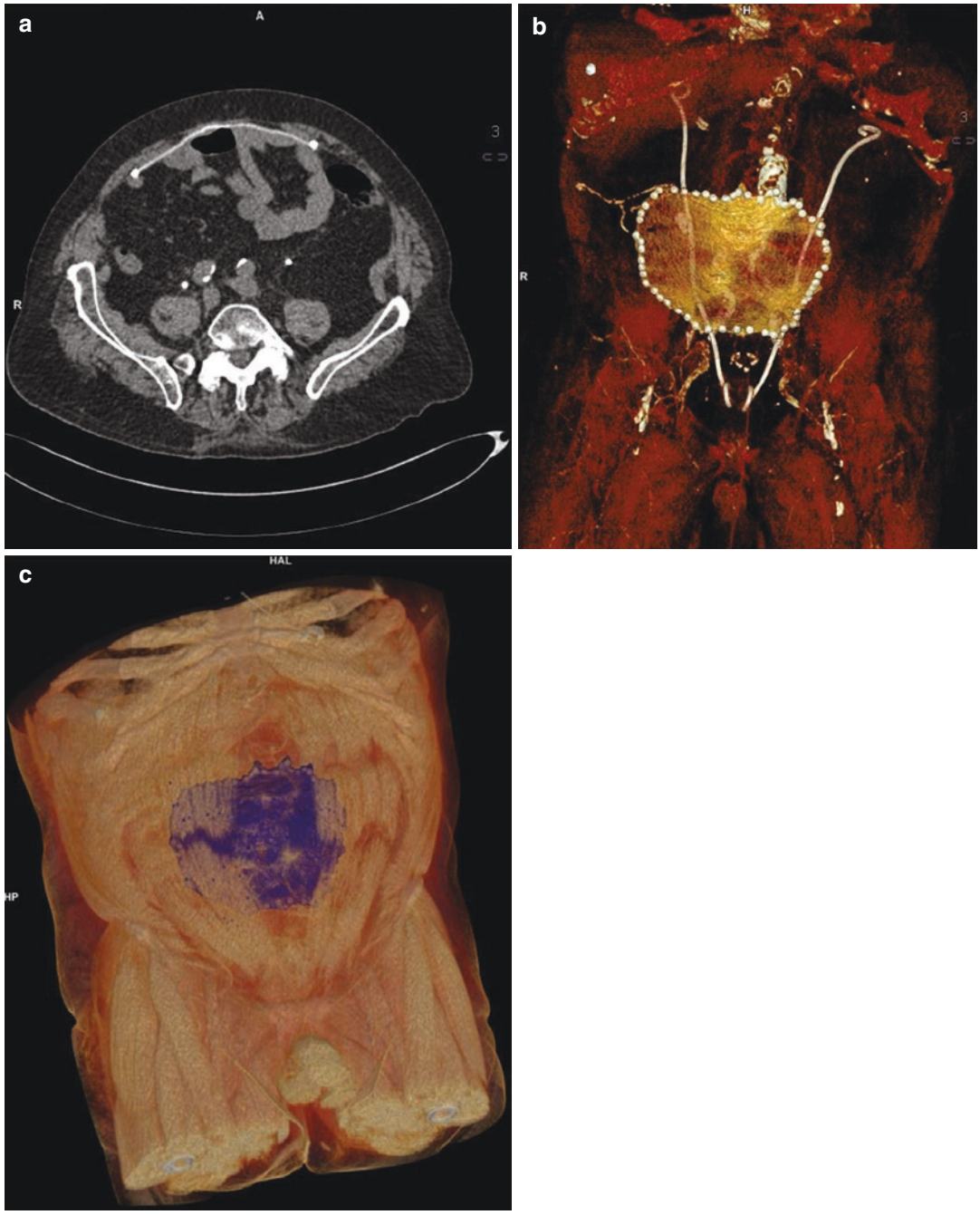

Fig. 10.12 Visibility of ePTFE mesh on CT. (**a**) Axial CT image. (**b**) Classic VRT. (**c**) Cinematic Rending technique image after isolation of mesh shows the relation between mesh and overlying rectus abdominus muscles as a result of partial transparency of abdominal wall and augmented intensity and brightness of the segmented mesh

prone position using the table built in posterior coil allows a complete evaluation of the ventral abdominal wall or groin MRI-visible mesh in less than 20 min. Furthermore, it is a safe investigation without the use of ionizing radiation or intravenous contrast injection that is highly reproducible. Main indications would be ruling out postoperative hematoma or other fluid collec-

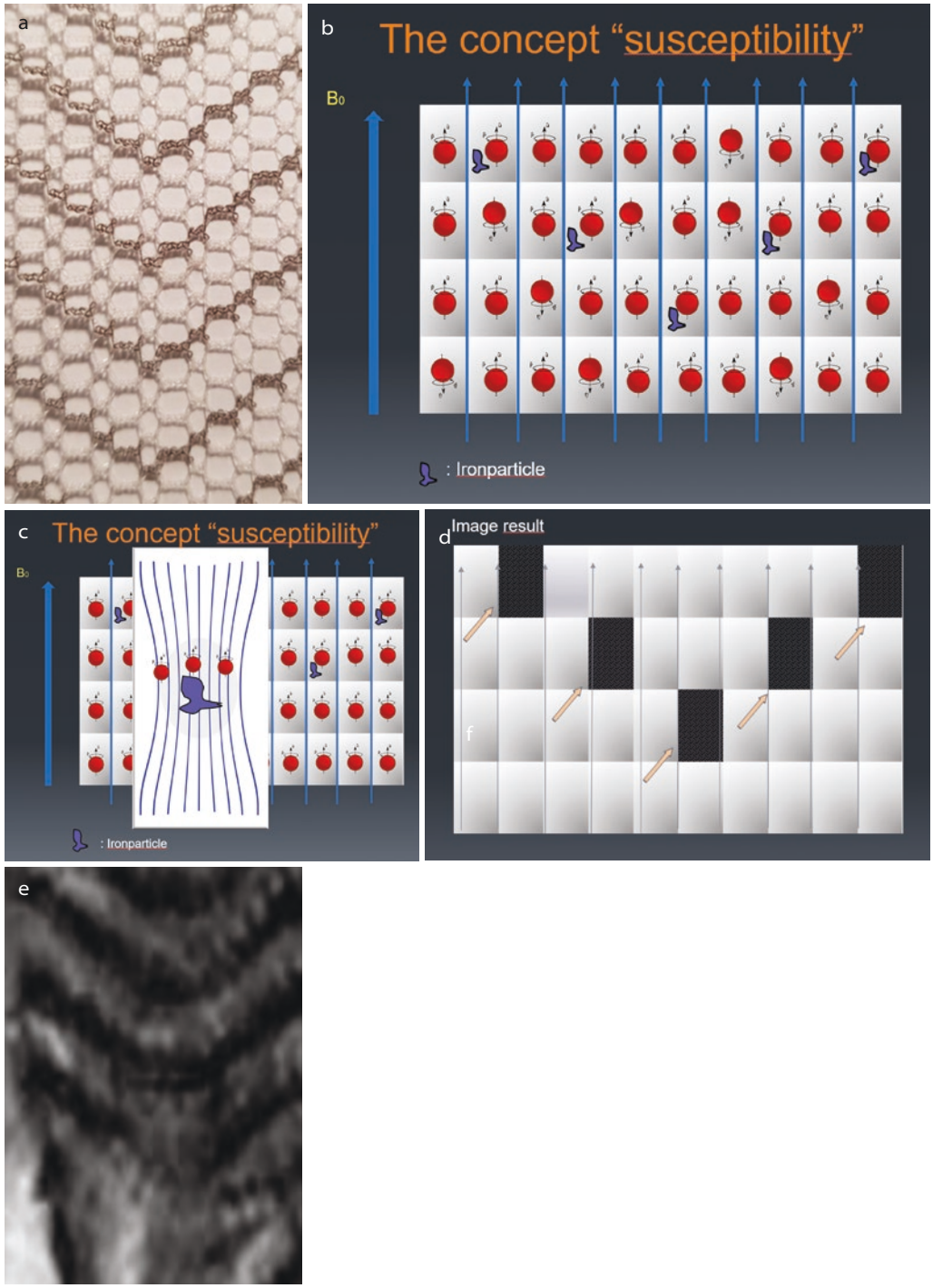

Fig. 10.13 Mechanism of iron-loaded mesh visualization. (**a**) Detailed picture of morphology of mesh containing incorporated iron particles. (**b**) Schematic presentation of mesh placed in external magnetic field B0. Small rectangles represent voxels containing H-nuclei however some also contain iron particles. Vertically extending arrows represent magnetic field lines. (**c**) Local disturbance of magnetic field nearby iron particles with the focal attraction of magnetic field lines (blue lines). (**d**) The resultant image will show dark "spots" at places of focal field disturbances. (**e**) Corresponding MR image of mesh

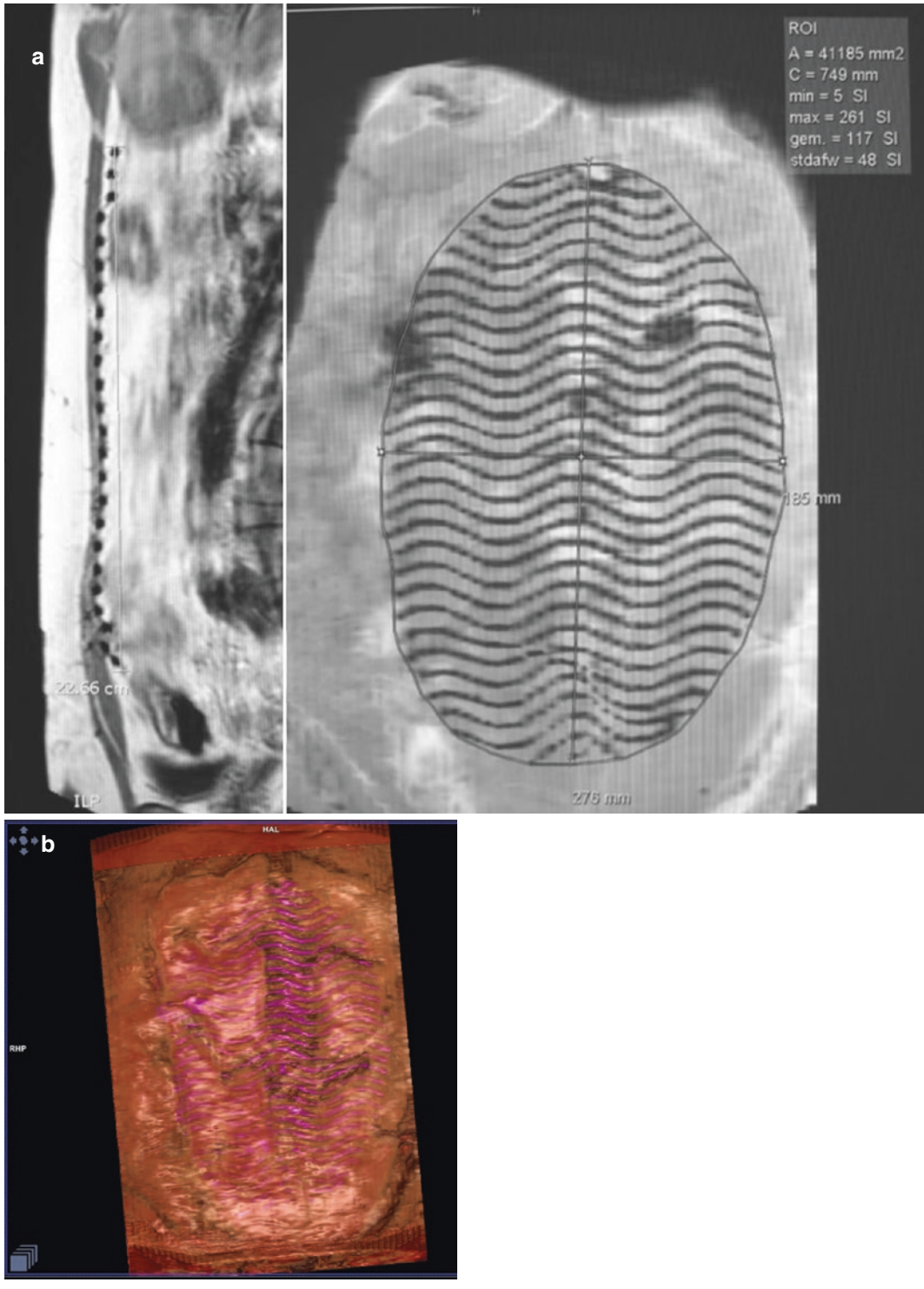

Fig. 10.14 (**a**) Left: Sagittal IF FFE native image slice (thickness 5 mm) through the anterior abdominal wall Right: Thick MiniP reconstruction (20–40 mm thickness) to determine projected surface, diameters, and circumference of MR-visible mesh. (**b**) Other patients as in a/3D VRT reconstruction out of 2D FFE Sagittal images. Partially transparent abdominal wall with increased intensity and brightness of segmented mesh

tions in cases of abdominal pain or discomfort and evaluation of mesh position with approximation of the mesh with the abdominal musculature using T2 and T1 gradient images.

A fast 3D T1 sequence with short TE and TR allows for nearly isotropic millimetric imaging and creates the basis for in-depth 3D analysis in mesh phantom imaging (Fig. 10.15) but also for clinical

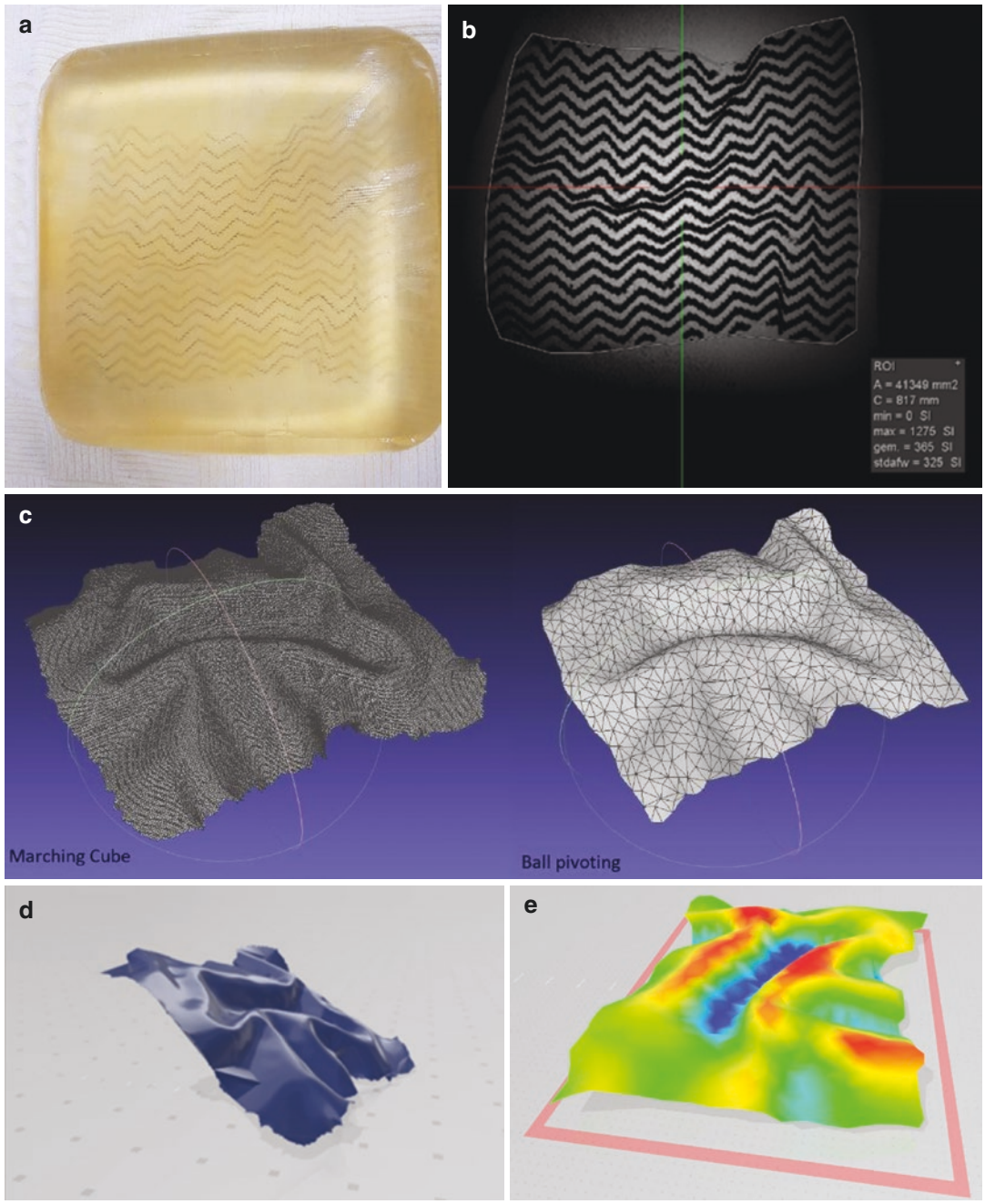

Fig. 10.15 (**a**) Agaragar incorporated mesh used for 3D T1 imaging. (**b**) Thick coronal MinIP projection of resultant 3D T1 image stack. (**c**) 3D reconstruction of the meshes using ball pivoting and marching cubes algorithm for surface calculation and curvature evaluation. (**d**) Corresponding 3D rendered model as STL file. (**e**) Color-coded surface curvature map (unpublished work in progress)

use. Thanks to a short TR and short TE (4.6 and 2.3 ms) more than 100 images can be made in less than 1 min. The strong contrast between mesh and surrounding tissue, such as fat and muscle, allows isolating the mesh out of this volume. Moreover, owing to the isotropic resolution, high-resolution 3D images can be calculated using various techniques. However, mesh isolation can be disturbed to a certain degree in the case of abutting intestinal air since it has an equal signal intensity.

For morphologic and basic geometric analysis the stack of images can be loaded into a dedicated workstation the same way as a CT volume (Fig. 10.16a). With appropriate window setting consisting of a reversed ramp and proper shading settings, the mesh can be made visible as an opaque structure. Manual editing of the mesh by removing other tissue results in the isolation of the mesh (Fig. 10.16b). Creating rotating image series or movies can help to increase the 3D

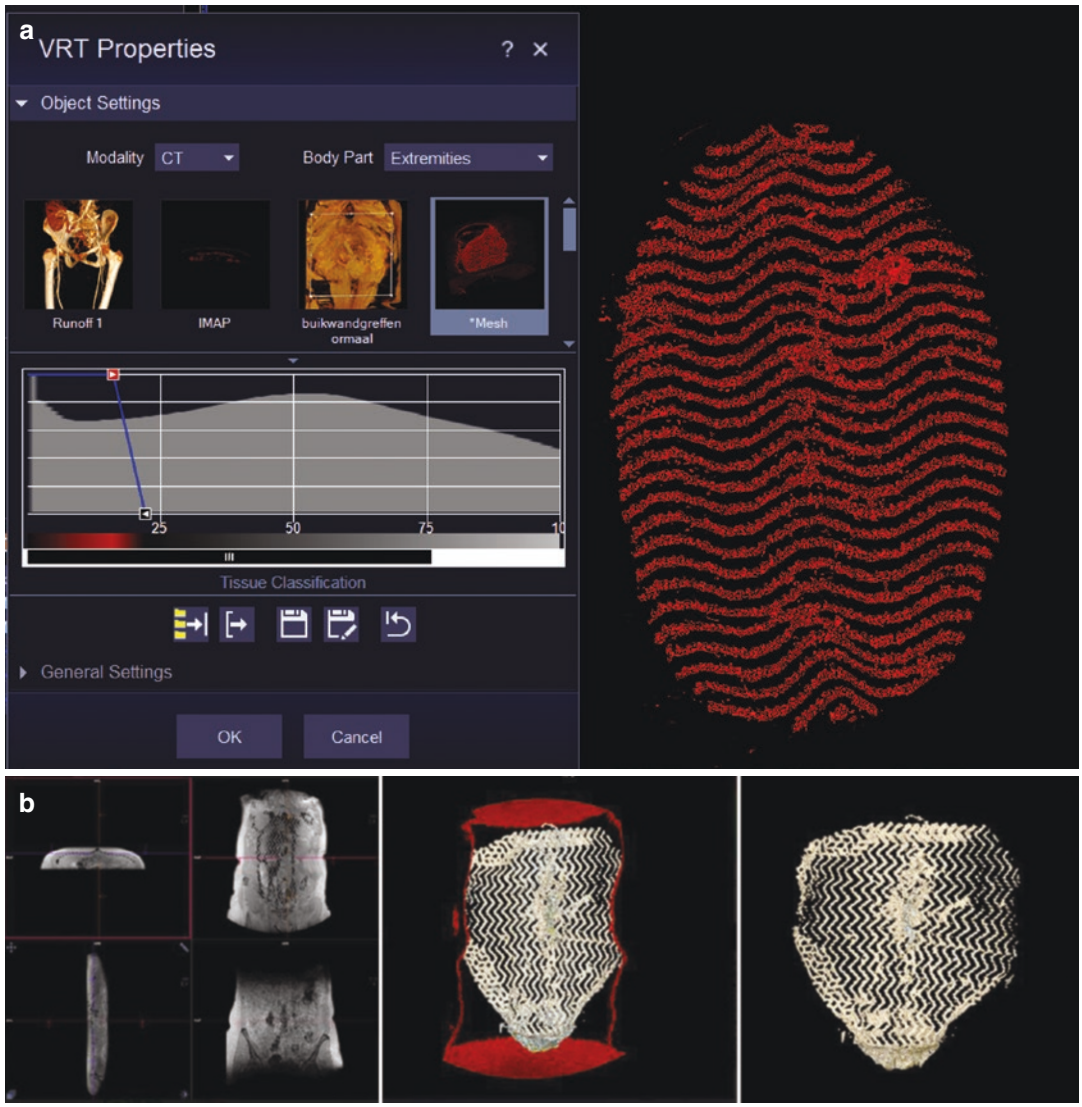

Fig. 10.16 (**a**) Mesh isolation out of 3D T1 stack by defining reversed ramp on histogram enabling to visualize only voxels with lowest signal intensity. (See also Video 10.5). (**b**) Step-by-step isolation of large abdominal wall mesh (i) 3D MPR view of native 3D T1 series, (ii) VRT result after choosing appropriate setting: the mesh becomes visible and can be isolated in only a few cutting steps (see also Video 10.6), and (iii) Final result

insight for the referring physician (Fig. 10.16c, Videos 10.5, 10.6).

Nowadays several commercial software packages are available that allow mesh isolation and extensive quantitative analysis starting from the 3D T1 sequences. Extra offered features include surface and curvature analysis and possibility to compare meshes surface over time allowing to visualize shrinkage or deformation (Fig. 10.17). Maybe less extended or merely morphologic

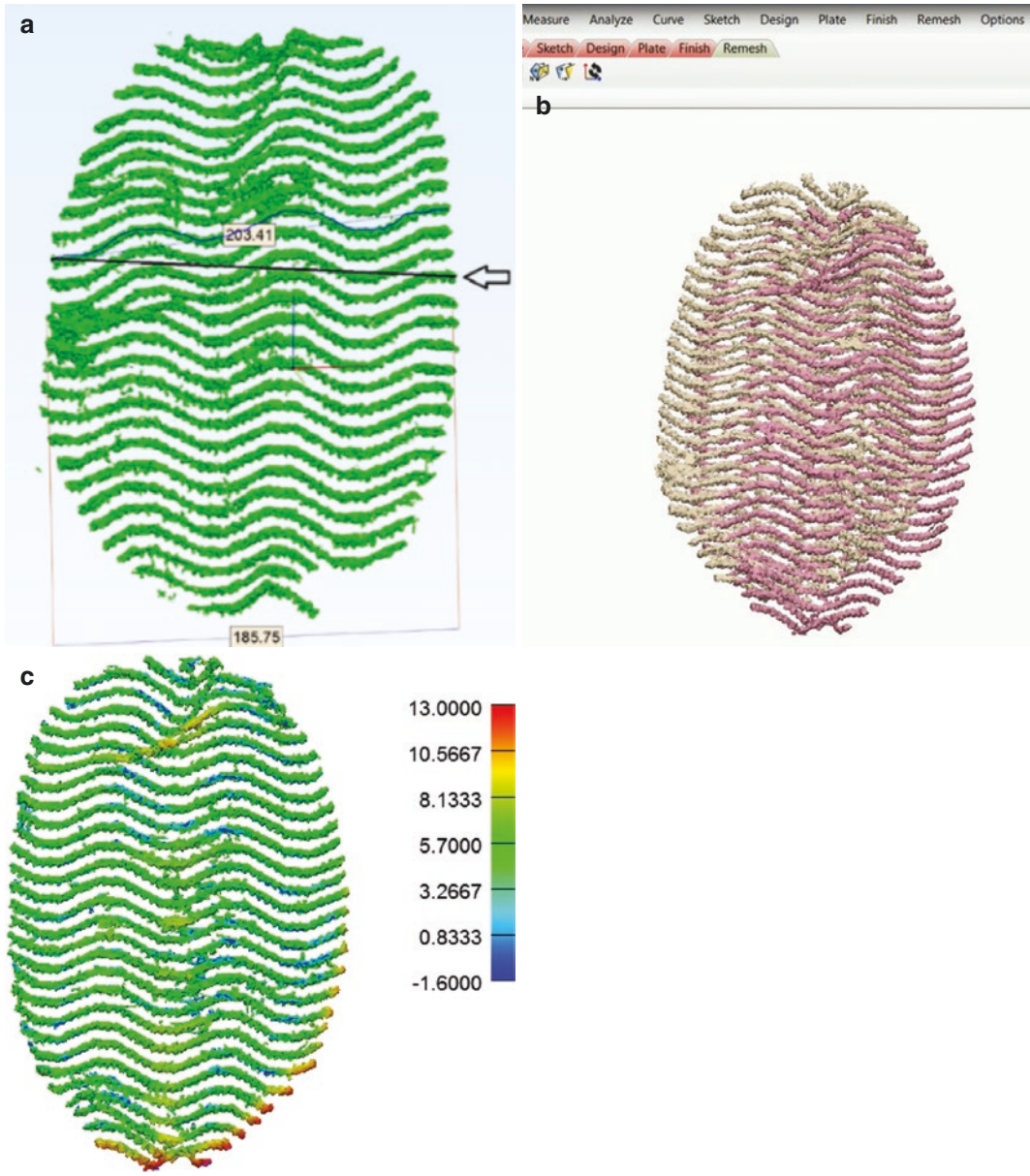

Fig. 10.17 Complex analysis of isolated abdominal wall mesh (Software used: Materialise Mimics Innovation Suite 20.0 Leuven Belgium): (**a**) Advanced quantitative mesh analysis comparing maximal projective transverse diameter with real filament length of mesh at the same level. (**b**) Same patient as in (**a**): Fusion of isolated meshes (yellow and pink) in same patient combining data with 12-month interval allowing qualitative and quantitative comparison. (**c**) Same patient as in (**a**): image parts in red show shrinkage over 12-month period time. (**d**) Example of time-resolved qualitative comparison of inguinal hernia mesh with 12-month interval

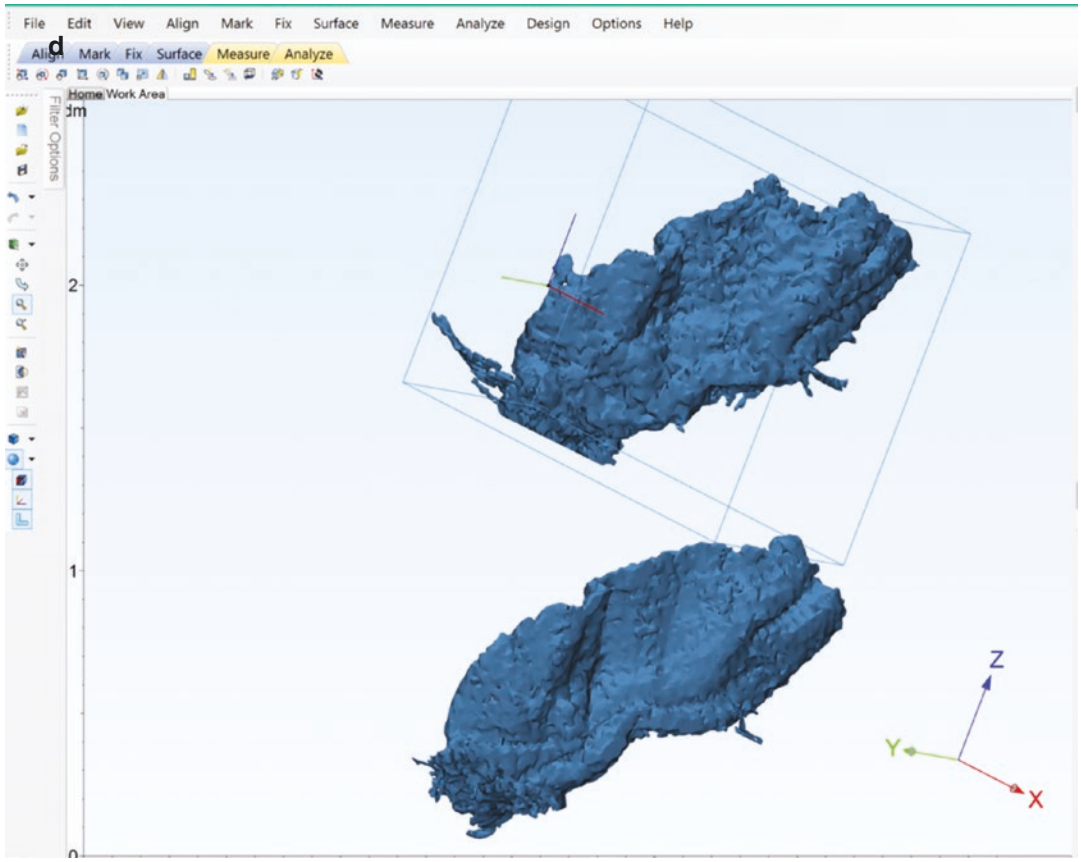

Fig. 10.17 (continued)

evaluation morphologic can be achieved with free available software (Slicer 3D—https://www.slicer.org/, SEG3D—https://www.slicer.org/) that allow for mesh isolation using several segmentation techniques. After isolation mesh results can be shared by images or movies, the object can be shared as an object or STL file or can be saved as a 3D PDF file.

Conclusion

Modern multidetector CT scans provide excellent data for extended morphologic and quantitative analysis of abdominal wall hernias using dedicated 3D software (Video 10.7). The use of additional 3D reconstructions derived from modern volume rendering techniques is truly an added value for comprehension of hernia and abdominal wall morphology as well as interrelationships with surrounding structures and can serve as a preoperative didactic tool. MRI has limited value in preoperative planning but has its value in evaluating position and morphology of iron-incorporated meshes.

Acknowledgement Disclosures of conflict of interest: R.B. disclosed no financial relationships, M.V. reports participation in the Advisory Board of Medtronic. F.M. reports having recieved research grants from Medtronic, Intuitive Surgical and FEG Textiltechnik besides speakers' honoraria from Medtronic, BD Bard, Intuitive Surgical and WL GORE, consultancy honoraria from Medtronic, CMR surgical and expert testimony from Sofradim. F.M. is proctor for Intuitive Surgical and participates in the Advisory Board of Medtronic.

References

1. Jenkins JT, O'Dwyer PJ. Inguinal hernias BMJ. 2008;336:269–336.
2. Burcharth J, Pedersen M, Bisgaard T, Perdersen C, Rosenberg J. Nationwide prevalence of groin hernia repair. Plos One. 2013:8.
3. Muysoms F, Miserez M, Berrevoet F, Campanelli G, Champault GG, Chelala E, Dietz UA, Eker HH, Nakadi IE, Hauters P, Hidalgo Pascual M, Hoeferlin A, Klinge U, Montgomery A, Simmermacher RKJ, Simons MP, Śmietańki M, Sommeling C, Tollens T, Vierendeels T, Kingsnorth A. Classification of primary and incisional abdominal wall hernia. Hernia. 2009;13:407–14.
4. Kingnorth A, LeBlanc K. Hernia's: inguinal and incisional. Lancet. 2003;362:1561–71.
5. Kalender WA, Seissler W, Klotz E, Vock P. Spiral volumetric CT with single-breath-hold technique, continuous transport, and continuous scanner rotation. Radiology. 1990;176:181–3.
6. Heiken JP, Brink JA, Vannier MW. Spiral (helical) CT. Radiology. 1993;189:647–56.
7. Rigauts H, Marchal G, Baert AL, Hupke R. Initial experience with volume CT scanning. J Comput Assist Tomogr. 1990;14(4):675–82.
8. Rydberg J, Buckwalter KA, Caldemeyer KS, Phillips MD, Conces DJ, Aisen AM Jr, Persohn SA, Kopecky KK. Multisection CT: scanning techniques and clinical applications. Radiographics. 2000;20:1787–806.
9. Geyer LL, Schoepf UJ, Meinel FG, Nance JW, Bastarrika G Jr, Leipsic JA, Paul NS, Rengo M, Laghi A, De Cecco CN. State of the art: iterative CT reconstruction techniques. Radiology. 2015;276:339–57.
10. Ehman EG, et al. Methods for clinical evaluation of noise reduction techniques in abdominopelvic CT. Radiographics. 2014;34:249–62.
11. Miletto A, Guimaraes LS, McCollough CH, Fletcher JG, Yu L. State of the art in abdominal CT: the limits of iterative reconstruction algorithms. Radiology. 2019;293:491–503.
12. Cody DD, Mahesh M. Technologic advances in multidetector CT with a Focus on Cardiac imaging. RadioGraphics. 2007;27:1829–37.
13. Habets J, Mali WPT, Budde RPJ. Multidetector CT angiography in evaluation of prosthetic heart valve dysfunction. Radiographics. 2012;32:1893–905.
14. Fishman EK, Drebin B, Magid D, Scott WW Jr, Ney DR, Brooker AF Jr, Riley LH Jr, St VJA, Zerhouni EA, Siegelman SS. Volumetric rendering techniques: applications for three-dimensional imaging of the hip. Radiology. 1987;163:737–8.
15. Levin DN, Xiaoping H, Tan KK, Galhotra S. Surface of the brain: three-dimensional MR images created with volume rendering. Radiology. 1989;171:277–80.
16. Heath DG, Soyer PA, Kuszyk BS, Bliss DF, Calhoun PS, Bluemke DA, Choti MA, Fishman EK. Three-dimensional Spiral CT during arterial portography: comparison of three rendering techniques. Radiographics. 1995;15:1001–11.
17. Calhoun PS, Kuszyk BS, Heath DG, Carley JC, Fishman EK. Three-dimensional volume rendering of spiral CT data: theory and method. Radiographics. 1999;19:745–64.
18. Lam DL, Mitsumori LM, Neligan PC, Warren BH, Shuman WP, Dubinsky TJ. Pre-operative CT angiography and three-dimensional image post processing for deep inferior epigastric perforator flap breast reconstructive surgery. Br J Radiol. 2012;85(1020):e1293–7.
19. Fishman EK, Ney DR, Heath DG, Corl FM, Horton KM, Johnson PT. Volume rendering versus maximum intensity projection in CT angiography: what works best, when, and why. Radiographics. 2006;26:905–9228.
20. Fellner FA. Introducing cinematic rendering: a novel technique for post-processing medical imaging data. J Biomed Sci Eng. 2016;9:170–5.
21. Johnson PT, Schneider R, Lugo-Fagundo C, Johnson MB, Fishman EK. MDCT angiography with 3D rendering: a novel cinematic rendering algorithm for enhanced anatomic detail AJR. 2017;209:309–12.
22. Comaniciu D, Engel K, Georgescu B, Mansi T. Shaping the future through innovations: from medical imaging to precision medicine. Med Image Anal. 2016;33:19–26.
23. Kavic SM, Segan RD, George IM, Turner PL, Roth JS, Park A. Classification of hiatal hernias using dynamic three-dimensonal reconstruction. Surg Innov. 2006;13:49–52.
24. Sabbagh C, Dumont F, Robert B, Badaoui R, Verhaeghe P, Regimpbeau JM. Peritoneal volume is predictive of tension-free fascia closure of large incisional hernias with loss of domain: a prospective study. Hernia. 2011;15:559–65.
25. Tanaka EY, Yoo JH, Rodrigues AJ Jr, Utiyama EM, Birolini D, Rasslan S. A computerized tomography scan method for calculating the hernia sac and abdominal cavity volume in complex large incisional hernia with loss of domain. Hernia. 2010;14:63–9.
26. Yao S, Li J-y, Liu F-d. Li juan Pei Significance of measurements of herniary area and volume and abdominal cavity volume in the treatment of incisional hernia: Application of CT 3D reconstruction in 17 cases. Comput Aided Surg. 2012;17: 1:40–5. link vervolledigen!!!!
27. Xu Z, Asman AJ, Baucam RB, Abramson RG, Poulose BK, Landman BA. Quantitative CT imaging of ventral hernias: preliminary validation of an anatomical labeling protocol. PLoS One. 2015;10:e0141671.
28. Koa AM, Ross SW, Otero J, Maloney SR, Prasad T, Augenstein VA, Heniford BT, Colavita PD. Use of computed tomography volumetric measurements to predict operative techniques in paraesophageal hernia repair. Surg Endosc. 2020;34:1785–94.
29. Winters H, Knaapen L, Buyne OR, Hummelinck S, Ulrich DJO, van Goor H, van Geffen E, Slater NJ. Pre-operative CT scan measurements for pre-

dicting complications in patient undergoing complex ventral hernia repair using the component separation technique. Hernia. 2019;23:347–54.
30. Elstner KE, Read JW, Saunders J, Cosman PH, Rodriguez-Acevedo O, Jacombs ASW, Martins RT, Ibrahim N. Selective muscle botulinum toxin A component paralysis in complex ventral hernia repair. Hernia. 2020;24:287–93.
31. del Olmo JCM, García-Vallejo L, Gestal J, Coello P, Antona F, Trincado M, González J, Esteban M, Colao L, Vaquero C, Carbajo M. The usefulness of magnetic resonance imaging in the preoperative study and postoperative control in the laparoscopic treatment of the incisional hernia. Surgical Science. 2015;6:376–82. https://doi.org/10.4236/ss.2015.68055.
32. Rakic S, LeBlanc KA. The radiologic appearance of prosthetic materials used in hernia repair and a recommended classification. AJR. 2013;201:1180–3.
33. Krämer NA, Donker HC, Otto J, et al. A concept for magnetic resonance visualization of surgical textile implants. Invest Radiol. 2010;45(8):477–83. https://doi.org/10.1097/RLI.0b013e3181e53e38.
34. Kuehnert N, Kraemer NA, Otto J, et al. In vivo MRI visualization of mesh shrinkage using surgical implants loaded with superparamagnetic iron oxides. Surg Endosc. 2012;26:1468–75.
35. Kraemer NA, Donker HC, Kuehnert N, et al. In vivo visualization of polymer-based mesh implants using conventional magnetic resonance imaging and positive-contrast susceptibility imaging. Invest Radiol. 2013;48(4):200–5. https://doi.org/10.1097/RLI.0b013e31827efd14.
36. Otto J, Busch D, Klink C, et al. In vivo MRI visualization of parastomal mesh in a porcine model. Hernia. 2014;18(5):663–70. https://doi.org/10.1007/s10029-014-1270-4.
37. Sindhwani N, Feola A, De Keyzer F, Claus F, Callewaert G, Urbankova I, Ourselin S, D'hooge J, Deprest J. Three-dimensional analysis of implanted magnetic-resonance-visible meshes. Int Urogynecol J. 2015;26:1459–65.
38. Brocker KA, Mokry T, Alt CD, Kauczor H-U, Lenz F, Sohn C, Delancey JO, Chen L. 3D reconstruction of MR-visible Fe3O4-mesh implants: pelvic mesh measurement techniques and preliminary findings. Neurol Urodyn. 2018:1–10.
39. Muysoms BR, Kyle-Leinhase I. Prospective cohort study on mesh shrinkage measured with MRI after laparoscopic ventral hernia repair with an intraperitoneal iron oxide-loaded PVDF mesh. Surg Endosc. 2018;32(6):2822–30.

Direct Inguinal Hernia

11

Joseph R. Imbus and Jacob A. Greenberg

Introduction and Relevant Anatomy

In the seventeenth and eighteenth centuries, anatomists and surgeons made great strides in understanding inguinal hernias. Lorenz Heister (1683–1758) is credited with differentiating the direct from indirect inguinal hernia during this era of anatomic discovery. Accounting for 15% of inguinal hernias, direct inguinal hernias represent a protrusion of parietal peritoneum and potentially abdominal viscera through an acquired weakening of the transversalis fascia in the posterior wall of the inguinal canal. These abdominal wall defects are more common in men compared to women, increase in incidence with increasing patient age, and are less likely to incarcerate or strangulate compared to indirect inguinal hernias. Uncommonly, direct inguinal hernias can develop concurrently with an indirect inguinal hernia. When this occurs, hernia sacs are present on both sides of the inferior epigastric vessels and thus referred to collectively as a "pantaloon hernia." Franz Hesselbach (1759–1816) described the now eponymous anatomic triangle which defines the location of direct inguinal hernias, that is, the region bound medially by the lateral edge of the rectus abdominus, inferiorly by the inguinal ligament, and superolaterally by the inferior epigastric vessels (Fig. 11.1). A sound understanding of inguinal anatomy is essential for clinicians evaluating inguinal hernias, and the relationship to the inferior epigastric vessels ultimately defines direct versus indirect hernias. A direct inguinal hernia

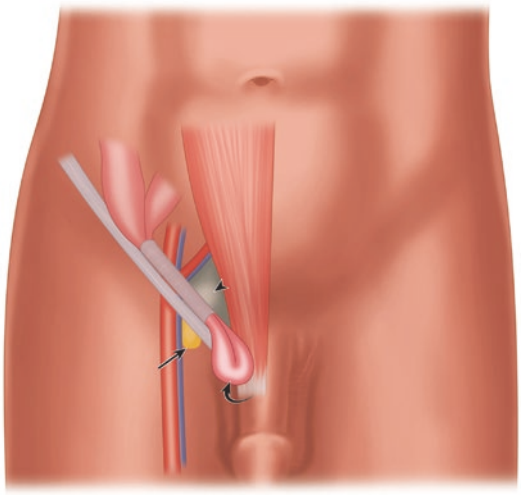

Fig. 11.1 Hesselbach's triangle (arrowhead); femoral ring (straight arrow); indirect inguinal hernia (curved arrow)

Supplementary Information The online version contains supplementary material available at https://doi.org/10.1007/978-3-031-21336-6_11.

J. R. Imbus
Division of Minimally Invasive Surgery, Department of Surgery, Duke University, Durham, NC, USA
e-mail: imbusjr@ucmail.uc.edu

J. A. Greenberg (✉)
Department of Surgery, University of Cincinnati College of Medicine, Cincinnati, OH, USA
e-mail: jacob.greenberg@duke.edu

S. Docimo Jr. et al. (eds.), *Fundamentals of Hernia Radiology*,
https://doi.org/10.1007/978-3-031-21336-6_11

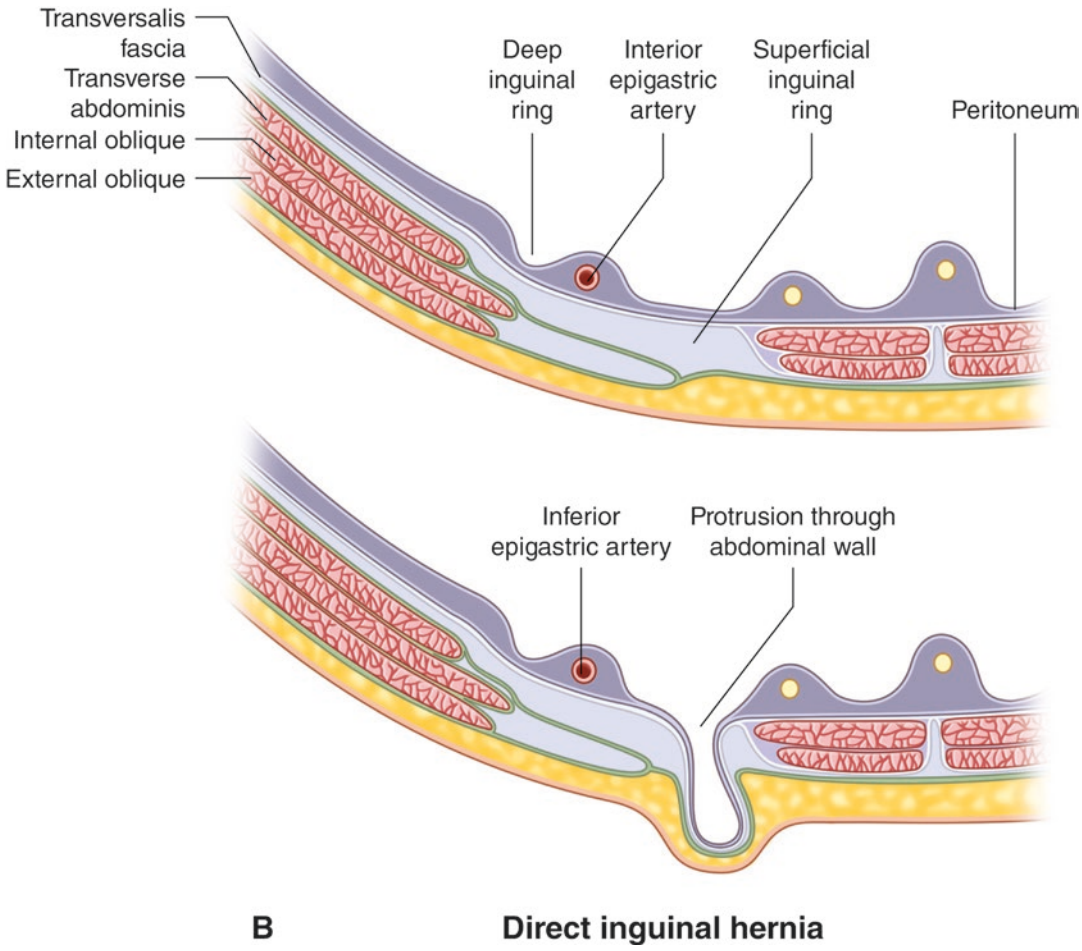

Fig. 11.2 A direct inguinal hernia protrudes medial to the inferior epigastric artery, and may extend into the superficial ring upon Valsalva

protrudes medial to the inferior epigastric artery and may extend into the superficial ring upon Valsalva (Fig. 11.2).

Role of Imaging for Direct Inguinal Hernia Diagnosis

Inguinal hernias commonly present as a painful bulge in the groin and a thorough history and physical exam are typically sufficient for diagnosis. Thus, the majority of patients should not require any imaging modality as part of their workup. However, patient and hernia factors including obesity and small hernia size can make diagnosis difficult without confirmatory imaging. Furthermore, the accuracy of physical examination in discriminating between direct and indirect inguinal hernias is debated in the literature, though is frequently not clinically relevant as both types of hernias should be routinely repaired via an open or minimally invasive approach. Preoperative differentiation of direct inguinal hernia from alternate pathologies, as well as definition of hernia sac contents, can be useful for surgical planning. Given the dynamic nature of inguinal hernias, ultrasonography (US) is the preferred imaging modality to evaluate inguinal hernias, but multidetector computed tomography (MDCT) and magnetic resonance imaging (MRI) are also potentially useful. In this chapter, we review US, MDCT, and MRI imaging for direct inguinal hernias, as well as postoperative imaging considerations.

Dynamic Ultrasound

Equipment and Technique

A high-frequency (≥10 MHz), long linear transducer operated by a skilled sonographer is recommended. For obese patients, a low-frequency curvilinear transducer (7–9 MHz) can improve imaging. Panoramic mode, if available, is useful to capture a more comprehensive anatomic view. Color Doppler capability aids in assessment of bowel perfusion for incarcerated hernias. Both still images and recorded video loops should be captured. The sonographer should use light pressure on the skin during imaging acquisition to avoid anatomic distortion. Compression can be intentionally used to assess reducibility and tenderness. Radiologist supervision is recommended to ensure quality and orientation of US imaging.

No patient preparation is required prior to inguinal US. The patient should first be imaged in a relaxed, supine position. Additional evaluation in the upright position should be performed to further evaluate any findings or to search for findings if supine examination is unremarkable. Several patient maneuvers to increase intra-abdominal pressure can be used to create dynamic images. These include the Valsalva maneuver—forced expiration against a closed glottis (i.e., "Blow on your thumb like a trumpet."), forceful cough, and raising one's head and shoulders off the bed from a resting position. Dynamic evaluation can reveal hernias otherwise occult at rest. In addition, hernias visible at rest generally become larger with Valsalva; a lack of dynamic movement may suggest incarceration.

Placement of the transducer transversely near the midpoint of the pubic tubercle and anterior superior iliac spine guides the identification of the key anatomic landmark of interest—the inferior epigastric artery. This technique identifies the origin of the inferior epigastric artery emanating from the external iliac artery. At this point, the inferior epigastric artery lies just medial to the deep inguinal ring. The inferior epigastric artery can also be identified with US reliably on the undersurface of the rectus abdominis midway between the pubic tubercle and umbilicus, and then traced down to its origin. At the origin, the transducer should be rotated such that images are obtained in planes parallel (long-axis) and perpendicular (short-axis) to the inguinal canal (Fig. 11.3).

Reporting

Radiologists should be systematic, consistent, and thorough in reporting dynamic US findings. Positive and negative findings should be reported in not only the direct hernia region but also the indirect and femoral regions of the patient. Synoptic reporting is encouraged to aid readability, interpretation, and use of reports for surgical planning and research purposes. Important elements to report include laterality, patient position and specific dynamic components utilized, presence/absence of hernia, hernia and hernia neck sizes, hernia contents, hernia reducibility, tenderness, and alternate pathology.

Interpretation of Imaging

Familiarity with the normal anatomic adynamic and dynamic long-axis and short-axis views of the inguinal region is useful for reference. Figure 11.4 shows normal male right groin anatomy in the long axis at rest. In this orientation, the male cord appears as a linear bundle of structures with variable echogenicity, and color Doppler can help confirm the cord vasculature. Based on body habitus, a variable amount of expected adiposity is observed enveloping the cord structures. Figure 11.5 shows normal left groin anatomy in the short-axis (anatomic sagittal view). Figure 11.6 shows the appearance of a right-sided direct inguinal hernia on US before and during Valsalva in both the long-axis and short-axis views.

Similarly, Fig. 11.7 shows a direct inguinal hernia during Valsalva in both axes, and annotated overlays are provided to highlight relevant anatomy. Note that in the short axis, a direct hernia displaces and compresses the spermatic cord anteriorly and laterally.

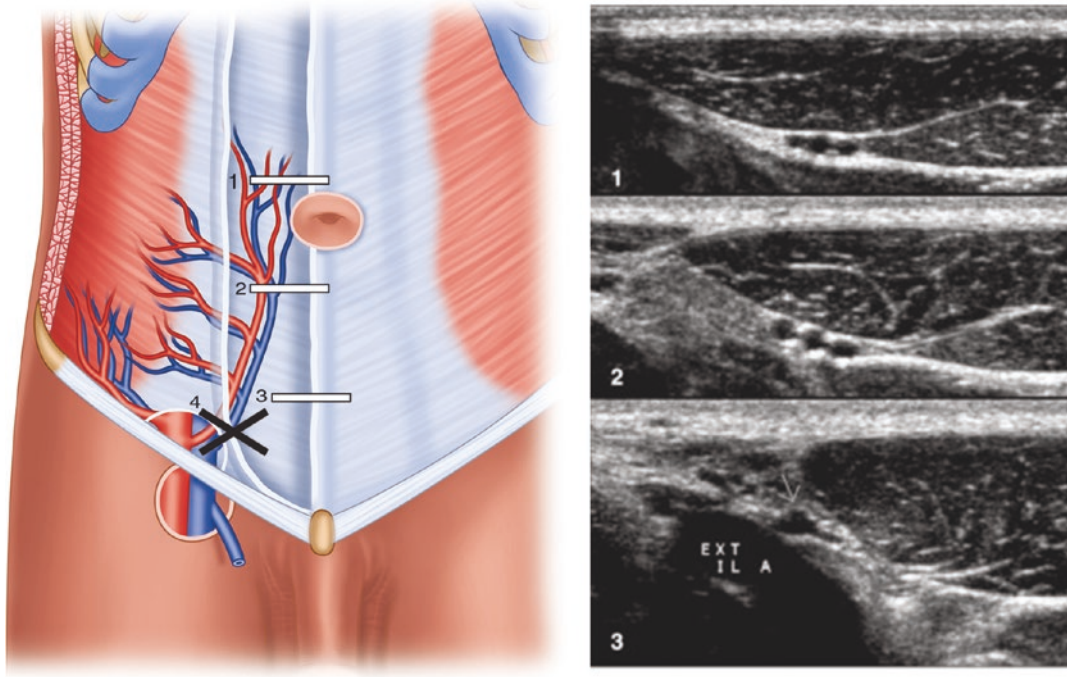

Fig. 11.3 Inferior epigastric vessels (IEVs) are the main landmarks for evaluating inguinal area
Image 1 was obtained in a transverse plane about halfway between the umbilicus and the pubic symphysis. The inferior epigastric artery and its paired veins lie along the midlateral posterior surface of the rectus abdominis muscle. Image 2 was obtained several centimeters inferiorly, and the IEVs lie more laterally. Image 3 was obtained at a level where the IEVs (arrow) lie at the edge of the rectus muscle. This is the level at which most spigelian hernias occur. Once the origin of the inferior epigastric artery is identified, the transducer should be rotated into planes that are parallel (see line 4 on the drawing) and perpendicular (see image 3) to the inguinal canal—long-axis and short-axis views
Modified from: Diagnostic Ultrasound. Dynamic Ultrasound of Hernias of the Groin and Anterior Abdominal Wall

In general, a direct inguinal hernia will bulge towards the US transducer on examination during Valsalva. Video 11.1 is an example of ultrasound use in hernia evaluation.

"Posterior inguinal wall insufficiency" or "conjoint tendon insufficiency" is an entity identifiable with US and considered a precursor to direct inguinal hernia. The conjoint tendon is comprised of the aponeuroses of the internal oblique and transversus abdominus muscles, with underlying transversalis fascia. Thinning and anterior bulging of the conjoint often occurs bilaterally but can cause symptoms unilaterally and/or progress to direct inguinal hernia if an overt tear or severe thinning occurs. This entity is often indistinguishable from direct inguinal hernia on the short-axis, but long-axis evaluation will show "posterior inguinal wall insufficiency" take on a semi-circular shape whereas a direct inguinal hernia protrudes inferiorly with a finger-like projection. This difference is illustrated in Fig. 11.8.

Given the poor negative predictive value of US for inguinal hernias, a negative study in a symptomatic patient warrants the pursuit of additional imaging modalities.

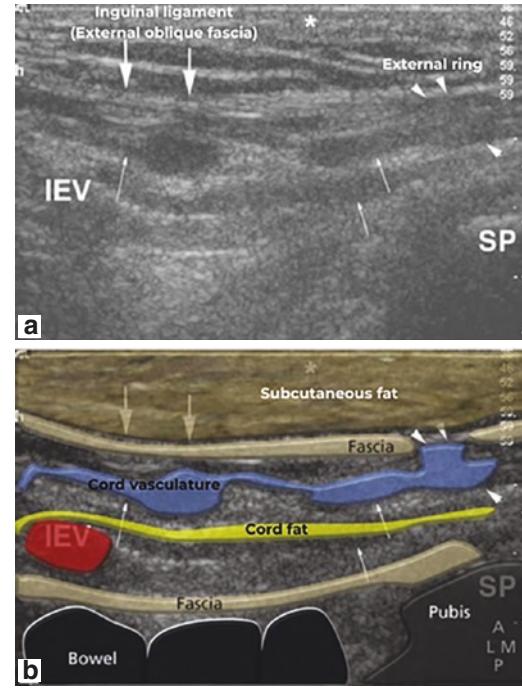

Fig. 11.4 Normal right inguinal canal, transverse sonogram. The IEVs lie medial to the internal ring. The thick echogenic inguinal ligament (large arrows) lies anteriorly, deep to the subcutaneous fat (*). Multiple tubular structures are seen (small arrows) passing medially towards the symphysis pubis (SP) and passing through the external ring where a defect (arrowheads) in the inguinal ligament can be visualized. With permission from: Practical Musculoskeletal Ultrasound [Philip Robinson]. Disorders of the Groin and Hip: Groin Pain

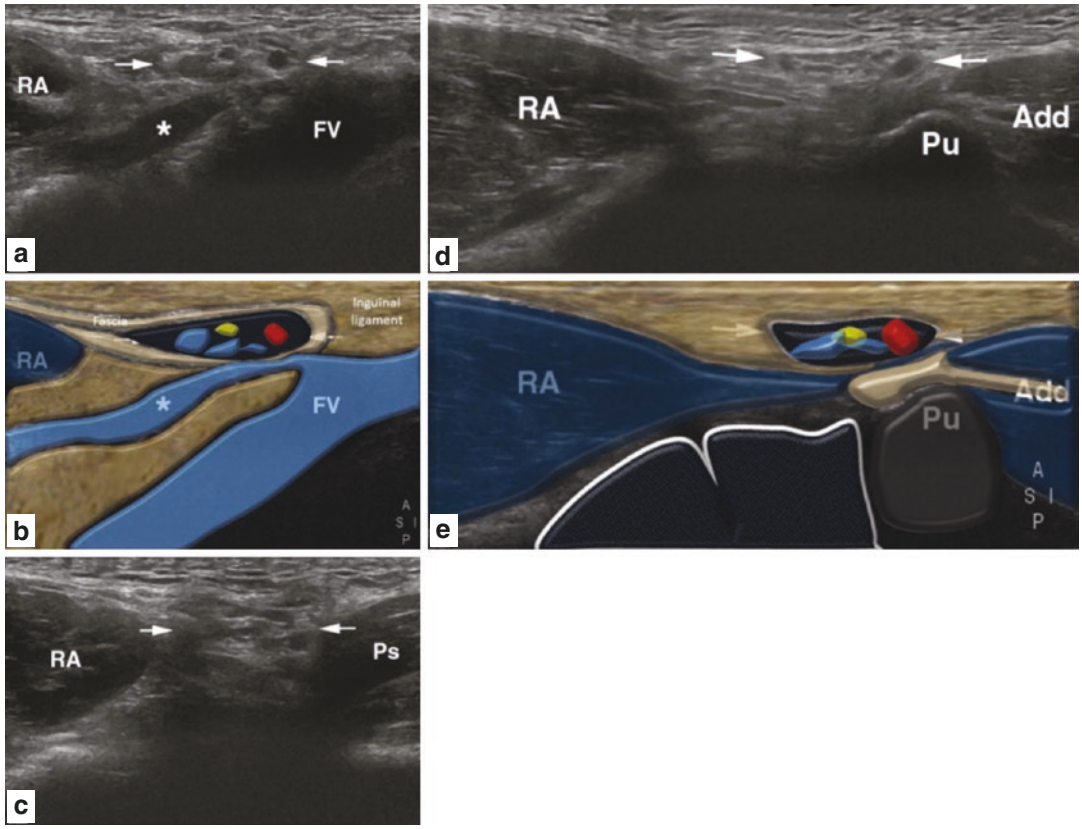

Fig. 11.5 Normal left inguinal canal, sagittal sonograms. (**a**, **b**) Image obtained at the level of the inferior epigastric vein (*) as it arises from the femoral vein (FV). The inguinal canal is seen as an oval-shaped soft tissue area containing multiple tubular structures (arrows) with rectus abdominis (RA) lying superiorly. (**c**) Medial to position in (**a**). (**d**, **e**) Medial to (**c**) at the level of the superficial ring as the contents (arrows) descend over the pubis (Pu) and adductor origin (Add)
With permission from: Practical Musculoskeletal Ultrasound [Philip Robinson]. Disorders of the Groin and Hip: Groin Pain

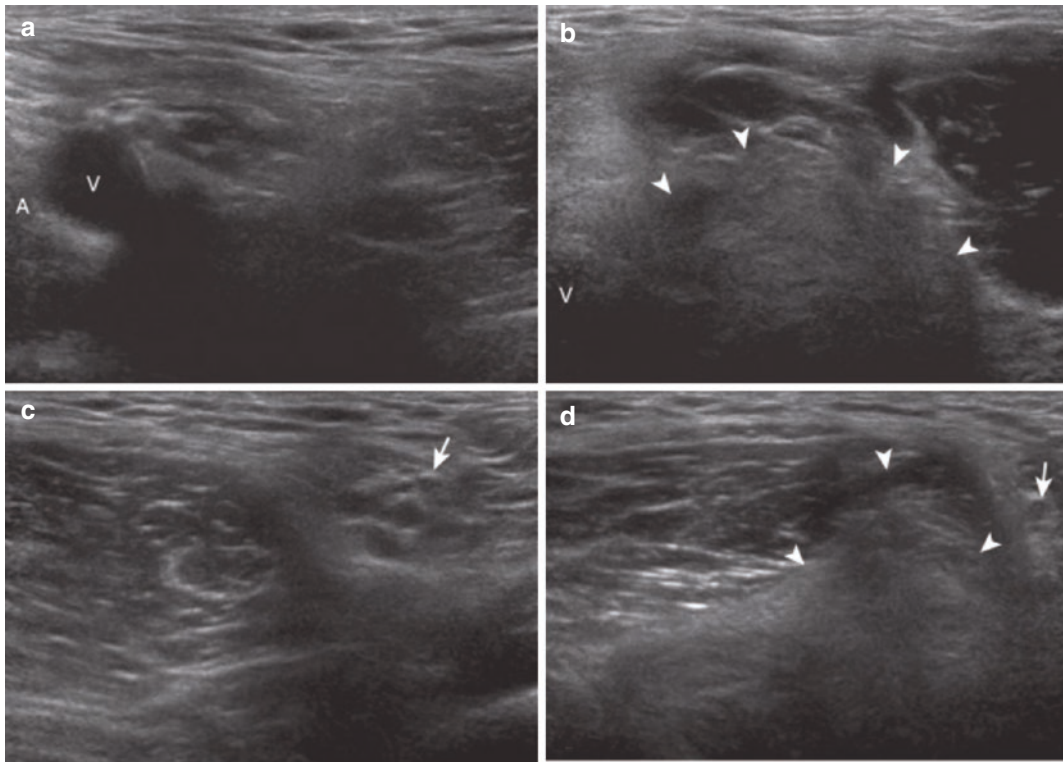

Fig. 11.6 Direct Inguinal Hernia
Ultrasound images parallel to the right inguinal canal (**a**) before and (**b**) during the Valsalva maneuver show abnormal echogenic intra-abdominal contents (arrowheads), which protrude anteriorly, medial to the external iliac vasculature (A and V) (left side of the image is lateral). Ultrasound images in short axis to the right inguinal canal (**c**) before and (**d**) during the Valsalva maneuver show abnormal echogenic intra-abdominal contents (arrowheads), which protrude anteriorly and displace the spermatic cord (arrow)
With permission from: Fundamentals of Musculoskeletal Ultrasound. Hip and Thigh Ultrasound

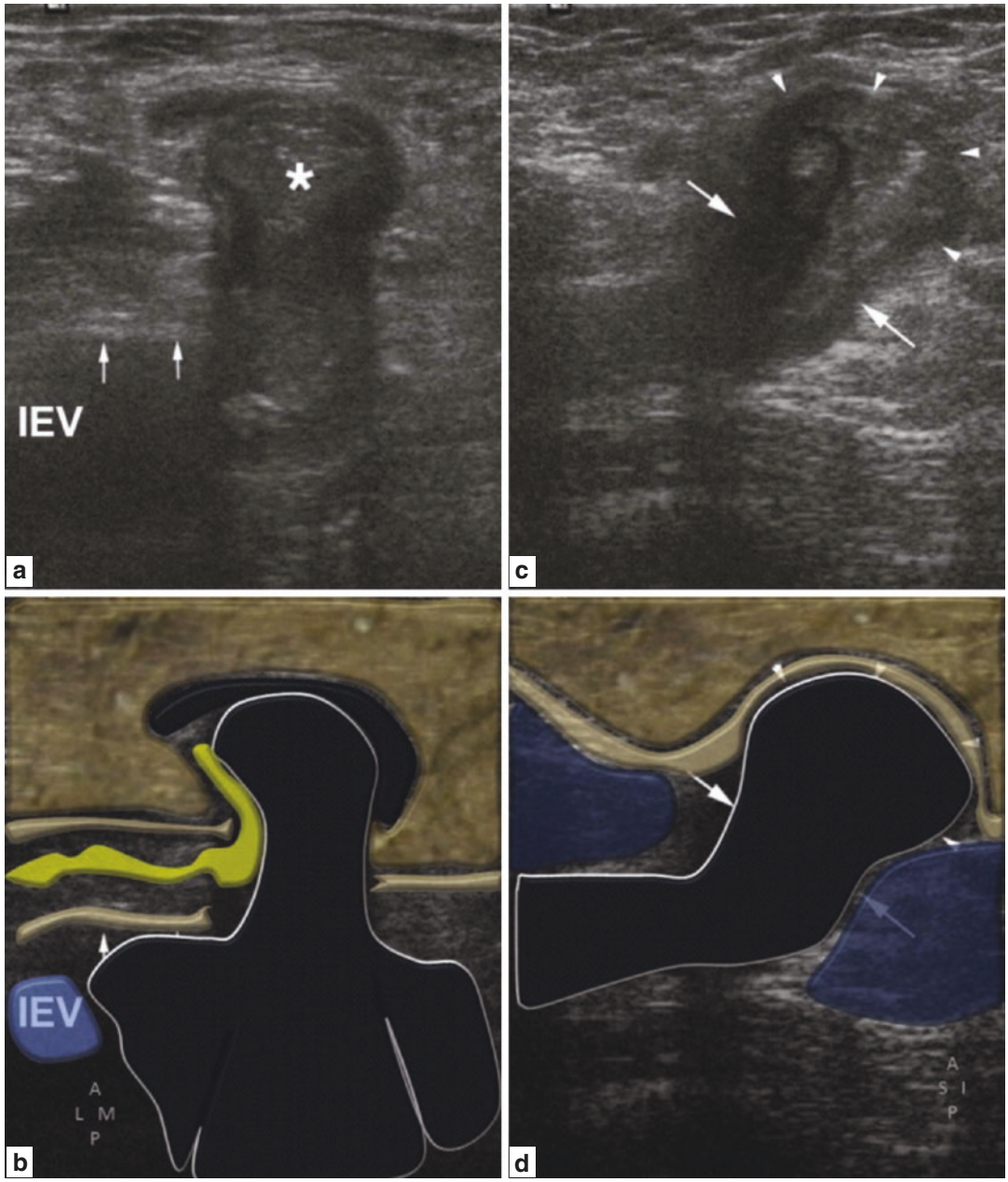

Fig. 11.7 Right direct hernia. (**a**, **b**) Transverse sonogram during straining shows the IEVs and adjacent transversus fascia (arrows) lateral to a hernia of bowel and fat (*) entering through the posterior wall defect. (**c**, **d**) Corresponding sagittal sonogram shows hypoechoic loop of bowel (small arrows) pushing through the posterior wall (large arrows)
With permission from: Practical Musculoskeletal Ultrasound [Philip Robinson]. Disorders of the Groin and Hip: Groin Pain

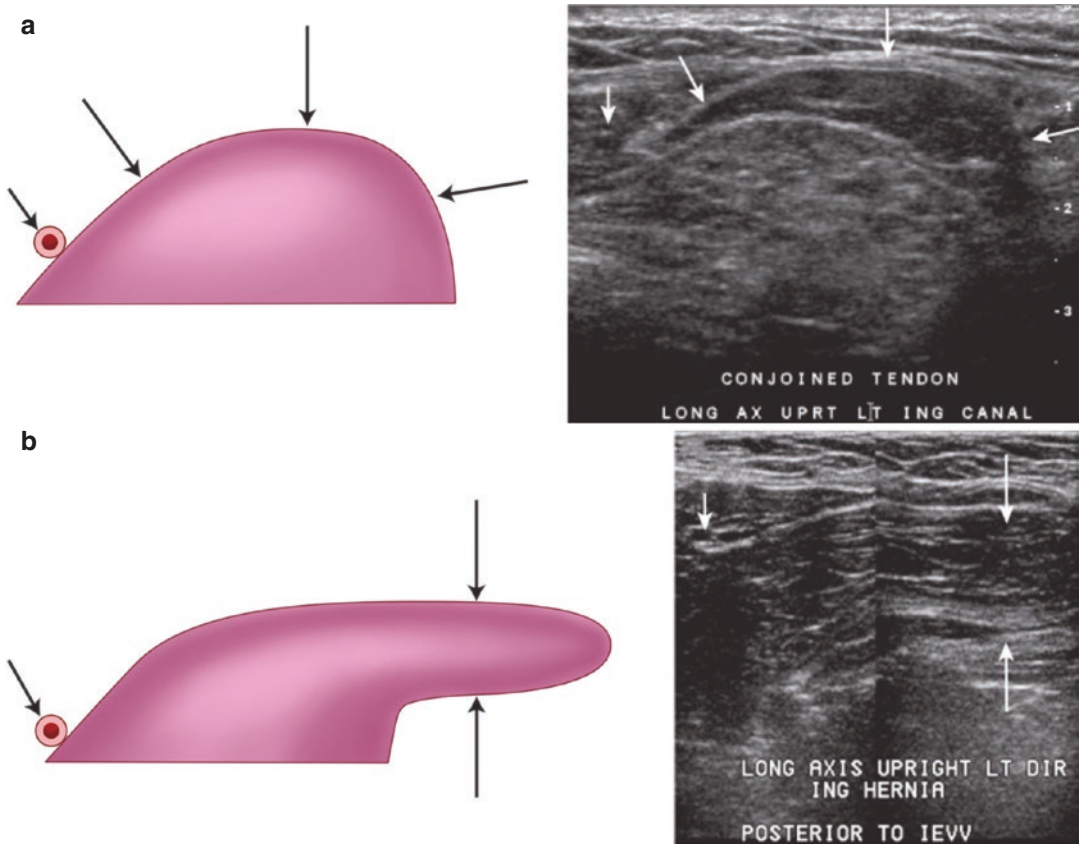

Fig. 11.8 Inguinal wall insufficiency versus direct inguinal hernia
Long-axis views show different appearance of posterior inguinal wall insufficiency and direct inguinal hernia. (**a**) Insufficiency of the posterior inguinal wall (long arrows). Short arrow is inferior epigastric artery. (**b**) Frank direct inguinal hernia extends distally within the inguinal canal in a finger-like projection (long arrows) posterior to the spermatic cord. At the level of the proximal inguinal canal, the distinction is possible only on long-axis views, because insufficiency and frank hernia appear identical on short-axis views obtained proximally. Short arrow is inferior epigastric artery
Modified from: Diagnostic Ultrasound. Dynamic Ultrasound of Hernias of the Groin and Anterior Abdominal Wall

Multidetector Computed Tomography

Technique

MDCT can be used as an alternative or adjunctive imaging modality to dynamic US. MDCT also finds many incidental inguinal hernias. Thin slice reconstruction (≤2.5 mm section) is recommended to optimize coronal and sagittal reformation. When planned, Valsalva maneuvers can be attempted during MDCT to increase detection. Intravenous contrast is necessary to visualize the interior epigastric vessels to differentiate different types of groin hernias. Similarly, oral contrast is used to visualize bowel loops which may be involved. Figure 11.9 shows coronal reformats to visualize a direct inguinal hernia.

Interpretation of Imaging

The Lateral Crescent sign is a radiographic finding to aid identification of direct inguinal hernias on MDCT. Lateral compression and stretching of inguinal canal adipose tissue and structures by an early direct inguinal hernia can manifest as a "moon-like" crescent as illustrated in Fig. 11.10.

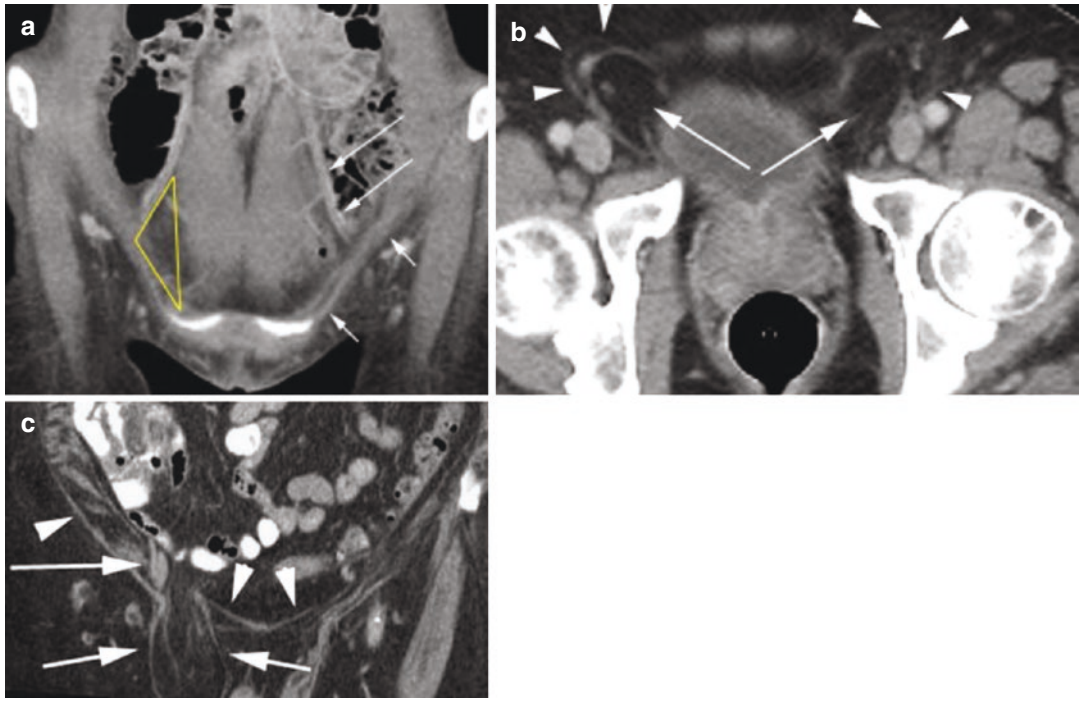

Fig. 11.9 (**a**) CT coronal reformat demonstrates the inguinal ligament (short arrows) and deep inferior epigastric vessels (long arrows). The Hesselbach's triangle is outlined in yellow on the right which superolaterally is marginated by the epigastric vessels, medially by the rectus abdominus, and inferiorly by the inguinal ligament. (**b**) Axial CT demonstrates a lateral crescent sign due to a fat containing direct inguinal hernias (arrows) displacing the contents of the inguinal canal laterally and the fat within it transformed into a crescent (arrowheads). (**c**) CT coronal reformat of a different patient demonstrates a fat containing direct inguinal hernia (short arrow) coursing above the inguinal ligament (arrowheads) with its neck medial to deep inferior epigastric vessels (long arrow)
With permission from: V. Trainer et al./Clinical Radiology 68 (2013) 388–389

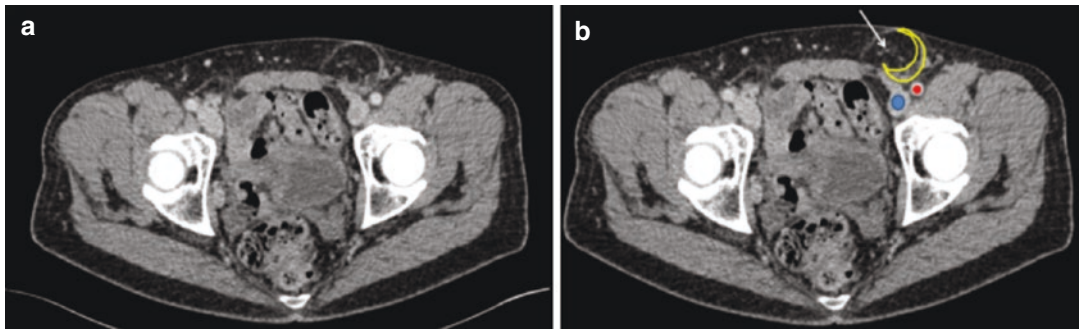

Fig. 11.10 Axial contrast-enhanced CT image (**a**). And color-coded image (**b**). Showing a left direct inguinal hernia. The fat and the other inguinal canal contents (outlined in yellow) are flattened by the herniated fat and omentum (arrow) into a thin lateral "moon-like" crescent. The common femoral artery (red dot) and vein (blue dot) are seen coursing laterally and posteriorly to the hernia
With permission from Schoettle A, Veillon F, Venkatasamy A. The lateral crescent sign. Abdominal Radiology 2018 11;43(11):3195–3196

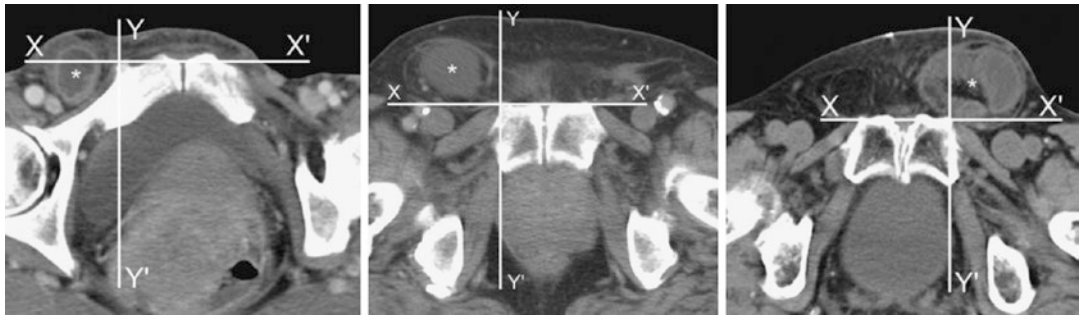

Fig. 11.11 (Left) Contrast-enhanced transverse CT scan at the level of the right pubic tubercle in a 68-year-old female patient. Right femoral hernia (white star), located dorsal to the *X*-axis (*X*–*X*′) and lateral to the *Y*-axis (*Y*–*Y*′), was correctly diagnosed. Middle) Unenhanced transverse CT scan at the level of the right pubic tubercle in an 80-year-old male patient. Right direct inguinal hernia (white star), located ventral to the *X*-axis (*X*–*X*′) and strictly to the *Y*-axis (*Y*–*Y*′), was correctly diagnosed. Right) Unenhanced transverse CT scan at the level of the left pubic tubercle in a 76-year-old male patient. Left indirect inguinal hernia (white star), located ventral to the *X*-axis (*X*–*X*′) and crossing medially the *Y*-axis (*Y*–*Y*′), was correctly diagnosed
With permission from (From: The pubic tubercle: a CT landmark in groin hernia. Delabrousse E, Denue PO, Aubry S, Sarlième P, Mantion GA, Kastler BA—Abdom Imaging—November 1, 2007; 32 (6); 803–6)

The pubic tubercle has been proposed as a landmark to differentiate direct from indirect and femoral hernias, particularly in instances when the inferior epigastric vessels are difficult to distinguish as a landmark. After drawing orthogonal lines on axial MDCT imaging at the level of the pubic tubercle as in Fig. 11.11, dorsal crossing of the *X*-axis suggests femoral origin and medial crossing of the *Y*-axis suggests an indirect inguinal hernia. Although this method has not been validated, it may provide insight for surgical planning in acute scenarios. Video 11.2 shows a CT scan of a patient with a right direct inguinal hernia.

Magnetic Resonance Imaging

MRI is a third-line imaging modality for hernia evaluation. However, compared to MDCT and US, MRI is far more sensitive, specific, and reliable for occult hernia identification. Compared to MDCT, MRI does not have ionizing radiation exposure or the potential consequences of iodinated intravenous contrast agents. As such, consider MRI when clinical suspicion is high despite negative prior studies when exam is non-congruent with reported symptoms, and for atypical presentations of groin pain. Limitations to MRI include cost and potentially limited accessibility, and variability in insurance coverage for hernia evaluation. In general, MRI is seldom used for the evaluation of direct inguinal hernias.

Imaging After Direct Inguinal Hernia Repair and Complications

Complications such as hernia recurrence, hematoma, seroma, mesh infection, and bowel obstruction can occur after direct inguinal hernia repair. A detailed discussion of surgical repairs for direct inguinal hernia is beyond the scope of this chapter, but non-surgeon clinicians and radiologists should have a basic understanding of repair approaches, techniques, prosthetic meshes, and expected postoperative changes when considering and interpreting imaging studies for suspected complications.

In general, inguinal hernia repairs are performed either from an anterior/open approach or a posterior/minimally invasive (laparoscopic or robotic) approach. After all minimally invasive repairs, some degree of subcutaneous and preperitoneal air is expected on cross-sectional imaging, as well as intraperitoneal air after lapa-

roscopic transabdominal pre-peritoneal (TAPP) repairs. Although some pneumoperitoneum is not abnormal after TAPP, the intra-abdominal nature and incising of the peritoneum during this approach create unique but rare risks including iatrogenic bowel injury and intestinal obstruction. With respect to obstruction, failure to reapproximate the peritoneal flaps created during repair can allow bowel entrapment in the pre-peritoneal space and potentially bowel obstruction or strangulation through an internal hernia in the peritoneal closure. Thus, given the gravity of consequences if unrecognized, patients with evidence of early postoperative obstruction or developing peritonitis warrant strong consideration for reexploration even if imaging is not confirmatory.

Most modern-day open and minimally invasive repairs involve the placement of prosthetic mesh in the affected groin for both direct and indirect repairs. Large pore polypropylene mesh is typical for use, and this material is invisible or poorly visible on MDCT due to its isoattenuation compared to the surrounding abdominal wall muscle and fascia. Polytetrafluoroethylene mesh, conversely, has higher attenuation and is readily visible on MDCT. Mesh-related infections in the groin are uncommon after both open and minimally invasive approaches without typical risk factors.

Postoperative fluid collections can be evaluated by MDCT and US. Seromas commonly occur in the inguinal canal and adjacent to prosthetic mesh postoperatively and are generally self-limited, resolving within weeks following the operation. MDCT is typically sufficient to differentiate simple fluid from abscess or hematoma; however, US can also establish this diagnosis as well by demonstrating anechoic fluid. Hematomas are characteristically hyperattenuating on MDCT versus hypoechoic and heterogeneous and complex on sonogram. Additionally, as most seromas will resolve spontaneously, imaging can be deferred if the seroma is decreasing in size on serial office examinations. Figure 11.12 demonstrates the US appearance of a postoperative hematoma after a direct inguinal hernia repair.

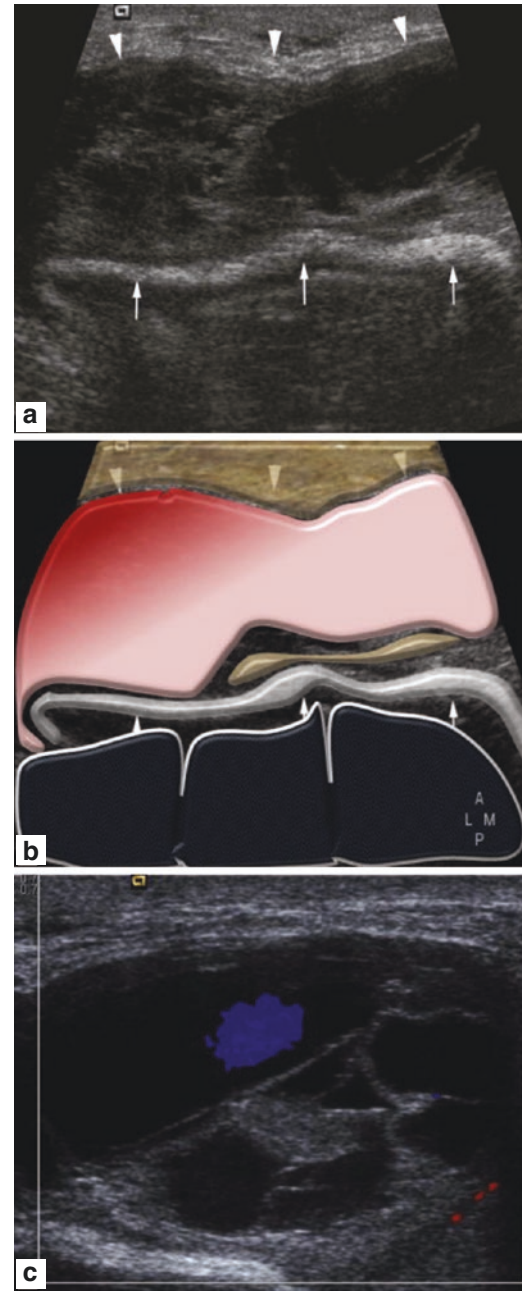

Fig. 11.12 Left inguinal mass after direct hernia repair, transverse sonograms. (**a**, **b**) A well-defined hyperechoic linear structure (arrows) lies on the deep aspect of the inguinal canal and has the typical appearance of a mesh placed over the posterior inguinal wall. However, filling the canal is a lobulated, predominantly heterogeneous soft tissue mass consistent with a postoperative hematoma (arrows). (**c**) Color Doppler shows no flow within the solid areas
With permission from: Practical Musculoskeletal Ultrasound [Philip Robinson]. Disorders of the Groin and Hip: Groin Pain

Conclusion

In summary, direct inguinal hernias occur in Hesselbach's triangle. Although a thorough history and physical exam obviate the need for radiologic evaluation of inguinal hernias in most situations, multiple imaging modalities exist to aid diagnosis when indicated. Dynamic US is the preferred modality to image direct inguinal hernias. MDCT and to some extent MRI are also useful in characterizing hernias and differentiating from non-hernia inguinal pathology. Finally, imaging can be useful when evaluating for complications after herniorrhaphy.

Further Readings

Delabrousse E, Denue P-O, Aubry S, Sarlième P, Mantion GA, Kastler BA. The pubic tubercle: a CT landmark in groin hernia. Abdominal Imaging. 2007;32(6):803–6.

Jacobson JA. Hip and thigh ultrasound, Chapter 6. In: Fundamentals of musculoskeletal ultrasound, pp. 223–283.e4.

Levine D, Napolitano L, Stavros AT. Dynamic ultrasound of hernias of the groin and anterior abdominal wall, Chapter 13. In: Diagnostic ultrasound, pp. 470–503.

Miller J, Cho J, Michael MJ, Saouaf R, Towfigh S. Role of imaging in the diagnosis of occult hernias. JAMA Surg. 2014;149(10):1077–80. https://doi.org/10.1001/jamasurg.2014.484.

Robinson P. Disorders of the groin and hip: groin pain, Chapter 17. In: Practical musculoskeletal ultrasound, pp. 177–192.

Schoettle A, Veillon F, Venkatasamy A. The lateral crescent sign. Abdominal Radiol. 2018;43(11):3195–6.

Indirect Inguinal Hernia

12

Oscar Gonzalo Talledo Zevallos, Kayla M. Watkins, Jason M. Wagner, and Laura E. Fischer

Introduction

Inguinal hernia repair is one of the most common general surgery procedures, with over 800,000 inguinal hernia repairs performed each year in the United States. One in three males will develop a hernia at some point during his lifetime. While groin hernias are more common in male patients, females can also develop inguinal hernias. Patients present in the elective, urgent, and emergent settings and ages range from less than 1 year to more than 80 years old. Sometimes, an inguinal hernia is obvious on physical exam; however, patients will often present with complaints consistent with a hernia, but a palpable defect is difficult to identify. The development of modern technology and advanced imaging has improved the diagnostic accuracy of challenging inguinal hernias. In this chapter, we will describe indirect inguinal hernia, the most common type of inguinal hernia, and its characteristics in multiple different imaging modalities. We discuss methods of diagnosis and best utilization practices for imaging modalities, specifically ultrasound (whether dynamic or standard), CT scan, or MRI.

Symptoms

The majority of inguinal hernias (in the non-emergent, clinic setting) are diagnosed based on a patient's history of present illness and their physical exam findings. There is a wide range of clinical presentations. In the non-emergent setting, generally, patients will present with a bulge or discomfort in the groin [1]. Occasionally, they will comment that they were straining and felt a pull or pop in the groin with discomfort following intermittently. Some patients will have a bulge that reduces spontaneously, some will reduce with lying down, pulling knees to chest and reducing manually, while others will be chronically incarcerated with the inability to reduce the hernia on exam.

In the emergent setting, we commonly see patients who come in with a bulge in the groin

Supplementary Information The online version contains supplementary material available at https://doi.org/10.1007/978-3-031-21336-6_12.

O. G. T. Zevallos
Department of MIS and Bariatric Surgery, UIHC, Iowa City, IA, USA

K. M. Watkins (✉) · L. E. Fischer
Department of Surgery, University of Oklahoma, Oklahoma City, OK, USA
e-mail: Laura-Fischer@ouhsc.edu

J. M. Wagner
Department of Radiological Sciences, University of Oklahoma, Oklahoma City, OK, USA
e-mail: Jason-wagner@ouhsc.edu

S. Docimo Jr. et al. (eds.), *Fundamentals of Hernia Radiology*,
https://doi.org/10.1007/978-3-031-21336-6_12

that has been "out" for a significant amount of time where it may have been reducible previously. We see symptoms of bowel obstruction including nausea, emesis, increasing pain, obstipation, and constipation. With these hernias, we may attempt reduction in the emergency department but most commonly have to take the patients to the operating room urgently for repair and examination of the incarcerated bowel for ischemia or necrosis.

In both settings, it is important to rule out other causes of a bulge or discomfort in the groin including hydrocele, lymphadenopathy, testicular torsion, or musculoskeletal strain.

Hernias are more common in males than females; however, of the different types of hernias, the most common among both genders is the indirect inguinal hernia.

Physical Exam Findings

As stated previously, most of the time a good history and physical exam is all that is needed to diagnose an inguinal hernia. An adequate physical exam has reported diagnostic sensitivities and specificities above 75%.

When performing an exam for a potential hernia in a male patient, the examiner invaginates the scrotum and places a finger through the external ring or into the inguinal canal (see below section for anatomy review). The examiner should then ask the patient to perform a Valsalva maneuver by either bearing down as if having a bowel movement or coughing to the side. Using this maneuver, a palpable defect or weakness in the inguinal floor may be identified, especially if a large hernia is not obvious on visual inspection. It is also useful to perform the groin examination in both the standing and supine positions, especially for female patients. Inguinal hernias in female patients are slightly more difficult to diagnose. During physical examination, the area lateral to the pubic tubercle should be palpated to assess for bulges or defects. A Valsalva maneuver may be performed here as well. In addition to checking both groins for defect, the umbilicus should be examined for potential hernia, as well.

The majority of patients who present with the typical symptoms will have a palpable defect or bulge on exam. A symptomatic bulge noted on physical exam is typically sufficent for diagnosis and operative planning. However, some patients have more vague symptoms or slower onset of pain or discomfort. In these instances, imaging studies can be very useful for confirming the suspected diagnosis and aiding in surgical planning [2].

Anatomy

The anatomy of the inguinal region is arguably one of the most challenging to understand and identify. There are three different types of inguinal hernias seen most commonly by general surgeons: indirect, direct, and femoral hernias. While the treatment or options for repair are relatively similar between these three considering all three defects are encompassed by the myopectineal orifice and covered completely by mesh during a laparoscopic or robotic repair, they differ in their anatomic relationships to important structures in the groin. Indirect inguinal hernias protrude through the internal inguinal ring into the inguinal canal and can be seen entering lateral to the epigastric vessels on imaging or during laparoscopy. Direct inguinal hernias protrude through a weak point in the transversalis fascia medial to the epigastric vessels—within the triangle of Hesselbach, which is bordered medially by the lateral border of the rectus, laterally by the epigastric vessels and inferiorly by the inguinal ligament. Femoral hernias, which are generally the most worrisome for potential obstruction, protrude inferior to the inguinal ligament and medial to the iliofemoral vessels.

The abdominal wall consists of multiple layers of muscle with associated fascia underneath the skin and subcutaneous adipose tissue. From superficial to deep, they are Scarpa and Camper fascia, the external oblique fascia and muscle, internal oblique fascia and muscle, and the transversus abdominis muscle [3]. The transversalis fascia is identified next followed by preperitoneal fat, peritoneum and then the peritoneal cavity housing the intestines, solid organs, etc.

The inguinal floor is made up of the abdominal wall muscles listed above and is located between the anterior superior iliac spine and the pubic tubercle. The inguinal canal is the space that contains the spermatic cord structures (testicular vessels and vas deferens) in men and round ligament in women. It is bounded by the external oblique fascia anteriorly (also known as the "roof" of the inguinal canal), the inguinal ligament inferiorly, the conjoint tendon superiorly, which is made up of the transversus abdominis and internal oblique, and the transversalis fascia posteriorly (also known as the "floor" of the inguinal canal). The internal and external rings are located at either end of the inguinal canal. In order to better understand the "roof" and "floor" designations, it is helpful to picture the patient in a supine position.

When performing a laparoscopic or robotic repair of an inguinal hernia the preperitoneal space is entered. It is in this plane that reduction of the hernia occurs, relevant anatomy is identified, the myopectineal orifice is cleared and mesh is placed to reduce future hernia recurrence. Two important anatomical spaces to identify during hernia repair are the triangles of doom and pain. The "tringle of doom" is bordered by the vas deferens medially, the gonadal vessels laterally, and the peritoneal reflection. Its contents are the external iliac vessels which if injured can lead to difficult to control bleeding. The "triangle of pain" is directly lateral to the "triangle of doom" and is bordered by the gonadal vessels medially, the iliopubic tract laterally, and the peritoneal reflection. This triangle contains the lateral femoral cutaneous nerve, the femoral branch of the genitofemoral nerve, and the femoral nerve. It is important to avoid excessive dissection and tacking within this anatomic triangle as chronic pain is a difficult to manage complication of this procedure [4].

Imaging

Although physical examination is the gold standard for the diagnosis of inguinal hernias, there are some scenarios in which a physical exam might not be conclusive, especially for patients who may be obese or have had multiple prior operations in the inguinal region. Diagnostic imaging options include ultrasound (still and dynamic), computed tomography scans, and magnetic resonance imaging.

Ultrasound

Ultrasound (US) is relatively inexpensive, noninvasive, portable, and fast; however, the sonographer's ability to perform the exam in both the supine and upright/standing position, as well as including a dynamic assessment, makes US particularly advantageous. Figure 12.1 demonstrates normal inguinal anatomy on ultrasound evaluation while Fig. 12.2 provides a view of a normal inguinal ligament, whereas Fig. 12.3 and Fig. 12.4 reveal indirect inguinal hernias containing small bowel and ascites, respectively. Figure 12.5 reveals both fluid and the appendix within the hernia sac consistent with an Amyand's hernia. In Fig. 12.6, we demonstrate the anatomy of an indirect inguinal hernia which was previously discussed. Here we see the inferior epigastric vessels which are circled in blue. Again, this is what differentiates an indirect, lateral to the vessels, from a direct hernia, medial to the vessels. Video 12.1 demonstrates physiologic soft

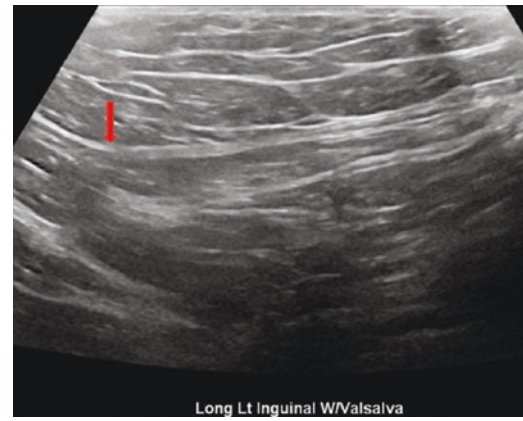

Fig. 12.1 Longitudinal ultrasound image of normal inguinal canal. The head of the patient is towards the left side of the picture. The internal inguinal canal is identified by the arrow

Fig. 12.2 Normal inguinal ligament of a young female. The pubic bone is towards the right side of the picture

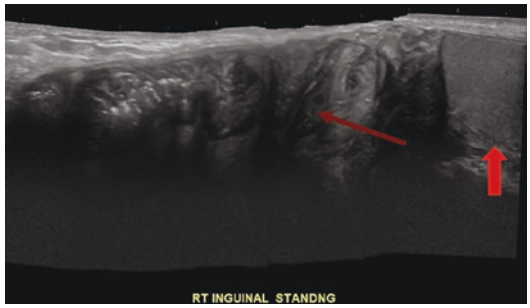

Fig. 12.3 Extended field of view longitudinal ultrasound image depicting a small bowel containing indirect inguinal hernia while the patient is in the standing position. The larger arrow identifies the testicle while the diagonal arrow identifies herniated small bowel

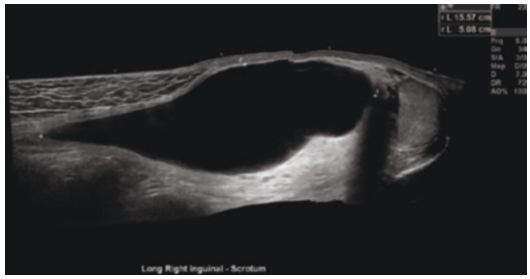

Fig. 12.4 Extended field of view longitudinal ultrasound image depicting hernia distended with ascites

tissue movement during a Valsalva maneuver, the same as performed during simple physical exam.

Dynamic inguinal ultrasound is described to have a diagnostic sensitivity of 98% and a specificity of 99% [5]. Usually performed in a standardized technique, the multifrequency linear transducer is placed vertically over the medial aspect of the groin to visualize the pubic tubercle and rectus muscle. Subsequently, it is placed diagonally over the inguinal canal (parallel to the cord structures) and the patient is, again, asked to perform the Valsalva maneuver allowing identification of a hernia sac parallel to the cord structures. Turning the probe 90 degrees will provide a perpendicular view of the spermatic cord and will help to localize the position of the hernia sac medial or lateral to the epigastric vessels. Lastly, the probe is placed longitudinally over the femoral and iliac vessels. Here, a protrusion of a hernia sac under the inguinal ligament parallel and medial to the iliofemoral vessels can be appreciated in a patient with a femoral hernia [6]. Video 12.2 demonstrates a longitudinal view of an indirect inguinal hernia with small bowel protrusion into the inguinal canal when the patient is asked to cough/perform Valsalva. Video 12.3 demonstrates longitudinal view of an indirect inguinal hernia during compression with ultrasound probe. Three other interesting ultrasound images are included below.

Computed Tomography

Computed tomography (CT) scans are particularly useful in the setting of larger hernias or patients with obesity. One advantage to CT scan is being able to better visualize the contents of the hernia. CT scans are also particularly useful in the setting of a recurrence where the clinical picture may not be as easily diagnostic of hernia as it would be for an initial evaluation. The disadvantages of a CT scan are cost, especially in comparison to the cheaper and readily available ultrasound, and the radiation dose, which is avoided with ultrasound.

When performing CT scans for evaluation of inguinal hernias, it is important to use intravenous contrast so that the vasculature is clearly delineated and we can evaluate for any other pathologies. A contrast CT scan of an inguinal hernia is particularly useful in the setting of a hernia recurrence and the position of previously placed mesh in relation to the vasculature is paramount in operative planning. Figure 12.7 is a still image extracted from a contrasted CT

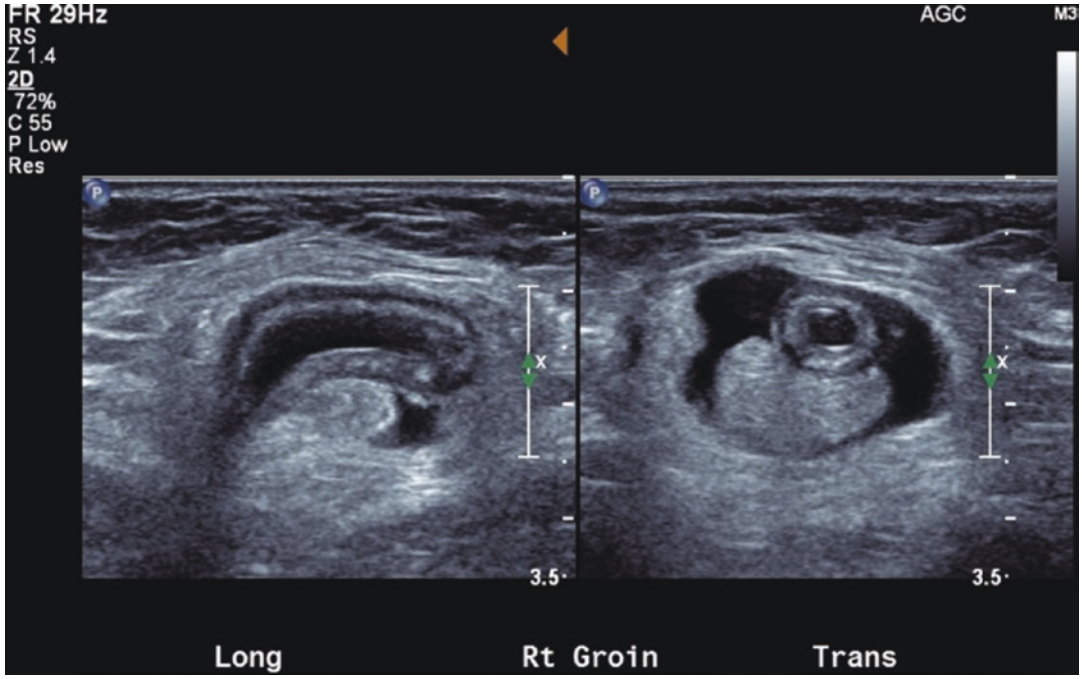

Fig. 12.5 Longitudinal and transverse images of fluid and the appendix within an inguinal hernia

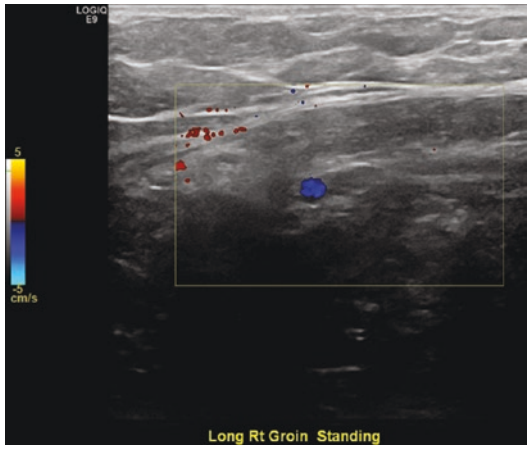

Fig. 12.6 Doppler longitudinal view of a fat containing indirect inguinal hernia. The inferior epigastric vessel is seen as a blue circular image

scan with normal anatomy while Fig. 12.8 shows an indirect inguinal hernia containing a loop of the small intestine. An advanced CT technique uses a protocol that takes images in the standard, supine position and compares them to images of the patient performing a Valsalva maneuver. This technique is similar to a dynamic ultrasound.

Fig. 12.7 Axial view of the pelvis with normal inguinal anatomy and no evidence of inguinal hernia

Magnetic Resonance Imaging

Magnetic resonance imaging (MRI) is advantageous in patients who present with symptoms of a defect that is difficult to palpate. It is also beneficial for patients in whom we would like to avoid the radiation dose of a CT scan, such as young adults or women of child-bearing age. MRI is also useful if the physician is suspecting a musculoskeletal issue or other pathology as the source of the patient's discomfort as this imaging modality is better for the evaluation and diagno-

Fig. 12.8 Axial view of a left inguinal hernia containing a loop of bowel

Fig. 12.9 MRI with bilateral inguinal hernias

sis of ligamentous injuries, strain, and lumbar spine/muscle abnormalities.

An obvious disadvantage to MRIs is the increased expense and longer time for examination as the average pelvic MRI takes approximately 30–60 min. While dynamic MRI may help make the diagnosis of an indirect inguinal hernia, this adds additional time to the standard MRI procedure. Figure 12.9 demonstrates bilateral inguinal hernias discovered with MRI.

X-ray

While x-rays are neither particularly sensitive nor specific for diagnosing inguinal hernias, we are sometimes able to identify bowel within a hernia sac by identifying bowel gas or haustra within the inguinal canal as shown in Fig. 12.10 below.

Fig. 12.10 Upright abdominal film with gas in bowel within inguinal hernia

Treatment

Many years ago, it was thought that all inguinal hernias should be repaired due to the risk of incarceration and strangulation, resulting in the need for an emergent operation. However, recently, there have been studies supporting observation in asymptomatic or minimally symptomatic hernias [7]. The only definitive treatment option for inguinal hernias, though, is operative intervention.

Previously, most initial and unilateral hernias were repaired using an open mesh technique. Recently, general surgeons are adopting a minimally invasive approach for initial hernias as it results in earlier return to work and the ability to evaluate bilateral groins during the same anesthetic. Larger or incarcerated hernias may be best treated with either robotic or open repairs, and sometimes even a combination of the two. A good rule of thumb for repairing recurrent inguinal hernias, which can occur up to 9.9% of open

mesh repairs [8], is to perform the repair from the opposite approach of the original procedure. For example, if a laparoscopic or robotic repair was performed initially, then an open repair should be performed for a recurrence and vice versa.

Conclusion

Indirect inguinal hernia is the most common hernia defect in adults and can be evaluated through the use of static and dynamic US, CT, and MRI for improved surgical care.

References

1. Cameron JL, Cameron A. Current surgical therapy. Philadelphia: Mosby Elsevier. 2017;12:623–9.
2. Fischer JE. Fischer's mastery of surgery. New Delhi: Wolters Kluwer Health/Lippincott Williams & Wilkins. 2012 (6):2063–90.
3. Miller HJ. Inguinal hernia: mastering the anatomy. Surg Clin N Am. 2018;98(3):607–21. https://doi.org/10.1016/j.suc.2018.02.005.
4. Dimick JB, Upchurch GR, Sonnenday CJ, Kao LS. Clinical scenarios in surgery: decision making and operative technique. Philadelphia: Wolters Kluwer. 2019 (1):3–20.
5. Niebuhr H, König A, Pawlak M, et al. Groin hernia diagnostics: dynamic inguinal ultrasound (DIUS). Langenbecks Arch Surg. 2017;402:1039–45.
6. Stavros AT, Rapp C. Dynamic ultrasound of hernias of the groin and anterior abdominal wall. Ultrasound Q. 2010;26(3):135–69.
7. Fitzgibbons RJ, Giobbie-Hurder A, Gibbs JO, et al. Watchful waiting vs repair of inguinal hernia in minimally symptomatic men: a randomized clinical trial. JAMA. 2006;295(3):285–92. https://doi.org/10.1001/jama.295.3.285.
8. Gopal SV, Warrier A. Recurrence after groin hernia repair-revisited. Int J Surg. 2013;11(5):374–7. https://doi.org/10.1016/j.ijsu.2013.03.012.

Femoral Hernia

13

Clayton C. Petro

Introduction

Femoral hernias have unique clinical characteristics attributable to their relevant anatomy. Most significant is that the femoral canal's entrance has rigid borders (Fig. 13.1) (Video 13.1):

- Anterior—Inguinal ligament or iliopubic tract
- Posterior—Pectineal or Cooper's ligament
- Lateral—Femoral vein
- Medial—Lacunar portion of the inguinal ligament

Typically, the space contains lymphatics and loose adipose connective tissue and its entrance is closed by a femoral septum of extraperitoneal tissue. Still, it is an area of weakness prone to hernia formation in aging patients, particularly women where the ring is relatively wider and loosens during pregnancy due to physical and hormonal changes. As such, femoral hernias are notoriously more common in females, by a ratio of 4:1. Since inguinal hernias, in general, are more common in men, femoral hernias account for less than 1% of defects in a male myopectineal orifice, while they account for 20% of groin hernias in women. Also—for unclear reasons—femoral hernias are almost twice as likely to be on the right. When the hernia sac of the peritoneum descends through the femoral canal, its caudal path is interrupted by the femoral sheath and insertion of the saphenous vein into the femoral vein. Consequently, the hernia sac typically turns forward and upward often reflecting back

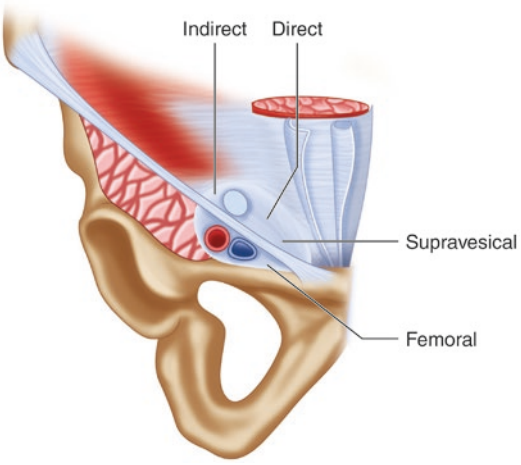

Fig. 13.1 Fruchaud's myopectineal orifice. Note the femoral space bound by the femoral vein medially, the iliac ligament superiorly, the lacunar ligament medially, and the pectineal ligament inferiorly. Modified from Skandalakis LJ, Skandalakis JE, Skandalakis PN. Surgical Anatomy and Technique: A Pocket Manual, 3rd ed. New York: Springer; 2009

Supplementary Information The online version contains supplementary material available at https://doi.org/10.1007/978-3-031-21336-6_13.

C. C. Petro (✉)
Department of General Surgery—Center for Abdominal Core Health, Cleveland Clinic, Cleveland, OH, USA
e-mail: PETROC@ccf.org

S. Docimo Jr. et al. (eds.), *Fundamentals of Hernia Radiology*,
https://doi.org/10.1007/978-3-031-21336-6_13

over the inguinal ligament. This explains the difficulty in clinically distinguishing a femoral from a direct or indirect hernia, despite the experience of the examining surgeon.

The aforementioned rigidity of the femoral canal entrance puts these patients at a particularly high risk of strangulation and emergent presentation. One group reported a 22% probability of strangulation within 3 months of diagnosis, escalating to 45% at 2 years. When compared to direct and indirect inguinal hernia, where watchful waiting of asymptomatic or minimally symptomatic patients is considered safe, the same cannot be said for femoral hernias. If appropriately identified in the elective setting, true femoral hernias should be repaired with a much greater sense of urgency. That said, many femoral hernias are encountered unexpectedly, mistaken for a direct or indirect inguinal hernia or when the clinician is distracted by an emergent presentation. For that reason, any general surgeon needs to be prepared to deal with this problem. While several options for repair will be discussed later, a comprehensive understanding of the relevant anatomy, close review of any preoperative imaging, and a high index of suspicion are ultimately going to facilitate appropriate identification and chosen operative approach.

Patient Selection

As was mentioned previously, most true femoral hernias should be fixed when they are diagnosed so as to avoid an emergent presentation. However, the designation of "true" is a subtle but important component of our institution's bias. Any patient with an easily palpable bulge or imaging (ultrasound or cross-sectional) that demonstrates intra-abdominal viscera in the femoral space should be repaired. Alternatively, surgeons should beware of a common clinical scenario—young patients presenting with groin pain but without a palpable bulge, and who subsequently undergo a dynamic ultrasound (US) of the groin (Video 13.2). Often, a well-meaning ultrasonographer will identify mobile pre-peritoneal fat in the femoral canal and assign the diagnosis of a femoral hernia. Even in the absence of a concomitant direct/indirect defect, this designation can begin a cascade of events that leads to the placement of mesh in the groin, but commonly will not alleviate—and may even exacerbate—the patient's pain. While the treatment of groin pain attributable to a "sports hernia" or athletic pubalgia is controversial and beyond the scope of this chapter, I do think it is worth acknowledging the stark contrast between these two ends of the clinical spectrum. The surgeon should recall that clinically meaningful femoral hernias are exceedingly more common in older patients and should be repaired expediently and that young patients with pain attributable to mobile fat in the femoral canal should be approached with caution—in our opinion non-operatively.

CT Scan Findings

CT scans can often reliably distinguish femoral hernias from direct or indirect inguinal hernias. While anatomic landmarks on cross-sectional imaging are useful, there are specific findings used by radiologists to identify a femoral hernia of which surgeons should be aware.

1. Since the femoral canal rests on the proximal insertion of the pectineus muscle, a femoral hernia is immediately anterior to Cooper's ligament (Fig. 13.2a, b). Admittedly, the specificity of this finding is unreliable as large direct inguinal hernias can have a similar appearance on axial cross-sections where it is not always possible to tell if the hernia is above or below the inguinal ligament.
2. To aid the aforementioned distinction, coronal CT cuts will often reliably distinguish whether a groin hernia is above (inguinal) or below (femoral) the inguinal ligament, even in the presence of inflammation (Fig. 13.2c, d).
3. Most femoral hernia sacs remain *lateral* to the pubic tubercle while direct and indirect hernia sacs will often track *medial* to the pubic tubercle (Fig. 13.2e).
4. A femoral hernia will emerge caudal, inferior, and medial to the origin of the inferior epigastric artery (Fig. 13.2a, b). While direct ingui-

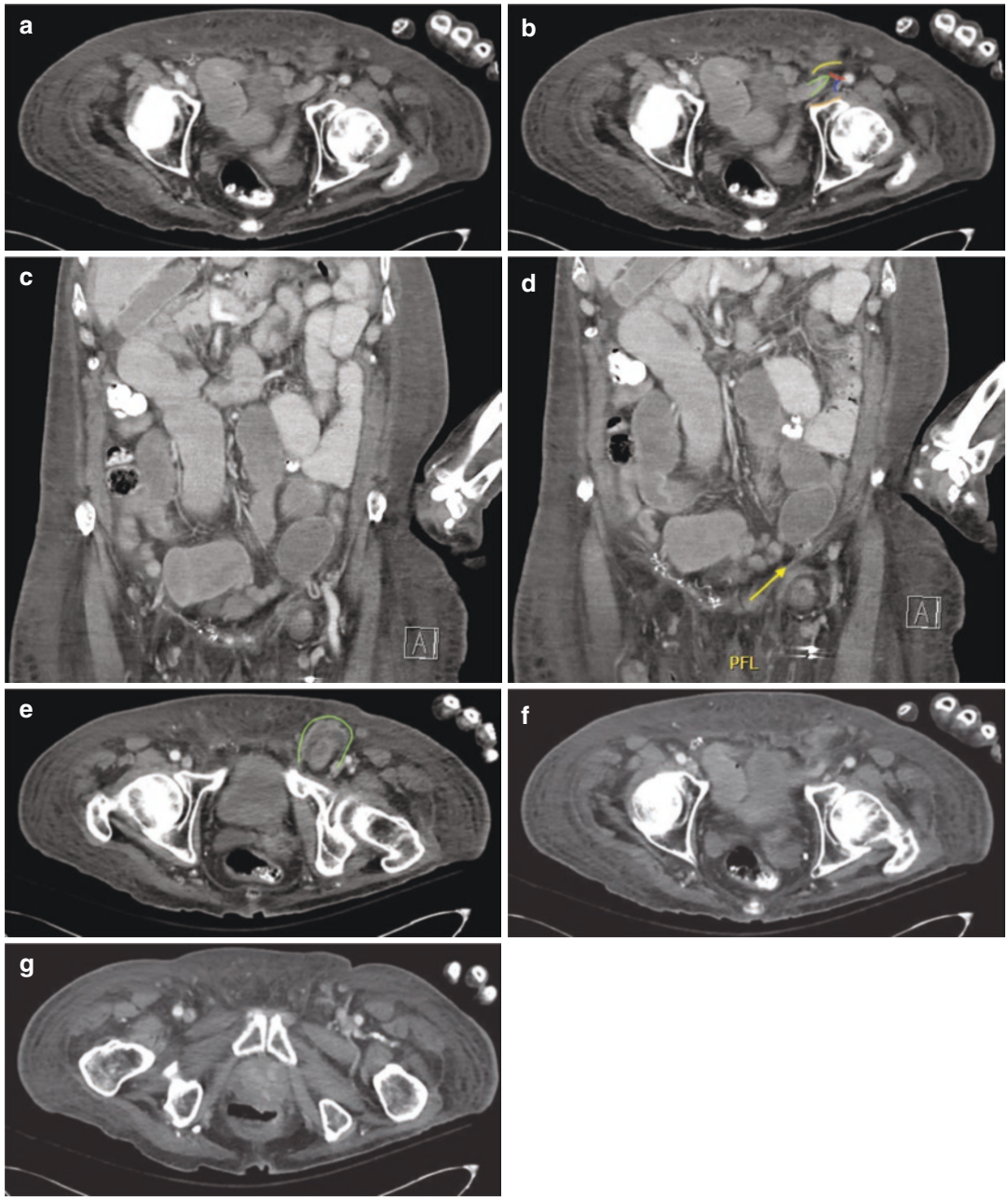

Fig. 13.2 CT scan of a left femoral hernia with strangulated small bowel. (**a/b**) Note: (i) The presence of the left femoral hernia sac (green) whose origin is inferior to the inguinal ligament (yellow) caudad to the inferior epigastric artery (red) and anterior to the pectineal ligament (orange). (ii) Significant compression of the left femoral vein (blue). (**c**) Femoral hernia seen just medial to femoral vessels. (**d**) This image is one slice ventral to the image in Fig. 13.3c, demonstrating that the inguinal ligament is ventral to the hernia sac, indicating a femoral defect. (**e**) Note that the hernia sac remains lateral to the pubic tubercle. Edema within the femoral hernia sac (green) surrounding a strangulated loop of small intestine. (**f**) Note almost complete compressions of the left femoral vein at the origin of the femoral canal. (**g**) Caudal to femoral vein compression, note collateral venous engorgement distinct from the contralateral side

nal hernias are also medial to the epigastric artery, their origin is cephalad to the inferior epigastric artery's takeoff from the iliac artery.
5. Given the high risk of strangulation for femoral hernias, significant edema surrounding incarcerated contents is common (Fig. 13.2e), but again not reliably specific.
6. **The most sensitive and specific finding for femoral hernias is compression of the femoral vein. Given the tight opening of the femoral canal and its rigid borders, a strangulated femoral hernia can have a significant mass effect, causing either concavity or almost complete compression of the adjacent femoral vein** (Fig. 13.2f).
7. A secondary finding caudal to venous compression is venous engorgement of the distal femoral vein and its collaterals (Fig. 13.2g).

Dynamic Groin Ultrasound

At our institution, we make liberal use of the dynamic groin US in several contexts. Most commonly, it is helpful to diagnose an inguinal hernia when the physical exam is equivocal. Likewise, it is also helpful to diagnose an occult recurrence or nerve entrapment, either of which could be the cause of chronic groin pain following repair. In the context of diagnosing a femoral hernia, we will specifically describe how a dynamic groin US is used.

1. After assessing the patient for a direct or indirect inguinal hernia, the ultrasonographer then makes a dedicated effort to determine if a femoral hernia is present. The patient remains in the supine position with the leg straight. While some begin this exam holding the transducer in the vertical or longitudinal position, we typically prefer to start with the transducer in the transverse position. This allows the user to quickly orient themselves by attaining a cross-section view of the femoral vessels. (Fig. 13.3a–c)
2. Next the transducer is moved towards the feet until the greater saphenous vein is identified medially as it empties into the femoral vein—this is the caudal extent of the exam. (Fig. 13.3d)
3. As the transducer—remaining in the transverse position—is moved cephalad, the femoral space is identified just anterior to the pectineus muscle, which inserts on the pectineal ligament. To widen this view, the patient's leg can be abducted (bent at the knee and relaxed laterally—"frog leg").
4. The patient is then asked to perform a Valsalva maneuver. If a femoral hernia is present, the ultrasonographer will note the protrusion of mobile fat or viscera above the pectineus muscle that compresses the adjacent femoral vein. (Fig. 13.3f–h).
5. If it is difficult to discern whether or not the protrusion is above or below the inguinal ligament—a direct or femoral hernia respectively—the transducer can then be turned to the vertical or longitudinal position to help clarify this. Additionally, as was mentioned in the discussion regarding CT scans, direct hernias typically emanate caudad to the takeoff of the inferior epigastric artery from the iliac artery. The takeoff of the epigastric artery is therefore the cephalad extent of this examination and its visualization should make the examiner pause to confirm that the associated hernia is not originating above the inguinal ligament.

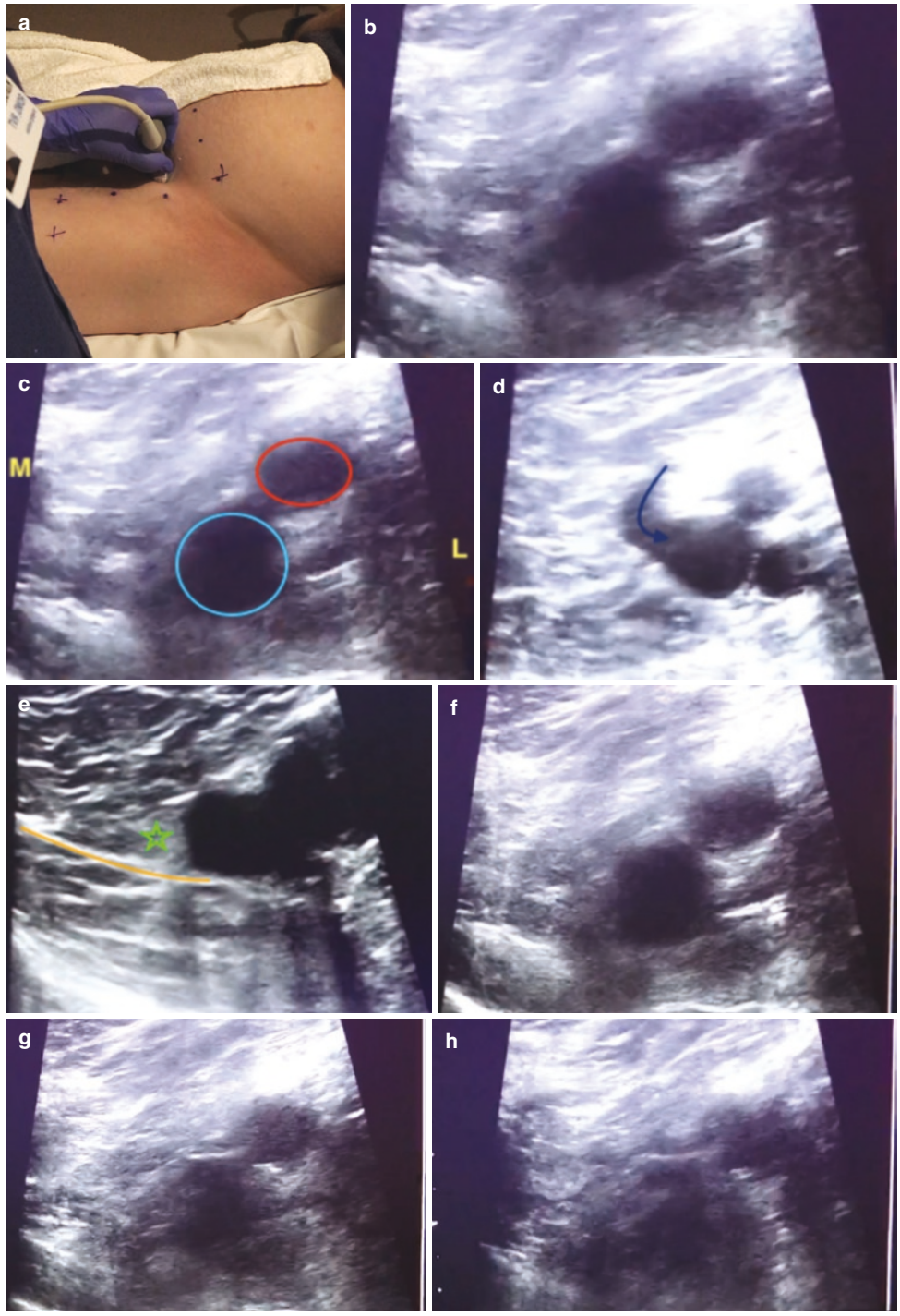

Fig. 13.3 Dynamic ultrasound to identify a femoral hernia. (**a**) The patient is supine with their leg straight and the ultrasound probe is held in the transverse position to obtain a cross-section of the femoral vessels. (**b**, **c**) Cross-section of the femoral vessels—for orientation medial and lateral (M & L) are marked. The femoral vein is marked in blue and the femoral artery is marked in red. (**d**) The greater saphenous vein empties medially into the femoral vein. This is the caudal extent of the exam. (**e**) The caudal extent of the potential femoral space (green star) is bordered inferiorly by the pectineus muscle (orange). (**f**–**h**) Note sequential compression of the femoral vein with Valsalva as fat moves into the femoral space

Clinical Pearls

Femoral hernia repair is not straightforward for several reasons. First, the somewhat frequent emergent presentation of these hernias can heavily dictate repair options. A strangulated piece of bowel may require a bowel resection and that added level of contamination may make the surgeon reluctant to place a piece of mesh. For that reason, a tissue repair is often necessary, and those techniques are typically not a routine part of most contemporary surgeons' practice. Even still, there are several options for open primary repair depending on whether the surgeon recognizes the femoral hernia diagnosis preoperatively and whether or not there is a concomitant direct/indirect defect as well. Next, even if the surgeon is comfortable with minimally invasive approaches, an incarcerated piece of small intestine causing an associated bowel obstruction may make a minimally invasive approach impossible or at least technically challenging. For these reasons, decision-making can be complex, yet the surgeon must be ready to deal with the many permutations of each scenario unexpectedly. It is not surprising that such cases—harkening back to traditional non-mesh repairs, which require a good understanding of inguinal anatomy—are often highlighted on surgical exams.

In the elective setting, a totally extraperitoneal (TEP) or transabdominal pre-peritoneal (TAPP) laparoscopic approach offers an advantageous perspective for identification of a femoral hernia as long as the surgeon recognizes its location below the inguinal ligament (Fig. 13.4a). Either pre-peritoneal approach does not differ in its ultimate execution, as mesh placement during this operation for an inguinal hernia should typically cover the opening of the femoral space as well (Fig. 13.4b). While minimally invasive approaches are possible during emergent presentations, exposure can be limited by bowel distention in the setting of incarceration and an associated obstruction. In these situations, the TEP approach should be avoided so that the incarcerated and potentially strangulated viscera can be assessed, reduced under direct visualization, and repaired/resected if needed. Those benefits are offered by the TAPP approach, assuming that there is sufficient working space. If the contents of the incarcerated hernia do not reduce with gentle traction, we recommend sharp division of the lacunar ligament (medially) or inguinal ligament (anteriorly) to widen the opening of the femoral canal. If the viscera reduces, the surgeon can assess the bowel laparoscopically and decide if a resection is necessary, and that can be done laparoscopically or through a small lapa-

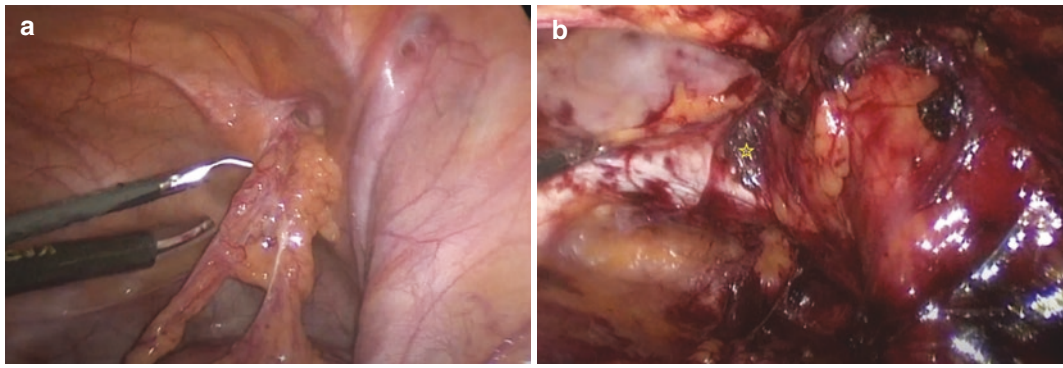

Fig. 13.4 Laparoscopic transabdominal pre-peritoneal repair of a femoral hernia. (**a**) Incarcerated omentum within a right femoral hernia during a transabdominal pre-peritoneal repair with a patient in Trendelenburg position. Note the tight size of the defect located anterior to Cooper's ligament, and just medial to the femoral vessels. (**b**) After developing the pre-peritoneal plane and reducing the femoral hernia sac, note the empty femoral space (yellow star) bounded medially by the lacunar ligament, inferiorly by Cooper's ligament, and anteriorly by the inguinal ligament

rotomy depending on the surgeon's preference. If a bowel resection is not necessary, a TAPP repair can be done with pre-peritoneal mesh placement. In the scenario where a bowel resection is done, some would consider the use of a permanent mesh as controversial in a contaminated setting. As such, laparoscopic primary closure of the femoral defect—sewing the anterior inguinal ligament to the posterior Coopers ligament—is a perfectly safe and acceptable way to temporize an emergent situation. As was highlighted, while laparoscopic approaches are favorable in the elective setting for identifying and repair femoral defects, there are numerous limitations in the emergent setting. Specifically, poor exposure or any difficulty reducing the hernia contents should prompt conversion to an open approach, and these techniques are discussed next.

Open approaches to femoral hernia repair are likewise heavily dictated by the context of the presentation. Occasionally, a femoral hernia is identified unexpectedly during an elective open inguinal hernia repair as a groin bulge on the medial thigh emanating below the inguinal ligament. Opening of the floor of the inguinal canal by dividing transversalis fascia to enter the pre-peritoneal plane allows for proper identification and some surgeons would suggest this practice be done routinely—particularly in women—so as not to miss an occult femoral hernia at the time of a concomitant inguinal hernia repair. Once identified, reduction can be difficult and as was mentioned previously, can be aided by division of the anterior inguinal ligament or medial division of the lacunar ligament. The latter can be complicated by an aberrant obturator vessel in 30% of cases and as such inguinal ligament division is considered preferable (Fig. 13.5). Once reduced, repair options are numerous. In an elective setting, one option is placement of a mesh plug in the femoral canal, which can be secured to the adjacent inguinal and pectineal ligaments. That said, our institution's experience with mesh plugs and their association with chronic pain has biased our use against these. Rather, the opening of the inguinal floor allows for the placement of a flat piece of synthetic mesh in the pre-peritoneal space that will reinforce the entire myopectineal orifice in a tension free manner. Securing the prosthetic to Cooper's ligament inferiorly will cover the opening of the femoral canal.

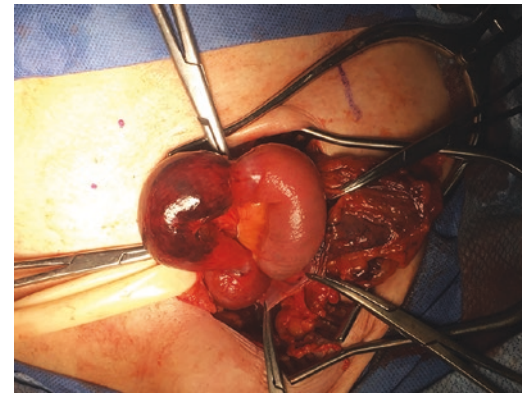

Fig. 13.5 Strangulated Small Bowel Liberated from a Femoral Defect. Strangulated intestine within a femoral hernia defect liberated by partially dividing the inguinal ligament anteriorly

In the emergent setting, where a bowel resection is necessary and gangrenous changes to the incarcerated contents obviate the placement of a synthetic mesh, options for primary repair are again numerous. If the floor of the inguinal canal was likewise opened by dividing the transversalis fascia as in a traditional inguinal hernia repair, the femoral space can be addressed in several ways. One option is simple suture repair by tacking the anterior inguinal ligament to Coopers's ligament posteriorly. Alternatively, a purse-string stitch can be used and secured to the inguinal, lacunar, pectineal ligaments, and femoral sheath. Finally, a Cooper ligament repair is my preference as its versatility addresses both inguinal and femoral hernias defects. Here, the conjoined tendon is secured to Cooper's ligament from medial to lateral and eventually transitioned to the shelving edge of the inguinal ligament when the femoral vein is encountered. While more traditionally described with simple interrupted silk sutures, my preference in a contaminated setting is to perform this with 2-0 slowly absorbable monofilament suture using a figure of 8's (Fig. 13.6). In anticipation of some tension on the repair, all sutures are placed before tying them down so as to distribute the tension evenly to each stitch and avoid tearing of the conjoined tendon. While a classic McVay repair

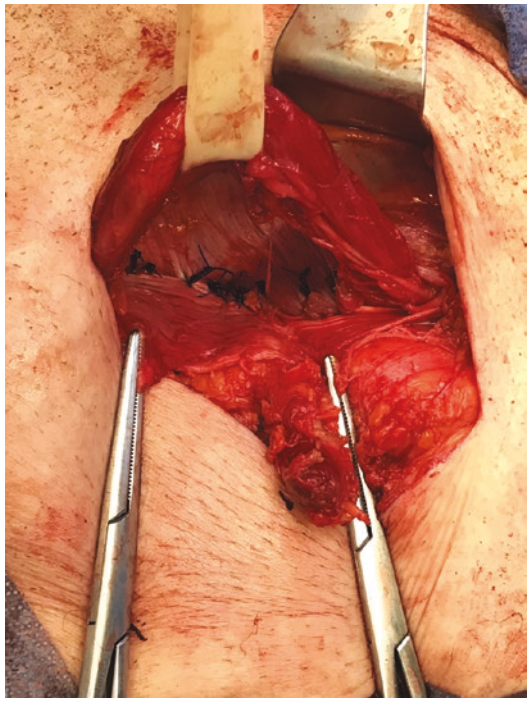

Fig. 13.6 Cooper Ligament Repair (Right). Right Cooper ligament repair—the conjoined tendon is secured to the pectineal ligament medially (right) and the inguinal ligament laterally (left). The entire myopectineal orifice is closed beneath the elevated spermatic cord

adds a relaxing incision of the external oblique as it inserts into the anterior rectus fascia for 4–5 inches from the pubic tubercle cephalad, I somewhat disagree with this philosophically. In modern times, these repairs are typically done in extremes and the goal is mostly to provide a temporizing solution for a patient in extremes that are offered by sturdy fixation of the conjoined tendon to Cooper's ligament regardless of the tension. Adding a 4–5-inch relaxing incision may ultimately lead to a more complex suprapubic defect and make a future repair more complex. I liken this to an emergent laparotomy in the context of a ventral hernia, where primary repair is often preferred to a separation of components.

Finally, a unique approach could be undertaken in the emergent setting if an isolated femoral hernia is encountered in the absence of a concomitant inguinal hernia and the surgeon is able to appreciate this preoperatively. Either a lower transverse or vertical incision can be made in the groin over the femoral bulge, caudal to the inguinal ligament. Rather than opening the inguinal canal as in a traditional inguinal hernia repair, the femoral hernia sac can be dissected and isolated as it exits the femoral canal (Fig. 13.7a).

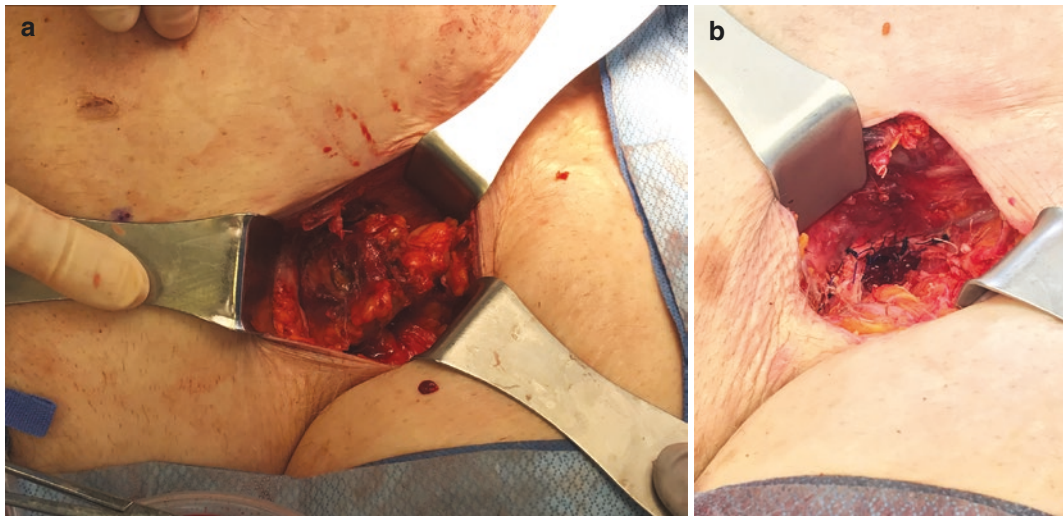

Fig. 13.7 Incarcerated femoral hernia contents. (**a**) Incarcerated femoral hernia contents approached by a vertical cut-down on the femoral hernia sac without entering the inguinal canal. (**b**) Primary closure of the inguinal ligament (anteriorly) to Cooper's ligament posteriorly

Again, the liberation of the hernia contents is most safely done by dividing some of the inguinal ligament anteriorly. I have also used a right angle to hook medial fibers of the lacunar ligament and divide them sharply but as was previously mentioned, this can be treacherous if aberrant obturator vessels are encountered. Once the hernia contents are liberated and reduced, the femoral space can be closed primarily by approximating the inguinal ligament to the pectineal ligament from this caudal perspective (Fig. 13.7b). A limitation of this approach is that if a bowel resection is required, the small space often makes reduction of an anastomosis challenging.

Literature Review

High-level evidence regarding femoral hernias is sparse, but the data that does exist is either extremely practical in terms of diagnosis or remarkably detailed from large prospectively maintained databases in Europe. These archives provide an enviable treasure trove of information that is necessary given the relative rarity of femoral hernias that precludes any prospective randomized trials.

In regards to the specific diagnosis of a femoral hernia by CT, one Japanese review of 215 groin hernia CTs found that the combined findings of femoral vein compression and a "localized" hernia sac lateral to the pubic tubercle successfully identified 11/11 femoral hernias and was exceedingly rare in inguinal hernias (1/92)—$p < 0.0001$ [1]. A separate Japanese study reviewed 75 groin hernias in 71 patients, of which 28 were femoral and 47 were inguinal. In 74/75 cases two separate radiologists were able to distinguish the femoral from inguinal defects using coronal images to clarify whether or not the defects were dorsal (femoral) or ventral (inguinal) to the inguinal ligament [2]. So to summarize, femoral hernias can be reliably diagnosed using CT by confirming that they are lateral to the pubic tubercle, associated with femoral vein compression, and coronal views delineate that the inguinal ligament is ventral to their path.

Regarding the utility of dynamic groin US, a German group reported 4951 cases where a clinical exam and US findings were prospectively collected (2010–2015) and compared with intraoperative findings [3]. In 3659 (73.9%) cases a hernia was diagnosed by both US and exam, and in 19.7% of cases no hernia was identified by either technique. So in 93.6% of instances exam and US correlated, and those patients with consistent positive findings were confirmed intraoperatively. In 292 (5.9%) cases, clinical detection of a small hernia was "ruled out" by US. After further investigation by CT or MRI to investigate for other causes of pain, 189 agreed to watchful waiting while 103 ultimately underwent diagnostic laparoscopy for the severity of symptoms. Of those who underwent surgery, 91% were found to have a hernia. Finally, in 25 (0.5%) cases, there was no hernia on exam but patients complained of inguinal pain, and dynamic US identified a femoral hernia in 19, small inguinal hernia in 3, and no findings in the last 3. In all 25 of these cases—specifically including the 19 diagnoses of a femoral hernia—the findings of the dynamic US were confirmed to be correct at the time of surgery. Ultimately, the sensitivity and specificity of dynamic US hernia detection could be defined as 97.6% and 99.8%, respectively.

As a final note in regards to diagnostic tools for completeness, a small series of 55 inguinofemoral hernias in 82 groins found that MRI identified 53 hernias with one false positive and 3 false negatives, offering a sensitivity of 94.5% and specificity of 96.3% [4]. While helpful, the added cost would typically not be justified given the reliability of CT and US.

As was mentioned, prospective randomized comparisons of repair technique for femoral hernias are not practical given their relative infrequency. Fortunately, the Danish Hernia Registry has had the capacity and completeness to capture one of the largest series of femoral hernia repairs allowing for valuable insight [5]. They retrospectively captured 3970 femoral hernia repairs done between 1998 and 2012 in Denmark. Notably, 39% were done emergently and 73% were done in women supporting the traditional demographic and clinical portrayals. Interestingly, there was

no difference in femoral hernia recurrence between elective and emergent repairs (3.1% vs 2.5%; $p = 0.51$). With a median follow-up of 82 months, a laparoscopic approach was found to require fewer reoperations when compared to an open elective approach (0.62% vs 3.4%; $p = 0.04$), and women were more than twice as likely to develop a recurrence requiring intervention (3.3% vs 1.5%; $p = 0.01$). While one could argue that these differences are clinically meaningful enough to pursue a laparoscopic approach in the elective setting, surgeons should view this data with reassurance as it would suggest that most repair techniques—even in open emergent scenarios—are ultimately durable >95% of the time.

References

1. Suzuki S, Furui S, Okinaga K, et al. Differentiation of femoral versus inguinal hernia: CT findings. AJR. Am J Roentgenol. 2007;189(2):W78–83.
2. Kitami M, Takase K, Tsuboi M, et al. Differentiation of femoral and inguinal hernias on the basis of anteroposterior relationship to the inguinal ligament on multidimensional computed tomography. J Comput Assist Tomogr. 2009;33(5):678–81.
3. Niebuhr H, Konig A, Pawlak M, Sailer M, Kockerling F, Reinpold W. Groin hernia diagnostics: dynamic inguinal ultrasound (DIUS). Langenbeck's Arch Surg. 2017;402(7):1039–45.
4. van den Berg JC, de Valois JC, Go PM, Rosenbusch G. Detection of groin hernia with physical examination, ultrasound, and MRI compared with laparoscopic findings. Investigat Radiol. 1999;34(12):739–43.
5. Andresen K, Bisgaard T, Kehlet H, Wara P, Rosenberg J. Reoperation rates for laparoscopic vs open repair of femoral hernias in Denmark: a nationwide analysis. JAMA Surg. 2014;149(8):853–7.

Further Readings

Fischer JE. Fischer's mastery of surgery. Chapters 195, 197, 201. 6th ed. Philadelphia: Wolters Kluwer Health/ Lippincott Williams & Wilkins; 2012.

Kitami M, Takase K, Tsuboi M, Rikimaru Y, Hakamatsuka T, Yamada T, et al. Differentiation of femoral and inguinal hernias on the basis of anteroposterior relationship to the inguinal ligament on multidimensional computed tomography. J Comput Assist Tomogr. 2009;33(5):678–81.

Ventral Hernias

14

MacKenzie Landin and Jin Yoo

Introduction

A "ventral hernia" is defined as the protrusion of loops of intestine, fat, or fibrous tissue through a weakened region of the abdominal wall (Fig. 14.1). The protrusion may involve preperitoneal fat, intestinal contents, or omentum [1]. Patients seek surgical repair when the develop symptoms. Some of these symptoms include abdominal pain, nausea, vomiting or a change in bowel habits. Ventral hernias are a core component of general surgery. The treatment strategy largely depends on the patient's clinical status, but can be influenced by imaging findings. If a patient has incarcerated bowel, then surgery is inevitable to prevent ischemia and perforation. What becomes more nuanced are the patients with large abdominal wall hernias who present with symptoms, but have no evidence of obstruction or perforation. The surgeon must decide which patient to offer surgery and what surgical approach is to be taken. Often that decision is guided by imaging. In this chapter, we will review ventral hernias and how radiography influences the surgical algorithm.

Fig. 14.1 Example of a ventral hernia containing bowel

History and Epidemiology:

Hernias were first described in the sixteenth century. Treatment at that time consisted of heat to "imprison the illness in the patient's body" [1]. With the evolution of medical education and technology, surgeons attempted repair. Dr. Pierre Nicholas Gerdy was the first surgeon to invert the hernia sac into the abdominal cavity. He sutured the edges together and injected ammonia to stimulate scar formation in 1836 [1]. As medicine

Supplementary Information The online version contains supplementary material available at https://doi.org/10.1007/978-3-031-21336-6_14.

M. Landin (✉)
Minimally Invasive/Bariatric Surgery (Division)/ Department of Surgery, University of Arizona-Phoenix, Phoenix, AZ, USA
e-mail: mackenzie.landin@bannerhealth.com

J. Yoo
Department of General Surgery, Duke University Health System, Durham, NC, USA
e-mail: Jin.s.yoo@duke.edu

S. Docimo Jr. et al. (eds.), *Fundamentals of Hernia Radiology*,
https://doi.org/10.1007/978-3-031-21336-6_14

developed, more patients were surviving their disease with treatment and hernias became a more relevant problem. Today, hernias are common. There is an estimated hernia prevalence of 5% of the general population. Hernias affect male patients more than females [2]. Patients can have a congenital defect or develop a hernia after physiologic stress. Patients have a 2–20% risk of developing an incisional hernia after laparotomy [1]. Wennergren et al. reported a rate of 9% of incisional hernias following surgery, of which at least a third are symptomatic [3]. Risk factors for developing a hernia include obesity, smoking, cancer, diabetes, pulmonary disease (where coughing creates a physical strain on the abdominal wall), and connective tissue disorders [1].

Technique

The first procedure developed to treat this disease was described by Dr. Pierre Nicholas Gerdy [1]. His technique was as stated above. Over time, other suture techniques and adjuncts, like mesh, were developed to aid in hernia repair such as mesh, to aid in repair. Perhaps what is more important than the type of prosthetic is its placement.

The main principle of hernia repair is reconstruction of the abdominal wall by restoring the muscle and fascial layers. This reconstruction should be done without any tension on the repair. Reconstruction is sometimes performed with suture alone, or with the addition of mesh. If the abdominal wall can be reconstructed without mesh, then it is known as a primary repair. Often, primary repairs are reinforced with prosthetic if the patient has risk factors for recurrence (smoking, diabetes, obesity, etc.). Prosthetics can be synthetic and permanent (e.g., polypropylene), synthetic and absorbable, or biologic and absorbable. If they are placed within the peritoneum, they are considered an intraperitoneal onlay mesh or an underlay. If they are below the layers of the abdominal wall, but above the level of the peritoneum, this is called a sublay. Mesh placed on top of the layers of the abdominal wall is an onlay mesh. The location of mesh placement is usually determined by hernia size, location, and degree of associated muscle atrophy.

As stated above, a primary repair is the closure of a fascial defect with suture alone. If the hernia is sufficiently small, the hernia sac is excised and the fascia sewn together. This is typically performed open. If the hernia is large, mesh is used to reinforce a repair. The surgical approach can be open or in a minimally invasive fashion depending on patient comorbidities, location of the hernia, and physician preference. We prefer a laparoscopic approach with an intraperitoneal onlay mesh placement with hernia defect closed to minimize the size of the incisions (compared to open) and to ensure adequate mesh placement and coaptation to the abdominal wall. Berger et al. reported a 10-year recurrence rate of 63% for suture repair versus 32% after mesh repair [4]. Mesh repair helps prevent some, but not all, recurrences. Reasons for recurrent hernias include patient factors (weight gain, tobacco, and diabetes) and technical errors (incorrect suture/mesh choice, mesh placement) or mesh failure [5, 6]. If a patient has failed a standard repair, they may be offered a complex repair to treat the recurrence.

For complex hernias (loss of abdominal domain, large hernias (greater than 10 cm), multiple organs involved in the hernia content, recurrent hernias (Fig. 14.2), consideration for component separation is given. Anterior component separation was originally described by Ramirez in 1990 [1]. Briefly, a large vertical midline incision is made, and the hernia contents are reduced after all adhesions are lysed. The sac is resected. The subcutaneous tissue is dissected off the rectus muscles and the semilunar lines are identified bilaterally. The external oblique is incised and separated from both

Fig. 14.2 Large ventral hernia containing bowel. The patient also has a loss of abdominal domain

the internal oblique and the space posterior to the rectus. This dissection allows the rectus muscles to be brought to the midline without tension (Figs. 14.3, 14.4, and 14.5). There are reports in the literature of a gain of 8–10 cm with this approach [1, 7, 8]. Many surgeons believe that a full anterior component separation yields the greatest amount of release and medialization of the rectus complex [9]. Typically, a piece of mesh is then placed as an onlay (Fig. 14.6). Issues with this repair are typically wound-related, due to the large subcutaneous flaps created to get to the external oblique dissection. Anterior component separation has a 7–32% hernia recurrence rate and a 50% complication rate. Aagain, most of the complications from anterior component separation are wound-related [9].

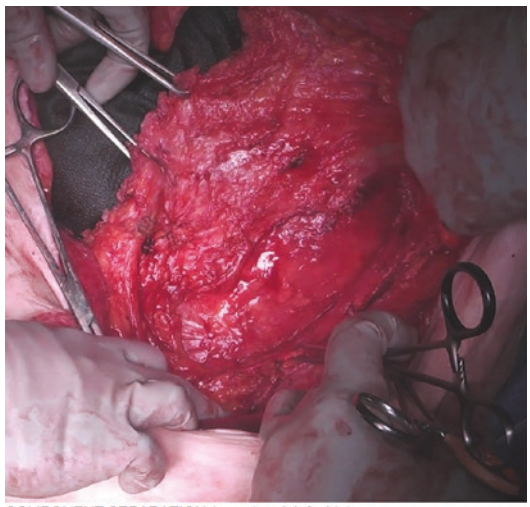

Fig. 14.3 The external oblique has been incised in an anterior component separation

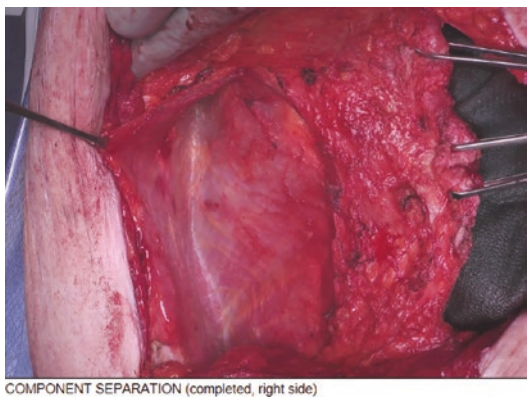

Fig. 14.4 The retromuscular space is dissected between the external and internal oblique

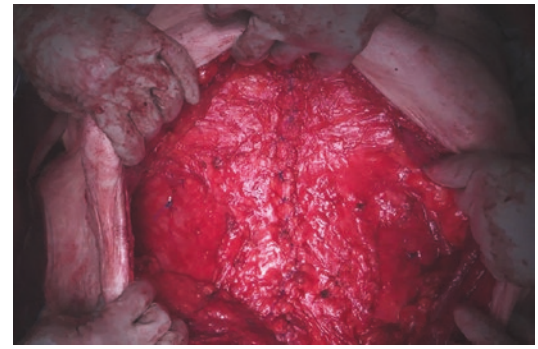

Fig. 14.5 With appropriate release of the muscle fibers, the rectus muscle can be advanced medially to close the abdomen in the midline

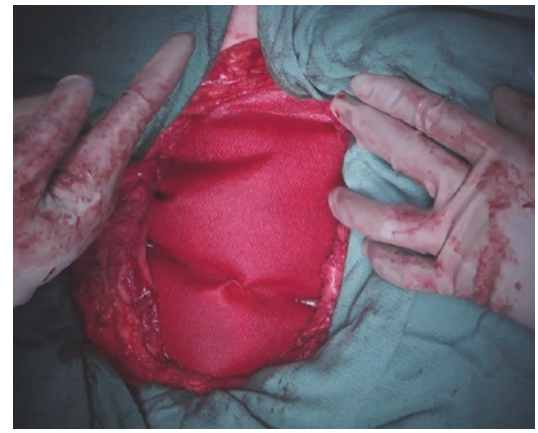

Fig. 14.6 After the abdominal muscles have been closed in the midline, a piece of mesh has been placed as an onlay to reinforce the repair

Case 1

The patient is a 71-year-old female with a history of an emergent sigmoidectomy with end colostomy for perforated diverticulitis. She later had her stoma reversed with a simultaneous repair of a parastomal hernia (on the left) with permanent mesh at the site of the ostomy. She developed a recurrence at the midline (Fig. 14.7a, b). She underwent a unilateral right-sided anterior component separation with laparoscopically placed coated permanent mesh. Due to the mesh within the left abdominal wall (from her prior

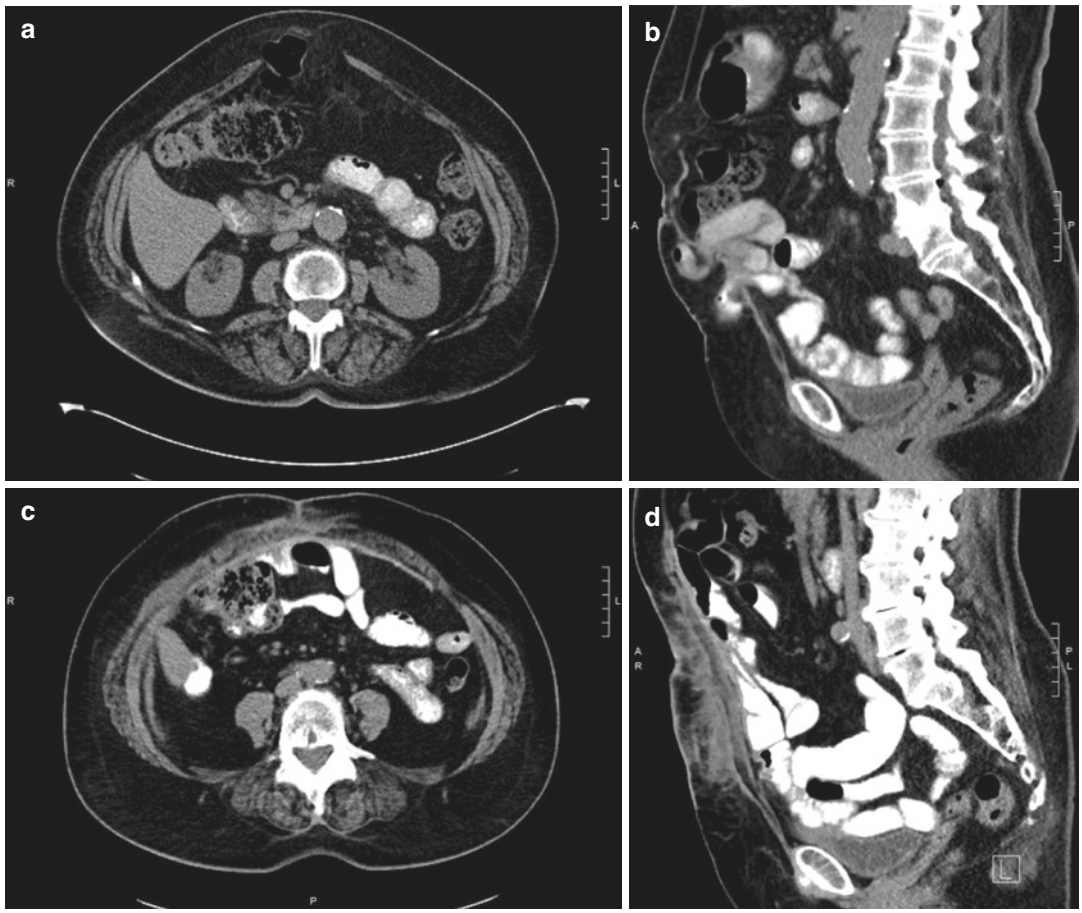

Fig. 14.7 (**a**) Hernia recurrence at the midline. (**b**) Sagittal view of hernia recurrence at the midline containing small bowel. (**c**) Edema within the site of the hernia repair. (**d**) Resolution of edema within the hernia repair site

parastomal hernia repair) and expected scar tissue as a result, a bilateral component separation was not offered. We sought to avoid creating a potential dead space for wound infection or hematoma. Her case was uneventful. She developed expected postoperative edema of the wound that resolved (Fig. 14.7c, d).

Carbonell et al. described an alternate approach to anterior component separation. In the posterior approach, the case is started with a midline laparotomy followed by lysis of adhesions and reduction of the hernia contents. Instead of incising the external oblique, the retromuscular space is dissected to the semilunar line and mesh is placed in this plane as a sublay. If additional tension needs to be relieved, a transverses abdominus muscle (TAM) release can be performed. A transversus abdominus muscle release is where the TAM is incised laterally (medial to the neurovascular bundle) allowing the posterior rectus sheath to come to midline and be closed with suture [10]. A meta-analysis by Holihan in 2015 showed that the sublay placement of mesh has the lowest risk for recurrence and surgical-site infection [11, 12]. The posterior component release alone has a 15% complication rate and 5% recurrence rate, as reported by Carbonell [13, 14]. If a TAR is included, there is a 45% wound complication rate, but recurrences are as low as 3% [1, 13, 15].

There are times that despite muscle release, the midline cannot be brought together. These are troubling scenarios for the surgeon. The typical approach to close the patient is with a bridging repair. In a bridging repair, a piece of mesh is

placed across the abdominal wall and secured laterally. The mesh bridges the gap between the recti. Mesh can be placed within the peritoneum or over the anterior abdominal wall, as an onlay. Placement again depends upon the size of the hernia, conditions of the operation, and prior surgical history. Risk of recurrence is thought to be high and can be exacerbated by patient comorbidities. Wennergren et al. evaluated hernia recurrence rates after primary fascial closure versus bridged mesh repair in laparoscopic ventral hernias. In a study of 196 patients, they saw no significant difference in recurrence, surgical-site infection, readmission, reoperation, or seroma formation between the two groups [3]. Holihan et al. studied this same question in open ventral hernia repair. They found there was a decrease in surgical-site infections and recurrences with primary fascial closure. Primary fascial closure appears to yield superior outcomes compared with bridged repairs in open ventral hernia repair [9]. In the acute setting, factors such as degree of contamination, patient stability, and volume status play a role in which approach to midline closure is taken. Skin closure alone or bridged repair to temporize the situation may be the safest choice [9].

Laparoscopic Repairs

The first laparoscopic ventral hernia repair was described by LeBlanc and Booth in 1993 [16]. The advantages of laparoscopic repair compared to the open approach include quicker rehab of the patient, less postoperative pain, less wound infections, and better perceived esthetic results [17, 18]. While the disadvantages are greater costs, longer learning curve, longer procedure time (due to tedious viscerolysis), reported accidental visceral and vascular damage, and a higher incidence of visceral-prosthetic fistulas [2, 16, 19]. This is somewhat of a controversial statement as several studies support and negate this. The Society of Alimentary and Gastrointestinal and Endoscopic Surgeons published guidelines in 2020 to provide recommendations for hernia surgeons. They published a lower rate of wound infections in laparoscopic ventral hernia repair, but similar rates of recurrence and postoperative pain between open and laparoscopic cases. Infections were 2.8% versus 21.9%; OR, 10.5; 95% CI, 2.3–48.2; $p = 0.003$ [11]. Laparoscopic repair becomes complex when the hernia defects are large (>10 cm), are in uncommon locations like the flank or suprapubic region, or if the patient has a preexisting medical condition that complicates the repair (ascites or pregnancy). Laparoscopic ventral hernia repair is typically contraindicated in enterocutaneous fistulas, patients with loss of domain and/or patients with prior skin grafts.

Robotic

Robotic hernia surgery has grown for several reasons. The robot most notably has six degrees of articulation that facilitate sewing in small spaces [20]. One of the drawbacks of laparoscopic ventral hernia repair is the technical difficulty in closing the midline fascia. If closure is not ergonomically feasible or time-efficient, it is often abandoned. As such, many laparoscopic ventral hernia repairs are essentially bridging hernia repairs [21]. With this comes mesh eventration and bulging at the hernia site. This is a common and chronic patient complaint [22]. With the robotic platform, the fascia can be repaired in a straightforward fashion. In a study of 106 patients over a four-year period, primary fascial closure was completed. Twenty-three percent of patients had component separations. Seventy-nine percent had sublays, which as discussed previously are associated with the lowest rates of recurrence [9, 13]. Of this group, 12% had hernia recurrence and 9% of those patients underwent a second robotic ventral hernia repair [22]. Two percent of patients developed seromas and 3% developed hematomas [22]. However, all the seroma patients required a subsequent procedure and half of the hematoma patients required surgery to address this complication [22]. Robotic ventral hernia repair is feasible. Robotic ventral hernia repair with component separation has lower morbidity and length of stay compared to open component separation [9, 22, 23].

Imaging

Imaging helps guide which type of repair is offered. The typical imaging study preferred for surgical planning is a CT (computed tomography) scan. CT scans are more commonly used for this purpose than magnetic resonance imaging [12]. They help determine the size and shape of a hernia as well as the contents of the hernia. CT scans allow surgeons to measure the dimensions of the hernia defect and estimate the volume of the hernia sac. This helps one plan whether the defect can be closed without tension. If there is a concern for tension, then the surgeon would consider adjunctive methods like botox injections to relax the abdominal wall and/or component separation. Additional features to consider with imaging includes degree of visceral (Fig. 14.8) and subcutaneous adiposity (Fig. 14.9) and the presence of rectus diastasis (Fig. 14.10). Visceral adiposity adds to the intra-abdominal pressure that will increase the risk of tension. Pre-operative weight loss may be offered to patients with excessive visceral adiposity. Subcutaneous adiposity is more important in terms of surgical access (laparoscopic or open) and risk of seroma formation. If a patient has a significant rectus diastasis, this likely needs to be addressed at the time of the hernia repair to minimize the risk of recurrence. As such, the plication of a diastasis requires a larger operation and/or wider mesh placement.

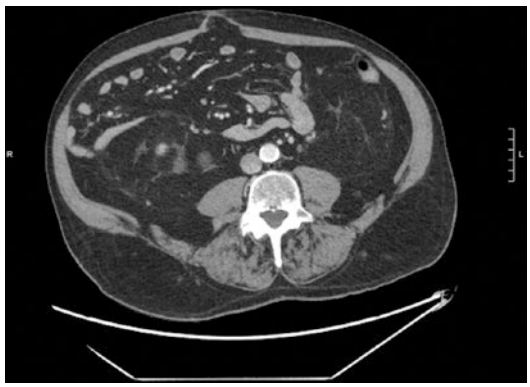

Fig. 14.8 Example of visceral adiposity

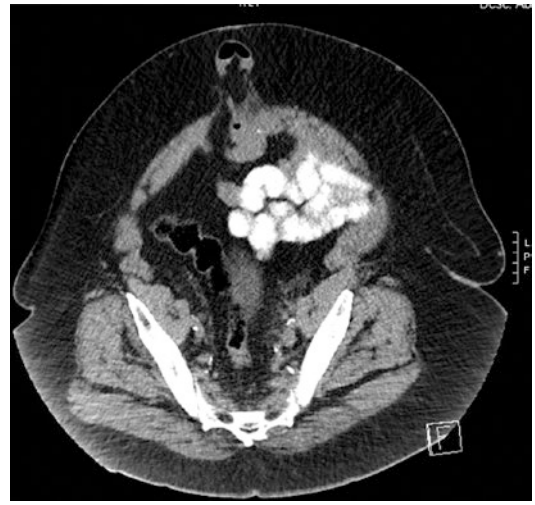

Fig. 14.9 Example of subcutaneous fat deposition

Fig. 14.10 In a rectus diastasis, the rectus muscles retract laterally and a gap forms in the midline. This can be symptomatic and present as a bulge. If the fascia is intact between the muscles, this is not a true hernia, but will often be misdiagnosed as one

Imaging is especially helpful when a hernia is in an unusual location (Fig. 14.11), such as the flank or the suprapubic region. Imaging can identify the potential need for the mesh to be anchored to bony structures, like the pelvis or ribs, depending on hernia location. When a hernia is located near the xiphoid process or the pelvis, a transversus abdominus release is often the preferred approach as it allows for better overlap of mesh in a sublay position.

CT scans help surgeons to determine the safest method of entry into the abdomen based on

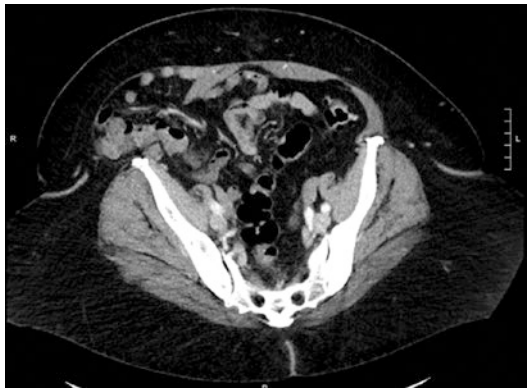

Fig. 14.11 Depiction of an "unusual hernia." In this image, small and large bowels are herniated through a fascial defect in the patient's right lower quadrant

Fig. 14.12 In this image, the hernia has dissected out a space in the subcutaneous tissue that is wider than the defect at the level of the fascia. This process creates a "mushroom" shape

the location of likely adhesions, size of hernia, and the organs involved. For example, if the defect within the fascia is small but the hernia sac itself is large and has been dissected out of the subcutaneous space (imagine the shape of a mushroom) (Fig. 14.12), dissection of the subcutaneous space should proceed with caution. Imaging will also help the surgeon estimate the degree of non-viable skin that will be present after the hernia is reduced and how much skin is to be removed. If the subcutaneous fat appears thick on imaging, a laparoscopic or robotic approach is preferred to minimize creation of dead space. However, if open surgery is the only feasible approach for a patient with obesity and a hernia, preoperative management utilizing weight loss surgery or medication is often indicated. Docimo et al. demonstrated that patients undergoing open component separation with a BMI $\geq$35 kg/m^2 were at an increased risk for surgical-site infections, minor complications, major complications, and hospital readmissions [24].

Often patients with prior surgical history have poor tissue quality. The presence and width of the rectus muscles are important features to know. A retrorectus repair is preferred when the rectus muscle is present and the space is wide, the idea being adequate mesh overlap laterally. If the rectus muscle is too narrow, the mesh overlap that would be obtained laterally from the midline closure may be inadequate. The surgeon would then need to perform a transversus abdominus muscle release to free this space or potentially convert to a sublay approach. Interestingly, De Silva et al. showed anterior component separation with external oblique release results in hypertrophy of the rectus, internal oblique, and transversus abdominus muscles [25]. They demonstrated in a subsequent study that posterior component separation with transversus abdominus release produces hypertrophy of the rectus, the external and internal obliques [25]. Both of these studies showed hypertrophy in open operations. There was no significant change in musculature with laparoscopic bridging ventral hernia repairs. The benefit of muscular hypertrophy is the theoretical increase of a functional abdominal wall. Therefore, in large and complex hernias, patients are likely to have a greater benefit from a component separation than a bridging repair [26].

CT is useful in diagnosing occult hernias, multiple fascial defects, as well as differentiating incarcerated hernias from abdominal wall neoplasms. In the patient with severe obesity, it can be difficult to detect a hernia on physical exam (Figs. 14.13, 14.14, and 14.15). In a retrospective review of 146 consecutive laparoscopic ventral hernia repairs, 48% of patients had occult defects not detected on preoperative physical exam [11]. When preoperative imaging is obtained and more than one defect is visualized, the surgeon can

Fig. 14.13 Anterior view of patient's abdomen. No obvious bulge is visible due to their level of adiposity

Fig. 14.14 Side view of the abdomen. Again, no obvious bulge on exam

modify the technique to incorporate the repair of the additional hernias. If this was not done preoperatively and additional hernias were only detected at the time of surgery, their discovery would likely cause the surgeon to modify his/her approach and may lead to patient dissatisfaction, especially if it prolongs postoperative recovery (e.g., they may choose to convert a laparoscopic case to an open one).

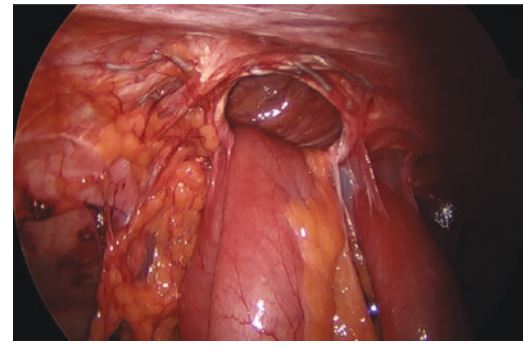

Fig. 14.15 Large ventral hernia that was not easily visible on exam, is easily visible laparoscopically

CT scans become even more helpful in the postoperative setting when patients return with chronic pain. Often the physical exam is limited by postoperative pain. If there is swelling at the site of the repair, it is difficult to discern if the swelling is expected fluid, a hematoma or worse, a recurrence. In one study, diagnosis of hernia recurrence after mesh repair was correct 88% of the time on physical exam, while CT was correct in 98% of cases [11]. Therefore, there are many reasons to obtain imaging in hernia patients. To interpret the results, one must have an understanding of the anatomy and of the hernia repairs themselves.

Postoperative Findings and Complications

Patients with hernias, especially large ones, will likely have significant pain postoperatively. Oftentimes, this pain is more than patients expect. Traditionally this is due to anchoring of the mesh and/or dissection of the muscles. Occasionally patients present to the emergency room where their workup includes imaging. CT used in conjunction with intravenous administration of iodinated contrast material is the best imaging examination to depict specific postoperative complications following abdominal wall repair with mesh [4]. When visible on CT, mesh appears as a fairly regular line, with moderate/high attenuation values similar to those of muscles [4]. If the patient has a thin abdominal wall or poor

muscle quality, it may be difficult to discern where the mesh is in relation to the layers of the abdominal wall. In the postoperative setting, it is normal to see edema of the subcutaneous tissues, small intraperitoneal air and tacks used to fixate the mesh during a laparoscopic repair [27].

Seroma

Seromas are commonly found within the dissection planes of hernia repairs. They are typically observed out of concern for potential contamination of sterile fluid with any aspiration attempt. In addition, 95% of seromas self-resolve [6]. If a seroma is aspirated and recurs, patients can be treated with a drain if symptomatic. Seromas are common enough that SAGES published guidelines stating, "seroma formation following laparoscopic hernia repair should be considered an expected outcome, rather than a complication" [11]. Incidence of seroma detected on the US or CT ranges from 95 to 100% in the early postoperative period. Seromas lasting beyond 90 days are around 20%. There is evidence to suggest that closure of the hernia defect reduces the rate of seroma formation as the potential space is reduced [4, 11]. Because of this principle, robotic hernia surgery has been pursued for large ventral hernias. CT will show a non-enhancing, homogenous collection with a density consistent with water [4]. If a seroma is infected, it will show a thick and well-vascularized wall with signs of inflammation [6].

Case 2

The patient was an 82-year-old male with a history of colon cancer. He underwent a laparoscopic right hemicolectomy one year prior to presentation. His complaint was an incisional ventral hernia (Fig. 14.16a). He had an open retrorectus approach with a 20 × 25 cm permanent mesh. This approach was chosen due to the poor quality of his musculature. He developed an asymptomatic seroma (Fig. 14.16b). It was observed and he recovered as expected.

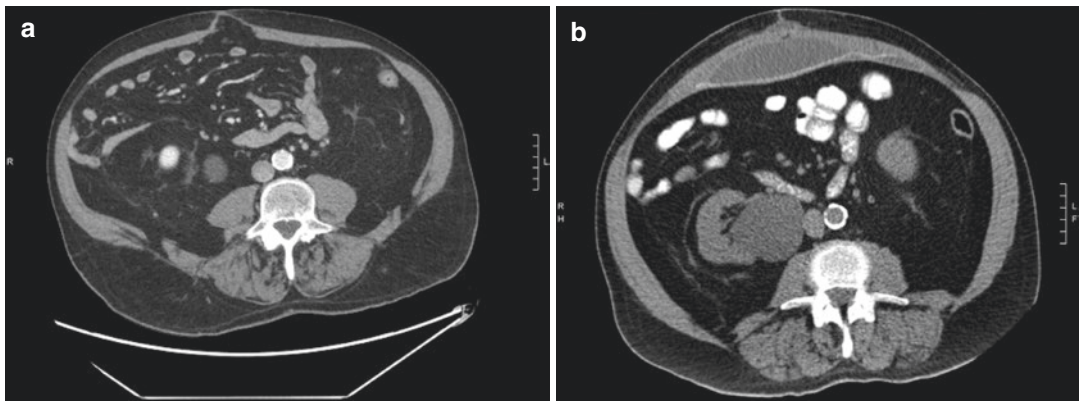

Fig. 14.16 (**a**) Imaging from CT of an 82-year-old patient with a history of right colectomy for cancer. An incisional ventral hernia is visible. This is the location of the extraction site of the colon specimen. (**b**) The patient developed a postoperative seroma in the location of the prior hernia

Hematomas

Hematoma occurs if there is inadequate hemostasis at the time of surgery, or if the patient develops postoperative bleeding in the surgical field (e.g., after restarting therapeutic anticoagulation). The incidence of hematoma is 0.4% as reported by Heniford [4]. On imaging, a hematoma appears as a hyperattenuating fluid collection within the dissection field. If there is contrast visible within the hematoma, this is concerning for active bleeding. Asymptomatic hematomas can be observed. Asymptomatic implies that the patient is hemodynamically stable and does not require any blood transfusions to be stable. In addition, there should be no concern about wound breakdown due to pressure necrosis from the hematoma of the overlying skin. Nor should there be the potential for bacterial contamination of the hematoma, which in turn could infect any underlying mesh. If there are wound concerns, the hematoma should be evacuated. Evacuation of the hematoma does put the mesh at risk of potential infection, which is a point to be considered by the surgeon. Hematomas may be drained. Again, drainage is avoided as any violation of the capsule of the hematoma creates a risk of seeding the wound with bacteria and converting a sterile field to an infected field. All management of hematomas include maintaining patient safety, while minimizing chance of infection. If active bleeding is suspected (change in vital signs, lab values, or contrast seen within collection on CT), the patient's surgeon should consider returning to the operating room for a wound exploration.

Case 3

The patient is a 47-year-old male with a history of rectal cancer who had a laparoscopic low anterior resection with diverting loop ileostomy 2 years prior to presentation. His ileostomy had been reversed. He presented with "swiss cheese" incisional ventral hernias (Fig. 14.17a). He had an open retrorectus incisional ventral hernia repair with a 20 × 20 cm permanent mesh. His postoperative course was complicated by a hematoma (Fig. 14.17b) which required a washout due to infection (Fig. 14.17c).

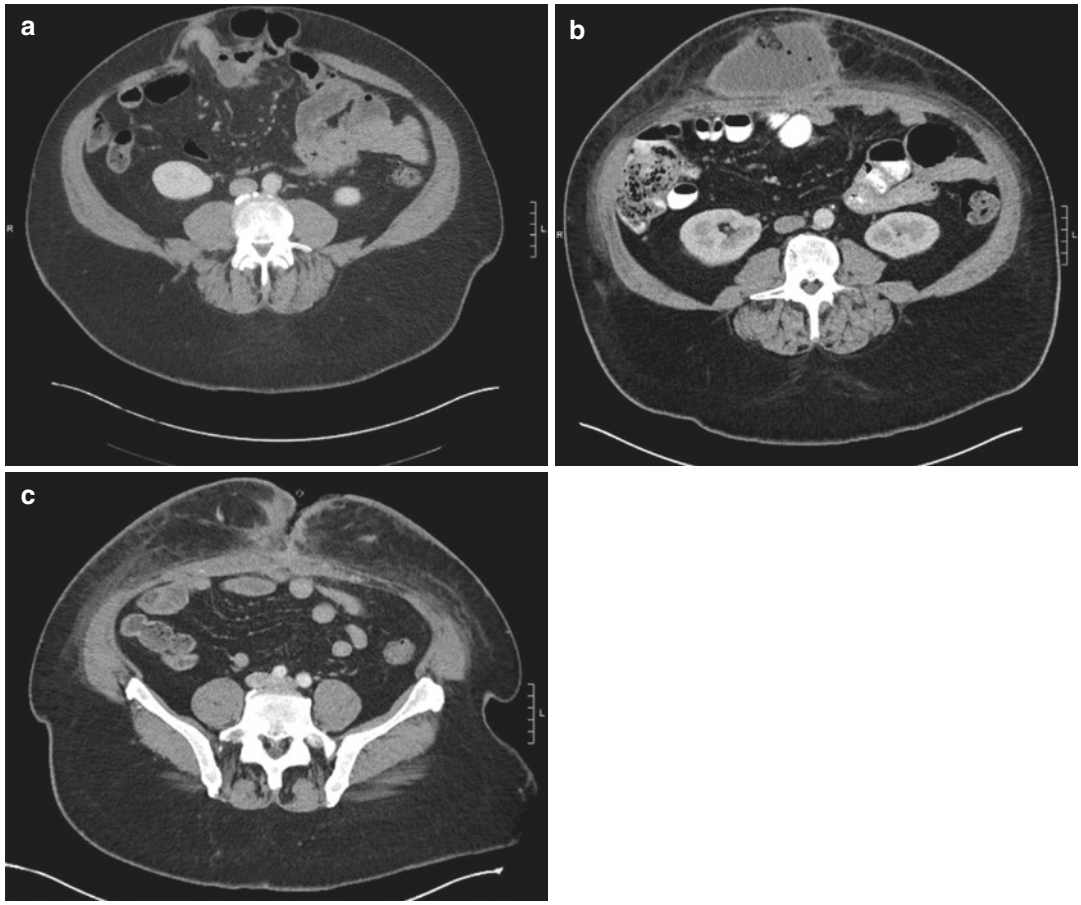

Fig. 14.17 (**a**) Example of a "swiss cheese" ventral hernia. A complex hernia comprised of multiple small defects in the fascia, some of these may not be appreciable on imaging. Often the surgeon detects other defects at the time of hernia repair. (**b**) After hernia repair, the patient developed a hematoma at the site of dissection. This hematoma is rim-enhancing and has foci of air within it, suggesting it is an infected hematoma. (**c**) CT scan performed after washout of the infected hematoma. There is resolution of the collection and no other radiographic signs of persistent infection

Enterotomy

Inadvertent enterotomy occurs in 6% of all laparoscopic ventral hernia repairs [4]. The management of enterotomies depends on the timing of recognition. If seen during the index operation and there is minimal contamination, there is evidence to support primary repair of the bowel with or without subsequent mesh placement [28]. Likewise, the enterotomy could be repaired and the hernia repair delayed several weeks to allow for a period of resolution with regard to the contamination. If the enterotomy is not recognized at the time of the ventral hernia repair, the patient may develop sepsis. Imaging typically shows free air and free fluid, which is difficult to interpret in the setting of a recent operation. However, a rising leukocytosis and tachycardia support the concern for missed enterotomy and should push the surgeon to explore the patient and explant any contaminated mesh. A hernia is accepted and definitive repair is deferred until the patient has recovered.

Case 4

The patient was a 60-year-old female who underwent a laparoscopic ventral hernia repair. Her postoperative course was complicated by delayed

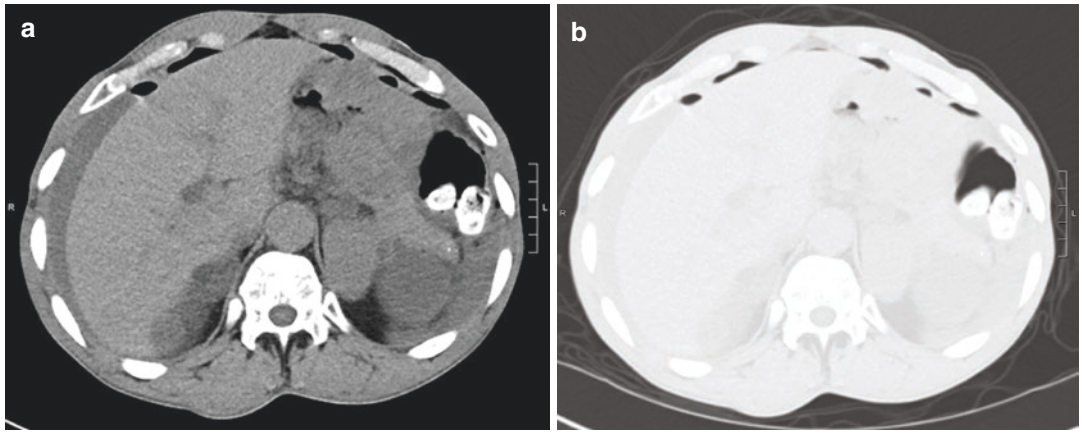

Fig. 14.18 (**a**) Free air is visible on this axial view of the abdomen. There is free fluid adjacent to the liver. (**b**) Free air is more easily visualized when the image settings are changed to "lung window"

return of bowel function. She had a history of hypertension for which she was taking a beta blocker. She developed a fever and a CT of the abdomen was obtained. What was notable about this scan was the amount of free air and free fluid seen on CT. It is difficult to interpret pneumoperitoneum and free fluid after an operation, but in cases where irrigation is not used and if the patient clinically is unwell, the surgeon should consider returning to the operating room. Missed enterotomy is largely a clinical diagnosis. The surgeon should assess the patient and monitor for tachycardia, fever, rising white count, and changes in physical exam. If imaging is obtained, consider a missed enterotomy when there is more free air than expected (Fig. 14.18a, b).

Mesh Infection

The risk of mesh infection is a possibility after any hernia repair. Fortunately, mesh infection is uncommon and occurs at a rate of 0.7% [4]. Some can be managed with antibiotics and aggressive wound care [29]. Others require serial debridement or worse, mesh explantation. Mesh infection has been reported to be less than 1% in laparoscopic ventral hernia repair [11]. Imaging findings of mesh infection include a heterogenous, peripherally enhancing fluid collection adjacent to the mesh [30]. The fluid collection often contains air [4].

Case 5

This patient is a 62-year-old female with an extensive past surgical history. Related to hernia repair, she had a prior emergent incarcerated umbilical hernia repaired primarily. She had a large recurrent incisional ventral hernia of incarcerated small and large bowel (Fig. 14.19a) that was repaired with an anterior component separation. She subsequently developed a mesh infection (Fig. 14.19b). The mesh was removed and she had a delayed open incisional ventral hernia repair with mesh. She unfortunately developed a third recurrence (Fig. 14.19c).

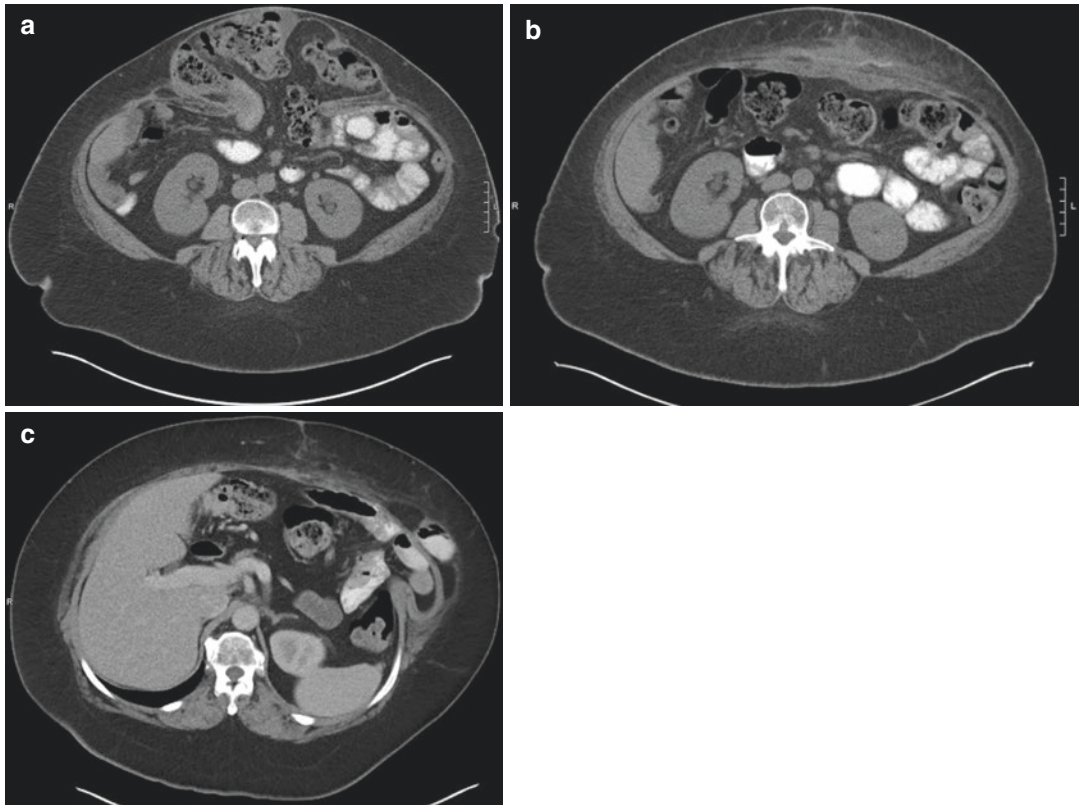

Fig. 14.19 (**a**) Imaging from Case 5. This patient has a large recurrent incisional ventral hernia of incarcerated small and large bowel. There are neither signs of obstruction (no transition points, no dilated loops) nor is there any free fluid or free air on this cut. (**b**) The patient underwent an anterior component separation. There is some subcutaneous edema and fat stranding seen on this image. Unfortunately, the patient had a mesh infection and required mesh explanation followed by a delayed hernia repair. (**c**) The patient developed a lateral recurrence. This is a known complication of recurrent hernia repairs, especially given the history of prior mesh infection

Fistula

An enterocutaneous fistula is a connection between the intestine and the skin. These typically occur if there is injury to the intestine during surgery leading to persistent inflammation and/or infection. Additionally, the presence of a foreign body (like mesh) can cause micro erosions into bowel perpetuating the cycle of inflammation and infection. On imaging, the patient will have inflammation of the subcutaneous tissues and there may be a visible connection between the skin and a segment of bowel (Fig. 14.20). Often these connections are not visible on imaging and patients require additional studies to identify the origin of their abdominal pain, recurrent abscesses, and wound drainage. Treatment strat-

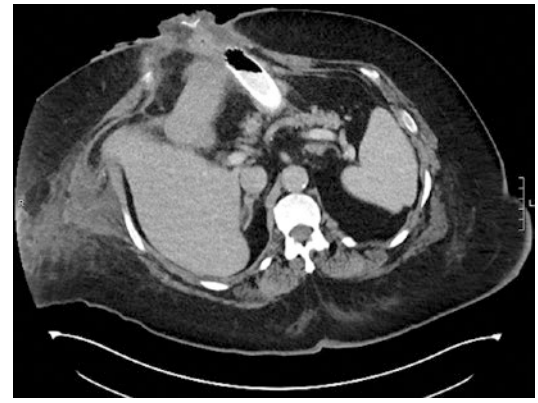

Fig. 14.20 An enterocutaneous fistula is a connection between a piece of the small intestine and the skin. On imaging, the patient will have inflammation of the subcutaneous tissues and there may be a visible connection between the skin and a segment of bowel. Often this connection is not seen without enteric contrast

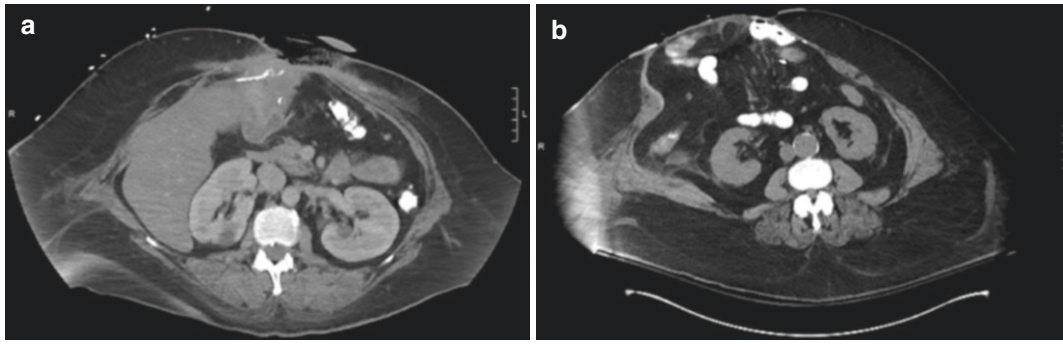

Fig. 14.21 (**a**) Ventral hernia after a duodenal switch. (**b**) Fistula between the alimentary limb of a roux-en-y gastric bypass and the skin

egy, once identified, is to attack the cause of the fistula. For example, if the cause is a mesh infection after a ventral hernia repair, then explantation of a non-salvageable mesh with bowel resection and anastomosis is likely indicated [31]. The patient will likely develop a recurrent hernia, which can be managed when they have recovered from the treatment of their fistula.

Case 6

In Fig. 14.21a, the patient had a duodenal switch which was complicated by a ventral hernia. She subsequently developed a duodenal-ileal fistula after the hernia was primarily repaired. In Fig. 14.21b, the patient had a roux-en-y gastric bypass several years prior and developed marginal ulceration at the anastomosis. She had a revision of her gastrojejunostomy due to ulcer disease and developed an anastomotic leak. She developed a chronic leak, which resulted in a fistula.

Fig. 14.22 Large recurrent incisional ventral hernia

Recurrence

Hernia recurrence is a known risk of any hernia repair (Fig. 14.22). At 1 year, 8% of patients will develop a recurrence if their BMI is less than 25 at the time of index repair [12]. Twenty-seven percent of patients will develop a recurrence if their BMI is greater than 35 [12]. Use of mesh in hernia repairs has reduced the recurrence rates compared to direct suturing. Even with mesh usage, inadequate fixation of the mesh and/or mesh shrinkage can lead to recurrent hernia [6]. When hernias recur, options for repair are often limited to what has not yet been attempted. Patients must be as invested as surgeons. If they have obesity, they must lose weight. If they smoke, they must quit. Any modifiable risk factor for failure must be addressed preoperatively.

Surgeons will frequently obtain preoperative imaging to help guide any repair as discussed above. Imaging often helps show the surgeon why the repair failed. The mesh may appear contracted or there may be increased adiposity compared to prior. However, prior mesh may not be visible on imaging [25]. The major factors that determine mesh visibility on CT are density, structure, and thickness [6]. Polypropylene, polyester-based mesh is isodense to muscle and hence not visualized unless with a fat interface or fixated with metallic tacks [6]. Polytetrafluoroethylene-based meshes are hyperdense and are easily seen [6]. Composite mesh has multiple layers and visibility will depend on its components. Collapsed mesh is best seen on ultrasound as a crumpled echogenic structure at an unexpected site or within a collection [6].

Case 7

This patient is a 58-year-old male with a history of colitis complicated by a cecal perforation, for which he had a subtotal colectomy 4 years prior to presentation. He was evaluated for a small bowel obstruction. He had a prior incisional ventral hernia repair and developed a recurrence at the midline (Fig. 14.23a) as well as a new parastomal hernia (Fig. 14.23b).

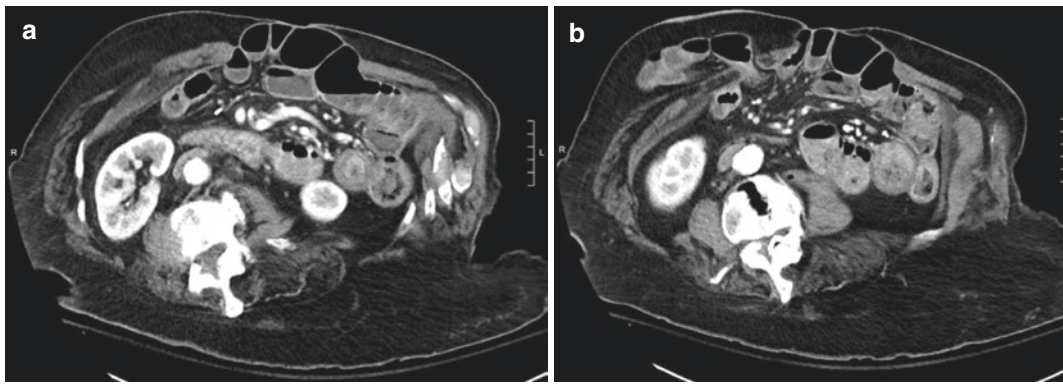

Fig. 14.23 (**a**) Recurrent incisional ventral hernia with dilated loops of bowel concerning obstruction. (**b**) Parastomal hernia in same patient with an incisional ventral hernia

Conclusion

In summary, ventral hernias exist on a gradient. They can be small and primary or complex with multiple organ involvement and recurrent. The approach of repair depends on the hernia morphology, the patient comorbidities, and the surgeon's comfort level. A large part of that skill set is understanding preoperative imaging to help guide surgery choice, but also postoperative imaging when things do not go according to plan. Radiology and surgery must continue to work together to evolve in parallel to provide the highest quality care for our patients. (Videos 14.1 and 14.2)

References

1. Faylona JM. Evolution of ventral hernia repair. Asian J Endosc Surg. 2017;10(3):252–8. https://doi.org/10.1111/ases.12392.
2. Basile F, et al. Surgical approach to abdominal wall defects: history and new trends. Int J Surg. 2013;11 https://doi.org/10.1016/s1743-9191(13)60008-4.
3. Wennergren JE, et al. Laparoscopic ventral hernia repair with primary fascial closure versus bridged repair: a risk-adjusted comparative study. Surg Endosc. 2015;30(8):3231–8. https://doi.org/10.1007/s00464-015-4644-5.
4. Lacour M, et al. CT findings of complications after abdominal wall repair with prosthetic mesh. Diagn Intervent Imaging. 2017;98(7-8):517–28. https://doi.org/10.1016/j.diii.2017.01.002.
5. Nieto E, et al. Obesity as a risk factor for complications and recurrences after ventral hernia repair. Int J Abdominal Wall Hernia Surg. 2020;3(1):1. https://doi.org/10.4103/ijawhs.ijawhs_35_19.
6. Patil AR, et al. Mind the gap: imaging spectrum of abdominal ventral hernia repair complications. Insights Imaging. 2019;10(1) https://doi.org/10.1186/s13244-019-0730-x.
7. Ivanics T, et al. Outcomes of component separation for ventral hernia repair in an emergent setting: analysis of the American College of Surgeons (ACS) NSQIP. J Am Coll Surg. 2017;225(4) https://doi.org/10.1016/j.jamcollsurg.2017.07.370.
8. Rosen MJ, et al. Multicenter, prospective, longitudinal study of the recurrence, surgical site infection, and quality of life after contaminated ventral hernia repair using biosynthetic absorbable mesh. Ann Surg. 2017;265(1):205–11. https://doi.org/10.1097/sla.0000000000001601.
9. Holihan JL, et al. Component separation vs. bridged repair for large ventral hernias: a multi-institutional risk-adjusted comparison, systematic review, and meta-analysis. Surg Infect. 2016;17(1):17–26. https://doi.org/10.1089/sur.2015.124.
10. Reinpold W. Transversus abdominis muscle release: technique, indication, and results. Int J Abdominal Wall Hernia Surg. 2018;1(3):79. https://doi.org/10.4103/ijawhs.ijawhs_27_18.
11. Earle, et al. Guidelines for laparoscopic ventral hernia repair. Society Gastrointest Endosc Surg. 2020. https://www.sages.org/publications/guidelines/guidelines-for-laparoscopic-ventral-hernia-repair/
12. Halligan S, et al. Imaging complex ventral hernias, their surgical repair, and their complications. Eur Radiol. 2018;28(8):3560–9. https://doi.org/10.1007/s00330-018-5328-z.
13. Carbonell AM, Cobb WS, Chen SM. Posterior components separation during retromuscular hernia repair. Hernia. 2008;12(4):359–62. https://doi.org/10.1007/s10029-008-0356-2.
14. Tastaldi LG, et al. Hernia recurrences after posterior component separation with transversus abdominis release: why they happen and how to fix them. J Am Coll Surg. 2018;227(4) https://doi.org/10.1016/j.jamcollsurg.2018.08.369.
15. Woeste G, et al. Wound morbidity in abdominal wall reconstruction can be reduced using transversus abdominis release compared to anterior component separation technique. J Am Coll Surg. 2016;223(4) https://doi.org/10.1016/j.jamcollsurg.2016.08.294.
16. Davies, et al. A comparative analysis between laparoscopic and open ventral hernia repair at a tertiary care center. Am Surg. 2012;28(8):888–92.
17. Ballem N, et al. Laparoscopic versus open ventral hernia repairs: 5 year recurrence rates. Surg Endosc. 2008;22(9):1935–40. https://doi.org/10.1007/s00464-008-9981-1.
18. Porecha M, et al. Comparative study of laparoscopic versus open ventral hernia repair. Internet J Surg. 2010;22(2)., http://ispub.com/IJS/22/2/7514
19. Ghali S, et al. Minimally invasive component separation results in fewer wound-healing complications than open component separation for large ventral hernia repairs. J Am Coll Surg. 2012;214(6):981–9. https://doi.org/10.1016/j.jamcollsurg.2012.02.017.
20. Oviedo RJ, et al. Robotic ventral hernia repair and endoscopic component separation: outcomes. JSLS J Society Laparoendosc Surg. 2017;21(3) https://doi.org/10.4293/jsls.2017.00055.
21. Gonzalez AM, et al. Laparoscopic ventral hernia repair with primary closure versus no primary closure of the defect: potential benefits of the robotic technology. Int J Med Robot Comput Assist Surg. 2014;11(2):120–5. https://doi.org/10.1002/rcs.1605.
22. Sharbaugh ME, et al. Robotic ventral hernia repair: a safe and durable approach. Hernia. 2019; https://doi.org/10.1007/s10029-019-02074-9.
23. Bittner JG, et al. Comparative analysis of open and robotic transversus abdominis release for ventral hernia repair. Surg Endosc. 2017;32(2):727–34. https://doi.org/10.1007/s00464-017-5729-0.

24. Docimo S Jr, Spaniolas K, Svestka M, Bates AT, Sbayi S, Schnur J, Talamini M, Pryor AD. Increased incidence of surgical site infection with a body mass index ≥ 35 kg/m2 following abdominal wall reconstruction with open component separation. Surg Endosc. 2019;33(8):2503–7. https://doi.org/10.1007/s00464-018-6538-9. Epub 2018 Oct 22
25. De Silva GS, et al. Comparative radiographic analysis of changes in the abdominal wall musculature morphology after open posterior component separation or bridging laparoscopic ventral hernia repair. J Am Coll Surg. 2014;218(3):353–7. https://doi.org/10.1016/j.jamcollsurg.2013.11.014.
26. Losanoff, et al. "Component separation" method for abdominal wall reconstruction. J Am Coll Surg. 2003;196(5):825–6.
27. Parikh KR, et al. Incisional hernia repair: what the radiologist needs to know. Am J Roentgenol. 2017;209(6):1239–46. https://doi.org/10.2214/ajr.17.18137.
28. Warren J, et al. Safety and efficacy of synthetic mesh for ventral hernia repair in a contaminated field. J Am Coll Surg. 2020;230(4):405–13. https://doi.org/10.1016/j.jamcollsurg.2019.12.008.
29. Augenstein V, et al. Optimal management of mesh infection: evidence and treatment options. Int J Abdominal Wall Hernia Surg. 2018;1(2):42. https://doi.org/10.4103/ijawhs.ijawhs_16_18.
30. Kugler NW, et al. A dual-stage approach to contaminated, high-risk ventral hernia repairs. J Surg Res. 2016;204(1):200–4. https://doi.org/10.1016/j.jss.2016.04.065.
31. Warren JA, et al. Factors affecting salvage rate of infected prosthetic mesh. Am J Surg. 2020; https://doi.org/10.1016/j.amjsurg.2020.01.028.

Subxiphoid Hernia

15

Sean C. O'Connor and Alfredo M. Carbonell

Introduction

The anatomy of the subxiphoid region is especially challenging due to the convergence of the chest wall, abdominal wall, and diaphragm. Hernias in this region (M1) can be generally categorized by the nature of their previous incision: Subxiphoid trocar site, sternotomy, subcostal, or midline laparotomy incisions. In this chapter, we will discuss the specific challenges in the repair of these hernias, as well as techniques used to optimize outcomes. Here we provide examples of each category with corresponding imaging and discuss how preoperative imaging can be used to optimize surgical technique.

Supplementary Information The online version contains supplementary material available at https://doi.org/10.1007/978-3-031-21336-6_15.

S. C. O'Connor
Mission Subspecialty Surgery, Mission Hospital, Asheville, NC, USA

University of North Carolina College of Medicine, Chapel Hill, NC, USA
e-mail: sean.oconnor2@hcahealthcare.com

A. M. Carbonell (✉)
Department of Surgery, Prisma Health-Upstate, Greenville, SC, USA

University of South Carolina School of Medicine-Greenville, Greenville, SC, USA
e-mail: Alfredo.Carbonell@prismahealth.org

Patient Selection

An intimate understanding of the subxiphoid anatomy is paramount to individualizing technique to each patient. As the costal margin moves midline and cephalad, the rectus muscle moves anterior to the ribs, ultimately inserting on the chest wall just inferior to the pectoralis muscle (Fig. 15.1). The transversus abdominis muscle has a very short course from its origin on the costal margin to its insertion on the posterior rectus sheath. The muscle body becomes thicker as it moves cephalad, making this an ideal place to begin the transversus abdominis release (TAR) without damaging the underlying peritoneum. Medially, the posterior rectus sheath inserts along the edges of the Xiphoid process. This can be taken down in order to enter the preperitoneal fat pad beneath the xiphoid process and will allow further dissection underneath the diaphragm in the preperitoneal space. (Fig. 15.2)

As discussed before, subxiphoid hernias can generally be categorized by the nature of their previous incision: Subxiphoid trocar site, sternotomy, subcostal, or midline laparotomy incisions. Subxiphoid trochars usually result in small hernias where the surrounding anatomy remains intact. These are amenable to suture repair or preperitoneal mesh placement, and not much consideration of the surrounding anatomy is required. Patients with previous sternotomy incisions have significant alterations of the anatomy that must

S. Docimo Jr. et al. (eds.), *Fundamentals of Hernia Radiology*,
https://doi.org/10.1007/978-3-031-21336-6_15

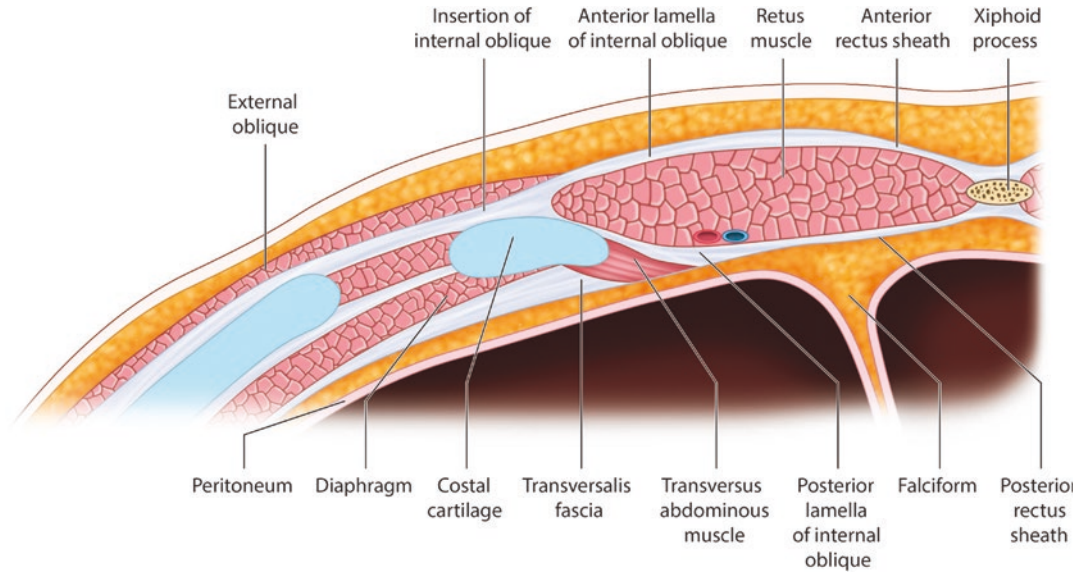

Fig. 15.1 Cross section of the abdominal wall at the level of the Xiphoid process

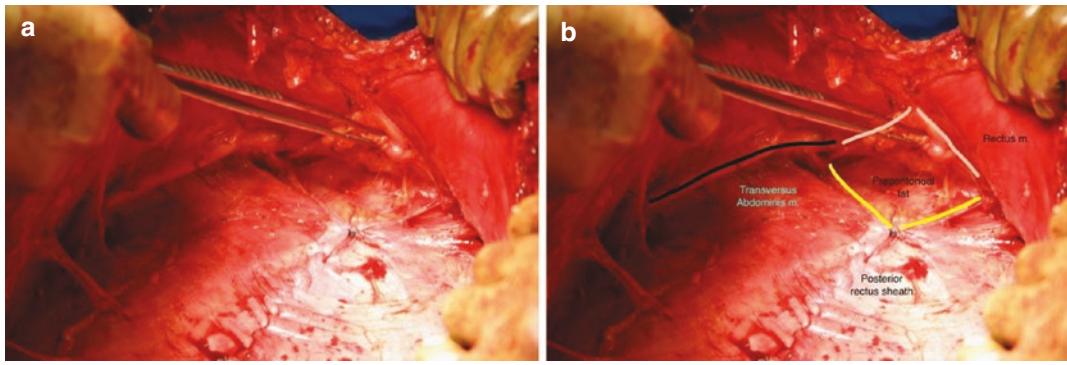

Fig. 15.2 (**a**) Intraoperative photo of subxiphoid component of abdominal wall reconstruction with posterior component separation. (**b**) Yellow highlights the cut edge of the posterior rectus sheath after it was transected from its insertion on the xiphoid process marked in tan. Black line highlights the costal margin with the Transversus abdominis M. inserting on the underside

be considered. These hernias occur quite cephalad along the abdominal wall and often protrude through the divided xiphoid process itself thus requiring a preperitoneal dissection under the diaphragm for proper overlap of mesh. Every effort must be made to ensure that previous wound infections have completely resolved as chronic osteomyelitis and sinus tracks are common. Omental or myofascial flaps that may have been used for wound coverage must also be considered.

In planning the repair of subcostal and midline laparotomy hernias, the subxiphoid region must be taken into account with the hernia defect as a whole. This is often the most difficult region to close, and proper approximation of the fascia in this region will direct the technique for the remainder of the defect. Preoperative imaging and intraoperative assessment of abdominal wall compliance should be used to tailor the technique to the patient. The ideal location for mesh however is in the retro rectus space where it is iso-

lated from the abdominal cavity as well as the overlying skin [1, 2].

Every effort should be made to optimize modifiable comorbidities (MCM) prior to surgery. Obesity (BMI >35), diabetes, and smoking have classically been described as the major risk factors affecting surgical site occurrence (SSO) after incisional hernia repair. This has been confirmed by a recent review of the Americas Hernia Quality Collaborative (AHSQC) showing that having one of these comorbidities increases a patient's risk of SSO, and having two or more increases the risk of SSO requiring procedural intervention (SSOPI). The relative risk of surgical site occurrences requiring procedural intervention (SSOPI) however was only 5%, corresponding to a number needed to treat 20 patients [3]. Therefore, in asymptomatic patients with reducible hernias, surgery can be delayed to optimize MCMs given the relative safety of watchful waiting in these patients [4]. Surgery should however not be delayed in patients with severe symptoms or recurrent obstructions since the benefits will clearly outweigh the risks. Patients in this circumstance should be informed of these statistics prior to consenting to surgery [5].

Case examples

Small Defect After Mediastinal Tubes

The simplest subxiphoid hernia is the small, incisional hernia that requires little or no mobilization of the anterior rectus sheath for closure. This is common at the subxiphoid port site from a laparoscopic cholecystectomy or mediastinal drains from a CABG [6]. If these incisions are not closed, preperitoneal fat can herniate and can eventually cause pain or an unsightly bulge in the epigastrium. The liver and falciform fat pad can prevent intra-abdominal contents from herniating, making the risk of obstruction or incarceration very low. These hernias are mostly safe to observe and the main indication for repair is unrelenting symptoms.

Though the repair is easy, finding the fascial defect can be difficult. In obese patients, they can be very hard to locate on physical exam and may require some exploration of the fascia to find the defect. A vertical incision is recommended in the open approach so that it can be extended during exploration of the fascia. Upon laparoscopic exploration, the defect may be hidden beneath the falciform ligament, and there may be no signs of the hernia from the intraperitoneal position. The falciform ligament should be taken down in order to fully expose the fascia to find the defect.

Non-contrasted CT imaging is helpful in these cases for several reasons. Small defects can be located by measuring the distance from the tip of the xiphoid, which is a reliable landmark even in obese patients. This can be done using the sagittal reformats, or by counting slices and multiplying by the slice thickness. Defects larger than 2 cm should be repaired with mesh to reduce the risk of recurrence, and an appropriate conversation with the patient can be had about the benefits and risks of preperitoneal mesh placement. In obese and diabetic patient, a laparoscopic preperitoneal mesh repair will allow for adequate mesh overlap while reducing the risk of infection. (Fig. 15.3)

Large Circular Defect After CAB

Subxiphoid hernias that are larger than 4 cm are more complex due to the wide area of dissection needed for mesh sublay. Fortunately, the falciform fat pad makes preperitoneal dissection easy to perform without damaging the peritoneum and the linea alba can often be approximated without further myofascial release. In this circumstance, a large preperitoneal plane should be created to allow for a minimum 5 cm of mesh sublay in all directions. A macroporous, uncoated permanent mesh can then be deployed in the preperitoneal plane and the linea alba can be approximated above it to complete the preperitoneal sublay.

The medialization of the anterior rectus sheath can often be limited by lateral tension from the costal margin on either side. In this scenario, myofascial release of the rectus muscle in a Rives-Stoppa fashion will allow for the tension-free approximation of the midline. The posterior rectus sheath is incised and the posterior rectus

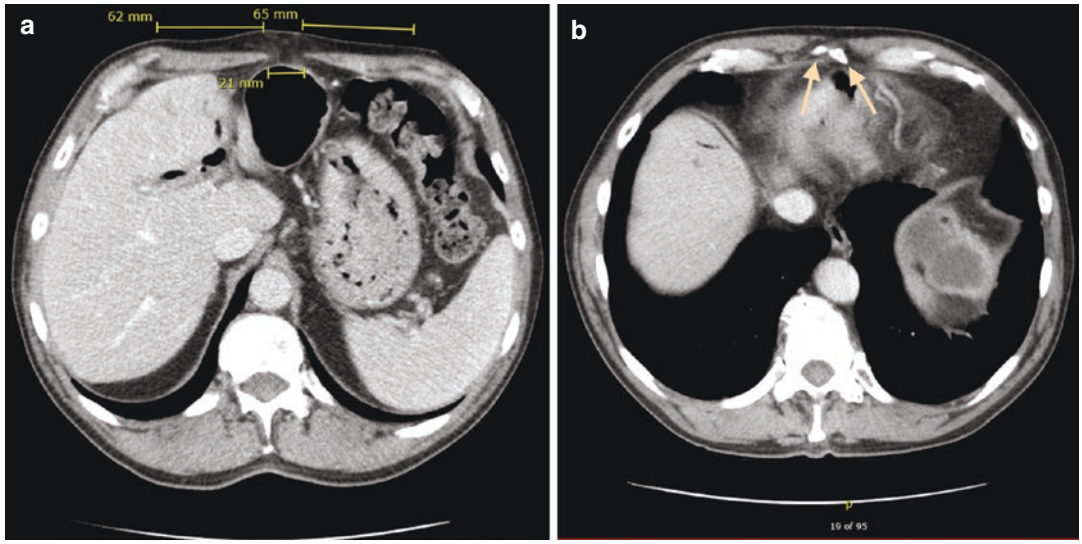

Fig. 15.3 (**a**) 2.1 cm defect from mediastinal drains after a CABG. Repaired by open approach with preperitoneal placement of mesh. (**b**) Xiphoid process is split from previous Sternotomy noted by arrows. Defect is 1.5 cm below the xiphoid process (3.75 mm × 4 slices)

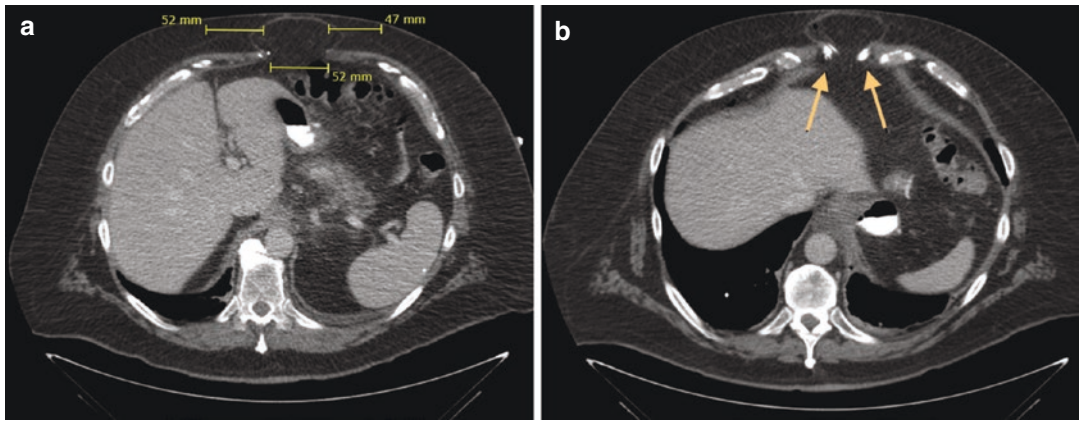

Fig. 15.4 (**a**) 5.2 cm subxiphoid defect after a CABG that was repaired by open preperitoneal approach. (**b**) Arrows point to the divided xiphoid from his previous sternotomy with the hernia sac protruding through the defect

space is entered. The posterior rectus sheath is then separated from linea alba to its insertion on the Xiphoid. It is important to completely detach the posterior rectus sheath from the xiphoid until the diaphragm muscle fibers can be seen anteriorly to allow the mesh to rest underneath the xiphoid process and the diaphragm if necessary (Fig. 15.2). Care must be taken here not to damage the diaphragm so that the mesh is not exposed to mediastinal structures. The abdominal wall is then closed in layers with the mesh placed in the posterior rectus space.

Figure 15.4 presents imaging 5.2 cm defect in the upper abdomen after a CABG. This defect should be closed with mesh and possibly a Rives-Stoppa dissection if the anterior rectus is difficult to medialize. Also, Fig. 15.4 shows the hernia going directly through the xiphoid process that has been split from his previous sternotomy. The dissection will need to be carried

in the preperitoneal plane under the diaphragm to allow for adequate mesh overlap under the xiphoid process.

Diaphragm and Sternal Defect After Omental Flap

Sternal wound infection overall is a rare event occurring in between 1 and 3% of cases; however, it can place patients at risk for developing a thoracoabdominal hernia extending through both the abdominal wall and sternum. This risk is compounded by the complex reconstruction effort requiring a well-vascularized flap to cover the sternum. Omental pedicle flaps can provide excellent, well-vascularized coverage of the sternal wound in cases where conservative measures fail [7]. The omentum is pulled through the debrided xiphoid and sternal cartilage, iatrogenically creating a Morgagni hernia through the anterior diaphragm to provide coverage for the exposed chest wall. Images of these hernias can be impressive, with herniation of colon, stomach, or small bowel high onto the chest wall (Fig. 15.5).

These hernias are unlikely to cause obstruction and the most common symptom requiring repair are pain or bulge. In a series of 415 reported cases, only 4 were reported to require repair due to symptoms [7]. The images in

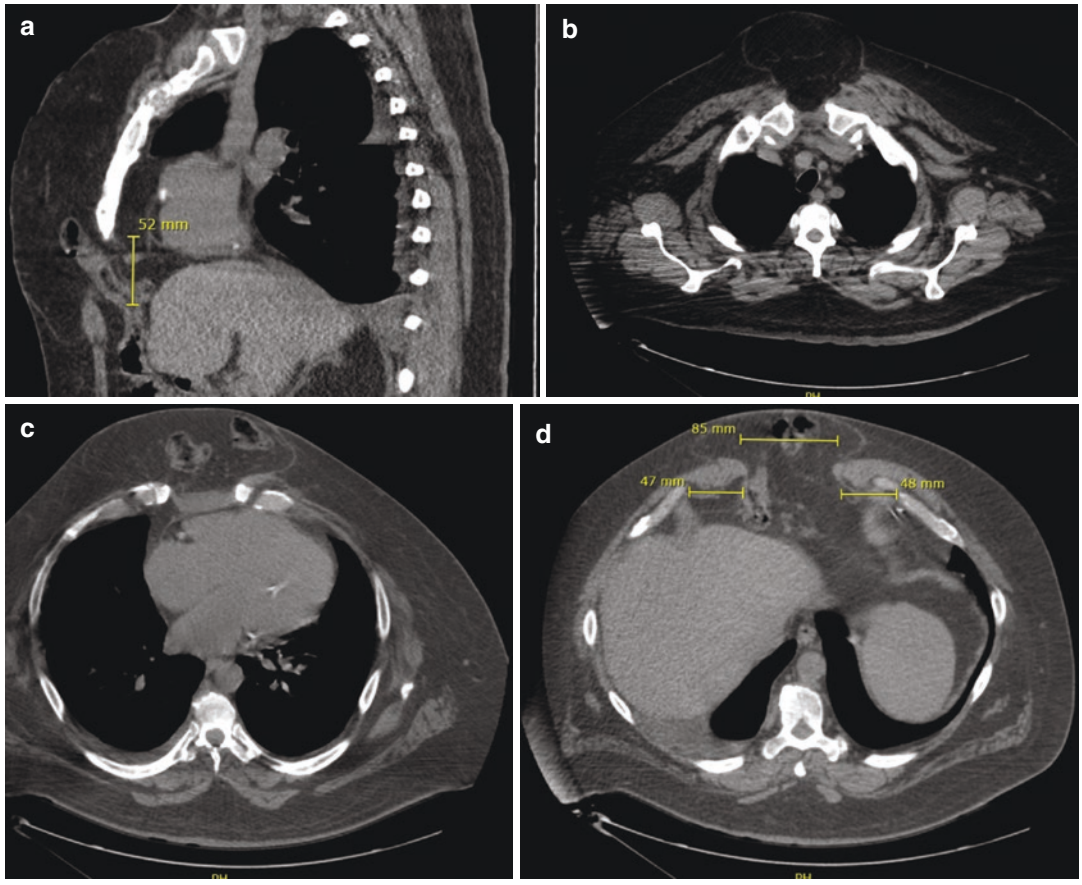

Fig. 15.5 (**a**) Sagittal view of the 5.2 cm defect with omentum and transverse colon herniated anterior to the sternum. (**b**) the omental pedicle flap extends the entire length of the sternum up to the sternal notch. Note the defect in the manubrium remaining from previous debridement. (**c**) Transverse colon herniated anterior to the sternal defect. (**d**) The rectus muscles are retracted laterally anterior to the costal margin with a wide 8.5 cm defect in the midline

Fig. 15.5 are of a patient who presented 18 months after CABG with sternal dehiscence requiring debridement and omental flap. As seen in Fig. 15.5, his chief complaint was the unsightly bulge overlying the sternum, with herniating omentum and transverse colon extending as high as the sternal notch. The patient had no obstructing symptoms however he reported the bulge became heavy on his chest, especially when lying down or coughing. Preoperative imaging can help guide the surgeon by indicating how much intrabdominal contents are herniated, and how far they extend above the diaphragm. It also will reveal any concomitant sternal or diaphragmatic defects that may not be detected clinically.

We recommend approaching these hernias robotically or laparoscopically, which provide excellent visualization and access to the upper abdomen and hiatus [8]. The omentum and transverse colon should first be reduced into the peritoneal cavity which may require division of the omentum. The preperitoneal plane can be entered starting at least 5 cm inferior to the fascial edge and is carried laterally beneath the rectus muscles to the costal margin and superiorly to the hernia defect. At this point, the preperitoneal plane can be continued beneath the diaphragm being careful to leave the muscle and central tendon of the diaphragm intact to prevent injury to the pericardium or diaphragm. It is important to remember that the central tendon constitutes the inferior wall of the pericardium, so sharp dissection without cautery should be used when peeling the peritoneum from this area. The preperitoneal plane is carried posteriorly on the diaphragm to achieve 5 cm of overlap or until the esophageal hiatus prevents further dissection. The defect can then be closed using a 1-0 absorbable, barbed suture, and a macroporous, permanent mesh can be fixated to the diaphragm and fascia using an absorbable suture. The peritoneal flap can then be closed using a 2-0 absorbable, barbed suture to completely isolate the mesh from the peritoneal cavity.

Midline Component of Subcostal Incision

Subcostal incisional hernias are most commonly found on the right side after open cholecystectomy or liver resection. However, they can extend bilaterally after a chevron incision for liver or pancreatic resection. Because the layers of the rectus fascia and obliques have been transected, the anatomy can be disorienting for many surgeons. The superior epigastric artery is ligated during the transection of the rectus muscle, leaving the muscle body at least partially devascularized below that point. This can cause the rectus muscle to atrophy and contract, creating scar within and reducing the size of the posterior rectus space. The proximity to the costal margin creates additional difficulty by limiting the mobility of the fascia and requiring dissection under the diaphragm for adequate mesh placement.

Though the subxiphoid component may be the presenting symptom, there can often be subclinical hernias lateral to midline along the length of the incision, even involving the semilunar line. Preoperative imaging will show the surgeon the full extent of the defects to ensure that all areas of weakness are repaired. The costal margin can often prevent medialization of the fascia, even with adequate myofascial release. If the hernia extends to and/or involves the semilunar line, the surgeon may want to consider closing the defect transversely to reduce tension. The example given in Fig. 15.6b shows extension of the hernia defect laterally; however, this hernia was still amenable to vertical closure. Figure 15.6a shows the robust rectus muscle above the level of the incision; however, it is almost completely absent at the level of the hernia and below. The retro rectus space will be contracted with dense adhesions, and care must be taken to preserve the hernia sac and posterior fascia during dissection.

Due to the lateral extension of these hernias, a TAR is almost always required on the affected side to obtain adequate mesh overlap. As in other subxiphoid hernias, the insertion of the posterior

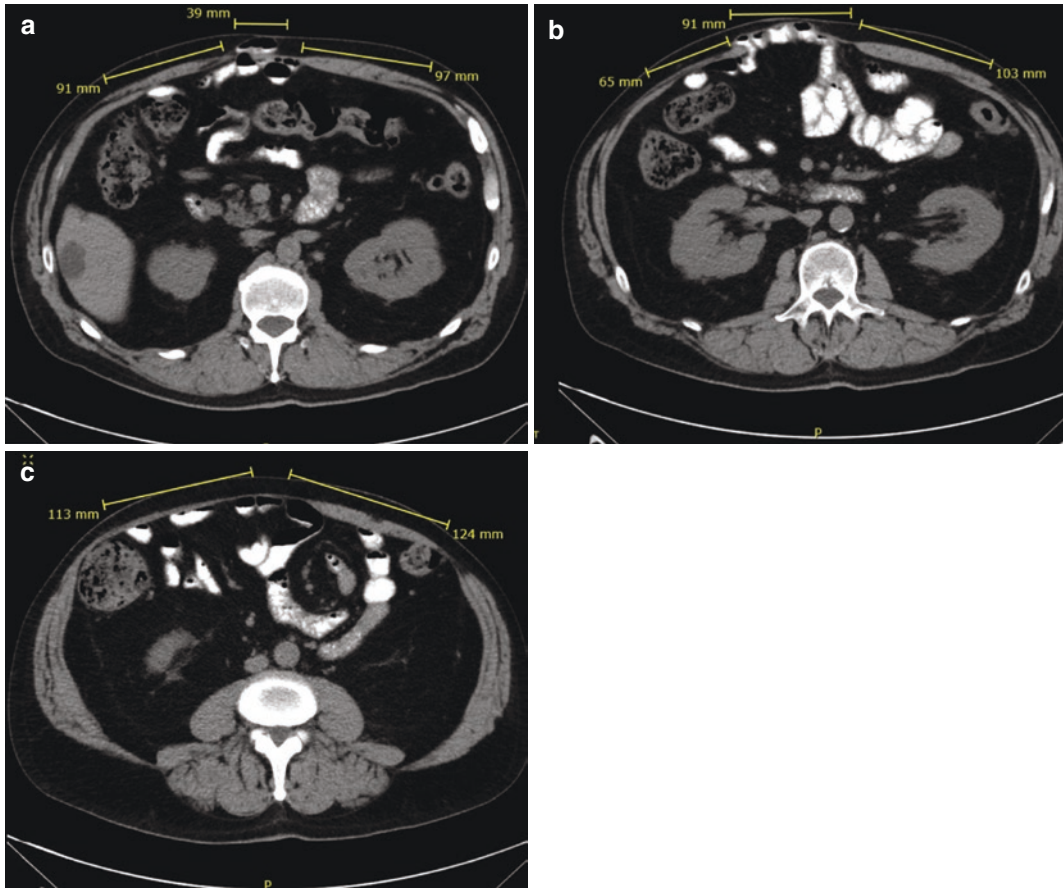

Fig. 15.6 (**a**) Subxiphoid component of a subcostal incision seen with a robust right rectus muscle above the level of the incision. (**b**) The hernia extends laterally along the length of the subcostal incision and the right rectus muscle is absent where it was transected at the index operation. (**c**) Below the level of the defect, the right rectus is clearly atrophic and retracted when compared to the left side. This makes the dissection in the posterior rectus plane difficult and limits medialization of the right abdominal wall

rectus sheath onto the xiphoid must be transected so that the dissection plane can be carried into the preperitoneal space under the diaphragm. The dissection should be extended under the diaphragm as well as into the retro rectus space on the contralateral side. This ensures proper mesh overlap in addition to proper tension reduction of the midline closure. The anterior rectus fascia can be closed either vertically or transversely depending on which direction produces the least tension.

Subxiphoid Component of Midline Incisional Hernia

As discussed previously, the subxiphoid (M1) region is often the most difficult portion of a midline incisional hernia during closure. The insertion of the obliques on the costal margin and retraction of the rectus over the chest wall limits the medialization of the fascia, leaving the upper portion of the abdominal wall with the least compliance. Dissection under the diaphragm for ade-

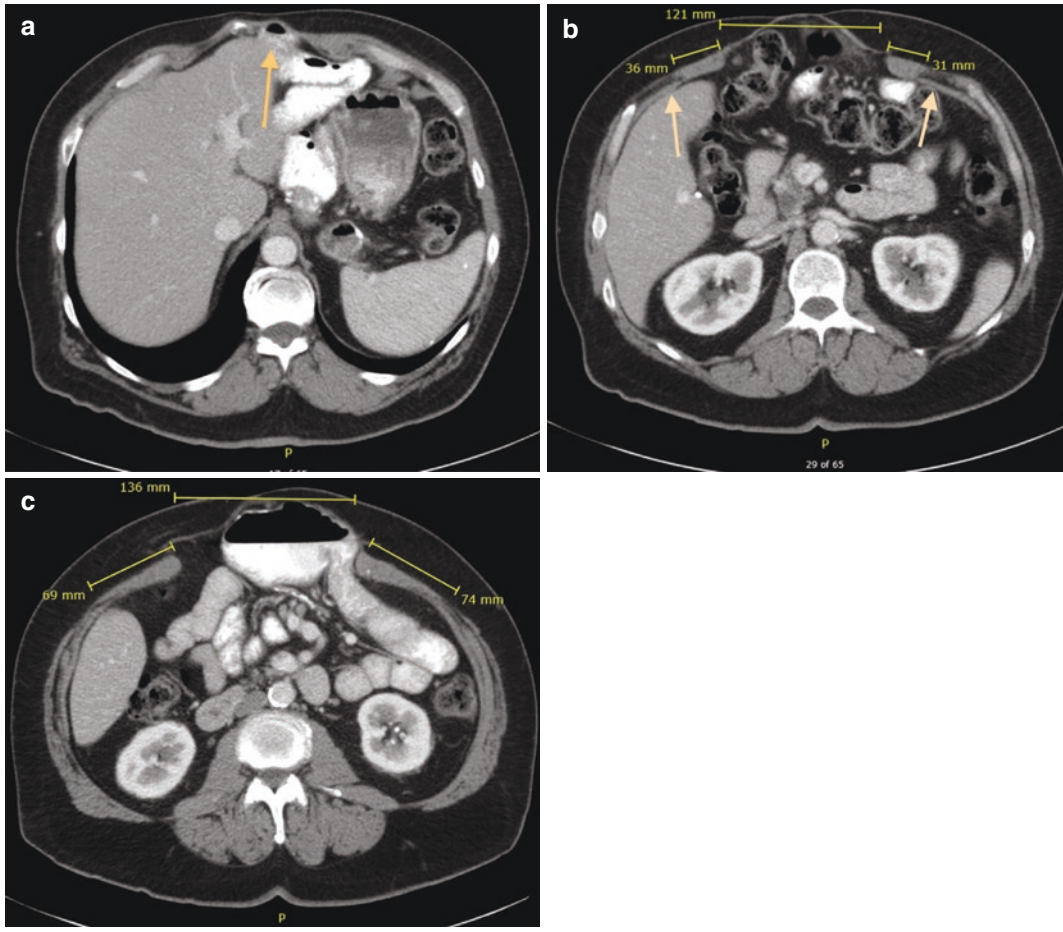

Fig. 15.7 (**a**) CT showing the hernia defect extending cephalad and to the left of the xiphoid process as a result of the previous laparotomy. (**b**) Retracted rectus muscles 3.6 and 3.1 cm respectively with a 12.6 cm defect. Arrows identify the transversus abdominis muscle originating on the costal margin and inserting onto the posterior rectus sheath bilaterally. (**c**) Below the costal margin the rectus muscles are less retracted at 6.9 cm or 7.4 cm respectively with 13.6 cm defect between

quate mesh overlap also adds complexity to the case and must be considered along with the closure of the defect as a whole.

Images below are of a patient with a large midline defect that extends up to the xiphoid process. Figure 15.7a shows a loop of small bowel herniating to the left of the xiphoid due to the patient's previous laparotomy extending cephalad, alongside the xiphoid. Figure 15.7b demonstrates the rectus muscles are retracted with approximately 3 cm of space within the rectus sheath and a 12 cm hernia defect between the muscles. At this level, the abdominal wall will have very little compliance due to the insertion of the rectus muscles on the costal margin. Medialization of the rectus muscles will be dependent on an adequate myofascial release. With narrow rectus muscles and a wide defect, it is unlikely that a Rives-Stoppa dissection alone will provide adequate mobilization, and a TAR may be required to close the defect. The oblique musculature is easily seen in Fig. 15.7b, with arrows pointing to the transversus abdominis muscle inserting on the posterior rectus sheath medially, and the costal margin laterally.

The transversus abdominis muscle and transversalis fascia can be incised along the costal margin starting as cephalad as possible to enter

the preperitoneal plane. This can be extended down the entire length of the hernia defect to allow for adequate release of tension as well as mesh overlap. At this point, the preperitoneal plain can be carried laterally to the retroperitoneum, and superiorly underneath the diaphragm. The insertion of the posterior rectus sheath onto the xiphoid will need to be taken down bilaterally to connect the right and left preperitoneal spaces. It is important to have one contiguous space so that the mesh can be placed flat in this plane.

Subxiphoid Component of Midline Hernia with Loss of Domain

Significant preoperative preparation is required in the case of true loss of abdominal domain. Volumetric analysis of the hernia sac volume to abdominal cavity volume based upon CT scan has been used to identify patients with significant loss of domain, and possibly referral for preoperative progressive pneumoperitoneum (PPP). This can be done by measuring the dimensions of the abdominal cavity and hernia sac and calculating the volume of an ellipse, or by utilizing specialized software commonly used in measuring liver volume [9]. The Tanaka method uses a hernia sac volume to abdominal cavity volume of 25% to identify patients that could benefit from PPP [10]. Though no randomized controlled trials exist, it is thought that PPP combined with botulinum toxin injection into the oblique musculature can both improve the compliance of the abdominal wall and also prepare the patient for the increased abdominal pressure they will experience after reconstruction.

Due to the wide defect and poor abdominal compliance, a TAR will not provide adequate mobilization of the rectus sheath for closure of these defects. This is especially true in the subxiphoid region where the transversus abdominis muscle travels a short distance to its origin on the costal margin, so division of this muscle and creation of a preperitoneal flap will not result in a sufficient enough release of the anterior rectus sheath. The external oblique however has its origin on the anterior chest wall lateral to the costal margin and insertion on the anterior rectus sheath. The division of the external oblique can be extended up the chest wall to the level of serratus anterior m., and a large interparietal flap can be raised laterally to allow medialization of the anterior rectus towards the midline. The ideal location for the mesh is still in the sublay retro rectus position, so dissection in the posterior rectus space is still required for placement of the mesh [11].

The images below represent a previous trauma patient who required delayed abdominal closure with absorbable mesh and skin graft coverage. The defect was wide with clear loss of domain and extended to the xiphoid process. The rectus muscles are retracted over the costal margin and foreshortened to 5.1 cm on the left and 3.9 cm on the right (Fig. 15.8b). Broadening these muscles with a retro rectus dissection alone failed to result in significant medialization. Even after skin flaps were raised, external oblique release, and retro rectus dissection, closure of the upper midline still proved difficult and was under some tension. (Video 15.1)

It is typically not recommended to perform both a TAR and division of the external abdominal oblique m. during the same operation due to potential destabilization of the abdominal wall. Therefore, it is a critical decision point to perform an anterior component separation (ACS) versus a posterior component separation (PCS). Preoperative imaging can be tremendously helpful with this decision, informing the surgeon prospectively of the distance that needs to be traversed and the nature of the abdominal wall musculature. In this patient with retracted rectus muscles and a wide defect up to the xiphoid, the decision to perform a Ramirez-style release was made preoperatively and confirmed by intraoperative assessment of tension.

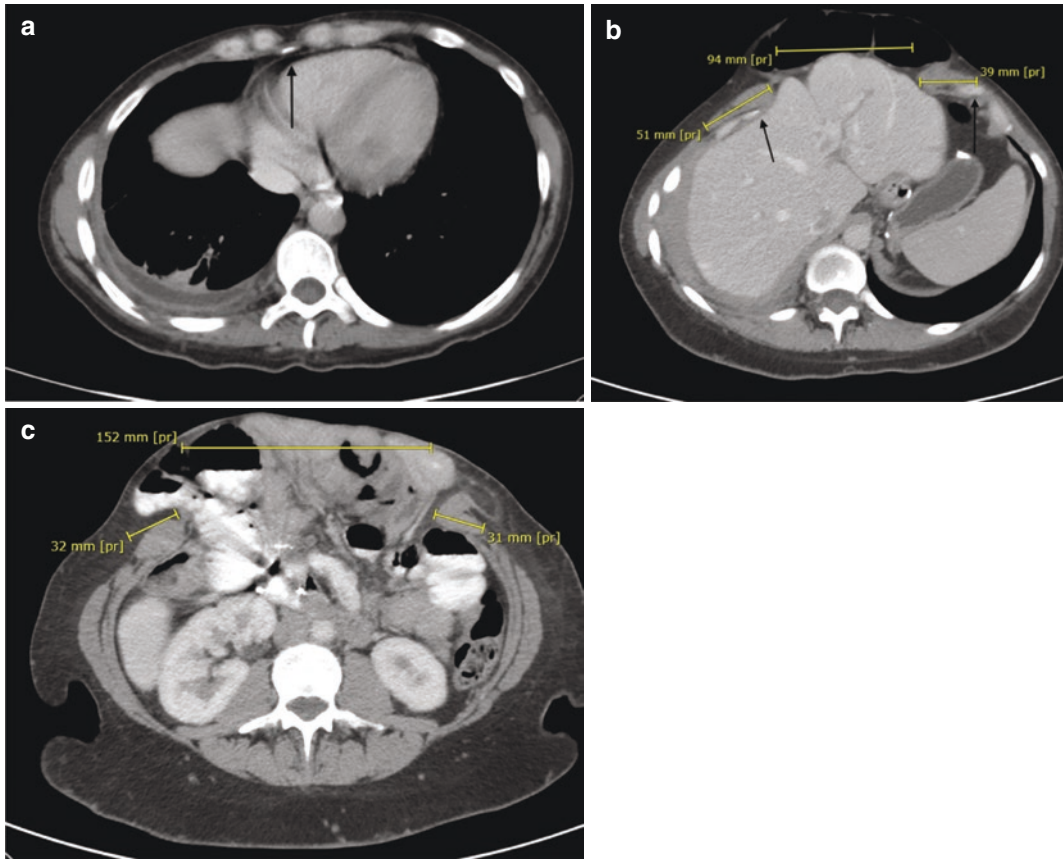

Fig. 15.8 (**a**) Upper portion of the abdominal wall with the hernia extending up to the xiphoid process. (**b**) The rectus muscles are retracted over the chest wall and foreshortened with a 9.1 cm defect between. (**c**) Significant retraction of the abdominal wall continues down the abdominal wall with narrow rectus muscles (3.2 and 3.1 cm) and a 15 cm defect. A large portion of the intraperitoneal volume is within the hernia sac suggesting loss of domain

Literature Review

As discussed previously, the majority of subxiphoid hernias are the result of previous surgery and therefore can be categorized by the nature of their operation. Hernias from laparoscopic trocars or mediastinal drainage tubes are the most common and simplest to repair. Laparoscopic cholecystectomy remains the most common surgery to utilize the subxiphoid incision with about a 1–3% risk of symptomatic hernia, likely due to extraction of the gallbladder through the epigastric port [12]. Meta-analysis of randomized trials comparing epigastric versus umbilical extraction of the gallbladder have shown no difference in hernia formation or wound infection between the two techniques, so the retrieval site remains the surgeon's choice [13, 14]. However, suture repair of the fascial defect at the extraction site is recommended to reduce the incidence of hernia formation. Often these hernias are small and contain only preperitoneal fat and are amenable to primary open repair if less than 2 cm. Larger hernias 2–4 cm may require open, laparoscopic, or robotic repair with mesh placed in the preperitoneal position with closure of the defect [15].

The second category of subxiphoid hernias are those occurring after median sternotomy. As the sternum is spread for exposure of the mediastinum, the fascial fibers inserted on either side of

the xiphoid process are split, leaving the subxiphoid region at high risk for hernia formation. These can often be complicated by concomitant diaphragm and sternal defects making repair challenging [7]. Patients who develop a sternal wound infection are at a particularly high risk of hernia development, although the exact incidence is underreported since these are often small, asymptomatic defects. Mackey et al. found that repair of these hernias without the use of mesh carried a 45% recurrence rate and 75% recurrence rate in patients who had a history of sternal wound infection [16]. Once contamination has been controlled, the lowest recurrence and SSO rate can be achieved with preperitoneal placement of microporous polypropylene mesh [17].

Subxiphoid component of abdominal incisions makes up the third and often most challenging category. This area is particularly challenging to reconstruct due to the short insertion of the obliques onto the costal margin and retraction of the rectus laterally over the chest wall. These hernias will often require a component separation in the form of Rives-Stoppa, Ramirez's anterior component separation (ACS) or TAR to achieve adequate mesh overlap and tension-free closure of the defect [18]. Majumder et al. recently used a fresh cadaver model to examine myofascial medialization after ACS vs PCS. They found that in both techniques, the subxiphoid region had the least myofascial medialization when compared to the mid and lower abdomen. Interestingly, PCS resulted in improved medialization over ACS (11.2 vs 8.2 cm, $p < 0.01$) in the subxiphoid region, suggesting that a PCS might be the technique of choice [19]. This challenges the idea that PCS results in inferior medialization; however, no human trials exist to confirm this finding. PCS also allows for extended overlap of the mesh superiorly and laterally under the diaphragm, while minimizing wound complications associated with raising subcutaneous flaps. However, in the case of loss of domain or poor abdominal compliance, many previous cadaver studies have reported that ACS results in superior medialization of the rectus muscles. After retro rectus dissection, surgeons should assess the compliance of the abdominal wall and make the decision for ACS vs PCS based on their intraoperative assessment of abdominal wall compliance [20].

Conclusion

Subxiphoid hernias are a complex subset of abdominal wall hernias. Preoperative planning utilizing radiographic analysis can assist surgeons in deciding if the need for a component separation may or may not be necessary. Radiographic evidence supporting the need for a component separation can guide the patient-surgeon conversation and also better prepare the surgeon for what he or she may encounter intraoperatively.

Conflicts of Interest Sean O'Connor, MD has no conflicts of interest to declare
Alfredo M. Carbonell, D.O. has received honoraria from W.L. Gore and Associates, Ethicon Inc. and Intuitive.

References

1. Holihan JL, Nguyen DH, Nguyen MT, Mo J, Kao LS, Liang MK. Mesh location in open ventral hernia repair: a systematic review and network meta-analysis. World J Surg. 2016;40(1):89–99. https://doi.org/10.1007/s00268-015-3252-9.
2. Carbonell AM, Criss CN, Cobb WS, Novitsky YW, Rosen MJ. Outcomes of synthetic mesh in contaminated ventral hernia repairs. J Am Coll Surg. 2013;217(6):991–8. https://doi.org/10.1016/j.jamcollsurg.2013.07.382.
3. Alkhatib H, Tastaldi L, Krpata DM, et al. Impact of modifiable comorbidities on 30-day wound morbidity after open incisional hernia repair. Surg (United States). 2019;166(1):94–101. https://doi.org/10.1016/j.surg.2019.03.011.
4. Kokotovic D, Sjølander H, Gögenur I, Helgstrand F. Watchful waiting as a treatment strategy for patients with a ventral hernia appears to be safe. Hernia. 2016;20(2):281–7. https://doi.org/10.1007/s10029-016-1464-z.
5. Pearson DG, Carbonell AM. Obesity and abdominal wall reconstruction: outcomes, implications, and optimization. Plast Reconstr Surg. 2018;142(3S):30S–5S. https://doi.org/10.1097/PRS.0000000000004845.
6. Erdas E, Dazzi C, Secchi F, et al. Incidence and risk factors for trocar site hernia following laparoscopic cholecystectomy: a long-term follow-up study.

Hernia. 2012;16(4):431–7. https://doi.org/10.1007/s10029-012-0929-y.
7. Izaddoost S, Withers EH. Sternal reconstruction with omental and pectoralis flaps: a review of 415 consecutive cases. Ann Plast Surg. 2012;69(3):296–300. https://doi.org/10.1097/SAP.0b013e31822af843.
8. Muysoms FE, Cathenis AKKJ, Hamerlijnck ARPHM, Claeys ADAB. Laparoscopic repair of iatrogenic diaphragmatic hernias after sternectomy and pedicled omentoplasty. https://doi.org/10.1007/s10029-009-0551-9
9. Parker SG, Halligan S, Blackburn S, et al. What exactly is meant by "'loss of domain'" for ventral hernia? systematic review of definitions. World J Surg. 43 https://doi.org/10.1007/s00268-018-4783-7.
10. Tanaka JH, Yoo AJ, Rodrigues Jr EM, Utiyama D, Birolini S, Rasslan EY. A computerized tomography scan method for calculating the hernia sac and abdominal cavity volume in complex large incisional hernia with loss of domain. https://doi.org/10.1007/s10029-009-0560-8
11. Heller L, McNichols CH, Ramirez OM. Component separations. Semin Plast Surg. 2012;26(1):25–8. https://doi.org/10.1055/s-0032-1302462.
12. Li M, Cao B, Gong R, et al. Randomized trial of umbilical incisional hernia in high-risk patients: Extraction of gallbladder through subxiphoid port vs. umbilical port after laparoscopic cholecystectomy. Wideochirurgia I Inne Tech Maloinwazyjne. 2018;13(3):342–9. https://doi.org/10.5114/wiitm.2018.76001.
13. Mongelli F, La Regina D, Zschokke I, et al. Gallbladder retrieval from epigastric versus umbilical port in laparoscopic cholecystectomy: a PRISMA-compliant meta-analysis. Surg Innov. 2019; https://doi.org/10.1177/1553350619890719.
14. Hajibandeh S, Hajibandeh S, Clark MC, et al. Retrieval of gallbladder via umbilical versus epigastric port site during laparoscopic cholecystectomy: a systematic review and meta-analysis. Surg Laparosc Endosc Percutaneous Tech. 2019;29(5):321–7. https://doi.org/10.1097/SLE.0000000000000662.
15. Kaufmann R, Halm JA, Eker HH, et al. Mesh versus suture repair of umbilical hernia in adults: a randomised, double-blind, controlled, multicentre trial. Lancet. 2018;391(10123):860–9. https://doi.org/10.1016/S0140-6736(18)30298-8.
16. Mackey RA, Brody FJ, Berber E, Chand B, Henderson JM. Subxiphoid incisional hernias after median sternotomy. J Am Coll Surg. 2005;201(1):71–6. https://doi.org/10.1016/j.jamcollsurg.2005.01.025.
17. Warren J, Desai SS, Boswell ND, et al. Safety and efficacy of synthetic mesh for ventral hernia repair in a contaminated field. J Am Coll Surg. 2020; https://doi.org/10.1016/j.jamcollsurg.2019.12.008.
18. Maloney SR, Schlosser KA, Prasad T, et al. Twelve years of component separation technique in abdominal wall reconstruction. Surgery. 2019; https://doi.org/10.1016/J.SURG.2019.05.043.
19. Majumder A, Martin-del-Campo LA, Miller HJ, Podolsky D, Soltanian H, Novitsky YW. Evaluation of anterior versus posterior component separation for hernia repair in a cadaveric model. Surg Endosc. 2019:0123456789. https://doi.org/10.1007/s00464-019-07046-9.
20. Hodgkinson JD, Leo CA, Maeda Y, et al. A meta-analysis comparing open anterior component separation with posterior component separation and transversus abdominis release in the repair of midline ventral hernias. Hernia. 2018;22(4):617–26. https://doi.org/10.1007/s10029-018-1757-5.

Suprapubic Hernias

16

Charlotte Horne and Ajita S. Prabhu

Suprapubic hernias present a unique challenge to a hernia surgeon due as their proximity to bony structures can make creating enough space for adequate mesh overlap technically challenging. Additionally, due to the atypical location of these hernias, understanding the normal anatomy as well as interpreting the variant anatomy is essential to achieving an adequate repair. Evaluating the imaging is essential when approaching the repair of these defects and the imaging provides essential information including defect size, proximity to vascular anatomy as well as the relationship to bony landmarks of the pelvis. Understanding these key findings on imaging preoperatively can allow the surgeon to successfully negotiate these planes intraoperatively and help the surgeon achieve an appropriate repair.

Suprapubic hernias are defined by the EHS guidelines as defects located from the pubic bone to 3 cm cranially [1]. These hernias can occur after Pfannenstiel incisions, lower midline incisions, low transverse incisions, trocar sites, or at previous suprapubic catheter insertion site. These are atypical hernias due to their relatively low incidence and their proximity to the pubis, major vascular structures as well as the bladder (Fig. 16.1).

Multiple imaging modalities are available to evaluate the anatomy in this region including ultrasound as well as cross-sectional imaging such as CT and MRI. While ultrasound can evaluate pelvic structures well, it is not routinely used in the evaluation of suprapubic hernias as the

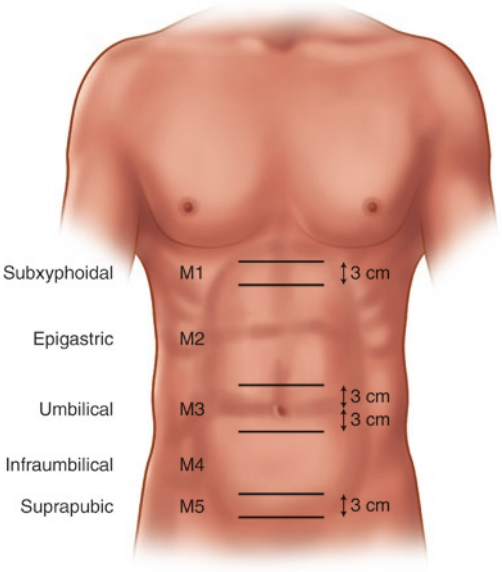

Fig. 16.1 Anatomic location of a suprapubic hernia. From *Techniques of Abdominal Wall Repair*, (pg 51) by B Alkhafaji, 2020, Springer, New Dehli. Copyright (2020) Springer Nature India Private Limited

C. Horne (✉)
Department of Minimally Invasive Surgery, PennState Health, Milton S. Hershey Medical Center, Hershey, PA, USA
e-mail: chorne1@pennstatehealth.psu.edu

A. S. Prabhu
Department of General Surgery, Cleveland Clinic Foundation, Cleveland, OH, USA
e-mail: prabhua@ccf.org

S. Docimo Jr. et al. (eds.), *Fundamentals of Hernia Radiology*,
https://doi.org/10.1007/978-3-031-21336-6_16

quality of the image can be limited by the patient's body habitus as well as the operator performing the ultrasound. An additional limitation is the inability of it to demonstrate the relationship of surrounding structures due to the focused image it provides.

Cross-sectional imaging is ideal as it allows for the evaluation of other concomitant intra-abdominal pathology as well as demonstrates the relationship of the hernia to both vascular and bony anatomy. Both MRI and CT scans can be utilized for this purpose. One drawback of obtaining an MRI for evaluation of suprapubic hernias is they are more time-consuming for a patient to undergo and can be more challenging to interpret. CT scans provide an abundance of information about hernia characteristics but also allow for the evaluation of concomitant pathology and other intra-abdominal structures. While normally, intravenous contrast may not be necessary for the evaluation of a hernia, it is important to note that due to the anatomic location of these hernias, contrast may be required to determine their relationship to major vascular structures in this region.

Normal Imaging

Interpreting imaging in a suprapubic hernia requires one to be aware of not only the abdominal wall muscles but also of the bony and vascular structures of the pelvis.

Inferior to the umbilicus in the suprapubic region the rectus muscles meet at midline with a very narrowed linea alba. The lateral abdominal wall is made of the external oblique, internal oblique, and transversus abdominis from superficial to deep, respectively. As one is below the arcuate line, the posterior rectus sheath is composed only of a thin layer of transversalis fascia and peritoneum (Fig. 16.2).

Inferiorly begin the bony aspects of the pelvis and the inguinal canal. Understanding these anatomic relationships is essential to allow for appropriate overlap as well as to determine if there are concomitant inguinal hernias associated with a suprapubic hernia.

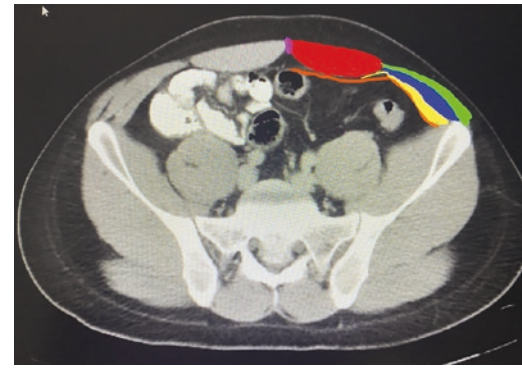

Fig. 16.2 Inferior to the umbilicus the linea alba (purple is narrow). The rectus muscles (red) are larger and meet at midline. The lateral abdominal wall consists of the external oblique (green), internal oblique (blue), and transversus abdominis (yellow). Below the arcuate line, the transversalis consists of a thin layer of fascia that is found at the lateral edge of the rectus muscle (yellow). The deepest layer is the peritoneum (orange)

In this area, the rectus muscle is found inserted medially at the pubic symphysis. Extending laterally from the pubic symphysis is the lacunar ligament which attaches to the pectineal line of the pubis medially and extends laterally to form Cooper's ligament. The epigastric vessels delineate the direct and indirect spaces.

The paired pyramidalis muscles are small triangular-shaped muscles that are not always present in patients, can be unilateral, and also vary in size. The muscles lie between the anterior surface of the rectus abdominis muscle and the posterior surface of the rectus sheath [2]. Their exact function remains unknown but it is theorized the muscle contract in order to tense the linea alba. The wider inferior ends of the pyramidalis muscles attach to the pubic symphysis and the pubic crests and the more narrow superior margins attach to the linea alba [2] (Figs. 16.3 and 16.4).

The major vascular anatomy in this region includes the inferior epigastric vessels which are found at the lateral border of the rectus muscles. The iliac vessels branch posterior into the internal and external iliac. The external iliac vein traverses anteriorly and is found at the lateral borders of the retropubic space. As it continues its medial course, it continues to the femoral

artery below the inguinal ligament which serves as an important landmark for femoral hernias (Fig. 16.5).

The space of Retzius or prevesicular space makes up the extraperitoneal retropubic space and is anterior to the bladder. This space is often exploited to create adequate mesh overlap at the pubis. Deep in the space of Retzius is the urinary bladder (Fig. 16.6).

Caudal to the inguinal ligament, the muscles of the pelvic floor and anterior thigh insert at the pubis to form the pelvic floor (Fig. 16.7). Knowledge of these muscles is relevant as obturator hernias may be present. While suprapubic hernias will originate above the pubic symphysis, the normal anatomic relationships may be disturbed by large hernias and understanding of normal anatomy is imperative to prevent injury during repair.

Fig. 16.3 The paired pyramidalis muscles are small triangular shaped. They are not always present and can be unilateral. The muscles lie between the anterior surface of the rectus abdominis muscle and the posterior surface of the rectus sheath

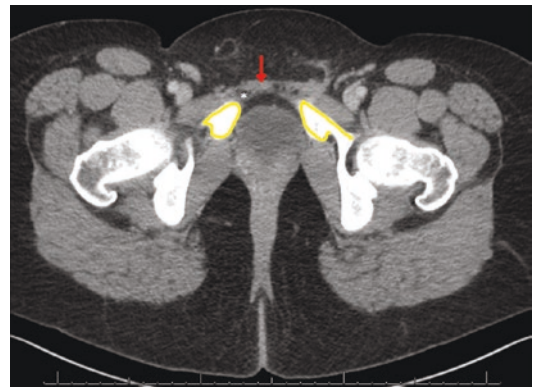

Fig. 16.4 The Rectus insertion to the pubis is marked by the red arrow. The pubis is outlined in yellow. The Lacunar ligament (Asterisk) extends laterally from the pubic symphysis

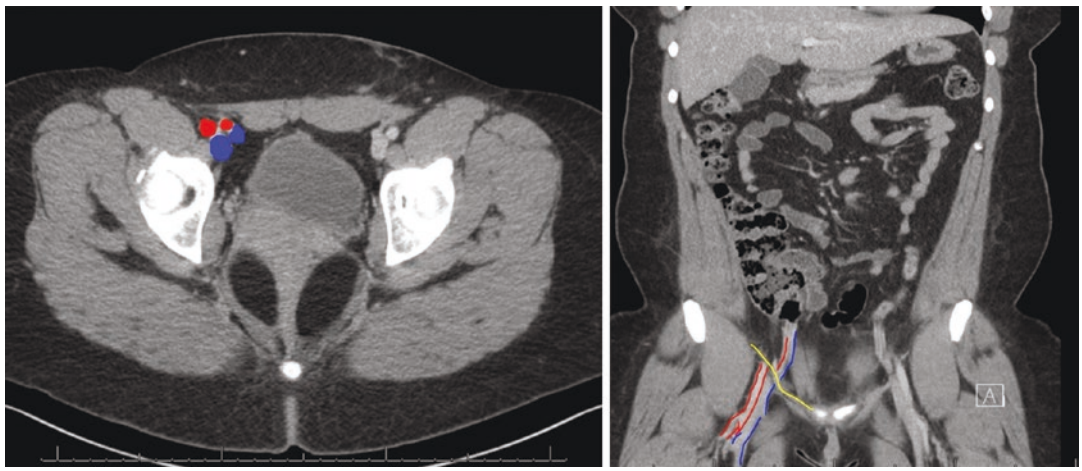

Fig. 16.5 Major Vascular anatomy of the suprapubic region. The Iliac vessels (left in blue) give rise to the inferior epigastric (right in red) at the lateral edge of the rectus muscle. On the right, we can see the relationship between the iliac and epigastric vessel in relation to the pubis and the inguinal ligament (yellow)

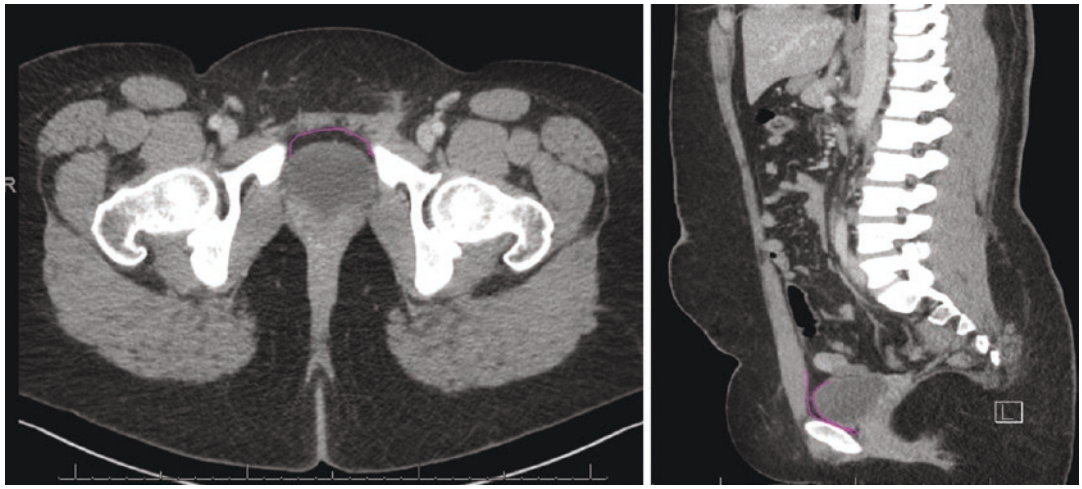

Fig. 16.6 The Space of Retzius is marked by the purple line. This space is a potential preperitoneal space that is anterior to the bladder which can be exploited to create room for adequate mesh overlap below the pubis

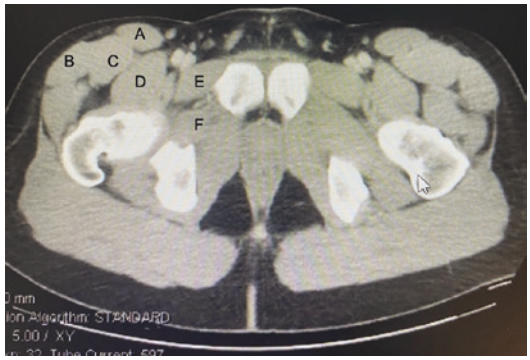

Fig. 16.7 Other muscles of the pubis. From front to back. Sartorius (A), Tensor Fascia Latae (B) Vastus Intermedius (C), Rectus Femoris (D), Pectineus muscle (E), External obturator muscle (F)

Fig. 16.8 Relationship between the hernia defect and the pubic symphysis on Sagittal view

Imaging Findings in Suprapubic Hernias

As described by Muysoms et al., one of the key determinations of suprapubic hernias is its location from the pubic symphysis [1]. While these are defined by their distance from the pubic symphysis, it is important to use imaging to determine their exact location defects that are just superior to the pubic symphysis will present unique challenges in obtaining appropriate mesh overlap when compared to those that are found at the superior aspect of this region. While axial cuts of cross-sectional imaging can demonstrate, the sagittal view can provide additional information about this anatomic relationship (Fig. 16.8).

Another important relationship that should be determined on imaging is the relationship between the defect and the rectus muscle (Fig. 16.9). As suprapubic hernias may occur in patients after Pfannenstiel incisions, tissue-based breast reconstructive procedures, cystectomies, and other prosthetic implants, determining the location of the rectus muscle in relation to the defect allow the surgeon to determine appropriate approach and overlap (Fig. 16.10).

Another important relationship that should be established on imaging is the relationship between the defect and the inferior epigastric vessels. This relationship is important to ascertain as these defects routinely encroach on these vessels. Understanding their proximity to the defect is essential as the epigastric vessels also mark the transition to the lateral aspect of the abdominal wall and can be found just medial to the linea semilunaris (Fig. 16.10). If near the lateral edge of the defect, there may be a need for a potential component separation to create a space that allows for adequate mesh overlap. As well as understanding the relationship between these vessels and the hernia defect is essential, especially in patients with multiple previous operations and incisions as these vessels as well as the periumbilical perforators supply the skin and soft tissue of the lower abdomen, and injury to both may lead to wound complications

Finally, it is important to ascertain the presence of concomitant hernias that will require repair. In addition to concomitant inguinal hernias, cross-sectional imaging should be evaluated for defects that may be located superior to the suprapubic area as those at significant distance away may necessitate variation of operative approach such as additional ports, incisions, or mesh to repair this defect (Fig. 16.11).

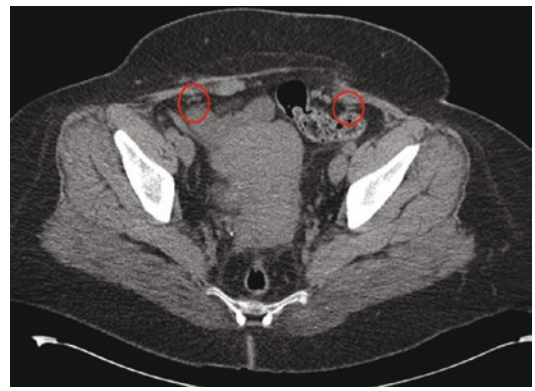

Fig. 16.10 Epigastric vessels in relationship to hernia defect. The epigastric vessels (circled in red) are just lateral to the edge of the defect on the patient's left. On the right side of the defect, they are more lateral and can be found at the lateral edge of the rectus muscle

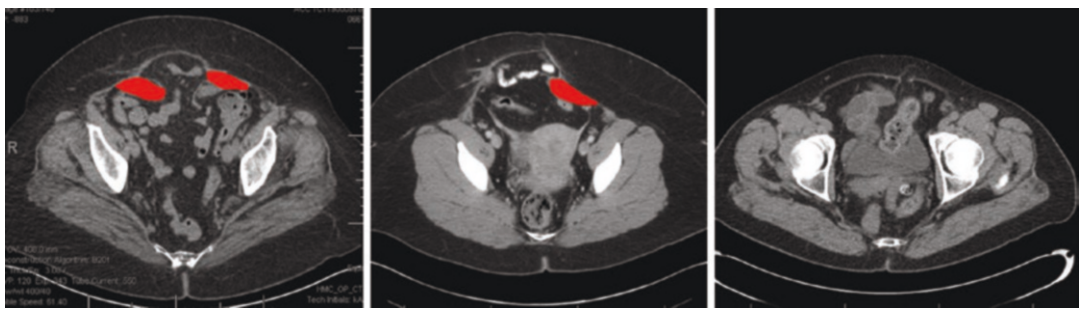

Fig. 16.9 Various types of suprapubic hernias. From left to right: Suprapubic hernia with rectus on either side (red). Absent right rectus muscle (middle). Absent bilateral rectus muscle (far right panel)

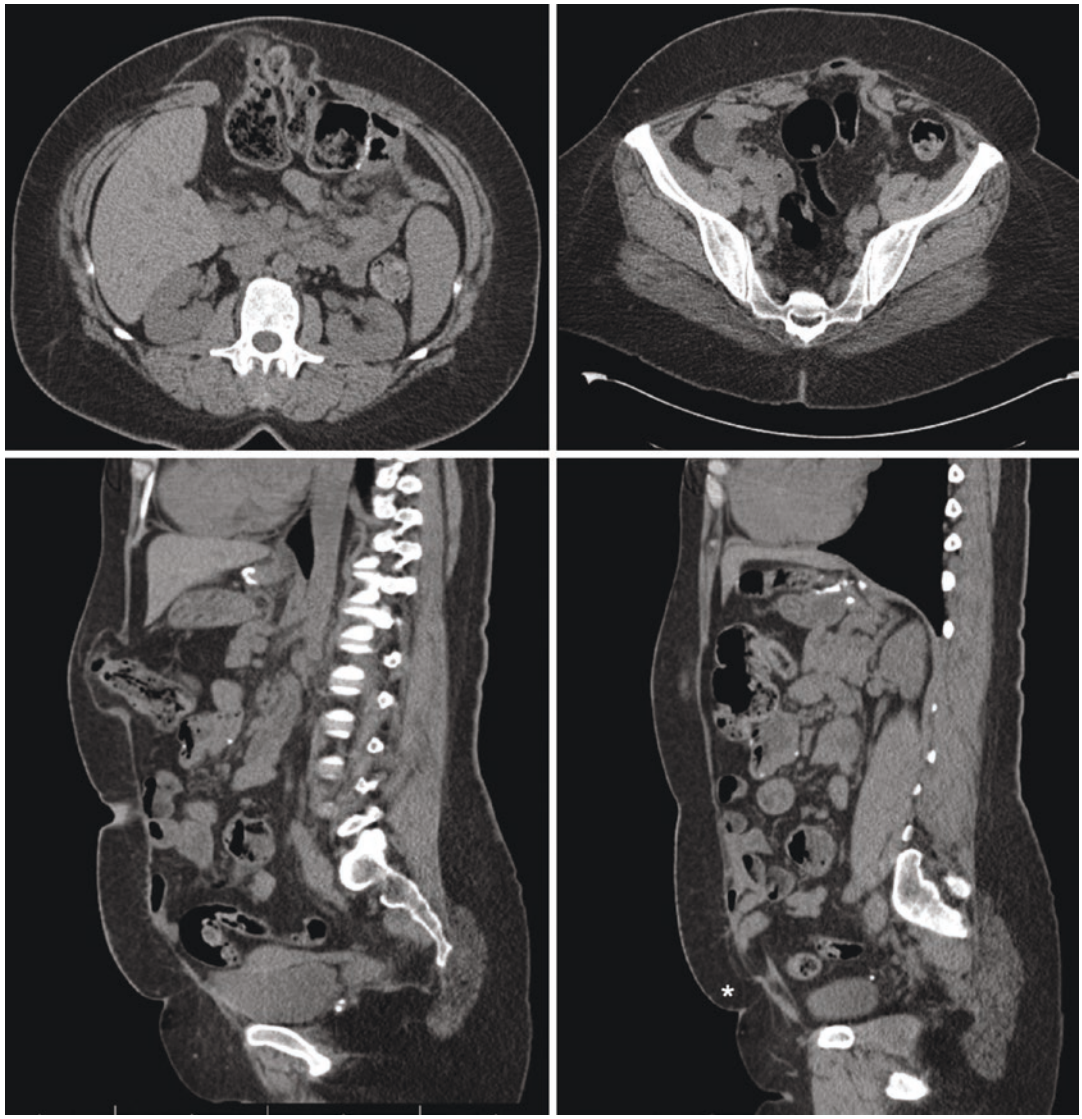

Fig. 16.11 Concomitant Hernias. This patient has a large epigastric hernia with transverse colon (left panels) with an associated suprapubic hernia (right panels)

Suprapubic Hernias After Pfannenstiel Incisions

While the incidence of a suprapubic hernia after a Pfannenstiel incision is low [3, 4], this incision is commonly used when performing Cesarean sections or for specimen retraction during a colorectal or gynecologic procedure. Suprapubic hernias occur after this incision as the pubis serves as the insertion point for the abdominal oblique aponeurosis, rectus muscle, and anterior fascia. Disruption or inadequate closure can result in a hernia through any one or all these layers. When evaluating imaging in patients after a Pfannenstiel incision, it is important to evaluate the relationship of defect to the pubis as this can help determine the need for appropriate overlap or aspects that may make this challenging. When

evaluating imaging in these situations it is also important to recognize concomitant defects, partial thickness defects, or other defects lateral of midline (Fig. 16.12).

It is also important to note that after a Pfannenstiel incision, there can be thinning of one or possibly both rectus muscles. Figure 16.13 demonstrates a patient with a hernia defect that is just off of midline to the right. While the patient has a robust right rectus muscle, the rectus muscle on the left is substantially attenuated.

Additionally, evaluating imaging for the presence or absence of fat planes can indicate areas that will be technically challenging due to dense scar tissue or adhesions. In suprapubic hernias loss of fat planes may indicate dense adhesions between the anterior abdominal wall and the bladder which is imperative to note preoperatively to prevent accidental injury to the bladder in these situations (Fig. 16.14).

Another unique imaging finding in the setting of suprapubic hernias after Pfannenstiel incisions is the presence of partial thickness hernias. This

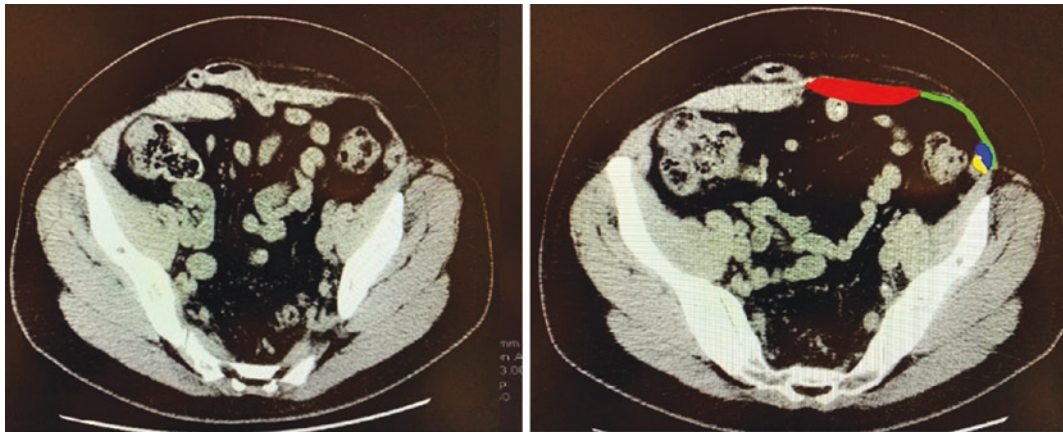

Fig. 16.12 Suprapubic hernia after previous Pfannenstiel incision. The left rectus muscle approaches midline and the defect is slightly lateral of midline. Concomitant partial thickness hernia with associated suprapubic hernia. The patient has an intact external oblique (green) but the internal oblique and transversus abdominis are no longer intact (blue and yellow, respectively)

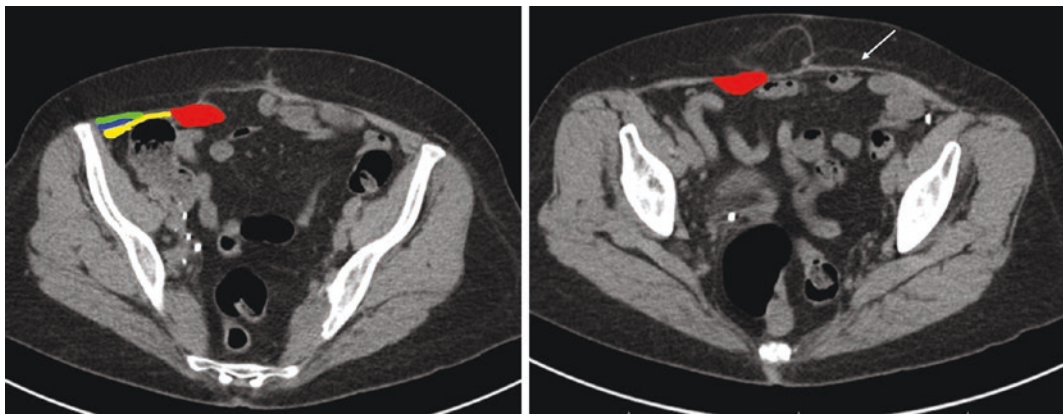

Fig. 16.13 Difference in the rectus muscles can be a common finding after Pfannenstiel incisions. Additionally, a lateral weakness or absence of a rectus muscle will not be seen as suprapubic hernia results after a midline incision

Fig. 16.14 Loss of normal anatomic fat planes. The white arrow demonstrates the loss of a normal anatomic fat plane between the anterior abdominal wall and the bladder from a previous incision. This can indicate dense scaring in this area

Fig. 16.15 Partial thickness hernia. While the anterior fascia is intact (white arrow), the sigmoid colon (asterisk) can be seen herniated through the rectus muscles

occurs when the anterior fascia is intact but there is a defect in the transversalis fascia allowing bowel or other pelvic content to herniate above the rectus muscle while remaining below intact external oblique fascia. Such hernias can be difficult to diagnose based on physical exam since a bulge may not be visible and a likely absence of a palpable fascial defect as the superior fascia is intact. However, these can be easily identified on cross-sectional imaging (Fig. 16.15). Here, there is continuity of the anterior fascia across the entirety of the lower abdomen; however, there is a separation of the rectus muscles deep to that and the sigmoid colon is seen herniating through this defect.

Imaging in Suprapubic Hernias in the Setting of Orthopedic Implants

The presence of adjacent orthopedic implants in the setting of suprapubic hernias can result in a very challenging hernia repair. Most of the time, orthopedic implants in the pelvic area involve hip prosthesis or spinal prosthesis which are not relevant to the repair. However, patients that have orthopedic implants of the anterior pelvis such as reconstruction of the pubic symphysis will have implants that will be in the surgical field and must be managed during the repair. Using imaging to evaluate critical pelvic structures in relation to these implants is key to ensure an appropriate repair with adequate overlap, mitigate risks of complications and prevent injury to the implant.

The first step when evaluating imaging in these situations is to understand what orthopedic prosthetic is in place and its components. These often can be easily identified on the scout films. Identifying the presence of plates and or screws and their locations on imaging is important as they can serve for anatomical landmarks in the OR. As these are fixed structures, understanding their anatomic relationships with other important structures can allow for easy identification of these critical structures intraoperatively (Fig. 16.16).

After the prosthetic components have been identified and their relationships to or involvement with critical structures has been determined, the next step in evaluating imaging is to understand the hernia characteristics and their relationship to the prosthetic. It is important to not only determine defect size but also proximity to the prosthetic, which will help determine whether appropriate overlap is possible, contents within

the hernia as well as the anatomy of the abdominal wall musculature in that area. Examining not only the axial views but as well as the sagittal and coronal images can allow the surgeon to create a 3D mental model of the location of the prosthetic in various dimensions. Sagittal and coronal views are helpful in examining vertical distance relationships from the prosthetic that may not be as apparent on the axial cross-sectional imaging (Figs. 16.17, 16.18, and 16.19).

Fig. 16.16 Understanding anatomic relationships. Here, the iliac vessels (red) are located lateral to the superior aspect of the pubic symphysis plate. In the operating room, any dissection medial and inferior to this can be done safely without concern for major vascular injury

Orthopedic hardware in the region of the pelvis presents a challenge when evaluating suprapubic hernias as oftentimes the presence of these implants results in a significant amount of artifact on imaging that can obscure relevant anatomy. These artifacts occur due to metal in the image plane as well as metal found in adjacent planes. In these situations, MRI can be utilized to minimize the amount of artifacts present in the image. A specific sequence called a metal artifact reduction sequence (MARS) can be utilized to reduce the intensity of the artifacts in the image. This sequence utilizes a lower magnetic field strength, spin echo as well as short T1 inversion recovery for fat suppression, thinner image slices as well as overall increased pixels. If there are significant artifacts present that limit the ability to interpret the suprapubic anatomy, we recommend utilizing MRI in these situations for the reasons listed above to allow for thorough image evaluation and operative planning.

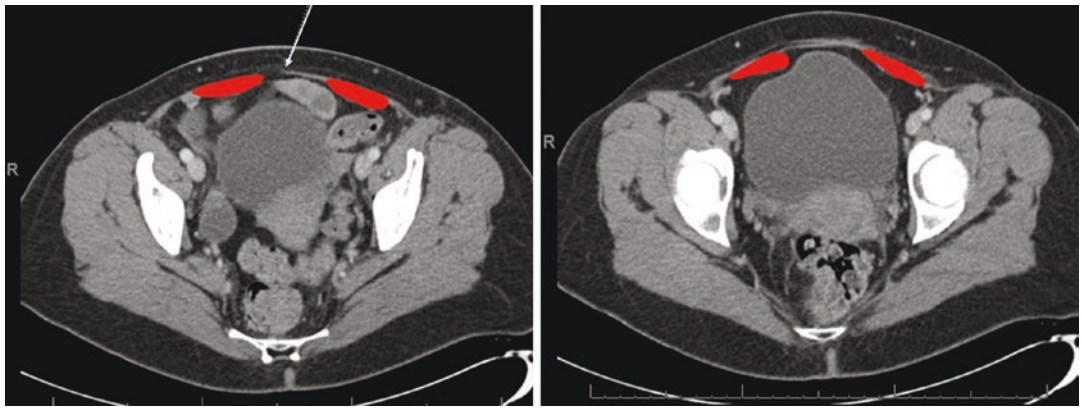

Fig. 16.17 Understanding anatomic relationships. A small defect is noted just inferior to the iliac crests (White arrow). Caudally to this, there is a partial thickness defect with intact anterior fascia with the anterior portion of the bladder above the rectus muscles. This is noted to be at the level of the femoral heads, and it is important to note the absence of any prosthetic implants in this area. Additionally, there is a clear flat plane anterior to the bladder indicating that there is a relative absence of scar tissue in this area and the bladder should be easily reduced from this defect

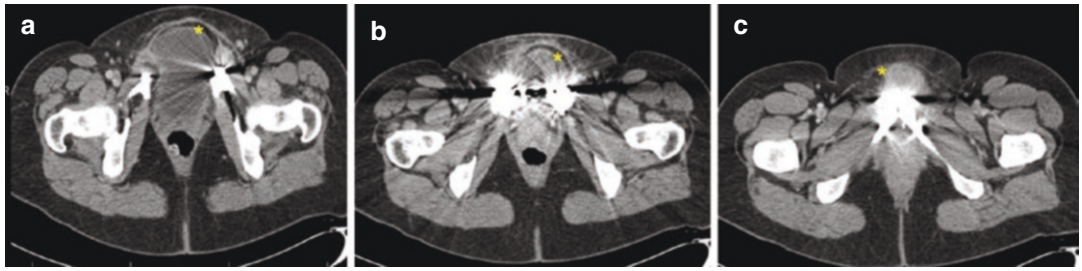

Fig. 16.18 These images demonstrate the bladder (yellow asterisk) herniating through the defect (**a**) but also is below the hardware (**b** and **c**). From these images, we can ascertain that appropriate inferior mesh overlap will be challenging due to its proximity to the hardware

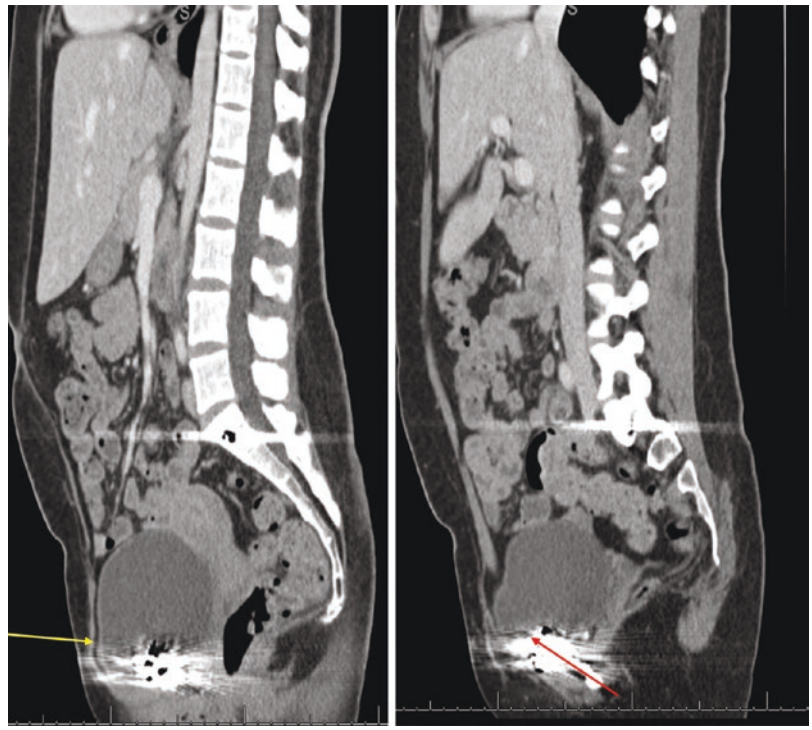

Fig. 16.19 The sagittal view helps to better characterize the distance of the defect to the implant as well as the amount of bladder herniating through the defect. Additionally, the anterior aspect of this bladder herniating through the defect demonstrates preserved fat planes, but we can see that posteriorly, just above the hardware, these fat planes are no longer present and may indicate that the bladder is densely adherent to this hardware

Suprapubic and Inguinal Hernias

Determining the difference between a suprapubic hernia or an inguinal hernia on exam, especially when large, is challenging since both hernias start superior to the pubis and can extended into the scrotum in males or below the pubis in females. However, when evaluating the cross-sectional imaging, several key imaging findings can be identified to delineate the difference between these two defects.

First, in patients with inguinal hernias, even if they are bilateral, the midline linea alba will be intact on imaging (Fig. 16.20). With the linea alba intact, it will be clear that the defects originate lateral to this. This can be seen on imaging by examining the relationship between the defect and the rectus muscles (Fig. 16.21 and 16.22).

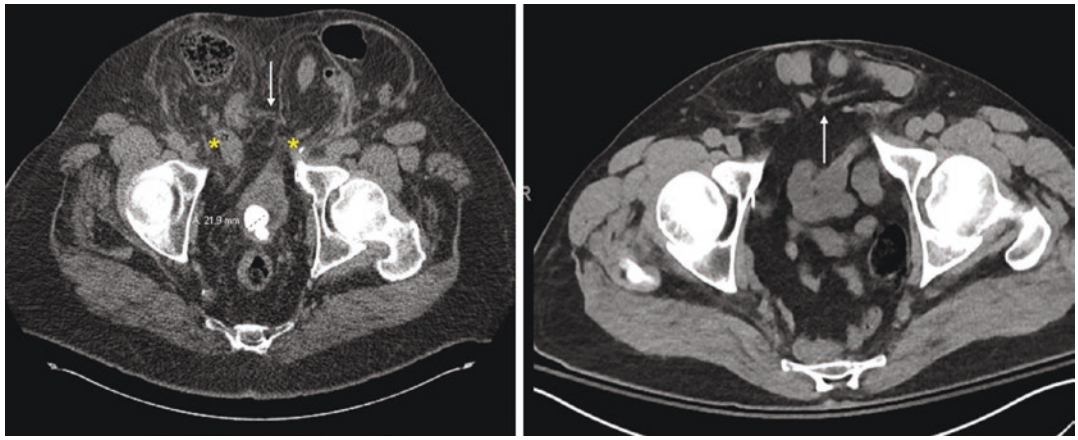

Fig. 16.20 Left panel: Bilateral inguinal hernias. Here the linea alba is intact (white arrow) and two discrete defects are seen lateral to this (yellow asterisks). Right panel: Suprapubic hernia. The linea alba is not intact and the bowel contents are seen herniating through this (white arrow)

Fig. 16.21 An inguinal hernia can be distinguished by its origin lateral to the rectus muscles (red)

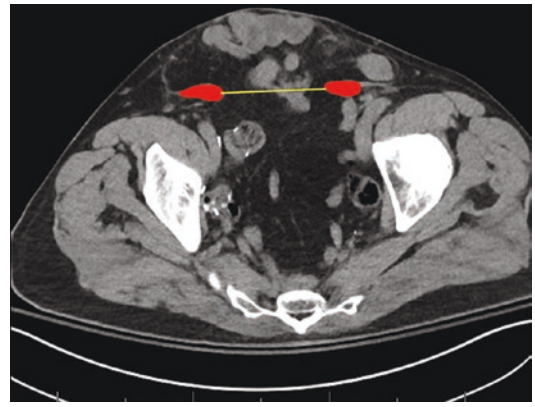

Fig. 16.22 Suprapubic hernias are located medial to the rectus muscles (red)

Inguinal hernias defects can be found lateral to the rectus muscles whereas suprapubic hernias will be located medially to the rectus muscles. In imaging done with contrast, another important anatomic landmark that may be helpful in characterizing the defect is the inferior epigastric vessels. Indirect inguinal hernias will be found lateral to these defects and suprapubic hernias will be found medially.

While the location of the rectus muscle can frequently be used as a key distinguishing feature to delineate the difference between a suprapubic and an inguinal hernia, this relationship does not hold true if the hernia is an incisional hernia from an off-midline incision in the lower abdomen. The relationship between these defects and the rectus muscle depends on where the incision is, in relation to the rectus muscle. These can be commonly mistaken for inguinal hernias in this situation when they are truly suprapubic incisional hernias.

Suprapubic Hernias as a Result of Other Defects

While lower midline incisions and Pfannenstiel incisions may be the most frequent cause of a suprapubic hernia, cystectomies for bladder can-

cer as well as tissue-based breast reconstruction in the form of transversus rectus abdominis (TRAM) flaps or a deep inferior epigastric perforator (DIEP) flap can result in suprapubic hernias. Imaging in each of these findings is unique and challenging due to the altered abdominal wall anatomy.

Tissue-based breast reconstruction requires the relocation of various components of the abdominal wall to provide a natural cosmetic breast reconstruction [5, 6]. However, with the removal of these components of the abdominal wall, resultant hernias are not uncommon. In the TRAM flap, the skin and rectus muscle are used to recreate the breast. If a suprapubic hernia occurs in the setting of a previous TRAM flap, one key imaging finding is the surgical absence of the inferior rectus muscle (Fig. 16.23).

Cystectomies are commonly performed for advanced bladder cancer, and while there has been a significant trend to minimally invasive procedures, suprapubic hernias after these surgeries may still occur [7, 8]. As the bladder is no longer present, bowel is often seen herniating through these defects. Also, as the peritoneum and transversalis fascia are removed in these situations to achieve an adequate oncologic margin, this can result in concomitant inguinal hernias and the imaging should be reviewed to confirm the presence or absence of this. The surgical removal of the tissue planes posterior to the rectus muscle commonly results in dense scarring between the rectus muscle and the herniated contents which can often be appreciated radiographically (Fig. 16.24).

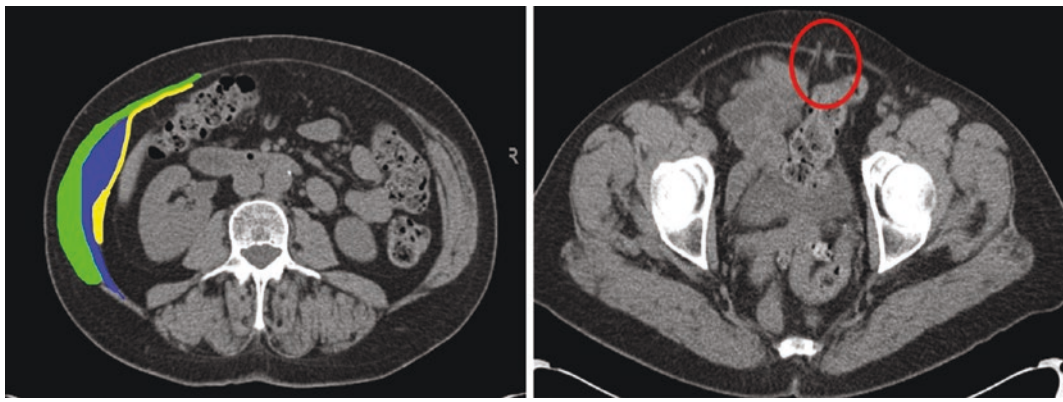

Fig. 16.23 Suprapubic hernia after bilateral TRAM flaps. The patient has bilateral absence of her rectus muscles but her lateral abdominal wall musculature remains intact. (External oblique, green, internal oblique, blue, transversus abdominis yellow). Inferiorly, there is a small amount of fat herniating through a true fascial defect (circled in red)

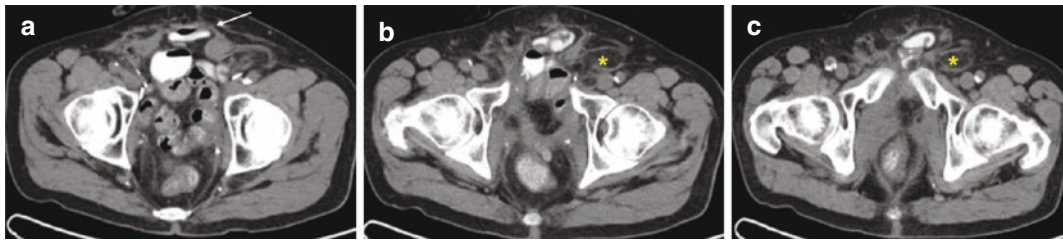

Fig. 16.24 Suprapubic hernia after cystectomy. There are multiple loops of small bowel herniated through the defect. These are noted to be densely adherent to the abdominal wall (Panel **a**). Additionally, this patient has a left inguinal hernia (yellow asterisk, panel **b** and **c**)

Suprapubic Hernias in the Setting of Pelvic Prosthetics

While suprapubic hernias are complex due to their anatomical location and relatively low incidence, another factor that makes these hernias uniquely complex is the involvement of permanent pelvic implants such as suprapubic catheters, reservoirs for penile prosthesis, or other pelvic implants. Imaging in these situations is essential to understand the relationship of the hernia defect to these implants. For those implants that cross from an extraperitoneal to a preperitoneal position, utilizing cross-sectional imaging allows the surgeon to understand the paths these take to minimize the risk of potential injury to these implants (Fig. 16.25). Additionally, imaging can be utilized to plan for appropriate overlap and determine the need for potential repositioning of these devices to ensure a durable repair and maintain prosthetic function. Again, reviewing the axial, coronal, and sagittal views allows one to fully visualize all the anatomic relationships between these implants to the hernia defect.

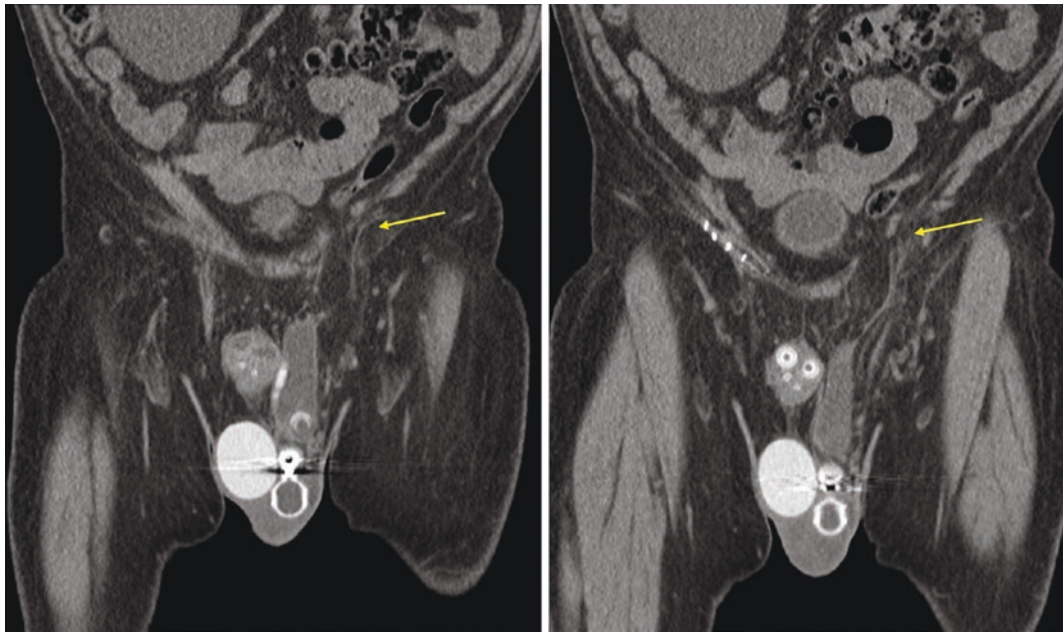

Fig. 16.25 Suprapubic hernia after penile prosthetic implant. The patient has herniated the reservoir as well as some preperitoneal fat through the defect (yellow arrow). Although this appears to be a direct inguinal defect, the defect is a result of the incision made to implant the prosthetic

Conclusion

Suprapubic hernias are challenging hernias to repair due to their atypical location, limits of overlap due to the bony pelvis as well as implants in these areas that must be considered when they are repaired. Cross-sectional imaging is a key part of the operative planning for these hernias as imaging in these situations provides a fund of knowledge about important anatomic relationships, concomitant defects, potential intraoperative challenges, and limitations to appropriate overlap.

References

1. Muysoms FE, Miserez M, Berrevoet F, Campanelli G, Champault GG, Chelala E, Dietz UA, Eker HH, El Nakadi I, Hauters P, Hidalgo Pascual M, Hoeferlin A, Klinge U, Montgomery A, Simmermacher RK, Simons MP, Smietański M, Sommeling C, Tollens T, Vierendeels T, Kingsnorth A. Classification of primary and incisional abdominal wall hernias. Hernia. 2009;13(4):407–14.
2. Lovering RM, Anderson LD. Architecture and fiber type of the pyramidalis muscle. Anat Sci Int. 2008;83(4):294–7. https://doi.org/10.1111/j.1447-073X.2007.00226.x.
3. deSouza A, Domajnko B, Park J, et al. Incisional hernia, midline versus low transverse incision: what is the ideal incision for specimen extraction and hand-assisted laparoscopy? Surg Endosc. 2011;25:1031–6.
4. Luijendijk RW, Jeekel J, Storm RK, Schutte PJ, Hop WC, Drogendijk AC, Huikeshoven FJ. The low transverse Pfannenstiel incision and the prevalence of incisional hernia and nerve entrapment. Ann Surg. 1997;225(4):365–9.
5. Shestak KC. Breast reconstruction with a pedicled TRAM flap. Clin Plast Surg. 1998;25(2):167–82.
6. Hauck S, Horch RE, Schmitz M, Arkudas A. Secondary breast reconstruction after mastectomy using the DIEP flap. Surg Oncol. 2018;27(3):513.
7. Chang SS, Bochner BH, Chou R, Dreicer R, Kamat AM, Lerner SP, Lotan Y, Meeks JJ, Michalski JM, Morgan TM, Quale DZ, Rosenberg JE, Zietman AL, Holzbeierlein JM. Treatment of non-metastatic muscle-invasive bladder cancer: AUA/ASCO/ASTRO/SUO guideline. J Urol. 2017;198(3):552–9.
8. Pignot G, Treacy P, Walz J. Growing evidence for benefits of minimally invasive radical cystectomy. Transl Androl Urol. 2020;9(6):2459–61.

Flank Hernia

17

Jordan A. Bilezikian, Justin D. Faulkner, Michael J. Bilezikian, Frederic E. Eckhauser, and William W. Hope

Abbreviations

AHSQC	American Hernia Society Quality Collaborative
CT	Computed tomography
DASH	Dynamic abdominal sonography for hernia
LAFS	Lumbar and flank sonography
MINORS index	Methodological index for non-randomized studies
MRI	Magnetic resonance imagery

Introduction

Flank hernias are rare clinical entities and account for only 1.5–2% of all abdominal wall defects [1]. They are often mentioned in conjunction with lumbar hernias, and the terminology in the literature is often considered interchangeable despite the European Hernia Classification providing anatomical distinction [2]. It is important to distinguish them from eventration, which is a separate clinical entity that can mimic a true hernia postoperatively and develops due to nerve damage and subsequent abdominal wall muscle laxity [3] (Figs. 17.1 and 17.2). Lumbar hernias occur in the area between the 12th rib and the iliac crest and are due to a defect in the posterior abdominal wall fascia. Flank hernias are most common in the fifth decade of life and are more

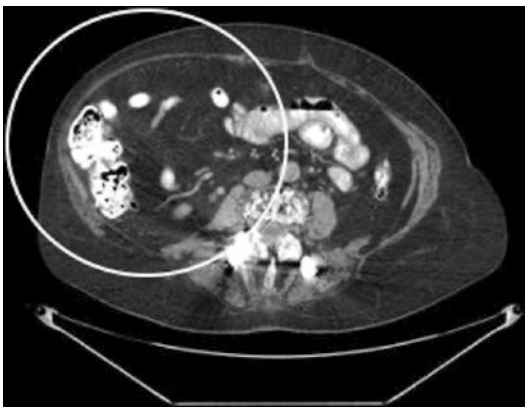

Fig. 17.1 Computed tomography scan showing eventration of the right lateral abdominal wall. The musculature on the right side has thinned out compared with the left side, which is the definition of eventration and causes bulging of the right flank on physical exam
©Photo produced by William W. Hope, MD, 2019

Supplementary Information The online version contains supplementary material available at https://doi.org/10.1007/978-3-031-21336-6_17.

J. A. Bilezikian · J. D. Faulkner · M. J. Bilezikian · F. E. Eckhauser · W. W. Hope (✉)
Department of Surgery, New Hanover Regional Medical Center, Wilmington, NC, USA
e-mail: Justin.Faulkner@nhrmc.org; Frederic.Eckhauser@nhrmc.org; William.Hope@nhrmc.org

S. Docimo Jr. et al. (eds.), *Fundamentals of Hernia Radiology*, https://doi.org/10.1007/978-3-031-21336-6_17

prevalent in males. Some authors claim that primary hernias are more common on the left side, although there is no good evidence to substantiate this claim [4, 5]. The majority of flank hernias are diagnosed due to previous surgery or trauma [6]. Understanding how these patients present and how to appropriately evaluate suspected flank hernias is important in clinical practice.

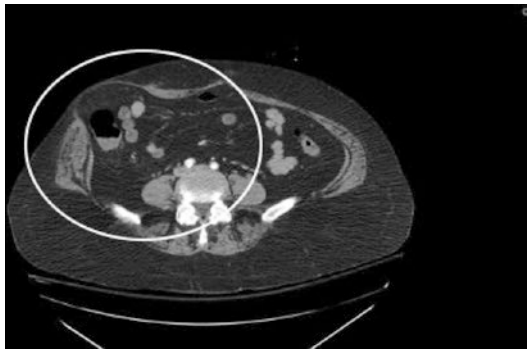

Fig. 17.2 Computed tomography scan showing eventration of the right flank. Although there is some muscle adjacent to this eventration, the fascial layer remains intact
©Photo produced by William W. Hope, MD, 2019

The two primary categories of flank hernias are congenital and acquired. Acquired flank hernias are a more common etiology and can be divided into primary and secondary categories based on etiology. Congenital flank hernias occur spontaneously, whereas secondary acquired flank hernias occur following trauma, surgery, or infection. Flank hernias occurring after surgical intervention do not correspond to typical anatomical landmarks.

There are three anatomically distinct types of flank hernias. They are classified based on the location of the hernia neck: superior flank hernia, inferior flank hernia, and diffuse type hernias.

A superior flank hernia occurs through the superior lumbar triangle, also referred to as the triangle of Grynfeltt-Lesshaft. The superior border of a superior flank hernia is the 12th rib, with the roof of the hernia consisting of the external oblique and latissimus dorsi muscles. The inferior aspect or the floor of the hernia consists of the transversalis fascia and the aponeurosis of the transversus abdominis muscle. The medial border is the quadratus lumborum muscle and the lateral border is the internal oblique muscle (Fig. 17.3).

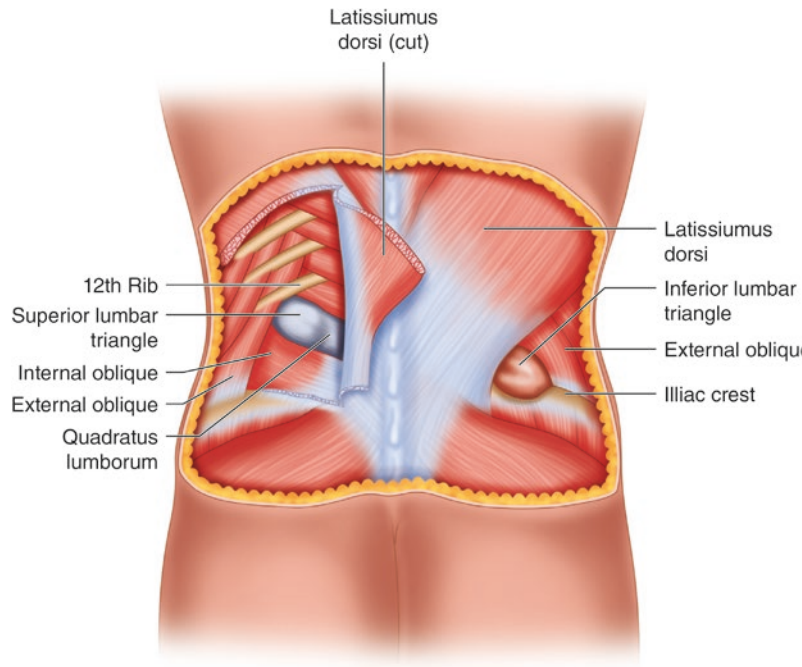

Fig. 17.3 Schematic drawing of a posterior view of lower back anatomy and relevant structures around the superior and inferior lumbar triangles

An inferior flank hernia occurs at the inferior lumbar triangle and is also referred to as Petit's triangle. The anterior border of this hernia space is the external oblique muscle, and the posterior border is the latissimus dorsi muscle. The floor consists of the internal oblique muscle, and the inferior border is the iliac crest (Fig. 17.3).

Diffuse lumbar hernias are not limited by the anatomical structures that define the superior and inferior types. They can be quite large and usually occur after a surgical procedure or traumatic event (Figs. 17.4 and 17.5) [7]. (Video 17.1)

Diagnosing flank hernias can be difficult due to their rarity in clinical practice. The remainder of this chapter explains the clinical presentation and diagnostic tools that are helpful in improving the understanding of flank hernias, patient selection, and the utility of available imaging modalities.

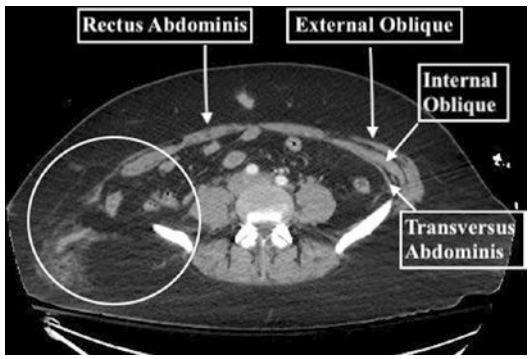

Fig. 17.4 Computed tomography scan of a traumatic flank hernia from a motor vehicle crash. The muscles of the right lateral abdomen have been traumatically avulsed from the attachments to the anterior superior iliac spine
©Photo produced by William W. Hope, MD, 2019

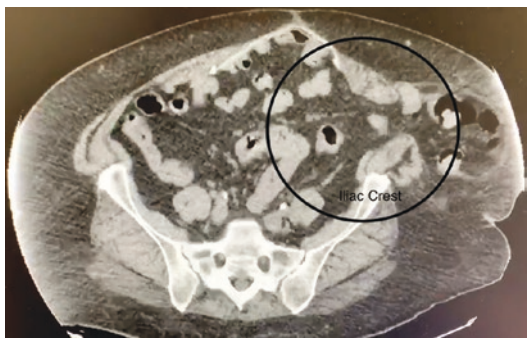

Fig. 17.5 Computed tomography scan demonstrating a true left flank hernia with a bowel protruding through the fascial defect
©Photo produced by William W. Hope, MD, 2019

Patient Selection

Flank hernias can be difficult to diagnose due to their nonspecific clinical signs and symptoms. When patients present with symptoms of flank pain or a suspicious bulge on clinical exam, they may be candidates for further diagnostic imaging. The differential diagnosis of a flank mass should include traumatic or postsurgical hematoma, abscess, lipoma, or another type of soft tissue tumor [4]. Rarely, patients present with signs and symptoms consistent with bowel obstruction. In this instance, imaging may demonstrate an incarcerated or strangulated flank hernia. Another common way that these hernias are diagnosed is incidentally through routine imaging after trauma. Finding an incidental flank hernia may guide a surgeon to the correct diagnosis before it becomes symptomatic.

The most common presenting sign consistent with a flank hernia is a bulge in the flank region [8]. Eighty percent of flank hernias are acquired and most commonly seen following surgical intervention in that region [6]. Postsurgical flank hernias are most often seen after trauma, iliac bone harvest, and retroperitoneal surgery for aortic disease, urologic/kidney pathology, or surgery for spine exposure [9]. Therefore, obtaining a good clinical history is an important step in diagnosing a suspected flank hernia. Patients typically describe low back pain lateralized to the affected side and/or abdominal pain. Symptoms can worsen, and patients may describe changes in the affected area with alterations in position, coughing, or straining. In rare cases, these hernias may become incarcerated or strangulated, and patients may describe skin changes, worsening pain, constipation, and/or other changes in bowel habits.

On physical exam, patients typically display a bulge in the flank region, which disappears when they assume a supine or decubitus position. Most flank hernias are reducible, but up to 24% of patients present with incarceration and 5% with

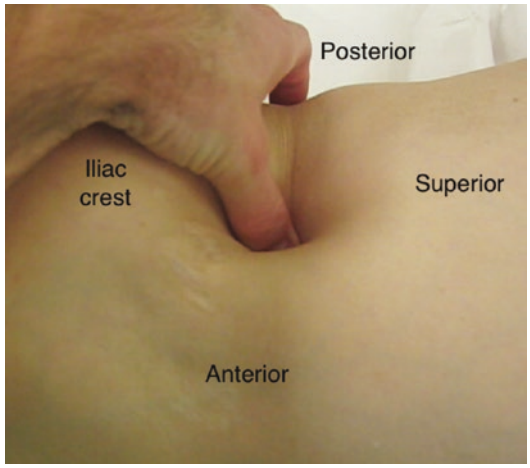

Fig. 17.6 Traumatic flank hernia located superior to the anterior superior iliac crest
©Photo by William W. Hope, MD, 2019

strangulation [10–12]. The patient in Fig. 17.6 is lying in a lateral decubitus position, and the hernia can be palpated just superior to the iliac crest. Although these hernias vary in size, acquired flank hernias typically occur just superior to the iliac crest, as depicted in the CT (Fig. 17.5). On exam, patients may have a surgical scar in the affected area and exhibit tenderness to palpation at the site. Unless the hernia is incarcerated, it should be reducible with gentle manipulation.

Clinical suspicion in a community setting is generally low when a patient presents with complaints of lower back pain and a bulge. This is due to the infrequency of the diagnosis in community practice. Flank hernias can be confused with an abscess, lipoma, tumor, or hematoma following trauma [13]. Understanding the associated symptoms and the anatomical location of flank hernias allows for more prompt diagnosis and timely referrals. If there is clinical suspicion for a flank hernia after a history and physical exam has been performed, then further imaging studies are indicated.

Ultrasound Scanning

Although computed tomography scanning is the most widely used imaging modality for flank hernias, ultrasonography may be used in certain cases. Ultrasound is a rapid, noninvasive, and inexpensive technique for detecting abdominal wall hernias [14–18]. In 2013, Beck et al. first published a standardized method called dynamic abdominal sonography for hernia (DASH). The sensitivity in this study was 98%, and the specificity was 88% for detecting abdominal wall hernias [18]. Although this method is designed for detecting hernias of the anterior abdominal wall, a similar method can be used in the flank and lumbar regions.

The patient should be placed in the lateral decubitus position with the side of concern facing up toward the examiner. The patient's head, neck, and shoulders should be placed in a comfortable position. The flank should be exposed, and an adequate amount of gel should be placed over the region of concern. A 12-MHz linear ultrasound probe should be positioned perpendicular to the patient's skin (Fig. 17.7). If there is an obvious bulge, the probe should be placed directly over it to look for a fascial defect with signs of herniated intra-abdominal contents. If there is not a bulge or if nothing is found during this initial examination, then a systematic scanning of the region should be done.

A modification of the originally described DASH method is called LAFS (lumbar and flank sonography). The linear ultrasound probe should be placed at the superior-medial portion of the

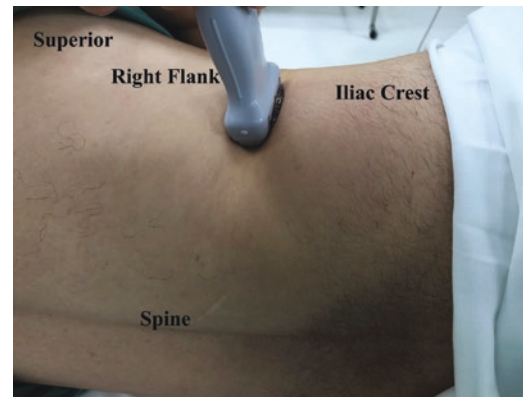

Fig. 17.7 The patient is placed in the left lateral decubitus position. Ultrasound probe placed on the flank to evaluate for hernia
©Photo by Jordan A. Bilezikian, MD, Justin D. Faulkner, MD, 2020

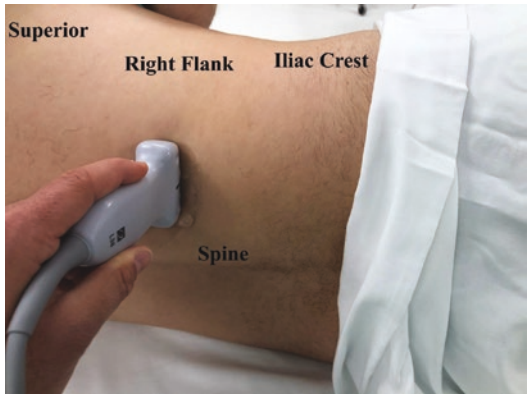

Fig. 17.8 The patient is placed in the left lateral decubitus position. The linear ultrasound probe being placed at the superior-medial portion of the superior lumbar triangle, just inferior to the 12th rib and just lateral to the spine to evaluate for a lumbar hernia. This is where the probe starts when employing the LAFS method
©Photo by Jordan A. Bilezikian, MD, Justin D. Faulkner, MD, 2020

superior lumbar triangle, just inferior to the 12th rib and just lateral to the spine (Fig. 17.8). The probe should be moved caudally to the iliac crest and then repositioned and moved adjacent and lateral to the location where the exam first began. The probe should be moved continually in a cephalad to caudal direction. Sonography is performed from cephalad to caudal in a series of adjacent lines until the mid-axillary line is reached. This systematic method should cover both the superior and inferior lumbar triangles in the examination.

Magnetic Resonance Imaging

There have been no studies that focus on the use of MRI specifically to diagnose or evaluate lumbar hernias [19]. However, it may be useful when radiation is contraindicated and when other diagnostic modalities have failed to delineate an adequate diagnosis. The disadvantages to this modality are that it is time-consuming and expensive and surgeons are usually less well-versed in reading these images as compared to computed tomography scanning.

Computed Tomography Scanning

Computerized tomography scanning is the gold standard for diagnosing flank and lumbar hernias [14]. This is likely due to the widespread availability of equipment, the speed of the exam, and the ubiquitous nature of CT scanning of the abdomen and pelvis for a variety of complaints. When CT scanning was gaining use as a novel imaging modality in the 1980s, it was shown in several case reports [8, 20] and several small case series [21–23] to be adequate for flank and lumbar hernia diagnosis. As CT scanning equipment became more efficient, it was increasingly used in clinical practice. The imaging modality is so common in modern medicine that patients routinely receive multiple CT scans for clinical scenarios such as traumatic events and abdominal pain. Often, CT scan findings suggest a hernia as the diagnosis explaining the patient's chief complaint. However, abdominal wall hernias are frequently also diagnosed as "incidental" findings.

Knowledge of abdominal wall anatomy along with a high-quality imaging study can allow surgeons to differentiate a true flank or lumbar hernia from eventration. When there is a fascial disruption with protrusion of intra-abdominal contents, this represents a true hernia. However, when there is a bulge that includes all layers of the abdominal wall at a given point, this is eventration. On the patient's left lateral side of Fig. 17.4, there is a good demonstration of the separate abdominal wall layers as they course along the flank. From superficial to deep, they are the external oblique fascia, internal oblique fascia, and transversalis fascia. The rectus abdominis muscles overly the anterior abdominal wall. As demonstrated in the patient's right lateral side in Fig. 17.4, there is traumatic disruption of these abdominal muscle layers with protrusion of intra-abdominal contents. This is a true hernia and is in stark contrast to the intact fascia present in an eventration, as depicted in Figs. 17.1 and 17.2. (Video 17.2)

Clinical Pearls

- Understanding the abdominal wall anatomy is critical in evaluating imaging for flank hernias. Surgeons should familiarize themselves with the muscle, fascia, and bony portions of the abdominal wall as well as the neurovascular anatomy.
- For surgeons adept at performing ultrasound, a modification of the well-described DASH [16, 18] technique called the LAFS (lumbar and flank sonography) technique can be used to quickly diagnose patients with flank hernias. (Video 17.3)
- Surgeons should become comfortable/familiar with reading CT scans related to flank hernias.
- CT scanning is recommended when evaluating flank hernias to help delineate anatomy, identify a true hernia versus an eventration of tissue, and to help with operative planning.
- Often, flank hernias caused by trauma or previous incisions represent an eventration of tissue due to loss of contractility of musculature in the flank area. These eventrations can be very difficult to repair surgically and can often be monitored if the patient is not having symptoms.

Literature Review

Overall, there is little high-quality literature concerning flank hernias, including imaging and management [24]. Most of the literature consists of case reports [20] and small case series[21–23].

Baker et al. in 1987 published a small case series of seven patients with lumbar hernias using CT as the main imaging modality before CT gained widespread use [8]. Prior to this, there were only three case reports with similar findings. In 1989, Faro et al. published the first case series including seven patients who were diagnosed using CT with acute post-traumatic lumbar hernias [22]. Since that time, most of the diagnostic imaging papers have focused on small case series at individual institutions or rare types of lumbar and flank hernias.

A 2008 report by Armstrong et al. demonstrated the utility of CT and MRI in the diagnosis of lumbar hernia when there was clinical suspicion [4]. Several high-quality photos were included in their report of two patients who initially presented for evaluation with complaints of painful flank lipomas.

In 1989, Siffring et al. described the first lumbar hernia diagnosis using ultrasound [17]. Although CT is the gold standard for diagnosis and operative planning of flank hernia, ultrasonography may be used as an initial screening tool in cases when the clinical diagnosis is unclear or questioned. In this chapter, we discuss a standardized method for ultrasound diagnosis of flank and lumbar hernias that is based on the well-described method for diagnosing ventral hernias [18]. This method, LAFS (lumbar and flank sonography), is analogous to the previously described DASH method by Beck et al. in 2013 [16, 18].

Van Steensel et al. published the first systematic review of the literature regarding primary lumbar hernias in 2019. After a review of 670 initial articles, the authors reported on 14 of these which met inclusion criteria [7]. The average quality of the articles that met inclusion criteria was 4.7 on the MINORS (methodological index for non-randomized studies) index (range from 0 to 16). The authors reported that incarceration was observed in 30.8% of patients and that 2% of patients developed a hernia recurrence postoperatively [7]. However, the studies included in this review focused primarily on diagnosis and treatment rather than on imaging techniques.

The most recent publication concerning flank hernias was a retrospective review of eight lateral abdominal wall hernias published by Katkhouda et al. [25]. This study focused on appropriate surgical management and highlighted the difficulty of studying such a rare clinical entity. Future studies should focus on prospectively analyzing flank and lumbar hernias using a multiple institutional approach. Databases such as the Abdominal Core Health Quality Collaborative (ACHQC) can be used to analyze larger pools of data. The imaging modalities used for diagnosis should be included in these data.

Conclusion

Although CT is the most commonly used modality for evaluating flank hernias, consideration should be given to using bedside ultrasound as an initial screening tool in cases when the clinical diagnosis is unclear or questioned. It is a quick, relatively inexpensive, and noninvasive tool. The LAFS method can be used to swiftly and accurately assess for flank or lumbar hernias in order to avoid unnecessary exposure to radiation and more expensive costs associated with other imaging modalities. However, if suspicion of a flank hernia remains and the US is equivocal, a CT for further evaluation is recommended.

Acknowledgments Figure 17.1, produced by William W. Hope, MD, published with permission, Copyright New Hanover Regional Medical Center 2019

Figure 17.2, produced by William W. Hope, MD, published with permission, Copyright New Hanover Regional Medical Center 2019

Figure 17.3, modified from illustration by Justin D. Faulkner, MD, and published with permission, 2020. Adapted from Harmouch M. LeBlanc KA. (2019) Lumbar Hernia. In: LeBlanc K. (eds), Robotic Assisted Hernia Repair. Springer, Cham.

Figure 17.4, produced by William W. Hope, MD, published with permission, Copyright New Hanover Regional Medical Center 2019

Figure 17.5, produced by Jordan A. Bilezikian, MD, Justin D. Faulkner, MD, published with permission, Copyright New Hanover Regional Medical Center 2020

Figure 17.6, produced by Jordan A. Bilezikian, MD, Justin D. Faulkner, MD, published with permission, Copyright New Hanover Regional Medical Center 2020

Figure 17.7, produced by William W. Hope, MD, published with permission, Copyright New Hanover Regional Medical Center 2019

Figure 17.8, produced by William W. Hope, MD, published with permission, Copyright New Hanover Regional Medical Center 2019

References

1. Alcoforado C, Lira N, Kreimer F, et al. Grynfelt hernia. Arq Bras Cir Dig. 2013;26(3):241–3.
2. Muysoms FE, Miserez M, Berrevoet F, et al. Classification of primary and incisional abdominal wall hernias. Hernia. 2009;13(4):407–14.
3. Huntington CR, Augenstein VA. Laparoscopic Repair of Flank Hernias. In: Novitsky Y. (eds) Hernia Surgery. Springer, Cham; 2016.
4. Armstrong O, Hamel A, Grignon B, et al. Lumbar hernia: anatomical basis and clinical aspects. Surg Radiol Anat. 2008;30(7):533–7; discussion 609-510.
5. Loukas M, Tubbs RS, El-Sedfy A, et al. The clinical anatomy of the triangle of Petit. Hernia. 2007;11(5):441–4.
6. Stamatiou D, Skandalakis JE, Skandalakis LJ, Mirilas P. Lumbar hernia: surgical anatomy, embryology, and technique of repair. Am Surg. 2009;75(3):202–7.
7. van Steensel S, Bloemen A, van den Hil LCL, et al. Pitfalls and clinical recommendations for the primary lumbar hernia based on a systematic review of the literature. Hernia. 2019;23(1):107–17.
8. Baker ME, Weinerth JL, Andriani RT, et al. Lumbar hernia: diagnosis by CT. AJR Am J Roentgenol. 1987;148(3):565–7.
9. Orcutt TW. Hernia of the superior lumbar triangle. Ann Surg. 1971;173(2):294–7.
10. Moreno-Egea A, Baena EG, Calle MC, et al. Controversies in the current management of lumbar hernias. Arch Surg. 2007;142(1):82–8.
11. Zhou X, Nve JO, Chen G. Lumbar hernia: clinical analysis of 11 cases. Hernia. 2004;8(3):260–3.
12. Hope WW, Cobb WS, Adrales GL. Textbook of hernia. Switzerland: Springer International Publishing; 2017.
13. Sarela AI, Mavanur AA, Bhaskar A, et al. Post traumatic lumbar hernia. J Postgrad Med. 1996;42(3):78–80.
14. Campanelli G, Bruni PG, Morlacchi A, et al. Flank Hernia. In: Campanelli, G. (eds) The Art of Hernia Surgery. Springer, Cham; 2018.
15. Young J, Gilbert AI, Graham MF. The use of ultrasound in the diagnosis of abdominal wall hernias. Hernia. 2007;11(4):347–51.
16. Baucom RB, Beck WC, Phillips SE, et al. Comparative evaluation of dynamic abdominal sonography for hernia and computed tomography for characterization of incisional hernia. JAMA Surg. 2014;149(6):591–6.
17. Siffring PA, Forrest TS, Frick MP. Hernias of the inferior lumbar space: diagnosis with US. Radiology. 1989;170(1 Pt 1):190.
18. Beck WC, Holzman MD, Sharp KW, et al. Comparative effectiveness of dynamic abdominal sonography for hernia vs computed tomography in the diagnosis of incisional hernia. J Am Coll Surg. 2013;216(3):447–53; quiz 510-441.
19. Lillie GR, Deppert E. Inferior lumbar triangle hernia as a rarely reported cause of low back pain: a report of 4 cases. J Chiropr Med. 2010;9(2):73–6.
20. McCarthy MC, Lemmon GW. Traumatic lumbar hernia: a seat belt injury. J Trauma. 1996;40(1):121–2.
21. Patel PP, Warren JA, Mansour R, et al. A large single-center experience of open lateral abdominal wall hernia repairs. Am Surg. 2016;82(7):608–12.

22. Faro SH, Racette CD, Lally JF, et al. Traumatic lumbar hernia: CT diagnosis. AJR Am J Roentgenol. 1990;154(4):757–9.
23. Killeen KL, Girard S, DeMeo JH, et al. Using CT to diagnose traumatic lumbar hernia. AJR Am J Roentgenol. 2000;174(5):1413–5.
24. Zhou DJ, Carlson MA. Incidence, etiology, management, and outcomes of flank hernia: review of published data. Hernia. 2018;22(2):353–61.
25. Katkhouda N, Alicuben ET, Pham V, et al. Management of lateral abdominal hernias. Hernia. 2020;24(2):353–8.

Further Readings

Armstrong O, Hamel A, Grignon B, Doye JM, Hamel O, Robert R, Rogez JM. Lumbar hernia: anatomical basis and clinical aspects. Surg Radiol Anat. 2008;30:533–7.
Kathouda N, Alicuben ET, Pham V, Sandhu K, et al. Management of lateral abdominal hernias. Hernia. 2020;24(2):353–8.
Van Steensel S, Bloemen A, van den Hil LCL, van den Bos J, Kleinrensink GJ, Bouvy ND. Pitfalls and clinical recommendations for the primary lumbar hernia based on a systematic review of the literature. Hernia. 2019;23:107–17.

Parastomal Hernias

18

Alexander T. Liu and Eric M. Pauli

Introduction

Stoma creation is an important surgical technique in elective and emergent alimentary tract operations, with over 100,000 in the US patients receiving colostomy or ileostomy each year [1]. One of the most common complications of having a stoma is the development of a parastomal hernia (PH). These are often complex hernias involving various aspects of the abdominal wall musculature and fascial tissue and prove to be a significant challenge in clinical assessment and operative repair. Many factors are considered when assessing and examining PH, including size, location, bowel involvement, stoma function, concomitant hernias, mesentery, and obstruction. These factors are often difficult or impossible to assess with the physical exam alone thus evaluation with computed tomography (CT) scans is crucial for understanding, assessing, and approaching the management of PH. This chapter provides an overview of CT imaging considerations for understanding and evaluating stomas and PH.

A. T. Liu
Department of Surgery, Penn State Milton S. Hershey Medical Center, Hershey, PA, USA

E. M. Pauli (✉)
Division of Minimally Invasive and Bariatric Surgery, Department of Surgery, Penn State Health Milton S. Hershey Medical Center, Hershey, PA, USA
e-mail: epauli@pennstatehealth.psu.edu

Incidence

The incidence of PH can vary greatly depending on the type of stoma. Based on a 2003 review, the incidence of hernias in end and loop ileostomies are as high as 28.3 and 6.2%, respectively; in colostomies, the incidence are as high as 48.1 and 30.8%, respectively. [2] A recent review of literature reported that overall PH occurrence can be as high as 56–58% with colostomies and as high as 35% with ileostomies. [3, 4] According to one review, there are approximately 87,000–135,000 stoma creation cases annually in the United States and approximately 20,000–35,000 patients (30–50%) develop PH. [5]

Challenges

One of the challenges in treating PH is the limitation of the physical exam. The contents within a PH are difficult to predict with just the surgeon's eyes and hands. Because there should be bowel in the abdominal wall, and because the patient generally has an ostomy appliance on for clinic examination, it is challenging if not impossible to know the PH contents for certain without the assistance of imaging. CT imaging can provide valuable information and details that support the physical exam; it can show the extent of the defect, the musculature and tissues involved, and the contents of the hernia. Knowing the visual details of a PH allows the surgeon to then plan the most appropriate operative repair.

S. Docimo Jr. et al. (eds.), *Fundamentals of Hernia Radiology*,
https://doi.org/10.1007/978-3-031-21336-6_18

Fig. 18.1 Normal end ileostomy; ileum traverses the mid-body of the right rectus abdominis muscle in a straight line without redundancy or twist

Fig. 18.2 Left-sided colostomy sited through the semilunar line has resulted in a disassociation of the internal oblique (arrow) and external oblique (arrowheads) muscles from the left rectus abdominis

Anatomy

Understanding the abdominal wall anatomy when creating stomas can help avoid complications such as the development of hernias. The location of the stoma often depends on the type of ostomy being formed. In general, stoma siting involves penetrating through the rectus abdominis muscle above the arcuate line without being too lateral or medial within the body of the rectus (Fig 18.1). [6] While seemingly simple, certain factors can limit appropriate locations for stoma creation such as body habitus, scars, posture, ostomy accessibility, or anatomy, and lead to bad siting.

Bad siting can disrupt the abdominal wall musculature and fascial tissue leading to large and complex defects; for example, an ostomy formed laterally in the rectus sheath may disconnect the lateral musculature from the rectus at the semilunar line and/or injure the innervation to the rectus muscle itself (Fig. 18.2). Bad sitting can lead to poor quality of life for the patient as a result of difficulties with bag fit or the ease with which they can change their appliance. The goal of surgery is to treat the patient while avoiding complications, and the best way to do that is by understanding the anatomy prior to performing the operation. In the case of PH, the purpose of understanding anatomy is to effectively repair the defect and restore function and anatomy.

Normal Radiographical Findings

Recognizing normal findings of stomas on CT can help understand abnormal findings after the development of PH. Recognizing what was not there prior to hernia development and identifying additional defects that may have developed will help with appropriate operative planning. The development of PH is often accompanied by the development of concomitant midline hernias or other abdominal wall changes (such as rectus denervation). Understanding normal stoma anatomy will provide an outline for repair.

Ileostomy and Colostomy

Ileostomy and colostomy are some of the most commonly created stomas. Normal radiographical findings should reflect the same operative findings and steps necessary to create the stoma. The site of the stoma is generally trans-rectus on the right or left side and above the infraumbilical fat mound (Fig. 18.3). The bowel and mesentery should penetrate the anterior and posterior rectus sheath in a perpendicular fashion without strangulation or redundancy. Small openings can cause ischemia or obstruction, while large openings can progress into PH. The stoma tract should ideally be through the mid body of the rectus abdominis muscle, avoiding the semilunar line or linea alba. [6, 7] While there has been no clear evidence to suggest that trans-rectus stoma creation technique is more effective than the lateral rectus positioning in reducing the incidence of PH [8–10], the complexity of the defect and dif-

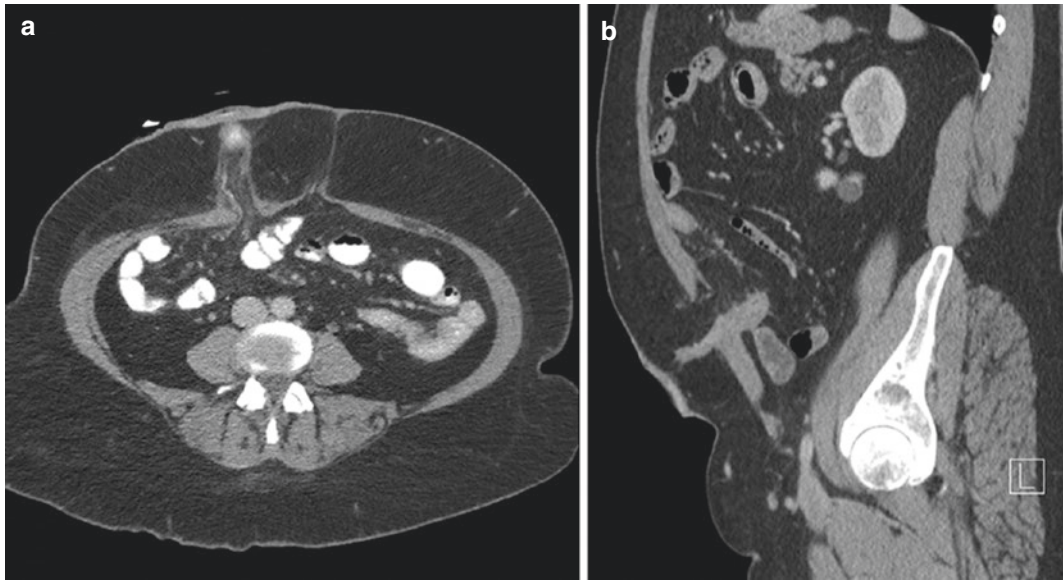

Fig. 18.3 (**a**) Normal end ileostomy (axial view). (**b**) Normal end colostomy (sagittal view)

ficulty of the repair from a laterally occurring PH can be more memorable for the surgeon because of the challenging location and abdominal wall components involved.

The colon generally has more bulk and may require wide mobilization before the stoma location is ultimately chosen; i.e., an end descending colostomy will sometimes require the mobilization of the left colon, splenic flexure, and transverse colon. On imaging, it is especially important to note the directionality of the mesentery in relation to the stoma site. A left-sided colostomy is limited by the mesentery on the same side and generally cannot cross midline should it need potential relocation. [6] The same principles apply to creating an enterostomy or ileostomy, which is often less bulky and easier to mobilize (with exception of patients with thick mesenteric fat or a foreshortened mesentery). An end ileostomy located on the contralateral side of its blood supply generally cannot be repaired without relocation in the event a PH develops.

One exception to the trans-rectus location of a colostomy is the transverse "blowhole" colostomy, generally formed in emergency situations in patients too unstable to tolerate a more prolonged operation. Such stomas are generally formed in the upper midline through the linea alba and therefore result in midline parastomal hernias (Fig. 18.4a, b).

Urostomy

Urinary diversion is performed in patients undergoing radical cystectomy for bladder cancer. The most common urinary diversion is the ileal conduit (Fig. 18.5). A 10–15 cm segment of ileum proximal to the ileocecal valve is isolated along with its mesentery for diversion. The remaining bowel is re-anastomosed to restore GI tract continuity. The right and left ureters are mobilized and anastomosed to the new ileal conduit. The distal end is then matured as the stoma, often in the right lower quadrant due to limitations on the length of the bowel mesentery. [11] Because the conduit is intentionally created from a short segment of bowel and is fixed (based on its mesentery and attachments to the ureters), relocating a urostomy to a new location is generally not feasible without significant effort.

Based on a systematic review, PH occurred in 17.1% of patients who underwent cystectomy and ileal conduit surgery and remains

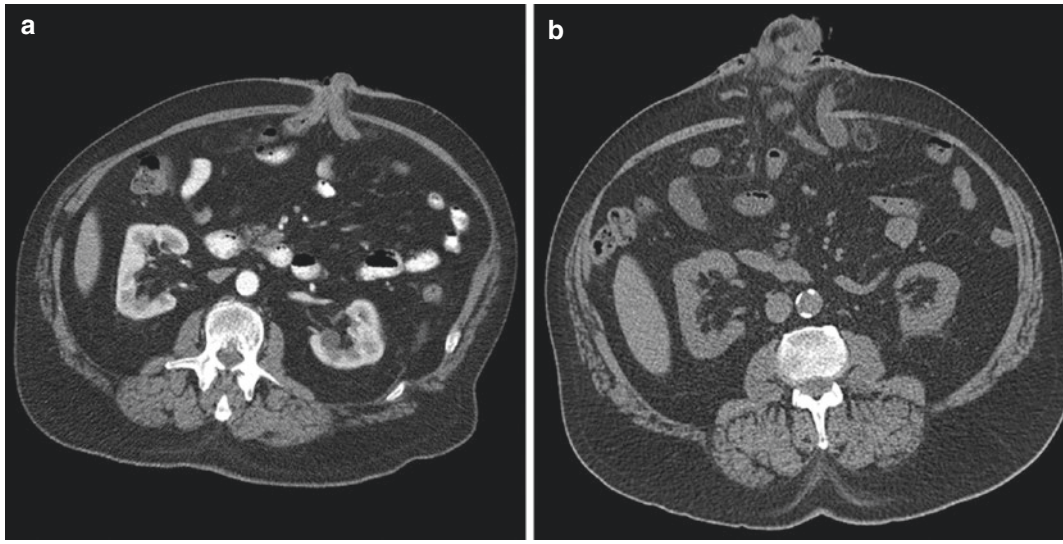

Fig. 18.4 (**a**) Transverse "blowhole" colostomy formed via the midline. (**b**) Midline parastomal hernia and colostomy prolapse

Fig. 18.5 Sagittal CT scan view of a normal urostomy (urinary conduit) through the right rectus abdominis. Intravenous contrast can be seen accumulating in the renal pelvis (arrow) and filling the urinary conduit (arrowheads) as it traverses from the pelvis to the skin

one of the most common complications of the operation. [12] Further studies found that female gender, high body mass index (BMI), and poor nutritional status were associated with the development of PH after radical cystectomy. [13] The relationship between the technical aspects of this operation and hernia development remains unclear, but it does not diminish an important surgical consideration in these patients, which is their postoperative anatomy.

In radical cystectomy for muscle-invasive bladder cancer, various aspects of the posterior rectus are resected along with the cystectomy specimen. [14] The exposed rectus muscle becomes a raw surface for adhesion development. The lack of posterior rectus sheath, transversalis fascia, peritoneum, and bladder also complicate any potential retromuscular hernia repair (as these elements of the abdominal wall have been resected surgically). Thus, development of PH around a urostomy becomes an underestimated complex issue to address in an already high-risk patient population.

Appendicostomy

A less common ostomy evaluated on imaging is the appendicostomy. These are typically created for patients with constipation issues requiring antegrade continence enemas (ACE) using the appendix as a conduit. They are often performed in the pediatric population, in patients with anorectal malformations, or in spina bifida patients requiring frequent enemas. The procedure involves mobilizing the appendix from the right lower quadrant and siting the stoma opening at the umbilicus or through the right rectus abdominis (Fig. 18.6a). On CT imaging, these are seen as a narrow channel linking the cecum to the skin. Hernias around appendectomies are uncommon but can occur (Fig. 18.6b).

Mesentery Considerations

A key consideration in approaching stoma anatomy, PH, and operative repair is understanding of location and orientation of the mesentery. This is crucial for both the stoma perfusion and initial siting. Knowing where the mesentery originates from and the limitations of where it can be mobilized to is a key part of deciding how a PH can/should be repaired.

The viability of a stoma is dependent on its perfusion via the mesentery. The location of the mesentery in relation to the stoma should be assessed with CT imaging. During stoma creation, both bowel and mesentery must be tension-free with a straight trajectory towards exit site. Any twist of the mesentery can jeopardize perfusion to the stoma. When looking at CT imaging, the surgeon should acknowledge whether the stoma is on the contralateral or ipsilateral side of the root of the mesentery, because this information will dictate the operative approach for repair. For example, a right-sided descending colostomy where the mesentery is crossing midline may not be a candidate for Sugarbaker repair due to tension on the bowel. The importance of having the CT scan is being able to correlate the findings back to the previous operative reports to understand the limitations of each surgical option and plan the optimal approach.

Classification of PH

There are two classifications that best describe the different types of PH seen on imaging. Both address some of the key radiographical findings when characterizing PH. These two classifications also best describe the hernias when discussing repair and are the most clinically applicable.

Rubin Classification

In 1993, Rubin described four types of PH based on anatomical findings that are radiographically correlated (Fig. 18.7). Type I is a true PH with a peritoneal sac traversing through enlarged stoma

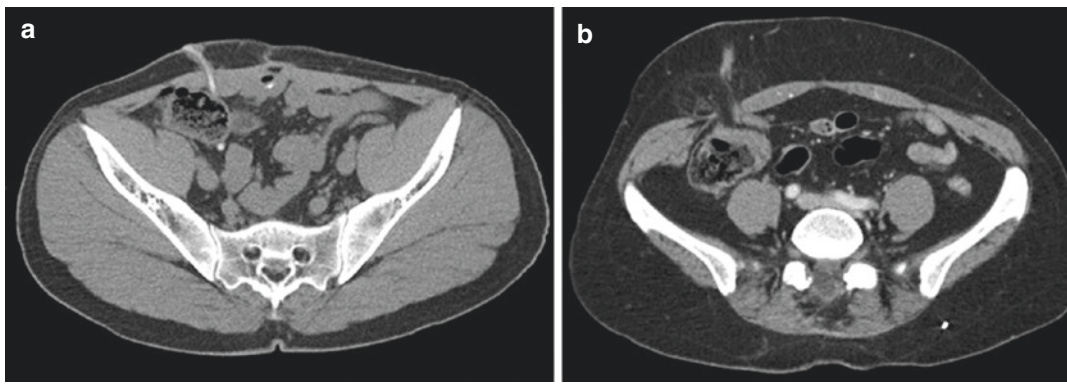

Fig. 18.6 (**a**) Normal appendicostomy formed through the right rectus abdominis. (**b**) Appendicostomy formed at the right linea semilunaris with a parastomal hernia containing inflamed omental fat

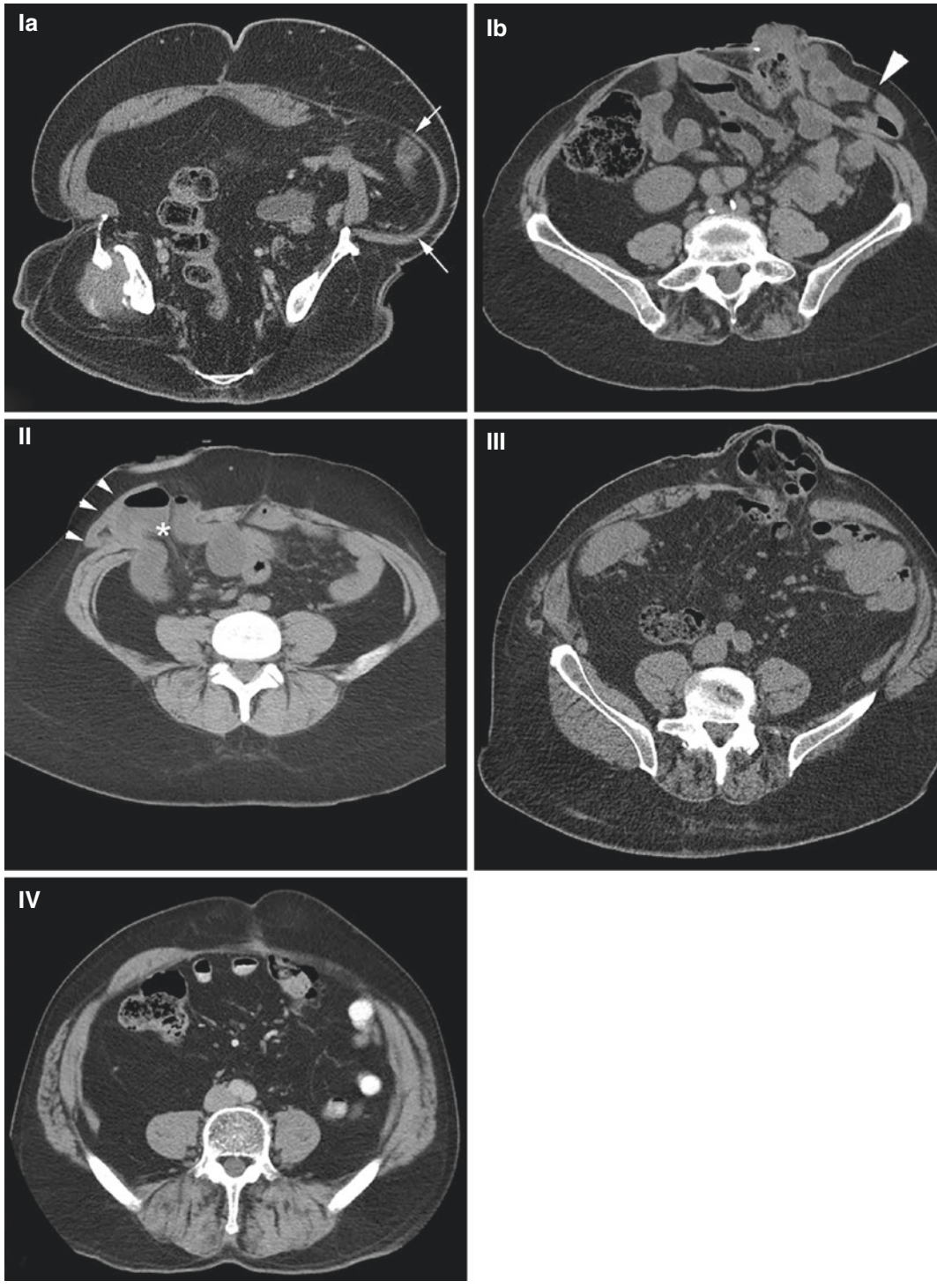

Fig. 18.7 Ruben classification of parastomal hernias; (**Ia**) Interstitial (intraparietal) hernia with bowel trapped between the internal and external (arrows) oblique muscles. (**Ib**) Subcutaneous hernia with small bowel (arrowhead) in the subcutaneous tissues. (**II**) Intrastomal hernia with dilated bowel (asterisk) within the wall of the ostomy loop (small arrowheads). (**III**) Subcutaneous prolapse of excess colon through an intact fascial ring forming a loop in the subcutaneous tissue. (**IV**) Pseudohernia (denervation of the left rectus) from an ostomy resulting in left-sided bulging with cough and Valsalva

tract. Type I is further subdivided into Type Ia: an interstitial hernia where the hernia sac lies within the layers of the abdominal muscle, and Type Ib: a subcutaneous hernia where the hernia sac lies in the subcutaneous tissue. Type II is an intrastomal hernia, where the hernia sac lies within the intestinal wall and in the everted intestine of a prolapsed stoma. Type III is a PH with a subcutaneous prolapse, where excess bowel forms a loop within the subcutaneous tissue with an intact fascial ring. Type IV is a pseudohernia such as ones associated with flank weakness or denervation typically located lateral to the rectus. [15, 16]

Gil and Szcepkowski Classification

In 2011, Gil and Szcepkowski published a classification based on structural criteria aimed to provide clinical applicability when describing PH. The classification is defined as follows: Type I is an isolated small PH that is less than 5 cm in diameter; Type II is a small PH less than 5 cm in diameter with a coexisting midline incisional hernia; Type III is an isolated large PH that is greater 5 cm in diameter; and Type IV is a large PH greater than 5 cm in diameter with a coexisting midline incisional hernia. [17] This classification scheme was later revised by Szepkowski into the European Hernia Society (EHS) classification of PH.

EHS Parastomal Classification

In 2014, members of the EHS board and subject matter experts released their classification scheme of parastomal hernias, defining four types (Fig. 18.8). [18]

Type I—small (<5 cm) parastomal hernia without concomitant incisional hernia

Type II—small (<5 cm) parastomal hernia with concomitant incisional hernia

Type III—large (>5 cm) parastomal hernia without concomitant incisional hernia

Type IV—large (>5 cm) parastomal hernia with concomitant incisional hernia

Their classification system also includes details about whether the hernia was recurrent after a previous PH repair or whether it was a primary PH. Although this classification system was developed to utilize intraoperative measurements, we have adopted it for preoperative purposes utilizing the CT scan imaging findings.

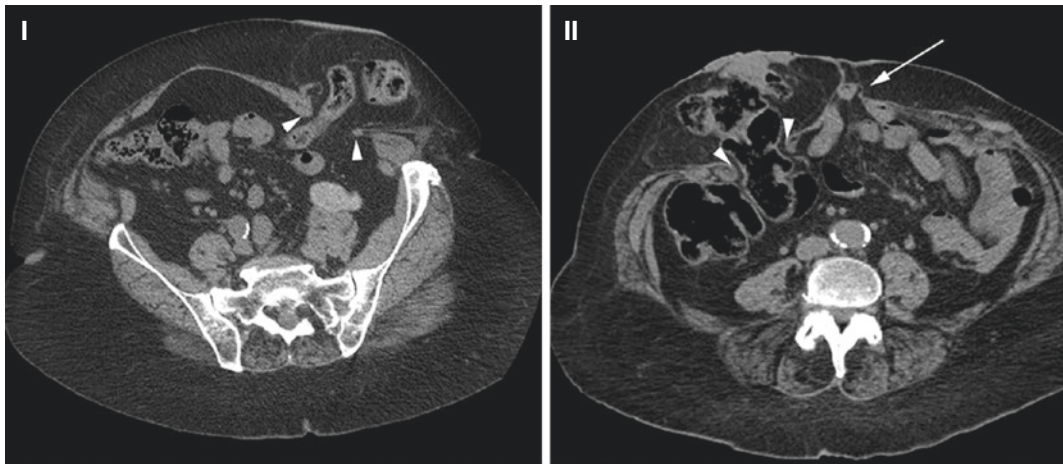

Fig. 18.8 European Hernia Society classification of parastomal hernias; (**I**) Small parastomal hernia (<5 cm gap in the rectus (arrowheads)) without concomitant incisional hernia. (**II**) Small parastomal hernia (<5 cm gap in the rectus (arrowheads)) with concomitant incisional hernia (arrow). (**III**) Large parastomal hernia (>5 cm gap in the rectus (arrowheads)) without concomitant incisional hernia. (**IV**) Large parastomal hernia (>5 cm gap in the rectus (arrowheads)) with concomitant incisional hernia (arrows)

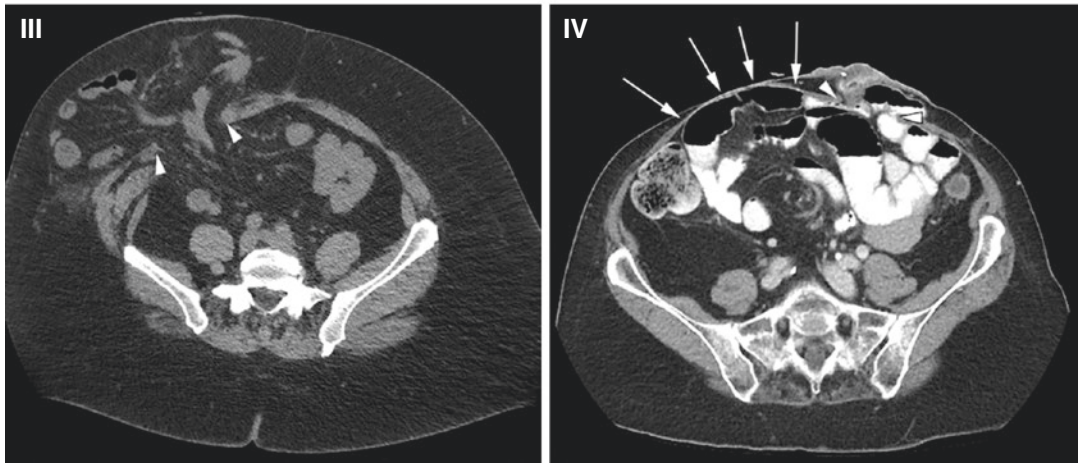

Fig. 18.8 (continued)

Clinical and Radiographical Significance

When looking at PH on CT imaging there are findings that can directly affect the patient's quality of life. While most PH are asymptomatic, patients have reported symptoms ranging from mild discomfort to life-threatening complications. [19, 20] In many cases, CT imaging provides the most accurate information for diagnosis and etiology. The following findings discussed are both relevant to the patient's symptoms as well as important for the surgeon to consider prior to planning any operative repair.

Fig. 18.9 End ileostomy with large hernia sac creating appliance fitment issues. Note the close proximity of the fascial defect (arrows) to the bony pelvis (arrowhead), which will make inferior-lateral mesh overlap during repair more difficult

Location

Location of the stoma or subsequent PH is one of the most important clinical and radiographical findings that affect the quality of life of the patient as well as their options of management. Stoma site is marked preoperatively away from bony landmarks, skin folds, scars, belt lines, and anticipated incisions. [21] A suboptimal location is often the root cause of stoma complications and patient symptoms. As discussed previously, stomas that are created along the semilunar line or further lateral can be both disruptive to the patient's quality of life as well as their surgical treatment options should they develop a PH (Figs. 18.2 and 18.7Ia). Stomas too lateral can lead to difficulties with fitting ostomy appliances resulting in leakage or skin excoriations; this is especially true in obese patients. [22] In the case of a lateral PH through the semilunar line or oblique muscles, repair is very difficult, and may require relocation. Similarly, PH that are located too close to the anterior superior iliac spine can cause appliance issues for the patient and may not be amenable to minimally invasive options such as laparoscopic repair (Fig. 18.9).

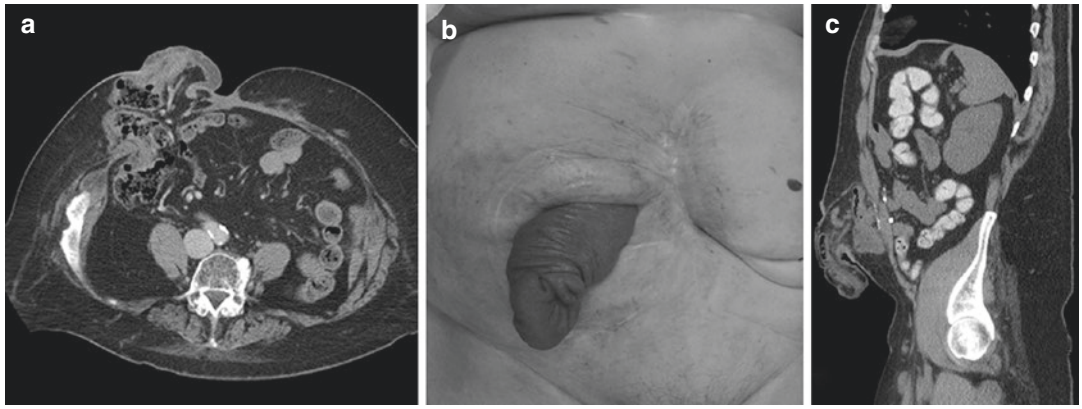

Fig. 18.10 Recurrent parastomal hernia with prolapse seen (**a**) radiographically on axial CT scan and (**b**) on physical examination (**c**) radiographically on sagittal CT scan

Prolapse

Prolapse occurs at a rate ranging from 5.4 to 6.8%; one study quotes the incidence of prolapse in loop transverse colostomy as high as 47%. [23, 24] Prolapse can be easily seen on imaging as redundant bowel protruding through the ostomy site and hanging outside the body (Fig. 18.10). Stoma prolapse can be unsightly for the patient and also cause physical discomfort or pain. While most prolapses are asymptomatic and do not require any intervention, some can develop stenosis, strangulation, and/or obstruction. From a surgical standpoint, prolapse can be associated with or worsened by the presence of a PH. If the surgeon is planning an operative repair, then the prolapse will also need to be addressed at the time of the operation.

Fig. 18.11 Small bowel obstruction in a patient with a urostomy with decompressed distal small bowel and colon (arrowhead) and multiple dilated loops of small bowel (arrows). Note the free fluid surrounding the bowel within the parastomal hernia sac

Small Bowel Obstruction

Small bowel obstruction is one of the most common symptomatic complications of abdominal surgery. In patients who have undergone surgeries resulting in a stoma and subsequent PH, it can occur in the setting of dense abdominal adhesions or within the hernia sac (Fig. 18.11). In patients with a stoma, one study reported an incidence of small bowel obstruction of 9.5%. [24] Ileostomy tends to be associated with a higher incidence compared to colostomy, 4.5% vs 0.75%. [25]

Small bowel obstruction can be diagnosed clinically and radiographically. Patients typically present with nausea, vomiting, minimal or no ostomy output, inability to pass flatus or stool, and abdominal pain. Radiographically, a transition point is typically seen where there is a change in the caliber of the bowel. In addition to

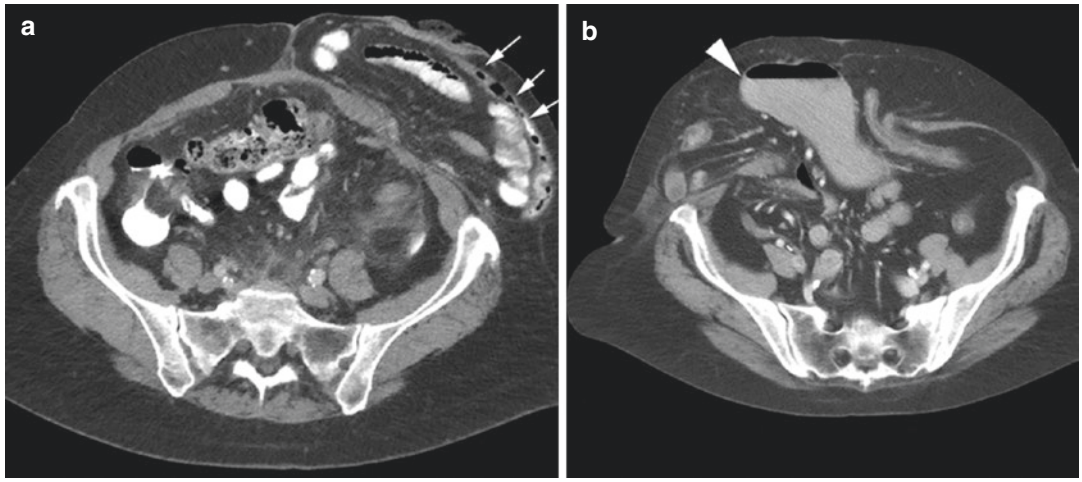

Fig. 18.12 (**a**) Significant amount of small bowel within a parastomal hernia displaces the end colostomy (arrows) laterally without causing an obstruction. (**b**) Obstructed stomach (arrowhead) as the result of a large hernia around a urostomy

adhesive disease, small bowel obstructions can be associated with PH. [26] In the presence of a large PH, where there are multiple loops of redundant bowel and mesentery within the hernia sac, the fascial defect can become a source of obstruction or strangulation for the bowel within the hernia sac. Small bowel entering and exiting the defect can become kinked at the level of the fascia.

Most isolated small bowel obstruction can be managed nonoperatively. However, an obstruction or strangulation associated with a PH is an indication of surgical repair. [26] It is therefore crucial to distinguish on CT scan whether the cause of the obstruction is due to the PH or at an isolated transition point elsewhere. In the latter case, a planned repair of the PH alone would not resolve the obstruction.

Additional Radiographical Considerations for Repair

Hernia Contents

Depending on the size, location, and type of defect, PH contents can include small bowel, colon, mesentery, omentum, and in rare cases, stomach (Fig. 18.12). [27] The importance is correlating the herniated contents on imaging with patient symptoms to plan an effective operation for repair.

Concomitant Hernias

As previously mentioned, the physical exam is limited in assessing PH. Subsequently, the use of imaging has contributed to higher detection of concomitant incisional hernias not apparent on physical exam. [19, 28, 29] According to Gil and Szcepkowski, 21% of PH in their study were discovered with coexisting incisional hernias (Type II and IV). [17] Their classification serves to better identify patients with PH requiring different surgical needs. A type I and II hernia may only require a laparoscopic Sugarbaker repair to be successful. Whereas, type III and IV may likely need a more comprehensive (open or robotic) abdominal wall reconstruction to effectively address the parastomal defect and/or midline incisional hernia. Regardless of classification, imaging often reveals additional defects that will ultimately need to be addressed at the time of the operation (Fig. 18.13). Knowing what to expect ahead of time can more effectively plan the operation for success.

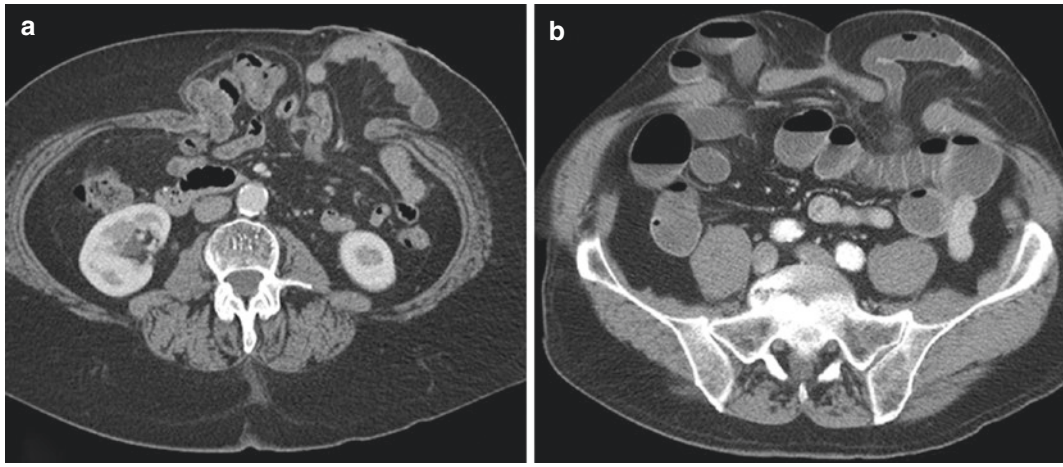

Fig. 18.13 (**a**) Parastomal hernia through the left rectus muscle with concomitant midline incisional hernia. (**b**) Parastomal hernia through the right rectus muscle with concomitant incisional hernia through the left rectus muscle at a prior ostomy site

Previous Repairs and Mesh Complications

PH is a recurrent disease, and some patients will undergo multiple operations before achieving long-term relief. It is essential to correlate imaging to previous operative reports in order to know and understand the layout of the patient's abdomen before making an incision. If the patient has undergone previous hernia repairs, there is often mesh already in place, which is important to note because additional repair may involve manipulation of the mesh and scar tissue (Fig. 18.14). Additionally, there can be complications associated with previous mesh implantation. Although mesh infection rates in PH are reported between 2 and 3% and overall wound infection rates of 4% [30], mesh erosions can occur and will alter how the repair can be performed (Fig. 18.15).

In some patients, mesh can be seen on imaging in patients without prior PH repairs. Within the literature, prophylactic mesh placement has been shown to decrease the incidence rate of PH. One study reported that the use of synthetic mesh was able to lower the occurrence of PH and be potentially more cost-effective when utilized prophylactically. [19, 22] However in practice, there remains to be a consensus among surgeons on prophylactic mesh placement, optimal mesh type, and mesh positioning. In particular, rates of prophylactic mesh differ between European and North American surgeons. Regardless of when mesh is placed, confirming on imaging what hardware is already present is an integral part of planning an operation.

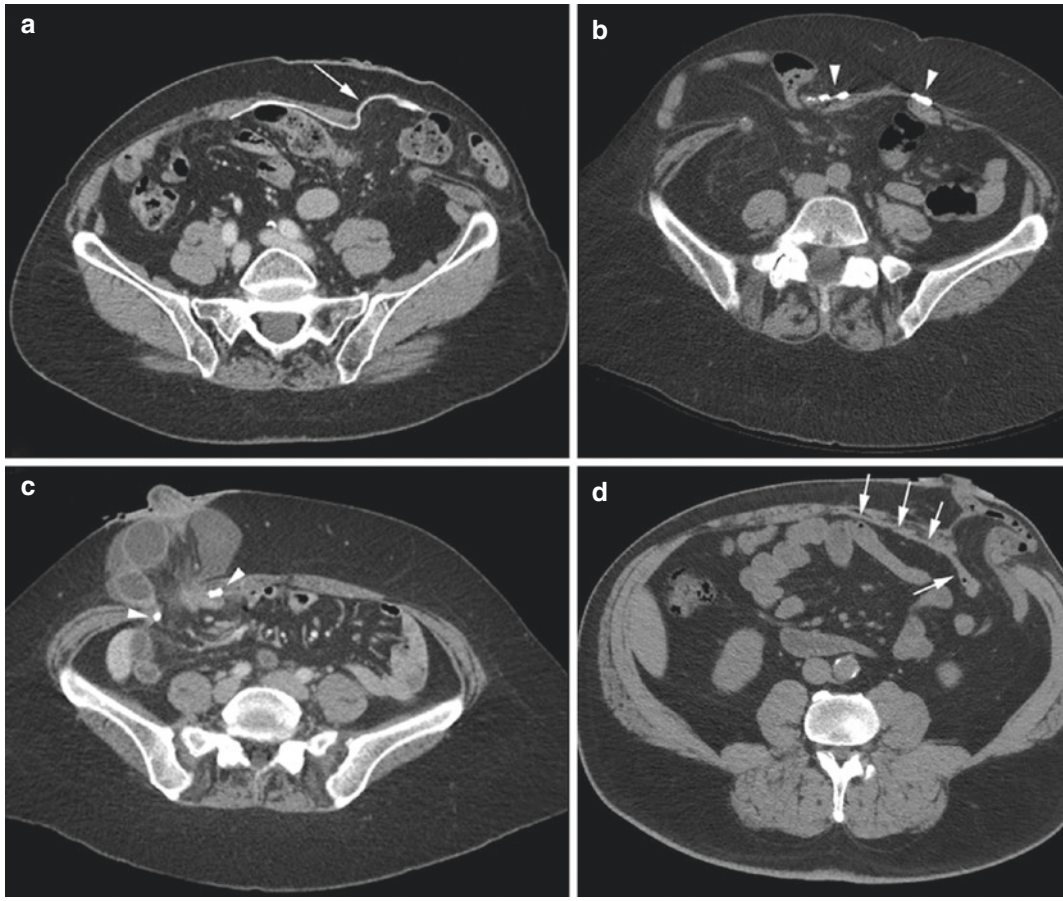

Fig. 18.14 Recurrent parastomal hernias following prior mesh repair; (**a**) failed IPUM Sugarbaker repair with expanded polytetrafluorethylene (ePTFE) mesh (arrow). (**b**) Failed keyhole repair with reduced-weight polypropylene mesh, identifiable only by radiopaque mesh fixation (arrowheads). (**c**) Failed IPUM keyhole repair with heavyweight polypropylene mesh, identifiable only by radiopaque mesh fixation (arrowheads). (**d**) Failed IPUM Sugarbaker repair with porcine small intestine submucosa (SIS) mesh (arrow)

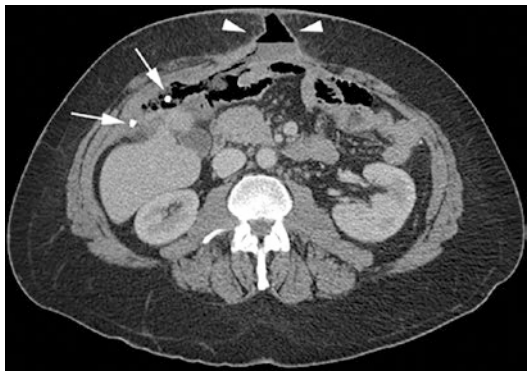

Fig. 18.15 Acute mesh erosion into an ileostomy following laparoscopic IPUM Sugarbaker repair as a result of over-aggressive lateralization maneuvers. Radiopaque mesh fixation (arrows) can be seen with an air fluid level (succus) tracking around the mesh and posterior abdominal wall towards the midline skin (arrowheads)

Radiographical Findings After PH Repair

Many PH can be managed conservatively. However, surgical repair is indicated when there is strangulation or obstruction present. PH is a complex disease and there are various surgical techniques that can be performed, including local revision, stoma relocation, or mesh repair (Sugarbaker, keyhole, cruciate, Stapled Transabdominal Ostomy Reinforcement with Retromuscular Mesh). Even after a successful repair, the recurrence rate of a PH is reported up to 50% across all techniques. [31] The techniques discussed in this section highlight the common operative findings on CT imaging after

the repair is performed; the operative steps of the repair will reflect the findings on imaging.

Sugarbaker and Keyhole Repair

Mesh implantation can be performed in several ways: onlay, sublay (retromuscular), or underlay (intraperitoneal). The intraperitoneal underlay mesh (IPUM) repair for PH can be performed using the Sugarbaker or the keyhole configuration mesh either open or via minimally invasive methods (laparoscopic or robotic-assisted). In the Sugarbaker technique, mesh is placed over the fascial defect and covers a segment of lateralized bowel with >5 cm overlap beyond the defect. The mesh is secured at all points except where the lateralized bowel exits, creating a valve flap to prevent further herniation. In the keyhole repair, mesh is placed over the fascial defect utilizing a slit in the mesh leading to a 2–3 cm trephine where the bowel passes. [2, 10, 19] Both techniques can be seen on imaging as mesh covering the fascial defect after successful reduction of the hernia contents. The Sugarbaker repair is distinguished by the presence of bowel exiting from the lateral edge of the mesh (Fig. 18.16); in a keyhole, the bowel traverses the center of the mesh. Studies have consistently reported a lower recurrence rate after the Sugarbaker repair than the keyhole [10, 19], making the Sugarbaker more preferred when possible.

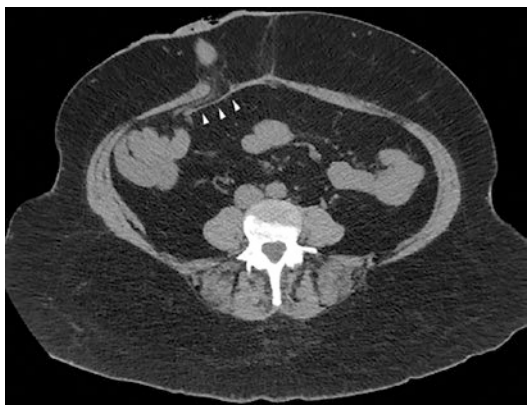

Fig. 18.16 Axial CT imaging of a successful laparoscopic IPUM Sugarbaker repair of an end ileostomy parastomal hernia. The lateralized bowel can be seen entering a tunnel of mesh (arrowheads) before traversing the rectus abdominis muscle and heading towards the mucocutaneous junction

Retromuscular Sugarbaker Repair (Pauli Parastomal Hernia Repair)

In 2016, Pauli et al. described a novel technique in open PH repair utilizing retromuscular dissection, posterior component separation via transversus abdominis release, and lateralization of the bowel utilizing a modified Sugarbaker mesh configuration within the retromuscular space. In this open repair, the bowel is lateralized within retromuscular space after the posterior component separation. Wide sublay mesh overlap reinforces the lateralized bowel, the midline incisional defect, and any concomitant incisional hernias at the time of repair. On imaging, the repair looks similar to a massive ventral hernia repair with mesh; the unique finding is the lateralized bowel within the retromuscular space reentering the peritoneal cavity further lateral from where the stoma exits (Fig. 18.17). [31] Since the initial description of this method, others have adapted the concept to laparoscopic and robotic platforms as well as

Fig. 18.17 Axial CT imaging of a successful retromuscular Sugarbaker operation (Pauli Parastomal Hernia Repair) of an end ileostomy parastomal hernia. The lateralized bowel (arrow) can be seen entering a tunnel of mesh before traversing the rectus abdominis muscle and heading towards the mucocutaneous junction. The mesh is not visualized because of its reduced weight and lack of radiopaque fixation

options to address isolated parastomal defects in a retromuscular fashion.

Stapled Transabdominal Ostomy Reinforcement with Retromuscular Mesh (STORRM)

In 2017, Novitsky et al. described a technique using the circular end-to-end stapler during open large PH repair to tunnel through mesh and abdominal wall layers, standardize sizing, fixate mesh, and reinforce the stoma aperture. After a transversus abdominis release is performed, the bowel is brought through the posterior sheath and delivered at the site of the new ostomy location for siting, all the layers including the mesh are aligned and fixed within the circular stapler, and the stapler is fired, securing anterior fascia to the mesh. This technique relocates the stoma but may lower the risk of acute mesh erosion into the bowel by fixating mesh to the anterior fascia and rectus abdominis thereby preventing "scissoring" within the retromuscular plane. On imaging, the stoma is in a new location, usually contralateral to the previous site, and the circular staple ring where the bowel traverses is distinctly recognizable (Fig. 18.18). [32]

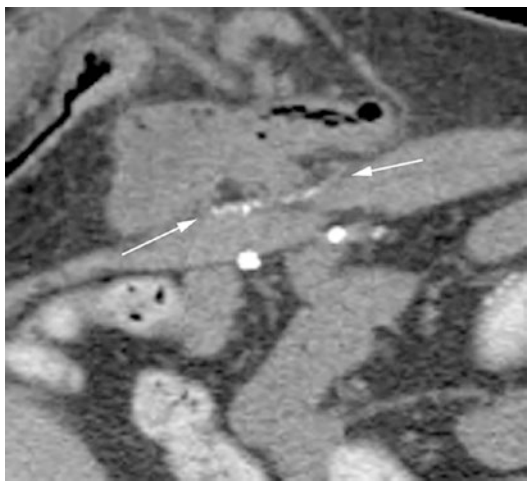

Fig. 18.18 Magnified CT imaging of a recurrent parastomal hernia following stapled transabdominal ostomy reinforcement with retromuscular mesh (STORRM). A circular ring of staples (arrows) can be seen at the level of the anterior rectus fascia as the result of using an EEA stapler to fixate the mesh at this level

Conclusion

Parastomal hernias are complex defects often associated with concurrent hernias, obstruction, loss of domain, and/or prolapse. They are difficult to assess by physical exam alone, and, therefore, CT imaging is essential for obtaining information to evaluate and plan an operative repair. When looking at CT imaging, there are various findings to consider before deciding on the optimal approach. The ones discussed include location, hernia contents, obstruction, concurrent hernias, and previous repairs. Additionally, imaging is helpful in planning these operations because they can identify if the stoma needs relocation, which mesh-based repair is most appropriate, or if a local revision will suffice. Imaging can further help classify the hernia in radiographically and clinically meaningful ways. Almost all the information regarding a hernia is gathered radiographically because very little is easily observable on physical exam. Cross-sectional imaging should be liberally applied in the diagnosis, preoperative assessment, and postoperative management of patients with PH.

References

1. Sheetz KH, Waits SA, Krell RW, et al. Complication rates of ostomy surgery are high and vary significantly between hospitals. Dis Colon Rectum. 2014;57(5):632–7. https://doi.org/10.1097/DCR.0000000000000038.
2. Carne PW, Robertson GM, Frizelle FA. Parastomal hernia. Br J Surg. 2003;90(7):784–93. https://doi.org/10.1002/bjs.4220.
3. Moreno-Matias J, Serra-Aracil X, Darnell-Martin A, et al. The prevalence of parastomal hernia after formation of an end colostomy. A new clinico-radiological classification. Colorectal Dis. 2009;11(2):173–7. https://doi.org/10.1111/j.1463-1318.2008.01564.x.
4. Rubin MS, Schoetz DJ, Matthews JB. Parastomal hernia: is stoma relocation superior to fascial repair? Arch Surg. 1994;129(4):413–9. https://doi.org/10.1001/archsurg.1994.01420280091011.
5. Styliński R, Alzubedi A, Rudzki S. Parastomal hernia—current knowledge and treatment. Wideochir Inne Tech Maloinwazyjne. 2018;13(1):1–8. https://doi.org/10.5114/wiitm.2018.72685.
6. Strong SA. The difficult stoma: challenges and strategies. Clin Colon Rectal Surg. 2016;29(2):152–9. https://doi.org/10.1055/s-0036-1580628.

7. Whitehead A, Cataldo PA. Technical considerations in stoma creation. Clin Colon Rectal Surg. 2017;30(3):162–71. https://doi.org/10.1055/s-0037-1598156.
8. Hardt J, Meerpohl JJ, Metzendorf MI, Kienle P, Post S, Herrle F. Lateral pararectal versus transrectal stoma placement for prevention of parastomal herniation. Cochrane Database Syst Rev. 2013;(11):CD009487. Published 2013 Nov 22. https://doi.org/10.1002/14651858.CD009487.pub2.
9. Hardt J, Meerpohl JJ, Metzendorf MI, Kienle P, Post S, Herrle F. Lateral pararectal versus transrectal stoma placement for prevention of parastomal herniation. Cochrane Database Syst Rev. 2019;4(4):CD009487. Published 2019 Apr 24. https://doi.org/10.1002/14651858.CD009487.pub3.
10. Glasgow SC, Dharmarajan S. Parastomal hernias: avoidance and Treatment in the 21st Century. Clin Colon Rectal Surg. 2016;29(3):277–84. https://doi.org/10.1055/s-0036-1584506.
11. Morrison CD, Kielb SJ. Use of bowel in reconstructive urology: what a colorectal surgeon should know. Clin Colon Rectal Surg. 2017;30(3):207–14. https://doi.org/10.1055/s-0037-1598162.
12. Narang SK, Alam NN, Campain NJ, et al. Parastomal hernia following cystectomy and ileal conduit urinary diversion: a systematic review. Hernia. 2017;21(2):163–75. https://doi.org/10.1007/s10029-016-1561-z.
13. Donahue TF, Bochner BH, Sfakianos JP, et al. Risk factors for the development of parastomal hernia after radical cystectomy. J Urol. 2014;191(6):1708–13. https://doi.org/10.1016/j.juro.2013.12.041.
14. Stein JP, Skinner DG. Radical cystectomy. BJU Int. 2004;94:197–221. https://doi.org/10.1111/j.1464-410X.2004.04981.x.
15. Devlin HB, Kingsnorth A. Management of abdominal hernias. London: Hodder Arnold Publishers; 1998. p. 177–8.
16. Rubin MS, Bailey HR. PH. In: MacKeigan JM, Cataldo PA, editors. Intestinal stomas: principles, techniques and management. 1st ed. St. Louis: Quality Medical Publishing; 1993. p. 245–67.
17. Gil G, Szczepkowski M. A new classification of parastomal hernia—from the experience at Bielański Hospital in Warsaw. Pol Przegl Chir. 2011;83(8):430–7. https://doi.org/10.2478/v10035-011-0067-8.
18. Śmietański M, Szczepkowski M, Alexandre JA, et al. European Hernia Society classification of parastomal hernia. Hernia. 2014;18(1):1–6. https://doi.org/10.1007/s10029-013-1162-z.
19. Celik S, Kocaay A, Akyol C. Parastomal hernia; 2017. https://doi.org/10.5772/intechopen.68876.
20. van Dijk SM, Timmermans L, Deerenberg EB, et al. Parastomal hernia: impact on quality of life? World J Surg. 2015;39(10):2595–601. https://doi.org/10.1007/s00268-015-3107-4.
21. Martin L, Foster G. Parastomal hernias. Ann R Coll Surg Engl. 1996;78(2):81–4.
22. Shellito PC. Complications of abdominal stoma surgery. Dis Colon Rectum. 1998;41(12):1562–72. https://doi.org/10.1007/BF02237308.
23. Cheung MT. Complications of an abdominal stoma: an analysis of 322 stomas. Aust N Z J Surg. 1995;65(11):808–11. https://doi.org/10.1111/j.1445-2197.1995.tb00566.x.
24. Nastro P, Knowles CH, McGrath A, Heyman B, Porrett TR, Lunniss PJ. Complications of intestinal stomas. Br J Surg. 2010;97(12):1885–9. https://doi.org/10.1002/bjs.7259.
25. Harris DA, Egbeare D, Jones S, Benjamin H, Woodward A, Foster ME. Complications and mortality following stoma formation. Ann R Coll Surg Engl. 2005;87(06):427–31.
26. Krishnamurty DM, Blatnik J, Mutch M. Stoma complications. Clin Colon Rectal Surg. 2017;30(3):193–200. https://doi.org/10.1055/s-0037-1598160.
27. Waheed A, Zeller PE, Bishop PJ, Robinson SK, Tuma F, Gastric PH. A case report of a rare yet fascinating clinical entity. Cureus. 2019;11(6):e4886. Published 2019 Jun 11. https://doi.org/10.7759/cureus.4886.
28. Cingi A, Cakir T, Sever A, Aktan AO. Enterostomy site hernias: a clinical and computerized tomographic evaluation. Dis Colon Rectum. 2006;49(10):1559–63. https://doi.org/10.1007/s10350-006-0681-4.
29. Hotouras A, Murphy J, Thaha M, Chan CL. The persistent challenge of parastomal herniation: a review of the literature and future developments. Colorectal Dis. 2013;15(5):e202–14. https://doi.org/10.1111/codi.12156.
30. Hansson BM, Slater NJ, van der Velden AS, et al. Surgical techniques for parastomal hernia repair: a systematic review of the literature. Ann Surg. 2012;255(4):685–95. https://doi.org/10.1097/SLA.0b013e31824b44b1.
31. Pauli EM, Juza RM, Winder JS. How I do it: novel parastomal herniorrhaphy utilizing transversus abdominis release. Hernia. 2016;20(4):547–52. https://doi.org/10.1007/s10029-016-1489-3.
32. Majumder A, Orenstein SB, Miller HJ, Novitsky YW. Stapled Transabdominal Ostomy Reinforcement with retromuscular mesh (STORRM): technical details and early outcomes of a novel approach for retromuscular repair of parastomal hernias. Am J Surg. 2018;215(1):82–7. https://doi.org/10.1016/j.amjsurg.2017.07.030.

Radiology of the Hiatal Hernia

19

Joseph Adam Sujka, Pete Peterson,
and Christopher DuCoin

Radiologic Classification

Hiatal hernias are typically broken down into four subtypes, 1 through 4 [1]. *Type 1* is also known as a sliding hiatal hernia. With this type, the gastroesophageal junction migrates through the diaphragm while the stomach stays in its normal alignment with the fundus remaining below the gastroesophageal junction [2]. Greater than 95% of hiatal hernias are categorized as *Type 1* and asymptomatic patients do not require repair as long-term studies have shown a lack of need for emergent repair [3, 4]. *Type 2–4* hiatal hernias are referred to as paraesophageal hernias because unlike Type 1 hernias, the posterolateral phrenoesophageal ligament is preserved around the gastroesophageal junction [5].

Type 2 paraesophageal hernias have the gastroesophageal junction in the normal anatomic position however a portion of fundus herniates adjacent to the esophagus into the thorax. Type 3 paraesophageal hernias are a combination of Type 1 and 2 with both the fundus and gastroesophageal junction herniating through the hiatus. Type 4 is a paraesophageal hernia that contains another organ in addition to a hiatal hernia. Among the paraesophageal hernia types, Type 3 is the most common making up 90% and Type 2 is the least common [2] (Figs. 19.1 and 19.2).

There is a more nebulously defined type of hiatal hernia, the "giant" paraesophageal hernia. Some have advocated for giant hiatal hernias to be defined as type 3 or 4 paraesophageal hernias. While others suggest that the amount of stomach contained in the chest, half the stomach or more, be used to define this type of hiatal hernia [8–10]. It is the opinion of the authors that a giant hiatal hernia is simply a large paraesophageal hernia requiring more mediastinal dissection than typically required for hiatal hernia repair. An additional type of hiatal hernia to consider is a hiatal hernia recurrence. Defining a recurrence begins with radiologic proof. However, clinical symptoms may not always accompany radiologic findings [11–13]. While there is no strict definition of what constitutes a radiologic recurrence some define a radiologic recurrence only when the recurrence is 2 cm in length [14]. Incidental discovery of a hiatal hernia recurrence and the reoperation should be balanced against the symptoms of the patient as most recurrences are small and asymptomatic [15]. Recurrence should be treated similarly to a newly diagnosed hiatal hernia with a thorough history and physical, imaging, and strict definition of the patient's symptoms.

J. A. Sujka (✉)
GI Surgery, University of South Florida,
Tampa, FL, USA
e-mail: josephsujka@usf.edu

P. Peterson · C. DuCoin
Department of Surgery, University of South Florida at
Tampa General Hospital, Tampa, FL, USA
e-mail: petepeterson@usf.edu; cducoin@usf.edu

S. Docimo Jr. et al. (eds.), *Fundamentals of Hernia Radiology*,
https://doi.org/10.1007/978-3-031-21336-6_19

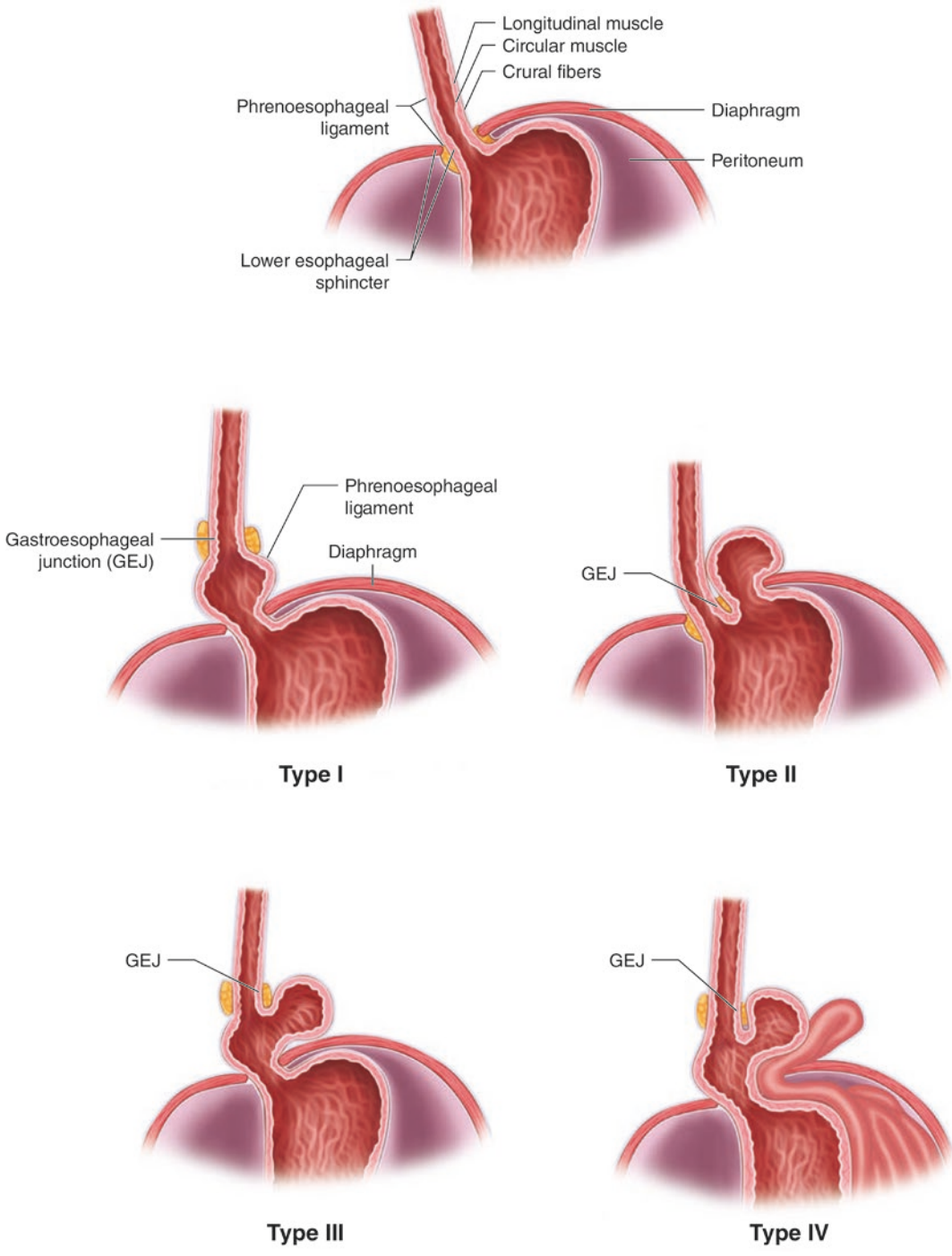

Fig. 19.1 Types of paraesophageal hernias. Modified from [6]

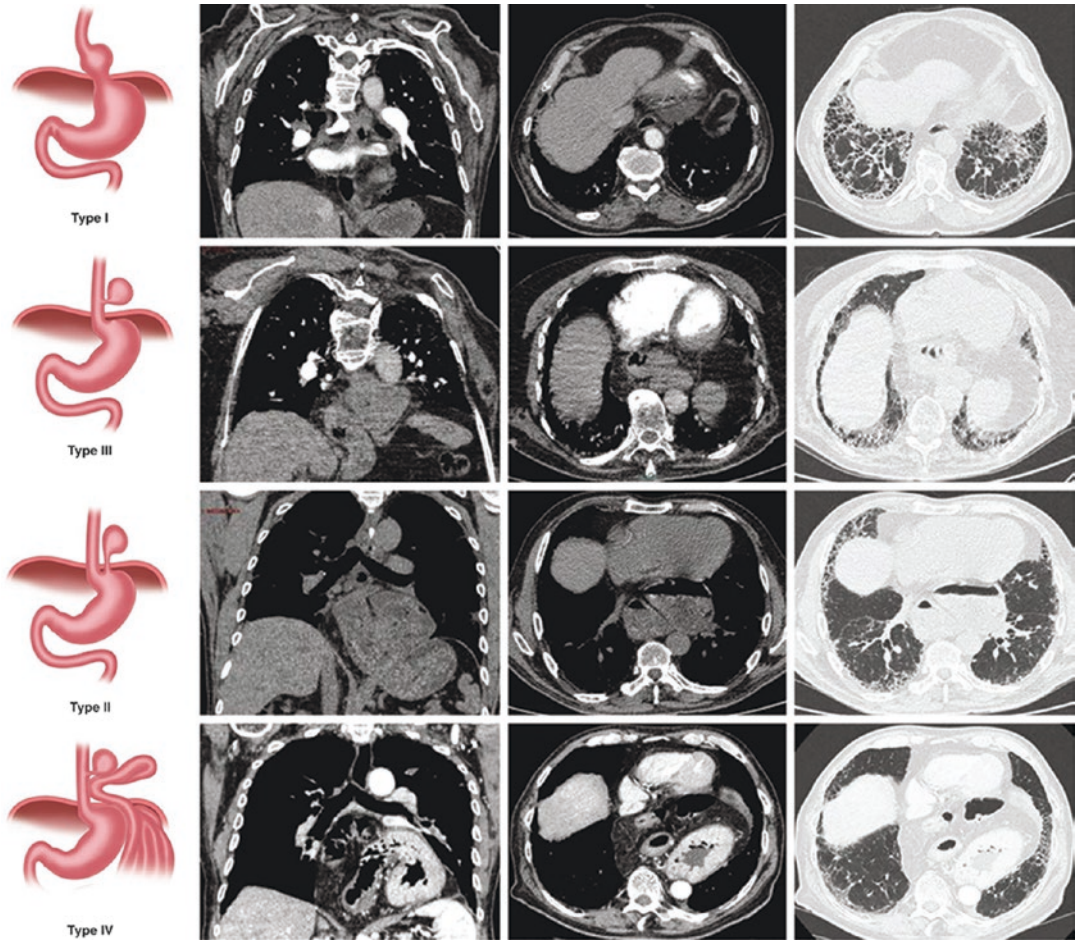

Fig. 19.2 Radiologic images for hiatal hernia types. Modified from [6, 7]

The final radiologic finding to take note of relating to a hiatal hernia is gastric volvulus. Gastric volvulus can occur in either the chest or the abdomen and is defined based on the axis of rotation. The two types of rotation are organoaxial and mesenteroaxial, with organoaxial being the more common of the two. Organoaxial rotation is when the stomach rotates on its longitudinal axis, from cardia to pylorus, where mesenteroaxial volvulus is when the stomach rotates around its transverse axis, from lesser to greater curve [3]. With complete gastric obstruction, the patient may present with Borchardt's triad—severe epigastric pain, unproductive retching, and the inability to pass a nasogastric tube [16]. Complete obstruction from gastric volvulus is a surgical emergency requiring operative exploration to avoid gastric ischemia or necrosis. However, patients with large hiatal hernias may present with incomplete obstruction from gastric volvulus and can be more completely worked up prior to operative intervention (Fig. 19.3).

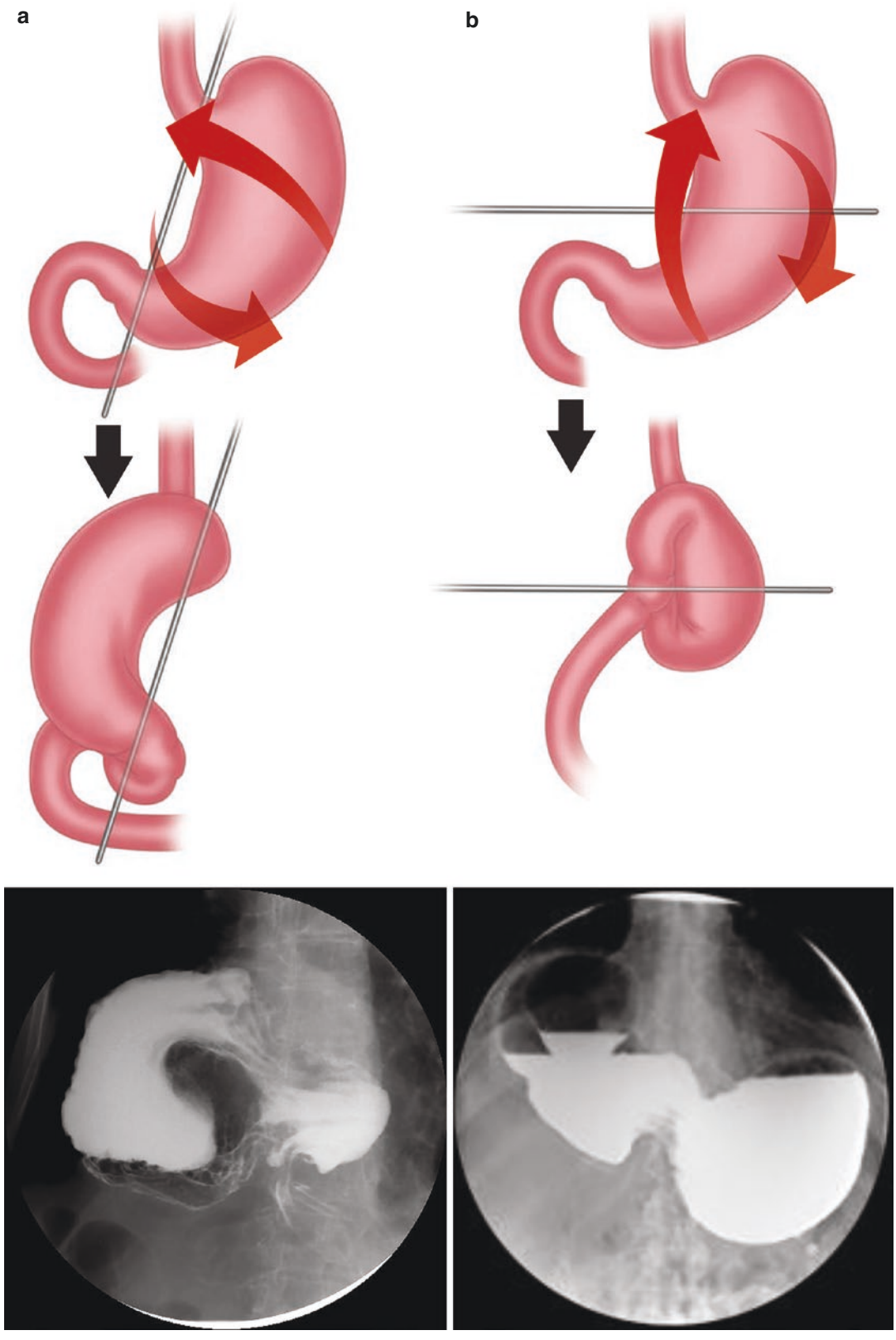

Fig. 19.3 Gastric volvulus: (**a**) Organoaxial, (**b**) Mesenteroaxial. Modified from [6, 17]

Diagnostic Workup and Preoperative Imaging

The diagnosis of a hiatal hernia can be completed through various radiologic tests. Once the diagnosis of a hiatal hernia has been completed no further testing is required for operative repair if the patient is symptomatic. Broadly speaking all patients should undergo esophagogastrodoudenoscopy (EGD) followed by pH testing if Los Angeles (LA) grade C or D esophagitis is not seen. Next, an upper gastrointestinal series (UGI) is performed to evaluate the size, motility, and emptying of the hernia. If there is any concern for dysmotility high-resolution manometry should also be used.

One of the first tests that can be utilized is a plain chest radiograph. Characteristic findings of a hiatal hernia include retrocardiac air-fluid levels, visceral gas in the mediastinum, loops of bowel running vertically towards the chest, and an upward displacement of the transverse colon if it is involved in the hernia [18]. While plain chest radiographs may suggest the presence of a hiatal hernia other studies are better able to characterize the size, contents, and functional difficulties these hernias represent (Fig. 19.4).

The next type of study that can be utilized is a contrasted study such as an upper gastrointestinal series (UGI). This test is useful for gauging the size of the hiatal hernia and localizing the gastroesophageal junction. It can also suggest dysmotility of the esophagus that would benefit from high-resolution manometry (HRM). An UGI can also increase suspicion for a short esophagus which may require esophageal lengthening procedures such as a Collis gastroplasty [20]. Finally, these dynamic studies give information on the transit of contrast into and out of the herniated stomach and can be particularly useful when trying to determine if a patient has complete gastric outlet obstruction. When performing an UGI barium should be used due to the risk of aspiration that can occur with larger partially obstructed hernias. If ionic water-soluble contrast, such as gastrografin, is used and aspirated it can lead to chemical pneumonitis in the lungs [21].

UGI can also be used to calculate the cross-sectional area of the herniated intrathoracic stomach as well as the hiatal surface area [22, 23].

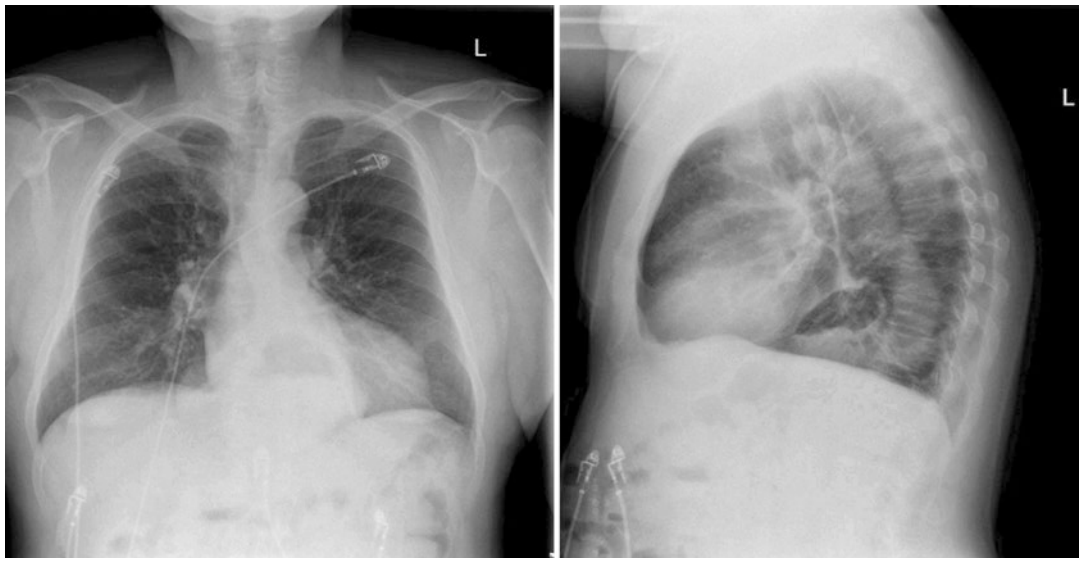

Fig. 19.4 Plain chest radiograph with hiatal hernia. Open access from [19]

However, the utility of this additional information appears to be limited at this time. One study by Swanstrom et al. examined 100 patients with chronic gastroesophageal reflux disease (GERD) who were planned for laparoscopic fundoplication. Prior to operative intervention, the patients underwent barium study to measure the presence of a hiatal hernia and they concluded that barium swallow had no correlation with hiatal surface area or hiatal hernia size for all patients [24]. Another study by Aye et al. looked at diaphragmatic tension radiologically and then intraoperatively to determine shapes of diaphragmatic hernias and their associated tension. Again, there was a limited correlation between the width of the hiatal opening and associated tension [25]. These limitations of UGI series may be due to their two-dimensional perspective but is more likely due to the complexity of the diaphragmatic hiatus and its mobility which makes quantification and characterization difficult.

Computed Tomography (CT) can be useful in the acute setting to determine complications related to a hiatal hernia but also in quantifying the size and complexity of a hiatal hernia. Unlike plain chest radiographs and UGI, a CT scan can clearly visualize the thoracic cavity and the hiatal hernia contents. Multi-slice CT scans with coronal, sagittal, and 3D reformatted images have been shown to increase the sensitivity of CT scans for diagnosis of hiatal hernias [26]. The larger the hernia the more useful a CT scan will be in the preoperative setting but in smaller and less complex hernias an UGI may be sufficient. Generally, with Type 3 or 4 paraesophageal hernias, or redo foregut surgery, a CT scan should be performed prior to operative intervention.

Other types of imaging studies have been performed for diagnosis of a hiatal hernia such as nuclear medicine studies [27], transesophageal echocardiogram [28], and endoscopic ultrasound; however, in the practical setting these modalities do not have a routine place in the diagnosis or management of hiatal hernias. In most hiatal hernias upper endoscopy and a contrast study will be sufficient testing prior to operative intervention.

Intraoperative Testing

Some centers utilize High-Resolution Manometry (HRM) prior to hiatal hernia repair. This is to characterize the contractility function of the esophagus as well as visualize a hiatal hernia. However, due to the configuration of the stomach it is sometimes impossible to cannulate the GEJ and some have begun to evaluate intraoperative tools for use during hiatal hernia repair [29]. Impedance planimetry, or Endoluminal functional lumen imaging probe (EndoFLIP), is a relatively new technology which can be used intraoperatively to evaluate the distensibility of the esophagus. This information may be used to characterize the esophagus both before and after repair with hopes of improving outcomes by individualizing operative repair based on intraoperative testing.

The specifics of the function of EndoFLIP may be found elsewhere, but briefly this modality introduces a balloon catheter into the esophagus, either 8 cm or 16 cm, then inflates to a fill volume of 30 or 40 mL, and measure pressure in a 360-degree fashion along the catheter. In the operating room, the catheter used is 8 cm as the area being measured is just the GEJ. Measurements are recommended to be taken after crural dissection and hernia reduction, after crural closure, and after fundoplication/magnetic sphincter augmentation. This provides multiple time points to evaluate the changes to the esophagus and distensibility at each step of operative repair. Target distensibility index (DI) is the value targeted by surgeons when evaluating their repair. This value represents the change in esophageal compliance. The DI can be measured both with or without pneumoperitoneum in the abdomen. Without pneumoperitoneum present, the DI should be between 2.0 and 3.5 mm^2/mmHg and with pneumoperitoneum should be >0.5 mm^2/mmHg [30, 31]. Other values that can be utilized by the surgeon include maximum diameter (Dmin) and cross-sectional area (CSA). One study demonstrated a decrease of Dmin $\leq$ 0.15 mm or a decrease in CSA $\leq$ 1.5 mm^2 resulted in persistent

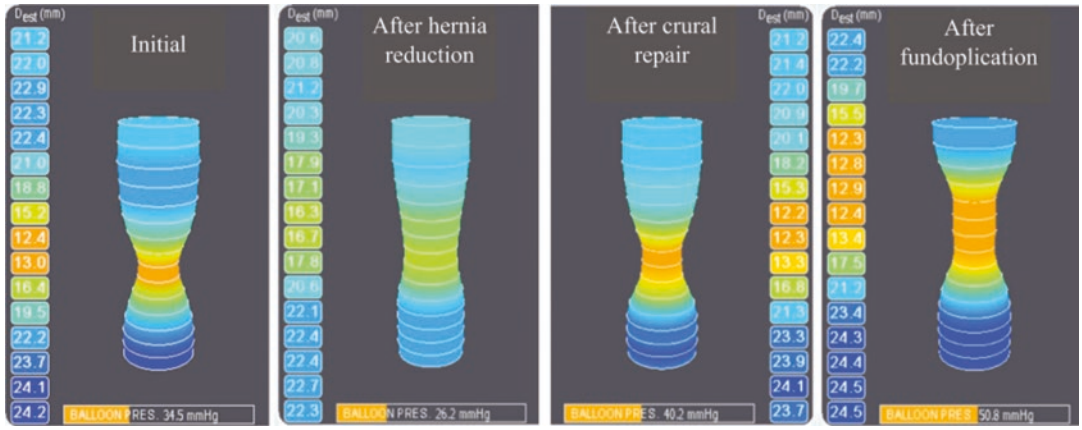

Fig. 19.5 Example of intraoperative EndoFLIP values. Modified from [30]

heartburn symptoms [32]. How all these values correlate with both short- and long-term outcomes is still an area of active research but it is possible that EndoFLIP may become a routinely used adjunct in the operating room for surgeons repairing hiatal hernias (Fig. 19.5).

Postoperative Imaging and Perioperative Findings

Imaging after hiatal hernia repair varies by provider. Some believe in routine postoperative imaging as a means of documenting the repair of the hiatal hernia and ruling out immediate complications. Others will selectively utilize imaging in patients with a difficult intraoperative dissection or a patient undergoing revisional surgery. While still others feel that symptoms should guide immediate postoperative imaging. The SAGES Guidelines for the management of hiatal hernia state that "routine postoperative contrast studies are not necessary in asymptomatic patients," citing a strong level of evidence [3]. If patients are symptomatic then UGI and CT scans are useful in ruling out key postoperative complications. These postoperative complications include immediate postoperative recurrence, severe dysphagia, pneumothorax, and esophageal/gastric leak.

Immediate postoperative recurrence can lead to transdiaphragmatic herniation of a fundoplication leading to ischemia and subsequent perforation. Elderly patients and those with atherosclerotic disease are at the highest risk of ischemia and perforation if wrap herniation occurs [33]. The incidence of wrap migration is 7–20% in the literature [34, 35]. Chest x-ray, UGI, and CT scan can be used to evaluate patients with findings of retrocardiac gas-filled structure with defined edges in continuity with the stomach being seen [36]. Patient with more chronic rehernia-tion of the fundoplication leads to postoperative failure including chronic postoperative reflux with or without dysphagia (Fig. 19.6).

In patients with immediate postoperative dysphagia, an UGI is helpful to determine the severity of any postoperative stenosis. Some postoperative dysphagia can be secondary to operative intervention and swelling but can also be secondary to an overly tight fundoplication or crural repair. Intolerance to saliva or liquids is concerning for dysphagia that will require intervention. Findings consistent with dysphagia that may not resolve with conservative management include contrast stasis with no transit into the stomach and esophageal dilation. Some surgeons are utilizing EndoFLIP intraoperatively as a means of avoiding postoperative dysphagia [37].

With the size of some hernias, an extensive mediastinal dissection is sometimes required. As a result, patients may develop pneumothorax, mediastinal air, and even mediastinal abscesses. Patients with pneumothorax will present with

Fig. 19.6 Plain chest X-ray, UGI, and CT scans consistent with herniated nissen fundoplication. Creative Commons [36]

hypoxia and possibly findings of tension physiology. These patients are treated with either a pigtail catheter or chest tube if clinically necessary. Smaller asymptomatic pneumothoraces do not require intervention if incidentally discovered on imaging for other reasons. In the setting of mediastinal air, consideration must be given to a possible leak even though pneumomediastinum may be normal in the immediate postoperative period. The same can be said of mediastinal fluid but this is more concerning for a mediastinal abscess or leak. UGI or CT scan with oral contrast can be used to further evaluate the mediastinum. Findings of air-fluid levels in the chest or a large contained fluid collection is concerning for a mediastinal abscess [33] (Fig. 19.7).

One of the most dreaded postoperative complications is an esophageal leak which can present on a spectrum. Presentations vary from tachycardia without any additional findings to a more pronounced presentation with high fevers, hypotension, and sepsis. UGI or CT scans with oral contrast are effective first-line tests to evaluate for a leak. Differentiation should be made between a pseudoleak, contained leak, and free perforation. A pseudoleak is not a true leak and will not present with sepsis or hemodynamic instability. It is seen on CT scan as a smooth variable defect in the region of the gastric fundus with a variable degree of edema at the GEJ. A contained or small leak will show up as linear tracks of contrast extending from the wrap. The most common position is in the posterior inferior border. Larger or free leaks will show up as large collections of contrast with adjacent inflammatory changes [33]. If there is any question of the location or severity of the leak and the patient is stable they can be taken for fluoroscopy to evaluate the leak in real time [38]. Typically, patients should undergo emergent surgical repair with any suspicion of a leak [39] (Fig. 19.8).

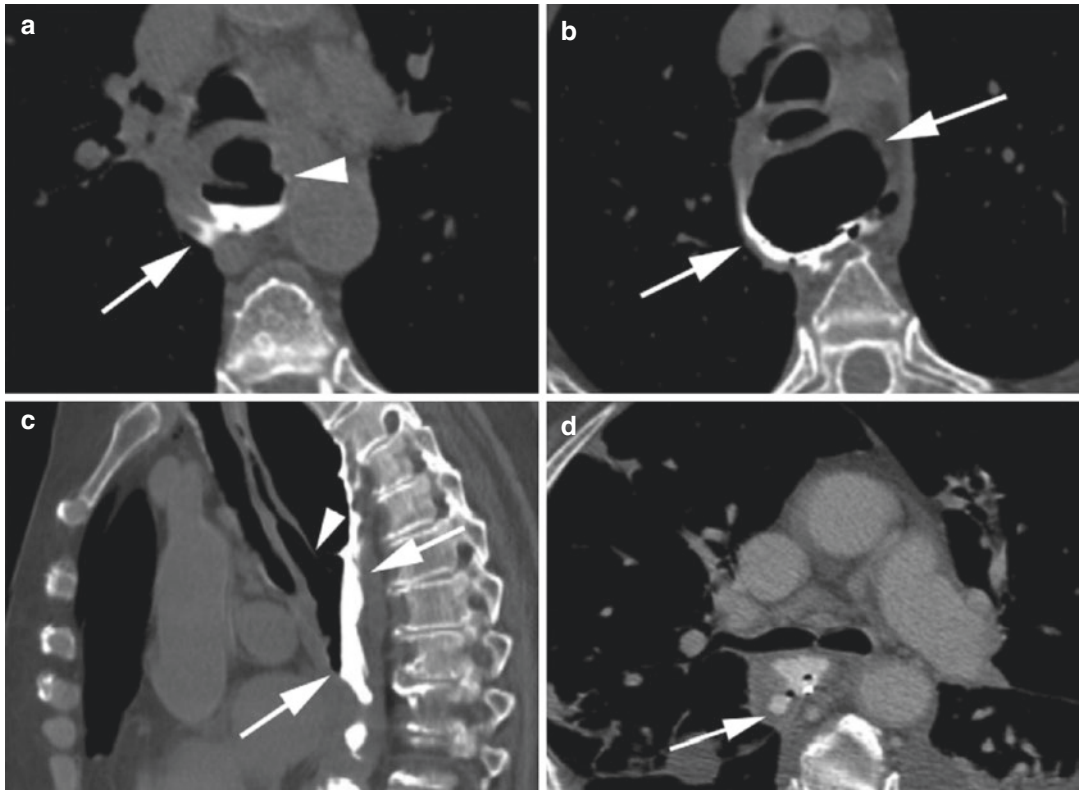

Fig. 19.7 CT scans with findings consistent with a mediastinal abscess (**a** and **b**) periesophageal fluid collection in the mediastinum (**c**) contrast leakage into the mediastinum (**d**) contrast leakage into the mediastinum. With permission from [33]

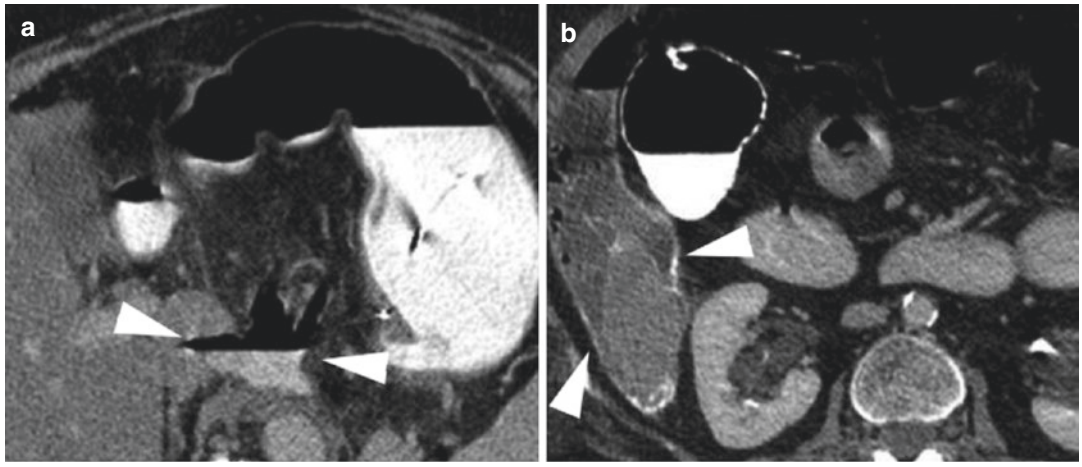

Fig. 19.8 Leak after nissen with Type 3 giant hiatal hernia repair, (**a**) shows a large irregular extraluminal collection, (**b**) contrast in the right paracolic gutter, (**c**) is an example of extraluminal fluid with air contrast levels, and (**d**) shows a drain in position. With permission from [33]

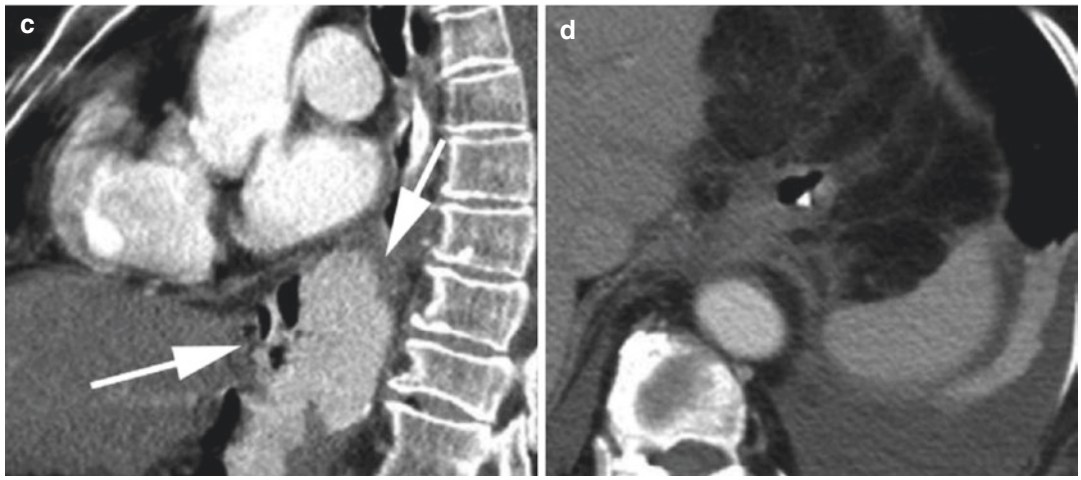

Fig. 19.8 (continued)

Conclusion

Patients with a hiatal hernia require some form of imaging preoperatively to evaluate both the size and severity of the hernia. Additional testing to evaluate the hernia may be necessary and intraoperative testing is becoming better characterized. Postoperatively patients without symptoms should not undergo imaging unless this is the practice of the provider or they become symptomatic.

References

1. Barrett NR. Hiatus hernia: a review of some controversial points. Br J Surg. 1954;42(173):231–43. https://doi.org/10.1002/bjs.18004217303.
2. Kavic SM, Segan RD, George IM, Turner PL, Roth JS, Park A. Classification of hiatal hernias using dynamic three-dimensional reconstruction. Surg Innov. 2006;13(1):49–52. https://doi.org/10.1177/155335060601300108.
3. Kohn GP, Price RR, DeMeester SR, et al. Guidelines for the management of hiatal hernia. Surg Endosc. 2013;27(12):4409–28. https://doi.org/10.1007/s00464-013-3173-3.
4. Ahmed SK, Bright T, Watson DI. Natural history of endoscopically detected hiatus herniae at late follow-up. ANZ J Surg. 2018;88(6):E544–7. https://doi.org/10.1111/ans.14180.
5. Landreneau RJ, Del Pino M, Santos R. Management of paraesophageal hernias. Surg Clin North Am. 2005;85(3):411–32. https://doi.org/10.1016/j.suc.2005.01.006.
6. Mulholland MW. Paraesophageal hernia repair: laparoscopic technique. In: Operative techniques in surgery. Wolters Kluwer; 2015. p. 136.
7. Tossier C, Dupin C, Plantier L, et al. Hiatal hernia on thoracic computed tomography in pulmonary fibrosis. Eur Respir J. 2016;48(3):833–42. https://doi.org/10.1183/13993003.01796-2015.
8. Awais O, Luketich JD. Management of giant paraesophageal hernia. Minerva Chir. 2009;64(2):159–68.
9. Litle VR, Buenaventura PO, Luketich JD. Laparoscopic repair of giant paraesophageal hernia. Adv Surg. 2001;35:21–38.
10. Mitiek MO, Andrade RS. Giant hiatal hernia. Ann Thorac Surg. 2010;89(6):S2168–73. https://doi.org/10.1016/j.athoracsur.2010.03.022.
11. Hazebroek EJ, Koak Y, Berry H, Leibman S, Smith GS. Critical evaluation of a novel DualMesh repair for large hiatal hernias. Surg Endosc. 2009;23(1):193–6. https://doi.org/10.1007/s00464-008-9772-8.
12. White BC, Jeansonne LO, Morgenthal CB, et al. Do recurrences after paraesophageal hernia repair matter?: Ten-year follow-up after laparoscopic repair. Surg Endosc. 2008;22(4):1107–11. https://doi.org/10.1007/s00464-007-9649-2.
13. Parameswaran R, Ali A, Velmurugan S, Adjepong SE, Sigurdsson A. Laparoscopic repair of large paraesophageal hiatus hernia: quality of life and durability. Surg Endosc. 2006;20(8):1221–4. https://doi.org/10.1007/s00464-005-0691-7.
14. Oelschlager BK, Pellegrini CA, Hunter J, et al. Biologic prosthesis reduces recurrence after laparoscopic paraesophageal hernia repair: a multicenter, prospective, randomized trial. Ann Surg. 2006;244(4):481–90. https://doi.org/10.1097/01.sla.0000237759.42831.03.

15. Jobe BA, Aye RW, Deveney CW, Domreis JS, Hill LD. Laparoscopic management of giant type III hiatal hernia and short esophagus. Objective follow-up at three years. J Gastrointest Surg Off J Soc Surg Aliment Tract. 2002;6(2):181–8.; discussion 188. https://doi.org/10.1016/s1091-255x(01)00067-1.
16. Cardile AP, Heppner DS. Gastric volvulus, Borchardt's triad, and endoscopy: a rare twist. Hawaii Med J. 2011;70(4):80–2.
17. Farber BA, Lim IIP, Murphy JM, Price AP, Abramson SJ, La Quaglia MP. Gastric volvulus following left pneumonectomy in an adolescent patient. J Pediatr Surg Case Rep. 2015;3(10):447–50. https://doi.org/10.1016/j.epsc.2015.08.014.
18. Eren S, Gümüş H, Okur A. A rare cause of intestinal obstruction in the adult: Morgagni's hernia. Hernia J Hernias Abdom Wall Surg. 2003;7(2):97–9. https://doi.org/10.1007/s10029-002-0099-4.
19. Farhat A, Towle D. Incidental hiatal hernia on chest X-ray. 2018. https://doi.org/10.21980/J8KP8S.
20. Mittal SK, Awad ZT, Tasset M, et al. The preoperative predictability of the short esophagus in patients with stricture or paraesophageal hernia. Surg Endosc. 2000;14(5):464–8. https://doi.org/10.1007/s004640020023.
21. Morcos SK. Review article: effects of radiographic contrast media on the lung. Br J Radiol. 2003;76(905):290–5. https://doi.org/10.1259/bjr/54892465.
22. Oelschlager BK, Pellegrini CA, Hunter JG, et al. Biologic prosthesis to prevent recurrence after laparoscopic Paraesophageal hernia repair: long-term follow-up from a Multicenter, prospective, Randomized Trial. J Am Coll Surg. 2011;213(4):461–8. https://doi.org/10.1016/j.jamcollsurg.2011.05.017.
23. Granderath FA, Schweiger UM, Pointner R. Laparoscopic antireflux surgery: tailoring the hiatal closure to the size of hiatal surface area. Surg Endosc. 2007;21(4):542–8. https://doi.org/10.1007/s00464-006-9041-7.
24. Koch OO, Schurich M, Antoniou SA, et al. Predictability of hiatal hernia/defect size: is there a correlation between pre- and intraoperative findings? Hernia J Hernias Abdom Wall Surg. 2014;18(6):883–8. https://doi.org/10.1007/s10029-012-1033-z.
25. Bradley DD, Louie BE, Farivar AS, Wilshire CL, Baik PU, Aye RW. Assessment and reduction of diaphragmatic tension during hiatal hernia repair. Surg Endosc. 2015;29(4):796–804. https://doi.org/10.1007/s00464-014-3744-y.
26. Eren S, Ciriş F. Diaphragmatic hernia: diagnostic approaches with review of the literature. Eur J Radiol. 2005;54(3):448–59. https://doi.org/10.1016/j.ejrad.2004.09.008.
27. Shih WJ, Milan PP. Gastric-emptying scintigraphy of type III hiatal hernia: a case report. J Nucl Med Technol. 2005;33(2):83–5.
28. Khouzam RN, Akhtar A, Minderman D, Kaiser J, D'Cruz IA. Echocardiographic aspects of hiatal hernia: a review. J Clin Ultrasound JCU. 2007;35(4):196–203. https://doi.org/10.1002/jcu.20312.
29. Lottrup C, McMahon BP, Ejstrud P, Ostapiuk MA, Funch-Jensen P, Drewes AM. Esophagogastric junction distensibility in hiatus hernia: EndoFLIP and hiatus hernia distensibility. Dis Esophagus. 2016;29(5):463–71. https://doi.org/10.1111/dote.12344.
30. Su B, Novak S, Callahan ZM, Kuchta K, Carbray J, Ujiki MB. Using impedance planimetry (EndoFLIP™) in the operating room to assess gastroesophageal junction distensibility and predict patient outcomes following fundoplication. Surg Endosc. 2020;34(4):1761–8. https://doi.org/10.1007/s00464-019-06925-5.
31. Shah A, Nguyen DT, Meisenbach LM, et al. A novel EndoFLIP marker during hiatal hernia repair is associated with short-term postoperative dysphagia. Surg Endosc. 2021. https://doi.org/10.1007/s00464-021-08817-z.
32. Turner B, Helm M, Hetzel E, Gould JC. Is that "floppy" fundoplication tight enough? Surg Endosc. 2020;34(4):1823–8. https://doi.org/10.1007/s00464-019-06947-z.
33. Devenney-Cakir B, Tkacz J, Soto J, Gupta A. Complications of Esophageal surgery: role of imaging in diagnosis and treatments. Curr Probl Diagn Radiol. 2011;40(1):15–28. https://doi.org/10.1067/j.cpradiol.2009.08.001.
34. O'Boyle CJ, Heer K, Smith A, Sedman PC, Brough WA, Royston CM. Iatrogenic thoracic migration of the stomach complicating laparoscopic nissen fundoplication. Surg Endosc. 2000;14(6):540–2. https://doi.org/10.1007/s004640000102.
35. Watson DI, de Beaux AC. Complications of laparoscopic antireflux surgery. Surg Endosc. 2001;15(4):344–52. https://doi.org/10.1007/s004640000346.
36. Moujir Sanchez A. Postoperative herniation of Nissen fundoplication. 2016. https://doi.org/10.1594/EURORAD/CASE.13708.
37. Nwokedi U, Nguyen DT, Meisenbach LM, et al. Short-term outcome of routine use of EndoFLIP during hiatal hernia repair. Surg Endosc. 2021;35(7):3840–9. https://doi.org/10.1007/s00464-020-07788-x.
38. Yoo C, Levine MS, Redfern RO, Laufer I, Buyske J. Laparoscopic Heller myotomy and fundoplication: findings and predictive value of early postoperative radiographic studies. Abdom Imaging. 2004;29(6):643–7. https://doi.org/10.1007/s00261-004-0182-7.
39. Singhal T, Balakrishnan S, Hussain A, Grandy-Smith S, Paix A, El-Hasani S. Management of complications after laparoscopic Nissen's fundoplication: a surgeon's perspective. Ann Surg Innov Res. 2009;3(1):1. https://doi.org/10.1186/1750-1164-3-1.

Lumbar Hernias

20

David J. Lourié

Introduction

Primary lumbar hernias, excluding those of incisional, traumatic, or infectious etiology, are dorsal rather than ventral hernias and occur between gaps in overlapping muscle groups of the low back. These herniate through two small anatomic areas both located between the lowest rib and the iliac crest and may contain fat, and retroperitoneal or peritoneal organs and tissues. They are divided into superior lumbar hernias and inferior lumbar hernias. Radiographically these can be distinguished by their specific surrounding muscle groups, and by their proximity and relationship to bony landmarks. Cross-sectional imaging, particularly Computed Tomography (CT) of the abdomen/pelvis (not lumbar spine), is the imaging modality of choice and is generally diagnostic [1–4]. Non-contrast scans are generally sufficient, though contrast scans may be requested to more accurately delineate associated renal, vascular, or intestinal content or evaluate other patient pathology. Ultrasound when CT scanning is not available can be utilized as an aid in the diagnosis, but is operator dependent, is less accurate in delineating surrounding landmark structures, has resulted in the misdiagnosis of lumbar herniated fat as subcutaneous lipomas, and is not recommended as the imaging modality of choice. Clinically these hernias present as external lumbar masses and can occasionally be painful [5–7]. Less than 10% present with obstruction [7–10]. On physical examination, a visible and palpable bulge is usually present off midline in the mid to lower back inferior to the 12th rib or superior to the iliac crest. These usually become more prominent with Valsalva or spinal flexion. As mentioned, lumbar hernias are at times mistaken for lipomas and occasionally initially mistreated as such [11, 12].

Normal Anatomy of the Lumbar Triangles

To recognize the pathology of lumbar hernias one must first understand the normal anatomy, and the boundaries of the two potential lumbar triangle gaps (Fig. 20.1, Video 20.1).

Supplementary Information The online version contains supplementary material available at https://doi.org/10.1007/978-3-031-21336-6_20.

D. J. Lourié (✉)
Department of Surgery, Huntington Hospital, Pasadena, CA, USA

S. Docimo Jr. et al. (eds.), *Fundamentals of Hernia Radiology*,
https://doi.org/10.1007/978-3-031-21336-6_20

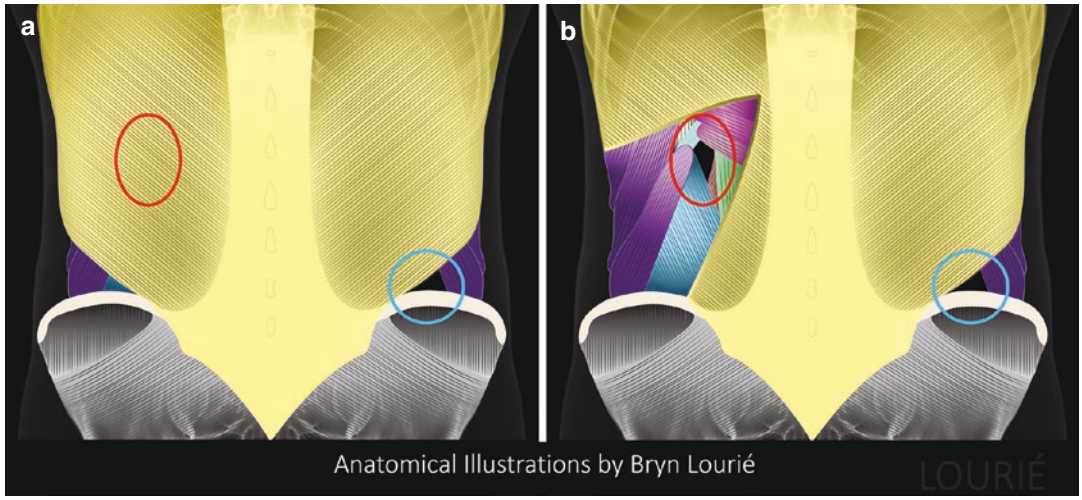

Fig. 20.1 Inferior and superior lumbar triangles. Circled in *blue*, the inferior lumbar triangle (Petit's triangle) is bordered by the iliac crest inferiorly, the external oblique muscle (*purple*) laterally, and the latissimus dorsi muscle (*yellow*) medially. Circled in *red*, the superior lumbar triangle (Grynfeltt-Lesshaft) lies deep to the latissimus dorsi in (**a**), which forms a roof or covering over it. The latissimus has been partially removed in (**b**) to show the deeper Grynfeltt-Lesshaft triangle, bordered superiorly by the 12th rib (*light blue*) and serratus posterior inferior muscle (*magenta*), medially by both the deeper quadratus lumborum (*brick red*) and the overlapping erector spinae complex (*green*), and laterally by the internal oblique muscle (*shiny blue*)

Superior Lumbar Hernias (Grynfeltt-Lesshaft Hernias)

Superior lumbar hernias, first described by Grynfeltt in 1866 [13] and soon thereafter in 1870 by Lesshaft [14], occur in the superior lumbar triangle bordered by the 12th rib and serratus posterior inferior muscle superiorly, the quadratus lumborum muscle and erector spinae muscle complex medially, and the internal oblique muscle laterally. The latissimus dorsi forms the roof of this superior triangle and the aponeurosis of the transversus abdominis forms its floor [15, 16].

Pathognomonic radiographic findings of a primary Grynfeltt-Lesshaft hernia are the relationship and proximity to the 12th rib and the appearance of the overlying latissimus dorsi forming a convex roof over the herniated contents. The author refers to this as the *latissimus balloon sign* (Figs. 20.2 and 20.3). Often these hernias are located posterior and lateral to the mid to inferior pole of the kidney which can be seen within the same axial cut (occasionally the kidney or the associated lateral conal, Gerota's or Zuckerkandl's fascias will be herniated into the defect) [17–19]. Video 20.2 details the CT interpretation of both superior and inferior lumbar hernias.

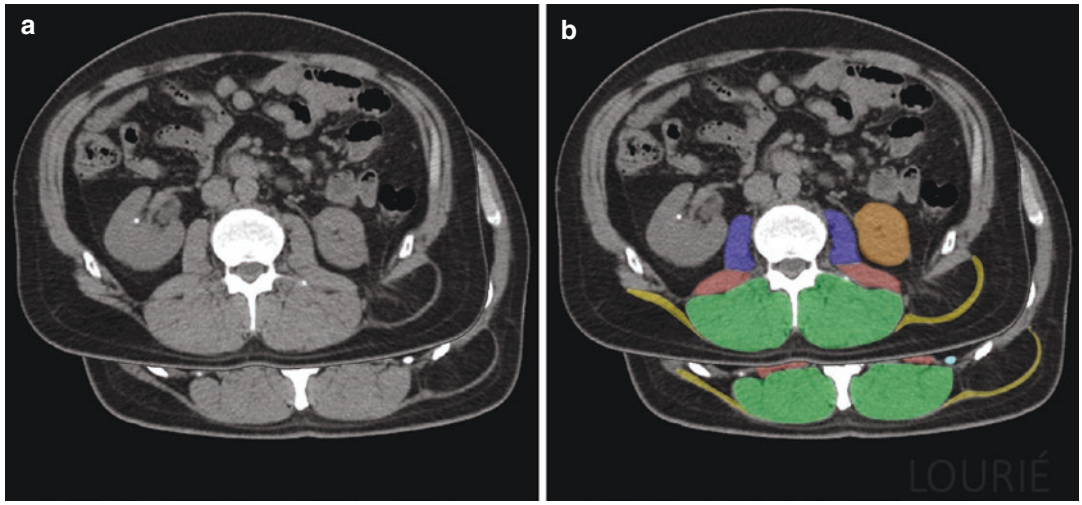

Fig. 20.2 Left-sided Grynfeltt-Lesshaft hernia. (**a**) Axial Computed Tomography (CT) abdomen cuts (*background slice more cranial*). (**b**) Same images, colored. Note the pathologic convexity of the left latissimus dorsi muscle (*yellow*) as it arches over the herniated contents (*latissimus balloon sign*) compared to the normal right latissimus contour. Also note the proximity of the kidney (*light orange*) to the hernia. Psoas muscles (*dark blue*), quadratus lumborum muscles (*red*), erector spinae muscle complex (*green*), and only in the cranial cut: the tip of 12th rib (*light blue*)

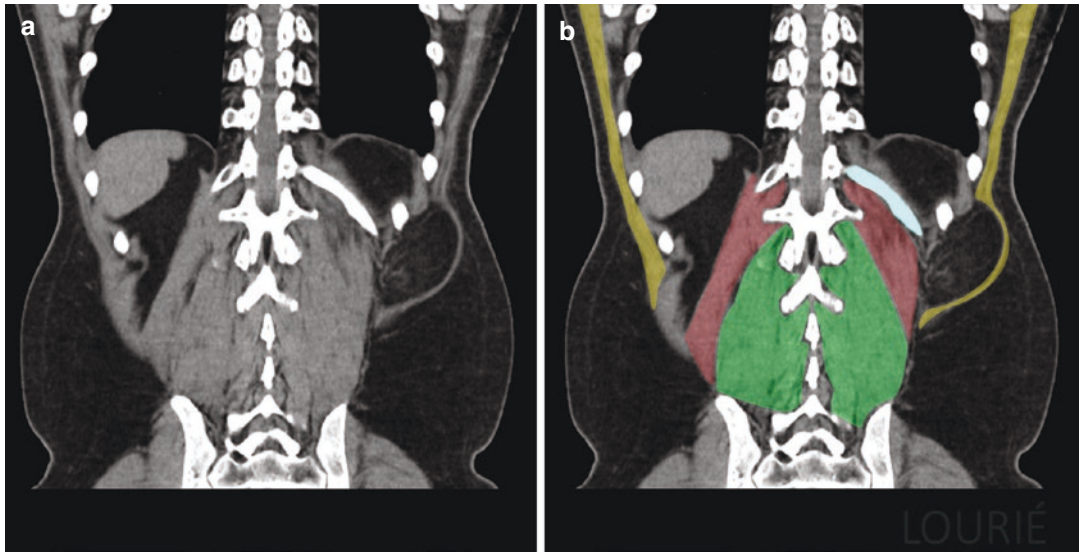

Fig. 20.3 Left-sided Grynfeltt-Lesshaft hernia. (**a**) Coronal CT abdomen cut, same patient as (Fig. 20.2) (**b**) Same image, colored. Note the hernia defect occurs inferior to the tip of the 12th rib (*light blue*). Note the pathologic convexity of the left latissimus dorsi muscle (*yellow*) as it arches over the herniated contents (*latissimus balloon sign*) compared to the normal right latissimus contour. Quadratus lumborum muscles (*red*), erector spinae muscle complex (*green*)

Inferior Lumbar Hernias (Petit's Hernias)

Inferior lumbar hernias, described by Jean Louis Petit (published posthumously in 1774, more than 90 years prior to the description of the superior lumbar triangle) [20], occur in the inferior lumbar triangle bordered by the iliac crest inferiorly, the latissimus dorsi medially, and the external oblique muscle laterally [15, 21] (Fig. 20.1). As this is a superficial defect, deep subcutaneous tissue forms the roof of the Petit's hernia. Its floor is formed by the internal oblique muscle layer as this merges into the thoracolumbar fascia. Petit's triangle represents the typical location of congenital lumbar hernias in infants (often associated with lumbocostovertebral syndrome and other developmental anomalies) [22–24]. In adults, inferior lumbar hernias are quite rare as primary acquired defects [25]. The interpreting physician should be aware that the overwhelming majority of hernias overlapping this same anatomic region will in fact be traumatic or incisional hernias [26, 27]. To distinguish a Petit's hernia look for contact with the iliac crest, herniation through a gap between the external oblique and latissimus dorsi muscle groups, and absence of an overlying latissimus dorsi (Figs. 20.4 and 20.5, Video 20.2).

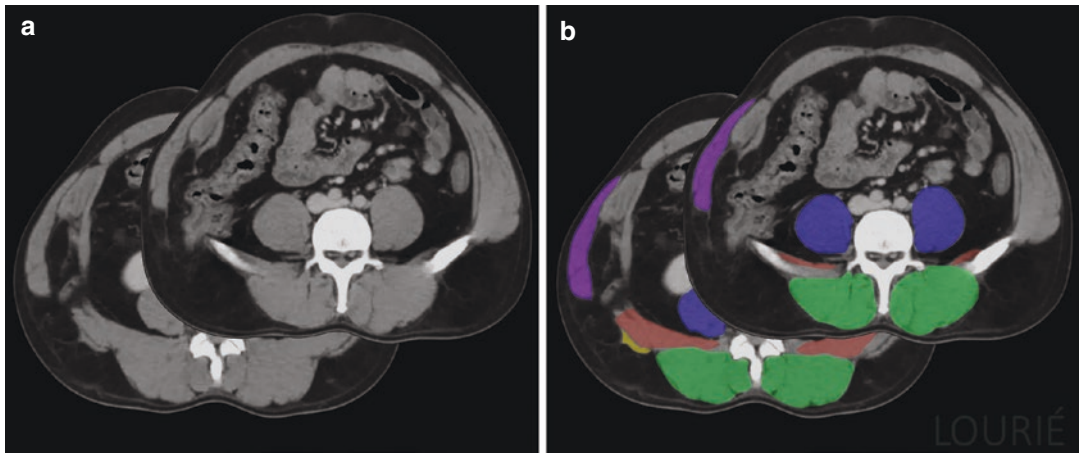

Fig. 20.4 Right-sided Petit's hernia. (**a**) Axial CT abdomen cuts (*background slice more cranial*). (**b**) Same images, colored. Note that the herniation occurs in the inferior gap between the superficial external oblique (*purple*) and latissimus (*yellow*) muscles, and contacts the iliac crest inferiorly. Psoas muscles (*dark blue*), quadratus lumborum muscles (*red*), erector spinae muscle complex (*green*). Original CT series courtesy of Dr. Nicolás Quezada

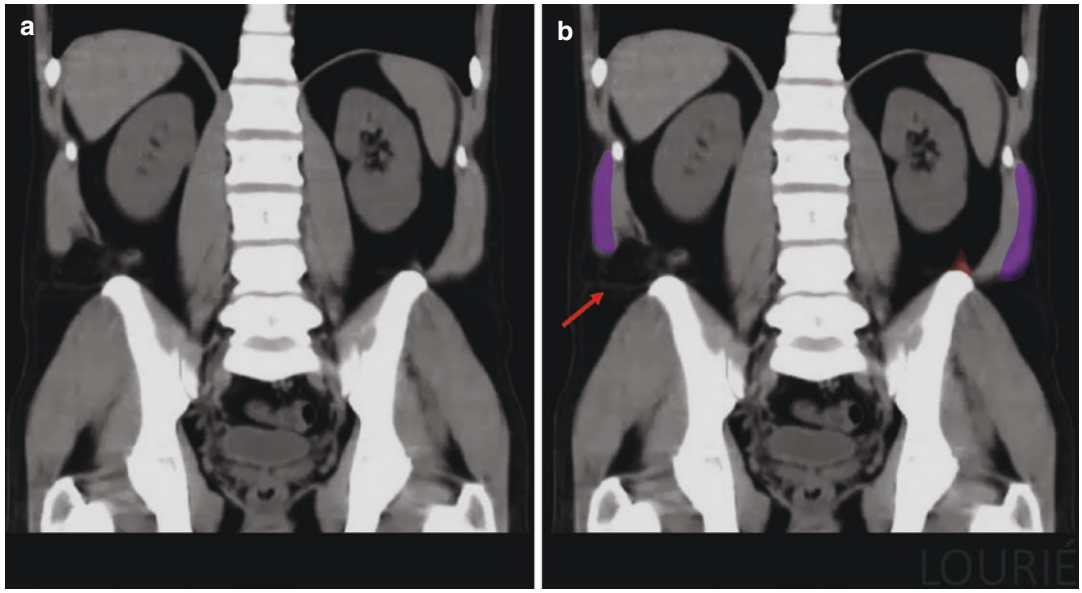

Fig. 20.5 Right-sided Petit's hernia. (**a**) Coronal CT abdomen/pelvis cut, same patient as (Fig. 20.4) (**b**) Same image, colored. Note that the herniation (*red arrow*) occurs in the gap medial to the external oblique muscle (*purple*), and contacts the iliac crest inferiorly. Original CT series courtesy of Dr. Nicolás Quezada

Importance of the Quadratus Lumborum as a Lumbar Landmark

The author proposes that radiographic interpreters and surgeons use the *quadratus lumborum muscle* as the key orienting and differentiating landmark to both lumbar hernias. As illustrated in Fig. 20.6 and Video 20.2, the lateral border of the quadratus lumborum muscle is in relative anterior-posterior alignment with that of the erector spinae at the level of a superior lumbar (Grynfeltt-Lesshaft) hernia. At the level of an inferior (Petit's) hernia, the lateral border of the quadratus lumborum muscle, in contrast, is far lateral to that of the erector spinae complex.

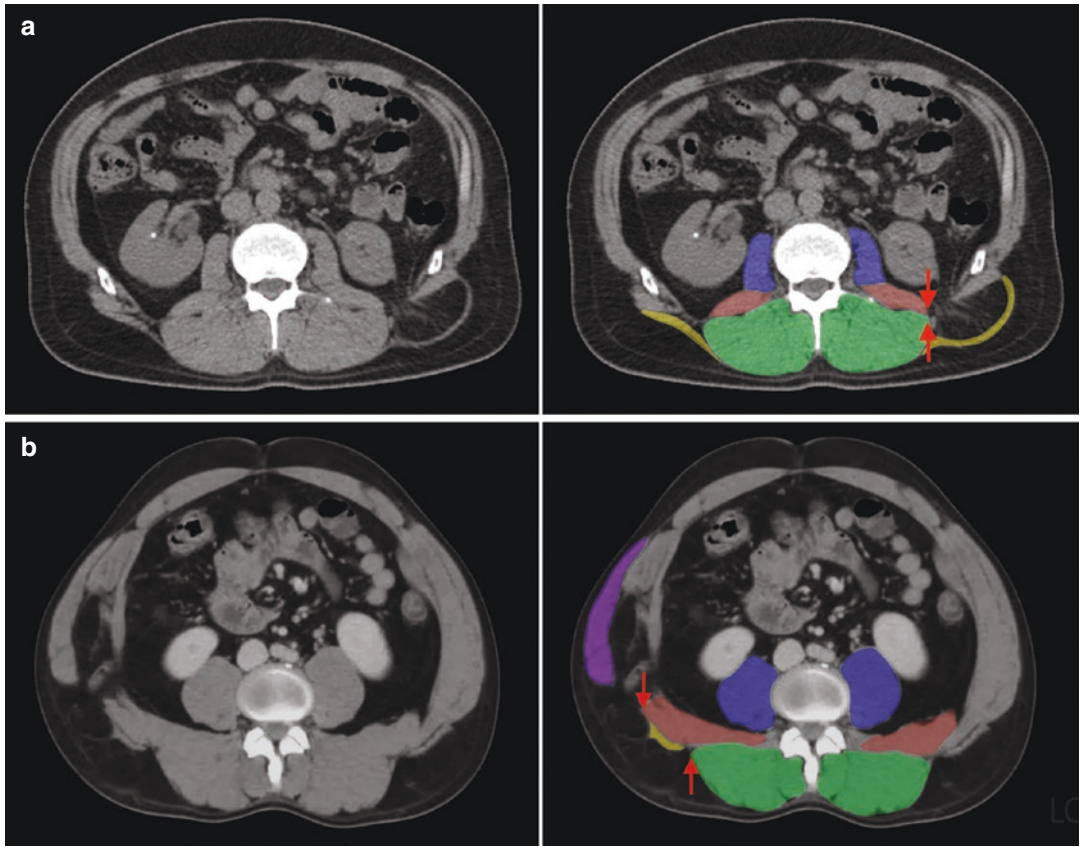

Fig. 20.6 Quadratus lumborum as orienting lumbar landmark. Axial CT abdomen cuts, with and without color highlights. Note, in (**a**) Grynfeltt-Lesshaft hernia, the lateral border of the quadratus lumborum muscle (*red*) lines up with that of the erector spinae complex (*green*) in the anterior/posterior plane (*arrows*). In (**b**) Petit's hernia, by contrast, the lateral border of the quadratus lumborum is much more lateral than that of the erector spinae complex (*arrows*). Petit's hernia image courtesy of Dr. Nicolás Quezada

Details of Importance to Surgeons

Beyond the specific location of the lumbar hernia, features that should be noted on cross-sectional imaging include the dimensional measurements of both the defect and the contents/sac/pseudosac, the organ(s) or tissue(s) forming the herniated contents, and other associated or adjacent abdominal wall hernias and pathology. In evaluating therapeutic candidacy and planning an operative repair, the surgeon will want to assess proximity and extent of any adjacent bone margin involvement, any associated muscular atony (more typical of incisional hernias), evidence of prior mesh if a recurrence, the anticipated area available for appropriate therapeutic mesh overlap, and the degree of surrounding adiposity.

Additional details which may or may not be apparent to the radiographic interpreter that are important to the surgeon include a history of specific prior surgery and patient medical comorbidities (including notably obesity, smoking, diabetes, coagulation, and cardiopulmonary status). Imaging studies may offer clues to some of the above, even when paramount patient history and exam findings are not available to the radiographic interpreter.

Epidemiology

Twenty percent of lumbar hernias are congenital and seen at birth or soon after, while 80% of lumbar hernias are acquired [7, 28–30]. Acquired hernias can be primary or secondary (incisional, traumatic, infectious) in etiology. Though incisional flank and lumbar hernias are not uncommon, true primary lumbar hernias are less so, making up fewer than 1% of all abdominal wall hernias [7, 27]. Primary superior lumbar (Grynfeltt-Lesshaft) hernias are much more common than primary inferior lumbar (Petit's) hernias in adults. Superior lumbar hernias are more often left sided, and seen more often in males [6, 7, 25, 28–30]. Traumatic hernias in the lumbar area more commonly affect the area crossing Petit's triangle, with those being caused by blunt force trauma, deceleration injury, and/or seat belt injury often associated with avulsion of the obliques off the iliac crest or disruption of a portion of the iliac crest itself [27, 31–33]. Bone graft harvest from the iliac crest is a well-documented precedent to incisional hernias near the inferior lumbar triangle [34, 35] (Fig. 20.7). Other operative procedures including renal surgery, spinal and vascular access, and latissimus dorsi harvesting for reconstructive flaps not uncommonly result in incisional hernias crossing the superior, inferior, or both (diffuse) lumbar areas [7, 36–39].

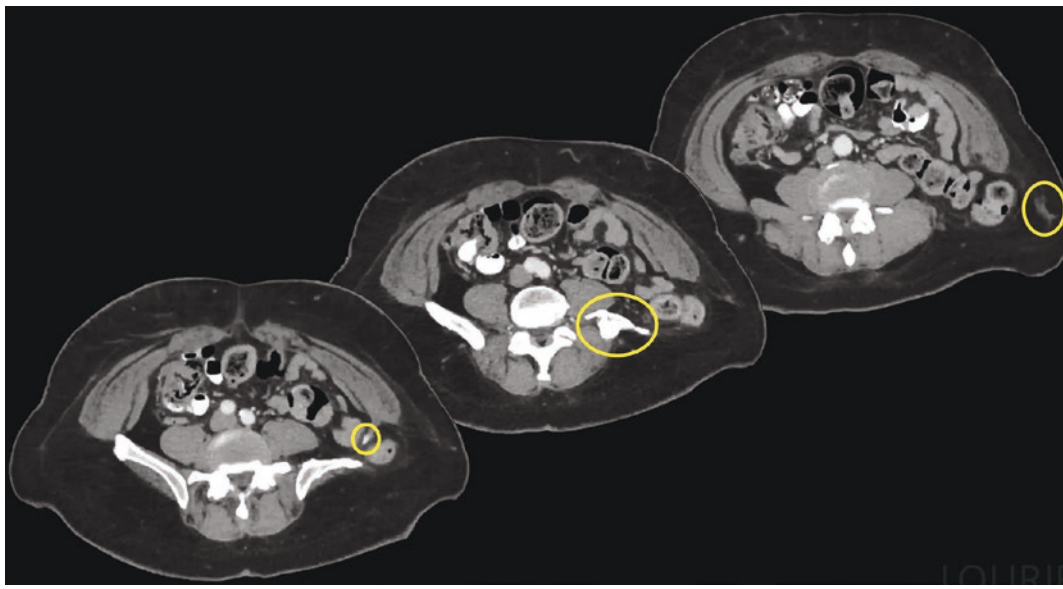

Fig. 20.7 Incisional left-sided hernia after iliac bone graft harvest. Axial CT abdomen/pelvis cuts (*background slices more cranial*). This incisional hernia crosses the area of Petit's triangle. Note encircled (*yellow*): the bone fragment attached to the internal oblique muscle, the marked deformity of the left iliac wing, and the subcutaneous stranding deep to Scarpa's fascia. These findings generally exclude the diagnosis of a primary or true Petit's hernia. Original CT series courtesy of Dr. Peter Santoro

Radiographic Findings Suggesting a Traumatic/Incisional/Infectious Etiology

The focus of this chapter is acquired primary lumbar hernias (see Chap. 18 on Flank Hernias for traumatic and incisional hernias impacting this region). Imaging clues as to traumatic, incisional, or infectious etiology are suggested by bone deformity or bone shrapnel, surrounding soft tissues fluid, stranding or density consistent with hemorrhage, hematoma, or abscess or detached adjacent oblique muscles [40] (Fig. 20.7). Other suspicious features include hernias which may cross the normal anatomic boundaries of the lumbar triangles, or the presence of adjacent muscular atrophy or eventration from sequelae of prior neuropathy. Surgically absent ipsilateral kidney, spinal deformity, hardware, or other suggestions of postoperative state in the adjacent area, may raise suspicion of a non-primary etiology. Hernias in this region which pass between ribs are intercostal, not primary lumbar, hernias.

Treatment

The treatment of lumbar hernias is surgical. Though tissue repairs (both primary and muscle flap) have been described in earlier decades, mesh repairs resulting in lower recurrence rates are now the standard of care. Mesh placement positions ranging from onlay to sublay to dual sandwich techniques (with mesh positioned in both planes at the same operation) have been reported. Open techniques with larger incisions, minimally invasive techniques (laparoscopic and robotic) using various preperitoneal approaches, and hybrid techniques combining open and minimally invasive approaches have also all been reported [15, 22, 26, 28–30, 41–45]. When possible, content reduction, primary defect closure especially when greater than 2.5 cm and wide overlap with mesh in the extraperitoneal space is generally the preferred repair [4, 25]. Thus, careful preoperative planning using the anatomy and pathology apparent in a well-performed and well-interpreted cross-sectional imaging study is crucial.

Summary

In this chapter, the *quadratus lumborum muscle* (an under-appreciated guide to the lumbar area) was presented as a key radiographic orienting and differentiating landmark to both lumbar hernias. With the insight provided in the above discussion and accompanying videos, the radiographic interpreter should be able to differentiate a primary superior lumbar hernia from an inferior lumbar hernia, even on a single axial CT cut through the hernia. In the case of a Grynfeltt-Lesshaft superior lumbar hernia, additional clues such as the *latissimus balloon sign*, and the proximity of the 12th rib and kidney to the hernia were highlighted. In a Petit's inferior lumbar hernia, confirmation of contact with the iliac crest, herniation between the external oblique and latissimus dorsi muscles, and the absence of the latissimus dorsi roof overlying the hernia were reviewed. The key imaging findings of importance to surgical planning and treatment were emphasized and should be clearly delineated in any radiographic interpretation and report concerning lumbar hernias.

References

1. Baker ME, Weinerth JL, Andriani RT, Cohan RH, Dunnick NR. Lumbar hernia: diagnosis by CT. Am J Roentgenol. 1987;148:565–7.
2. Martin J, Mellado JM, Solanas S, Yanguas N, Salceda J, Cozcolluela MR. MDCT of abdominal wall lumbar hernias: anatomical review, pathologic findings and differential diagnosis. Surg Radiol Anat. 2012;34:455–63.
3. Killeen KL, Girard S, DeMeo JH, Shanmuganathan K, Mirvis SE. Using CT to diagnose traumatic lumbar hernia. Am J Roentgenol. 2000;174:1413–5.
4. Cavallaro G, Sadighi A, Paparelli C. Anatomical and surgical considerations on lumbar hernias. Arch Surg. 2007;142:82–8.
5. Bonner CD, Kasdon SC. Herniation of fat through the lumbodorsal fascia as a cause of low-back pain. N Engl J Med. 1954;251:1102–4.
6. Zhou X, Nve JO, Chen G. Lumbar hernia: clinical analysis of 11 cases. Hernia. 2004;8:260–3.

7. Moreno-Egea A, Baena EG, Calle MC, Martínez JA, Albasini JL. Controversies in the current management of lumbar hernias. Arch Surg. 2007;142:82–8.
8. Fokou M, Fotso P, Ngowe Ngowe M, Essomba A, Sosso M. Strangulated or incarcerated spontaneous lumbar hernia as exceptional cause of intestinal obstruction: case report and review of the literature. World J Emerg Surg. 2014;9:44.
9. Ka I, Gueye ML, Thiam O, Akpo LG, Toure AO. Strangulated lumbar hernias in adults: a case report and review of the literature. Ann R Coll Surg Engl. 2016;98:160–1.
10. Teo KA, Burns E, Garcea G, Abela JE, McKay CJ. Incarcerated small bowel within a spontaneous lumbar hernia. Hernia. 2010;14:539–41.
11. Zadeh JR, Buicko JL, Patel C, Kozol R, Lopez-Viego MA. Grynfeltt hernia: a deceptive lumbar mass with a lipoma like presentation. Case Rep Surg. 2015;2015:954804.
12. Kadler B, Shetye A, Patten DK, Al-Nowfal A. A primary inferior lumbar hernia misdiagnosed as a lipoma. Ann R Coll Surg Engl. 2019;101:e96–8.
13. Grynfeltt JC. Quelques mots sur la hernie lombaire à l'occasion d'un fait observé dans le service de clinique chirurgicale de M. le professeur Bouisson. Montpellier Méd. 1866;16:329–70.
14. Lesshaft P. Die lumbalgegend in anatomisch-chirurgischer hinsicht. Arch Anat Physiol Wiss Med. 1870; 37:264–99.
15. Stamatioui D, Skandalakis JE, Skandalakis LJ, Mirilas P. Lumbar hernia: surgical anatomy, embryology, and technique of repair. Am Surg. 2009;75:202–7.
16. Loukas M, El-Zammar D, Shoja MM, Tubbs RS, Zhan L, Protyniak B, Krutoshinskaya Y. The clinical anatomy of the triangle of Grynfeltt. Hernia. 2008;12:227–31.
17. Presti JC, Narayan P. Lumbar herniation of the kidney. J Urol. 1988;140:586–7.
18. Fogarty JD, Hafron JM, Melman A. Renal obstruction caused by herniation of renal pelvis and ureteropelvic junction through superior triangle hernia (Grynfeltt hernia). Urology. 2006;67:620–1.
19. Pesce A, Puleo S. A rare case of herniated renal cyst through Grynfeltt's triangle. J Gastrointest Dig Syst. 2015;5:304.
20. Petit JL. Traité des maladies chirurgicales, et des opérations qui leur conviennent. Ouvrage posthume. Vol. 2. Paris: Didot Le Jeune; 1774. p. 256–8.
21. Loukas M, Tubbs RS, El-Sedfy A, Jester A, Polepalli S, Kinsela K, Wu S. The clinical anatomy of the triangle of Petit. Hernia. 2007;11:441–5.
22. Dowd CN. Congenital lumbar hernia at the triangle of Petit. Ann Surg. 1907;45:245–8.
23. Hancock BJ, Wiseman NE. Incarcerated congenital lumbar hernia associated with lumbocostovertebral syndrome. J Pediatr Surg. 1988;23:782–3.
24. Wakhlu A, Wakhlu AK. Congenital lumbar hernia. Pediatr Surg Int. 2000;16:146–8.
25. van Steensel S, Bloemen A, van den Hil LCL, van den Bos J, Kleinrensink GJ, Bouvy ND. Pitfalls and clinical recommendations for the primary lumbar hernia based on a systematic review of the literature. Hernia. 2019;23:107–17.
26. Hafner C, Wylie J Jr, Brush BE. Petit's lumbar hernia: repair with Marlex mesh. Arch Surg. 1963;86:180–6.
27. Netto FA, Hamilton P, Rizoli SB, Nascimento B Jr, Brenneman FD, Tien H, Tremblay LN. Traumatic abdominal wall hernia: epidemiology and clinical implications. J Trauma. 2006 Nov;61:1058–61.
28. Thorek M. Lumbar hernia. J Int Coll Surg. 1950;14:367–93.
29. Goodman EH, Speese J. Lumbar hernia. Ann Surg. 1916;63:548–60.
30. Orcutt TW. Hernia of the superior lumbar triangle. Ann Surg. 1971;173:294–7.
31. Burt BM, Afifi HY, Wantz GE, Barie PS. Traumatic lumbar hernia: report of cases and comprehensive review of the literature. J Trauma. 2004;57:1361–70.
32. Balkan M, Kozak O, Gulec B, Tasar M, Pekcan M. Traumatic lumbar hernia due to seat belt injury: case report. J Trauma. 1999;47:154–5.
33. Esposito TJ, Fedorak I. Traumatic lumbar hernia: case report and literature review. J Trauma. 1994;37:123–6.
34. Stevens KJ, Banuls M. Iliolumbar hernia following bone grafting. Eur Spine J. 1994;3:118–9.
35. Velchuru VR, Satish SG, Petri GJ, Sturzaker HG. Hernia through an iliac crest bone graft site: report of a case and review of the literature. Bull Hosp Jt Dis. 2006;63:166–8.
36. Osman T, Emam A, Farouk A, ElSaeed K, Tawfeek AM, AbuHalima A. Risk factors for the development of flank hernias and bulges following surgical flank approaches to the kidney in adults. Arab J Urol. 2018;16:453–9.
37. Moon HK, Dowden RV. Lumbar hernia after latissimus dorsi flap. Plast Reconstr Surg. 1985;75:417–9.
38. Varban O. Lumbar hernia after breast reconstruction. Int J Surg Case Rep. 2013;4:869–71.
39. Chatterjee S, Nam R, Fleshner N, Klotz L. Permanent flank bulge is a consequence of flank incision for radical nephrectomy in one half of patients. Urol Oncol. 2004;22:36–9.
40. Faro SH, Racette CD, Lally JF, Willis JS, Mansoory A. Traumatic lumbar hernia: CT diagnosis. Am J Roentgenol. 1990;154:757–9.
41. Heniford BT, Iannitti DA, Gagner M. Laparoscopic inferior and superior lumbar hernia repair. Arch Surg. 1997;132:1141–4.
42. Meinke AK. Totally extraperitoneal laparoendoscopic repair of lumbar hernia. Surg Endosc. 2003;17:734–7.
43. Moreno-Egea A, Alcaraz AC, Cuervo MC. Surgical options in lumbar hernia: laparoscopic versus open repair. A long-term prospective study. Surg Innov. 2013;20:331–44.
44. Bigolin AV, Rodrigues AP, Trevisan CG, Geist AB, Coral RV, Rinaldi N, Coral RP. Petit lumbar hernia-a double-layer technique for tension-free repair. Int Surg. 2014;99:556–9.
45. Beffa LR, Margiotta AL, Carbonell AM. Flank and lumbar hernia repair. Surg Clin North Am. 2018;98:593–605.

Spigelian Hernia

21

Allie E. Steinberger and Sara E. Holden

Introduction

Spigelian hernias are exceedingly rare with an incidence ranging from 0.12–2.4% of all abdominal wall hernias [1]. They result from a defect in the Spigelian fascia which is composed of the transversus abdominis and internal oblique aponeuroses. Anatomically, the aponeurosis lies lateral to the rectus muscle and medial to the linea semilunaris, where the external oblique becomes the anterior rectus sheath. It extends longitudinally from the ninth rib to the pubic tubercle. A congenital or acquired weakening in this fascia permits deeper intra-abdominal contents such as preperitoneal fat, peritoneum, or intra-abdominal organs to protrude through the transversus abdominis aponeurosis and in most cases, the internal oblique aponeurosis as well. However, Spigelian hernias do not penetrate or disrupt the overlying external oblique aponeurosis, which often makes them diagnostically challenging to ascertain on physical exam. While these hernias can occur anywhere along the Spigelian aponeurosis, 90% arise inferior to the arcuate line in the "Spigelian hernia belt." The belt is approximately 6 cm in length and located between horizontal lines drawn just distal to the umbilicus cranially—where the linea semilunaris bisects the arcuate line—and at the anterior superior iliac spines (i.e., horizontal interspinous plane) caudally. The increased incidence of herniation in this region has been attributed to multiple factors including the absence of posterior sheath below the arcuate line, the parallel interdigitation of the contributing fascial layers at this level, and the Spigelian fascia being penetrated and weakened by the inferior epigastric vessels [2–5]. A schematic of the relevant abdominal wall anatomy for Spigelian hernias is shown in Fig. 21.1.

The risk factors for Spigelian hernias are similar to those associated with the development of other types of abdominal wall hernias. Perhaps the most recognized is abdominal wall strain secondary to sustained increases in intra-abdominal pressure. Causes include, but are not limited to, marked obesity, multiparity, chronic cough, heavy lifting, and ascites. Additionally, there are a number of predisposing conditions that inherently attenuate the aponeurotic strength layer of the abdominal wall, such as connective tissue disorders, smoking, poor nutritional status, significant weight loss, and exogenous steroid use. Defects in the Spigelian fascia can also occur in the setting of trauma or previous abdominal sur-

Supplementary Information The online version contains supplementary material available at https://doi.org/10.1007/978-3-031-21336-6_21.

A. E. Steinberger · S. E. Holden (✉)
Department of Surgery, Washington University in St. Louis, St. Louis, MO, USA
e-mail: allie.steinberger@wustl.edu; holdensara@wustl.edu

S. Docimo Jr. et al. (eds.), *Fundamentals of Hernia Radiology*,
https://doi.org/10.1007/978-3-031-21336-6_21

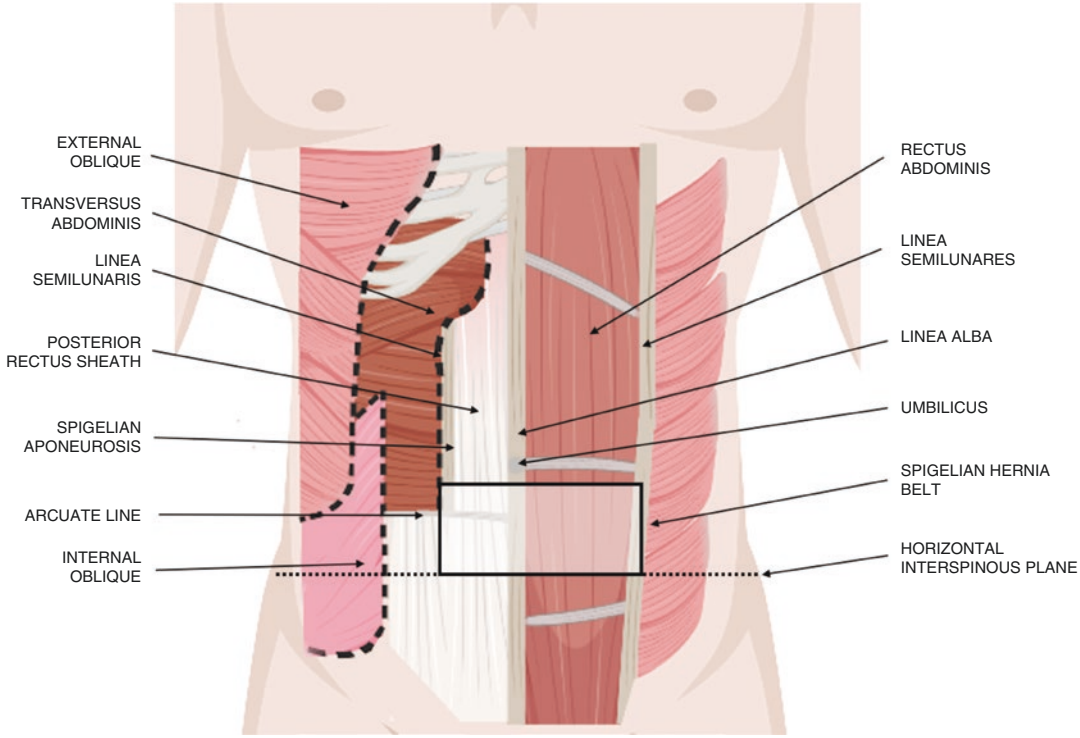

Fig. 21.1 Schematic illustration showing the pertinent abdominal wall anatomy

gery (e.g., drain placement, laparoscopic port sites, peritoneal dialysis catheters, and previous stomas). While the literature reports that nearly 50% of patients with Spigelian hernias have had previous abdominal surgery, there remains some debate as to whether these should be classified as true primary Spigelian hernias or secondary lateral incisional hernias. Certainly, this is an important distinction given the proven differences in patient complexity and postoperative morbidity between the groups [6, 7].

The interparietal nature and vague symptomatology of Spigelian hernias make them particularly difficult to identify on history and physical exam alone. When these hernias are suspected but clinically occult, various imaging studies have proven to be valuable diagnostic adjuncts. Ultrasonography (US) allows for an inexpensive, noninvasive, and dynamic assessment of the soft tissues of the abdominal wall. Though it is the preferred first-line imaging modality for Spigelian hernias, its accuracy is somewhat limited by operator dependency and body habitus. Computed tomography (CT) has the highest sensitivity and positive predictive value among radiologic investigations. It also gives clinicians the opportunity to visualize important anatomy and diagnose any concomitant intra-abdominal pathology. The major disadvantage of CT is the exposure to ionizing radiation. Magnetic resonance imaging (MRI) is a more costly option without much-added benefit. While historically herniography has been utilized in the setting of Spigelian hernias, it has largely fallen out of favor given the risk of visceral organ injury and potential allergic reaction to the injected contrast medium. Lastly, when a definitive diagnosis remains elusive, some surgeons will opt to proceed straight to laparoscopy which permits real-time identification of any hernia defects along with immediate surgical repair.

Patient Selection

Spigelian hernias generally occur in the fourth to seventh decades of life, though there are rare reports of congenital Spigelian hernias in the pediatric population. The male-to-female ratio is negligible at 1:1.18, and the majority are unilateral with a slight predominance on the right side [8–10]. There are a few notable comorbidities that confer an increased risk of developing a Spigelian hernia including chronic obstructive pulmonary disorder, collagen disorders such as Ehlers-Danlos, ascites, and morbid obesity.

While there is a diverse range of symptom patterns, the most common presentation among patients is intermittent lower abdominal pain with or without a reducible, palpable mass along their side. This pain is typically postural, worse when standing, and reproducible during provocative maneuvers such as Valsalva. As previously described, the physical exam does not reliably reveal a discrete bulge as the external oblique aponeurosis is often intact thus obscuring the underlying fascial defect. Identification can also be greatly confounded by obesity. Figure 21.2 shows an example of a left-sided Spigelian hernia. In the absence of a definable abnormality on clinical grounds, preoperative imaging should be performed to confirm the suspected diagnosis of Spigelian hernia.

Fig. 21.2 Clinical image of a patient with a left-sided Spigelian hernia

While the majority of patients describe a vague, indolent course, the rate of incarceration and strangulation in Spigelian hernias is quite high at 17–24% [11, 12]. As such, clinicians should maintain a high index of suspicion when confronted with a chief complaint of lateral abdominal wall pain and bulge. Definitive operative management is recommended for all Spigelian hernias upon diagnosis.

Ultrasound Scanning

The ultrasound examination of a Spigelian hernia should be performed with the patient in an upright, standing position. The study is primarily done using linear transducers with frequencies of 7–12 MHz. However, for obese patients, 3.5–5 MHz convex transducers may prove useful [12].

Diagnosis of a Spigelian hernia with ultrasonography requires a discrete understanding of the abdominal wall anatomy. The differential echogenicities of the various layers help the operator orient themselves and define the appropriate planes. At the most superficial position, skin is echogenic below which is a stratum of hypoechoic subcutaneous fat of variable thickness. Deep to the fat, the muscle layers can be identified with the paired rectus abdominis at midline and the external oblique (EO), internal oblique (IO), and transversus abdominis (TA) muscles anterolaterally. The muscles connote a medium-level echogenicity and have a discernible lamellar pattern to their fibers. Finally, there is a second layer of preperitoneal fat before peritoneum is encountered.

The abdominal wall musculature is held together by a fortified network of fascia. The aponeuroses of the anterolateral EO, IO, and TA travel medially to encase the rectus muscles as the rectus sheath. The rectus sheath consists of two layers, anterior and posterior, until the level of the arcuate line, below which the posterior leaflet disappears. The arcuate line is located approximately half of the distance from the

umbilicus to the pubic crest. The anterior and posterior rectus sheaths fuse at the midline to form the linea alba which separates the two rectus muscles. Lateral to the rectus muscles and medial to the obliques, the rectus sheath forms the vertical semilunar lines bilaterally.

A systematic approach to the sonographic examination of the abdominal wall should be performed at each evaluation, starting first with the aponeurotic borders. The linea alba should be carefully assessed from xiphoid to pubic symphysis including the umbilicus, followed by an interrogation of the semilunar lines bilaterally from costal margins to pubis. Next, attention should be turned to both inguinal regions to rule out direct and indirect inguinal as well as femoral hernias. It is also recommended to assess all previous surgical scars for the presence of incisional hernias. Any defects that are discovered should be characterized in terms of greatest dimension, contents of the hernia sac, and reducibility under transducer compression. Lastly, due to the inherent mobility of non-incarcerated hernias, the examination should be repeated during cough test and Valsalva maneuvers [12].

Spigelian hernias are confirmed sonographically by the presence of a well-defined orifice or defect along the semilunar lines or Spigelian fascia. Defects will appear as interruptions in the echo line of the aponeurosis. The majority are small, measuring less than two centimeters in diameter. Since the external oblique aponeurosis is often intact, ultrasound will demonstrate a dynamic spreading of hernia contents below the external oblique muscle or within the rectus sheath. This makes identification of the three anterolateral muscle layers crucial for diagnosis. Findings of echogenic mesentery and omentum or shadowing from air-filled bowel in the anterior abdominal wall also lend themselves to the diagnosis. Dynamic maneuvers such as the Valsalva will often show widening of the hernia orifice and greater protrusion of sac contents with narrowing and intra-abdominal recession upon relaxation. Figure 21.3 demonstrates a schematic of the pertinent abdominal wall anatomy in regards to a Spigelian hernia with the corresponding sono-anatomy side by side.

Clinical Pearls

Spigelian hernias have a highly variable clinical picture and therefore lack a characteristic set of signs and symptoms. A patient's presentation could range from asymptomatic to vague lower

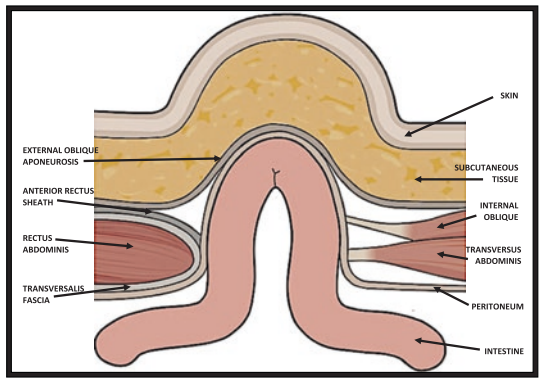

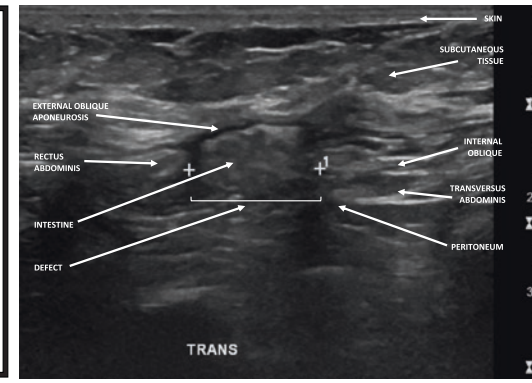

Image Acknowledgement: Vincent M. Mellnick, MD
Abdominal Imaging Division, Mallinckrodt Institute of Radiology
Washington University School of Medicine, St. Louis, MO

Fig. 21.3 Schematic illustration of a Spigelian hernia and anterior abdominal wall layers in the axial plane with the corresponding sono-anatomy side by side

abdominal pain to overt obstruction depending on the hernia contents. The sac itself is typically composed of extraperitoneal fat and peritoneum with or without abdominal viscera. Reports of various organs found within Spigelian hernias include omentum, small bowel, colon, stomach, bladder, appendix, ovaries, and testes. Infrequently, a Richter-type Spigelian hernia may be seen where the antimesenteric border of the intestine protrudes through the defect. The diagnostic uncertainty of Spigelian hernias is further exacerbated by subtle or even absent findings on physical exam. Spigelian hernias are considered interparietal or interstitial, meaning the defect and its contents spread along the planes between the oblique musculature making a bulge difficult to detect. Only half of the patients will actually have a lump along the lateral abdominal wall on inspection or palpation thus requiring a strong clinical suspicion to diagnose accurately. The differential diagnosis of a Spigelian hernia is broad. Consideration should be given both to abdominal wall lesions (benign and malignant neoplasms, rectus sheath hematoma, spontaneous rectus muscle rupture, seromas, granulomas, other abdominal wall, or high groin hernias) as well as intra-abdominal pathologies (appendicitis, diverticulitis, Meckel's diverticulum, gallbladder disease, intermittent bowel obstruction, ovarian cysts, abscesses, tumor implants). Certainly, in older patients with intermittent pain or swelling in the ventrolateral abdominal wall in the setting of increased intra-abdominal pressure or previous surgery, the concern for Spigelian hernia should be high.

If a Spigelian hernia is suspected but not confirmed on physical exam, additional radiographic investigations are warranted given the high incidence of incarceration. Owing to its relative accuracy, inexpensive cost, low risk, and lack of radiation exposure, ultrasonography should be performed first line in the majority of cases. For those in whom ultrasound is equivocal, CT scan should be obtained next. It is recommended that the CT be done with oral contrast as it provides better visualization of the bowel contour. Figures 21.4 and 21.5 demonstrate CT findings of right and left-sided Spigelian hernias, respectively. Lastly, if both US and CT are negative, MRI can be a valuable imaging modality for visualizing any soft tissue abnormalities in the ventral abdominal wall.

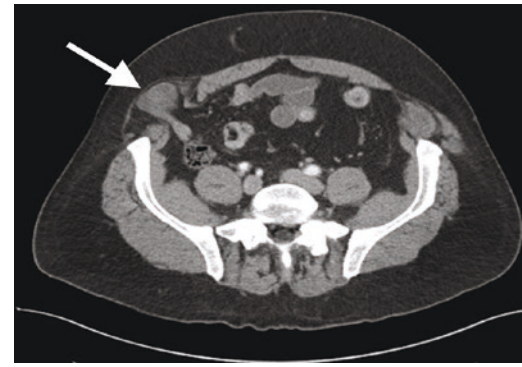

Fig. 21.4 CT scan of a right Spigelian hernia causing a partial small bowel obstruction. The hernia was reduced at the bedside and the patient underwent a semi-elective minimally invasive hernia repair with mesh

Fig. 21.5 CT scan of a small, fat-containing left Spigelian hernia in an elderly patient with an extensive surgical history. This was repaired in an open onlay fashion with mesh

It is critical to understand the sonographic signs of strangulation. Findings indicative of compromised visceral contents include a thickened hernia sac and bowel wall, diminished or absent blood flow, and lack of normal peristaltic movement. Failure to recognize incarcerated and strangulated bowel can cause delay of definitive surgical intervention leading to increased morbidity and mortality. While the operative approach (minimally invasive vs. open, primary vs. mesh) should be determined on a case-by-case basis, long-term outcomes are excellent with low rates

of recurrence and complications across repairs. Video 21.1 demonstrates a robotic preperitoneal repair of a right-sided Spigelian hernia with mesh.

Literature Review

While Spigelian hernias comprise only 0.12–2.4% of all abdominal wall hernias, they confer a 17–24% risk of incarceration, strangulation, and obstruction. As such, identification is the indication for operative intervention. The literature is punctuated with the numerous diagnostic challenges associated with this type of hernia in particular. Only half are diagnosed preoperatively [13, 14]. Furthermore, in one series, nearly 50% of patients who underwent hernia repair on the basis of clinical examination alone had no defect present. As such it is strongly recommended that clinicians utilize imaging adjuncts to optimize their diagnostic yield prior to surgery.

A few reports have attempted to characterize the true sensitivity and specificity of the common imaging modalities used in association with Spigelian hernias. In these reports, neither US nor CT had 100% sensitivity. Namely, there were a number of false negative scans in patients who ultimately went on to have clear evidence of a Spigelian hernia at the index operation. It should be noted though, that most of these false negatives were from the earliest time points in the retrospective review periods when imaging was less accurate and Spigelian hernias were less of a consideration. As far as correlation with operative findings, CT has the highest sensitivity and positive predictive value (PPV) at 100%. Ultrasound has a sensitivity of 90% and a PPV of 100%; the slight inferiority is attributable to user dependence and body habitus [15]. These were both markedly better than the clinical exam alone, which had a sensitivity of 100% (only if a palpable bulge was present) and a PPV of 36%.

Upon review of the literature, there are notable accounts of extensive, noninvasive radiologic workups failing to provide a conclusive diagnosis of Spigelian hernia. In light of this, several case reports and series have gone on to describe the beneficial use of laparoscopy in this setting [16]. This minimally invasive surgical technique permits a thorough, real-time assessment of the entire intra-abdominal cavity allowing for localization of hernia defects, identification of contemporaneous pathologies (including occult bilaterality), and definitive repair [17]. These findings are further reinforced by the only prospective trial to directly compare open versus laparoscopic repair of Spigelian hernias [18]. This study concluded that laparoscopy led to statistically significant reductions in both morbidity and hospital stay with no difference in recurrence rate at a mean follow-up of 3.4 years. Moreover, a minimally invasive approach could be safely performed on an outpatient basis, similar to other types of laparoscopic ventral hernia repairs. With diagnosis being the primary indication for repair, the literature supports the use of laparoscopy as a feasible and effective way to both diagnose and treat Spigelian hernias [19, 20].

Conclusion

Spigelian hernias comprise a rare subtype of ventral hernia. They are the consequence of congenital or acquired defects in the fascial layer bound by the rectus muscle and the linea semilunaris. These hernias present a diagnostic challenge as an intact external oblique aponeurosis often precludes frank protrusion at the most superficial layers of the abdominal wall. As with other hernias, predisposing conditions include those of increased intra-abdominal pressure and decreased connective tissue tensile strength. While their onset is often insidious and symptomatology highly variable, Spigelian hernias confer a high risk of incarceration and strangulation. As such, imaging is often necessary for diagnostic confirmation, starting first with US and progressing to CT or MRI if findings are equivocal. Sonographic evidence of disruption along the semilunar lines or dynamic spreading of sac contents below the external oblique or within the rectus sheath is highly suggestive of a Spigelian hernia.

Identification is the primary indication for surgical intervention. Fortunately, both open and minimally invasive repairs of Spigelian hernias yield low rates of recurrence and peri-operative complications.

References

1. Polistina FA, Garbo G, Trevisan P, Frego M. Twelve years of experience treating Spigelian hernia. Surgery. 2015;157(3):547–50.
2. Webber V, Low C, Skipworth RJE, Kumar S, de Beaux AC, Tulloh B. Contemporary thoughts on the management of Spigelian hernia. Hernia. 2017 Jun;21(3):355–61.
3. Montes IS, Deysine M. Spigelian and other uncommon hernia repairs. Surg Clin North Am. 2003; 83:1235.
4. Skandalakis PN, Zoras O, Skandalakis JE, Mirilas P. Spigelian hernia: surgical anatomy, embryology, and technique of repair. Am Surg. 2006;72:42.
5. Stavros AT, Rapp CT. Dynamic ultrasound of hernias of groin and anterior abdominal wall. In: Rumack CM, Wilson SR, Charbonneau JW, et al., editors. Diagnostic ultrasound, vol. 1. 4th ed. Philadelphia, PA: Elsevier Mosby; 2011. p. 486–523.
6. Kroese LF, Gillion JF, Jeekel J, et al. Primary and incisional ventral hernias are different in terms of patient characteristics and postoperative complications—a prospective cohort study of 4,565 patients. Int J Surg. 2018;51:114.
7. Subramanian A, Clapp ML, Hicks SC, et al. Laparoscopic ventral hernia repair: primary versus secondary hernias. J Surg Res. 2013;181:e1.
8. Larson DW, Farley DR. Spigelian hernias: repair and outcome for 81 patients. World J Surg. 2002;26:1277–81.
9. Vos DI, Scheltinga MR. Incidence and outcome of surgical repair of Spigelian hernia. Br J Surg. 2004;91(5):640–4.
10. Houlihan TJ. A review of Spigelian hernias. Am J Surg. 1976;131:734–5.
11. Artioukh DY, Walker SJ. Spigelian herniae: presentation, diagnosis and treatment. J R Coll Surg Edinb. 1996 Aug;41(4):241–3.
12. Smereczyński A, Kołaczyk K, Lubiński J, Bojko S, Gałdyńska M, Bernatowicz E. Sonographic imaging of Spigelian hernias. J Ultrason. 2012;12(50):269–75.
13. Mittal T, Kumar V, Khullar R, et al. Diagnosis and management of Spigelian hernia: a review of literature and our experience. J Minim Access Surg. 2008;4(4):95–8. https://doi.org/10.4103/0972-9941.45204.
14. Opson RO, Davis WC. Spigelian hernia: rare or obscure? Am J Surg. 1968;116:842–6.
15. Martell EG, Singh NN, Zagorski SM, Sawyer MA. Laparoscopic repair of a Spigelian hernia: a case report and literature review. JSLS. 2004;8:269–74.
16. Light D, Chattopadhyay D, Bawa S. Radiological and clinical examination in the diagnosis of Spigelian hernias. Ann R Coll Surg Engl. 2013;95:98–100.
17. Paajanen H, Ojala S, Virkkunen A. Incidence of occult inguinal and Spigelian hernias during laparoscopy of other reasons. Surgery. 2006;140:9–12.
18. Moreno-Egea A, Carrasco L, Girela E, Martin JG, Aguayo JL, Canteras M. Open versus laparoscopic repair of spigelian hernia: a prospective randomized trial. Arch Surg. 2002;137:1266–8.
19. Sabiston DC, Townsend CM. Sabiston textbook of surgery: the biological basis of modern surgical practice. Philadelphia, PA: Elsevier; 2012.
20. Cameron JL. Current surgical therapy. 13th ed. Elsevier; 2020.

Umbilical and Epigastric Hernia

22

Jesse Bandle and Alisa M. Coker

Introduction

Umbilical and epigastric hernia are common disorders evaluated and treated by general surgeons. The prevalence of umbilical hernia has been noted to be as high as 23% in patients screened using ultrasound (US) [1]. Though studies have demonstrated that epigastric hernias are less common, accounting for only 1–5% of abdominal wall hernias, they were noted in up to 10% of subjects in an autopsy study, demonstrating a combination of underdiagnosis and the frequently asymptomatic nature of the defect [2, 3]. This group of hernias contributes a significant cost burden to our health system. In the United States, more than 350,000 ventral midline hernias are repaired every year, at least 75% of which are classified as primary umbilical or epigastric hernias at a cost of over $2.4 billion [4–6].

Umbilical hernias occur due to an inadequate closure of the orifice that transmits the umbilical cord in-utero. According to the European Hernia Society classification system, umbilical hernias are located within 3 cm inferior or superior to the umbilicus (Fig. 22.1) [6]. The inferior portion of the umbilicus is typically more protected from herniation due to the fibrotic remnants of the vitelline duct, umbilical vein, and paired umbili-

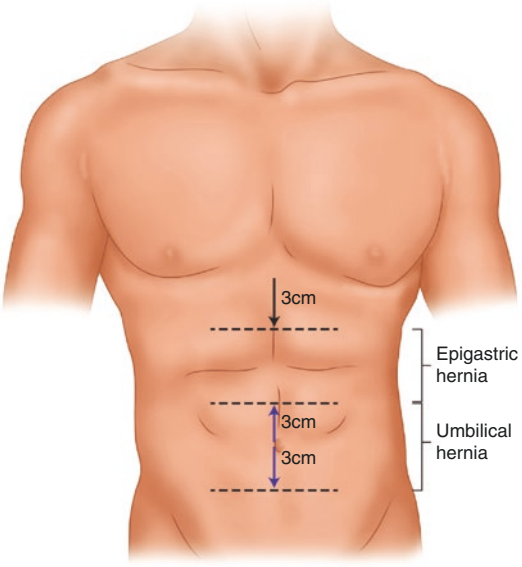

Fig. 22.1 Definition of umbilical and epigastric hernias based on the European Hernia Society classification system [6]

Supplementary Information The online version contains supplementary material available at https://doi.org/10.1007/978-3-031-21336-6_22.

J. Bandle
Department of General Surgery, Naval Medical Center San Diego, San Diego, CA, USA
e-mail: jesse.bandle.mil@mail.mil

A. M. Coker (✉)
Department of Surgery, Johns Hopkins University School of Medicine, Baltimore, MD, USA
e-mail: ACoker5@JHMI.edu

S. Docimo Jr. et al. (eds.), *Fundamentals of Hernia Radiology*,
https://doi.org/10.1007/978-3-031-21336-6_22

cal arteries. The superior portion of the umbilicus however has a thinner aponeurosis which makes it more vulnerable to the stress of increased intra-abdominal pressure over time.

The risk factors for umbilical hernia are well described and include obesity, pregnancy, ascites, and other conditions that increase intrabdominal pressure. Umbilical hernias were traditionally thought to occur far more frequently in women than men (3:1) owing to the greater risk incurred from pregnancy however more recent studies demonstrate that men are actually more likely to have an umbilical hernia repair [7, 8].

Epigastric hernias are located in the anterior midline starting 3 cm inferior to the xiphoid process and extending to 3 cm superior to the umbilicus (Fig. 22.1) [6]. These hernias are typically in the linea alba, linea semilunaris, or are associated with one of the linea transversus of the rectus sheath [9, 10]. Reported risk factors for epigastric hernias are extensive physical training or coughing (from unrelated lung pathology), obesity, steroid use, and smoking. Up to 20% of epigastric hernias are found to have multiple defects [10]. A recent large Danish population-based study demonstrated that epigastric hernias were repaired equally among men and women [11].

Several studies have attempted to elucidate the origin of epigastric hernias—which were originally believed to be congenital but likely have a more complex etiology. Focusing on cadaveric specimens, investigations have highlighted the importance of fascial patterns of decussation and the three-dimensional structured meshwork of collagen fibers in the linea alba and rectus sheath as an underlying issue [12]. Ultimately, conclusions about the pathologic origins of epigastric hernias remains unclear but seem to correspond to underlying fascial weakness in the face of sustained increased intra-abdominal pressure over time.

Umbilical hernias most commonly present with a reducible bulge near the umbilicus with varying degrees of tenderness to palpation. Epigastric hernias may also present with a bulge but commonly the presenting symptom is pain at the site of the hernia. The pain is frequently out of proportion to the relative size of the hernia, which may represent the early increased risk of incarceration of preperitoneal fat through a very small defect [10]. Both hernias can also result in acute incarceration of omentum, which can present with increased pain and overlying skin erythema. Bowel obstruction and perforation may result if incarceration and/or strangulation of digestive tract viscera occurs. It may be difficult to estimate the size of the defect with physical exam alone due to obesity, incarcerated contents, or tenderness of the hernia with palpation. Imaging of these hernias may be useful in both diagnostic capacity and in guiding surgeon choice of repair. Repair of umbilical and epigastric hernias can be achieved using an open, laparoscopic, or robotic approach depending on patient factors and surgeon experience.

Selection Criteria

Previous generations of physicians had only a history and physical exam to rely upon when diagnosing a hernia. With the increase in availability and prevalence of imaging, both computed tomography (CT) and ultrasound have become very common diagnostic tools for hernia detection and characterization. The benefit of imaging may seem clearer in more complex hernias such as recurrent or incisional hernias—these are topics addressed in chapters within this book. One could argue that the primary umbilical or epigastric hernia does not require any imaging. This may be true for some patients and we would urge the reader to use imaging selectively, rather than reflexively, when it will add value. There are many situations however where the value of imaging is present—even for this "simple" class of hernias.

It should also be noted there are many patients that may present to you from a referring provider with imaging already obtained. If you are a surgeon, we would encourage you to communicate with your referring providers about your algorithms and desire for imaging in order to avoid unnecessary imaging and cost to the patient. Even if you would not have required or obtained imaging yourself, the images can still be beneficial in your operative planning or simply in discussing the diagnosis with the patient.

There are situations where imaging may be required for diagnosis or beneficial in operative

planning. The first group of patients is that in which the diagnosis is not clear. If the clinician suspects a hernia, but is unable to definitely appreciate this on exam, imaging is useful in confirming this. This would include patients that do not tolerate an exam given tenderness produced on palpation, and those that are patients with obesity and you are simply unable to appreciate a hernia given the excessive subcutaneous fat. This diagnostic imaging can also be useful in ruling out other mimicking pathologies such as seromas, hematomas, abscesses, and desmoid tumors. While these pathologies would be discovered intraoperatively you can save the patient a potentially unnecessary procedure with the correct diagnosis preoperatively.

The second group which may benefit from imaging are those patients we would classify as complex. They may be complex because of the characteristics of the hernia itself or patient characteristics. This includes recurrent hernias, very large hernias, or those with multiple hernias suspected or appreciated on exam. The latter is also included in the third group of patients: those who benefit from imaging for preoperative planning. An example would be a patient with a larger defect, diastasis, and suspected additional hernias. Imaging allows the surgeon to plan procedure type based on the ability to close the defect and potentially address diastasis and additional defects. While some of these decisions can be made intraoperatively, the knowledge ahead of time is useful for informed consent and scheduling.

Choosing a Modality

There are several considerations when choosing a specific imaging modality. If the purpose is simply to confirm the existence of a hernia you cannot appreciate otherwise, and you do not feel more information would change your operative approach, an ultrasound will often suffice. If your main intent is to further define anatomy and determine the best approach to repair, a computed tomography will provide much more detailed information. While imaging can provide a wealth of information, the associated risks and benefits should be considered. Unfortunately, we cannot ignore the financial impact on both our healthcare system and our patients. While the specific financial impact will vary greatly, often influenced by payer contracts, ultrasound is generally a much cheaper modality than CT [13].

Patient factors may also contribute to your choice of imaging. CT is generally performed with intravenous iodinated contrast to enhance image contrast by increasing the attenuation of the x-ray beam. Given concerns of nephrotoxicity associated with this administration, the risks should be carefully considered when dealing with patients with preexisting renal insufficiency [14]. Radiation exposure should be considered as well. The actual dose is dependent on many patient and protocol factors. For a comparative understanding, a CT of the abdomen pelvis exposes the patient to about 8.7 mSv, whereas chest radiography is about 0.1 mSv [15]. While a single scan may certainly outweigh the small increased risk of cancer, the clinician should consider alternative methods in a young patient or one with an extensive imaging history as the dose is cumulative.

This chapter concentrates on ultrasound and computed tomography, as these are generally the modalities of choice for surgeons. It should be noted however that other modalities can be useful. Plain radiographs, particularly when combined with enteric contrast, can confirm the presence of a hernia with incarcerated bowel and provide information regarding the state of that bowel. They can also demonstrate a resulting bowel obstruction but they provide little information about the actual hernia defect causing the obstruction [16]. Magnetic resonance imaging (MRI) has significant drawbacks that include high cost and long scan times (30–60 min) [13, 14]. It does provide superior soft tissue contrast but this is generally not required for the purpose of identifying and defining the extent of a hernia. Additionally, most surgeons are trained on interpretation of computed tomography but not MRI. Thus, US and CT remain the preferred modalities.

If you are responsible for placing the order for the imaging, keep in mind the overall benefit of the study will also depend on appropriate communication between the ordering provider, the radiologist, and technologist performing the test.

Details provided by the ordering provider give the radiologist a clinical context that will be useful in focusing attention on relevant anatomy. They will also help explain what you are looking for, particularly important when ordering dynamic studies.

Modality: Ultrasound

The vast majority of umbilical hernias can be diagnosed by physical exam and history. There are however several situations in which US may provide additional, useful, information in diagnosis and operative planning. This is especially true for obese patients for whom the physical exam may be challenging as well as for pediatric patients where ultrasound provides improved diagnostic accuracy without the need for the ionizing radiation of a CT scan. A study by Bloemen et al. demonstrated that the addition of US to physical exam findings increased the detection of ventral hernia by more than 20% [17]. When physical exam is inconclusive, and there is a concern for differential pathology, ultrasonographic appearance may help narrow your differential (Table 22.1). Finally, the use of US in the clinic may help to improve patient understanding of their pathologic process, as they can actively participate in diagnostic elements of the exam and see their own study in real time.

The advantages of US for umbilical and epigastric hernias include:

1. Accessible exam: can even be performed during a clinic visit or at bedside.
2. No ionizing radiation.
3. The ability to scan the patient in multiple positions.
4. Incorporation of real-time dynamic maneuvers to observe the motion of hernia contents and recognize occult defects.
5. Ruling out mimicking pathology when the clinic exam is inconclusive.

While diagnosing the presence, or absence, of a hernia is the primary goal of the US examination, additional useful information can be obtained

Table 22.1 Differential diagnosis of abdominal soft tissue mass

Diagnosis	Ultrasonographic findings
Lipoma	Circumscribed hypo or hyperechoic soft tissue swelling commonly ovoid or spindle shape with interlacing echogenic fibrous bands giving a feathery appearance (Fig. 22.2)
Endometrioma	Typically following abdominal gynecologic surgery; sonographically has different shapes varying from simple cystic, complex cystic, and even solid mass-like lesions
Hematoma	A recent hematoma has a heterogenous echogenic pattern with possible layering fluid or fluid-fluid levels. Older hematomas tend to be partially absorbed or liquefied giving a cystic appearance
Abscess	Complex fluid collection with debris and low- to medium-level internal echoes. Irregular walls, marginal vascularity, and the surrounding inflammatory changes may help to differentiate abscess from hematoma
Metastasis	Melanoma, bronchogenic carcinoma, or lymphoma are most common. Appears as an ill-defined hypoechoic mass with increased internal vascularity
Neurogenic Tumors	Either schwannoma or neurofibroma—appear as well-circumscribed fusiform or ovoid swellings with tapering ends to the parent nerve
Urachal cyst	Fluid-filled, septated mass with thickened walls and faintly echogenic fluid running from the bladder superiorly to the umbilicus in the midline
Vascular malformations	Intercommunicating cystic spaces are found and may show by color Doppler either a pure venous flow (low-flow type) or evidence of arteriovenous shunting (high-flow)
Desmoid tumor	Appears as a poorly circumscribed, hypoechoic soft tissue lesion that infiltrates the abdominal wall muscles and may present internal vascularity. Lesions typically do not cross the midline

There are several masses which may be confused with a hernia on exam. Ultrasound findings as described above may be useful in discriminating these hernia-mimicking pathologies [18–22]

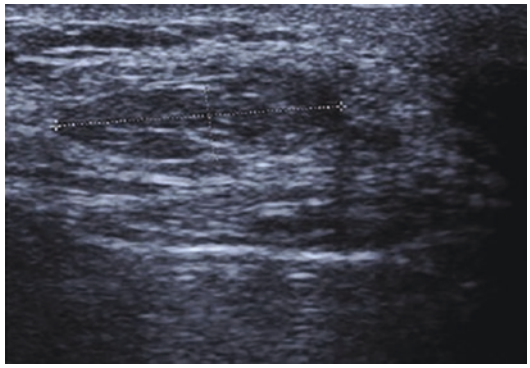

Fig. 22.2 Sonographic appearance of a subcutaneous lipoma

during the study. Identifying the composition and reducibility of herniated contents is helpful for surgical planning. Additionally, US images can clearly identify the size of the hernia defect in multiple dimensions gaining useful information for selecting a surgical approach as well as guiding the selection of mesh needed for the repair.

Gaining experience and comfort utilizing US in the clinical settings can open opportunities to expand its use in operative and perioperative settings. Estimating the thickness of the abdominal soft tissue in obese patients can assist in planning incision location as well as confirm the expected depth of Veress needle insertion for insufflation of the abdomen. Becoming facile with US can also provide the opportunity to perform adjunctive periprocedural anesthesia such as image-guided regional nerve blocks.

Ultrasound Anatomy of the Anterior Abdominal Wall

Reading an US of the abdominal wall requires a rudimentary understanding of the principles of acoustic physics. At the most basic level, an ultrasound transducer sends a sound wave through a substance and then receives the "echoes" back. The echoes contain spatial and contrast information due to changes in amplitude and the frequency shift in the returning sound waves from the interface of each tissue plane [23].

Table 22.2 Tips for viewing ultrasound images

1.	Top is always the skin side
2.	Fluid does not reflect sound waves, making it anechogenic (black)
3.	Calcified structures (such as foreign bodies) may cause acoustic shadowing
4.	Comparison with normal anatomy is useful and can help improve the identification of pathology (e.g., Normal bowel vs thickened, dilated bowel incarcerated in a hernia)

Radiologists will report on the echogenicity of the various structures in the scan; frequently referring to hyper- or hypoechoic structures which correspond to the viewer as whiter or darker images, respectively.

There are some basic guidelines that are useful in reading an US (Table 22.2). Chapter 7 of this book is dedicated to normal anatomy seen in US and is worth reviewing. In brief, US imaging of the normal anterior midline abdominal wall will demonstrate three tissue layers. The skin and subcutaneous fat appear as a thin hyperechogenic structure with variably thick underlying ovoid hypoechoic nodules separated by echogenic septa and perforating vessels. The rectus muscles have a medium echogenicity (grey) and are surrounded by the more echogenic fascia. The anterior and posterior fascial lines will join at the midline and form a thicker plane at the linea alba. The preperitoneal fat layer is typically thin and has similar echogenicity to the subcutaneous fat [24].

Abdominal wall hernias appear as a break in the otherwise smooth contour of the hyperechoic fascia and are highlighted by the mixed echogenicity of the hernia contents. Omental or preperitoneal fat may be slightly more hyperechoic and intestinal loops may have gas which will have a "dirty" acoustic shadow on US (Fig. 22.3). In healthy small bowel you expect to see symmetric, clear, and relatively thin wall layers surrounding a central lumen and peristaltic motion may be witnessed. US findings consistent with incarceration include free fluid in the hernia sac, bowel wall thickening within the hernia, fluid within the herniated loop of bowel, and dilated loops of bowel in the abdomen. Studies have demonstrated that if two or more of these findings are noted, US pro-

Fig. 22.3 Ultrasound of bowel containing umbilical hernia demonstrating "dirty" acoustic shadowing resulting from gas within loops of bowel

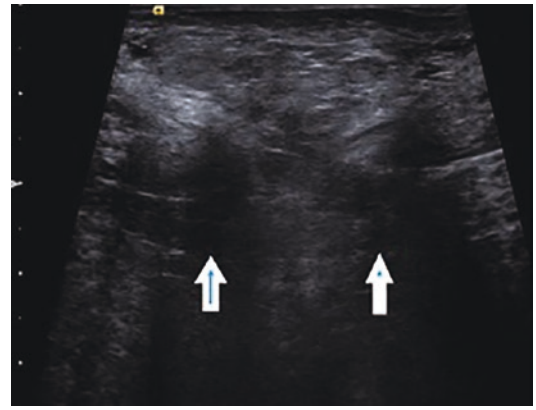

Fig. 22.4 Ultrasound of umbilical defect. Arrows indicate the edges of the fascial defect

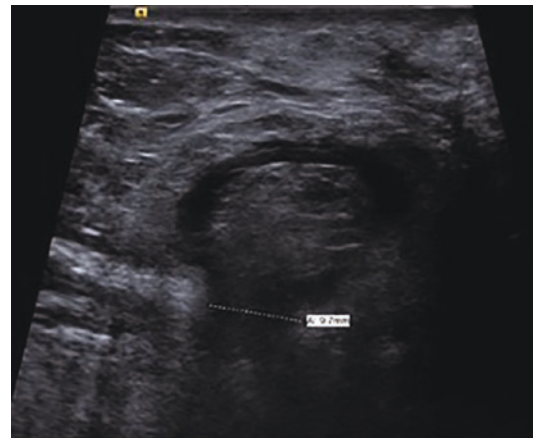

Fig. 22.5 Sagittal view of a fat-containing supraumbilical hernia. Dotted line demonstrates the craniocaudal measurement of the defect

vided 100% sensitivity and 100% specificity for the detection of incarceration [25]. The use of color doppler blood flow in the evaluation of the herniated bowel and absence of peristalsis has not demonstrated adequate sensitivity or specificity to inform clinical decision-making.

Technique for Clinic Use of Ultrasound

For most patients, a high-frequency (7-MHz or greater, 50 mm long) linear transducer is used. In obese patients however a lower frequency curved array transducer may be helpful [26, 27]. The general steps for midline abdominal ultrasound use are listed below:

1. Identify landmarks (rectus abdominus), attempting to display the medial margin of both muscles/fascia in the same image (Fig. 22.4).
2. Work cephalad to caudad along the linea alba with the probe in the transverse orientation in a slow and deliberate manner. The DASH (Dynamic Abdominal Sonography for Hernia) technique of sequential craniocaudal passes of the probe in vertical "columns" can be used as a systematic approach for US evaluation of the entire anterior abdominal as described by Beck et al. [28]. A sagittal view can help to estimate the superior/inferior dimension of the defect (Fig. 22.5; Video 22.1).
3. Repeat with the patient in a provocative posture or with Valsalva if needed (Fig. 22.6).
4. Measure the neck and assess reducibility by applying pressure manually or with the probe to a relaxed abdomen.

Begin scanning in the supine position and transition the patient to the position (standing, straining, etc.) that is associated with symptoms if the hernia is difficult to detect or you would like to better evaluate what hernia contents are present

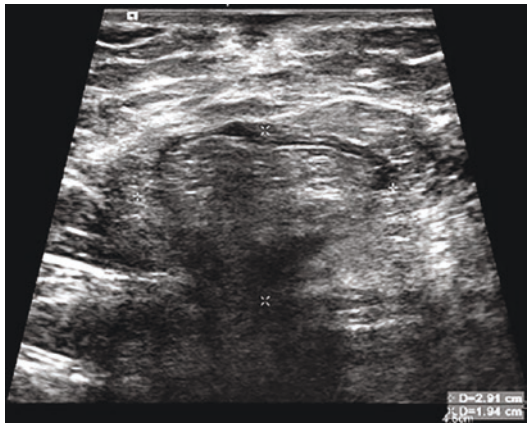

Fig. 22.6 Supraumbilical hernia with omental fat protruding through defect with Valsalva maneuver

during that activity. Care should be taken not to apply too much pressure with the transducer initially, as reduction of any hernia contents may make it more difficult to appreciate small hernias. Starting your scan distant from the obvious hernia may help to identify additional asymptomatic lesions, especially for smaller epigastric hernias that may have multiple midline defects [10]. Identification of these lesions can influence surgical approach or identify the need for a preoperative CT scan to further clarify the anatomy.

There are limitations to the use of US in umbilical and epigastric hernia diagnosis. Learning how to properly use your institution's particular machine, or multiple machines, can require an investment of time. If you are relying on the selected images from your US tech or the radiologist, you may not get all the information you would like from the exam and the images. Training in an US course can be helpful to overcome the initial learning curve and gain confidence in the equipment and technique. Close communication with your radiologist/US tech or your presence during the exam can help ensure you get the desired information from the exam.

Modality: Computed Tomography

When more detailed anatomic description of a hernia is desired, CT is the modality of choice for cost and efficiency considerations. Benefits include gathering detailed anatomic description of both the hernia and the patient's anatomy at baseline that can be useful in planning an operative repair. As with US, the clinician may also choose to obtain a CT because they were unable to appreciate the defect on exam but have high clinical suspicion. This is very common in the obese patient population where excess subcutaneous fat makes palpating a defect more difficult (Fig. 22.7).

We cannot stress the importance of looking at your own imaging enough. Additionally, we recommend reviewing the images with your patients. This can be a wonderful adjunct to informed consent as patients can gain a better understanding of their pathology and the planned repair. Our preferred approach to evaluation is to start with the axial views. Most hernias will easily be seen in this view and you can see where on the abdomen the hernia lies relative to other landmarks. From this view, we measure the width of the fascial defect. This has implications in operative planning as the size may influence whether to use mesh, help plan for appropriate size of mesh needed for adequate overlap, and determine whether a fascial closure will be possible without additional tissue manipulation such as a rectus sheath release.

Many of these umbilical hernias will be the simple "bread and butter" hernias that many clinicians see. These are a single defect right at the umbilicus and may have a narrow (Fig. 22.8) or a wide base (Fig. 22.9). The smaller hernias tend to present with pain as preperitoneal or omental fat herniates through the defect. The larger hernias may present with pain as well, but commonly the chief complaint is the more notable bulge. The imaging of many umbilical hernias however will reveal the defect is actually several defects that are directly adjacent to each other (Fig. 22.10).

Note that some radiologists, when reporting the hernia size report the size of the hernia contents. We recommend against this practice and instead stress the importance of measuring the actual fascial defect as this is what is relevant to operative planning. Figure 22.11 depicts an umbilical hernia with a small to moderate defect but a large amount of herniated omentum. This was described in the report as a 9.9 cm by 8 cm hernia, which is misleading as the actual hernia defect is only 3.5 cm wide by 3 cm long.

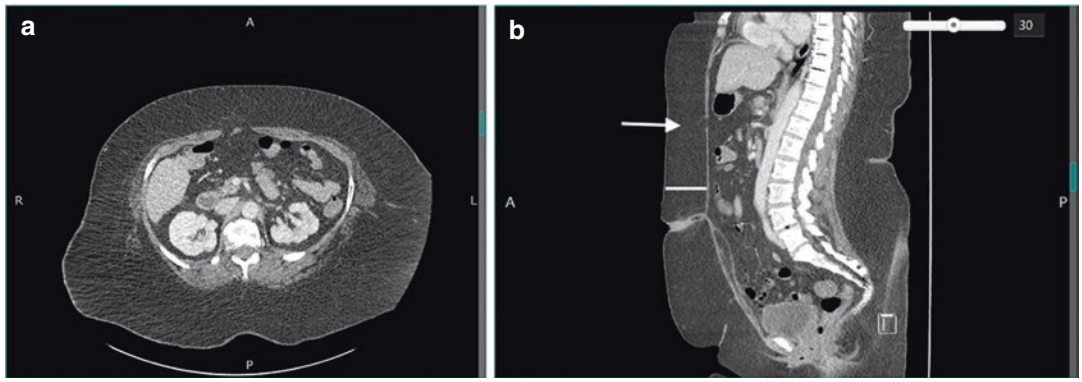

Fig. 22.7 (**a**) Axial and (**b**) sagittal views of an epigastric hernia (arrow) in a patient with obesity (BMI 50 kg/m^2). Hernia consists of multiple defects spanning 4 cm wide by 15 cm long. Subcutaneous fat (line) is 6 cm deep

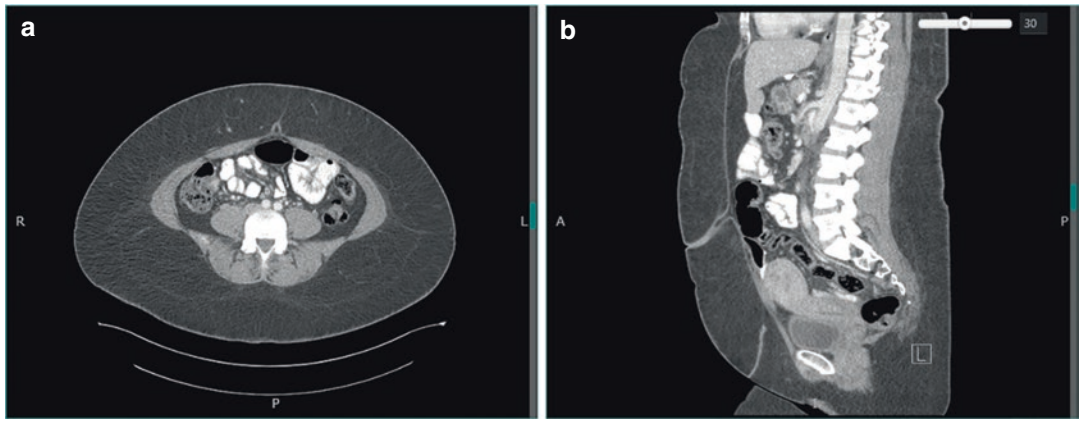

Fig. 22.8 (**a**) Axial and (**b**) sagittal view of a narrow-based umbilical hernia

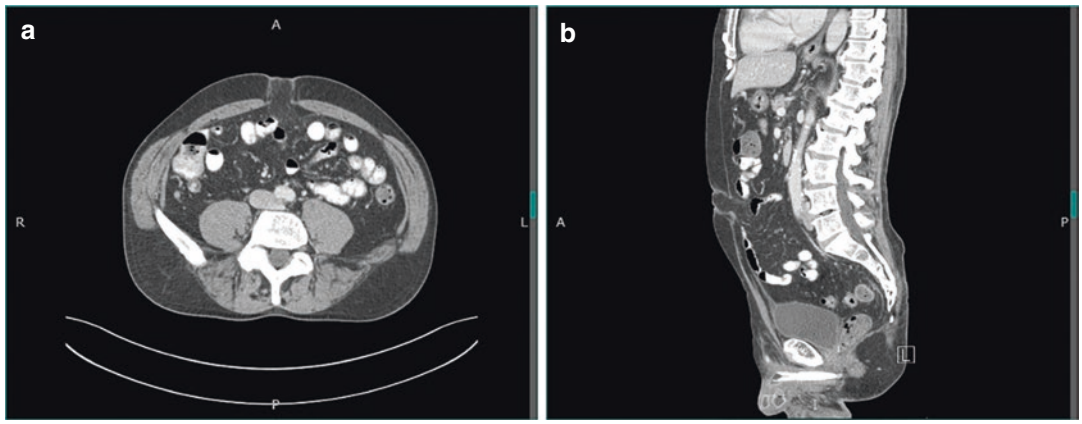

Fig. 22.9 (**a**) Axial and (**b**) sagittal view of a wide-based umbilical hernia

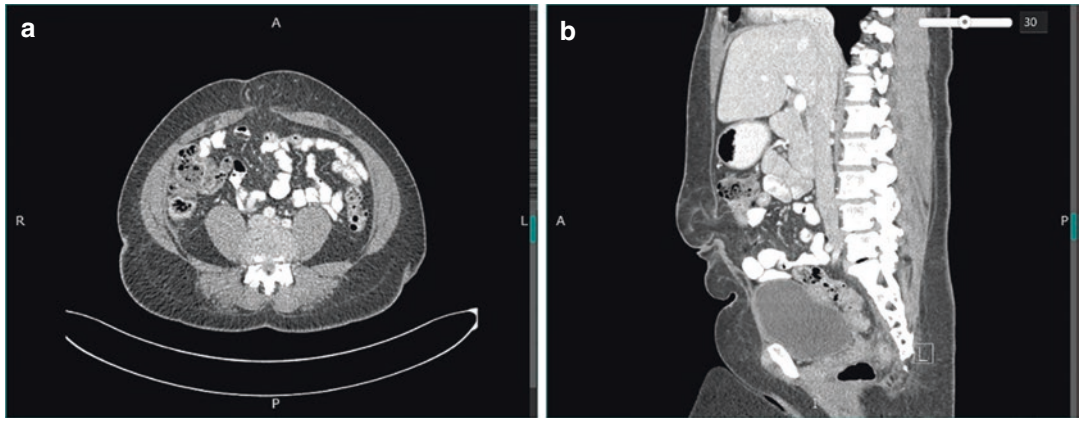

Fig. 22.10 (**a**) Axial view of a fat-containing umbilical hernia. (**b**) Sagittal view reveals two hernias are present directly adjacent to each other

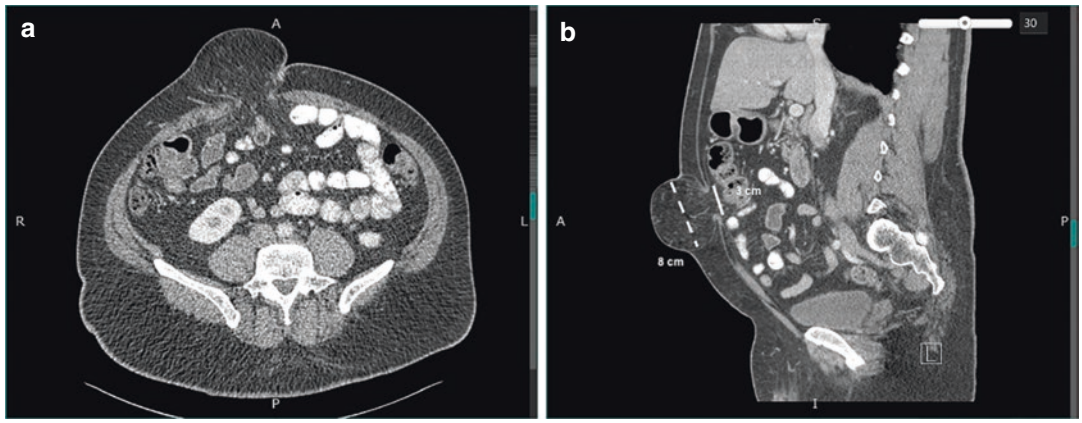

Fig. 22.11 (**a**) Axial and (**b**) sagittal views of a fat-containing umbilical hernia. The fascial defect (solid line) is only 3 cm long while the herniated omentum (dashed line) is 8 cm in diameter

The axial view will also provide a nice view of the rectus abdominus muscles. The width and position of these provide potentially useful information (Fig. 22.12). For example, if the width is diminutive, certain approaches—such as an extended view totally extraperitoneal (eTEP) repair—can be difficult given the limited space. For larger defects, the rectus width in relation to defect size can also help the surgeon recognize, preoperatively, that a separation of components may be necessary to achieve fascial closure. In normal anatomy, these muscles run parallel with minimal separation. In some patients, usually associated with prior pregnancy or obesity, these separate over time and result in a diastasis (Fig. 22.13). This is worth noting as within this weakened area the clinician may find additional, occult defects (Video 22.2). The debate over whether diastasis should be plicated at the time of hernia repair is beyond the scope of this chapter, but the reader should be aware that some do advocate this in hopes of decreasing recurrence rates and improving cosmetic outcome [29].

After reviewing the axial images, we routinely review the sagittal images. This view will allow easy measurement of the length of the fascial defect. Probably more important however this view allows for easy identification of occult defects that may have been difficult to appreciate in the axial view. Given umbilical and epigastric hernias occur frequently together, it is worth looking carefully for these (Fig. 22.14) [2]. Missing one of these hernias can lead to unnecessary reoperations for the patient.

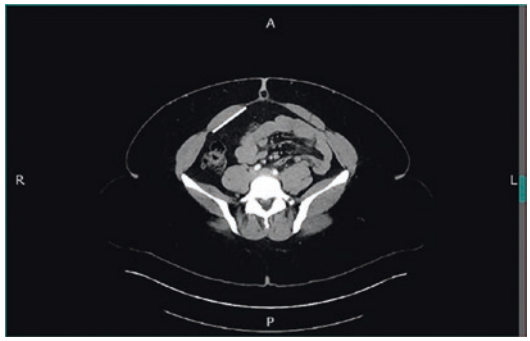

Fig. 22.12 Axial view of a small, fat-containing umbilical hernia. The width of the rectus abdominus muscle (right side highlighted with a line) can be useful in preoperative planning

Fig. 22.13 Axial view of an epigastric hernia containing fat. There is a diastasis recti present (line) measuring 6 cm in width

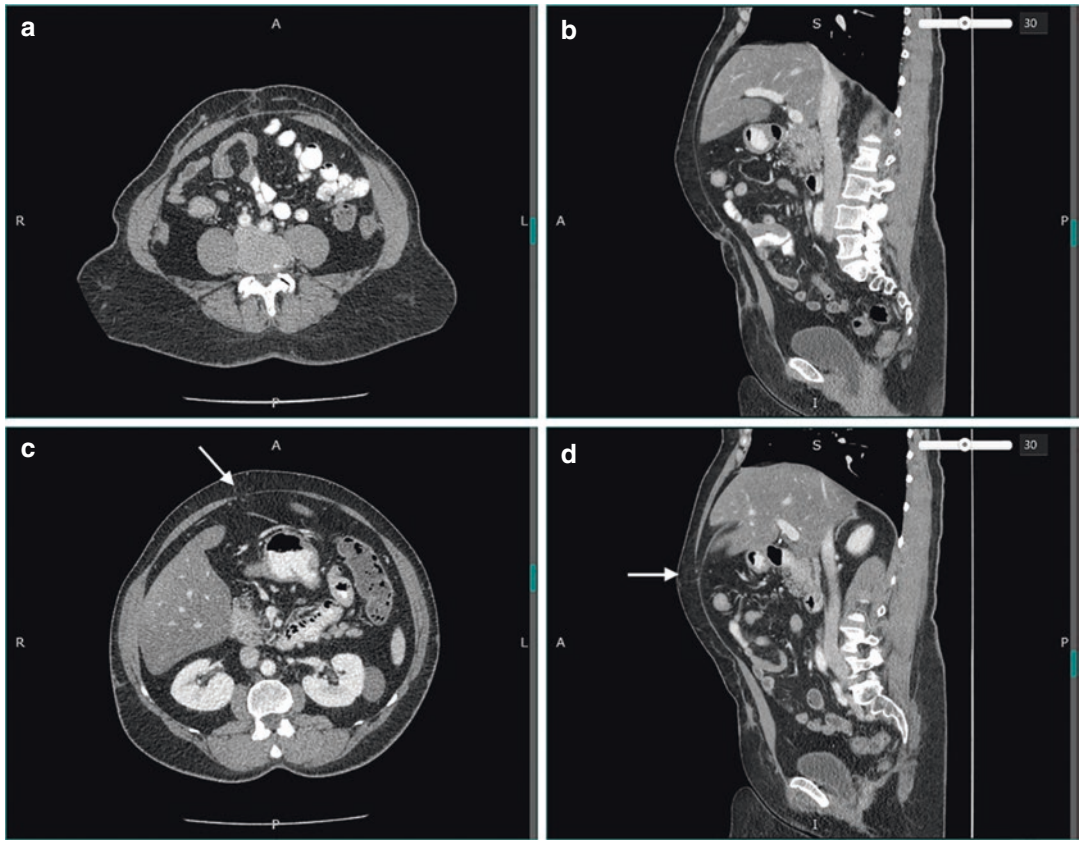

Fig. 22.14 CT images of a patient with both a tiny fat-containing umbilical and epigastric hernia. (**a**) Axial and (**b**) sagittal view demonstrating a small fat-containing umbilical hernia. (**c**) Axial view of the epigastric hernia as seen by only a tiny fascial defect (arrow). (**d**) Sagittal view of the same epigastric hernia. Herniated fat is seen protruding through the fascial defect (arrow)

Failure to carefully evaluate for a defect can lead to significant distress to the patient as well. Particularly when you add in complexity factors such as obesity and diastasis, a small defect may be overlooked. Figure 22.15 highlights the case of a patient that suffered from abdominal pain for over 3 years as her initial CT scan was interpreted as no hernia when in fact there was an umbilical hernia present within a massive diastasis. This highlights the importance of both having a high clinical suspicion for these small umbilical and epigastric hernias and for carefully reviewing images yourself and not relying only on a dictated interpretation if you are the ordering clinician.

A patient may present with a concurrent hernia in other locations as well. Figure 22.16 demonstrates a patient that presented with an umbilical hernia and CT demonstrated both the umbilical hernia and a fat-containing right inguinal hernia. Knowing about these ahead of time allows the surgeon to offer a concurrent repair and the approach may be influenced by knowing both hernias need to be addressed.

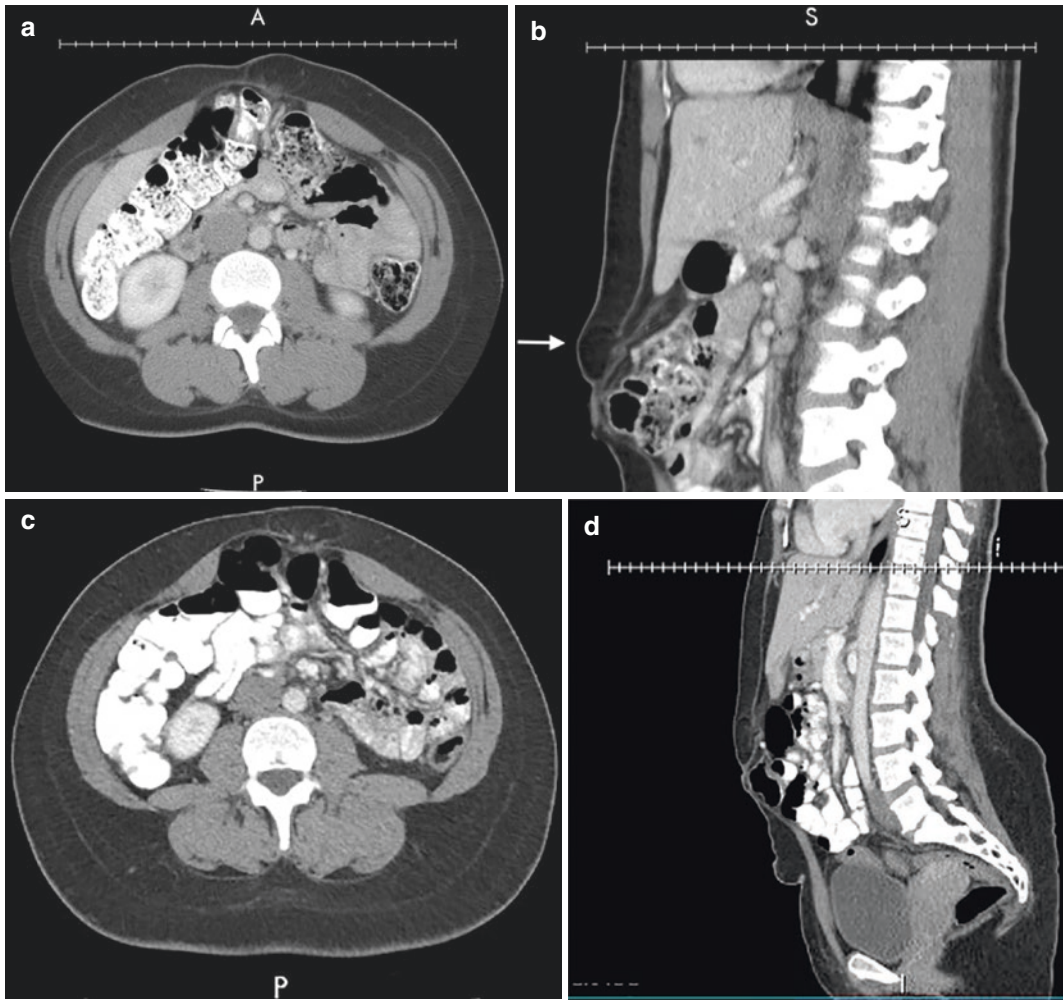

Fig. 22.15 Patient with significant diastasis who initially presented with supraumbilical pain. A CT was obtained at that time and the final interpretation was "no hernia present." On axial image (**a**) a small fascial defect is seen within the large diastasis with a faint outline demonstrating herniated fat. This defect (arrow) is seen in a supraumbilical position in the sagittal view (**b**) 3 years later, the patient had repeat imaging for the ongoing pain, the axial (**c**) and sagittal (**d**) views demonstrate a slightly larger defect, still with herniated fat present

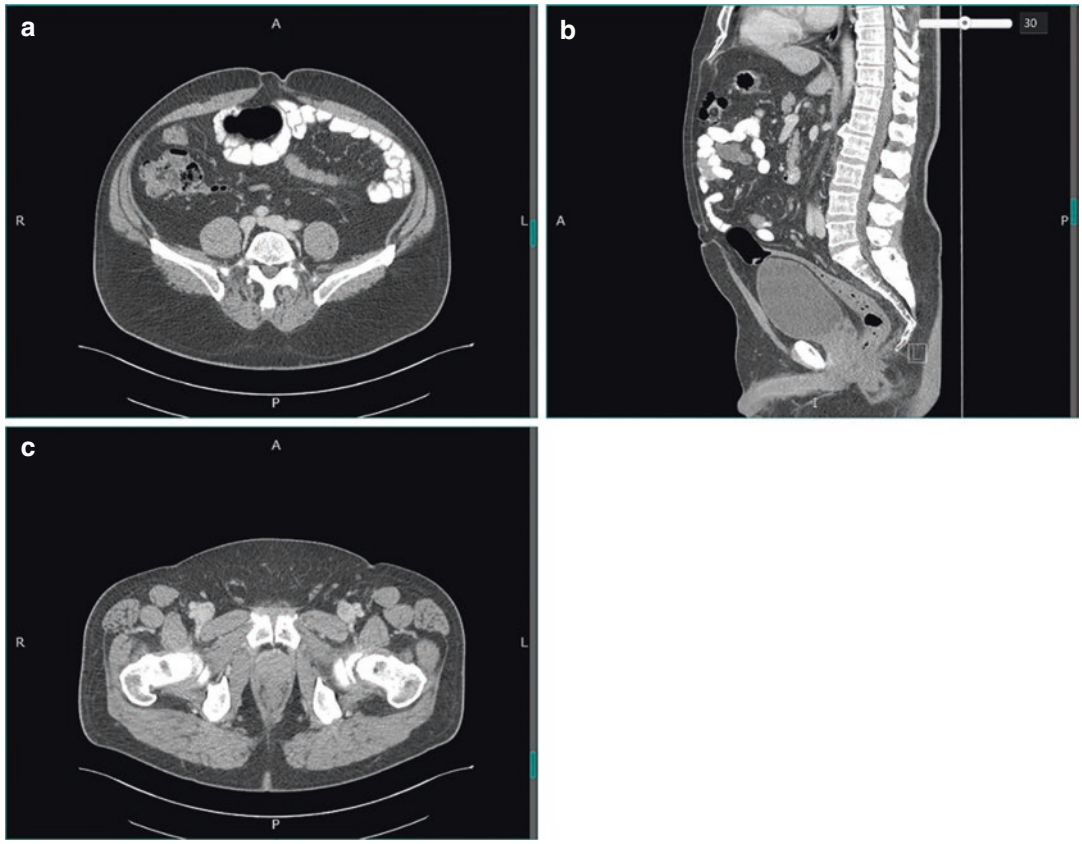

Fig. 22.16 CT images of a patient that presented complaining of an umbilical hernia but was found to have both an umbilical and an inguinal hernia. (**a**) Axial and (**b**) sagittal view of a fat-containing umbilical hernia measuring 2 cm wide by 1.5 cm long. (**c**) Axial view demonstrating right-sided fat-containing inguinal hernia

We have seen several examples of both fat and bowel-containing umbilical and epigastric hernias. When the hernia contains bowel, the clinician must often rely upon signs and symptoms the patient is exhibiting to determine urgency of repair. A patient in distress, with a hernia which cannot be reduced, should not have intervention delayed. Some of these images however may have just captured a transient moment of bowel herniation. The condition of the bowel on imaging can also point to the urgency. Figure 22.17 depicts an infra-umbilical hernia with a herniated loop of the small bowel. There is no evidence of obstruction as contrast is present throughout and there are no dilated loops of bowel. This patient was seen in the clinic weeks after this image, in no distress, and with a reduced hernia. In contrast, Fig. 22.18 depicts an umbilical hernia containing multiple loops of bowel. This patient came in emergently with an irreducible hernia and the CT demonstrates a small bowel obstruction resulting from the incarcerated hernia.

Like any modality, computed tomography has its limitations. As previously mentioned, it carries risks of radiation exposure, is more expensive than ultrasound, and it cannot be performed at bedside. Notably different from US, it is also a static image and the supine positioning may result in spontaneous reduction of hernia contents. While this may make the hernia less obvious, it stresses the importance of looking carefully at the fascia for any defects and not relying on herniated fat or bowel to reveal the hernia.

Fig. 22.17 Sagittal view of small bowel herniated through an infra-umbilical defect without evidence of obstruction

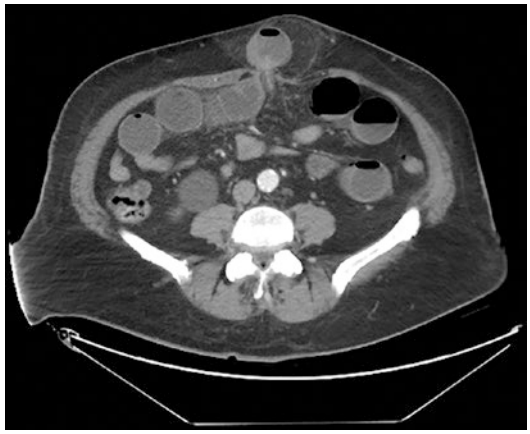

Fig. 22.18 Axial view of small bowel herniated through an umbilical defect. Within the abdomen the obstruction results in fluid-filled and dilated small bowel

Conclusion

We would argue that for most umbilical and epigastric hernias, imaging is not a necessity but is a luxury. There are patients where imaging is a nice adjunct and may assist with diagnosis when there is high clinical suspicion or patients whose operative plan may be influenced by imaging. It is critical that the clinician know when and what to order to obtain the desired information, and for radiologists to understand what critical information is to be obtained from these images. Careful review of imaging and understanding of anatomy will only enhance the patient's experience and operative outcome.

References

1. Bedewi MA, El-Sharkawy MS, Al Boukai AA, Al-Nakshabandi N. Prevalence of adult paraumbilical hernia. Assessment by high-resolution sonography: a hospital-based study. Hernia. 2012;16(1):59–62.
2. Lang B, Lau H, Lee F. Epigastric hernia and its etiology. Hernia. 2002;6(3):148–50.
3. Klinge U, Prescher A, Klosterhalfen B, Schumpelick V. Development and pathophysiology of abdominal wall defects. Chirurg. 1997;68(4):293–303.
4. Nguyen MT, Berger RL, Hicks SC, Davila JA, Li LT, Kao LS, et al. Comparison of outcomes of synthetic mesh vs suture repair of elective primary ventral herniorrhaphy: a systematic review and meta-analysis. JAMA Surg. 2014;149(5):415–21.
5. Poulose BK, Shelton J, Phillips S, Moore D, Nealon W, Penson D, et al. Epidemiology and cost of ventral hernia repair: making the case for hernia research. Hernia. 2012;16(2):179–83.
6. Muysoms FE, Miserez M, Berrevoet F, Campanelli G, Champault GG, Chelala E, et al. Classification of primary and incisional abdominal wall hernias. Hernia. 2009;13(4):407–14.
7. Koebe S, Greenberg J, Huang LC, Phillips S, Lidor A, Funk L, et al. Current practice patterns for initial umbilical hernia repair in the United States. Hernia. 2021;25(3):563–70.
8. Dabbas N, Adams K, Pearson K, Royle G. Frequency of abdominal wall hernias: is classical teaching out of date? JRSM Short Rep. 2011;2(1):5.
9. Hotchkiss LVI. Epigastric hernia. Ann Surg. 1911;54(1):78–82.
10. Powell BS, Voeller GR. Umbilical, epigastric, and Spigelian hernias. In: Kingsnorth AN, LeBlanc KA, editors. Management of Abdominal Hernias. 4th ed. London: Springer; 2013. p. 299–308.

11. Burcharth J, Pedersen MS, Pommergaard HC, Bisgaard T, Pedersen CB, Rosenberg J. The prevalence of umbilical and epigastric hernia repair: a nationwide epidemiologic study. Hernia. 2015;19(5):815–9.
12. Muschaweck U. Umbilical and epigastric hernia repair. Surg Clin North Am. 2003;83(5):1207–21.
13. Saini S, Seltzer SE, Bramson RT, Levine LA, Kelly P, Jordan PF, et al. Technical cost of radiologic examinations: analysis across imaging modalities. Radiology. 2000;216(1):269–72.
14. Zaer NF, Amini B, Elsayes KM. Overview of diagnostic modalities and contrast agents. In: Elsayes KM, Oldham SAA, editors. Introduction to diagnostic radiology. New York, NY: McGraw-Hill; 2014.
15. Mettler FA, Mahesh M, Bhargavan-Chatfield M, Chambers CE, Elee JG, Frush DP, et al. Patient exposure from radiologic and nuclear medicine procedures in the United States: procedure volume and effective dose for the period 2006-2016. Radiology. 2020;295(2):418–27.
16. Miller PA, Mezwa DG, Feczko PJ, Jafri ZH, Madrazo BL. Imaging of abdominal hernias. Radiographics. 1995;15(2):333–47.
17. Bloemen A, van Dooren P, Huizinga BF, Hoofwijk AG. Comparison of ultrasonography and physical examination in the diagnosis of incisional hernia in a prospective study. Hernia. 2012;16(1):53–7.
18. Baz AAM, El-Azizi HMS, Mohamed MSQ, Abdeldayem AYI. Role of high-resolution ultrasound in the assessment of abdominal wall masses and mass-like lesions. Egypt J Radiol Nucl Med. 2019;50(1):1–0.
19. Devareddy MM, Devakar S, Chetan M. Evaluation the sonographic appearance of spectrum of anterior abdominal wall lesions and to compare the sonological features with pathological and operative diagnosis: a cross-sectional study. Int J Sci Stud. 2016;4(7):112–9.
20. Ahn SE, Park SJ, Moon SK, Lee DH, Lim JW. Sonography of Abdominal Wall masses and Masslike lesions: correlation with computed tomography and magnetic resonance imaging. J Ultrasound Med. 2016;35(1):189–208.
21. Gokhale S. High resolution ultrasonography of the anterior abdominal wall. Indian J Radiol Imaging. 2007;17(4):290–8.
22. Lee RK, Cho CC, Tong CS, Ng AW, Liu EK, Griffith JF. Ultrasound of the abdominal wall and groin. Can Assoc Radiol J. 2013;64(4):295–305.
23. Enriquez JL, Wu TS. An introduction to ultrasound equipment and knobology. Crit Care Clin. 2014;30(1):25–45. v
24. Jain N, Goyal N, Mukherjee K, Kamath S. Ultrasound of the abdominal wall: what lies beneath? Clin Radiol. 2013;68(1):85–93.
25. Rettenbacher T, Hollerweger A, Macheiner P, Gritzmann N, Gotwald T, Frass R, et al. Abdominal wall hernias: cross-sectional imaging signs of incarceration determined with sonography. AJR Am J Roentgenol. 2001;177(5):1061–6.
26. Jacobson JA, Khoury V, Brandon CJ. Ultrasound of the groin: techniques, pathology, and pitfalls. AJR Am J Roentgenol. 2015;205(3):513–23.
27. Jamadar DA, Jacobson JA, Morag Y, Girish G, Dong Q, Al-Hawary M, et al. Characteristic locations of inguinal region and anterior abdominal wall hernias: sonographic appearances and identification of clinical pitfalls. AJR Am J Roentgenol. 2007;188(5):1356–64.
28. Beck WC, Holzman MD, Sharp KW, Nealon WH, Dupont WD, Poulose BK. Comparative effectiveness of dynamic abdominal sonography for hernia vs computed tomography in the diagnosis of incisional hernia. J Am Coll Surg. 2013;216(3):447–53. quiz 510–1
29. Bittner R, Bain K, Bansal VK, Berrevoet F, Bingener-Casey J, Chen D, et al. Update of guidelines for laparoscopic treatment of ventral and incisional abdominal wall hernias (international Endohernia society (IEHS)): part B. Surg Endosc. 2019;33(11):3511–49.

Thoracoabdominal Hernia

23

Michael Genz, John Childress III,
and Vedra A. Augenstein

Introduction

Thoracoabdominal hernias are rare and therefore not well represented in the literature. Thoracoabdominal hernias can be congenital or acquired, the latter usually the result of blunt trauma or forceful coughing; however, thoracic and retroperitoneal surgery also account for iatrogenic causes [1–4]. The hernia literature consists of relatively few case reports of thoracoabdominal hernias. In one literature review, 14 total cases were published in the literature spanning a period of 30 years, from 1977 to 2017 [5]. A separate study from 2014 reported on 19 thoracoabdominal hernias [2]. More recently, a two-institution series was published consisting of 16 patients, all with spontaneous, cough-induced thoracoabdominal hernias. This particular series focused on the physiology and optimal surgical repair of these rare hernias [4].

The exact definition of a thoracoabdominal hernia is vague. For the purpose of this chapter, thoracoabdominal hernia is defined as a hernia that involves a defect in the region of the "thoracoabdominal zone," which is the area bounded superiorly by the fourth intercostal space; anteriorly by the sixth intercostal space; laterally by the eighth intercostal space; and inferiorly by the costal margin [6]. A commonality of all thoracoabdominal hernias is an intercostal defect (Fig. 23.1).

In addition to the intercostal defect, disruption of the diaphragm may also be present, often with herniation of abdominal visceral contents into the chest and subsequently through the intercostal defect. If a diaphragmatic hernia defect is present, the term "transdiaphragmatic intercostal hernia" (TDIH) has been proposed (Fig. 23.2) (Videos 23.1, 23.2, 23.3, and 23.4). In the absence of a diaphragmatic hernia, the term "abdominal intercostal hernia" has been suggested as an apt descriptor [7]. Involved visceral organs described in the literature include liver, small and large bowel, omentum, and gallbladder [8] (Videos 23.5 and 23.6). The term thoracic intercostal hernia is reserved for a hernia that involves a protruding thoracic organ, most commonly the lung, through an intercostal defect in the thoracoabdominal zone in the presence of an intact diaphragm [9].

Supplementary Information The online version contains supplementary material available at https://doi.org/10.1007/978-3-031-21336-6_23.

M. Genz
Department of General Surgery, Atrium Health—Carolinas Medical Center, Charlotte, NC, USA
e-mail: Michael.genz@atriumhealth.org

J. Childress III
Atrium Health CMC, Radiology (Charlotte Radiology), Charlotte, NC, USA
e-mail: john.childress@charlotteradiology.com

V. A. Augenstein (✉)
General Surgery, Atrium Healthcare, Charlotte, NC, USA

S. Docimo Jr. et al. (eds.), *Fundamentals of Hernia Radiology*,
https://doi.org/10.1007/978-3-031-21336-6_23

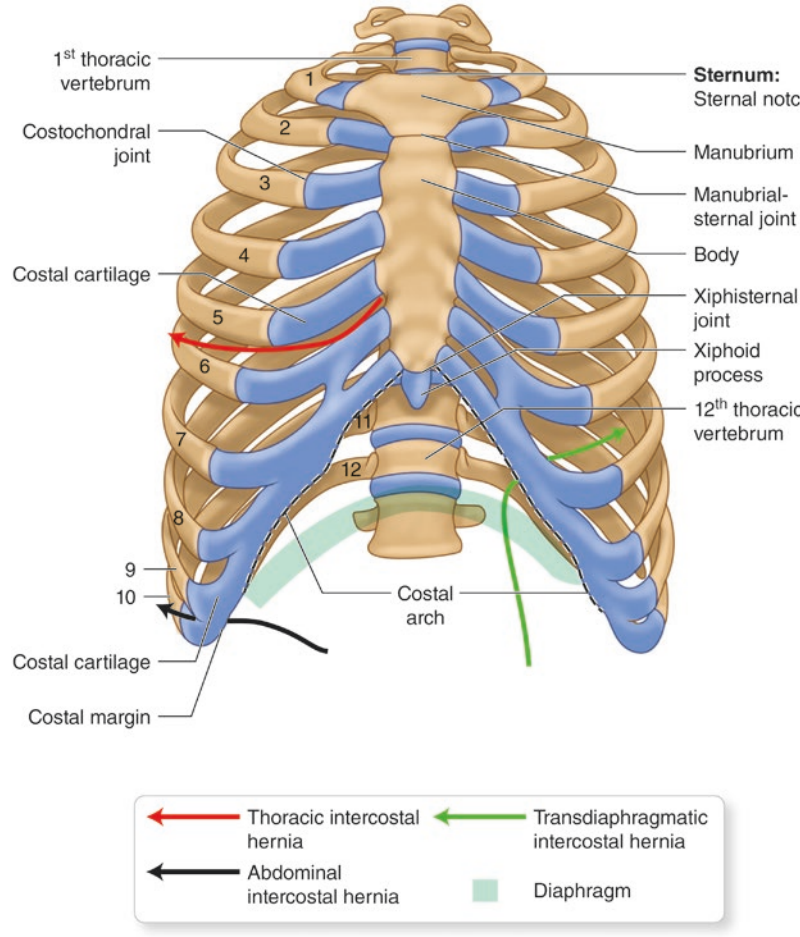

Fig. 23.1 Thoracoabdominal zone

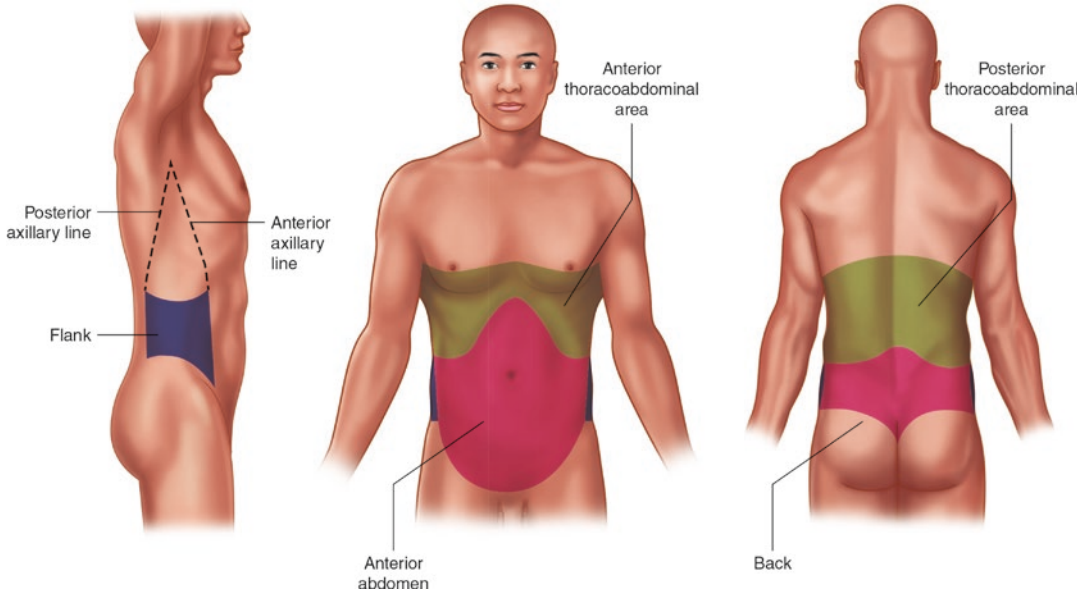

Fig. 23.2 TDIH

Pathophysiology

Acquired thoracoabdominal hernias are more commonly caused by trauma or previous surgery although can rarely be caused by forceful coughing. Ribs are often fractured in acquired thoracoabdominal hernias, allowing for a separation of the intercostal space that results in a hernia. One proposed mechanism for cough-induced rib fractures is that the intrathoracic and intra-abdominal force applied to the chest wall during a forceful cough exceeds the elasticity of the bone. A second proposed theory is that the opposing forces of the intercostal muscles, abdominal wall muscles, and diaphragm muscle result in sufficient force to fracture an adjacent rib [5]. The intrathoracic pressure generated during a forceful cough has been described as a "modified Valsalva maneuver," with pressures of 140–300 mm Hg and expiratory velocities reaching 28,000 cm/s [10]. For the sake of comparison, chest compressions during cardiopulmonary resuscitation generate intrathoracic pressures of approximately 75 mm Hg [11].

Comorbidities thought to contribute to spontaneous thoracoabdominal hernias include chronic lung diseases such as chronic obstructive pulmonary disease and cystic fibrosis, respiratory infections and smoking, and corticosteroid use [4].

When a diaphragmatic defect is present, abdominal viscera can migrate into the chest and subsequently through an intercostal defect (if present) above the diaphragm. This migration occurs due to a pressure gradient generated by the mechanics of breathing. During inspiration, the diaphragm and intercostal muscles contract, resulting in negative intrapleural pressure. This negative pressure results in a gradient that facilitates the migration of the intra-abdominal visceral contents into the chest. Upon expiration, the intrapleural pressure reverts to positive pressure, in effect "pushing" the abdominal visceral contents through the intercostal defect [12]. Of note, the chest wall is weaker between the costochondral junction and sternum anteriorly, and the costal angle posterior to the spine, due to the lack of external intercostal muscle mass and intercostal muscle mass, respectively [13]. These inherent weaknesses in the chest wall could contribute to the development of abdominal intercostal hernias.

Presentation

Most patients will present with a palpable mass on exam. It is often possible to appreciate the hernia defect along the rib edges and due to rib separation. Patients often complain of pain as the hernia defect enlarges and the gap between the involved intercostal space increases. There are reports of complicated small bowel obstructions secondary to thoracoabdominal hernias, occasionally associated with bowel strangulation [14]. In a TDIH, the mass should be prominent on inspiration and less so on expiration if the hernia contents are components of the abdominal viscera. The opposite is true when lung is herniated [13].

Radiological Assessment

Diagnosis of a thoracoabdominal hernia requires a high index of suspicion. Chest radiograph may reveal a pleural effusion or bowel gas in the base of the thorax as well as intercostal space widening in patients with associated rib fractures. Comprehensive computed tomography (CT) of the chest and abdomen with axial, coronal, and sagittal reconstructions will aid in surgical planning. Although CT is not optimal for detecting a diaphragm injury and can in some cases miss thoracoabdominal defects (Fig. 23.3), multidisciplinary review including radiology and thoracic surgery may be helpful.

Surgical Management:

Given the low incidence of thoracoabdominal hernias, there is no standard technique for the repair of thoracoabdominal hernias. Open and minimally invasive approaches to these repairs have been described [15]. In addition, primary suture repair with and without mesh reinforcement, and the reapproximation of ribs utilizing peri-costal/peri-ostial sutures have been described [7, 16]. In 2004, *Losanoff* et al. repaired an inter-

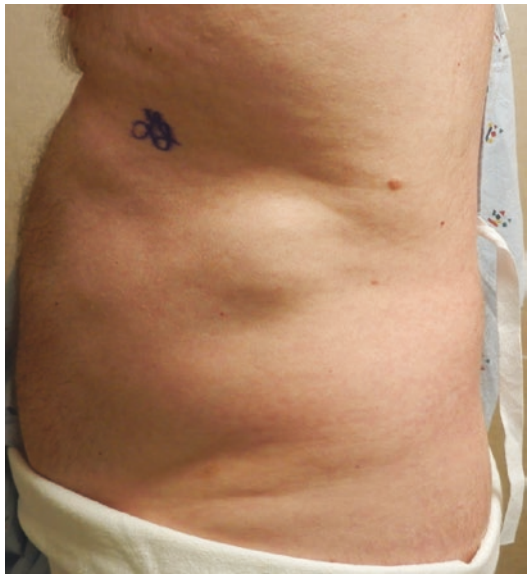

Fig. 23.3 Left thoracoabdominal bulge present on exam

costal hernia with steel cables which was found to be more durable than peri-costal sutures or wires [17]. In our experience, we have noted that thoracoabdominal hernias repaired by suture alone had unacceptable recurrence rates with long-term follow-up [4]. Further examination and consultation led to the implementation of rib fixation utilizing titanium plates and steel cables.

In the operating room, the patient is positioned in the lateral decubitus position using a bean bag. A double lumen tube may be used after the induction of general endotracheal anesthesia. The entirety of the chest wall, from the sternum medially to the spine posteriorly, as well as the ipsilateral hemi-abdomen is prepped in a sterile fashion. An incision is made over the area of the hernia defect. Access to the chest wall is gained by either dividing or retracting the latissimus dorsi muscle and splitting or dividing the serratus anterior. Next, the diaphragm is identified and assessed for a defect. It is also important at this time to identify any possible rib fractures. If a diaphragmatic defect is present, it can be repaired primarily with permanent sutures and reinforced with mesh if possible. It may also be necessary to transpose the diaphragm to a rib located more cranially. In our practice, mesh is typically placed in the preperitoneal plane. As with abdominal hernias, enough preperitoneal dissection needs to be performed circumferentially around the defect, in order to allow for wide mesh overlap in all directions. Mesh is fixated in the usual fashion. Titanium rib fixation plates are placed and secured with screws on the separated ribs. The specific numbers and sizes of plates used vary depending on the associated fracture present, as well as the number of levels involved. Screws are placed in intended spaces, leaving a few empty spaces to pass multistrand cables (available in stainless steel and titanium) later in the operation. Metal crimpers are used to secure the cables in place and reconstruct the chest wall injury. We have found that simple wire repair of the ribs alone is not durable and should be avoided. Hernia cavity drains are placed, and chest tubes are placed as needed if there was a diaphragm repair. Chest wall muscles are then closed in layers with absorbable sutures.

Repair of the abdominal wall defect is performed in conjunction. Patients subsequently undergo routine postoperative care.

Cases

Case 1

Patient is a 68-year-old male who presented to the clinic in July 2018 with left thoracoabdominal pain and bulge (Fig. 23.3). He first noticed the bulge in 2016 after an episode of severe coughing. This was followed by severe left chest wall pain and bruising. Shortly thereafter, he noticed a bulge in this region which was lifestyle-limiting. He had a medical history notable for hypertension, renal stones, and gastroesophageal reflux disease. Cross-sectional imaging was obtained in the form of computed tomography and demonstrated a left intercostal hernia (Figs. 23.4, 23.5, and 23.6). He was subsequently taken to surgery the following month for a left thoracoabdominal hernia repair. The hernia was repaired with polypropylene mesh placed in the preperitoneal plane, extending from the umbilicus to the psoas muscle. The ribs were reapproximated by open reduction and internal fixation with titanium plates and steel cables (Figs. 23.7, 23.8, 23.9, and 23.10).

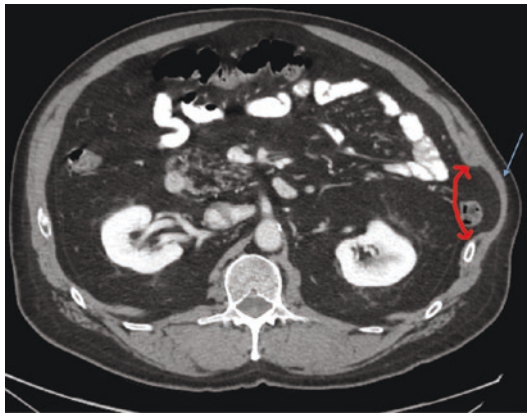

Fig. 23.4 Axial image demonstrating the hernia neck (red double arrow) and the hernia defect containing a portion of the descending colon. The external oblique muscle demonstrates eventration and attenuation (blue arrow)

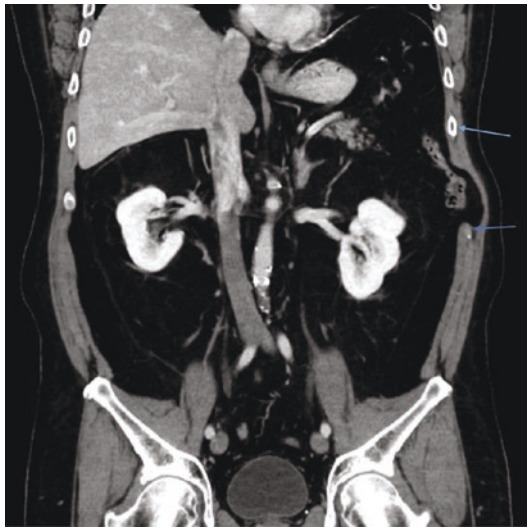

Fig. 23.5 Coronal image demonstrating the intercostal defect. Rib separation is depicted (blue arrows)

Postoperative chest x-ray demonstrated proper positioning of the rib plates (Fig. 23.11). He was discharged on postoperative day 5 after a relatively uncomplicated postoperative course.

Case 2

Patient is a 64-year-old male who presented to the clinic with an enlarging acquired left thora-

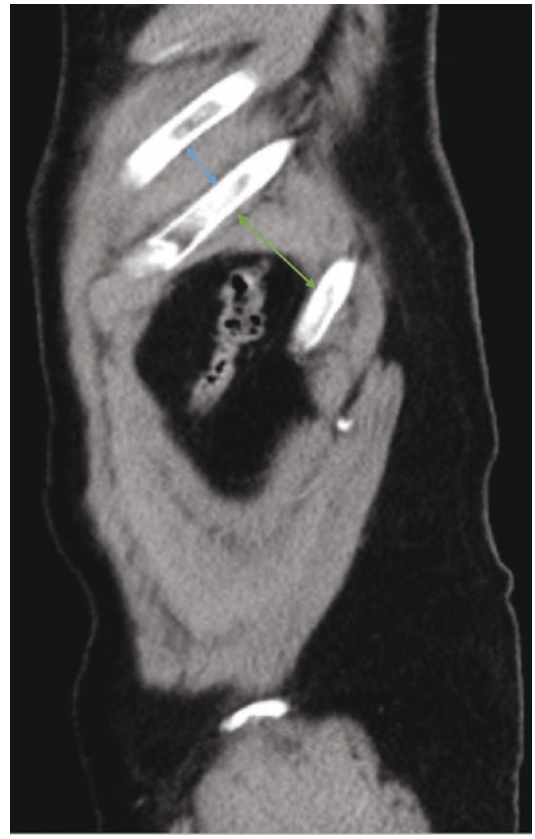

Fig. 23.6 Sagittal image of the intercostal defect. Highlighted is the separation of the interspace between ribs 9 and 10 (green double arrow). It is noticeably wider compared to the more superior intercostal space (blue double arrow)

Fig. 23.7 Development of the preperitoneal space

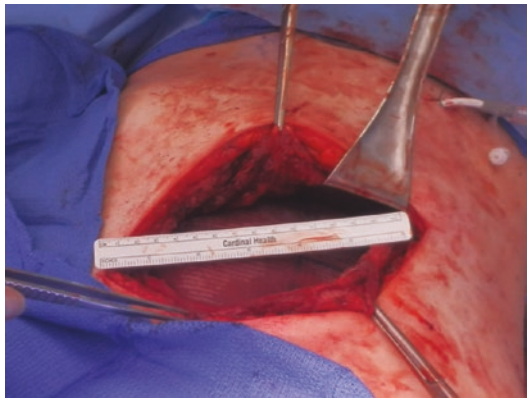

Fig. 23.8 Preperitoneal mesh placement with transabdominal suture fixation

Fig. 23.9 Placement of rib plates adjacent to hernia defect

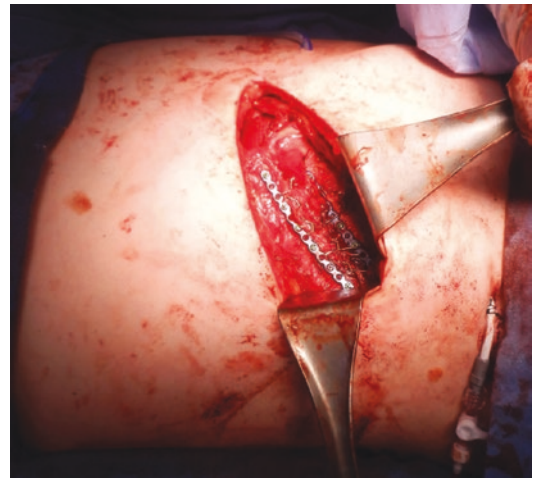

Fig. 23.10 Rib plates with intercostal wires secured between plates

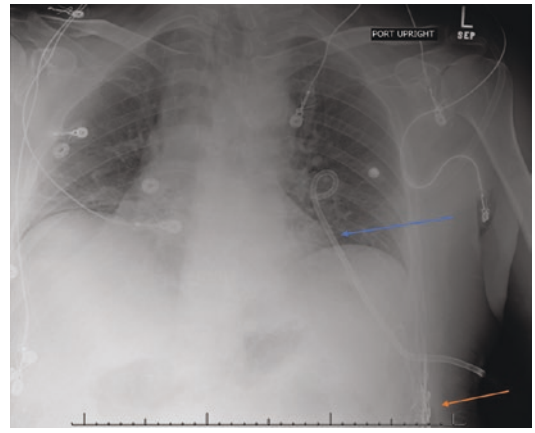

Fig. 23.11 Pigtail catheter in the left pleural space (blue arrow). Rib plates in the right lower portion of the image about inferolateral left ribs (orange arrow)

coabdominal hernia. His past medical history included hypertension, obesity, chronic obstructive pulmonary disease, and smoking. Five years earlier, the patient developed a violent coughing episode and then felt a "pop" that was associated with significant pain. Cross-sectional imaging demonstrated a hernia in the area of the left thoracoabdominal region. The patient was initially taken to surgery for resection of a fractured, necrotic rib and did not have the hernia addressed. The patient then presented to our clinic with chronic pain due to enlargement. Cross-sectional imaging was obtained in the form of computed tomography and demonstrated a left abdominal intercostal hernia (Figs. 23.12, 23.13, and 23.14)

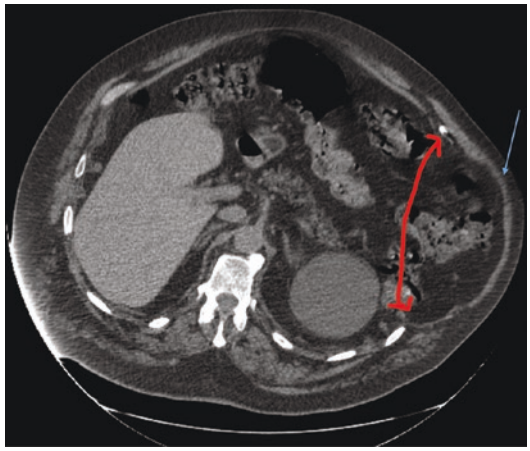

Fig. 23.12 Axial image demonstrating a large hernia defect (red double arrow) containing colonic splenic flexure with overlying attenuated external oblique muscle (blue arrow)

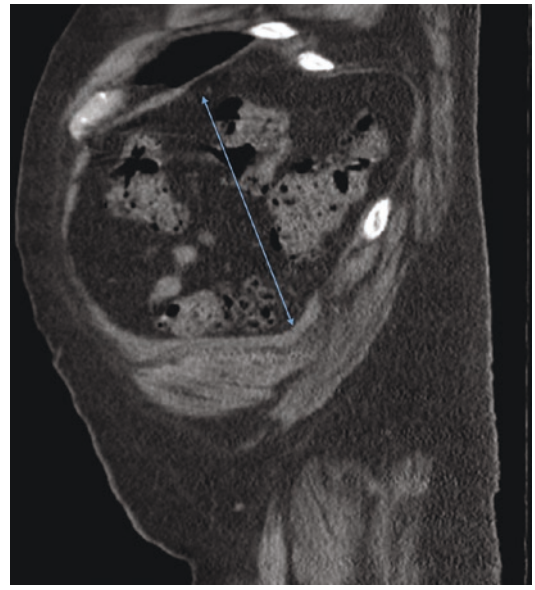

Fig. 23.14 Sagittal image demonstrating the extent of the hernia defect; 11 cm in craniocaudal dimension

Fig. 23.13 Coronal image demonstrating herniation of the left hemidiaphragm into the defect (blue arrows)

Fig. 23.15 Axial image of a right intercostal hernia between ribs 10 and 11. Liver is depicted herniating through the defect (blue arrow)

Case 3

The patient is a 54-year-old female with a history of prior right radical nephrectomy for renal cell carcinoma followed by resection of a disease recurrence with laparoscopic right thoracoabdominal hernia repair after each operation. She presented with a recurrent incisional thoracoabdominal hernia. Cross-sectional imaging was obtained and demonstrated a right intercostal hernia containing colon and liver (Figs. 23.15 and 23.16). In the operating room, she underwent old mesh explantation, open reduction, and internal fixation of the adjacent ribs with plates and wires and implantation of a large polypropylene mesh.

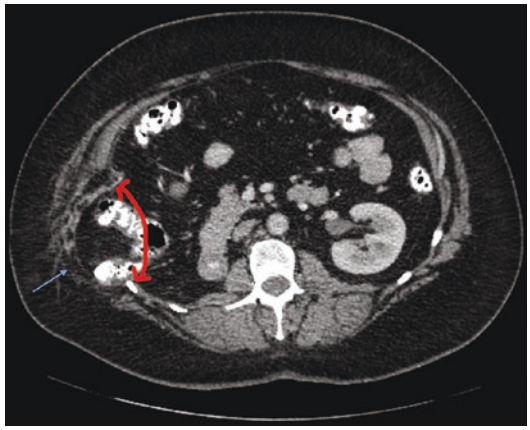

Fig. 23.16 Axial image of the hernia demonstrating hepatic flexure herniated through the defect (red double arrow). The defect includes intercostal musculature and the abdominal wall oblique muscles (blue arrow)

References

1. Benizri EI, Delotte J, Severac M, Rahili A, Bereder JM, Benchimol D. Post-traumatic transdiaphragmatic intercostal hernia: report of two cases. Surg Today. 2013;43(1):96–9. https://doi.org/10.1007/s00595-012-0197-6.
2. Erdas E, Licheri S, Calò PG, Pomata M. Acquired abdominal intercostal hernia: case report and systematic review of the literature. Hernia. 2014;18(5):607–15. https://doi.org/10.1007/s10029-014-1232-x.
3. Bendinelli C, Martin A, Nebauer SD, Balogh ZJ. Strangulated intercostal liver herniation subsequent to blunt trauma. First report with review of the world literature. World J Emerg Surg. 2012;7(1):1–4. https://doi.org/10.1186/1749-7922-7-23.
4. Alayon-Rosario M, Schlosser K, Griscom T, et al. Primary thoracoabdominal hernias. Hernia. 2020;25(6):1621–8. https://doi.org/10.1007/s10029-020-02194-7.
5. Chapman AA, Duff SB. A case of spontaneous Transdiaphragmatic intercostal hernia with contralateral injury, and review of the literature. Case Reports in Surgery. 2017;2017:7416092. https://doi.org/10.1155/2017/7416092.
6. Parreira JG, Rasslan S, Utiyama EM. Controversies in the management of asymptomatic patients sustaining penetrating thoracoabdominal wounds. Clinics. 2008;63(5):695–700. https://doi.org/10.1590/S1807-59322008000500020.
7. Bobbio A, Ampollini L, Prinzi G, Sarli L. Endoscopic repair of an abdominal intercostal hernia. Surg Laparosc Endosc Percutan Tech. 2008;18(5):523–5. https://doi.org/10.1097/SLE.0b013e31817f2883.
8. Smith E, Spain L, Ek E, Farrell S. Post-traumatic intercostal liver herniation. ANZ J Surg. 2008;78(7):615–6. https://doi.org/10.1111/j.1445-2197.2008.04586.x.
9. Iwata T, Yasuoka T, Hanada S, et al. Inverted intercostal hernia of soft tissue manifested as slow-growing chest wall tumor after thoracotomy. Ann Thorac Surg. 2010;90(4):1355–7. https://doi.org/10.1016/j.athoracsur.2010.04.042.
10. Irwin RS. Complications of cough: ACCP evidence-based clinical practice guidelines. Chest. 2006;129(1 SUPPL):54S–8S. https://doi.org/10.1378/chest.129.1_suppl.54S.
11. Schultz DD, Olivas GS. The use of cough cardiopulmonary resuscitation in clinical practice. Hear Lung J Acute Crit Care. 1986;15(3):273–82.
12. Mehdi SB, Madi S, Sudworth J. Non-traumatic transdiaphragmatic intercostal hernia and cor pulmonale in a patient with poorly controlled obstructive sleep apnoea. BMJ Case Rep. 2016;2016:bcr2016216841. https://doi.org/10.1136/bcr-2016-216841.
13. Kalles V, Dasiou M, Doga G, et al. Posttraumatic transdiaphragmatic intercostal hernia: report of a case and review of the literature. Int Surg. 2015;100(3):444–9. https://doi.org/10.9738/INTSURG-D-13-00272.1.
14. Akinduro OO, Jones F, Turner J, Cason F, Clark C. Rare case of a strangulated intercostal flank hernia following open nephrectomy: a case report and review of literature. Int J Surg Case Rep. 2015;17:143–5. https://doi.org/10.1016/j.ijscr.2015.11.015.
15. Luqman MQ, Mughal A, Waldron R, Khan IZ. Laparoscopic IPOM repair of an acquired abdominal intercostal hernia. BMJ Case Rep. 2018;2018:bcr2018227158. https://doi.org/10.1136/bcr-2018-227158.
16. Yodonawa S, Kobayashi K, Yoshida S, et al. Transdiaphragmatic intercostal hernia following blunt trauma. Gen Thorac Cardiovasc Surg. 2012;60(7):459–61. https://doi.org/10.1007/s11748-012-0020-8.
17. Losanoff JE, Richman BW, Jones JW. Recurrent intercostal herniation of the liver. Ann Thorac Surg. 2004;77(2):699–701. https://doi.org/10.1016/S0003-4975(03)00749-5.

Diaphragmatic Hernia

24

Samuel J. Zolin, Aldo Fafaj, and Diya Alaedeen

Anatomy and Embryology

The diaphragm separates the abdominal and thoracic cavities, with three main orifices allowing the passage of the inferior vena cava (IVC) at the level of T8, the esophagus at T10, and the aorta, azygos vein, thoracic duct, and splanchnic nerves at T12 (Fig. 24.1). The diaphragm consists of three major muscle groups and a large central tendon. The sternal, costal, and lumbar muscle groups are attached to their corresponding bones anterolaterally, and the arcuate ligaments posteriorly. The esophageal hiatus is made up of the right crus muscle bundles, which arise from L1–3 of the lumbar vertebrae, and the left crus muscle bundles, which arise from L1–2. The right crus muscle fibers split, with some passing anteriorly to the esophagus, and some passing posterior and medially. The left crus muscle fibers meet with the right crus fibers anterior to the esophagus, and the fibers of both crura attach to the central tendon of the diaphragm. The fusion of endoabdominal and endothoracic fascias constitutes the phrenoesophageal membrane, which circumferentially connects to the esophagus at the squamocolumnar junction, and helps to fix the esophagus to the crura. The anatomy of the esophageal hiatus is particularly important, as this is the most common site at which acquired diaphragmatic hernias occur (Fig. 24.2).

Blood supply to the majority of the diaphragm comes from the left and right phrenic arteries, which arise directly from the abdominal aorta. Additional perfusion is provided from branches of the internal mammary arteries. Venous drainage follows the arterial supply, ultimately leading medially into the IVC. Innervation of the diaphragm is almost exclusively from the right and left phrenic nerves, which originate from cervical nerves 3–5. Each nerve divides into four trunks that innervate the anterolateral, posterolateral, crural, and sternal areas of the diaphragm. Injury to either phrenic nerve results in an elevated hemidiaphragm and impaired respiration, while injury to both phrenic nerves results in complete diaphragmatic paralysis.

The diaphragm begins to develop during the fourth to seventh weeks of gestation and completes its development by the 10th–12th week. Four structures comprise the diaphragm during embryogenesis: (1) the muscular body wall along the periphery, (2) the esophageal mesentery asso-

Supplementary Information The online version contains supplementary material available at https://doi.org/10.1007/978-3-031-21336-6_24.

S. J. Zolin
Cleveland Clinic Foundation, Digestive Disease and Surgery Institute, Cleveland, OH, USA
e-mail: zolins@ccf.org

A. Fafaj (✉) · D. Alaedeen
Department of General Surgery, Cleveland Clinic, Cleveland, OH, USA
e-mail: fafaja@ccf.org; alaeded@ccf.org

S. Docimo Jr. et al. (eds.), *Fundamentals of Hernia Radiology*,
https://doi.org/10.1007/978-3-031-21336-6_24

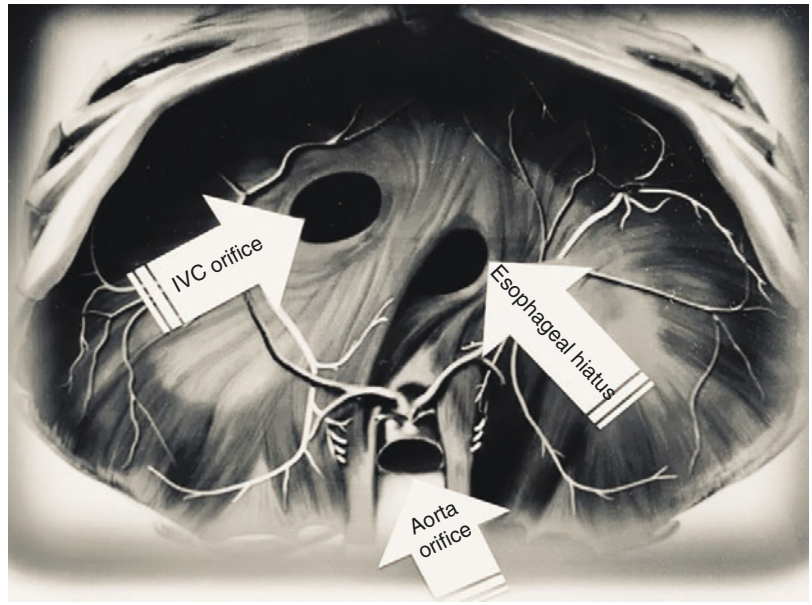

Fig. 24.1 The natural orifices of the diaphragm

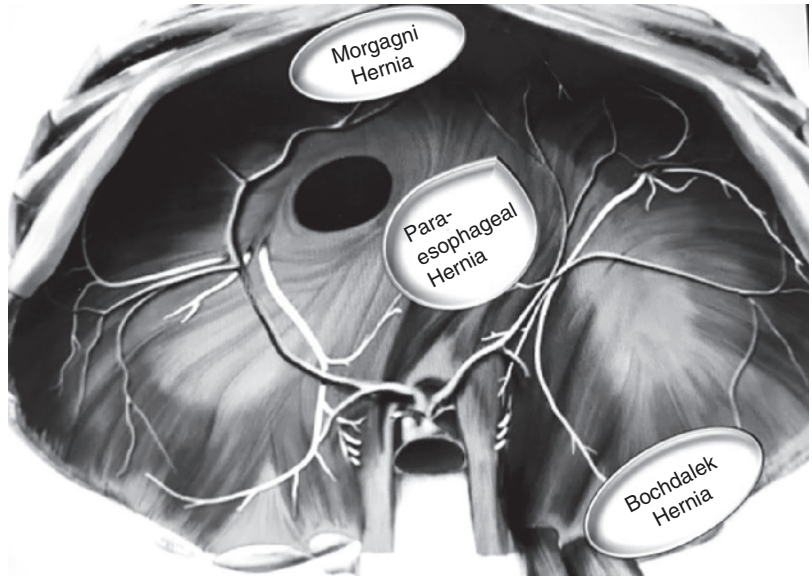

Fig. 24.2 Typical locations of common diaphragmatic hernias

ciated with the esophagus, the IVC, and the aorta, (3) the left and right pleuroperitoneal folds located posteriorly, and (4) the transverse septum anteriorly. The central tendon is formed from the septum transversum, while the posteromedial portion of the diaphragm develops from the dorsal mesentery of the esophagus, and the right and left pleuroperitoneal membranes grow medially to fuse with the central tendon. Migration of the neuromuscular components completes diaphragmatic development. The myocytes migrate from the third, fourth, and fifth cervical myotomes, and the bilateral phrenic nerves evolve from the third, fourth, and fifth cervical nerves. While embryologic development of the diaphragm is generally very consistent, aberrant maturation can lead to congenital hernias. Furthermore, diaphragmatic hernias can also be acquired in the

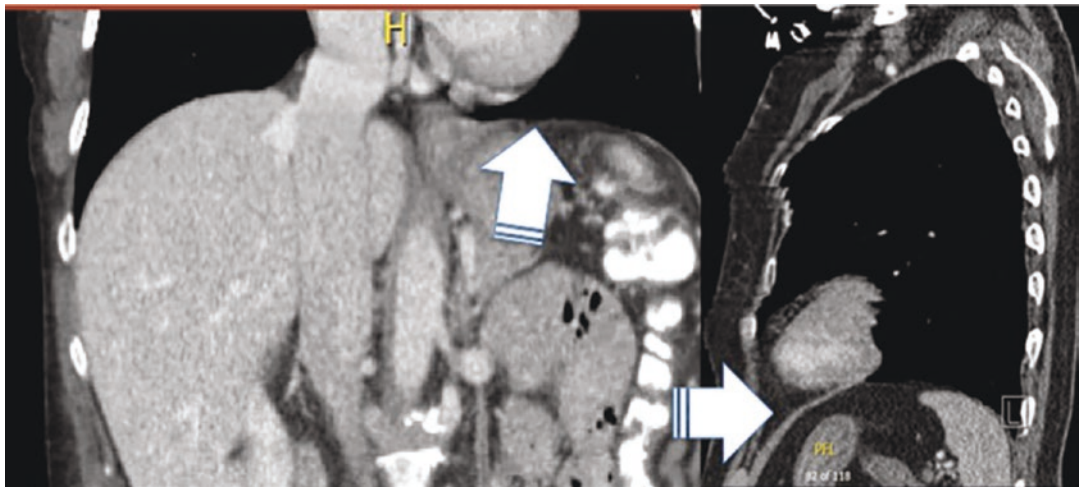

Fig. 24.3 Normal coronal and sagittal CT appearance of the diaphragm (arrows)

context of injury or secondary to age- or disease-related weakening of the phrenoesophageal membrane (Fig. 24.2) [1].

Many imaging modalities, including fluoroscopy, magnetic resonance imaging (MRI), and ultrasound, have been utilized to visualize the diaphragm. However, computed tomography (CT) remains the most widely used modality for diaphragmatic evaluation, especially in the adult population. Figure 24.3 shows the normal CT appearance of the diaphragm. The diaphragm usually has a smooth contour with increased thickness at its edges. Diaphragmatic slips, or folds, are normal anatomic variants and should not be confused with defects of the diaphragm [2].

Bochdalek Hernia

Initially described by anatomist Vincent Bochdalek in a population of newborns who experienced significant abnormalities of respiration, Bochdalek hernia is the term used to refer to posterolateral diaphragmatic hernias (Fig. 24.2). These hernias are thought to result from failure of fusion of the pleuroperitoneal folds and the transverse septum, leading to a diaphragmatic hernia in a posterior and lateral location [3].

Bochdalek hernias are estimated to constitute approximately 90% of congenital diaphragmatic hernias (CDHs). Despite this, they are relatively rare overall, estimated to occur at a rate between 1 in 12,500 and 1 in 2200 live births. Bochdalek hernias are described as having a left-sided predominance, with an approximate 75–90% incidence on the left side (Fig. 24.2) [4]. It is possible that the presence of the liver, preventing herniation of viscera into the chest on the right, is the reason left-sided defects are more prevalent.

The presence of abdominal viscera in the thoracic cavity during development may lead to pulmonary hypoplasia as well as vascular and cardiac abnormalities. This can lead to the development of severe pulmonary symptoms at birth. While rates of neonatal mortality associated with CDH were an estimated 50% in the 1980s and 1990s, these have declined to less than 30% as of 2013 [5].

Though CDH may be diagnosed prenatally or shortly after birth in many, some individuals progress to adulthood without being diagnosed, and therefore it is difficult to estimate the number of asymptomatic adults who may have a Bochdalek hernia. One retrospective review of all abdominal CT scans performed in a single year at the Massachusetts General Hospital estimated the prevalence of Bochdalek hernia in adults to be 0.17% [6]. In contrast, a significantly higher prevalence of Bochdalek hernia has been reported elsewhere in the literature, with 5% of patients

between ages 40 and 49, 15% of patients between ages 50 and 69, and 35% of patients age 70 or older being estimated to have Bochdalek hernias. This age-related increase in Bochdalek hernia prevalence suggests that small congenital defects may enlarge over time [7]. Furthermore, conditions that raise intra-abdominal pressure such as coughing, chronic obstructive pulmonary disease, vigorous activity, chronic constipation, pregnancy, and childbirth have been suggested to act as precipitating factors for the manifestation of Bochdalek hernias [8].

The literature is replete with case reports describing acute and sometimes dramatic presentations of Bochdalek hernias in adults, including reports of volvulus, strangulation, and perforation secondary to these hernias. A recent review of 226 reported cases of Bochdalek hernias indicates that most commonly patients present with abdominal pain (62%) and pulmonary symptoms (40%). Additionally, obstructive symptoms occur in 36% and bowel strangulation in 26% [8]. Together, these data suggest that diaphragmatic hernia must be considered in the differential diagnosis of patients presenting with bowel obstruction. Although rates of surgical emergencies attributable to Bochdalek hernia may be slightly inflated due to publication bias, it is likely that elective repair of these hernias is warranted when they are discovered incidentally. Furthermore, because of their age-related increase in prevalence, Bochdalek hernias cannot be excluded on the basis of previously normal imaging.

Most CDHs are diagnosed by neonatal ultrasound before the 25th week of gestation. Polyhydraminos, a poor prognostic sign, is present in 80% of cases. The presence of the stomach in the left hemithorax, with a right shift in the mediastinum, is the most common ultrasound finding. Fetal MRI can further identify the location, contents, and effect of the CHD on adjacent structures (Fig. 24.4).

With regard to imaging findings in adults, chest x-ray may demonstrate evidence of Bochdalek hernia, including elevation of the left hemidiaphragm and potentially intestinal air-fluid levels in the hemithorax. Radiographs are not always diagnostic, and other disease processes including pulmonary, pleural, mediastinal, diaphragmatic, or paravertebral masses may be confused for Bochdalek hernias. Furthermore, a chest x-ray without obvious evidence of a diaphragmatic hernia does not rule out this diagnosis [9]. Upper gastrointestinal (UGI) studies may be useful in determining whether there is a volvulus or malrotation of involved hollow viscera, particularly if consideration is being given to a thoracic approach for repair (Fig. 24.5).

CT scan remains the most diagnostic imaging modality for Bochdalek hernia in adults. Cross-

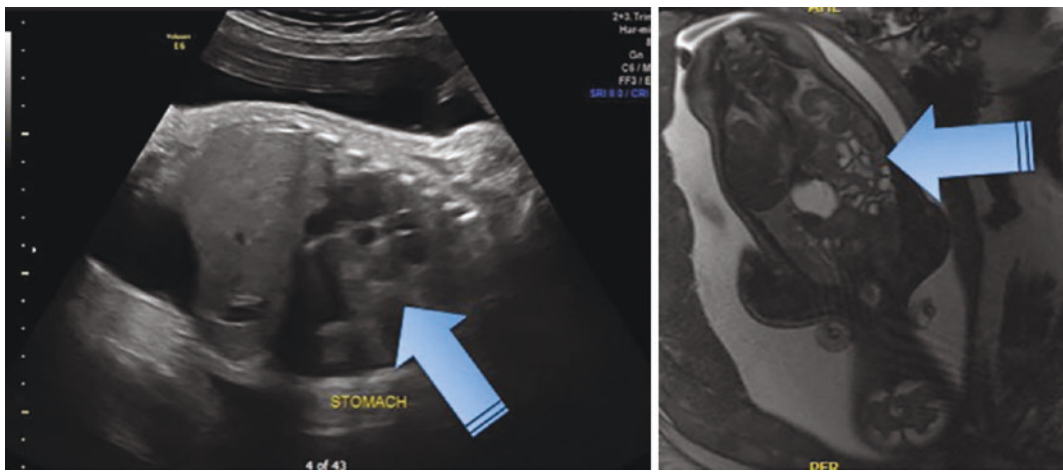

Fig. 24.4 Ultrasound (left) and MRI (right) images revealing Bochdalek hernia in an infant in utero. The arrows point to the stomach and intestine in the left hemithorax

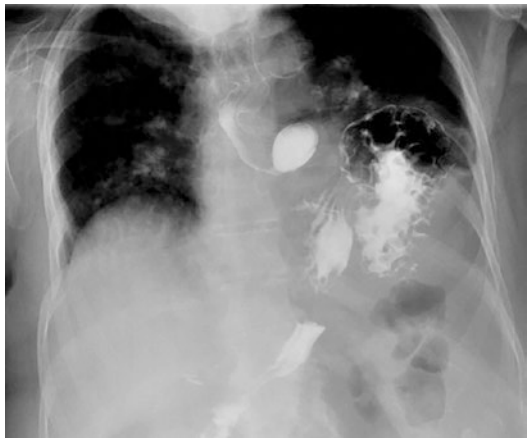

Fig. 24.5 An upper GI study in an adult patient presenting with congenital Bochdalek hernia. There is elevation of the left hemidiaphragm, and the stomach is seen within left thoracic cavity

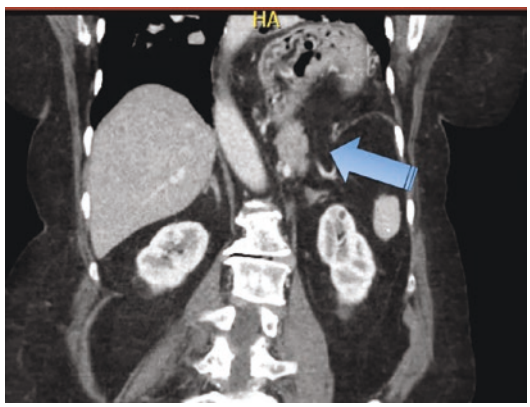

Fig. 24.6 The coronal CT of the same adult patient depicted in Fig. 24.5. The arrow points to the diaphragmatic defect of this Bochdalek hernia

sectional imaging will demonstrate a posterior diaphragmatic defect occurring lateral to the crura. Small defects may contain only retroperitoneal fat, while larger defects may contain other abdominal viscera (Fig. 24.6) [10]. Fat or soft tissue may be visualized above the diaphragm, with a mass adjacent to the diaphragmatic defect and a continuous density over and under the discontinuity of the diaphragm [8].

Due to the risk of emergent presentation, it is generally recommended that Bochdalek hernias be repaired in patients who are candidates for surgery [9]. Historically, many Bochdalek hernias in adults were repaired via the open approach. However, the safety and feasibility of minimally invasive repairs make this approaches a popular option.

Morgagni Hernia

In 1769 the Italian anatomist Giovanni Morgagni described an abnormal defect that exists between the diaphragm and the sternum, and subsequently, anteromedial subcostosternal defects have been termed Morgagni hernias (Fig. 24.2). Morgagni hernias constitute fewer than 10% of all CDHs and result from an embryological defect in fusion of the transverse septum to the lateral body wall [3]. The foramen of Morgagni is covered by the pericardium on the left, leading to an estimated 90% prevalence of rightward herniation (Fig. 24.2) [11]. Although this is a congenital hernia, it is more commonly diagnosed in adults as they become symptomatic later in life, or incidentally discovered on radiological studies. It is thought that increased abdominal pressure related to obesity, pregnancy, constipation, and chronic cough, as well as trauma or substantial core effort, may contribute to these hernias increasing in size across one's lifespan [12]. These hernias commonly contain omentum, colon, stomach, liver, or small intestine [10]. The term "Morgagni hernia" may also be used to refer to an acquired, iatrogenic anterior diaphragmatic hernia that may occur most commonly after cardiac surgery, although in this context the term is used imprecisely.

While some patients with Morgagni hernias are asymptomatic, symptomatic Morgagni hernias may present a diagnostic challenge. Diagnosis may be delayed due to the presence of nonspecific symptoms including epigastric and lower sternal discomfort or vague cardiorespiratory and gastrointestinal symptoms [12]. It has been reported that pulmonary symptoms are the presenting symptom of Morgagni hernia in more than a third of cases, suggesting that normal gastrointestinal function does not exclude this diagnosis [13].

Findings on chest x-ray (CXR) are dependent on the organ or organs involved. If omentum

alone is involved, Morgagni hernia may be seen as a smooth, well-defined opacity in the right anterior cardiophrenic angle. If the hernia is large enough to contain bowel, gas shadowing may appear in the right cardiophrenic angle, or may even obliterate the cardiac silhouette in anteroposterior views. In this case, lateral views may reveal loops of intestine herniating into the chest posterior to the sternum. The CXR may also reveal marked elevation of the right hemidiaphragm (Fig. 24.7) [10].

Upper gastrointestinal series or contrast enemas may reveal herniated bowel in the right chest depending on whether the intestine is involved and whether it is small or large bowel, but CT scan is usually the most diagnostic. The CT will show the diaphragmatic defect, and axial and sagittal images may clearly demonstrate the presence of abdominal fat and potentially bowel anterior to the heart. Additionally, a high-riding transverse colon may also be seen if omentum is present in the hernia and exerts upward traction (Fig. 24.8, Video 24.1) [10, 14].

While it has been proposed that all Morgagni hernias should be repaired, even in asymptomatic patients, the rarity and heterogeneity of this condition and its clinical presentations have prevented a standardized approach from being developed. Both transabdominal and transtho-

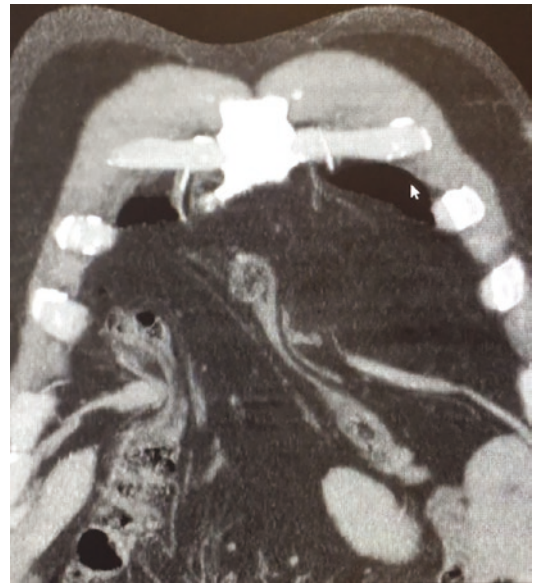

Fig. 24.8 Coronal CT scan of the same patient depicted in Fig. 24.7 revealing large left diaphragmatic defect, with herniating transverse colon into the left posterior thoracic cavity

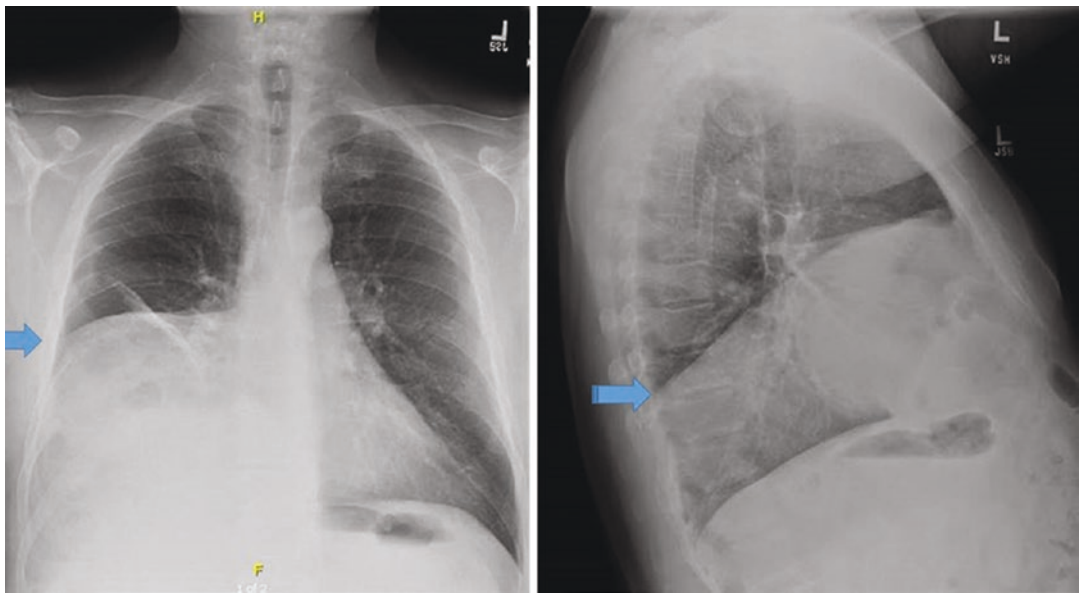

Fig. 24.7 Postero-anterior and lateral CXR revealing marked elevation of the right hemidiaphragm (arrows) in an adult patient with Morgagni hernia

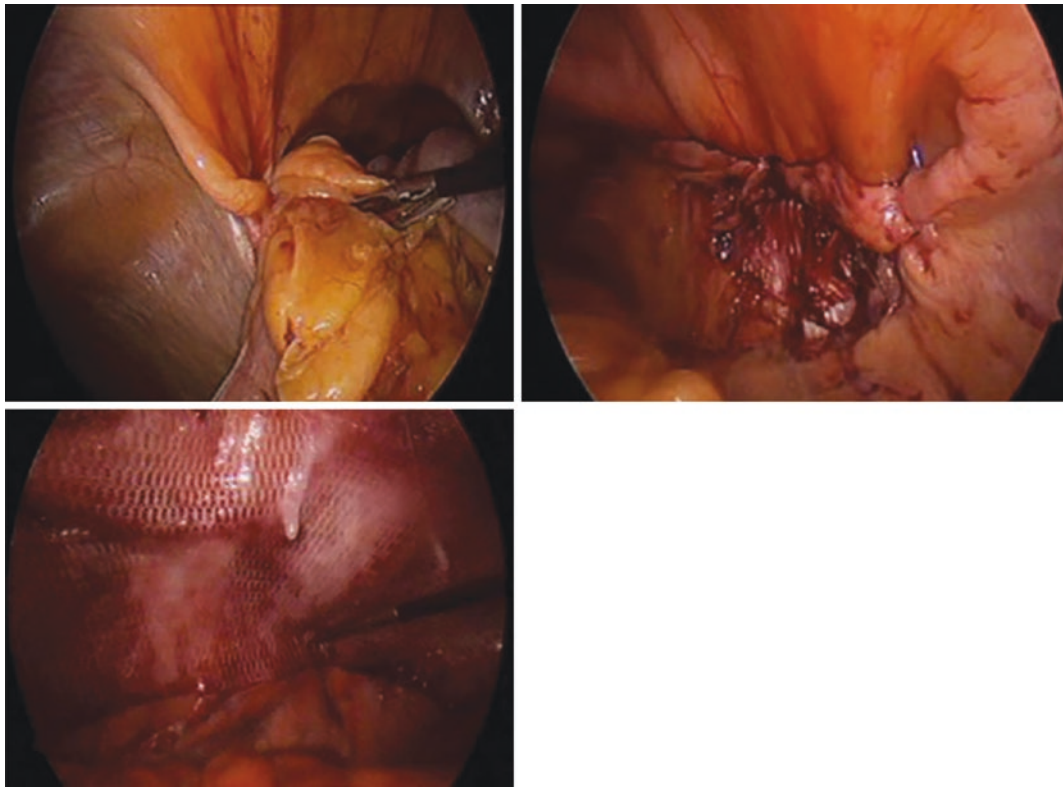

Fig. 24.9 Laparoscopic views of a large Morgagni hernia. The repair proceeded with primary closure of the defect and then mesh reinforcement

racic approaches have been reported, and both minimally invasive and open approaches from both the abdomen and the chest have been described (Fig. 24.9). While prosthetic mesh reinforcement during Morgagni hernia repair has been reported, particularly in contexts of large hernias or where primary repair was not possible, there is generally a lack of long-term data to guide the decision-making when a tension-free primary repair is feasible [12]. Ultimately, operative strategy will depend on the clinical situation and surgeon's preference.

Traumatic Diaphragmatic Hernia

Traumatic diaphragmatic hernias are acquired hernias resulting from herniation of abdominal contents through a diaphragmatic injury. It should be noted that diaphragmatic injury and traumatic diaphragmatic hernia are not synonymous. Diaphragmatic injury may occur without development of herniation. Though, unrecognized diaphragmatic injury may subsequently lead to development of a traumatic diaphragmatic hernia. Therefore, absence of a diaphragmatic hernia immediately after injury does not exclude the presence of a diaphragmatic injury. While the etiology of diaphragmatic injury in the context of penetrating mechanisms is straightforward, diaphragmatic injury is thought to occur in blunt mechanisms secondary to sudden increases in intrathoracic or intra-abdominal pressure against a fixed diaphragm. Fractured ribs may also cause diaphragmatic injury through penetration of the diaphragm or due to avulsion of the diaphragm from its peripheral attachment [9].

Traumatic diaphragmatic injury (TDI) is thought to be relatively rare; however, the true incidence is uncertain as these injuries may be difficult to diagnose. In the largest examination of TDI to date, 833,309 patients in the 2012

National Trauma Data Bank were reviewed for diagnosis of TDI [15]. The overall incidence of TDI was 0.46%, with TDI being diagnosed more often after penetrating injury than blunt injury (67% vs. 33% of patients with TDI). Patients with blunt TDI tended to be older and had greater overall injury severity. Blunt TDI was more commonly associated with thoracic aortic, pulmonary, splenic, and bladder injuries, whereas penetrating TDI was more often associated with hollow viscus injury, hemothorax, esophageal, gastric, pancreatic, and hepatic injuries. Mortality in the population of patients with penetrating TDI was 8.8%, and 19.8% for blunt TDI. The substantially higher mortality rate associated with blunt TDI is likely secondary to higher burden of severe injury. Given increasing nonoperative management of abdominal injuries, particularly for blunt mechanisms, it is possible that the incidence of TDI is higher than this estimate and small TDI are simply not being detected with imaging. While TDI is a rare clinical entity, it is clear that its occurrence and diagnosis is often a marker of injury severity.

Left-sided TDI is described more often in the literature than right-sided TDI. This may be due to the presence of the liver on the right, which could prevent other viscera from herniating into the chest, and hence prevent right-sided injuries from being readily diagnosed [16]. Additionally, left-sided injury may be more common with sharp penetrating mechanisms due to greater prevalence of right-handed assailants.

The evolution of diaphragmatic injury into a diaphragmatic hernia has been posited to have three stages: (1) the acute phase, from the time of injury to apparent recovery from the most life-threatening concomitant injuries, which may include states of shock, respiratory insufficiency, respiratory injury, and acute head injury, (2) the latent phase, in which abdominal viscera begin to occupy the defect and herniate into the hemithorax, producing symptoms including upper gastrointestinal complaints, left upper quadrant and/or left shoulder pain, and shortness of breath, and (3) the obstructive phase, which consists of visceral obstruction or ischemia [17]. While identification of all injuries a patient has is a key goal of early trauma management, the clinical signs that a patient has a diaphragmatic injury may be subtle, and many patients may not be identified as having a diaphragmatic injury until it results in a diaphragmatic hernia of substantial size. Clinically, when herniation is manifested, patients may experience chest or abdominal pain, dyspnea, respiratory failure, and ventilation difficulty. On physical exam, it may be possible to auscultate bowel sounds over the thorax. If a chest tube is placed, abdominal viscera may be seen or palpated during chest tube insertion.

In the acute setting, traumatic diaphragmatic hernias may be suspected on chest x-ray when the diaphragmatic contour is irregular or obscured, with a persistent opacity in the lower hemidiaphragm, elevation of the hemidiaphragm more than 4 cm higher than the contralateral side, and contralateral mediastinal shift without an effusion or pneumothorax. Clearer evidence of a traumatic diaphragmatic hernia includes obvious stomach or bowel loops in the chest, or extension of the tip of a correctly placed gastric tube from below to above the diaphragm [16, 18].

In the modern era, most TDIs are identified on CT scan. CT scan has been estimated to have a sensitivity and specificity of 0.77 and 0.91 for TDI, respectively [19]. CT scan may reveal a sharp cutoff of the diaphragm, herniated abdominal viscera (including stomach, small bowel, large bowel, omentum, spleen, and kidney), narrowing of abdominal viscera through the site of herniation (the so-called collar sign), and contact between the stomach, bowel, spleen, or upper one-third of the liver with the posterior ribs (the so-called dependent viscera sign). It may be helpful to review coronal and sagittal reconstructions of scans to identify subtle defects, particularly looking for the collar sign [10, 11]. (Fig. 24.10, Video 24.2).

While CT is relatively sensitive for these injuries, diagnostic laparoscopy may be indicated for a subset of patients who are not otherwise undergoing abdominal or thoracic exploration in whom there exists a high likelihood of TDI (Fig. 24.11).

Management of TDI and subsequent hernia is dependent on how the injury or hernia is discovered, including in the context of other injuries

Fig. 24.10 Coronal CT images of posttraumatic left flank and diaphragmatic hernias after blunt abdominal trauma. The stomach can be seen herniating into the left hemithorax

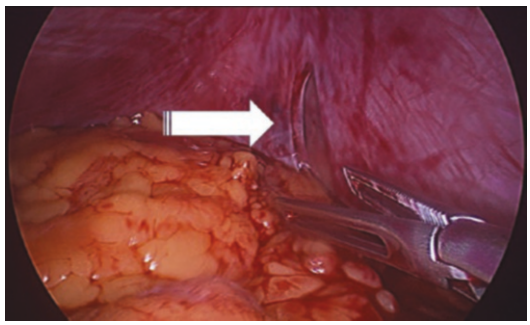

Fig. 24.11 Laparoscopic view of a left traumatic diaphragmatic injury after penetrating trauma

being managed. If diaphragmatic injury is discovered during laparotomy or thoracotomy, repair may be performed at that point in time and from either approach. If diaphragmatic injury is the indication for operation in the acute setting, then an abdominal approach is typically favored as other intra-abdominal injuries may be addressed at that time, and reduction of viscera may be easier. In the context of delayed recognition of a traumatic diaphragmatic hernia, surgical dogma has typically recommended a thoracic approach for chronic traumatic hernias, as it may be easier to address intrathoracic adhesions from the chest. However, this dogma has been challenged and many surgeons are now addressing chronic traumatic diaphragmatic hernias transabdominally and with minimally invasive approaches [18].

Hiatal and Paraesophageal Hernias

Hiatal hernias are hernias in which abdominal viscera extrude into the mediastinum between the diaphragmatic crura at the esophageal hiatus. Hiatal hernias are most commonly classified as type I–IV, with the degree of involvement of the stomach and other intra-abdominal organs distinguishing between types:

- Type I hiatal hernias involve herniation of the gastroesophageal junction (GEJ) above the diaphragm, and are also known as sliding hiatal hernias.
- Type II hiatal hernias involve herniation of the gastric fundus above the diaphragm, with the GEJ remaining in its anatomical position.
- Type III hiatal hernias involve herniation of both the GEJ and the stomach into the chest.
- Type IV involves herniation of the stomach and another abdominal organ—commonly the colon, small bowel, omentum, or spleen—above the diaphragm.

Collectively, type II–IV hiatal hernias are known as paraesophageal hernias (PEH). Type I hiatal hernias are estimated to account for approximately 95% of hiatal hernias, while PEH constitute the remaining 5% [20].

The exact mechanism or mechanisms by which hiatal hernias occur remain uncertain. At this point, most evidence supports the concept that structural changes of the periesophageal ligaments and muscular crura at the esophageal hiatus lead to the formation of hiatal hernias [21]. Increased intra-abdominal pressure, esophageal shortening from fibrosis or excess vagal stimulation, and enlargement of the hiatus from congenital defects or acquired molecular/cellular changes are posited to contribute to the development of

these hernias, and it is likely that this is multifactorial [22]. Incidence of hiatal herniation also increases with age, with hiatal hernia found on cross-sectional imaging in approximately 5% of patients under 40, 30% of patients between 40 and 59, and 65% between 60 and 79 years old [7].

The symptomatology and clinical presentation of patients with hiatal hernias can vary drastically. Sliding hiatal hernias are sometimes asymptomatic, but when symptoms manifest, they most commonly consist of gastroesophageal reflux disease (GERD) due to displacement of the GEJ into the mediastinum. For PEH, some asymptomatic patients are discovered incidentally during imaging studies for other conditions, while other patients with PEH may be severely affected by symptoms including dysphagia, GERD, postprandial abdominal pain, regurgitation, chest pain, and/or shortness of breath, which result from abnormal location of the GEJ, intermittent gastric outlet obstruction, and mass effect on the intrathoracic organs. Cameron lesions related to hiatal hernias—linear ulcers or erosions of the gastric mucosal folds at the site of diaphragmatic indentation—may lead to gastrointestinal bleeding and anemia and are more common with larger hernia size [23]. Rarely, large PEH may present acutely with gastric volvulus leading to obstruction, incarceration, and ultimately strangulation. This presentation may be suggested by Borchardt's triad, consisting of epigastric pain, inability to vomit, and failure to pass a nasogastric tube into the stomach [20], and constitutes a surgical emergency. Consequences of longstanding GERD related to hiatal hernias include esophagitis, Barrett's metaplasia, and esophageal cancer.

A variety of radiographic tests are helpful in the workup of hiatal hernias and may be supplemented by other endoscopic studies. The utility of chest x-ray may be limited based on the type of hiatal hernia. For sliding hiatal hernias with only upward GEJ displacement, there may be no obvious findings on chest x-ray. With larger PEH, chest x-ray may reveal a retrocardiac mass with an air-fluid level (Fig. 24.12a). In these cases, a lateral view is helpful to distinguish between a Morgagni hernia and a hiatal hernia, which may be differentiated by the position of air-fluid levels relative to the position of the heart (Fig. 24.12b).

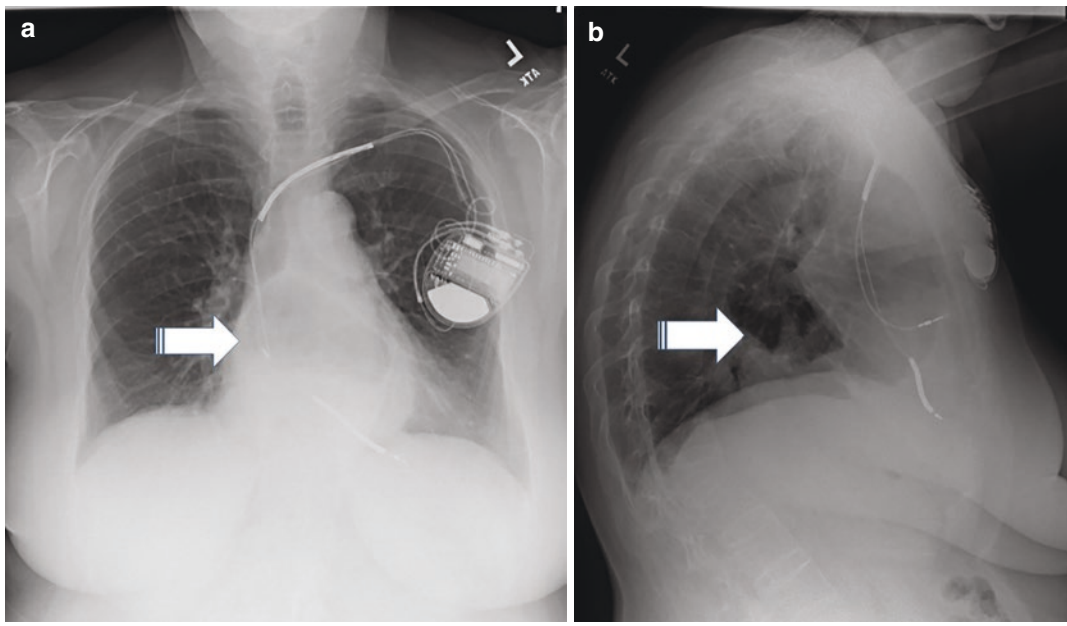

Fig. 24.12 (**a**, **b**) Posterio-anterior and lateral CXR illustrating retrocardiac air-fluid levels (arrows) seen in a patient with a large paraesophageal hernia

In the setting of gastric volvulus, two retrocardiac air-fluid levels may be present due to gastric rotation and obstruction [24].

Barium upper GI studies yield a large amount of useful information related to hiatal hernias (Fig. 24.13). These may demonstrate presence and relative size of a hiatal hernia, as well as presence of any esophageal strictures secondary to GERD. As these can be performed as dynamic tests, they may also demonstrate reducibility of the hiatal hernia as well as any abnormalities of esophageal motility. Because of this, upper GI studies are highly valuable in planning for elective hiatal hernia repair and may assist with the decision of whether further workup is needed and whether or not to perform a fundoplication. Typically, the finding of the GEJ 2 cm above the diaphragm on upper GI is used to define presence of a sliding hiatal hernia [24–26].

While CT scan does not provide a substantial amount of information in the setting of sliding hiatal hernias, it can distinguish between these and PEH. For PEH specifically, CT scan is useful for distinguishing the relative size of the hernia, whether organs other than the stomach are involved and their orientation in the mediastinum, and the relative size of the defect at the esophageal hiatus. If a diagnosis of acute gastric volvulus is suspected, CT scan is helpful as a rapid test to distinguish between gastric volvulus and the myriad other causes of acute abdominal pain. As with other diaphragmatic hernias, a review of sagittal and coronal images can be particularly helpful in delineating the involved anatomy (Fig. 24.14a, b, Video 24.3) [10].

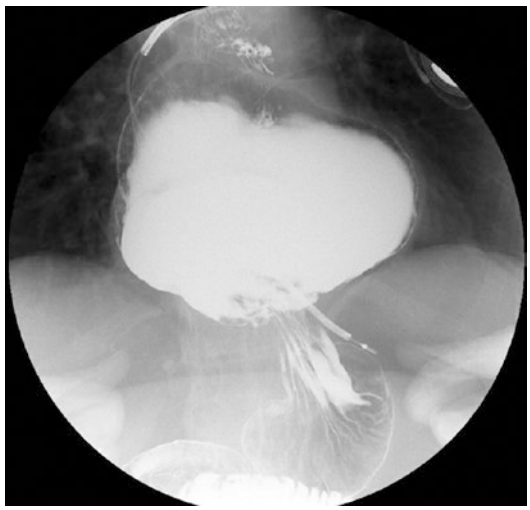

Fig. 24.13 An upper GI revealing a large fixed paraesophageal hernia containing the entire gastric fundus and a portion of the gastric body

Several invasive tests are helpful for supplementing the workup of hiatal hernias. Esophagogastroduodenoscopy (EGD) may demonstrate esophageal length, presence of esophagitis, Barrett's changes, or esophageal neoplasm, and gastric abnormalities including ulcers and gastritis, and is therefore a key test in the evaluation and management of hiatal hernia [20]. Esophageal manometry provides information about lower esophageal sphincter position, contraction, and relaxation, as well as esophageal motility. Again, this can influence the decision of whether further workup is needed and whether a partial or full fundoplication should be performed, if at all. A pH probe test is not necessary in most cases but may help in the setting of sliding hiatal hernias without endoscopic evidence of increased acid exposure. This test provides information about whether a patient's subjective symptoms correspond to objective decreases in pH; this can help to avoid unnecessary fundoplication and its potential complications in an individual whose symptoms are not attributable to acid reflux [24, 25].

Management of hiatal hernias is dependent on the type of hiatal hernia present as well as the symptoms. The Society of American Gastrointestinal and Endoscopic Surgeons (SAGES) guidelines recommend that repair of type I hiatal hernia in the absence of reflux disease is not necessary, while all patients with types II–IV hiatal hernias who have symptoms should undergo repair [25]. Asymptomatic patients with PEH may not require repair, although many patients will report at least mild symptoms depending on how questions are posed. A full discussion of operative approaches is beyond the scope of this chapter; however, both transabdominal and transthoracic approaches are possible, with a laparoscopic transabdominal repair being the preferred operation for most patients with hiatal hernias [25, 26].

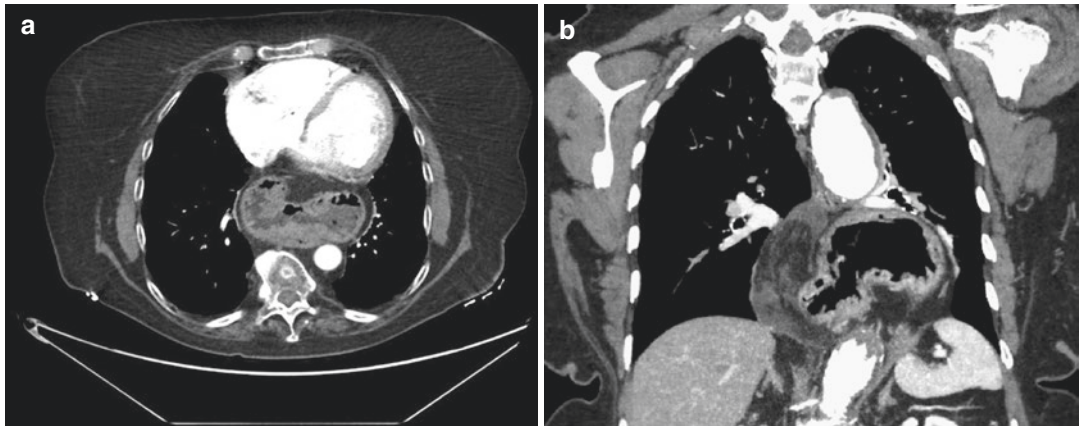

Fig. 24.14 (**a**, **b**) Axial and coronal CT scan images revealing paraesophageal hernia with the stomach in the retrocardiac mediastinal cavity

Conclusion

Congenital and acquired diaphragmatic hernias are less common, but advanced imaging technologies, and the recent increase in their utilization, have increased the detection of these hernias. Cross-sectional imaging, namely CT scan, remains the most widely used modality for diaphragmatic evaluation in adults, while UGI studies may be essential in evaluating hiatal hernias. The repair of these hernias via the minimally invasive approach has been feasible, safe, and effective.

References

1. Maish MS. The diaphragm. Surg Clin North Am. 2010;90:955–68. https://doi.org/10.1016/j.suc.2010.07.005.
2. Sandstrom CK, Stern EJ. Diaphragmatic hernias: a spectrum of radiographic appearances. Curr Probl Diagn Radiol. 2011;40:95–115. https://doi.org/10.1067/j.cpradiol.2009.11.001.
3. Nason LK, Walker CM, McNeeley MF, et al. Imaging of the diaphragm: anatomy and function. Radiographics. 2012;32:E51–70. https://doi.org/10.1148/rg.322115127.
4. Mallik K, Rodgers BM, McGahren ED. Congenital diaphragmatic hernia: experience in a single institution from 1978 through 1994. Ann Thorac Surg. 1995;60:1331–6. https://doi.org/10.1016/0003-4975(95)00617-T.
5. Harting MT, Lally KP. The congenital diaphragmatic hernia study group registry update. Semin Fetal Neonatal Med. 2014;19:370–5. https://doi.org/10.1016/j.siny.2014.09.004.
6. Mullins ME, Stein J, Saini SS, Mueller PR. Prevalence of incidental Bochdalek's hernia in a large adult population. Am J Roentgenol. 2001;177:363–6. https://doi.org/10.2214/ajr.177.2.1770363.
7. Caskey CI, Zerhouni EA, Fishman EK, Rahmouni AD. Aging of the diaphragm: a CT study. Radiology. 1989;171:385–9. https://doi.org/10.1148/radiology.171.2.2704802.
8. Machado NO. Laparoscopic repair of Bochdalek diaphragmatic hernia in adults. N Am J Med Sci. 2016;8:65–74. https://doi.org/10.4103/1947-2714.177292.
9. Gulamhusein T, Obeid NR, Pryor AD. Surgical management: other diaphragmantic hernias in adults. In: The SAGES manual of foregut surgery. Cham: Springer; 2019. p. 273–97.
10. Walker CM, Chung JH, Godwin JD. Diaphragm. 2nd ed. Elsevier; 2020.
11. Gore RM, Ghahremani GG, Marn CA. Hernias and abdominal wall pathology. 4th ed. Elsevier; 2008.
12. Sanford Z, Weltz AS, Brown J, et al. Morgagni hernia repair: a review. Surg Innov. 2018;25:389–99. https://doi.org/10.1177/1553350618777053.
13. Horton JD, Hofmann LJ, Hetz SP. Presentation and management of Morgagni hernias in adults: a review of 298 cases. Surg Endosc Other Interv Tech. 2008;22:1413–20. https://doi.org/10.1007/s00464-008-9754-x.
14. Webb WR. Pleura, chest wall, and diaphragm. 5th ed. Elsevier; 2006. p. 157–74.
15. Fair KA, Gordon NT, et al. Traumatic diaphragmatic injury in the American College of Surgeons National Trauma Data Bank: a new examination of a rare

diagnosis. Am J Surg. 2015;209:864–9. https://doi.org/10.1016/j.amjsurg.2014.12.023.
16. Hanna WC, Ferri LE. Acute traumatic diaphragmatic injury. Thorac Surg Clin. 2009;19:485–9. https://doi.org/10.1016/j.thorsurg.2009.07.008.
17. Grimes OF. Traumatic injuries of the diaphragm. Am J Surg. 1974;128:175–81. https://doi.org/10.1016/0002-9610(74)90090-7.
18. Scharff JR, Naunheim KS. Traumatic diaphragmatic injuries. Thorac Surg Clin. 2007;17:81–5. https://doi.org/10.1016/j.thorsurg.2007.03.006.
19. McDonald AA, Robinson BRH, Alarcon L, et al. Evaluation and management of traumatic diaphragmatic injuries: a practice management guideline from the eastern Association for the Surgery of Trauma. J Trauma Acute Care Surg. 2018;85:198–207. https://doi.org/10.1097/TA.0000000000001924.
20. Oleynikov D, Jolley JM. Paraesophageal hernia. Surg Clin North Am. 2015;95:555–65. https://doi.org/10.1016/j.suc.2015.02.008.
21. Weber C, Davis CS, Shankaran V, Fisichella PM. Hiatal hernias: a review of the pathophysiologic theories and implication for research. Surg Endosc. 2011;25:3149–53. https://doi.org/10.1007/s00464-011-1725-y.
22. Saad AR, Corey BL. Classification and evaluation of diaphragmatic hernias. In: SAGES manual of foregut surgery. Cham: Springer; 2019. p. 225–39. https://doi.org/10.1007/978-3-319-96122-4_18.
23. Maganty K, Smith RL. Cameron lesions: unusual cause of gastrointestinal bleeding and anemia. Digestion. 2008;77:214–7. https://doi.org/10.1159/000144281.
24. Kohn GP. Preoperative diagnostic workup for GERD and hiatal hernia: an evidence and experience-based approach. In: Hiatal hernia surgery: an evidence based approach. Cham: Springer; 2017. p. 51–72. https://doi.org/10.1007/978-3-319-64003-7_4.
25. Kohn GP, Hons M, Fracs M, et al. SAGES–hiatal hernia management. 2013.
26. Chan EG, Sarkaria IS, Luketich JD, Levy R. Laparoscopic approach to Paraesophageal hernia repair. Thorac Surg Clin. 2019;29:395–403. https://doi.org/10.1016/j.thorsurg.2019.07.002.

25

Obturator, Perineal, Sciatic, Internal, and Paraduodenal Hernias

Yang Lu, David C. Chen, and Ian T. MacQueen

Introduction

As groin and anterior abdominal wall hernias constitute the majority of hernias encountered in practice, most providers are familiar with these hernias and there is an abundance of expertise in the diagnosis and management of these conditions. In contrast, there exists a range of less common hernias which pose significant diagnostic and therapeutic challenges, mainly stemming from the rarity and relative obscurity of these afflictions. Despite the low prevalence of these hernias, it is crucial that primary care physicians, radiologists, and surgeons be familiar with these rare hernias and maintain a high degree of suspicion when a patient's clinical presentation is consistent with one of these diagnoses. This chapter seeks to describe several of these uncommon hernias, with a focus on anatomy, epidemiology, clinical presentation, diagnostic workup, and treatment.

Obturator Hernias

An obturator hernia is present when peritoneal contents protrude through the obturator canal, within the obturator foramen. The obturator foramen is a large opening situated between the ischium and pubis, filled almost completely by the obturator internus and externus muscles. The obturator canal is a passageway through the obturator foramen and is bordered by the obturator muscles. The canal is approximately 1/3 cm in size and allows for the passage of the obturator nerve, artery, and vein from the pelvis to the medial thigh. An obturator hernia passes immediately adjacent to these structures within the obturator canal.

Though it is an extremely rare form of abdominal wall hernia (<1%), the obturator hernia carries one of the highest mortality rates [1]. It has earned the moniker "little old ladies' hernia," because the classic patient is an elderly, thin woman. Typical presentation includes repeated episodes of bowel obstruction accompanied by weight loss. Other risk factors include those associated with pelvic laxity, such as multiparity, and conditions that increase intra-abdominal pressure, such as chronic constipation or ascites. An obturator hernia occurs more often unilaterally

Supplementary Information The online version contains supplementary material available at https://doi.org/10.1007/978-3-031-21336-6_25.

Y. Lu
Department of Surgery, David Geffen School of Medicine at UCLA, Los Angeles, CA, USA
e-mail: yanglu@mednet.ucla.edu

D. C. Chen · I. T. MacQueen (✉)
Department of Surgery, Lichtenstein Amid Hernia Clinic at UCLA, Santa Monica, CA, USA
e-mail: dcchen@mednet.ucla.edu; imacqueen@mednet.ucla.edu

S. Docimo Jr. et al. (eds.), *Fundamentals of Hernia Radiology*,
https://doi.org/10.1007/978-3-031-21336-6_25

and on the right side because the left obturator foramen is often shielded by the sigmoid colon. The rarity of obturator hernias often leads to a delay in diagnosis and thus results in gangrenous bowel requiring surgical resection in half of all cases [2]. Clinical symptoms depend on the size of the hernia and its contents. While most patients present with subtle symptoms of pelvic discomfort, those with mechanical obstruction will endorse crampy abdominal and pelvic pain, nausea, and vomiting.

On physical examination, tenderness may be elicited upon palpation of the obturator foramen. A visible or palpable bulge on the medial thigh is only found in 20% of patients. The Howship-Romberg sign is a pathognomic exam finding which describes referred pain down the medial aspect of the thigh during medial rotation of the hip, due to compression of the cutaneous branch of the obturator nerve [3, 4]. Pain is often exacerbated by provocative maneuvers such as coughing or extension, adduction, and medial rotation of the hip. It may be relieved by flexion of the hip. Another exam finding suggestive of an obturator hernia is the Hannington-Kiff sign, which is characterized by the loss of thigh adductor reflex in the presence of a positive patellar reflex.

Although physical examination is important in the diagnosis of this challenging hernia, most cases of asymptomatic obturator hernias are discovered incidentally during laparoscopic surgery for a separate indication. In a symptomatic individual, the diagnosis of an obturator hernia can be readily made on cross-sectional imaging including CT or MRI, in which fluid or bowel can be traced along the obturator canal to lie in the medial upper thigh (Figs. 25.1 and 25.2, Video 25.1). The treatment of obturator hernias is surgical repair, either via transabdominal, inguinal, or obturator approaches [4, 5]. For patients presenting with bowel obstruction, a transabdominal approach is preferred because of the possible need for bowel resection.

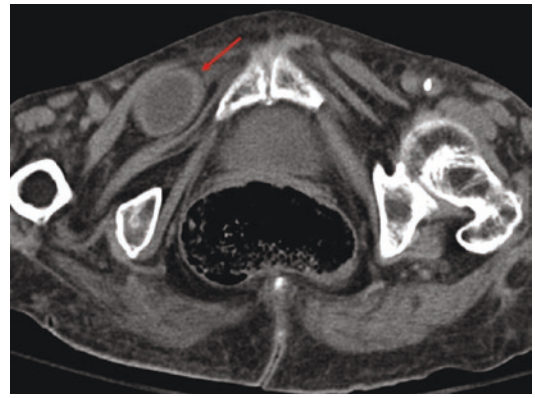

Fig. 25.1 Obturator hernia. A 94-year-old female presents with abdominal distention. The red arrow indicates a right obturator hernia with an incarcerated loop of the bowel, along with significant free fluid in the hernia sac

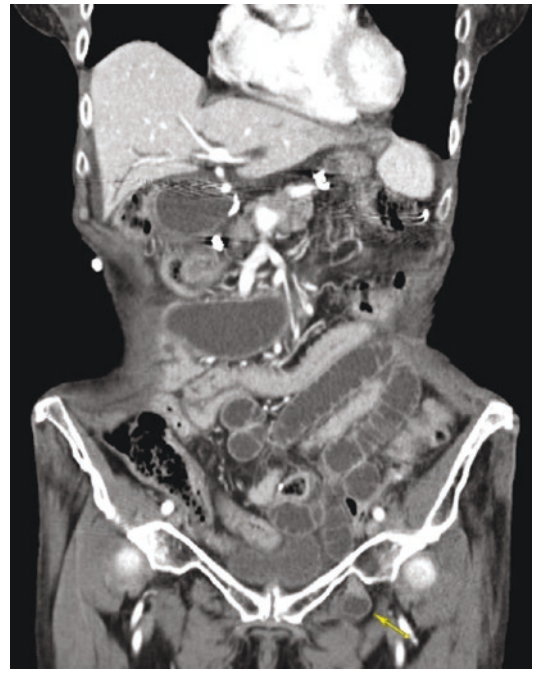

Fig. 25.2 Obturator hernia. A 76-year-old female with a history of gastric bypass presented with generalized abdominal pain. CT demonstrated high-grade obstruction of the pancreaticobiliary limb with transition point (marked by yellow arrow) within a small left obturator hernia containing a small portion of bowel

Perineal Hernias

A perineal hernia is a protrusion of visceral contents through a defect in the pelvic floor, either anterior or posterior to the superficial transverse perineal muscles. Perineal hernias may be primary or secondary based on the occurrence of prior surgery. Primary perineal hernias are extremely rare and may be due to a failure of regression of the peritoneal cul de sac of the embryo, leading to a relatively weakened pelvic floor [6]. Acquired perineal hernias may occur later in life through an accumulation of risk factors associated with increased intra-abdominal pressure, such as chronic constipation and multiparity. Primary perineal hernias have also been described after pelvic fractures following major trauma such as a motor vehicle accident. Secondary perineal hernias are complications following major pelvic surgery such as abdominoperineal resection, pelvic exenteration, or orthopedic operations that remove the coccyx or distal sacrum without adequate reconstruction.

Patients typically describe symptoms including pelvic pain, which is often exacerbated by standing up and may be associated with impaired urination or defecation. Perineal hernias tend to have a wide neck, and strangulation or obstructive symptoms are relatively uncommon [6]. On physical examination, perineal hernias may be palpated on bimanual rectal-vaginal examination. Pelvic ultrasound and CT imaging may be used to further evaluate the severity of a perineal hernia. Due to the location of perineal hernias, skin erosion and problems with urination and defecation often necessitate surgical repair. Various techniques have been described to correct this difficult problem, including perineal, transabdominal, and combined abdominoperineal approaches. The defect in the pelvic diaphragm may be closed primarily or by using autogenous material or synthetic mesh.

Sciatic Hernias

A sciatic hernia is the protrusion of intra-abdominal contents through the greater or lesser sciatic foramen of the pelvis. The greater sciatic foramen is bounded by the ilium, sacroiliac ligament, sacrospinous ligament, and sacrotuberous ligament. The piriformis muscle passes through and nearly fills this foramen. Hernias through the greater sciatic foramen may occur in the supra-piriform space (adjacent to the superior gluteal vessels and nerve) or in the infra-piriform space (adjacent to multiple vessels and nerves including the sciatic nerve). The lesser sciatic foramen is bounded by the sacrospinous ligament, the sacrotuberous ligament, and the ischial tuberosity. Lesser sciatic hernias occur adjacent to the multiple nerves and vessels that traverse this foramen, including the internal pudendal vessels and the pudendal nerve. Regardless of whether they occur in the supra-piriformis, infra-piriformis, spinotuberous location, and sciatic hernias are typically overlaid by the gluteus maximus and only large sciatic hernias protrude from under the distal aspect of the muscle. In female patients, sciatic hernia defects are generally found in the ovarian fossa. In males, the internal topography of sciatic hernias is less consistent, but they may frequently be found laterally and posteriorly to the rectum [7].

Sciatic hernias are one of the rarest forms of pelvic hernias and their presentation is highly variable. When symptomatic, patients may complain of dull, pressure sensation in the pelvis, radiating to the gluteal muscle or posterior thigh. Patients may also experience sharp pain traveling down the posterior thigh related to compression of the sciatic nerve. Due to the sciatic hernia's location deep in the gluteal maximus muscle, early detection of a bulge is rare. Palpation of a tender, reducible mass with a cough can be diagnostic of a sciatic hernia. Digital rectal or vaginal

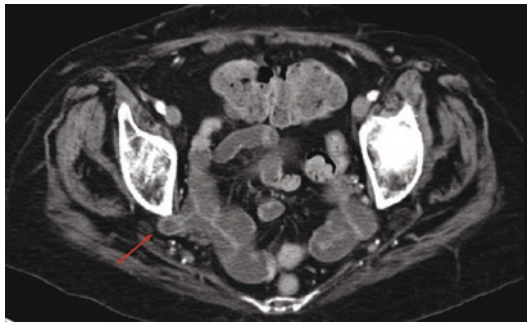

Fig. 25.3 Sciatic hernia. A 68-year-old female with an incidentally found sciatic hernia on cross-sectional imaging. The red arrow indicates a small right sciatic notch hernia with protrusion of small bowel into the greater sciatic foramen

examination may also be performed to facilitate a diagnosis, as a mass may be felt within the sciatic region. As with the other types of hernias described in this chapter, a definitive diagnosis is most frequently made on cross-sectional imaging (Fig. 25.3, Video 25.2). CT with water-soluble rectal contrast may be helpful in characterizing a sciatic hernia containing colon. In addition, an excretory urography can be useful in diagnosing a ureteric sciatic hernia. In such a study, a curling ureter, also known as the "curlicue ureter" sign, is considered pathognomonic and is seen when the herniated ureter passes laterally to the medial wall of the pelvis. Surgical management of sciatic hernias can be performed via transgluteal, transabdominal, or combined approaches.

Internal Hernias

An internal hernia is a protrusion of viscus through a foramen or retroperitoneal fossa within the abdominal cavity. Internal hernias may be congenital or acquired. Acquired internal hernias are frequently due to surgically created foramina or mesenteric defects, which may be formed after bowel surgery such as Roux-en-Y procedure or liver transplantation (Figs. 25.4 and 25.5) [8]. Internal hernias are frequently found in the following locations: paraduodedunal, pericecal, foramen of Winslow, parasigmoid, transmesenteric, pelvic, and transomental (Fig. 25.6) [9].

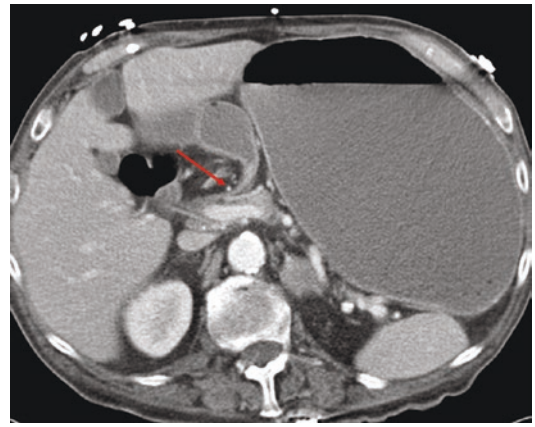

Fig. 25.4 Internal hernia. A 89-year-old male presents with severe abdominal pain and vomiting. The red arrow marks an internal hernia in the transverse mesocolon, causing significant gastric outlet obstruction in this patient

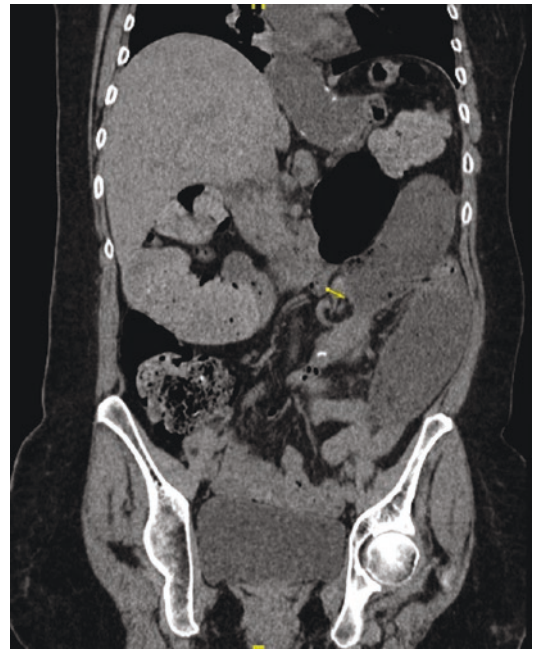

Fig. 25.5 Internal hernia. A 48-year-old female with a history of Roux-en-Y gastric bypass presents with symptoms of bowel obstruction. CT demonstrates dilated distal esophagus, stomach and proximal loops of small bowel with the yellow indicator pointing to a transition point in the left central abdomen

Internal hernias are rare and have an autopsy incidence of <1%, but account for nearly 5% of all cases of small bowel obstruction [8, 10].

Paraduodenal 53%

Pericecal 13%

Foramen of Winslow 8%

Transmesenteric 8%

Perisigmoid 6%

Pelvic and supravesical 6%

Transomental 4%

Fig. 25.6 Common locations and relative frequencies of internal hernias. Paraduodenal 53%, Pericecal 13%, Foramen of Winslow 8%, Transmesenteric 8%, Perisigmoid 6%, Pelvic and supravesical 6%, Transomental 4%

Fig. 25.7 Axial and coronal views of a paraduodenal hernia. A 27-year-old female presents with diffuse abdominal pain. The small bowel can be seen herniating into a large left paraduodenal hernia through the fossa of Landzert

Paraduodenal Hernias

Paraduodenal hernias account for over half of all internal hernias. They occur with a male-to-female predominance of 3:1, and may occur at any age [8, 10]. Patients classically present with symptoms of intermittent post-prandial abdominal pain and weight loss. Paraduodenal hernias occur more frequently on the left side (75%), where visceral contents protrude through the fossa of Landzert, a congenital defect which is found just left of the duodenojejunal junction [8, 11]. The defect is bordered anteriorly by peritoneal tissue overlying the inferior mesenteric vein and ascending left colic artery. A small bowel loop may enter through the mesocolic defect and become entrapped in the fossa of Landzert. On computed tomography, herniated small bowel loops can be visualized posterior to the ascending left colic artery near the ligament of Treitz (Figs. 25.7 and 25.8, Video 25.3) [12]. Additional signs of bowel compromise include vessel engorgement, bowel-wall thickening, and absence of wall enhancement after contrast injection.

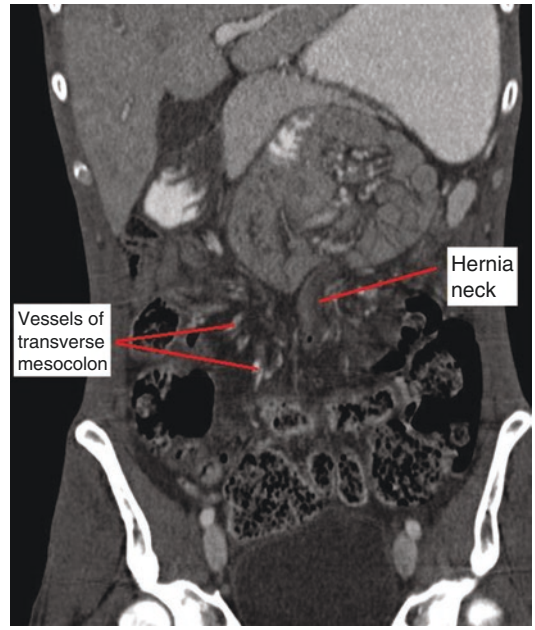

Fig. 25.8 Axial and coronal views of a paraduodenal hernia. A 27-year-old female presents with diffuse abdominal pain. The small bowel can be seen herniating into a large left paraduodenal hernia through the fossa of Landzert

Twenty-five percent of paraduodenal hernias occur on the right side, where viscera herniate through the fossa of Waldeyer within the proximal jejunal mesentery [8, 13]. Right paraduodenal hernias are congenital disorders that result from absent or malrotation of the midgut. In these cases, the small bowel is located to the right of the superior mesentery artery (SMA) and may be entrapped as it tunnels into a peritoneal recess

posterior to the SMA. CT imaging reveals small bowel loops posterior to the SMA or branches of the ileocolic arteries positioned within the fossa of Waldeyer.

Pericecal Hernias

Pericecal hernias make up 6–13% of all internal hernias and frequently present with entrapment of ileum through the paracolic sulcus posterior to the cecum, which is bordered by the parietocecal fold laterally and the mesentericocecal fold medially [8]. Clinical symptoms related to pericecal hernias include intense right lower quadrant pain, which may mimic appendicitis, but will often also include obstructive symptoms such as nausea, vomiting, obstipation, and abdominal distension. On barium enema or computed tomography, pericecal hernias can be identified by visualizing fixed and dilated small bowel loops posteriorlateral to a normal-appearing cecum, with extension into the right paracolic gutter [13].

Foramen of Winslow Hernias

The foramen of Winslow is a normal peritoneal opening situated in the portacaval space and bordered by the portal vein anteriorly and inferior vena cava posteriorly. Factors that predispose herniation of viscera through the foramen of Winslow include an abnormally enlarged foramen and extended bowel mesentery. Herniation of small bowel contents through this space is most commonly reported, but there have also been reported cases of hernias including colon and gallbladder. On computed tomography, the presence of bowel and mesenteric fat tracking from lateral to medial between vena cava and porta hepatis, extending into the lesser sac and anteriorly displacing the stomach supports the diagnosis of a foramen of Winslow hernia.

Transmesenteric, Petersen Defect, Parasigmoid, and Transomental Hernias

In adults, transmesenteric hernias are frequently related to prior abdominal operations, particularly when Roux-en-Y anatomy is created (Fig. 25.9) [12]. Transmesenteric defects causing internal hernias most commonly occur in the transverse mesocolon and may occasionally be found in the small bowel mesentery. Roux-en-Y anatomy may result in a transmesenteric defect in the small bowel mesentery as well as a "Petersen defect," which is a potential space found between the transverse mesocolon and the small bowel mesentery, and may be present in any patient with a gastrojejunostomy. In children, transmesenteric hernias are a leading cause of internal hernias, usually through a congenital defect in the small bowel mesentery near the ileocecal segment [12]. In a unique case shown in Fig. 25.10, a closed-loop small bowel obstruction developed from herniation of small bowel into a mesenteric defect in a young patient without prior abdominal surgery.

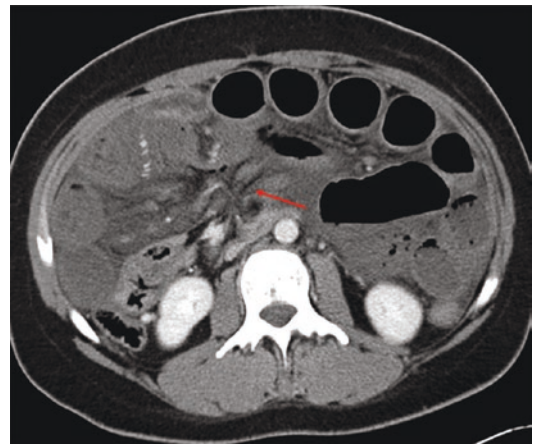

Fig. 25.9 Internal hernia. A 31-year-old female with a history of Roux-en-Y gastric bypass presents with abdominal pain. The red arrow indicates an internal hernia containing ischemic small bowel

Fig. 25.10 Internal hernia. A 38-year-old male with no prior surgical history presents with abdominal pain. The red arrow indicates small bowel herniation through what was suspected to be a mesenteric defect. On laparoscopy, an adhesive band was seen between mesentery and epiploic appendage, which created a small defect that led to a closed-loop bowel obstruction

Parasigmoid hernias make up 6% of all internal hernias [8]. Due to the redundant nature of sigmoid colon, an intersigmoid fossa may be formed between two neighboring loops, through which a segment of small bowel may become entrapped, resulting in obstruction. In a separate process, a transmesosigmoid hernia results when there is protrusion of viscera through a direct defect in the sigmoid mesocolon. Finally, a transomental hernia, which accounts for approximately 4% of internal hernias, describes protrusion of viscera through the greater or lesser omentum and is usually congenital in nature [14]. Treatment for internal hernia consists of transabdominal reduction of hernia contents with surgical closure of the internal foramen through which the hernia occurred.

Conclusion

Obturator, perineal, sciatic, internal, and paraduodenal hernias are a complex and difficult group of hernias to diagnose accurately and in a timely fashion due to the rarity of their presentation. However, understanding their clinical and radiographic presentation is paramount in order to provide appropriate and timely treatment in order to avoid significant morbidity and mortality.

Acknowledgement The author would like to acknowledge the following people for their support in this chapter, especially in the contribution of cross-sectional imaging of these rare hernias: Dr. Victor Sai, Dr. Katrina Beckett, and Dr. Barbara Kadell.

References

1. Nasir BS, Zendejan B, Ali SM, Groenewald CB, Heller SF, Farley DR. Obturator hernia: the Mayo Clinic experience. Hernia. 2012;16:316–9.
2. Lo CY, Lorentz TG, Lau PW. Obturator hernia presenting as small bowel obstruction. Am J Surg. 1994;167:396–8.
3. Pandey R, Maqbool A, Jayachandran N. Obturator hernia: a diagnostic challenge. Hernia. 2009;13:97–9.
4. Shipkov CD, Uchikov AP, Grigoriadis E. The obturator hernia. Hernia: difficult to diagnose, easy to repair. Hernia. 2004;8:155–7.
5. Mandarry MT, Zeng SB, Wei ZQ, Zhang C, Wang ZW. Obturator hernia- a condition seldom thought and hence seldom sought. Int J Color Dis. 2012;27(2):133–41.
6. Stamatiou D, Skandalakis JE, Skandalakis LJ. Perineal hernia: surgical anatomy, embryology, and technique of repair. Am Surg. 2010;76(5):474–9.
7. Losanoff JE, Basson MD, Gruber SA, Weaver DW. Sciatic hernia: a comprehensive review of the world literature (1900-2008). Am J Surg. 2010;199(1):529.
8. Salar O, El-Sharkaway AM, Singh R, Speake W. Internal hernias: a brief review. Hernia. 2013;17(3):373–7.
9. Takeyama N, Gokan T, Ohgiya Y, Satoh S, Hashizume T, Hataya K, Kushiro H, Nakanishi M, Kusano M, Munechika H. CT of internal hernias. Radiographics. 2005;25:997–1005.
10. Ghahremani GG. Abdominal and pelvic hernias. In: Gore RM, Levine MS, editors. Textbook of gastrointestinal radiology. 2nd ed. Philadelphia, PA: Saunders; 1994.
11. Martin LC, Elmar MM, Thompson WM. Review of internal hernias radiographic and clinical findings. Am J Roentgenol. 2006;186:703–17.
12. Janin Y, Stone AM, Wise L. Mesenteric hernia. Surg Gynecol Obstet. 1980;150:747–54.
13. Blachar A, Federle MP, Dodson SF. Internal hernia: clinical and imaging findings in 17 patients with emphasis on CT criteria. Radiology. 2001;218:68–74.
14. Blachar A, Federle MP. Internal hernia: an increasingly common cause of small bowel obstruction. Semin Ultrasound CT MR. 2002;23(2):174–83.

Diastasis Recti

26

Bianca J. Molina and Jeffrey E. Janis

Abbreviations

AP	Antero-posterior
BMI	Body mass index
CT	Computed tomography
IEHS	International Endohernia Society
MHz	Megahertz
MRI	Magnetic resonance imaging
US	Ultrasound

Introduction

Anatomy of the Linea Alba

Diastasis recti, otherwise known as rectus diastasis, can be understood as a separation between the rectus abdominis muscles at the midline of the abdomen due to attenuation of the linea alba. It is important to note that rectus diastasis does not constitute a true hernia, as there is no fascial defect or hernia sac encountered in these patients.

The linea alba comprises the midline confluence of the aponeuroses of the musculature of the abdominal wall. In the midline, the linea alba extends from the xiphoid process superiorly to the pubic symphysis inferiorly. There is a triangular reinforcement inferiorly termed the *adminiculum lineae albae*, which is composed of the aponeuroses of the external oblique, internal oblique, and transversus abdominis. There are also anatomic variations of the linea alba, for instance, in a minority of the population, the linea alba may not be present at the origin of the xiphoid, but rather found more lateral on the costal margin [1, 2]. The linea alba is also composed of both obliquely and transversely oriented fibers. Variation of composition has been shown between males and females, and in general the male linea alba is thicker, whereas the female linea alba is wider [3]. Additionally, anatomic studies have shown the linea alba to vary in deformability, elasticity, and width along its supero-inferior course [4]. Above the umbilicus, the linea alba has generally been found to be wider in this region compared to points at or below the umbilicus [1, 4]. Although width varies along the length of the linea alba, differences in physical properties of resistance to linear traction and deformability between the supra- or infra-umbilical regions have not been found [4].

Supplementary Information The online version contains supplementary material available at https://doi.org/10.1007/978-3-031-21336-6_26.

B. J. Molina · J. E. Janis (✉)
Department of Plastic and Reconstructive Surgery, The Ohio State University Wexner Medical Center, Columbus, OH, USA
e-mail: Jeffrey.Janis@osumc.edu

S. Docimo Jr. et al. (eds.), *Fundamentals of Hernia Radiology*,
https://doi.org/10.1007/978-3-031-21336-6_26

Etiology of Rectus Diastasis

The linea alba may become attenuated and the inter-rectus distance widened due to various reasons. A common cause in females is pregnancy, as the increased intra-abdominal force outwards causes attenuation and thinning of the fibers of the linea alba, changes which can be permanent. Another common contributor to increased intra-abdominal pressure is obesity, seen in both male and female patients. A history of previous abdominal surgery is also associated with this condition. Generally, the inter-rectus distance is smaller in nulliparous females compared to males and parous females [5].

Congenital lateral insertion of the paired rectus abdominis muscle also leads to an increase in the inter-rectus distance, though the true incidence of this, and any associated symptomatology is not known. This is clinically important in that the etiology of rectus diastasis can dictate surgical management strategies [2, 6].

Less commonly, congenital conditions have been implicated in causing thinning and widening of the linea alba in neonates. *Prune Belly Syndrome* is one such condition, wherein hypoplasia of the abdominal wall musculature is caused by genitourinary tract obstruction (urethral obstruction sequence). This leads to massive fetal abdominal wall distention. *Prune Belly Syndrome* occurs in approximately 1/40,000 live births, with over 95% of patients being male. *Pseudo Prune Belly Syndrome* is used to describe patients with partial or unilateral abdominal wall deficiency, unilateral undescended testis, or female neonates with significant abdominal wall laxity. It is difficult to determine the true incidence of this, though it is estimated to occur in 3–5% of those with *Prune Belly Syndrome* [7]. A separate clinical entity—*familial abdominal wall muscular hypoplasia*—has been described as an isolated finding in case reports, and not as part of the *Prune Belly Syndrome* or sequence. In one case report of this, a 3-year-old male was noted to have significant rectus diastasis associated with bowel and bladder dysfunction [8].

Vertical transmission of non-syndromic anterior abdominal wall deficiency has also been described in case reports. Linea alba weakness and rectus diastasis have been shown to exhibit familial segregation with autosomal dominant transmission. Considering the embryologic process of ventral abdominal wall closure, disordered ventral migration of mesenchyme leads to a spectrum of known congenital abnormalities such as *Cantrell pentalogy*, bladder extrophy, omphalocele, and weakness or hypoplasia of the rectus and linea alba. It is possible for weakness of the linea alba and diastasis rectus to be due to maturational deficiency and not occur as part of a sequence or syndrome [8, 9].

Clinical Significance of Rectus Diastasis

Rectus diastasis is a clinically important entity. Increased inter-rectus distance due to attenuation of the linea alba potentially contributes to symptoms of abdominal pain and weakness, low back pain, and impairments with urologic function. The literature suggests that a diastasis wider than 3 cm may benefit from repair from a functional, pain, and cosmetic standpoint [10]. Postpartum female patients have been shown to have an improvement in symptoms of back pain and urinary incontinence after undergoing traditional abdominoplasty to repair rectus diastasis [11]. The International Endohernia Society (IEHS) guidelines state the goal of reconstruction of the linea alba to more normal anatomy is to restore functionality of the abdominal wall, with the added secondary benefit of improved cosmesis [12].

Classification Systems of Rectus Diastasis

There are various classification systems that attempt to define pathologic or clinically significant inter-rectus distances. By the simplest definition, pathologic rectus diastasis can be considered present when the inter-rectus distance is greater than 2 cm. Currently established classification systems include: (1) Beer, (2) Rath, and (3) Nahas

classifications (Tables 26.1, 26.2, and 26.3). These named classifications aim to expand beyond one simple measurement in distinguishing a normal linea alba from one considered pathologically widened. Various clinical characteristics have been considered and included in these three classifications in an attempt to create a more meaningful and clinically useful construct.

Table 26.1 Beer classification

Level	Average width (mm)	Maximum normal width (mm)
Xiphoid process	7 ± 5	15
3 cm above umbilicus	13 ± 7	22
2 cm below umbilicus	8 ± 6	16

Beer et al. set the maximum inter-rectus distance that can be considered normal based on a study of 150 nulliparous females aged 20–45 years, with a body mass index (BMI) less than 30 kg/m^2 and no history of significant weight loss or previous surgery. The width of the linea alba was measured at three points using ultrasound. Measurements falling within the 10–90 percentile were considered "normal." Maximum normal widths are listed. According to this investigation, the linea alba is consistently widest at a point 3 cm above the umbilicus [1]

Table 26.2 Rath classification

Level	Age < 45 years		Age > 45 years	
–	Normal (mm)	Pathologic (mm)	Normal (mm)	Pathologic (mm)
Above umbilicus	5–6	10	12–14	15
At umbilicus	19–23	27	19–23	27
Below umbilicus	5–6	9	9–11	14

The Rath classification was developed from the comparison between gross measurements of the inter-rectus distance in male and female cadavers, and those obtained by CT. Patients fall into two age groups: under 45 years, and over 45 years. There are three points of interest: (1) supra-umbilical (halfway between xiphoid and umbilicus), (2) at the umbilicus, and (3) infra-umbilical (halfway between the umbilicus and pubic symphysis). Normal and pathologic ranges of the inter-rectus distances at these three points are given, according to age [4]

Table 26.3 Nahas classification

Type	Etiology	Corrective measure
A	Pregnancy	Anterior rectus sheath plication
B	Lateral, infra-umbilical myoaponeurotic laxity	Anterior rectus sheath + external oblique plication
C	Congenital lateral insertion of rectus abdominis	Rectus abdominis advancement
D	Obesity	Anterior sheath plication + external oblique advancement

The Nahas classification describes rectus diastasis according to the etiology of myofascial defects. Corrective measures are recommended based on the etiology of the diastasis, which takes into account various anatomic causes for the rectus diastasis. Type A deformity due to pregnancy is most common and is best repaired with standard abdominoplasty techniques using anterior rectus sheath plication [6, 13]

Beer Classification

The Beer classification is the most recently published classification system (2009) which sets a maximum inter-rectus distance that can be considered normal in females. The Beer system defines the maximum normal width of the linea alba based on measurements obtained from a study population of 150 nulliparous females aged 20–45 years, with a body mass index (BMI) less than 30 kg/m^2, and without a history of significant weight loss or previous surgery. The width of the linea alba (or inter-rectus distance) was measured at three points along its length from superior to inferior, including: (1) at its origin at the xiphoid, (2) 3 cm above the umbilicus, and (3) 2 cm below the umbilicus. Measurements of the inter-rectus distances at these points were obtained via ultrasound using a high-resolution linear array transducer.

Measurements within the range of the 10–90 percentile dictate "normal" widths of the linea alba at the respective points. Maximum "normal"

widths are defined as 15 mm at the xiphoid; 22 mm at 3 cm above the umbilicus; and 16 mm at 2 cm below the umbilicus. Average widths at the xiphoid were 7 mm ± 5; at 3 cm above the umbilicus the average width was 13 mm ± 7; and at 2 cm below the umbilicus, the average width was 8 mm ± 6. According to this investigation, the linea alba is consistently widest at a point 3 cm above the umbilicus. This classification system does not include other variables, such as age, body habitus, or height, as these were not found to be statistically correlated with the width of the linea alba in the study population [1] (Table 26.1).

Rath Classification

The Rath classification was developed and published in 1996 as part of an early anatomic and radiologic study of the linea alba, using both male and female cadavers. This classification system was borne out of cross-comparisons between gross anatomic measurements of the inter-rectus distance and measurements obtained by computed tomography (CT). In this classification system, the age of the patient is considered in determining whether an increased inter-rectus distance should be defined as pathologic. Two age groups are included: one of patients under 45 years of age and the other including patients above 45 years of age. Using the fixed anatomic reference points of the xiphoid, umbilicus, and pubic symphysis, three points are included along the supero-inferior extension of the linea alba: (1) supra-umbilical, or halfway between the xiphoid and umbilicus, (2) at the umbilicus, and (3) infra-umbilical, or halfway between the umbilicus and pubic symphysis.

Normal ranges of the inter-rectus distances, or linea alba width, in the supra-umbilical region are 5–6 mm before age 45 and 12–14 mm after the age of 45. Normal ranges at the umbilicus are 19–23 mm, without a difference for age. Normal ranges below the umbilicus are 5–6 mm before 45 years and 9–11 mm after age 45.

The Rath classification defines rectus diastasis in those aged 45 years or younger as an inter-rectus distance greater than 10 mm above the umbilicus (halfway between xiphoid and umbilicus), 27 mm at the umbilicus, and 9 mm below the umbilicus (halfway between the umbilicus and pubic symphysis). In those older than 45 years, cut-offs for abnormal inter-rectus distances are 15 mm, 27 mm, and 14 mm, respectively. Generally, the width of the supra-umbilical linea alba increases with age and is wider in females [4] (Table 26.2).

Nahas Classification

The Nahas classification describes rectus diastasis according to the etiology of myofascial defects and recommends appropriate surgical intervention for each type of rectus diastasis. Deformities are given type, A through D. Type A deformity is due to pregnancy and according to this classification is best repaired with anterior rectus sheath plication. Type B deformity is due to myoaponeurotic laxity, and recommended surgical repair includes anterior rectus sheath and external oblique plication. Type C deformity is due to congenital defects, and should be approached with rectus abdominis muscle advancement. Type D deformity is due to obesity, and should be approached with both anterior sheath plication and external oblique muscle advancement [6, 13] (Table 26.3).

Overall, agreement and standardization among these three classification systems are currently lacking both in the literature and in practice [14, 15]. Attempts have been made by major hernia societies, such as the International Endohernia Society (IEHS) and the German Hernia Society, to more clearly delineate and propose formal guidelines. Even after forming a working group to review the literature on rectus diastasis and its treatment, no clear guidelines or agreed-upon definitions were discovered [15]. Nevertheless, the three classification systems—Beer, Rath, and Nahas—do provide a framework for the diagnosis and management of rectus diastasis.

Diagnostic Imaging

Imaging has a role in accurately diagnosing rectus diastasis by proving objective measurements of the inter-rectus distance [14]. While it is possible to measure the inter-rectus distance using physical exam and direct measurement techniques, there is a lack of standardization to these techniques. For instance, in the preoperative setting, the finger breadth test characterizes the distance based on the number of finger breadths wide the medial edges of the rectus muscles are palpably separated, which is obviously variable among individuals. The use of calipers or tape measures provides more quantitative information, although unless performed directly in situ during surgical abdominoplasty, these tools may also give inconsistent results as a result of the inability to accurately identify the actual medial border of the rectus [16] (Figs. 26.1 and 26.2). These issues may be overcome with imaging techniques that are able to accurately and clearly identify fascial borders.

In terms of assessing reliability and reproducibility of the various techniques used to measure the inter-rectus distance, the relaxation or contraction state of the abdominal wall should be taken into account. There may be variations of the inter-rectus distance as a result of muscle relaxation or paralytics used during surgery, though this has not been shown definitively to contribute to measurable changes in the inter-rectus distance [17]. When using imaging modalities, respiratory variations and the imposed tension or laxity that occurs naturally with inspiration and expiration may also cause the inter-rectus distance to vary at certain points in the respiratory cycle [18]. Attention should be paid to these variables in patients requiring comparisons of repeat or serial imaging to ensure control.

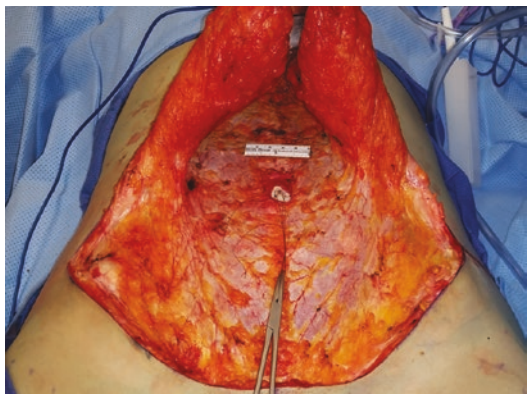

Fig. 26.1 Direct intra-operative measurements of the inter-rectus distance can be done using tools such as a ruler or caliper. In this patient with rectus diastasis noted on clinical exam preoperatively, the inter-rectus distance was directly measured to be 5 cm. The ruler sits with its edges at the medial borders of the rectus abdominis muscles

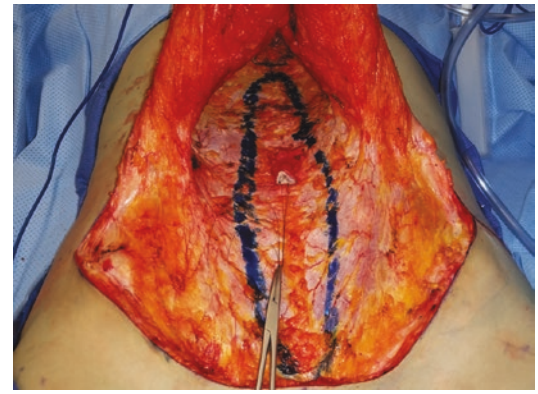

Fig. 26.2 The medial borders of rectus abdominis muscles are outlined with ink along their entire length, revealing separation of the muscle bellies away from the midline

Radiograph (X-Ray)

Radiograph, or X-ray, may be used to measure the linea alba and inter-rectus distance both in patients with suspected rectus diastasis or in those who have undergone corrective surgery who require postoperative imaging. The use of plain abdominal radiograph taken in the supine position has been described for these purposes.

The only reported method for imaging the linea alba with X-ray is by using metal or radio-opaque clips or markers. Placement of radio-opaque clips may be done in situ during surgical repair of rectus diastasis, wherein these clips are placed along the medial edge of the rectus after plication is performed. In addition to measuring

the distance between the medial edges of the rectus muscle, the vertical distance of the linea alba may also be discerned. Shortening of the vertical length of the linea alba is also achieved during surgical plication and is clinically important in achieving tightening and stabilization of the abdominal wall. Radio-opaque markers placed at the cranial and caudal ends of the linea alba after surgical plication provide landmarks for assessing the vertical length.

Direct measurements of the distance between clips on the actual radiograph do not necessarily correlate with the actual in situ distance between clips. Radiographic magnification should be corrected by comparing the actual length of the clip (known at the time of placement) to the measured length of the clip on the radiograph. Using the appropriate multiplier, the in situ distance between clips can be calculated. In this way, the inter-rectus distance or the vertical length of the linea alba can later be imaged in the case of suspected clinical recurrence of rectus diastasis, or for study purposes.

The longest reported follow-up imaging using X-ray was obtained 1 year postoperatively after abdominal wall plication. It is unclear if the accurate representation of significant diastasis (> 3 cm) is able to be captured using radiographs alone. Agreement between independent raters has been reported to be acceptable, though this methodology of assessing rectus diastasis using metal markers and radiographs has not been validated [19–21]. Although feasible, current advancements in imaging techniques make the use of X-rays less likely to be utilized for the purpose of imaging rectus diastasis or for obtaining anatomic measurements of the inter-rectus distance.

Ultrasound

Ultrasound (US) is a frequently employed imaging modality to evaluate rectus diastasis. There are more data in the literature evaluating ultrasound measurement of the inter-rectus distance than any other imaging modality. Overall, ultrasound has been shown to be reliable when used by a sonographer with experience in imaging the abdominal wall [16]. Level 4 evidence shows that high-frequency US is helpful in diagnosing and measuring rectus diastasis, and the IEHS recommends its use [12, 16].

There are anatomic considerations when using ultrasound to image the anterior abdominal wall structures. On ultrasound, fascia will appear hyperechoic (bright) and muscle will appear hypoechoic (dark). The medial border of the rectus can be easily identified based on this, as the anterior and posterior rectus sheaths fuse into the linea alba at the midline (Fig. 26.3, Video 26.1). Intrinsic muscle quality changes with age or disease, so there may be a replacement of the normal water content with fibro-fatty tissue, causing muscle to appear more hyperechoic and blurring the sharp demarcation between muscle and fascia [22]. Moving from the umbilicus inferiorly towards the pubic symphysis, there is a normal thinning and then absence of the posterior rectus sheath. This causes a loss of echogenicity and may contribute to increased difficulty in visualizing the fascial borders in this area. This has been shown to result in greater variability in measurements of the inter-rectus distances at these levels [23]. Additionally, there may be significant limitations in using ultrasound to measure the inter-rectus distance in patients with significant abdominal wall adiposity

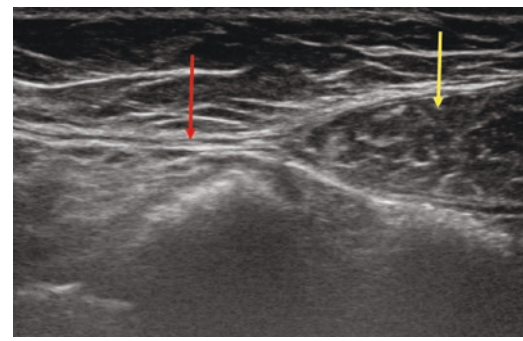

Fig. 26.3 Ultrasound is a frequently used imaging modality and is able to easily demonstrate the hypoechoic rectus abdominis muscle belly (yellow arrow) and the hyperechoic fascia of the linea alba (red arrow). Note the medial confluence of the anterior and posterior rectus sheaths in the midline which form the linea alba. The inter-rectus distance in this patient is widened (medial edge of the contralateral rectus muscle is not visible)

or a BMI of 30 kg/m^2 or greater. It is also important to note the surgical history of the patient, as postsurgical scarring can contribute to difficulty in accurately defining the borders of the rectus. This can be particularly so in patients who are postpartum and have undergone Cesarean section, further contributing to difficulty in imaging the infraumbilical region [24–27].

Patient positioning should be considered when using ultrasound to evaluate rectus diastasis. While resting supine with the arms at the side and the knees bent at 90 degrees, the patient is arguably relaxed with no contraction of the abdominal wall musculature. This is the most commonly described patient position. Attention should also be paid to when in the respiratory cycle measurements are taken [28]. Image capture at the end of passive exhalation arguably gives a picture of the most relaxed state of the abdominal wall [29].

There are a multitude of ultrasound probes and settings available to image the soft tissue of the anterior abdominal wall. Two-dimensional brightness (B) mode is the most frequently described, wherein sound waves are reflected back towards the probe in different intensities based on the intrinsic properties of the tissues. High-frequency linear transducers consisting of 3–10 megahertz (MHz), 4–13 MHz, and 5–10 MHz probes have been described in the literature for the purpose of assessing the inter-rectus distance specifically. Linear probe sizes range in width and length and there are various sizes appropriate for this type of abdominal wall imaging [24, 27, 29].

Operator technique plays a role in any ultrasound exam, and also applies to imaging of rectus diastasis. The ultrasound transducer can be positioned transversely (perpendicular to the axis of the linea alba) in the midline of the abdominal wall at set points, and then moved laterally to the medial edge of the rectus. Image distortion can occur if movement of the transducer by the operator is not smooth or steady [24]. The examiner should also be cognizant of the external pressure being placed on the abdominal wall, as significant downward pressure may cause flattening or widening of the rectus, thereby changing the inter-rectus distance [29].

Ultrasound use may be difficult if the inter-rectus distance is very wide. In patients with severe rectus diastasis with widths up to or greater than 5 cm, the entire width of the rectus may not be captured on a standard ultrasound probe. Ultrasound techniques to increase the field of view include the use of an acoustic standoff pad, which increases the distance between the probe surface and underlying tissue in question, in this case, the linea alba and the distance between the rectus muscles [12, 24]. Another way to extend the field of view is by panoramic technology, wherein multiple adjacent images are synthesized to create a final composite image over a distance that is larger than able to be captured singly by the probe. These techniques have been used in imaging other larger muscle bellies such as the quadriceps. Conventional ultrasound and extended field-of-view techniques have been compared for both validity and internal consistency with regard to imaging the anterior abdominal wall for rectus diastasis. Both panoramic ultrasound and use of an acoustic standoff pad to extend the field of view have been deemed equivalent and reliable compared to standard ultrasound imaging techniques for evaluating the inter-rectus distance. Of note, there is a decrease in image quality when using an acoustic standoff pad, likely due to artifacts imposed by the additional physical barrier of the standoff pad and from signal attenuation, as a result of the increased distance the sound waves must travel [24].

Ultrasound is the only imaging modality that is able to capture both static and dynamic images in real time. Its use has been described to evaluate the movement of the rectus edges and the changes in the linea alba as a result of various active movements. Exercise tasks such as abdominal crunch, drawing in of the abdominal wall, pelvic floor contraction, and head lift all cause changes in the inter-rectus distance. These tasks generally lead to contraction of the rectus abdominis muscles and the shortening of the inter-rectus distance. Conversely, activation of the transversus abdominis muscles acts to pull the abdominal wall in the transverse direction (lateral vector of pull) and leads to widening of the linea alba.

Variations in linea alba appearance during a task have been described as minimally distorted, following a smooth curved path ventrally or dorsally, or as having an undulating appearance. In addition, during tasks where the inter-rectus distance is shortened, this may lead to increased overall distortion of the line alba (in the ventral-dorsal plane), though this does not appear to functionally affect abdominal wall stability.

Generally, the inter-rectus distance is smaller in nulliparous females compared to males and parous females, and this has been seen in both the resting and contractile states [5]. Ultrasound measurements obtained during these active tasks have been compared to direct measurement and produce reliable and comparable results [25, 29, 30]. There has been variation reported at the infra-umbilical level, where ultrasound measurements of the inter-rectus distance may not correlate as well to other methodologies [22]. These imaging findings are used to guide targeted therapy for musculoskeletal rehabilitation in patients with rectus diastasis [31].

Ultrasound measurements have also been applied to ascertain the physical characteristics of the linea alba in patients with rectus diastasis. Shear-wave elastography is an ultrasound technique that is able to measure tissue stiffness or deformability and has been applied to the linea alba specifically. The distortion index is a calculation based on the area of the linea alba seen on ultrasound. This index estimates linea alba distortion at the time of tension and measures the average deviation of the path of the linea alba from the shortest path between its attachments. Women with rectus diastasis have been shown to have a lower measure of stiffness and a significant distortion of the linea alba on exercise tasks compared to individuals without diastasis. In women without pathologic rectus diastasis, the stiffness of the linea alba is greatest during exercise tasks [31–33].

Ultrasound measurements have been compared against direct intraoperative measurements of the inter-rectus distance. Direct intraoperative measurement is performed using calipers or a ruler at the time of surgical intervention, where the rectus fascia and linea alba are exposed directly after elevating the subcutaneous tissue and skin during abdominoplasty. There may be variability in measurements obtained in these two settings when looking at the region below the umbilicus. Methods of direct intra-operative or in situ measurement may also yield greater inter-rectus distances compared to ultrasound, though the magnitude of difference has been reported to be small [26, 28].

Ultrasonography has been used to provide anatomic measurements in preoperative planning and has been described for use in children with congenital abdominal wall anomalies, such as omphalocele with associated rectus diastasis. Ultrasound in this case is able to provide ample information on the abdominal wall anatomy for preoperative planning and is useful in complicated patients such as those planning to undergo repair of omphalocele defects [34].

Ultrasound can also be used in the postoperative phase to confirm the suspected clinical recurrence of rectus diastasis [35, 36]. It also can be used to guide physical therapy in patients undergoing abdominal wall strengthening for rectus diastasis. In pregnant patients, abdominal wall activation with rectus contraction (abdominal crunch) has been shown over time to decrease the inter-rectus distance at points above and below the umbilicus. Conversely, drawing in, or repeated activation of the transversus abdominis muscle can lead to a widening of the inter-rectus distance below the umbilicus, which is likely explained by the anatomy in this region as the linea alba thins out [23].

Computed Tomography (CT)

Computed tomography (CT) is widely used today in imaging the abdomen. The use of intravenous contrast is not required to assess rectus diastasis or to measure the inter-rectus distance, as there is high attenuation between the muscle and fascia at baseline. Standard CT imaging using millimeter cuts is sufficient for evaluating rectus diastasis (Figs. 26.4, 26.5, and 26.6). It is possible in cooperative patients to obtain CT images during various points of the respiratory cycle, which affects

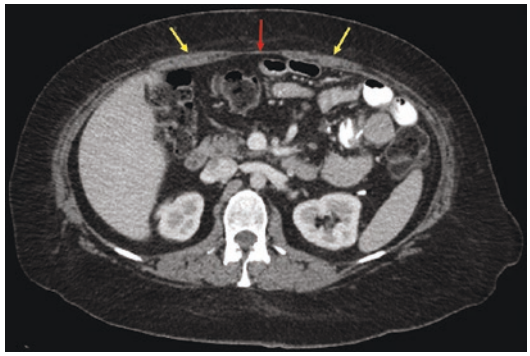

Fig. 26.4 CT abdomen in a patient with ventral hernia and concomitant rectus diastasis. This axial cut shows the thinned rectus abdominis muscle bellies (yellow arrows) and a widened linea alba between them (red arrow)

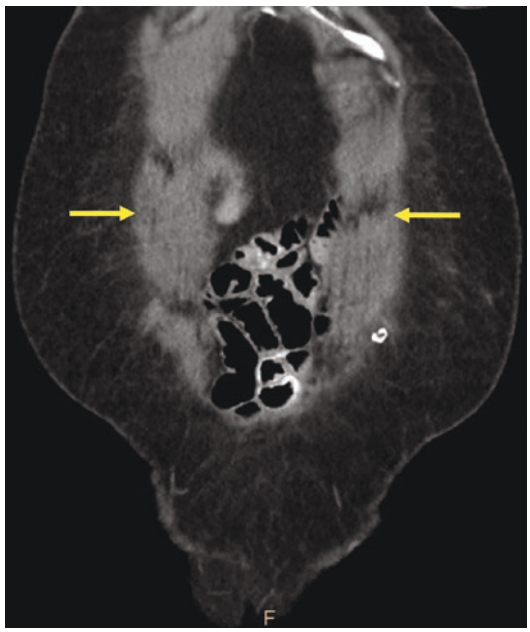

Fig. 26.5 CT abdomen in the same patient in the sagittal plane showing a splaying of the rectus abdominis muscles (yellow arrows)

the intra-abdominal pressure and the inter-rectus distance. CT also has the added benefit of ruling out any associated intra-abdominal pathology or hernias in patients where there is clinical concern. In addition, CT scan of the abdomen is not overly time-consuming to perform, and there is no operator dependency as with ultrasound (Video 26.2).

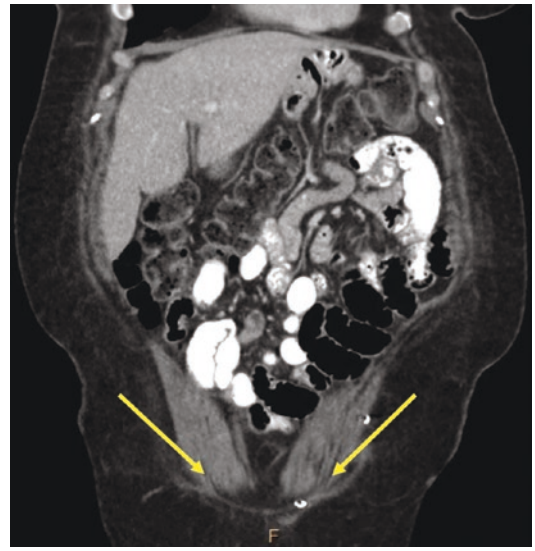

Fig. 26.6 CT abdomen in the same patient displaying the inferior attachment of the paired rectus abdominis muscles (yellow arrows) at the pubic symphysis, and a widening of the inter-rectus distance

The downsides to CT imaging include cost and patient exposure to radiation. There are ways to decrease radiation exposure from CT, such as obtaining single slice images at predefined points of interest along the linea alba. These points can be tagged within the imaging system using a bony landmark for reference, as the bony landmark is not mobile and will allow for repeat imaging at the same axial level. These prespecified points can be imaged at multiple time points or after an intervention that has addressed the diastasis [37]. Despite the ability to limit the amount of radiation exposure with single slice imaging, CT still may not be the best imaging choice in patients requiring repeated interval assessment of rectus diastasis, nor is it advised in pregnant patients. However, CT is generally the preferred imaging modality in patients with suspected hernias and may incidentally capture information about a rectus diastasis as well, either alone (if the patient is obese and physical exam is confounded), or within the context of a true hernia (Fig. 26.7).

As with ultrasound, variability in measuring the infra-umbilical inter-rectus distance has also

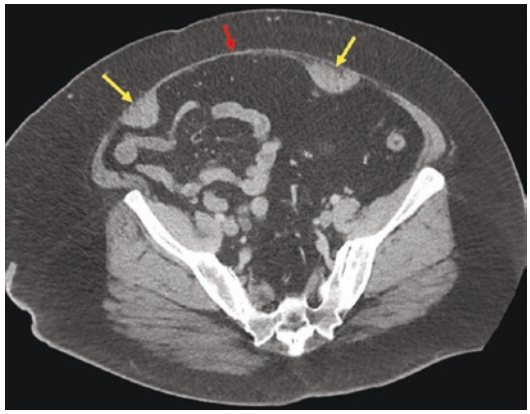

Fig. 26.7 CT abdomen showing severe rectus diastasis with significant displacement of the rectus abdominis muscle bellies (yellow arrows). This patient also had a large ventral wall hernia inferior to the level shown

been reported when using CT exam at various distances between the umbilicus and pubic symphysis. These variations were noted when comparing direct measurement techniques to CT-obtained measurements, with some reports of underestimation of the inter-rectus distance on CT. In one study, the largest variation reported between measurement modalities was 0.3 cm, which is unlikely to translate to clinical relevance in the operative setting [38, 39].

Magnetic Resonance Imaging (MRI)

Reports of the use of magnetic resonance imaging (MRI) for the assessment of musculoskeletal abdominal wall characteristics are limited. This is possibly due to numerous factors, such as the increased cost and time required to perform this exam. On the other hand, there is no radiation exposure risk to the patient, nor is there operator dependency as there is in ultrasound. This may make MRI a more desirable choice for patients undergoing repeat studies for investigative research purposes.

MRI may have more use in neonates with congenital abdominal wall deformities. There has been case reports of this use in patients with *Prune Belly Syndrome (Eagle-Barrett Syndrome)* and *Pseudo Prune Belly Syndrome*. MRI was specifically used in these cases to define anatomy related to the abnormal anterior abdominal wall, in addition to aiding in preoperative planning [7]. Ultrasound does have a similarly effective use in these patients as well.

The use of MRI to investigate rectus diastasis and to measure the inter-rectus distance has been described similarly to other imaging techniques. Various points along the linea alba between the xiphoid, umbilicus, and pubic symphysis are able to be targeted for measurement in both pre- and post-intervention states. Both T1- and T2-weighted thin slice images can be used. MRI also has the benefit of being able to image the entire abdomino-pelvic anatomy, much like CT scan (Figs. 26.8 and 26.9). MRI has also been

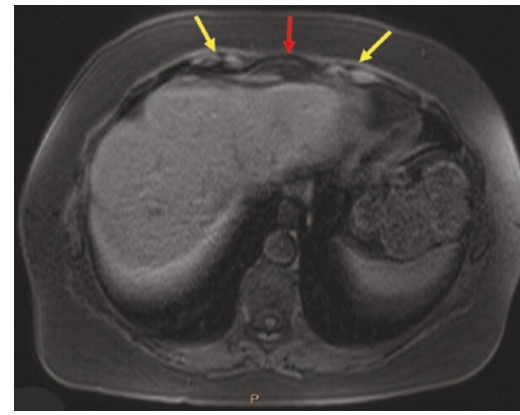

Fig. 26.8 MR image performed in the T1 phase. In this phase, the rectus abdominis muscles (yellow arrows) are bright

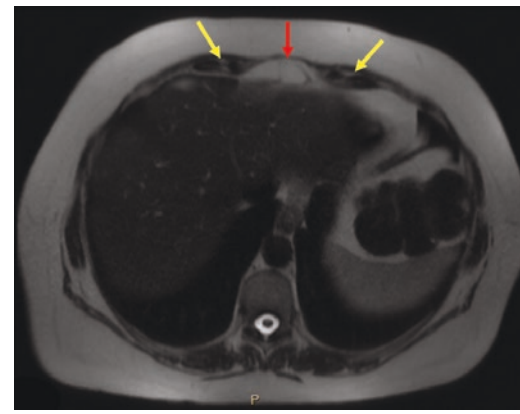

Fig. 26.9 MR image performed in the T2 phase in the same patient displaying rectus diastasis (red arrow). The rectus muscles (yellow arrows) appear dark due to high water content

used to compare pre- and postoperative abdominal girth in the antero-posterior (AP) and transverse dimensions in patients undergoing surgical repair of rectus diastasis [17].

Operative Repair of Rectus Diastasis and Appearance on Imaging

There are various techniques described for the repair of rectus diastasis [40]. It is important to know the surgical history in patients undergoing postoperative imaging after rectus diastasis repair, as there may be differing appearances on imaging based on the repair performed.

The most commonly employed and traditional method of repair is standard abdominoplasty where the subcutaneous tissue and skin are elevated revealing the anterior abdominal wall fascia and linea alba directly. The attenuated linea alba is then plicated and the inter-rectus distance is shortened by bringing the medial borders of the rectus back to midline. This is done using single or multilayer permanent sutures. Suture plication is generally done vertically, from xiphoid to pubic symphysis, leaving the umbilical stalk free to be reset on the anterior abdominal wall. Depending on the laxity and excess of the attenuated linea alba, plication can also be done horizontally, obliquely, or in combination (Figs. 26.10 and 26.11). Afterward, the skin and subcutaneous tissue are redraped, pulled taught, and the excess tissue trimmed. The new position of the umbilicus is marked on the skin and a hole is cut out so that the umbilicus can be fixed in place [41]. "Stapler abdominoplasty" is described mostly in the setting of minimally invasive endoscopic approaches wherein a linear cutting stapler is used to trim and remove the excess attenuated linea alba fascial tissue [42]. Permanent sutures are not likely to be visible on imaging techniques, though staple lines will be. In either, the medial borders of the paired rectus with interposing fascia will be identifiable after diastasis repair, as it is preoperatively. Additionally, when the existing linea alba is only plicated and not resected, infolding of that fascial tissue will be visible and identifiable, giving hint to the radiologist that surgical plication was performed.

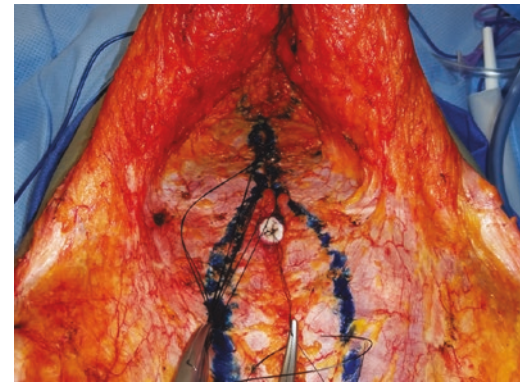

Fig. 26.10 Traditional abdominoplasty involves elevation of the subcutaneous tissue and skin off of the anterior abdominal wall fascia revealing the attenuated linea alba at the midline. The entire length of the rectus diastasis is exposed, from xiphoid process to pubic symphysis. Standard surgical repair techniques for rectus diastasis include single or double-layer plication with permanent sutures. This is performed from the xiphoid process superiorly, coursing around the umbilicus, and completing the plication all the way down to the pubic symphysis

Fig. 26.11 Final postoperative view after abdominal plication for rectus diastasis. The medial edges of the rectus have been brought back to midline, decreasing the inter-rectus distance and tightening the abdominal wall. By nature of the plication, the vertical distance of the linea alba is effectively decreased as well, contributing to abdominal wall stability

Repair of rectus diastasis with the use of mesh also commonly occurs. Mesh reinforcement,

placed either open or minimally invasively (laparoscopic or endoscopic) has been deemed safe in the correction of rectus diastasis and may have use in more severe cases. Mesh may be placed in multiple different planes along the abdominal wall [10]. Mesh may be used in the repair of concomitant ventral hernias and can be located in the retrorectus plane, intra-peritoneal, or in preperitoneal plane. Mesh can also be placed as an onlay, sitting on top of the anterior rectus fascia and reinforcing an underlying primary repair of diastasis [42, 43].

Various mesh material may be used in the ventral abdominal wall, both permanent and absorbable. Depending on the time frame of imaging and the type of mesh used, mesh may or may not be visible on imaging studies, or may have the appearance of scar tissue. Mesh may also be seen in various planes of the abdominal wall (Fig. 26.12). In addition, mesh fixation can be done with permanent or semi-permanent suture material, absorbable or nonabsorbable tacks, or glue products [44]. These possibilities should be noted as fixation methods also may or may not be visible on currently available imaging modalities. Surgical drains are commonly used in these surgical procedures and may also be placed in various planes, so their presence should be noted during postoperative imaging exams as well [45, 46].

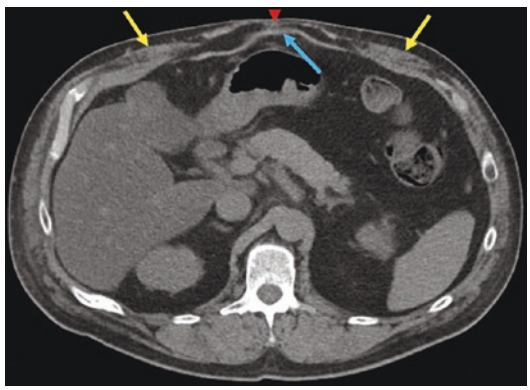

Fig. 26.12 CT abdomen showing significant splaying of the rectus abdominis muscles (yellow arrows), an attenuated linea alba (red arrow), and an intra-peritoneal inlay mesh (blue arrow). In this case, a biologic mesh was used and is visible on this CT scan performed 1 year postoperatively

Assessing Clinical Outcomes

Postoperative imaging (US, CT, MRI) has been used in the literature to provide objective outcome measures after surgical intervention for rectus diastasis [14, 37].

Recurrence of rectus diastasis after surgical repair is a possibility and is concerning to both patient and clinician. Confirmation of a postoperative recurrence may be difficult as the clinical exam alone may not be as reliable in the postoperative state. In the immediate months after standard abdominoplasty, there is anterior abdominal wall swelling that may be particularly or asymmetrically prominent above the umbilicus. This can persist for months, and it is difficult in this time frame to assess unanticipated recurrence of rectus diastasis or failure of surgical repair [2]. Imaging in this case is able to provide a detailed view of the abdominal wall and inter-rectus distance, where physical exam and direct measurement cannot.

The use of ultrasound, CT, and MRI for the detection of postoperative recurrence of rectus diastasis has been reported. Overall, the longevity and durability of rectus diastasis repair is good with current surgical repair techniques. This has been confirmed by multiple studies using various imaging techniques to provide objective measurements of the inter-rectus distance [17, 35, 37, 39, 40, 44, 47, 48].

It may not be possible to compare a patient's pre- and postoperative inter-rectus distance. Many patients do not routinely undergo preoperative imaging prior to abdominoplasty, nor is the inter-rectus distance measured routinely as part of the surgical procedure. In cases with concern for possible postoperative recurrence, imaging will provide an accurate measure of the inter-rectus distance, but it is difficult to know how this may have compared to preoperative values. In these instances, the classification systems described earlier in this chapter may be useful in determining the pathologic widening of the diastasis. Studies have used classification systems as well to define recurrence [2, 49, 50].

Postoperative complications other than recurrence of rectus diastasis can also occur, and the

presence of pain, new onset swelling, or other concerning symptoms warrants investigation. CT scan is the most commonly performed test for imaging the symptomatic abdomen, and may be beneficial over ultrasound exam as it gives a more global picture and is better able to rule out serious intra-abdominal pathology. In patients who have undergone diastasis repair, seroma is one of the more common complications and is readily imaged on US and CT scans [41, 51–53].

Conclusion

Agreement and standardization of the classification of rectus diastasis is currently lacking in the literature and in practice. Overall, published literature dating back from the 1980s on the topic of rectus diastasis and surgical repair is mostly case-based and retrospective, with few prospective studies. Imaging studies most commonly used to image the musculoskeletal abdominal wall are CT and US. These imaging modalities are able to provide detailed images and specific measurements of the inter-rectus distance under varying conditions, and can aid in operative planning. There is a large role for postoperative imaging to provide objective outcome measures, to compare different types of surgical intervention, and to assess complications [14, 15, 54, 55].

References

1. Beer GM, Schuster A, Seifert B, Manestar M, Mihic-Probst D, Weber SA. The normal width of the linea alba in nulliparous women. Clin Anat. 2009 Sep;22(6):706–11. https://doi.org/10.1002/ca.20836.
2. Nahas FX, Ferreira LM, Mendes JA. An efficient way to correct recurrent rectus diastasis. Aesthet Plast Surg. 2004;28(4):189–96.
3. Axer H, von Keyserlingk DG, Prescher A. Collagen fibers in linea alba and rectus sheaths. J Surg Res. 2001;96(2):239–45.
4. Rath AM, Attali P, Dumas JL, Goldlust D, Zhang J, Chevrel JP. The abdominal linea alba: an anatomo-radiologic and biomechanical study. Surg Radiol Anat. 1996;18(4):281–8.
5. Chiarello CM, McAuley JA, Hartigan EH. Immediate effect of active abdominal contraction on inter-recti distance. J Orthop Sports Phys Ther. 2016;46(3):177–83. https://doi.org/10.2519/jospt.2016.6102. Epub 2016 Jan 26
6. Nahabedian MY. Management strategies for diastasis recti. Semin Plast Surg. 2018;32(3):147–54. https://doi.org/10.1055/s-0038-1661380. Epub 2018 Jul 24
7. De Bernardo G, Giordano M, De Brasi D, Esposito F, De Santis R, Sordino D. Pseudo prune belly syndrome: a case report with unilateral abdominal defect. Radiol Case Rep. 2019;14(8):941–5. https://doi.org/10.1016/j.radcr.2019.05.019. eCollection 2019 Aug.
8. Chan YC, Bird LM. Vertically transmitted hypoplasia of the abdominal wall musculature. Clin Dysmorphol. 2004;13(1):7–10.
9. Digilio MC, Capolino R, Dallapiccola B. Autosomal dominant transmission of nonsyndromic diastasis recti and weakness of the linea alba. Am J Med Genet A. 2008;146A(2):254–6.
10. Bittner R, Bain K, Bansal VK, Berrevoet F, Bingener-Casey J, Chen D, et al. Update of guidelines for laparoscopic treatment of ventral and incisional abdominal wall hernias (International Endohernia Society (IEHS)): Part B. Surg Endosc. 2019;33(11):3511–49. https://doi.org/10.1007/s00464-019-06908-6. Epub 2019 Jul 10
11. Taylor DA, Merten SL, Sandercoe GD, Gahankari D, Ingram SB, Moncrieff NJ, et al. Abdominoplasty improves low back pain and urinary incontinence. Plast Reconstr Surg. 2018;141(3):637–45. https://doi.org/10.1097/PRS.0000000000004100.
12. Bittner R, Bain K, Bansal VK, Berrevoet F, Bingener-Casey J, Chen D, et al. Update of guidelines for laparoscopic treatment of ventral and incisional abdominal wall hernias (International Endohernia Society (IEHS))-Part A. Surg Endosc. 2019;33(10):3069–139. https://doi.org/10.1007/s00464-019-06907-7. Epub 2019 Jun 27
13. Nahas FX. An aesthetic classification of the abdomen based on the myoaponeurotic layer. Plast Reconstr Surg. 2001;108(6):1787–95.
14. Akram J, Matzen SH. Rectus abdominis diastasis. J Plast Surg Hand Surg. 2014;48(3):163–9. https://doi.org/10.3109/2000656X.2013.859145. Epub 2013 Nov 21
15. Reinpold W, Köckerling F, Bittner R, Conze J, Fortelny R, Koch A, et al. Classification of rectus diastasis - a proposal by the German Hernia Society (DHG) and the International Endohernia Society (IEHS). Front Surg. 2019;6:1. https://doi.org/10.3389/fsurg.2019.00001. eCollection 2019.
16. van de Water AT, Benjamin DR. Measurement methods to assess diastasis of the rectus abdominis muscle (DRAM): A systematic review of their measurement properties and meta-analytic reliability generalisation. Man Ther. 2016;21:41–53. https://doi.org/10.1016/j.math.2015.09.013. Epub 2015 Oct 3
17. Elkhatib H, Buddhavarapu SR, Henna H, Kassem W. Abdominal musculoaponeuretic system: magnetic resonance imaging evaluation before and after vertical plication of rectus muscle diastasis in conjunction with lipoabdominoplasty. Plast Reconstr

Surg. 2011;128(6):733e–40e. https://doi.org/10.1097/PRS.0b013e318230c8a1.
18. Nahas FX, Augusto SM, Ghelfond C. Should diastasis recti be corrected? Aesthet Plast Surg. 1997;21(4):285–9.
19. Birdsell DC, Gavelin GE, Kemsley GM, Hein KS. "Staying power"—absorbable vs nonabsorbable. Plast Reconstr Surg. 1981;68(5):742–5.
20. Netscher DT, Wigoda P, Spira M, Peltier M. Musculoaponeurotic plication in abdominoplasty: how durable are its effects? Aesthet Plast Surg. 1995;19(6):531–4.
21. Veríssimo P, Nahas FX, Barbosa MV, de Carvalho Gomes HF, Ferreira LM. Is it possible to repair diastasis recti and shorten the aponeurosis at the same time? Aesthet Plast Surg. 2014;38(2):379–86. https://doi.org/10.1007/s00266-014-0272-z. Epub 2014 Jan 30
22. Chiarello CM, McAuley JA. Concurrent validity of calipers and ultrasound imaging to measure interrecti distance. J Orthop Sports Phys Ther. 2013;43(7):495–503. https://doi.org/10.2519/jospt.2013.4449. Epub 2013 Apr 30
23. Mota P, Pascoal AG, Carita AI, Bø K. The immediate effects on inter-rectus distance of abdominal crunch and drawing-in exercises during pregnancy and the postpartum period. J Orthop Sports Phys Ther. 2015;45(10):781–8. https://doi.org/10.2519/jospt.2015.5459. Epub 2015 Aug 24
24. Keshwani N, Mathur S, McLean L. Validity of inter-rectus distance measurement in postpartum women using extended field-of-view ultrasound imaging techniques. J Orthop Sports Phys Ther. 2015;45(10):808–13. https://doi.org/10.2519/jospt.2015.6143. Epub 2015 Aug 24
25. Barbosa S, de Sá RA, Coca Velarde LG. Diastasis of rectus abdominis in the immediate puerperium: correlation between imaging diagnosis and clinical examination. Arch Gynecol Obstet. 2013;288(2):299–303. https://doi.org/10.1007/s00404-013-2725-z. Epub 2013 Feb 24
26. Mendes Dde A, Nahas FX, Veiga DF, Mendes FV, Figueiras RG, Gomes HC, et al. Ultrasonography for measuring rectus abdominis muscles diastasis. Acta Cir Bras. 2007;22(3):182–6.
27. Keshwani N, McLean L. Ultrasound imaging in postpartum women with diastasis recti: intrarater between-session reliability. J Orthop Sports Phys Ther. 2015;45(9):713–8. https://doi.org/10.2519/jospt.2015.5879. Epub 2015 Jul 10
28. Gama LJM, Barbosa MVJ, Czapkowski A, Ajzen S, Ferreira LM, Nahas FX. Single-layer plication for repair of diastasis recti: the most rapid and efficient technique. Aesthet Surg J. 2017;37(6):698–705. https://doi.org/10.1093/asj/sjw263.
29. Sancho MF, Pascoal AG, Mota P, Bø K. Abdominal exercises affect inter-rectus distance in postpartum women: a two-dimensional ultrasound study. Physiotherapy. 2015;101(3):286–91. https://doi.org/10.1016/j.physio.2015.04.004. Epub 2015 May 6
30. Theodorsen NM, Strand LI, Bø K. Effect of pelvic floor and transversus abdominis muscle contraction on inter-rectus distance in postpartum women: a cross-sectional experimental study. Physiotherapy. 2018;105(3):315–20. https://doi.org/10.1016/j.physio.2018.08.009. Epub 2018 Oct 25
31. Lee D, Hodges PW. Behavior of the linea alba during a curl-up task in diastasis rectus abdominis: an observational study. J Orthop Sports Phys Ther. 2016;46(7):580–9. https://doi.org/10.2519/jospt.2016.6536.
32. Taljanovic MS, Gimber LH, Becker GW, Latt LD, Klauser AS, Melville DM, et al. Shear-wave elastography: basic physics and musculoskeletal applications. Radiographics. 2017;37(3):855–70. https://doi.org/10.1148/rg.2017160116.
33. Beamish N, Green N, Nieuwold E, McLean L. Differences in linea alba stiffness and linea alba distortion between women with and without diastasis recti abdominis: the impact of measurement site and task. J Orthop Sports Phys Ther. 2019;49(9):656–65. https://doi.org/10.2519/jospt.2019.8543. Epub 2019 Mar 26
34. van Eijck FC, van Vlimmeren LA, Wijnen RM, Klein W, Kruijen I, Pillen S, et al. Functional, motor developmental, and long-term outcome after the component separation technique in children with giant omphalocele: a case control study. J Pediatr Surg. 2013;48(3):525–32. https://doi.org/10.1016/j.jpedsurg.2012.08.010.
35. Passamai de Castro EJ, Radwanski HN, Pitanguy I, Nahas F. Long-term ultrasonographic evaluation of midline aponeurotic plication during abdominoplasty. Plast Reconstr Surg. 2013;132(2):333–8. https://doi.org/10.1097/PRS.0b013e3182958ad2.
36. Tadiparthi S, Shokrollahi K, Doyle GS, Fahmy FS. Rectus sheath plication in abdominoplasty: assessment of its longevity and a review of the literature. J Plast Reconstr Aesthet Surg. 2012;65(3):328–32. https://doi.org/10.1016/j.bjps.2011.09.024. Epub 2011 Oct 20
37. Nahas FX, Ferreira LM, Augusto SM, Ghelfond C. Long-term follow-up of correction of rectus diastasis. Plast Reconstr Surg. 2005;115(6):1736–41; discussion 1742-3.
38. Emanuelsson P, Dahlstrand U, Strömsten U, Gunnarsson U, Strigård K, Stark B. Analysis of the abdominal musculo-aponeurotic anatomy in rectus diastasis: comparison of CT scanning and preoperative clinical assessment with direct measurement intraoperatively. Hernia. 2014;18(4):465–71. https://doi.org/10.1007/s10029-014-1221-0. Epub 2014 Feb 1
39. Nahas FX, Augusto SM, Ghelfond C. Nylon versus polydioxanone in the correction of rectus diastasis. Plast Reconstr Surg. 2001;107(3):700–6.

40. ElHawary H, Abdelhamid K, Meng F, Janis JE. A comprehensive, evidence-based literature review of the surgical treatment of rectus diastasis. Plast Reconstr Surg. 2020;146(5):1151–64. https://doi.org/10.1097/PRS.0000000000007252. PMID: 33136963.
41. Gutowski KA. Evidence-based medicine: abdominoplasty. Plast Reconstr Surg. 2018;141(2):286e–99e. https://doi.org/10.1097/PRS.0000000000004232.
42. Köckerling F, Botsinis MD, Rohde C, Reinpold W, Schug-Pass C. Endoscopic-assisted linea alba reconstruction: new technique for treatment of symptomatic umbilical, trocar, and/or epigastric hernias with concomitant rectus abdominis diastasis. Eur Surg. 2017;49(2):71–5. https://doi.org/10.1007/s10353-017-0473-1. Epub 2017 Mar 10
43. Cheesborough JE, Dumanian GA. Simultaneous prosthetic mesh abdominal wall reconstruction with abdominoplasty for ventral hernia and severe rectus diastasis repairs. Plast Reconstr Surg. 2015;135(1):268–76. https://doi.org/10.1097/PRS.0000000000000840.
44. Rangwani SM, Kraft CT, Schneeberger SJ, Khansa I, Janis JE. Strategies for mesh fixation in abdominal wall reconstruction: concepts and techniques. Plast Reconstr Surg. 2021;147(2):484–91. https://doi.org/10.1097/PRS.0000000000007584. PMID: 33235048.
45. Khansa I, Khansa L, Meyerson J, Janis JE. Optimal use of surgical drains: evidence-based strategies. Plast Reconstr Surg. 2018;141(6):1542–9. https://doi.org/10.1097/PRS.0000000000004413.
46. Barchi LC, Franciss MY, Zilberstein B. Subcutaneous videosurgery for abdominal wall defects: a prospective observational study. J Laparoendosc Adv Surg Tech A. 2019;29(4):523–30. https://doi.org/10.1089/lap.2018.0697. Epub 2018 Dec 31
47. Bellido Luque J, Bellido Luque A, Valdivia J, Suarez Gráu JM, Gomez Menchero J, García Moreno J, et al. Totally endoscopic surgery on diastasis recti associated with midline hernias. The advantages of a minimally invasive approach. Prospective cohort study. Hernia. 2015;19(3):493–501. https://doi.org/10.1007/s10029-014-1300-2. Epub 2014 Aug 21
48. Nahas FX, Ferreira LM, Ely PB, Ghelfond C. Rectus diastasis corrected with absorbable suture: a long-term evaluation. Aesthet Plast Surg. 2011;35(1):43–8. https://doi.org/10.1007/s00266-010-9554-2. Epub 2010 Nov 25
49. van Uchelen JH, Kon M, Werker PM. The long-term durability of plication of the anterior rectus sheath assessed by ultrasonography. Plast Reconstr Surg. 2001;107(6):1578–84.
50. Nahas FX. Pregnancy after abdominoplasty. Aesthet Plast Surg. 2002;26(4):284–6.
51. Emanuelsson P, Gunnarsson U, Dahlstrand U, Strigård K, Stark B. Operative correction of abdominal rectus diastasis (ARD) reduces pain and improves abdominal wall muscle strength: a randomized, prospective trial comparing retromuscular mesh repair to double-row, self-retaining sutures. Surgery. 2016;160(5):1367–75. https://doi.org/10.1016/j.surg.2016.05.035. Epub 2016 Jul 27
52. Emanuelsson P, Gunnarsson U, Strigård K, Stark B. Early complications, pain, and quality of life after reconstructive surgery for abdominal rectus muscle diastasis: a 3-month follow-up. J Plast Reconstr Aesthet Surg. 2014;67(8):1082–8. https://doi.org/10.1016/j.bjps.2014.04.015. Epub 2014 May 2
53. Janis JE, Khansa L, Khansa I. Strategies for postoperative seroma prevention: a systematic review. Plast Reconstr Surg. 2016;138(1):240–52. https://doi.org/10.1097/PRS.0000000000002245.
54. Hickey F, Finch JG, Khanna A. A systematic review on the outcomes of correction of diastasis of the recti. Hernia. 2011;15(6):607–14. https://doi.org/10.1007/s10029-011-0839-4. Epub 2011 Jun 18
55. Mommers EHH, Ponten JEH, Al Omar AK, de Vries Reilingh TS, Bouvy ND, Nienhuijs SW. The general surgeon's perspective of rectus diastasis. A systematic review of treatment options. Surg Endosc. 2017;31(12):4934–49. https://doi.org/10.1007/s00464-017-5607-9. Epub 2017 Jun 8

Athletic Pubalgia

27

Matthew Peacock and Brian P. Jacob

Introduction

There are a variety of terms used synonymously with athletic pubalgia including "sports hernia" or "hockey groin" and "Gilmore's groin." These describe a condition characterized by persistent pain in the groin without a definitive hernia typically in competitive athletes which has gained increasing attention since its first description in 1980 as a source of disability and time lost from athletics [1]. The interchangeable use of these terms can confound the imaging evaluation, but the term sports hernia has come to refer to a posterior inguinal wall deficiency whereas athletic pubalgia is a general term for groin pain in athletes rather than a specific diagnosis. The true incidence of athletic pubalgia is difficult to evaluate given the lack of uniform definition, but it is estimated to be in approximately 50–80% of athletic patients presenting with chronic groin pain of unknown etiology [2, 3]. Sports hernias are more common in men and in athletes participating in sports including but not limited to hockey, soccer, rugby, and football in which athletes tend to bend or lean forward. Risk factors for injury were assessed in hockey players and found players with prior injury, those who did not aggressively train in off season and age as factors predictive of groin injury [4].

Mechanism/Presentation

There are several hypotheses for the mechanisms of athletic pubalgia including increased tension in the groin due to strenuous activity which causes tears to the supporting structures of the inguinal area to loss of hip motion causing pubic symphysis stress and instability [5]. Another proposed mechanism is nerve compression or conjoined tendon inflammation which was supported in a study using radiofrequency denervation (RFD) of the ilioinguinal nerve and inguinal ligament. This study found RFD treatment to be associated with significant improvement above baseline at an interval of up to 6 months using pain and function scoring systems. Although multiple hypotheses exist, the underlying etiology is abnormal tension in the inguinal canal causing pain which may present as tears in the external oblique, conjoined tendon, inguinal ligament, or posterior abdominal wall weakness without true herniation (Fig. 27.1) [6].

Supplementary Information The online version contains supplementary material available at https://doi.org/10.1007/978-3-031-21336-6_27.

M. Peacock (✉)
Department of General Surgery, Mount Sinai Hospital, New York, NY, USA
e-mail: matthew.peacock@mountsinai.org

B. P. Jacob
Department of Surgery, Laparoscopic Surgical Center of New York, New York, NY, USA

S. Docimo Jr. et al. (eds.), *Fundamentals of Hernia Radiology*,
https://doi.org/10.1007/978-3-031-21336-6_27

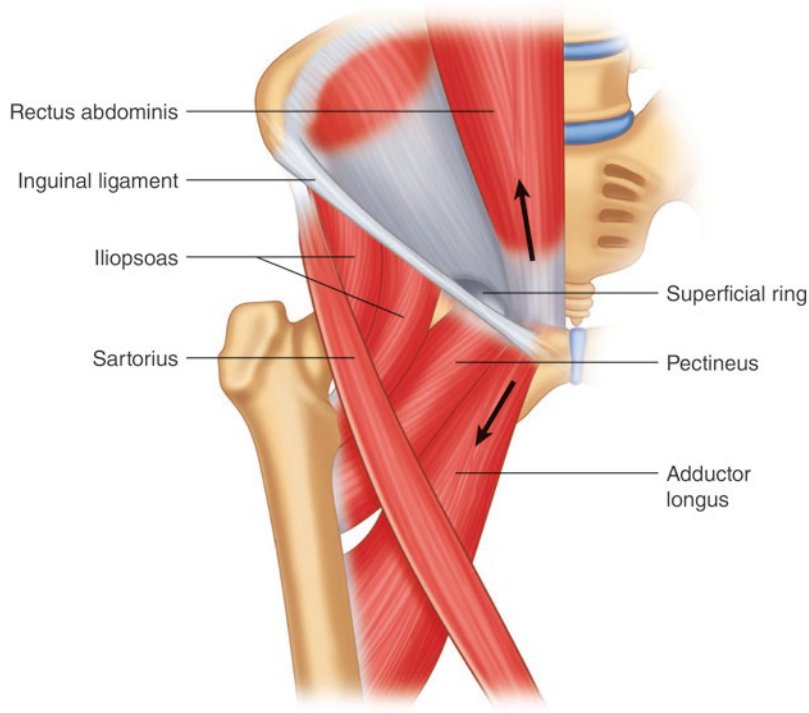

Fig. 27.1 Inguinal anatomy. Injury at tendons (arrows) implicated in athletic pubalgia

The presentation of patients can be variable but typically patients complain of gradually increasing activity-related lower abdominal or adductor-related pain. Symptoms may be exacerbated by coughing and athletes may complain of radiation of pain to the groin or thigh possibly representing nerve entrapment. Patients with lateral pain with sitting, flexion, or abduction should be evaluated for intra-articular hip pathology as well.

Diagnosis

Eliciting patient history is the first step in diagnosis and it is important to determine the location of the patient's pain. Diagnosis of sports hernia can be made based on the following history and exam findings

1. Supra-inguinal exercise-related groin pain.
2. Tenderness to palpation at the pubic tubercle or at the deep inguinal ring or at the adductor longus tendon.
3. Abnormal conjoint tendon on imaging or physical exam and a bulge of the posterior inguinal wall when contracting the abdominal muscles on dynamic imaging.

The first imaging modality chosen is usually radiographs of the pelvis and hip to evaluate the osseous structures and rule out other diagnosis [7]. Ultrasound and computed tomography (CT) are useful in delineating the anatomy and can show an inguinal bulge that is not appreciated on examination [8]. Magnetic resonance imaging (MRI) typically is considered the gold standard for the evaluation of musculoskeletal pelvic pain.

Evaluation: Imaging Modalities

Magnetic Resonance Imaging

Given the small nature of the inguinal region, subtle changes can be missed with a standard pelvis protocol. Although it is institution-specific,

generally a 3 mm slice thickness and anterior surface coil are recommended and gadolinium can be given to highlight capsular and tendinous inflammation although its routine use is not required [8]. MRI was associated with a sensitivity of 68% and 100% specificity for rectus abdominis tendon injury and 86% sensitivity and specificity of 89% for adductor tendon injury in a retrospective review [9]. Attention is focused initially on the pubic symphysis for bone marrow edema location and symmetry and for degenerative changes such as subchondral sclerosis and osseous erosions [10]. The presence of an accessory cleft reflecting an adductor enthetic microtear may be present as fluid or near fluid signal under the anterior or inferior pubic bone and often identifies the site of pain [11]. The morphology and signal intensity of the rectus abdominis attachments to the superior pubic rami, adductor tendon origins, and the inguinal canal are reviewed.

Osteitis Pubis

Osteitis pubis represents painful inflammation and/or degenerative changes at the area of the pubic symphysis and/or parasymphyseal bone which is thought to be a result of repetitive microtrauma. Traditionally osteitis pubis has been investigated using anteroposterior radiographs and 99mTc-methylenediphosphonate triple-phase bone scans [12]. Findings on radiograph include widening of the symphysis, sclerosis, cystic changes, or marginal erosions in the subchondral bone. Flamingo view x-rays can be obtained to evaluate for pelvic instability defined as vertical shift greater than 2 mm, widening greater than 7 mm across the pubic symphysis while standing on one leg [12]. MRI has become the imaging modality of choice as it has superior visualization of soft tissue and changes within the bone marrow than radiographs. Findings on MRI of osteitis pubis include bilateral subchondral bone marrow edema reminiscent of osteoarthritis with higher intensity corresponding to the side of pain (Figs. 27.2 and 27.3). It is important to differentiate between acute osteitis pubis which includes findings of bone marrow edema that can be seen as a linear high T2 signal intensity in the parasymphyseal pubis or fluid within the pubic symphysis and chronic osteitis which include findings of subchondral sclerosis, bony irregularity, and osteophytes [13, 14]. The bone marrow edema seen in the pubic bones is usually relatively symmetric in osteitis pubis in athletes [14]. A distinct band of linear high T2 signal at the parasymphyseal bone parallelling the subchondral bone plate at the pubis has been

Fig. 27.2 Patient with chronic right groin pain found to have right-sided osteitis pubis. MRI finding of higher intensity on the right consistent with bone marrow edema

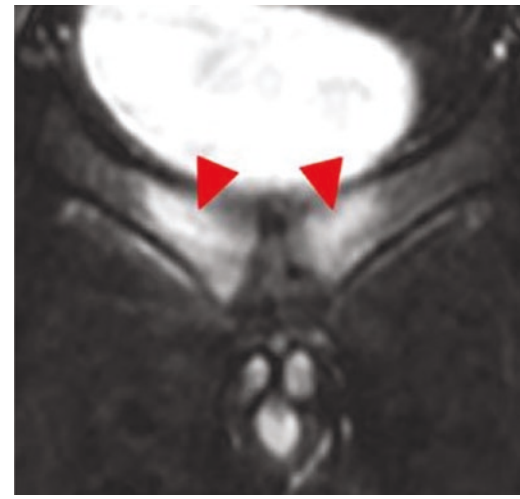

Fig. 27.3 Bone marrow edema spanning the joint anterior to posterior. Bilateral osteitis pubis (red arrow corresponding to the area of inflammation)

described in most symptomatic athletes and may be more clinically relevant than bone marrow edema [15].

Rectus Abdominis and Adductor Pathology

Rectus abdominis and adductor longus pathology are one of the common causes of athletic pubalgia as injury to the common aponeurosis between rectus and adductor can result in groin pain (Fig. 27.4). Acute and chronic rectus abdominis strain injury can be differentiated by evaluating the signal of the caudal rectus abdominis muscle in which acute injury would have abnormal T2 signal and chronic appearance being hypertrophic or atrophic morphology. Focus on the caudal tendinous attachment is important as this is commonly a source of pain and instability at the pubic symphysis when a tear is present [10]. Rectus abdominis commonly extends into the adductor longus origin and findings on MRI include enlargement and signal abnormalities which can represent acute injury such as osseous avulsion at tendon origin or myotendinous strains. MRI was evaluated in a series of 52 athletes with chronic groin pain and the extent and laterality of the anterior pubis and adductor longus enthesis abnormality demonstrated reproducible correlation with the athletes' symptoms [16]. A distal rectus abdominis tear or detachment with an adductor longus origin tear is one of the most frequently encountered lesions on MRI done for athletic pubalgia and likely reflects the previously described sportsman hernia (Fig. 27.5) [17]. This injury also frequently involves a lateral edge defect at the caudal aspect of the rectus abdominis extending into the origin of the adductor longus manifesting as an interstitial tear [10]. Patients with this injury are more likely to be treated with surgery than with isolated adductor or rectus injury [18].

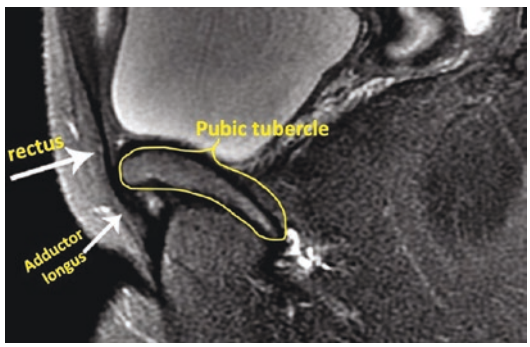

Fig. 27.4 Rectus abdominis and adductor longus anatomy on sagittal view: pathology here is one of the common causes of athletic pubalgia

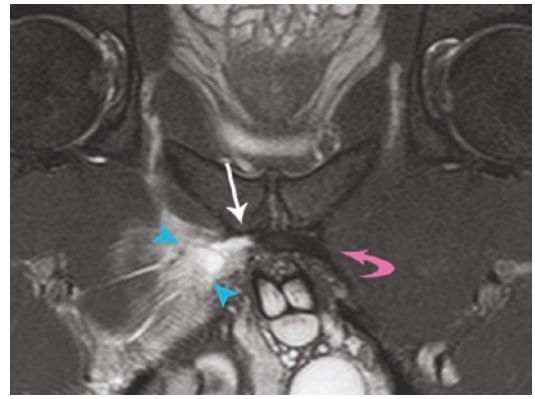

Fig. 27.5 A distal rectus abdominis tear or detachment with an adductor longus origin tear is one of the most frequently encountered lesions on MRI. The aponeurosis has been avulsed from the pubic tubercle (white arrow) with edema extending well into the adductor compartment (blue arrowheads)

Rectus Abdominis/Adductor Aponeurotic Plate Disruption

Bilateral caudal rectus detachment that spans midline is a consistent finding on MRI for an aponeurotic plate disruption [19]. It is important to exclude extension across the midline and involvement of the contralateral rectus abdominis if a unilateral aponeurosis lesion is identified. Osteitis pubis is also commonly seen in association with these lesions (Figs. 27.6 and 27.7). Surgical intervention is common in athletes with these findings as it is rare to return to optimal performance without intervention.

Postoperative MRI

Unilateral pelvic floor repair in patients with athletic pubalgia is estimated to have approximately 4% chance of developing contralateral groin injury or recurrent ipsilateral pubalgia [18]. One of the most frequently encountered injuries after

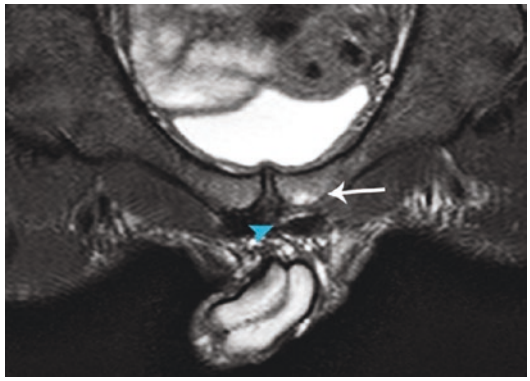

Fig. 27.6 Chronic left rectus and adductor aponeurotic detachment with subendothelial bone marrow edema at the left pubic tubercle (white arrow) and T2 hyperintense gap between the aponeurosis and pubic periosteum (blue arrowhead)

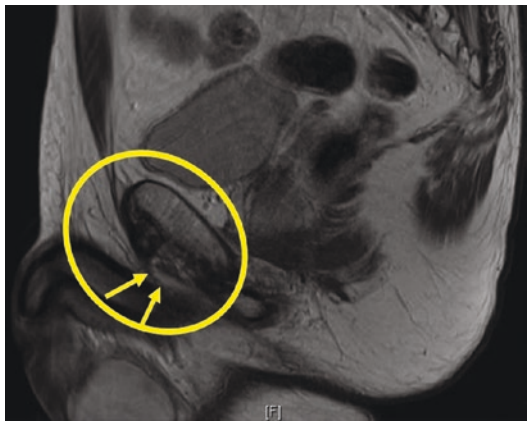

Fig. 27.7 Sagittal view of aponeurotic plate avulsion

repair is a myotendinous strain in the thigh adductor compartment and commonly at the proximal myotendinous junction of the adductor longus. Because of this, it is important for any postoperative MRI for athletic pubalgia to include imaging of the proximal thigh. The extent of edema secondary to osteitis pubis is a useful indicator of the success of surgical treatment [10]. Bone marrow edema typically decreases after surgery since the preoperative MRI in the majority of patients and in one series subjects who had worsening osteitis on postoperative MRI were ultimately diagnosed with a new rectus abdominis/adductor aponeurosis tear [20]. MRI secondary cleft on the side of surgery is expected after repair of aponeurosis tear but should exhibit intensity less than that of fluid on T2-weighted fat suppressed musculoskeletal imaging [10].

Ultrasound

Ultrasound has some advantages when compared to MRI including flexible fields-of-view and dynamic imaging techniques that can make it a useful adjunct in the diagnosis of patients with athletic pubalgia [21]. Ultrasound also has the advantage of correlating findings in real time with a patient's location of symptoms and the ability to image during a valsalva maneuver. Initial evaluation includes the rectus abdominis muscle in both axial and sagittal planes and assessment of the aponeurosis in two sets of orthogonal planes (Fig. 27.8) The transducer is moved to an oblique sagittal orientation to assess the adductor longus and then turned 90 degrees to assess the adductor longus tendon in the transverse plane [21]. It is important to aim the transducer as parallel as possible to the long axis of the tendon to minimize anisotropy which may result in artifactual hypoechogenicity which can be misinterpreted as tendinosis or a tear [22]. The inguinal region is then examined for inguinal or femoral hernias during static assessment and during valsalva maneuver. A thin echogenic band

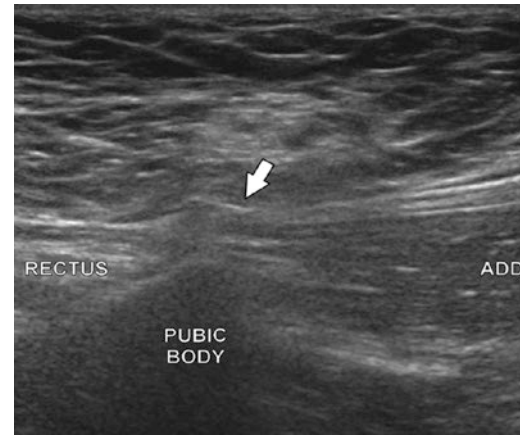

Fig. 27.8 Normal sonographic appearance of the aponeurosis (white arrow). Rectus and adductor longus (ADD) muscles shown

with parallel fibers represents the inguinal ligament and the posterior wall of the canal is assessed for bulging with valsalva which is associated with athletic pubalgia [23]. Targeted sonographic examination should then be performed at any focal reported area of pain.

Osteitis Pubis

Ultrasound is limited in its assessment of bony structures relative to MRI as it does not penetrate the osseous cortex. There are still several sonographic findings for osteitis pubis based on surface morphology including subchondral plate irregularity, pubic symphyseal effusion, spurring, and diastasis of the symphysis [23]. Doppler imaging is also useful and may reveal periarticular hyperemia indicating active associated arthropathy [21].

Rectus Abdominis-Adductor Longus Aponeurosis Injury

The rectus abdominis-adductor longus aponeurosis is imaged from an anterior approach with the patient in supine position with hips abducted and externally rotated (Fig. 27.8). Finding of a tear on MRI corresponded to a secondary cleft at the inferior margin of the anterior pubic body and the analogous finding on ultrasound includes a focal anechoic defect at the origin of the adductor longus aponeurosis [21]. The adductor tendon can also be found to be completely avulsed from the pubis in some cases. Tendon hypoechogenicity, thickening, and loss of normal fibrillar echotexture can be seen in areas of tendinosis. Tendon mineralization can be seen and if pronounced may be the etiology of pain from calcific tendinosis. Color doppler can find periarticular hyperemia and other findings to support an injury including spurring of the pubic body or pubic symphyseal effusion. Injury to the rectus abdominis portion of the aponeurosis can be seen as an anechoic defect on sonography similar to the adductor longus findings previously described.

Sports Hernia on Dynamic Sonogram

Ultrasound examination allows for the assessment of the transversus muscle and rectus abdominis muscle in normal condition and also in the presence of a sports hernia during increased intra-abdominal pressure. During the operation for sports hernias, a subjective finding of weakness of the posterior inguinal wall has been described and dynamic conditions such as coughing and valsalva maneuver during sonography can elicit this laxity [24]. Several studies have also described a posterior wall bulge of preperitoneal fat through the deep inguinal ring or Hasselbach's triangle during increased abdominal pressure (Figs. 27.9 and 27.10) [25, 26]. Ultrasound is also useful to exclude the diagnosis of inguinal hernia which is in the differential diagnosis of patients with groin pain (Video 27.1). Findings of a conjoint tendon tear or external oblique aponeurosis tear have also been described on sonogram and can be seen as a localized hypoechoic thickening of the conjoint tendon [27].

Ultrasound-Guided Intervention

Sonography provides an ideal modality for image-guide interventions for athletic pubalgia given the real-time imaging and lack of radiation. Intra-articular injection in the pubic symphysis for osteitis pubis and injections into the adductor longus tendon are the most commonly performed interventions [28]. Typically, a high-frequency linear probe is placed cephalad at the pubis and the needle is advanced to the probe with injection of anesthetic and cortisone into the symphysis. An adductor tendon injection is performed with sagittal oblique positioning of the transducer to image the tendon in longitudinal axis with the target typically at the origin of the pubic tubercle [29].

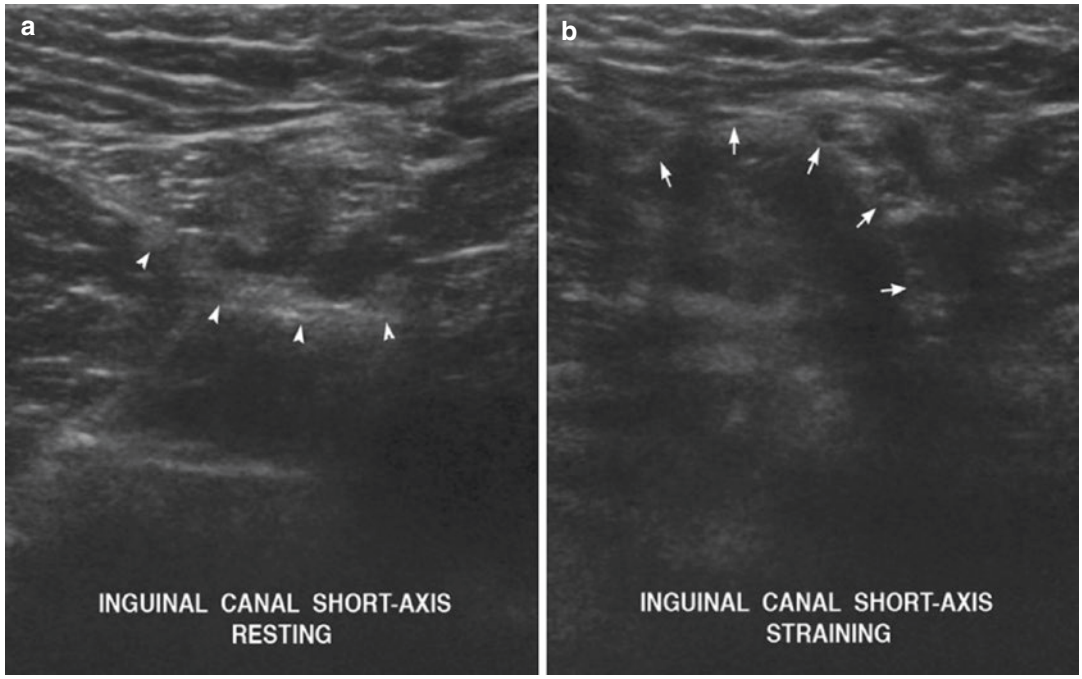

Fig. 27.9 Dynamic ultrasound showing posterior wall bulge of preperitoneal fat through the deep inguinal ring or Hasselbach's triangle during increased abdominal pressure. (**a**) is the canal when resting showing no posterior wall bulge. (**b**) is during valsalva/straining showing the bulge representing wall axity

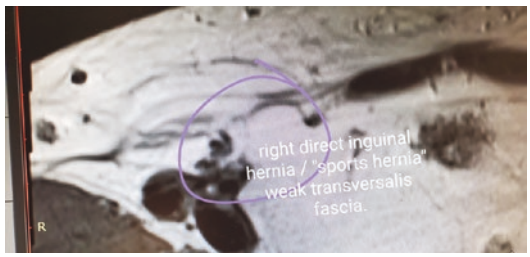

Fig. 27.10 Sports hernia on MRI

Computed Tomography Arthrography

CT-guided pubic symphyseal injection and concurrent arthrography has been proposed as an imaging modality to help identify tendon and aponeurosis tears that were not evident on MRI [30]. CT arthrography is both diagnostic and therapeutic as the protocol used in a study used 3-mm slice thickness for imaging and a 22-gauge spinal needle was advanced approximately 1 cm into the central cleft of the pubic symphysis fibrocartilaginous disk for injection. The position of the needle was confirmed using intermittent CT fluoroscopy. Approximately 0.5 mL of iodinated contrast was injected into the pubic symphysis to reveal the morphology of the disk and potentially reproduce the patient's pain. A therapeutic injection was then performed of triamcinolone aerosol solution at a dose of 40 mg/mL and 1.0 mL of 0.5% bupivacaine. A post-procedure CT was then performed of the symphysis with multiplanar reformatting at a slice thickness of 1 mm [30]. CT arthrography was helpful in evaluating for secondary clefts when MRI was insufficient to explain the cause of groin pain. Overall, CT-guided injection is a reliable diagnostic tool that can provide short-term symptomatic relief during conservative treatment and the addition of CT arthrography can help in identifying more subtle aponeurotic tears [30].

Treatment and Outcomes

There are a wide variety of treatment options available and recommendations generally are the choice of surgery and operative approach be based on surgeon experience [6]. Physical therapy and conservative management are often attempted between 2 and 6 months prior to surgical treatment. Initial management includes range-of-motion exercises and core muscle strengthening while avoiding deep hip flexion. Little prospective data is available on the efficacy of nonoperative treatment, but one randomized study comparing athletes with sports hernias undergoing physical therapy versus surgical laparoscopic repair found 7 of 30 patients in the nonsurgical group switching to the surgical arm and only 50% returning to sports at 1 year compared to 29 of 30 athletes returning to full sports after surgery [31]. Surgical intervention is typically recommended after failure of nonoperative rehabilitation and for sports hernias can be performed through open or minimally invasive techniques (Figs. 27.11 and 27.12) (Video 27.2). Open techniques have been compared with laparoscopic repairs with respect to timing to return to sports and open repairs showed a mean of 5 weeks versus 3 weeks for laparoscopic repairs [32]. A minimally invasive technique has been described which includes opening the posterior abdominal wall with the repair of the transversalis fascia for a tension-free suture repair

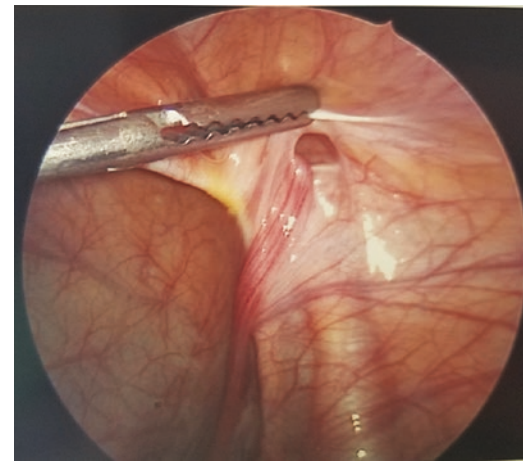

Fig. 27.11 Patient with chronic groin pain taken for diagnostic laparoscopy found to have hernia defect after negative imaging

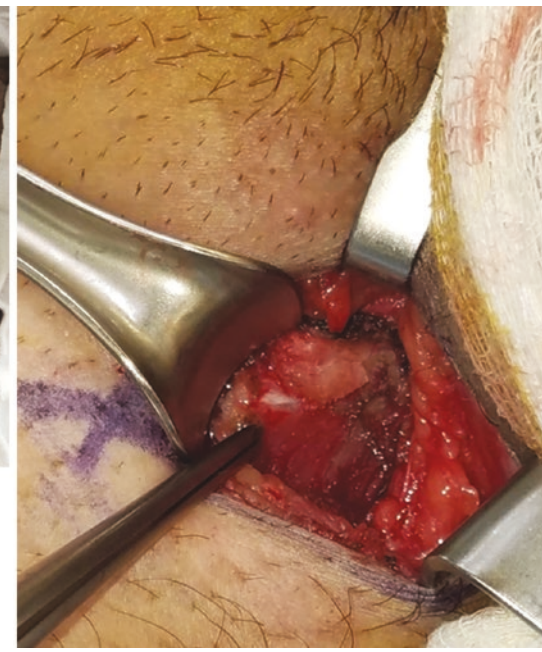

Fig. 27.12 Isolated right adductor tear: right AL tendonotomy. Patient with chronic right groin pain with right adductor tear taken to the operating room for tendonotomy

of the posterior inguinal wall and decompression of the genital branch of the genitofemoral nerve which has shown a faster return to sports activity at a mean of 4 weeks [33]. Sports hernia with associated acetabular impingement is a poor predictor of successful sports hernia repair and a staged procedure incorporating both hernia repair and arthroscopy led to improved outcomes calling for a multidisciplinary approach between general and orthopedic surgery in these cases [34]. Radiofrequency denervation of the ilioinguinal nerve and ligament has also been explored and was successful in treating groin pain for 6 months compared to injection only which provided relief for approximately 1 week [35]. Given most studies report only short-term follow-up and end point of return to sports, it is difficult to identify a superior surgical technique and the recommendation from the British Hernia Society is for the choice of surgery and operative approach to be based on surgeon experience [6].

References

1. Hopkins JN, Brown W, Lee CA. Sports hernia: definition, evaluation, and treatment. JBJS Rev. 2017;5(9):e6. https://doi.org/10.2106/JBJS.RVW.17.00022.
2. Lovell G. The diagnosis of chronic groin pain in athletes: a review of 189 cases. Aust J Sci Med Sport. 1995;27(3):76–9.
3. Malycha P, Lovell G. Inguinal surgery in athletes with chronic groin pain: the 'sportsman's' hernia. Aust N Z J Surg. 1992;62(2):123–5.
4. Emery CA, Meeuwisse WH. Risk factors for groin injuries in hockey. Med Sci Sports Exerc. 2001;33:1423.
5. Rambani R, Hackney R. Loss of range of motion of the hip joint: a hypothesis for etiology of sports hernia. Muscles Ligaments Tendons J. 2015;5(1):29–32.
6. Sheen AJ, Stephenson BM, Lloyd DM, Robinson P, Fevre D, Paajanen H, de Beaux A, Kingsnorth A, Gilmore OJ, Bennett D, Maclennan I, O'Dwyer P, Sanders D, Kurzer M. 'Treatment of the sportsman's groin': British hernia Society's 2014 position statement based on the Manchester consensus conference. Br J Sports Med. 2014;48(14):1079–87. Epub 2013 Oct 22
7. Larson CM. Sports hernia/athletic pubalgia: evaluation and management. Sports Health. 2014;6(2):139–44.
8. Robinson P, Bhat V, English B. Imaging in the assessment and management of athletic pubalgia. Semin Musculoskelet Radiol. 2011;15(1):14–26. https://doi.org/10.1055/s-0031-1271956. Epub 2011 Feb 17
9. Zoga AC, Kavanagh EC, Omar IM, Morrison WB, Koulouris G, Lopez H, Chaabra A, Domesek J, Meyers WC. Athletic pubalgia and the "sports hernia": MR imaging findings. Radiology. 2008;247(3):797–807.
10. Mullens FE, Zoga AC, Morrison WB, Meyers WC. Review of MRI technique and imaging findings in athletic pubalgia and the "sports hernia". Eur J Radiol. 2012;81(12):3780–92. https://doi.org/10.1016/j.ejrad.2011.03.100. Epub 2011 Sep 3
11. Cunningham PM, Brennan D, O'Connell M, et al. Patterns of bone and soft tissue injury at the symphysis pubis in soccer players: observations at MRI. Am J Roentgenol. 2007;188:W291–6.
12. Fricker PA, Taunton JE, Ammann W. Osteitis pubis in athletes: infection, inflammation or injury? Sports Med. 1991;12(4):266–79.
13. O'Connell MJ, Powell T, McCaffrey NM, O'Connell D, Eustace SJ. Symphyseal cleft injection in the diagnosis and treatment of osteitis pubis in athletes. AJR Am J Roentgenol. 2002;179:955–9.
14. Hiti CJ, Stevens KJ, Jamati MK, Garza D, Matheson GO. Athletic osteitis pubis. Sports Med. 2011;41(5):361–76.
15. Braun P, Jensen S. Hip pain: a focus on the sporting population. Aust Fam Physician. 2007;36(6):406–8. 410–3
16. Robinson P, Barron DA, Parsons W, Grainger AJ, Schilders EM, O'Connor PJ. Adductor-related groin pain in athletes: correlation of MR imaging with clinical findings. Skeletal Radiol. 2004;33(8):451–7.
17. Omar IM, Zoga AC, Kavanagh EC, et al. Athletic pubalgia and "sports hernia": optimal MR imaging technique and findings. Radiographics. 2008;28:1415–38.
18. Meyers WC, McKechnie A, Philippon MJ, et al. Experience with "sports hernia" spanning two decades. Ann Surg. 2008;248(4):656–65.
19. Walheim G, Olerud S, Ribbe T. Mobilityofthepubicsymphysis, measurements by an electromechanical method. Acta Orthop Scand. 1984;552:203–8.
20. Zoga AC, Morrison WB, Roth CG, Horner M, Meyers WC. MR findings in athletic pubalgia: normal postoperative appearance and reinjury patterns after pelvic repairs and releases for "sports hernia". In: Proceedings of the Radiologic Society of North America. 2009.
21. Morley N, Grant T, Blount K, Omar I. Sonographic evaluation of athletic pubalgia. Skeletal Radiol. 2016;45(5):689–99. https://doi.org/10.1007/s00256-016-2340-8. Epub 2016 Feb 10
22. Jamadar DA, Robertson BL, Jacobson JA, Girish G, Sabb BJ, Jiang Y, et al. Musculoskeletal sonography: important imaging pitfalls. AJR Am J Roentgenol. 2010;194(1):216–25.

23. Orchard JW, Read JW, Neophyton J, Garlick D. Groin pain associated with ultrasound finding of inguinal canal posterior wall deficiency in Australian rules footballers. Br J Sports Med. 1998;32(2):134–9.
24. Hackney RG. The sports hernia: a cause of chronic groin pain. Br J Sports Med. 1993;27:58–62.
25. Santilli OL, Nardelli N, Santilli HA, Tripoloni DE. Sports hernias: experience in a sports medicine center. Hernia. 2016;20:77–84.
26. Jamadar DA, Jacobson JA, Morag Y, Girish G, Ebrahim F, Gest T, et al. Sonography of inguinal region hernias. AJR Am J Roentgenol. 2006;187:185–90.
27. Malycha P, Lovell G. Inguinal surgery in athletes with chronic groin pain: the "Sportsman's" hernia. Aust NZ J Surg. 1992;62:123–5.
28. Lee SC, Endo Y, Potter HG. Imaging of groin pain: magnetic resonance and ultrasound imaging features. Sports Health. 2017;9(5):428–35. https://doi.org/10.1177/1941738117694841. Epub 2017 Mar 8
29. Balconi G. US in pubalgia. J Ultrasound. 2011;14(3):157–66. https://doi.org/10.1016/j.jus.2011.06.005.
30. McArthur TA, Narducci CA, Lopez-Ben RR. The role of pubic symphyseal CT arthrography in the imaging of athletic pubalgia. AJR Am J Roentgenol. 2014;203(5):1063–8.
31. Paajanen H, Brinck T, Hermunen H, Airo I. Laparoscopic surgery for chronic groin pain in athletes is more effective than nonoperative treatment: a randomized clinical trial with magnetic resonance imaging of 60 patients with sportsman's hernia (athletic pubalgia). Surgery. 2011;150:99–107.
32. Ingoldby CJ. Laparoscopic and conventional repair of groin disruption in sportsmen. Br J Surg. 1997;84:213–5.
33. Economopoulos KJ, Milewski MD, Hanks JB, Hart JM, Diduch DR. Sports hernia treatment: modified Bassini versus minimal repair. Sports Health. 2013;5(5):463–9.
34. Larson CM, Pierce BR, Giveans MR. Treatment of athletes with symptomatic intra-articular hip pathology and athletic pubalgia/sports hernia: a case series. Art Ther. 2011;27(6):768–75.
35. Comin J, Obaid H, Lammers G, Moore J, Wotherspoon M, Connell D. Radiofrequency denervation of the inguinal ligament for the treatment of 'sportsman's hernia': a pilot study. Br J Sports Med. 2013;47(6):380–6. Epub 2012 Sep 5

Imaging Approach to Chronic Postoperative Inguinal Pain

28

Aldo Fafaj, Samuel J. Zolin, Michael C. Forney, and David M. Krpata

Introduction

With the advent of prosthetic materials and refinement of tension-free repairs contributing to reduced recurrence rates, chronic postoperative pain has become the primary focus when discussing outcomes of inguinal hernia repair [1]. Chronic postoperative inguinal pain (CPIP) is defined as pain lasting more than 3 months following inguinal hernia repair. [2] This pain can be severe, potentially affecting activities of daily living in up to one-third of patients with CPIP [3]. Determining the etiology of CPIP can present a diagnostic challenge for any surgeon, often delaying diagnosis and treatment. Unlike the initial presentation of inguinal hernias, when the diagnosis is often made only with the history and physical exam, the cause of CPIP may be subtle. Thus, other than in unique cases where the reason is evident on physical exam, imaging becomes an essential tool for diagnosis and treatment. Here we discuss the different imaging modalities (ultrasound, computed tomography, and magnetic resonance) in the context of the most encountered causes for this complication. Of note, primary groin pain will not be addressed here, as it will be discussed in a separate chapter.

Pathophysiology of CPIP

The pathophysiology of CPIP is complex, given the heterogeneity of the types of pain. In general, pain can be broadly categorized as neuropathic, nociceptive, somatic, and visceral. Neuropathic pain involves nerve entrapment or direct damage during dissection or mesh fixation. The most commonly involved nerves include ilioinguinal, iliohypogastric, and the genital branch of the genitofemoral nerve. Additionally, the implanted prosthetic material can migrate, shrink, or fold, which may also lead to nerve entrapment. Nociceptive pain has been described as a persistent inflammatory response to tissue injury and

Supplementary Information The online version contains supplementary material available at https://doi.org/10.1007/978-3-031-21336-6_28.

A. Fafaj (✉)
Department of General Surgery, Cleveland Clinic, Cleveland, OH, USA
e-mail: fafaja@ccf.org

S. J. Zolin
Cleveland Clinic Foundation, Digestive Disease and Surgery Institute, Cleveland, OH, USA
e-mail: zolins@ccf.org

M. C. Forney
Section of Musculoskeletal Imaging, Cleveland Clinic Foundation, Imaging Institute, Cleveland, OH, USA

D. M. Krpata
Department of Surgery, Cleveland Clinic, Cleveland, OH, USA
e-mail: krpatad@ccf.org

S. Docimo Jr. et al. (eds.), *Fundamentals of Hernia Radiology*,
https://doi.org/10.1007/978-3-031-21336-6_28

the implanted foreign body where endogenous inflammatory mediators cause exaggerated responses to normal stimuli [4]. Somatic pain is thought to be caused by damage to the periosteum of the pubic tubercle [5], while visceral pain refers to post-ejaculatory pain caused by venous congestion of the spermatic cord from prosthetic material encasement [6]. Finally, some patients develop hernia recurrence, which also may contribute to pain. To add to the complexity of these cases, patients may have multiple factors contributing to CPIP. Thus, radiologic imaging to identify the cause(s) of CPIP becomes critically important.

Imaging Modalities

Ultrasound is a widely available, noninvasive imaging modality that does not subject patients to radiation. Thus, it is typically the first imaging modality used to evaluate the CPIP patient (Figs. 28.1 and 28.2). In order to increase the accuracy, the ultrasound exam must be performed dynamically with the patient lying supine and in an upright position, both at rest and during straining by performing the Valsalva maneuver. In addition, ultrasound can also be used to perform local analgesic blocks, which can help to identify and treat inguinal neuralgia [7].

If the ultrasound is non-diagnostic, then cross-sectional computed tomography (CT) or magnetic resonance imaging (MRI) may be helpful in determining the etiology of CPIP. Of note, MRI is currently considered the best imaging tool for evaluating the causes of inguinal pain, and some argue that it should be considered as a first-line imaging modality when evaluating the postoperative groin [8, 9]. The advantages of this modality are superior soft tissue evaluation coupled with accurate and reproducible identification of groin anatomic structures in several planes [10, 11]. Although it may be a limitation in some centers, both CT and MRI scans should be performed dynamically if possible, to increase the likelihood that any occult pathology is demonstrated [12]. However, high-level evidence comparing ultrasound with CT or MRI in the context of CPIP is lacking.

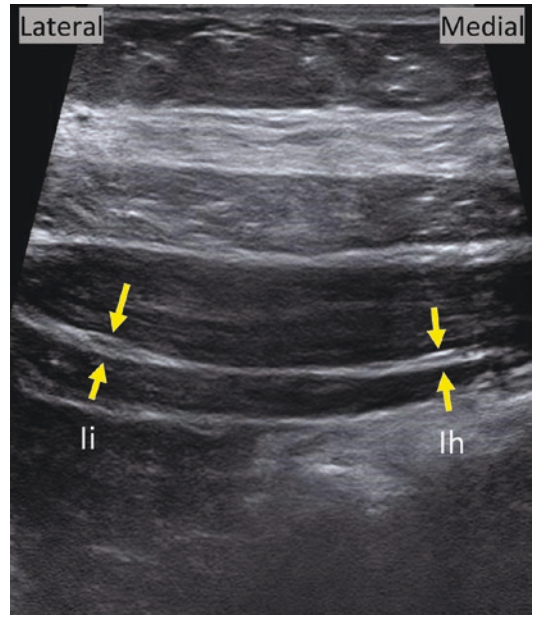

Fig. 28.1 Transverse image (short axis) of normal-appearing ilioinguinal (arrows, Ii) and iliohypogastric (arrows, Ih) nerves using a 9 MHz ultrasound probe. When normal, at times, these nerves can be difficult to identify, but anatomically located between the internal oblique and transversus abdominus muscles. Doppler imaging can be used to differentiate the nerves from adjacent vessels

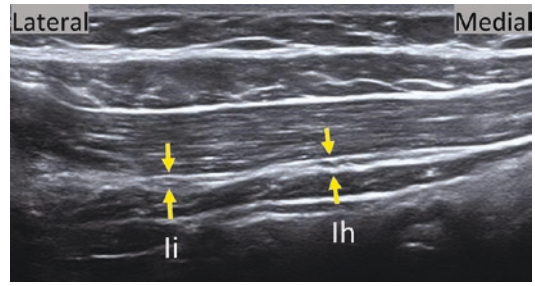

Fig. 28.2 Transverse image of normal-appearing ilioinguinal (arrows Ii) and iliohypogastric (arrows, Ih) nerves (short axis) using an 18 MHz ultrasound probe. Compared with the 9 MHz probe, the detail is greater with the 18 MHz probe; however, a fundamental trade-off exists between image resolution and depth of imaging in ultrasound. So, for patients with high body mass index, the resolution will need to be sacrificed to achieve adequate imaging depth

All three imaging modalities are limited by operator-dependability and the availability of radiologists who are familiar with dynamic groin imaging [13]. To maximize the yield of these studies, imaging protocols should be standardized and performed by radiologists who are specialized in groin anatomy and post-herniorrhaphy changes. More importantly, the surgeon and the radiologist must work closely together, ideally in a multidisciplinary team, to ensure proper diagnosis and treatment options, regardless of which diagnostic imaging modality is used.

Commonly Encountered Pathology

Recurrence

If recurrence is suspected as the cause of pain, dynamic ultrasound is best suited as the initial test. Although non-dynamic ultrasound has a high sensitivity for detecting inguinal hernias, it cannot reliably exclude occult ones. The sensitivity of ultrasound increases when performed dynamically, as described above, by a radiologist who specialized in groin anatomy. If clinical suspicion is high for recurrence, negative ultrasound should prompt further cross-sectional imaging. However, it should be pointed out that inguinal hernias have been poorly reported on routine CT and MRI, leading to delay in diagnosis [14]. Reasons for these missed hernias include non-dynamic imaging and inconsistent reads by radiologists who do not routinely read these scans. Often the initial radiology reports for evaluation of groin pain may have significant shortcomings, as shown by Miller and colleagues [14]. Strikingly, two out of three CT or MRI radiology reports incorrectly identified groin pathology when those scans were subsequently reviewed by a radiologist specializing in hernia-related pathology. Most importantly, the surgeon must not rely solely on the imaging report. Reviewing the scans closely with the radiologist will not only improve the accuracy of these tests but may also ameliorate diagnostic delays.

Mesh Complications

Given the variability in mesh position based on the surgical approach and surgeon preference, a thorough review of prior surgical reports is critical when evaluating the postoperative groin for mesh abnormalities. Ultrasound has been used to assess implanted mesh [15]; however, its reliability has been questioned for detecting mesh that has folded or turned into a meshoma [9]. On CT scan, some meshes may be difficult to distinguish from the surrounding tissue given their nonradiopaque material. In addition, polypropylene meshes, which are the most commonly used prosthetics in inguinal hernia repair, have densities similar to surrounding muscle, so they appear invisible or poorly visible on CT [16]. This material is readily seen on MRI, however. Unfortunately, mesh manufacturers do not provide information regarding the radiopaque properties of the prosthetic materials they offer, so that information is missing unless surgeons or radiologists have self-categorized them based on past experiences [16].

Initial folding of the mesh can lead to a continuous process where the mesh forms into a ball, commonly referred to as a meshoma [17] (Video 28.1). This structure can lead to mechanical compression of nerves and cord structures, causing pain. CT and MRI can readily reveal this structure and aid the surgeon with operative planning. However, due to the lack of radiology literature regarding this topic, meshoma is often interpreted as nonspecific postoperative changes. [17] Repair techniques that involve anterior and posterior components such as the plug, the plug-and-patch, or the Prolene® Hernia system present unique challenges. The posterior component of the mesh is inserted beyond the internal ring, which may appear as an irregular mass often misdiagnosed as free fluid, bowel-containing hernia, and lymphadenopathy [18] (Video 28.2). This highlights, again, the importance of close collaboration between the surgeon and the radiologist. Furthermore, nonspecific radiographic images should be rereviewed by a radiologist familiar

with both groin anatomy and CPIP pathology. This may prevent further exposure to ionizing radiation and may reduce cost by minimizing the workup.

Nerve Damage

Thorough knowledge of the groin neuroanatomy is critical not only to avoid nerve damage during the initial repair but also when evaluating for causes of CPIP. Unlike the evaluation for recurrence or meshoma, nerve pathology is not as readily displayed on an ultrasound or CT scan. Radiologic expertise is critically important to recognize the often-subtle changes. Figures 28.3 and 28.4 show the ilioinguinal and iliohypogastric nerves, respectively, in two patients with a history of inguinal hernia repair. Compared to normal nerves shown in Figs. 28.1 and 28.2, these nerves appear abnormally enlarged. Ultrasound images of the cord structures may also aid in identifying abnormal nerve pathology. Figure 28.5 shows transverse images of the spermatic cord after inguinal hernia repair. Here the spermatic cord can be visualized close to the implanted mesh, and the genital branch of the genitofemoral nerve has a normal appearance. In contrast, Fig. 28.6 shows the abnormally enlarged genital branch of the genitofemoral nerve in longitudinal and transverse images of the spermatic cord after inguinal hernia repair. In addition to direct visualization, neuropathic causes may be indirectly implied by the presence of meshoma or fixation devices along the predicted anatomic path of the nerves [9].

MRI has more utility as this modality may identify nerve entrapment or neuromas. In addition, MRI neurography can also be used to visualize the involved nerves. This is an imaging technique that can capture the intrinsic signal of nerves [19]. This technique can identify nerve compression; however, similar to other imaging modalities, it is radiologist-dependent [7].

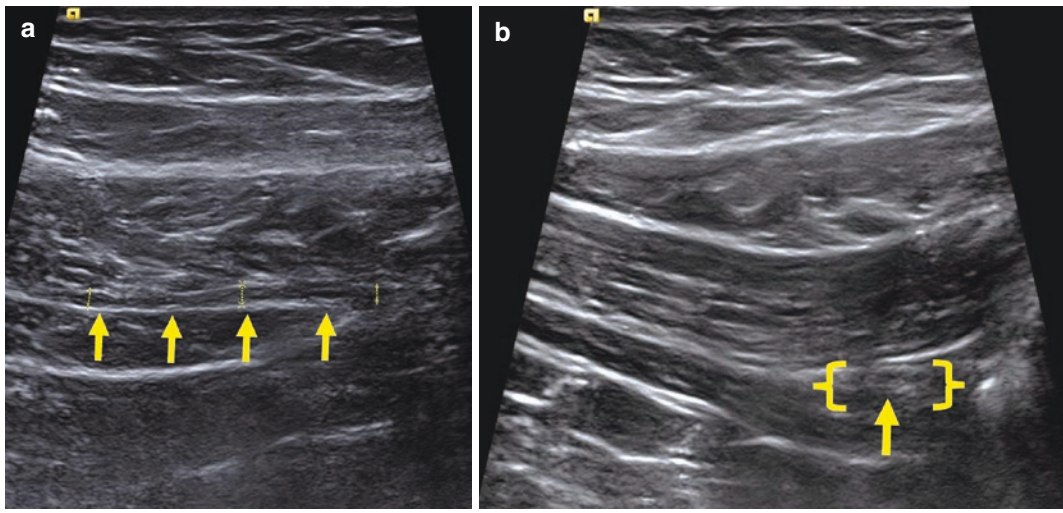

Fig. 28.3 Longitudinal (**a**) (arrows) and transverse (**b**) (arrow and brackets) images of the ilioinguinal nerve. In this post-hernia repair patient, the nerve is abnormally enlarged. Of note, imaging abnormalities of nerves do not always correspond with clinical symptoms

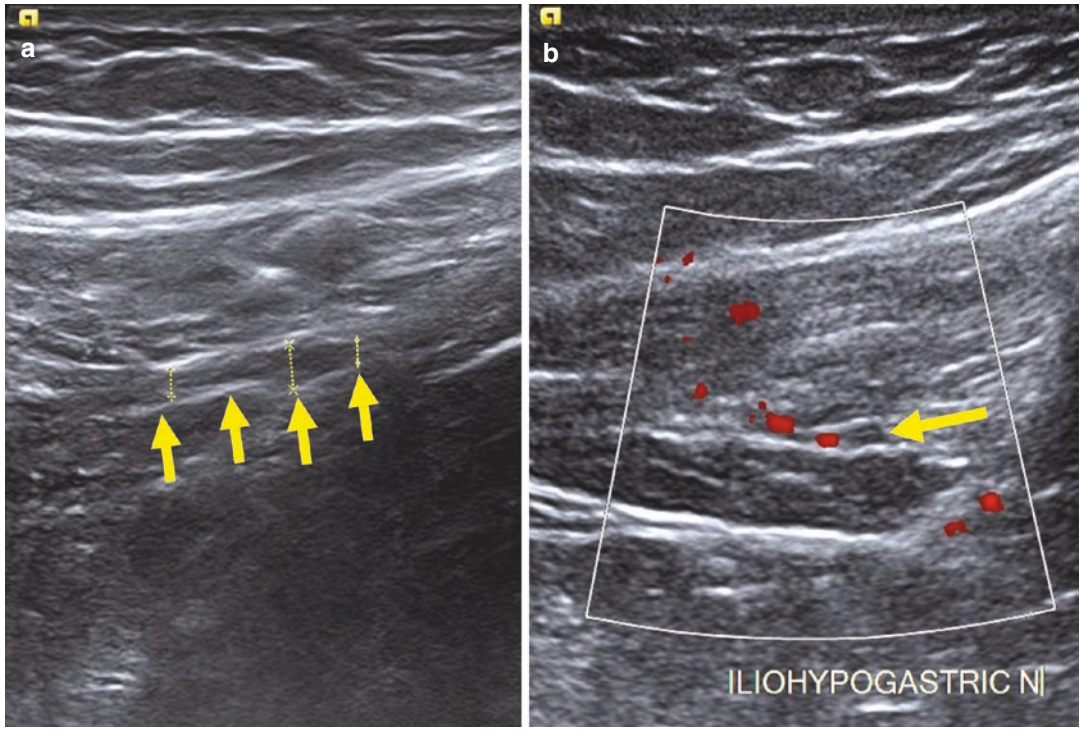

Fig. 28.4 Longitudinal (**a**) and transverse (**b**) images of the iliohypogastric nerve (arrows). In this post-hernia repair patient, the nerve is abnormally enlarged. The iliohypogastric nerve is seen more medial than the ilioinguinal nerve when scanning in an oblique plane, roughly parallel with the ilioinguinal ligament

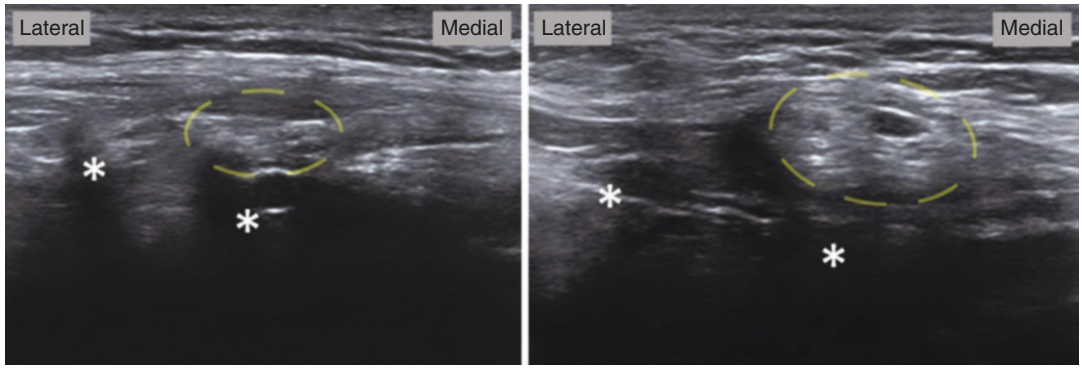

Fig. 28.5 Transverse images of the spermatic cord (dashed oval) near the hernia repair mesh (asterisks). In this case, the spermatic cord has a normal appearance without focal enlargement of the genital branch of the genitofemoral nerve

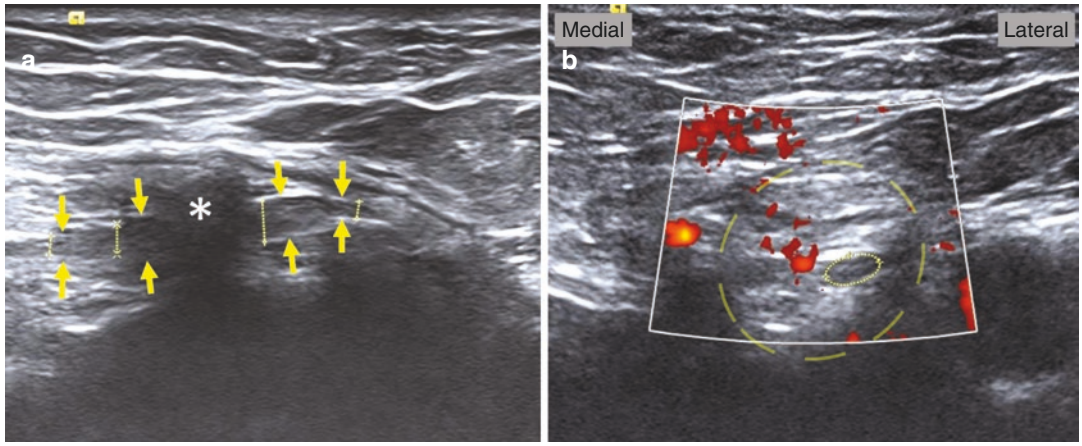

Fig. 28.6 Longitudinal (**a**) and transverse (**b**) images of the spermatic cord in a patient status post inguinal hernia repair. In the longitudinal plane, the genitofemoral nerve (arrows) is abnormally enlarged near the hernia repair mesh (asterisks). Although sometimes difficult to uniquely identify within the spermatic cord, the genitofemoral nerve is also enlarged in the transverse plane in this case (small dashed oval)

Conclusion

Chronic postoperative inguinal pain can present a diagnostic and therapeutic challenge for any surgeon, which prolongs treatment. Several imaging modalities can be used with varying degrees of success for detecting complex groin pathology. Perhaps more important than the test used is the establishment of a close surgeon-radiologist relationship, ideally in a multidisciplinary setting. This close collaboration will optimize both the diagnosis and treatment of the CPIP patient.

References

1. van Hout L, Bökkerink WJV, Ibelings MS, Heisterkamp J, Vriens PWHE. Outcomes of surgery on patients with a clinically inapparent inguinal hernia as diagnosed by ultrasonography. Hernia. 2018;22:525–31. https://doi.org/10.1007/s10029-018-1744-x.
2. Charalambous MP, Charalambous CP. Incidence of chronic groin pain following open mesh inguinal hernia repair, and effect of elective division of the ilioinguinal nerve: meta-analysis of randomized controlled trials. Hernia. 2018;22:401–9. https://doi.org/10.1007/s10029-018-1753-9.
3. Nienhuijs S, Staal E, Strobbe L, Rosman C, Groenewoud H, Bleichrodt R. Chronic pain after mesh repair of inguinal hernia: a systematic review. Am J Surg. 2007;194:394–400. https://doi.org/10.1016/j.amjsurg.2007.02.012.
4. Kehlet H, Jensen TS, Woolf CJ. Persistent postsurgical pain: risk factors and prevention. Lancet. 2006;367:1618–25. https://doi.org/10.1016/S0140-6736(06)68700-X.
5. Cunningham J, Temple WJ, Mitchell P, Nixon JA, Preshaw RM, Hagen NA. Cooperative hernia study. Pain in the postrepair patient. Ann Surg. 1996;224:598–602. https://doi.org/10.1097/00000658-199611000-00003.
6. Hakeem A. Current trends in the diagnosis and management of post-herniorraphy chronic groin pain. World J Gastrointest Surg. 2011;3:73. https://doi.org/10.4240/wjgs.v3.i6.73.
7. Nguyen DK, Amid PK, Chen DC. Groin pain after inguinal hernia repair. Adv Surg. 2016;50:203–20. https://doi.org/10.1016/j.yasu.2016.04.003.
8. Hu QL, Chen DC. Approach to the patient with chronic groin pain. Surg Clin North Am. 2018;98:651–65. https://doi.org/10.1016/j.suc.2018.02.002.
9. Miller JM, Ishimitsu DN. The SAGES manual of groin pain. In: SAGES man groin pain. Springer; 2016. p. 257–265. https://doi.org/10.1007/978-3-319-21587-7.
10. van den Berg JC, Go PM, de Valois J, Rosenbusch G. Preoperative and postoperative assessment of laparoscopic inguinal hernia repair by dynamic MRI. Investig Radiol. 2000;35:695–8. https://doi.org/10.1097/00004424-200011000-00008.
11. Burgmans JPJ, Voorbrood CEH, Van Dalen T, Boxhoorn RN, Clevers GJ, Sanders FBM, et al. Chronic pain after TEP inguinal hernia repair, does MRI reveal a cause? Hernia. 2016;20:55–62. https://doi.org/10.1007/s10029-015-1448-4.

12. HerniaSurge Group. International guidelines for groin hernia management. Hernia. 2018;22:1–165. https://doi.org/10.1007/s10029-017-1668-x.
13. Leander P, Ekberg O, Sjöberg S, Kesek P. MR imaging following herniography in patients with unclear groin pain. Eur Radiol. 2000;10:1691–6. https://doi.org/10.1007/s003300000555.
14. Miller J, Tregarthen A, Saouaf R, Towfigh S. Radiologic reporting and interpretation of occult inguinal hernia. J Am Coll Surg. 2018;227:489–95. https://doi.org/10.1016/j.jamcollsurg.2018.08.003.
15. Gavrilov SG, Son DA, Churikov DA, Shuliak GD. Ultrasound appearance of mesh after transabdominal Preperitoneal inguinal hernia repair. J Laparoendosc Adv Surg Tech A. 2020;00:1–7. https://doi.org/10.1089/lap.2019.0689.
16. Rakic S, LeBlanc KA. The radiologic appearance of prosthetic materials used in hernia repair and a recommended classification. AJR Am J Roentgenol. 2013;201:1180–3. https://doi.org/10.2214/AJR.13.10703.
17. Amid PK. Radiologic images of Meshoma. Arch Surg. 2004;139:1297. https://doi.org/10.1001/archsurg.139.12.1297.
18. Aganovic L, Ishioka KM, Hughes Cassidy F, Chu PK, Cosman BC. Plugoma: CT findings after prosthetic plug inguinal hernia repairs. J Am Coll Surg. 2010;211:481–4. https://doi.org/10.1016/j.jamcollsurg.2010.06.001.
19. Filler A. Magnetic resonance neurography and diffusion tensor imaging: origins, history, and clinical impact of the first 50,000 cases with an assessment of efficacy and utility in a prospective 5000-patient study group. Neurosurgery. 2009;65:A29–43. https://doi.org/10.1227/01.NEU.0000351279.78110.00.

29 Therapeutic Ultrasonography: TAP Block and BOTOX, Collections, Nerve Injections

Verghese T. Cherian

Introduction

The successful repair of an abdominal hernia would depend on various factors including, but not limited to, the site and the type of defect, the size of the hernia, the tone of the musculature, and the contents of the hernia sac. Surgical repair of an extremely large hernia or a recurrent incisional hernia pose added challenges such as inadequate or incompetent muscle cover, significant postoperative pain, potential respiratory compromise due to high intra-abdominal pressure, increased tension of the muscles of the lateral abdominal wall which can lead to early recurrence [1].

Acute pain following abdominal hernia repair can be controlled by blockade of the nerves of the anterior abdominal wall with local anesthetic [2, 3]. The analgesia reduces the involuntary guarding of the abdominal muscles, improves respiratory excursions, and promotes postoperative recovery. Over the last decade, there have been clinical reports of the use of Botulinum toxin (Btox) for analgesia after hernia surgery [4] and also to temporarily paralyze the lateral abdominal muscles, to facilitate primary closure of open abdomen [5] and repair of complex incisional hernia [1, 6].

A seroma is a common and challenging postoperative complication after extensive dissection of tissues needed to repair complex recurrent hernia. This accumulation of lymph and inflammatory fluids in surgically created dead space prevents the apposition and adhesion of tissue surfaces [7]. The disruption of lymphatic channels and blood vessels is believed to play a central role in the accumulation of the exudative fluid that results in seroma, and so does the local inflammatory reaction to the mesh used for repair of the hernia [7, 8].

Patient Selection

Injection of Btox stretches the lateral abdominal muscles which can benefit two groups of patients.

1. Patients with large incisional hernia following previous wound infection or major trauma can have significant loss of abdominal muscle mass and the hernial sac is made up of scar tissue and devoid of muscle. Stretching of the lateral muscles could provide the muscle cover to strengthen the repair.

Supplementary Information The online version contains supplementary material available at https://doi.org/10.1007/978-3-031-21336-6_29.

V. T. Cherian (✉)
Department of Anesthesiology and Perioperative Medicine, Penn State Health Milton S Hershey Medical Center, Hershey, PA, USA
e-mail: vcherian@pennstatehealth.psu.edu

S. Docimo Jr. et al. (eds.), *Fundamentals of Hernia Radiology*,
https://doi.org/10.1007/978-3-031-21336-6_29

2. Patients with extremely large hernias could have a significant rise in intra-abdominal pressure when the contents of the hernial sac are returned to the abdomen. The lengthening and the thinning of the muscle mass would decrease the wall tension and increase the available intra-abdominal space to accommodate the hernial contents.

Postoperative analgesia after abdominal surgery can be supplemented by blocking the muscular and cutaneous nerves of the abdomen, proximal to the site of surgery. Therefore, the choice of the nerve block depends on the extent of tissue dissection for the repair of the hernia and to place the surgical mesh and also the sites for insertion of the laparoscopic instruments. The choices available to block the abdominal nerves are the Erector Spinae Plane (ESP) [9], the Quadratus Lumborum (QL) [10], the Transversus Abdominis Plane (TAP) [11], the Rectus sheath (RS), the ilio-inguinal, and the ilio-hypogastric nerve blocks. The use of liposomal bupivacaine can prolong the duration of the block compared to plain bupivacaine or ropivacaine [11, 12]. Alternatively, a catheter can be placed in the proximity of the nerve and an automated pump used to infuse local anesthetic continuously or in boluses.

Most seromas are asymptomatic and resolve in a short time, but the few that linger may get lined with fibrous tissue and become pseudocysts. Although expectant management is the usual initial treatment, the symptomatic and the chronic ones need aspiration of fluid or open surgery. Injection of sclerosing agents such as talc, doxycycline, and alcohol have been shown to obliterate the space [7].

Ultrasound Scanning

Ultrasound imaging is a convenient technique to delineate the abdominal wall muscles and the fascial planes. It can also be used to detect intra-abdominal hernias and herniation through defects in abdominal wall muscles such as the Spigelian and the lumbar hernias. Prior to performing the nerve block or the Btox injection, it is prudent to do a diagnostic ultrasound scanning to identify the muscle layers and the exact location to perform the injection (Fig. 29.1). Real-time ultrasonography is a valuable tool to confirm the correct placement of the needle tip before injecting the medication. Ultrasonography is valuable in delineating the extent of a seroma and in guiding the needle used to aspirate it. A high-frequency linear ultrasound probe is ideal since the target of interest is superficial. However, in an obese patient a curvilinear probe may be used.

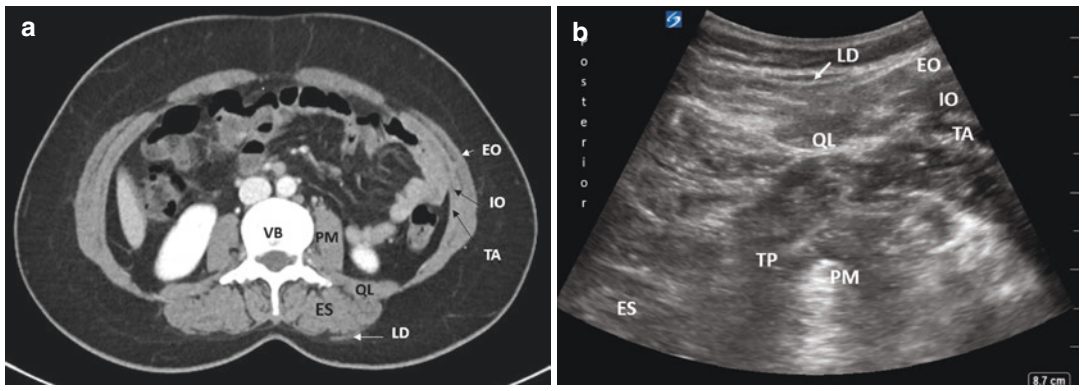

Fig. 29.1 The muscles and the fascial layers of the abdominal wall as seen by computed tomography (**a**) and ultrasonography (**b**). *PM* psoas major, *QL* quadratus lumborum, *LD* latissimus dorsi, *EO* external oblique, *IO* internal oblique, *TA* transversus abdominis, *VB* vertebral body, *TP* transverse process

Ultrasound Procedure

Botulinum Toxin (Btox) Injection: (Video 29.1)

Btox when injected into a muscle makes the neuro-muscular junction dysfunctional [13]. The muscles of the lateral abdominal wall are the usual site for injection. Mild sedation and local anesthetic infiltration of the injection site should suffice to perform this procedure. Although the patient may be supine if bilateral block is required, it helps to turn the patient slightly lateral by placing a folded blanket under the flank, especially if the hernia is large or the patient is obese. The patient's abdomen is cleaned with a standard antiseptic solution and then using the ultrasound probe *three* points are located along the anterior axillary line between the costal margin and the iliac crest where all three muscles, namely the external oblique (EO), the internal oblique (IO), and the transversus abdominis (TA) are seen (Fig. 29.2a). The procedure is repeated on the opposite side by turning the patient the other way.

Once the skin and the superficial fascia are infiltrated with a local anesthetic, the needle is passed through the muscles and the location within the muscle is confirmed by injecting about 0.5 mL of normal saline. An aliquot of 11 mL of diluted Btox (200 units of Btox is diluted into 200 mL of normal saline; 1 U/mL) is injected into each of the three muscles, starting with the deeper one (Fig. 29.2b). It may be prudent to observe the patient for any allergic reactions after the first aliquot is given. The needle insertion can be "in-plane" or "out-of-plane" to the ultrasound probe, depending on the surface contour and the available space between the costal margin and the iliac crest. Once the three muscles at each of the three sites, on both sides are injected, the patient may be transferred to the recovery area and observed for an hour before being discharged.

Nerve Blocks: (Video 29.2)

The thoracic (T) and the lumbar (L) nerves, namely the intercostal (T7–T12), the ilio-inguinal (L1), and the ilio-hypogastric (L1) nerves, provide the sensory and the muscular innervation to the abdominal wall. The rectus abdominis is innervated by the lower six intercostal nerves and the cutaneous nerves follow the dermatomal distribution. The T10 nerve aligns along the umbilicus with the area between the xiphoid and the umbilicus and is innervated by T7–T9 nerves and the cutaneous branches of T11–L1 supplying the area from the umbilicus to the pubis.

All these nerves arise from the ventral rami of the thoracic and the lumbar spinal nerves (T7–L1) and run ventral to the vertebral transverse

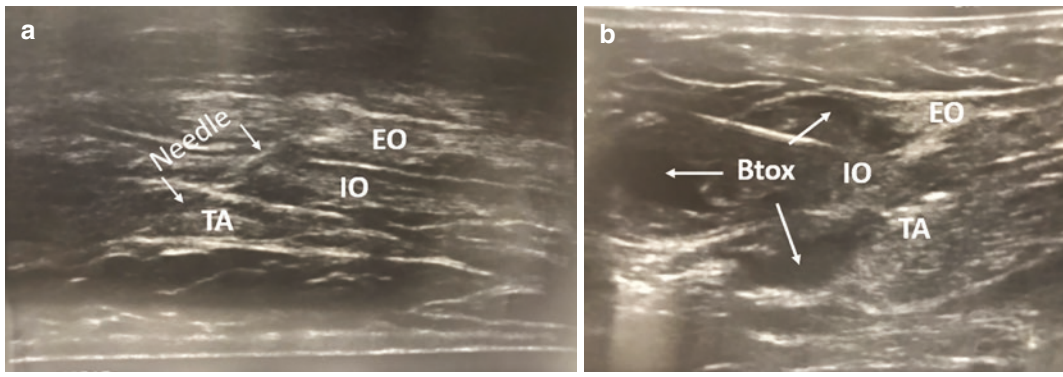

Fig. 29.2 Ultrasound scan of the lateral abdominal wall showing the external oblique (EO), internal oblique (IO), and the transversus abdominis (TA) muscles, before (**a**) and after (**b**) the injection of the Botulinum toxin (Btox) into each muscle layer

processes, pass between the psoas major and the quadratus lumborum muscles and enter the fascial plane between the internal oblique and the transversus abdominis. The ilio-inguinal and the ilio-hypogastric nerves pierce the internal oblique muscle, near the anterior superior iliac spine, and traverse between it and the external oblique to supply the inguinal region.

These nerves can be blocked at various sites along its path; namely, anterior to the erector spinae muscle (ESP), anterior to the quadratus lumborum (QL), in the transversus abdominis plane (TAP) or within the rectus sheath (RS) (Fig. 29.3). Using real-time ultrasonography, the block needle is guided into the correct plane to either inject a bolus dose of local anesthetic (plain, with adjuvants or the liposomal bupivacaine) or place a catheter to enable continuous or on-demand infusion of local anesthetic through it.

Seroma

Percutaneous aspiration of the fluid collection under ultrasound guidance is usually therapeutic, but if it recurs, injection of a sclerosing agent after the aspiration is shown to be effective. Figure 29.4a demonstrates a seroma collection noted on ultrasound as well as drain placement under ultrasound guidance (Fig. 29.4b).

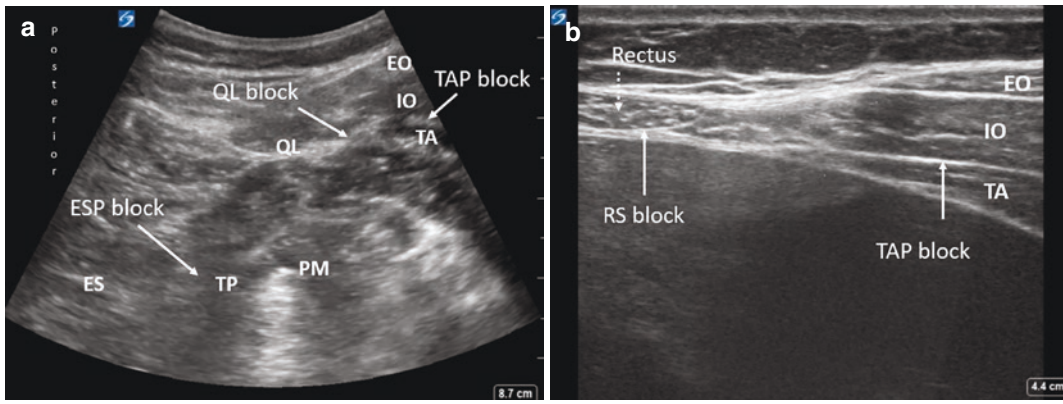

Fig. 29.3 The ultrasound scanning of the posterior (**a**) and anterior (**b**) abdominal walls showing the site for Erector Spinae Plane (ESP), Quadratus Lumborum (QL), Transversus Abdominis Plane (TAP), and Rectus sheath (RS) blocks. *PM* psoas major, *QL* quadratus lumborum, *EO* external oblique, *IO* internal oblique, TA transversus abdominis

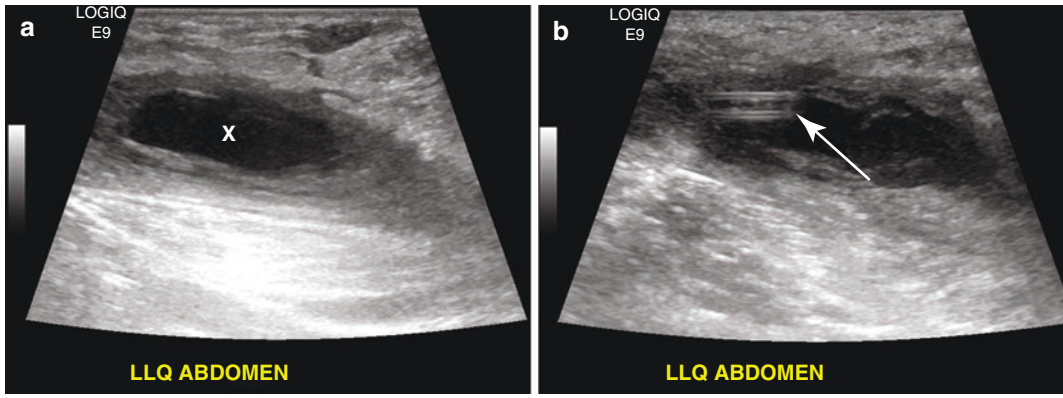

Fig. 29.4 Ultrasound scan of needle aspiration of a seroma following the repair of an incisional hernia (**a**) Seroma collection (X) seen on ultrasound (**b**) Aspiration and insertion of drain (*arrow*) into a seroma under ultrasound guidance

Clinical Pearls

A subcostal TAP block can anesthetize the T6–T9 nerves and would be indicated if the hernia is epigastric or supra-umbilical. Similarly, a rectus sheath block would be effective in a midline hernia such as para-umbilical or the divarication of the rectus. Blocking the ilio-inguinal and the ilio-hypogastric nerves would be needed for repair of the hernias in the inguino-scrotal region.

As the Btox has to be injected into the belly of the muscle, the ultrasound should be used to locate the site with the thickest portion of all the three muscles (EO, IO, TA), preferably along the anterior axillary line.

When the needle is inserted out of plane, the ultrasound probe should be angulated towards the needle to locate the needle tip and then, as the needle is advanced, the probe should be slowly straightened to follow it. At times when the deeper muscle is injected with Btox, it may compress the superficial muscle and may necessitate moving the probe slightly to visualize an unflattened section of the muscle.

In patients who have had multiple surgeries for recurrent hernia, the scar tissue may appear as fascial planes giving the impression of more than three layers of abdominal muscles. In such a situation, Btox may be injected at more than one site of the same muscle.

Literature Review

When Btox is injected into the muscle, it binds to the glycoprotein on the cholinergic nerve terminal. It gains access to the nerve and cleaves the protein responsible for the transport of acetylcholine to the synaptic cleft. Thus, the mechanism of action of Btox is preventing the release of acetylcholine from the nerve ending leading to muscle paralysis. This interruption of the synaptic transmission is temporary. The onset of muscle weakness occurs within 2–3 days, reaching the maximum effect by 2 weeks and it gradually starts to wear off after 10 weeks [13].

Btox application decreases the thickness and increases the length of the lateral abdominal muscles which assists in the closure of incisional hernia secondary to open abdomen management [14].

The repair of a recurrent abdominal incisional hernia is a surgical challenge, both in the process of closing the defect and also in keeping it from dehiscing. Farooque et al. injected 50 units of Btox into the external oblique, internal oblique, and transversus abdominis muscles at three sites on each side of the lateral abdominal wall (total dose 300 units) and demonstrated a significant increase in the mean length of the lateral abdominal wall from 18.5 cm to 21.3 cm on computed tomography [1].

The "open abdomen" management or the inability to close the abdomen after an urgent damage control laparotomy can lead to severe morbidity and mortality. In a novel technique of "chemical component separation," Zielinski et al. have shown remarkable success by creating flaccid paralysis of the lateral abdominal wall by injecting Btox, within 24 h of their initial surgery [5].

In the management of a seroma, perhaps the best strategy is to prevent it by using closed-suction drains until their output volume is minimal and the use of sharp or ultrasonic dissection rather than cautery [8]. Although the use of sclerosants at the initial operation actually increased the risk of seroma [8], injection of a sclerosing agent along with a negative pressure wound therapy system has been shown to be effective for a chronic and recurrent seroma [7, 15].

Summary

Ultrasonography is a valuable tool to identify the muscular and the fascial layers of the abdominal wall and to guide the needle used for the procedure to the correct location.

References

1. Farooque F, Jacombs AS, Roussos E, Read JW, Dardano AN, Edye M, Ibrahim N. Preoperative abdominal muscle elongation with botulinum toxin A for complex incisional ventral hernia repair. ANZ J Surg. 2016;86:79–83.
2. Leem JG. Ultrasound-guided nerve blocks for post-hernia repair pain. Korean J Pain. 2010;23:227–9.
3. Yarwood J, Berrill A. Nerve blocks of the anterior abdominal wall. Contin Educ Anaesth Crit Care Pain. 2010;10:182–6. https://doi.org/10.1093/bjaceaccp/mkq035.
4. Smoot D, Zielinski M, Jenkins D, Schiller H. Botox a injection for pain after laparoscopic ventral hernia: a case report. Pain Med. 2011;12:1121–3.
5. Zielinski MD, Goussous N, Schiller HJ, Jenkins D. Chemical components separation with botulinum toxin A: a novel technique to improve primary fascial closure rates of the open abdomen. Hernia. 2013;17:101–7.
6. Zendejas B, Khasawneh MA, Srvantstyan B, Jenkins DH, Schiller HJ, Zielinski MD. Outcomes of chemical component paralysis using botulinum toxin for incisional hernia repairs. World J Surg. 2013;37:2830–7.
7. Sood A, Kotamarti VS, Therattil PJ, Lee ES. Sclerotherapy for the management of seromas: a systematic review. Eplasty. 2017;17:e25.
8. Janis JE, Khansa L, Khansa I. Strategies for postoperative seroma prevention: a systematic review. Plast Reconstr Surg. 2016;138:240–52.
9. Chin KJ, Adhikary S, Sarwani N, Forero M. The analgesic efficacy of pre-operative bilateral erector spinae plane (ESP) blocks in patients having ventral hernia repair. Anaesthesia. 2017;72:452–60.
10. Blanco R, Ansari T, Riad W, Shetty N. Quadratus lumborum block versus transversus abdominis plane block for postoperative pain after cesarean delivery: a randomized controlled trial. Reg Anesth Pain Med. 2016;41:757–62.
11. Stokes AL, Adhikary SD, Quintili A, Puleo FJ, Choi CS, Hollenbeak CS, Messaris E. Liposomal bupivacaine use in transversus abdominis plane blocks reduces pain and postoperative intravenous opioid requirement after colorectal surgery. Dis Colon Rectum. 2017;60:170–7.
12. Bhakta A, Glotzer O, Ata A, Tafen M, Stain S, Singh P. Analgesic efficacy of laparoscopic guided transverse abdominis plane block using liposomal bupivacaine in bariatric surgery. Am J Surg. 2018;215:643–6.
13. Dressler D. Clinical applications of botulinum toxin. Curr Opin Microbiol. 2012;15:325–36.
14. Ibarra-Hurtado TR, Nuño-Guzmán CM, Miranda-Díaz AG, Troyo-Sanromán R, Navarro-Ibarra R, Bravo-Cuéllar L. Effect of botulinum toxin type A in lateral abdominal wall muscles thickness and length of patients with midline incisional hernia secondary to open abdomen management. Hernia. 2014;18:647–52. https://doi.org/10.1007/s10029-014-1280-2.
15. Daoud F, Thayer A, Daswani GS, Maraqa T, Perinjelil V, Mercer L. Management of chronic abdominal wall seroma with doxycycline sclerotherapy using a negative pressure wound therapy system KCI--V.A.C.Ulta™—a case report. Int J Surg Case Rep. 2018;51:25–8.

Radiographic Appearance of Mesh

30

Sabrina Drexel and Ryan Michael Juza

Introduction

The surgical management of hernias has evolved over time and the introduction of mesh reinforcement can be considered one of the biggest paradigm shifts in the field. While the use of mesh has led to a reduction in hernia recurrence, the use of a foreign body in the abdominal wall creates unique challenges and carries specific risks. A surgeon who performs hernia repairs should therefore be well versed in these pathologies, and imaging studies are an essential tool in the diagnosis and management of them. In this chapter, we will cover the use of imaging studies to detect hernioplasty mesh. We will describe the importance of radiographic mesh identification and explain how it can be used to guide surgical decision-making and planning.

Imaging Modalities in Hernia Surgery

Hernia surgery is rapidly evolving as new technology, mesh, and techniques are introduced. Imaging modalities also continue to advance with improved resolution and access. Hernias can be evaluated by a variety of imaging modalities including computed tomography (CT), ultrasound, or magnetic resonance imaging (MRI) [1].

Abdominal surgeons are most familiar with CT, as it is commonly used to evaluate a variety of intra-abdominal pathologies. CT imaging can provide adequate visualization of the abdominal wall musculature as well as hernia architecture, including location, dimensions, and contents [2]. It is relatively inexpensive, rapid, and well tolerated by patients. Computed tomography has become ubiquitously available over the past two decades and the most frequently used modality for the evaluation of hernias [3]. CT is typically performed with the patient supine; if a hernia is suspected, techniques to increase intra-abdominal pressure can be performed, such as the Valsalva maneuver, to better visualize subtle hernias [4]. Contrast is often not necessary to assess the integrity of a hernia repair postoperatively, as the muscle and fascial layers of the abdominal wall are readily apparent on CT imaging. However, IV contrast enhances visualization of the abdominal wall and adjacent organs by outlining the vascular supply, which can be particularly helpful in cases where mesh is

Supplementary Information The online version contains supplementary material available at https://doi.org/10.1007/978-3-031-21336-6_30.

S. Drexel (✉)
Department of General Surgery, University Hospitals Cleveland Medical Center, Cleveland, OH, USA

R. M. Juza
Department of Surgery, University Hospitals Cleveland Medical Center, Cleveland, OH, USA
e-mail: Ryan.Juza@UHHospitals.org

S. Docimo Jr. et al. (eds.), *Fundamentals of Hernia Radiology*,
https://doi.org/10.1007/978-3-031-21336-6_30

Fig. 30.1 CT pelvis with intravenous contrast to highlight vessels. Mesh plug (circle) placed in the femoral space adjacent to the femoral vessels (bracket). Patient had chronic pain resolved by surgical removal of the plug

placed for groin hernias (Fig. 30.1). If a bowel obstruction is suspected, oral contrast should be used to better characterize loops of bowel [2] in relation to the mesh (Fig. 30.2).

However, CT imaging does expose the patient to radiation and can be suboptimal in the evaluation of tissue planes due to artifacts or implants. Patients can also have adverse reactions to contrast dyes if they are used. These factors should be considered when debating whether to order CT imaging for hernia evaluation and whether to use contrast.

Ultrasound can be used to accurately diagnose and monitor a hernia [5, 6] It is very inexpensive and does not expose the patient to radiation. It is also the only imaging modality that can provide dynamic and real-time information, such as tissue movement around mesh or other foreign bodies [7]. However, it is operator dependent and typically does not provide nearly as much detail regarding hernia architecture or abdominal wall musculature as a CT. Results are difficult to replicate in patients with obesity or very large defects, and images can be obscured by bowel distention or underlying structures.

While MRI can also precisely visualize abdominal wall musculature and hernia location, it is the most expensive of the three studies and often the least familiar to surgeons. MRI is not readily available at many institutions, is time-consuming, and is not well tolerated by patients due to the confined nature of the imaging system. Additionally, MRI is contraindicated in patients with metal implants. Limited data exists for the use of MRI for hernia evaluation. Inter-observer variability has been shown to be quite high among radiologists reviewing MRI imaging after hernia repair [8]. Therefore, most hernia surgeons prefer CT as the modality of choice for preoperative planning and assessment of postoperative complications.

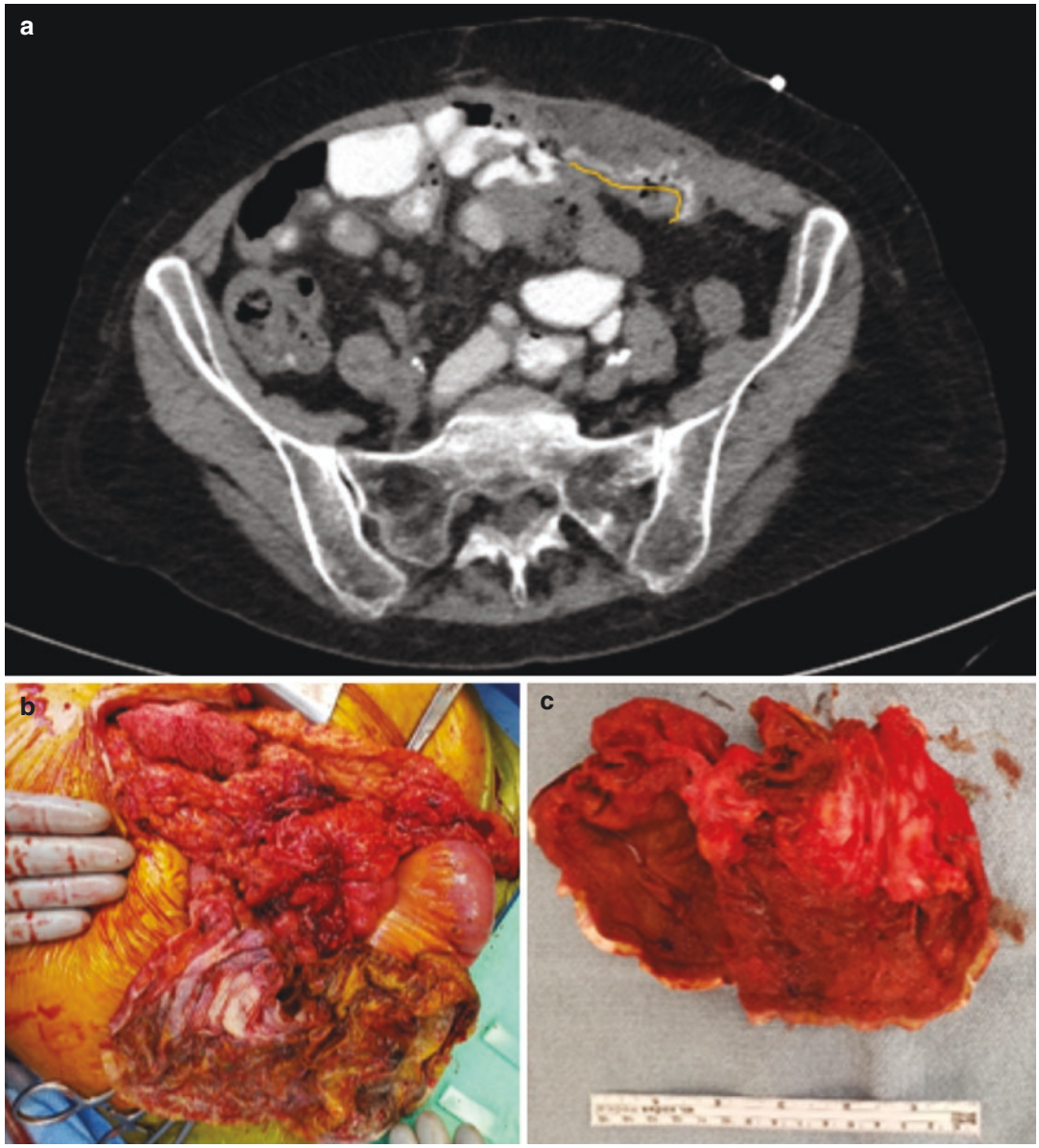

Fig. 30.2 (**a**) CT imaging with oral contrast demonstrates contracted wrinkled mesh (outlined in yellow) with erosion into underlying bowel, creating entero-prosthesis-atmospheric fistula demonstrated by efflux of contrast at the site of the fistula and surrounding soft tissue inflammatory response and fluid. (**b**) Intraoperative finding of mesh erosion into the bowel confirms findings on preoperative imaging. (**c**) En bloc resection of small bowel, fistula, and mesh

Importance of Mesh Identification on Imaging

The introduction of mesh into the abdominal wall, particularly in ventral herniorrhaphy, creates adhesions, alters natural anatomic planes, and generates barriers to any future abdominal surgeries. Mesh-based herniorrhaphy also carries the risk of mesh-specific complications. These risks include hernia recurrence, mesh erosion, mesh dislodgement, and mesh rejection, among others. Preoperative imaging can successfully be used to evaluate and diagnose many of these problems.

Recurrence

Recurrence is an unfortunate complication of hernia surgery. Substantial efforts have been made to study and evaluate the factors that predict failure in hernia surgery and help guide future surgery. In the case of recurrence, not all recurrences are created equal. The type of mesh, location of mesh, and cause of failure all factor into subsequent management options. Assessing preoperative imaging can help determine the best operative approach for repairing the recurrence. In this section, we will cover some of the main types of hernia recurrence.

Central mesh fracture after hernia repair is a known complication of mesh-based repairs, particularly in cases utilizing lightweight synthetic mesh [9] or bridged fascial defects. Central mesh fracture occurs when the burst strength of the mesh is insufficient to resist intra-abdominal pressure and the mesh tears or fractures in the central portion. Evaluating a patient for "recurrence," when it is deemed to be mesh failure, will impact the nature of the subsequent repair. With central fracture of the mesh, the fractured edges of the mesh can come in contact with the bowel making adhesiolysis challenging and increasing the risk of bowel injury. Bowel injury raises the wound class and increases the risk of surgical site infection and mesh contamination. As a case comparison, consider two patients who were found with mesh fracture after prior herniorrhaphy. In Fig. 30.3, the patient had synthetic mesh placed in the sublay position. Despite hernia recurrence due to mesh fracture, the mesh was well incorporated and not in direct contact with the bowel. Contrast that with Fig. 30.4, where the patient had prior intraperitoneal mesh placement. At the time of surgery, dense adhesions were noted to the mesh necessitating a more extensive adhesiolysis.

Recurrences also happen when the mesh separates from the abdominal wall allowing intra-

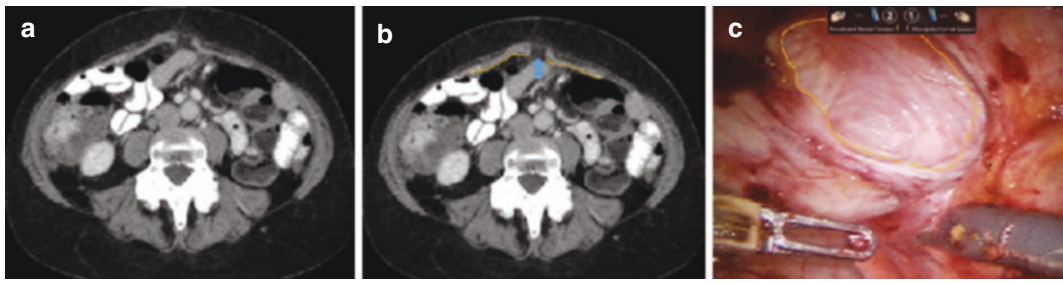

Fig. 30.3 (**a**, **b**) Central mesh fracture (blue arrow) of lightweight polypropylene mesh (yellow line) placed in the sublay position. Mesh is identified by local tissue changes and scar formation. The fracture is readily apparent by the break in the line with fat herniated between. Despite the mesh fracture, there is evidence of a layer of fat between the mesh layer and the underlying bowel. The evidence of maintained tissue planes and the lack of direct contact with the mesh reduces the chance of dense adhesion formation. This can be interpreted on preoperative imaging and guide operative planning. Intraoperatively, a site was chosen lateral to the border of the mesh and optical access was used to enter the abdomen. (**c**) Central mesh fracture seen on laparoscopic view corroborates preoperative CT imaging. The yellow line follows the fractured edges of the mesh which have expanded in a circular pattern as the force is distributed. The mesh is entirely covered by peritoneum with no exposed edges. Minimal adhesions were noted intraoperatively and the recurrence was repaired without issue.

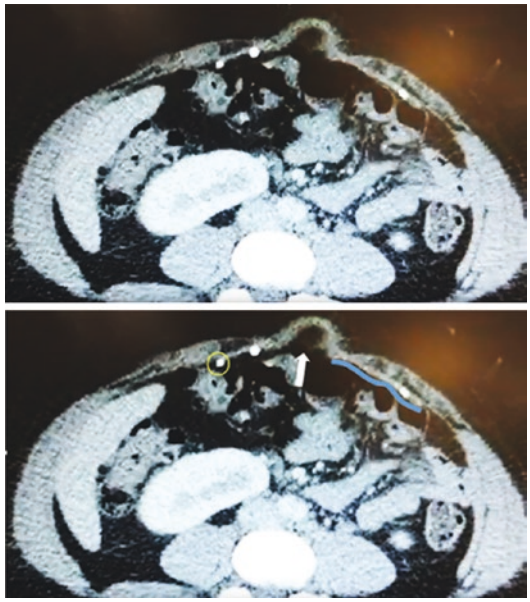

Fig. 30.4 Synthetic mesh fracture (white arrow) of intraperitoneal onlay mesh (blue line left side) and metal tacks (yellow circle). On imaging, bowel is herniated between the fractured edges of mesh and appears in direct contact. An open approach was chosen. At reoperation, dense adhesions were noted along the edges of mesh requiring extensive adhesiolysis. The fractured mesh was removed and sublay mesh was placed to repair the recurrence

abdominal contents to herniate around the edge. Consider the following case represented in Fig. 30.5. In this case, preoperative imaging provided several crucial details: it demonstrated that the recurrence was caused by the cephalad border of the mesh dislocating from the anterior abdominal wall and that fat had herniated to the uncoated side of the mesh. Contact with the uncoated side of the mesh can create dense adhesions. The fact that the bowel was not herniated above the mesh and therefore not in direct contact with the uncoated side meant adhesions would be more manageable. A minimally invasive approach was chosen. Intraoperatively, our preoperative interpretation of the imaging was substantiated. The herniated fat was densely adherent to the uncoated side of the mesh but no bowel was at risk during adhesiolysis. Adhesiolysis was carried out carefully but with the liberal use of a vessel sealing device. The mesh was removed in its entirety and the recurrence was repaired with primary defect closure. Had the bowel been demonstrated to herniate above the mesh, as shown in Fig. 30.6, more consideration would have been given to an open approach to aid in safe adhesiolysis.

"False Recurrence"

Imaging can also help identify a true recurrence versus a "false recurrence," such as orphaned fat above the mesh. The definition of hernia recurrence on imaging is not well-defined and orphaned fat above a prior repair may be interpreted as hernia recurrence despite an intact repair (Figs. 30.7 and 30.8). In these particular cases, the ability to accurately interpret CT imaging prevented an unnecessary surgical intervention and was essential in educating and managing expectations in a patient who had been told they had a hernia recurrence and may have felt they needed another operation (Video 30.1).

Access

Abdominal access and intra-abdominal adhesions can be particularly challenging in patients who have previously undergone a hernia repair with mesh. In these cases, evaluation of preoperative imaging can guide operative planning and direct procedural modifications such as determining laparoscopic versus open approach, incision type, and port placement. These technical decisions can mean the difference between a straightforward case and a very challenging one and can prevent significant complications such as chronic mesh infection and hernia recurrence. In the following case (Fig. 30.9), the patient was scheduled for planned cesarean delivery; however, in preoperative planning, the obstetrics team was concerned the patient's prior mesh-based ventral hernia repair would prevent a low Pfannenstiel incision and general surgery was consulted. After reviewing prior images it was determined the patient's mesh would not impede the planned operation, but a general surgeon would be standing by. As an additional measure of precaution, the patient was scheduled at the earliest recom-

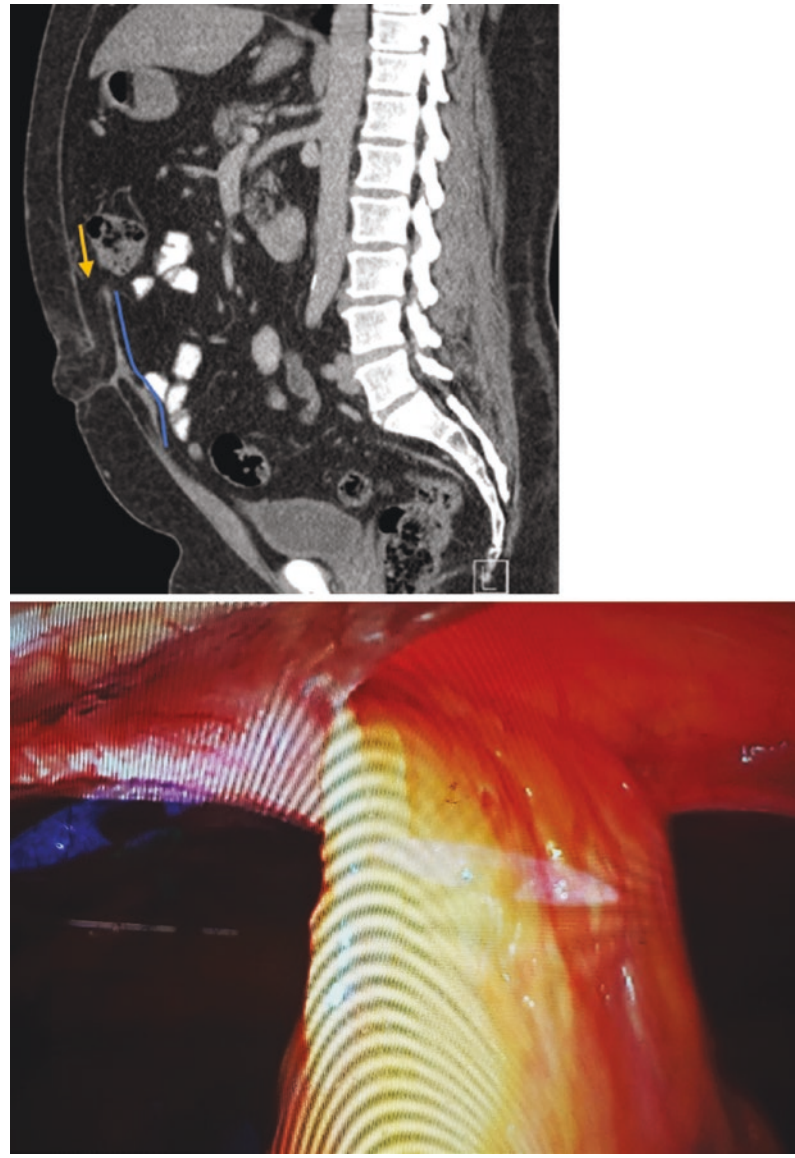

Fig. 30.5 Preoperative imaging demonstrated hernia recurrence (yellow arrow) due to the superior edge of mesh (blue line) separating from the abdominal wall with intra-abdominal fat herniation above the mesh. Note that there was no evidence of bowel above mesh which would have complicated reoperation. Intraoperative picture corroborated the CT image finding of omental fat herniated above the mesh but no bowel

mended gestational age to decrease the risk of an unplanned emergent surgical delivery.

Adhesions to indwelling mesh also impact surgical access and can be assessed on preoperative imaging in conjunction with prior operative reports. Mesh that has been placed in the underlay or intraperitoneal position is, by definition, in direct contact with intra-abdominal structures and will result in adhesion formation. The use of anti-adhesive barriers can minimize those adhesions but does not completely prevent them. Patients with a robust omentum may have a visible fat plane between the mesh and the bowel but often several loops of bowel are in direct contact. Mesh that has been placed in the onlay or sublay position is not as likely to be in direct contact with the bowel and typically a fat plane is visible between the mesh and the bowel (Fig. 30.10).

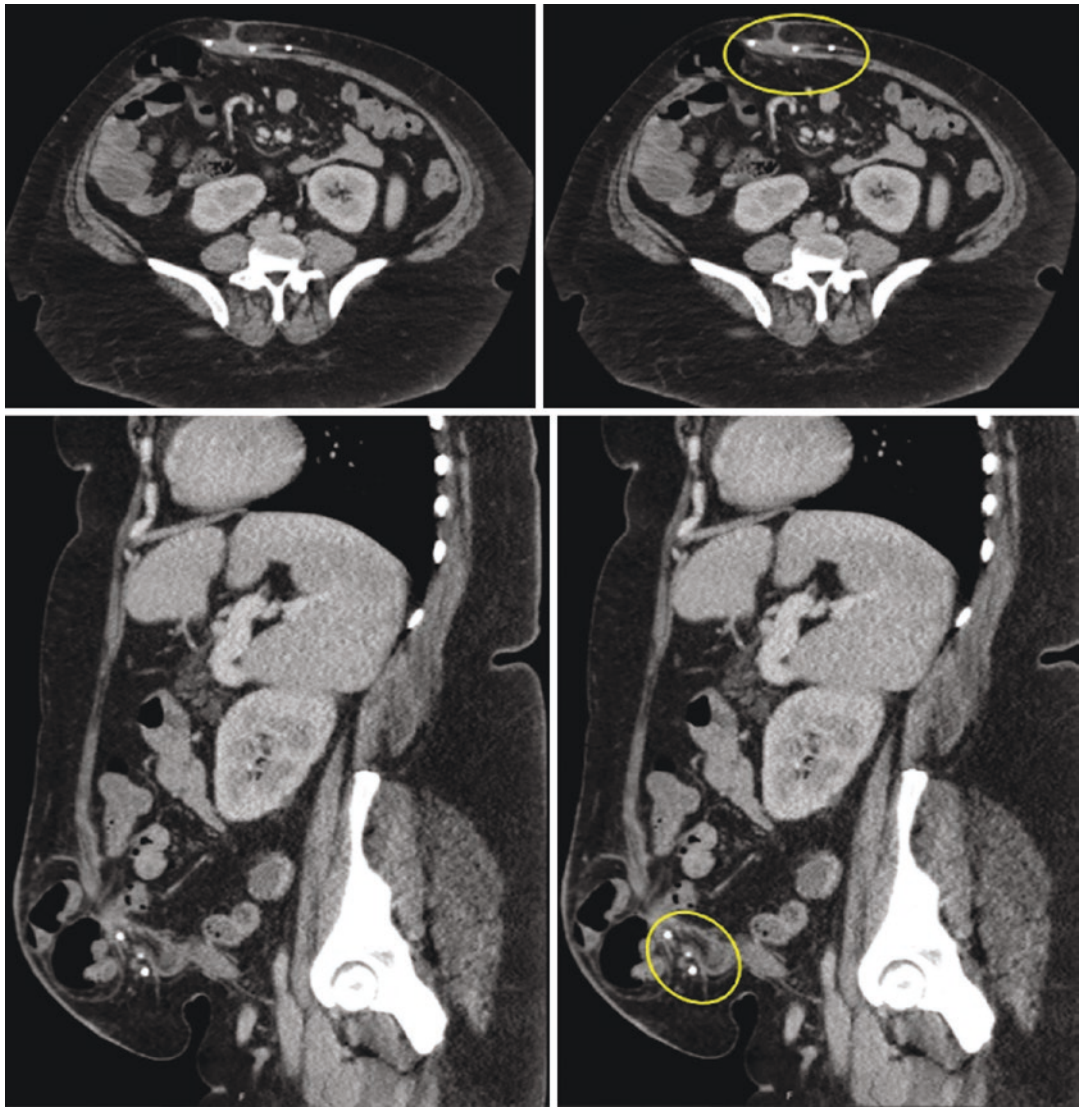

Fig. 30.6 A 43-year-old female with a history of five prior ventral incisional hernia repairs now with recurrence. Patient had onlay mesh and tacks (yellow circle) in close proximity to bowel within her recurrent hernia

Mesh Complications

Patient concerns about mesh complications are becoming increasingly common, spurred by the regular advertisements for mesh litigation on television. While some patients do have complications from mesh, the majority do not. Imaging studies are essential to identifying those that have problems and those that do not. Patients that come into the office with mesh concerns frequently have nonspecific complaints of abdominal pain or of "feeling the mesh," sparking their concern that a complication is pending. Determining when a patient has true complication versus when they do not is the difference between gentle reassurance and an unnecessary operation. In most cases, physical examination is limited in the information it

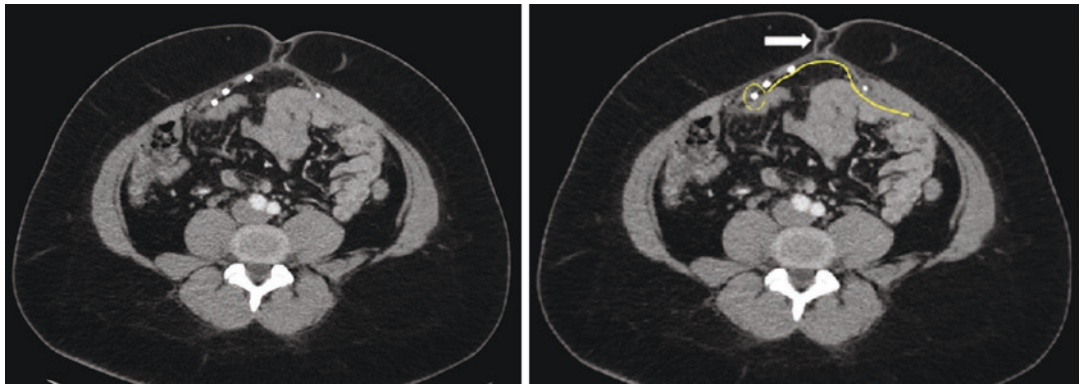

Fig. 30.7 A 30-year-old patient referred by her primary care provider for "recurrent" umbilical hernia after prior laparoscopic ventral hernia repair. The patient reported a nonreducible bulge at her umbilicus. CT imaging was obtained and interpreted as recurrent ventral hernia. On further review of the imaging, the patient's mesh repair and tacks were intact (yellow line and circle). Comparing with preoperative imaging, it was determined the patient had preperitoneal fat orphaned in the umbilical defect at the time of her original operation. The patient was counseled on this and no further surgery recommended. If the patient had pain or discomfort from the orphaned fat, an open approach with amputation of the hernia sac and contents would be recommended to avoid disrupting the intact repair

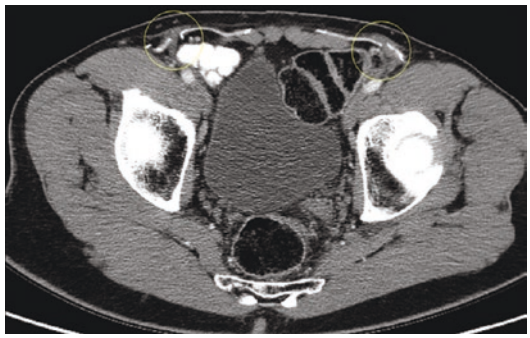

Fig. 30.8 This patient was referred after an unrelated CT scan was interpreted as recurrent inguinal hernias through fractures in the mesh. On evaluation the patient was asymptomatic. On review of the images, it was determined the "recurrence" was actually the slit in the keyhole mesh to permit the cord structures (yellow circles)

can provide. Imaging is largely necessary not only to completely evaluate the symptoms but also to assuage the patient's fears. When evaluating for mesh complications, several questions should be answered; is the hernia still repaired? is the mesh in correct location? and is the mesh well incorporated?

Seroma formation following herniorrhaphy is common, self-limited, and typically resolves spontaneously. In some cases, a reactive seroma may form adjacent to the mesh and prevent the mesh from incorporating or may form as a result of mesh not incorporating. These chronic fluid collections can be bothersome to the patient and may intermittently drain or become secondarily infected (Figs. 30.11 and 30.12).

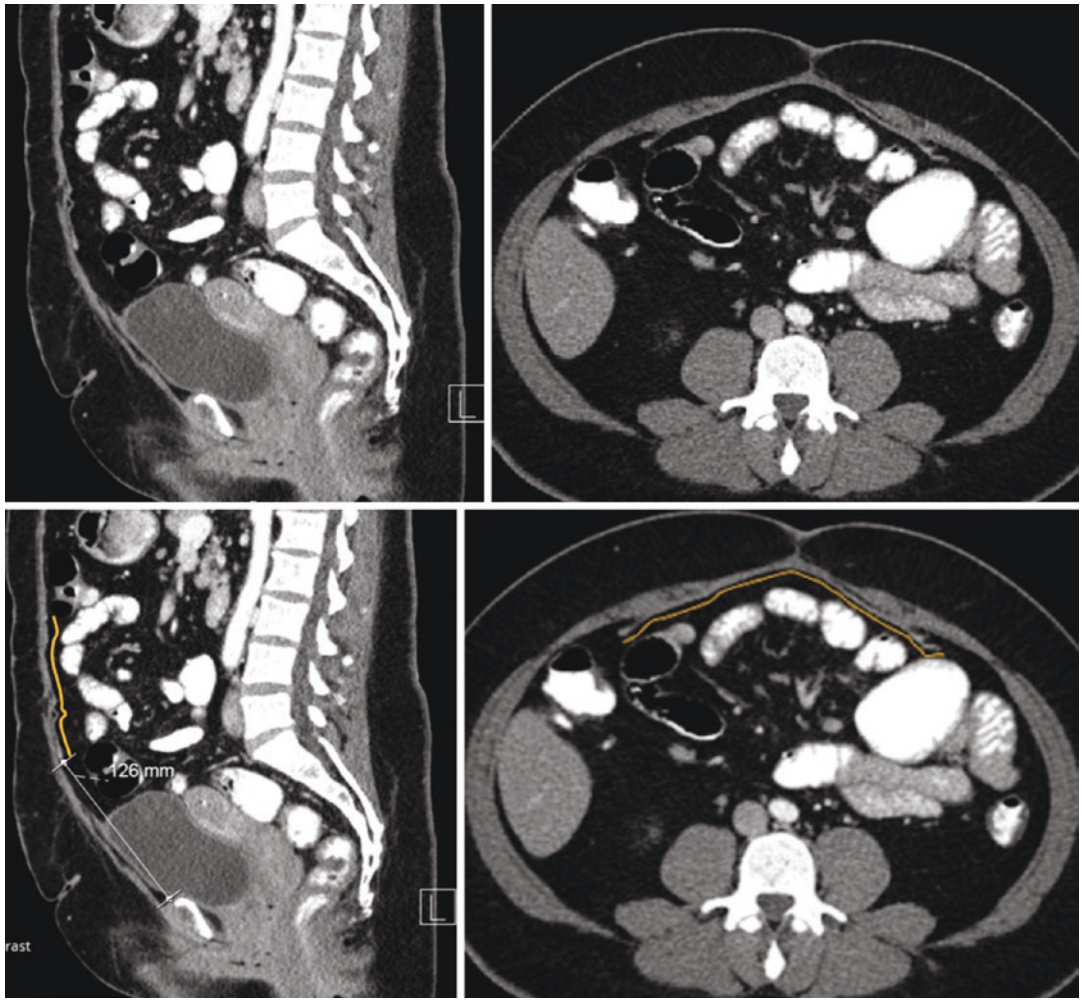

Fig. 30.9 A 42-year-old female who had previous open repair of a large ventral hernia with underlay Dualmesh (W.L Gore, Flagstaff, AZ) placement. She was scheduled for planned cesarean section and general surgery was consulted for abdominal access due to the history of intraperitoneal mesh. After reviewing preoperative imaging, it was determined the inferior edge of the mesh was 12.6 cm above the pubic symphysis in the nonpregnant abdomen. Based on those measurements, a low midline was not advised due to the risk of mesh involvement and mesh contamination. A low Pfannenstiel incision was therefore chosen and successful cesarean section was performed without mesh involvement. General surgery was standing by, but ultimately not needed

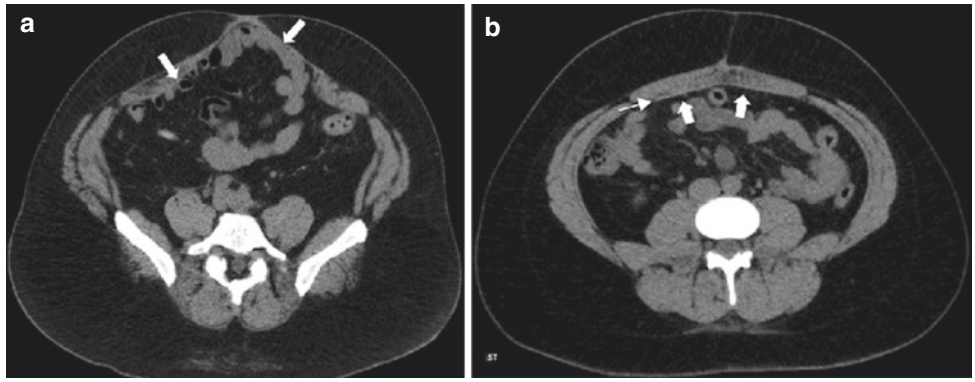

Fig. 30.10 (**a**) Synthetic mesh in contact with bowel. The lack of a fat plane (arrows) between the mesh and the bowel predicts a challenging adhesiolysis with dense adhesions and increases the risk of enterotomy. (**b**) Intact bioabsorbable mesh (thin arrow) in the sublay position with a fat plane between the mesh and intra-abdominal contents (thick arrows)

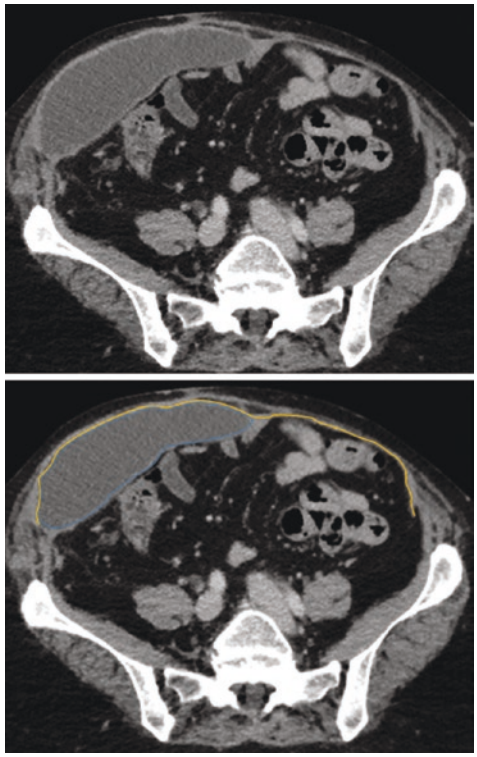

Fig. 30.11 Female patient with a history of bilateral transverse rectus abdomnis muscle (TRAM) flap for breast cancer with abdominal wall reconstruction with heavyweight polypropylene mesh. The mesh (yellow line) is visible on the patient's left side but is more difficult to see on the right due to underlying reactive seroma (blue outline). This seroma caused longstanding abdominal discomfort, inability to bend at the waist or wear tight clothing, and intermittently drained through a prior drain site

Fig. 30.12 Lightweight polypropylene mesh infection with complicated collection in the sublay position. The mesh is not directly visible due to the surrounding collection

Mesh Migration/Erosion

Despite fixation and scar formation, mesh can migrate leading to mesh erosion into adjacent structures and subsequent complications. Preoperative imaging is useful to determine the location of the mesh and identify the cause for migration. Chronically infected mesh or chronic seroma formation inhibits local tissue ingrowth and creates an enlarged pocket within which the mesh can move and migrate to remote sites (Fig. 30.13). When mesh migrates, it increases the risk of recurrence and complications of the mesh such as erosion into the bowel or surrounding structures.

Fig. 30.13 Migrated heavyweight polypropylene mesh eroding through the umbilical port site (arrow) due to chronic mesh infection after laparoscopic inguinal herniorrhaphy

Appearance of Mesh on Computed Tomography

The interpretation of mesh on imaging has become increasingly difficult with the plethora of hernia repair products on the market. Manufacturers of hernia mesh do not routinely publish information regarding mesh radiographic characteristics; however, the major properties that determine visibility on CT are density, structure (woven, knitted, or homogenous), and thickness [10]. These known characteristics can provide a foundation to infer visibility. The inflammatory response created by the prosthetic implant also affects the radiopaque properties [11]. The visibility of mesh on imaging ranges from not visible to completely visible. A classification scheme was recommended by prior authors [7], and a similar classification of meshes based on radiographic visibility is displayed in Table 30.1.

Table 30.1 Mesh classifications based on radiographic visibility

Visibility on imaging	Material	Mesh product	Manufacturer	Properties
Readily visible				
	ePTFE	Dualmesh, dualmesh plus	WL gore	Synthetic 2-sided laminar sheet (1–2mm thickness)
Partially visible: Due to coated side of mesh				
Composite meshes	Polypropylene mesh with ePTFE coating	Composix	BD	Synthetic macroporous or microporous mesh
	Polypropylene mesh with ePTFE coating	Ventralex	BD	Synthetic mesh for small defects
	ePTFE	Dulex	BD	Synthetic 2-sided laminar sheet
Indirectly visible: Can be seen due to inflammatory response and/or incorporation of mesh				
	Polypropylene	Bard mesh, bard soft mesh	BD	Synthetic heavyweight or lightweight, microporous or macroporous
	Polypropylene	Prolene, prolene soft	Ethicon	Synthetic heavyweight or lightweight, microporous or macroporous
Composite meshes	Polyester with collagen-polyethylene glycol coating	Parietex composite	US surgical/ covidien/ medtronic	Synthetic medium weight, macroporous
	Polypropylene and polydioxanone mesh with regenerated cellulose coating	Proceed	Ethicon	Synthetic lightweight, macroporous

(continued)

Table 30.1 (continued)

Visibility on imaging	Material	Mesh product	Manufacturer	Properties
	Polypropylene and polyglycolic acid mesh with CMC-HA-PEG[a] coating	Sepramesh	BD	Synthetic medium weight, macroporous
	Polypropylene mesh with Polyvinylidenefluoride coating	DynaMesh	DynaMesh	Synthetic medium weight or heavy weight, macroporous
	Polypropylene mesh with titanium coating	TiMesh	PFM medical	Medium weight or lightweight; macroporous
Biologic meshes	Porcine dermis	Strattice	LifeCell	1.76mm thick, non-cross linked
	Porcine dermis	XenMatrix	BD	1.95mm thick, non-cross linked
	Human dermis	FlexHD	Ethicon	1.15mm thick, non-cross linked
	Porcine dermis	Permacol	Medtronic	0.91mm thick, cross linked
Bioabsorbable meshes	92% polyglycolic acid, 8% polylactic acid	Vicryl	Ethicon	Absorbable, woven
	67% polyglycolic acid, 33% trimethylene carbonate	Bio-A	WL gore	Absorbable, multifilament laminar sheet, microporous
	Poly-4-hydroxybutyrate (P4HB)	Phasix	BD	Absorbable, monofilament, macroporous
	40% PGA-PLA-TMC matrix, 60% PLA-TMC matrix[b]	TIGR matrix	Novus scientific	Absorbable, knitted, dual-filament
Not visible				
	Polypropylene mesh with poliglecaprone	Ultrapro	Ethicon	Partially resorbable lightweight, macroporous
	Polypropylene with Polyglactin	Vypro	Ethicon	Partially resorbable lightweight, macroporous
	Polyester mesh with polylactic acid	ProGrip	Covidien/ medtronic	Partially resorbable medium weight, macroporous
Composite mesh	Polypropylene mesh with poliglecaprone coating	Physiomesh	Ethicon	Synthetic lightweight, macroporous

[a]CMC-HA-PEG: carboxymethylcellulose-sodium hyaluronate-polyethylene glycol
[b]PGA-PLA-TMC Matrix: polyglycolic acid-polylactic acid-trimethylene carbonate

Synthetic Mesh

There are three main groups of synthetic mesh based on material: polypropylene (PP), polyester (PET), and polytetrafluoroethylene (PTFE) [12]. Each of these meshes has different properties which influence whether they are visible on high-resolution imaging.

Polypropylene and polyester meshes have a similar density to native tissue. The majority of these meshes are knitted (porous), making them less dense than a homogenous mesh and enabling tissue ingrowth. These properties make them difficult to visualize as they are well incorporated with surrounding tissues. Polypropylene meshes such as Surgipro (Covidien, Minneapolis, MN) and Prolene (Ethicon, Cincinnati, OH) are conventionally not visible on CT [13, 14]. However, polypropylene mesh can range in weight from 36 g/m^2 for ultra-lightweight mesh to 110 g/m^2 for heavy weight mesh [15]. Traditional heavyweight mesh can generate a robust inflammatory

response, which may make the mesh indirectly visible on imaging. Polyester mesh can be lightweight (33–40 g/m^2) or medium-weight (46–78 g/m^2). Knowledge of the type of mesh placed can be extremely valuable when reviewing CT scans.

In contrast, PTFE is typically much denser than lightweight or medium-weight polypropylene or polyester implants (65–70 g/m^2 for PTFE versus 35–85 g/m^2 for PP or PET meshes) [15]. PTFE is constructed utilizing solid laminar sheets to create a homogenous structure. It has been shown to produce a significant inflammatory response with encapsulation instead of tissue integration [16]. All of these properties make PTFE meshes such as Dualmesh or Dualmesh PLUS (W. L. Gore, Newark, DE) readily visible on CT imaging [17, 18].

For laparoscopic repairs of ventral and incisional hernias, the abdominal side of the synthetic mesh must be coated to minimize adhesion formation between the bowel and the abdominal wall, while the opposite side will typically contain a porous surface to facilitate tissue ingrowth. These are typically known as "composite meshes." Some of these meshes will consist of a polypropylene matrix with an expanded PTFE (ePTFE) coating to prevent adhesions. In this instance, the thickness of the ePTFE coating can affect the overall mesh visibility. TiMesh (PFM Medical, Carlsbad, California) has a polypropylene mesh coating with titanium; however, the applied titanium layer ranges from 30 to 50 nm, which has minimal impact on the overall visibility of this mesh. Therefore, composite meshes are typically partially visible or indirectly visible, depending on the composition of the anti-adhesive coating.

Biologic Mesh

Biologic meshes are derived from human, porcine, or bovine dermis. There is limited data regarding the visibility of these meshes on high-resolution imaging. As they are derived from native tissues, they are roughly the same density as surrounding tissues and can be difficult to visualize. They are designed to enable mesh integration and are processed to be immunologically inert, although biologic mesh can induce a disproportionate inflammatory response, leading to significant scarring and encapsulation [19]. Some meshes do become incorporated, resulting in neovascularization, or completely degraded, with no trace of the mesh implant over time [20]. Imaging adjuncts such as the operative note and prior imaging can help identify the mesh location. One study utilizing alloderm biologic mesh spacers in the abdomen and pelvis to protect viscera from radiation showed increased attenuation of the biologic mesh over time, suggesting neovascularization [21]. Therefore, we consider these meshes to be indirectly visible, depending upon the location, inflammatory response, and degree of tissue integration.

Bioabsorbable Mesh

Several bioabsorbable meshes have been popularized recently due to their ability to resist infection in a contaminated field and decrease cost compared to biologic meshes, with acceptable hernia recurrence rates and improved quality of life [22]. They are synthesized from absorbable materials but are not comprised of tissue-derived materials. They are relatively new to the hernia market and therefore information regarding imaging findings for these meshes remains sparse. Some can generate a robust inflammatory response, and using adjuncts, such as the operative report to note location and size, they can also be indirectly visible on imaging.

Vicryl (Ethicon) is an absorbable mesh comprised of polyglycolic acid (PGA). It is degraded by hydrolysis and completely absorbed within 3 months [23]. However, vicryl mesh is known to induce a strong host inflammatory response which may hinder tissue integration, so it may be indirectly visible on imaging prior to complete absorption [24].

Phasix (BD, Franklin Lakes, NJ) mesh is comprised of poly-4-hydroxybutyrate (P4HB), which

is a naturally derived polymer and is absorbed by hydrolysis over 18 months. It has been shown to produce a mild to moderate inflammatory response [25], which can aid in the detection of the mesh on imaging. In one patient 5 months postoperatively from a bridging Phasix abdominal wall reconstruction, the mesh could be visualized due to inflammatory stranding surrounding the implant (Fig. 30.14).

Other bioabsorbable meshes include Bio-A (W.L. Gore) and TIGR Matrix (Novus Scientific, Uppsala, Sweden). These are also degraded by hydrolysis, but Bio-A is absorbed in 6 months versus TIGR Matrix which takes 3 years for complete resorption. Presumptively, these meshes can be visualized by indirect means, such as inflammatory changes and known placement, prior to absorption as well.

Mesh Locations in Hernia Repair

Consensus guidelines have been established by the International Hernia Collaboration for terminology regarding mesh placement [26]. Correct descriptions of mesh location in relation to the abdominal musculature is helpful for identifying the mesh on imaging. Briefly, an *onlay* mesh is located above the anterior rectus sheath, while an *inlay* mesh is bridged between the rectus muscles. *Sublay* mesh is behind the muscle; either in a *retrorectus* repair where the mesh lies above the posterior rectus sheath but below the rectus muscles, or a *retromuscular* position after a posterior component separation. Mesh can also be placed in the *preperitoneal* space, or within the abdominal cavity as an *intraperitoneal* (IPOM) repair (Fig. 30.15).

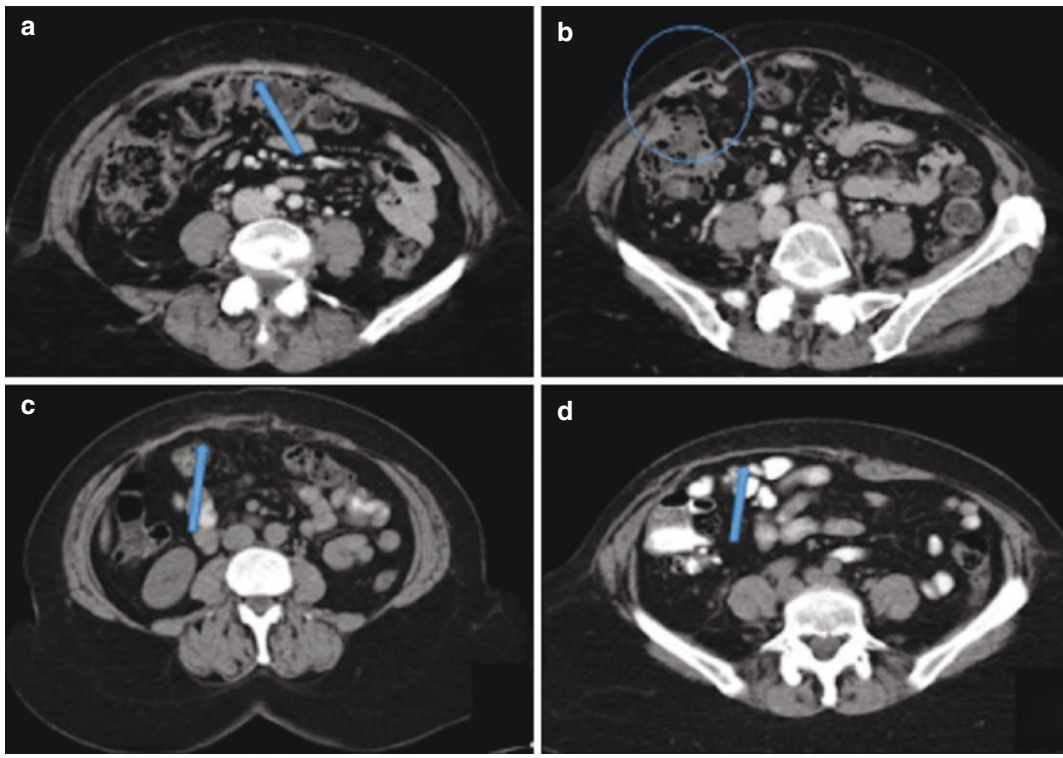

Fig. 30.14 Patient underwent transverse rectus abdominis myocutaneous (TRAM) flap after left mastectomy in 2017. Polypropylene mesh was placed at the time of TRAM flap in her rectus sheath defect in an inlay fashion between the left rectus and right semilunaris. She subsequently developed a hernia at the semilunar line and underwent ventral hernia repair with a 15x20cm piece of Phasix mesh in an inlay technique. (**a**) Appearance of polypropylene mesh (blue arrow) 13 months after placement. (**b**) Hernia defect at the semilunar line where the mesh has separated (blue circle). (**c**) Inflammatory response around Phasix inlay mesh (blue arrow) 5 months after placement. (**d**) Inferior axial image of Phasix inlay mesh (blue arrow) with minimal inflammatory reaction

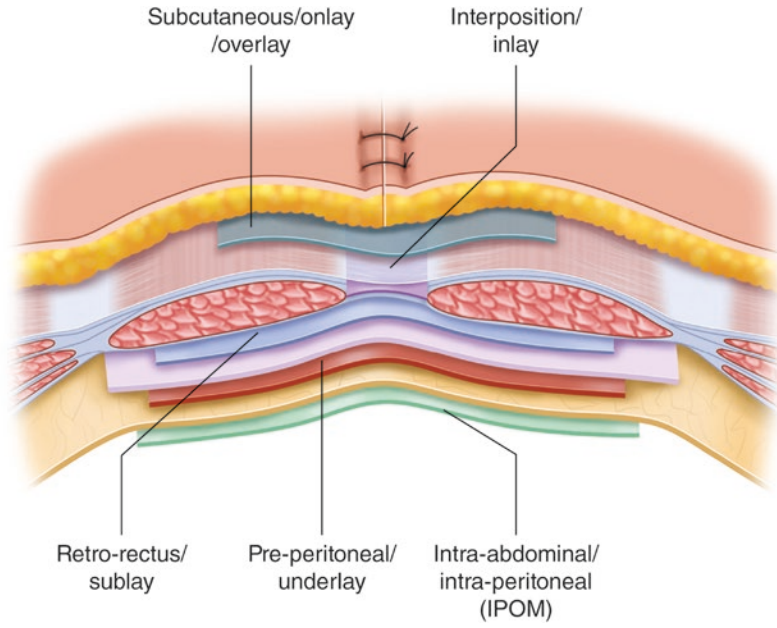

Fig. 30.15 Illustration of the abdominal wall showcasing the different planes mesh can be placed. (Modified from [27])

Adjuncts to Mesh Identification

In cases where mesh is not directly visible on CT imaging, indirect signs can be used to identify the location of the mesh. Metal tacks or other radiopaque devices are often used to secure the mesh to the abdominal wall. Additionally, mesh is a foreign body that creates local reaction and alterations to the surrounding tissues, some more subtle than others. The ability to recognize these indirect signs can help in the identification of the mesh for surgical decision-making. This section will highlight some of those adjuncts to mesh identification when the material itself is radiolucent.

Tissue Distortion

As a foreign body, mesh is a flat sheet of material placed in direct contact with the abdominal wall. The mesh may be placed above, below, or between the myofascial planes as detailed in the previous section (Fig. 30.15). Local tissue reaction results in scar formation and fibrosis in the repaired area resulting in non-anatomic contortions in the local tissues. These undulations and distortions of the surrounding tissue can be readily visible if you are looking for them. Once detected, the abnormal plane can be followed to reveal the extended footprint of the mesh (Video 30.2).

Metallic Tacks/Staples

Metallic tacks and staples are often used to fixate mesh at the time of placement. Typically, a circumferential ring around the periphery is used to secure the mesh to the abdominal wall to prevent herniation around the edge of the mesh. These radiopaque markers act as fiducials to identify the outline of the mesh on the abdominal wall (Fig. 30.16). Future operative plans can be altered to avoid encountering the indwelling mesh on initial access. In Fig. 30.17, abdominal access may be most easily achieved through the right upper quadrant to avoid the prior ventral hernia repair, which appears to be misplaced toward the left upper quadrant.

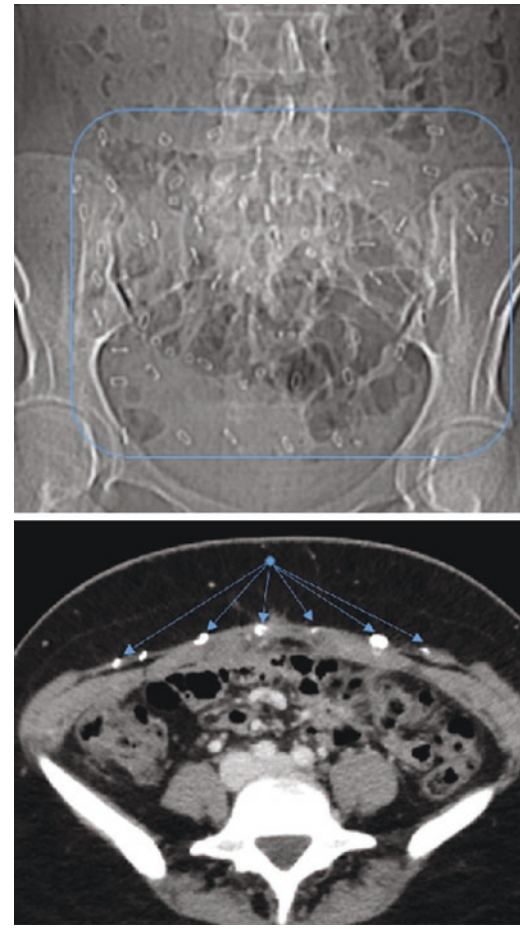

Fig. 30.16 A 40 year old female with prior open onlay mesh repair following abdominal wall resection of endometrial deposits. Plain abdominal X-ray demonstrates staples used to secure the mesh to the abdominal wall (blue outline). CT imaging confirms the mesh is placed in the onlay fashion based on the location of staples above the rectus muscles. In this situation, future abdominal access could be planned above the superior edge of the mesh with the expectation that intra-abdominal adhesions would not be affected by the prior mesh repair

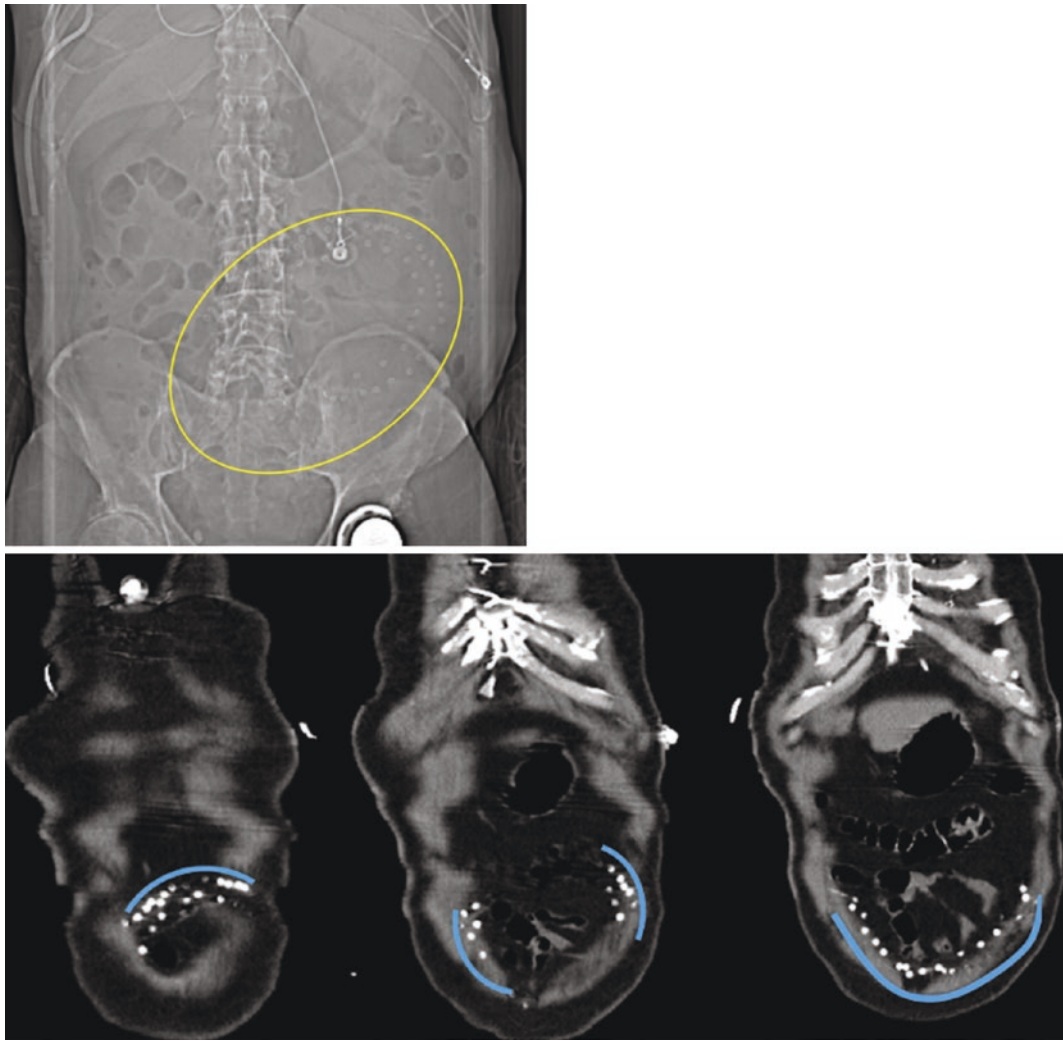

Fig. 30.17 This patient had a laparoscopic intraperitoneal repair secured with metal tacks in two concentric rings along the periphery of the mesh. The tacks are visible on plan radiograph or CT imaging. Following the tacks through sequential cuts on coronal views (Images left to right are anterior to posterior) can give the outline of the mesh

Conclusion

Identification of mesh on imaging is a crucial step in the assessment of the abdominal wall and is a vital component of a hernia surgeon's knowledge base as it relates to the evaluation and management of patients with hernioplasty mesh. In this chapter, we covered many of the techniques that can be used to directly or indirectly identify mesh on imaging and discussed how this information can aid in surgical planning and decision-making. We hope the real-world examples in this chapter illustrate the decision-making process the authors use in everyday practice and that you find these techniques useful and applicable to your own practice.

References

1. Patil AR, Nandikoor S, Mohanty HS, Godhi S, Bhat R. Mind the gap: imaging spectrum of abdominal ventral hernia repair complications. Insights. Imaging. 2019;10(1):40. https://doi.org/10.1186/s13244-019-0730-x.
2. Aguirre DA, Santosa AC, Casola G, Sirlin CB. Abdominal wall hernias: imaging features, complications, and diagnostic pitfalls at multi-detector row CT. Radiographics. 2005;25(6):1501–20. https://doi.org/10.1148/rg.256055018.
3. Parikh KR, Al-Hawary M, Millet JD, Burney R, Finks J, Maturen K. Incisional hernia repair: what the radiologist needs to know. AJR Am J Roentgenol. 2017;209(6):1239–46. https://doi.org/10.2214/AJR.17.18137.
4. Emby DJ, Aoun G. CT technique for suspected anterior abdominal wall hernia. AJR Am J Roentgenol. 2003;181(2):431–3. https://doi.org/10.2214/ajr.181.2.1810431.
5. Jamadar DA, Jacobson JA, Girish G, et al. Abdominal wall hernia mesh repair: sonography of mesh and common complications. J Ultrasound Med. 2008;27(6):907–17. https://doi.org/10.7863/jum.2008.27.6.907.
6. den Hartog D, Dur AH, Kamphuis AG, Tuinebreijer WE, Hermans JJ, Kreis RW. Pre-, intra-, and postoperative sonography of the abdominal wall in patients with incisional hernias repaired via a three-layered operative suture method. J Clin Ultrasound. 2009;37(7):394–8. https://doi.org/10.1002/jcu.20606.
7. Jain N, Goyal N, Mukherjee K, Kamath S. Ultrasound of the abdominal wall: what lies beneath? Clin Radiol. 2013;68(1):85–93. https://doi.org/10.1016/j.crad.2012.05.016.
8. Aasvang EK, Jensen KE, Fiirgaard B, Kehlet H. MRI and pathology in persistent postherniotomy pain. J Am Coll Surg. 2009;208(6):1023–9. https://doi.org/10.1016/j.jamcollsurg.2009.02.056.
9. Petro CC, Nahabet EH, Criss CN, et al. Central failures of lightweight monofilament polyester mesh causing hernia recurrence: a cautionary note. Hernia. 2015;19(1):155–9. https://doi.org/10.1007/s10029-014-1237-5.
10. Rakic S, LeBlanc KA. The radiologic appearance of prosthetic materials used in hernia repair and a recommended classification. AJR Am J Roentgenol. 2013;201(6):1180–3. https://doi.org/10.2214/AJR.13.10703.
11. Kokotovic D, Burcharth J, Helgstrand F, Gögenur I. Systemic inflammatory response after hernia repair: a systematic review. Langenbecks Arch Surg. 2017;402(7):1023–37. https://doi.org/10.1007/s00423-017-1618-1.
12. Rastegarpour A, Cheung M, Vardhan M, Ibrahim MM, Butler CE, Levinson H. Surgical mesh for ventral incisional hernia repairs: Understanding mesh design. Plast Surg (Oakv). 2016;24(1):41–50. https://doi.org/10.4172/plastic-surgery.1000955.
13. Lin BH, Vargish T, Dachman AH. CT findings after laparoscopic repair of ventral hernia. AJR Am J Roentgenol. 1999;172(2):389–92. https://doi.org/10.2214/ajr.172.2.9930789.
14. Silvestre AC, de Mathia GB, Fagundes DJ, Medeiros LR, Rosa MI. Shrinkage evaluation of heavyweight and lightweight polypropylene meshes in inguinal hernia repair: a randomized controlled trial. Hernia. 2011;15(6):629–34. https://doi.org/10.1007/s10029-011-0853-6.
15. Orenstein S. Chapter 5. Permanent prosthetics: polypropylene, polyester, ePTFE, and Hybride Mesh. In: The sages manual of hernia surgery. 2nd Ed. 2019. https://doi.org/10.1007/978-3-319-78411-3.
16. Orenstein SB, Saberski ER, Kreutzer DL, Novitsky YW. Comparative analysis of histopathologic effects of synthetic meshes based on material, weight, and pore size in mice. J Surg Res. 2012;176(2):423–9. https://doi.org/10.1016/j.jss.2011.09.031.
17. Wassenaar EB, Schoenmaeckers EJ, Raymakers JT, Rakic S. Recurrences after laparoscopic repair of ventral and incisional hernia: lessons learned from 505 repairs. Surg Endosc. 2009;23(4):825–32. https://doi.org/10.1007/s00464-008-0146-z.
18. Schoenmaeckers EJ, van der Valk SB, van den Hout HW, Raymakers JF, Rakic S. Computed tomographic measurements of mesh shrinkage after laparoscopic ventral incisional hernia repair with an expanded polytetrafluoroethylene mesh. Surg Endosc. 2009;23(7):1620–3. https://doi.org/10.1007/s00464-009-0500-9.
19. Novitsky YW, Rosen MJ. The biology of biologics: basic science and clinical concepts. Plast Reconstr Surg. 2012;130(5 Suppl 2):9S–17S. https://doi.org/10.1097/PRS.0b013e31825f395b.

20. Novitsky YW. Biology of biological meshes used in hernia repair. Surg Clin North Am. 2013;93(5):1211–5. https://doi.org/10.1016/j.suc.2013.06.014.
21. Hedgire SS, Elmi A, Kambadakone AR, Yoon S, Blake M, Harisinghani MG. MDCT imaging of Alloderm biologic mesh spacers in the abdomen and pelvis--preliminary experience. Clin Imaging. 2014;38(3):279–282. https://doi.org/10.1016/j.clinimag.2013.12.020.
22. Rosen MJ, Bauer JJ, Harmaty M, et al. Multicenter, prospective, longitudinal study of the recurrence, surgical site infection, and quality of life after contaminated ventral hernia repair using biosynthetic absorbable mesh: the COBRA study. Ann Surg. 2017;265(1):205–11. https://doi.org/10.1097/SLA.0000000000001601.
23. Arnold MR, Kao AM, Augenstein VA. Chapter 6. Biologic and absorbably prosthetic: when, why, and where are we going. In: The SAGES manual of hernia surgery. 2nd ed. 2019. https://doi.org/10.1007/978-3-319-78411-3.
24. Laschke MW, Häufel JM, Scheuer C, Menger MD. Angiogenic and inflammatory host response to surgical meshes of different mesh architecture and polymer composition. J Biomed Mater Res B Appl Biomater. 2009;91(2):497–507. https://doi.org/10.1002/jbm.b.31423.
25. Deeken CR, Matthews BD. Characterization of the mechanical strength, resorption properties, and histologic characteristics of a fully absorbable material (poly-4-hydroxybutyrate-PHASIX Mesh) in a porcine model of hernia repair. ISRN Surg. 2013;2013:238067. https://doi.org/10.1155/2013/238067.
26. Muysoms F, Jacob B. International hernia collaboration consensus on nomenclature of abdominal wall hernia repair. World J Surg. 2018;42(1):302–4. https://doi.org/10.1007/s00268-017-4115-3.
27. Parker SG, Wood CPJ, Sanders DL, Windsor ACJ. Nomenclature in abdominal wall hernias: is it time for consensus? World J Surg. 2017;41(10):2488–91. https://doi.org/10.1007/s00268-017-4037-0.

Acute and Chronic Postoperative Hernia Complications and Changes

31

Alaa Sada, Mazen Iskandar, and Omar M. Ghanem

Introduction

Hernia is one of the most commonly encountered surgical pathologies that surgeons have to tackle on a daily basis. Despite the remarkable advancement in the approach to hernias as well as the wide variety of open and minimally invasive performed techniques, hernia repair complications are still deemed inevitable. In general, acute complications are those occurring in the immediate postoperative period whereas chronic complications occur weeks to months after an operation. It is of paramount importance for surgeons to recognize and treat the inescapable complications early and to be able to manage their patients' expectations. In addition to a history and physical exam, imaging modalities serve as a valuable adjunct in identifying or ruling out potential complications. The need for the surgeon to review each imaging study cannot be over-emphasized.

In this chapter, we will discuss the most common acute and chronic complications in inguinal, ventral, and hiatal hernia repairs along with their radiographic presentation.

Acute Inguinal Hernia Complications

The overall complication rate of inguinal hernia repair is relatively low irrespective of the technique performed. The most common acute complications and their radiological presentations are highlighted below.

Seroma

A postoperative seroma occurs when fluid accumulates in the dead space following inguinal hernia reduction and repair. The incidence of seroma is dependent on the surgical approach used as minimally invasive techniques are associated with higher seroma rates compared to open [1, 2]. Complicating about 9–12% of inguinal repair cases, it rarely requires intervention [1]. Mostly, the diagnosis can be made clinically as acute postoperative seroma tends to present with a groin bulge in the early postoperative period causing patient discomfort. However, in some

Supplementary Information The online version contains supplementary material available at https://doi.org/10.1007/978-3-031-21336-6_31.

A. Sada · O. M. Ghanem (✉)
Department of Surgery, Mayo Clinic, Rochester, MN, USA
e-mail: Sada.alaa@mayo.edu; Ghanem.omar@mayo.edu

M. Iskandar
Department of General Surgery, Baylor Scott and White Center for Hernia Surgery, Waxahachie, TX, USA
e-mail: Mazen.Iskandar@bswhealth.org

S. Docimo Jr. et al. (eds.), *Fundamentals of Hernia Radiology*, https://doi.org/10.1007/978-3-031-21336-6_31

cases, it is not as easy to differentiate between early hernia recurrence and seroma thus necessitating radiological confirmation [2]. An ultrasound (US) or computed tomography (CT scan) can be obtained to confirm the diagnoses. In US, a seroma appears as hypo- or anechoic simple fluid collection while on CT scan it appears as a simple, homogeneous, water-density fluid collection with no septations or rim enhancement [3]. Management is usually conservative, especially in the acute phase.

Hematoma

Hematoma formation following inguinal hernia repair develops in about 4–6% of cases [4]. It can present as a wound or scrotal hematoma with a higher incidence in patients on anti-coagulation therapy [5]. The majority of hematomas present as a groin or scrotal mass and discomfort due to blood collection in the dead space that develops after hernia reduction [4]. Similar to seroma, most postoperative hematomas can be diagnosed clinically and they usually resolve without intervention. However, an US or CT scan may be necessary to rule out other complications. On US, acute hematoma appears as hyperechoic or heterogeneously echoic lesion while on CT scan it appears as a fluid collection with high attenuation on non-contrast images (Fig. 31.1) [6]. Hematomas if large and symptomatic may require reoperation for evacuation but are commonly observed.

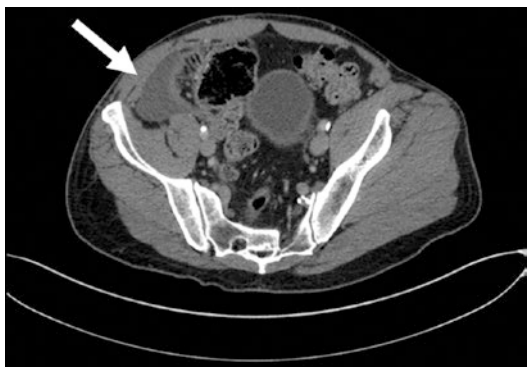

Fig. 31.1 A CT scan axial image showing a hyperattenuating simple collection (white arrow) status post inguinal hernia repair in a patient on antiplatelet therapy. The absence of rim enhancement or gas suggests a hematoma

Surgical Site Infections

Other acute complications following inguinal hernia repair include surgical site infection which develops in 1–3% of the cases. Features consistent with acute infection make this occurrence a clinical diagnosis as well [1, 7]. US or CT scan have a limited role and are only obtained to rule out a deep extension of the infection or an abscess. An abscess on US shows as a hypoechoic fluid collection with or without septa and with hyperechoic rim. On CT scan, a deep infection or abscess appears as a fluid collection with hyperenhanced rim, surrounding soft tissue edema and fat stranding [6, 8]. The presence of gas pockets within the collection can be a distinctive feature in the appropriate clinical setting. Acutely, abscess in the groin in proximity to mesh prosthesis is managed with surgical drainage and mesh explantation.

Small Bowel Obstruction

While the risk of small bowel obstruction in inguinal hernia repair is very low, the incidence is higher in laparoscopic repair including extraperitoneal and transabdominal approaches [9–13]. Small bowel obstruction can develop due to early adhesion formation or small bowel herniation into a trocar site [11]. Obstruction with barbed sutures or intraparietal hernia has also been reported [14]. Diagnosis can be made clinically along with an abdominal X-ray or CT scan suggesting intestinal obstruction pattern including dilated loops of bowel with air-fluid levels on X-ray or dilated and decompressed loops of bowel on CT scan with a transition point [8]. The location of the transition point in addition to the utilized intraoperative technique can help identify the cause and dictate the management. For example, acute bowel obstructions due to trocar site hernia mandates operative exploration.

Ischemic Orchitis

Vascular injuries during inguinal hernia repair are mostly due to venous compromise and can lead to ischemic orchitis and testicular atrophy in about 0.2–1.1% of cases [15, 16]. This complication usually presents with acute scrotal pain and diagnosis is confirmed with a Doppler US. Absence of blood flow to the testicle is pathognomonic (Fig. 31.2) [17]. Orchiectomy is often needed once the diagnosis is established.

Early Recurrence

There is no standard definition for early hernia recurrence. However, some studies define early recurrence when a hernia developes within 2 months after surgery [18]. In contrast to late recurrence, early recurrence is mainly the result of technical failures rather than patient's risk factors [18–20]. Early recurrence usually presents as a bulge and can be diagnosed clinically. When exam is not conclusive, US or CT scan can differentiate recurrences from seromas or hematoma and may provide some insight into the cause of the recurrence. As shown in Fig. 31.3, recurrence appears as a hernia defect with protruding hernia sac contents on US or CT scan. The old mesh can be appreciated at times on imaging [6].

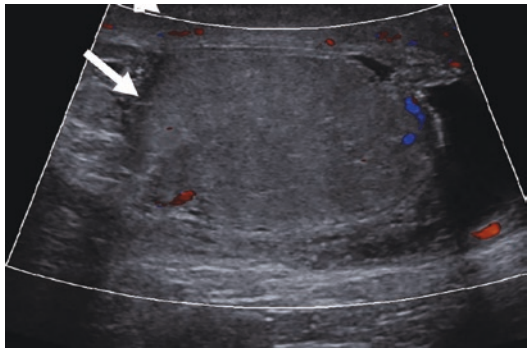

Fig. 31.2 Doppler US showing an edematous testicle (white arrow) 4 days after inguinal hernia repair. Since no arterial flow was established, a trans-scrotal orchiectomy was indicated

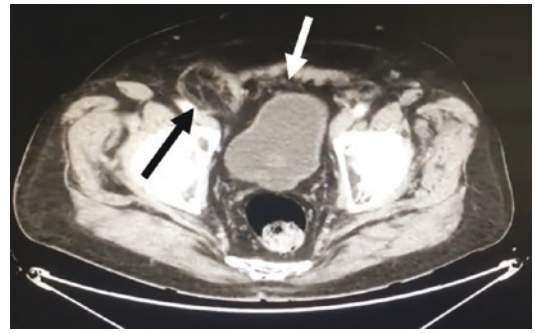

Fig. 31.3 CT scan obtained within 2 months after right inguinal hernia repair with mesh. An obvious fat-containing recurrence (black arrow) is observed. The mesh can be noted within the space of Retzius (white arrow)

Bladder Injury

Despite its rare occurrence, bladder injury in inguinal hernia repair has been described following both open and laparoscopic approaches [21, 22]. The reported incidence is less than 0.07% [22]. Bladder injury can occur during trocar insertion or dissection in the space of Retzius especially in reoperative cases [23–25]. If encountered and noted intraoperatively, bladder repair with absorbable sutures can be performed [26]. Missed bladder injuries usually present in the first week after surgery with pelvic discomfort and distension. Bladder injury can be suspected on US or CT showing paravesicular fluid collection and can be confirmed with a CT cystogram which can show free intraperitoneal or focal pre-peritoneal contrast extravasation (Video 31.1) [27].

Chronic Inguinal Hernia Complications

Chronic Pain

Chronic pain can complicate as much as 10% of inguinal hernia repairs [28]. The rate of debilitating pain affecting daily life is 0.5–6% [28]. The most common mechanisms for chronic pain include intraoperative nerve injury, inflammation leading to nerve entrapment by mesh as well as

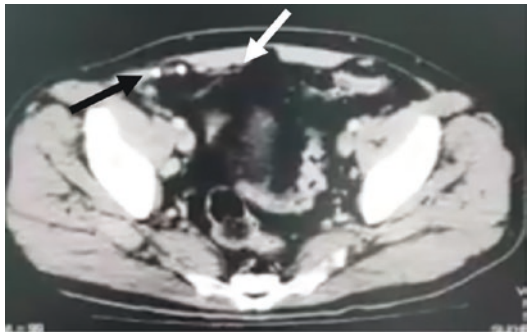

Fig. 31.4 Patient with severe groin pain post laparoscopic hernia repair with mesh. Metallic tacks are seen below the level of anterior superior iliac spine (black arrow). Mesh is noted medially (white arrow)

mesh migration and meshoma [28, 29]. While the diagnosis of chronic pain is made clinically with a good history and physical exam including dermatome mapping, diagnostic imaging is often obtained to rule out other causes such as seroma, hematoma, infection, or recurrence. CT scans can provide helpful details in the diagnostic work-up for chronic pain including anatomy, mesh location, and presence of tacks which can be suspected as a cause of chronic pain if found along the nerve tracks (Fig. 31.4).

Recurrence

Inguinal hernia recurrence rates range between 1.4 and 5% [4, 30]. The risk of late recurrence is directly related to the patient's specific risk factors and technical differences including approaches, type and size of mesh, and surgeon's experience/volume [4, 30]. Late recurrence can be diagnosed clinically or with an US or CT scan showing hernia defect with protruding content (bowel, pre-peritoneal fat, etc.) [6].

Chronic Seroma

Chronic seroma formation after inguinal hernia repair is far less common than acute seroma. An US or CT is needed to differentiate between chronic seroma and hernia recurrence. In US, chronic seroma appears as hypoechoic septated fluid collection while on CT scan, it appears as homogeneous fluid collection abutting the mesh [3, 6].

Mesh Infection and Erosion

While chronic mesh infection following inguinal hernia repair is rare, it is a devastating complication as it can require reoperation for mesh removal and subsequent reconstruction [31–33]. The incidence of chronic mesh infection is reported around 0.35%, and is usually suspected clinically. It presents with localized infection signs. However, and in some cases, systematic signs such as fever are seen [31]. If mesh erodes into bowel, it can result in enterocutaneous fistula [34]. When mesh infection is suspected, the patient needs to be started on broad spectrum antibiotics and diagnostic tests are obtained for confirmation. An US can show hypoechoic fluid collection with hyperechoic rim concerning for an abscess formation. On the other hand, CT scan findings include a heterogeneous fluid collection and an enhanced rim abutting the mesh (Fig. 31.5). Other CT findings concerning infection include tissue edema and fat stranding [35].

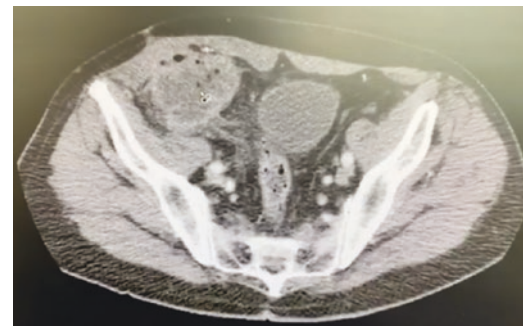

Fig. 31.5 Patient presenting months after minimally invasive right inguinal hernia repair with mesh. Seen in the image is a right groin abscess in proximity to the mesh presumably due to an intra-abdominal pathology/infection

Acute Ventral Hernia Complications|

In the United States, the estimated number of ventral hernia repair cases is 348,000 annually and the number of cases continue to rise [36]. It is critical for clinicians and surgeons to be familiar with the common ventral hernia repair complications.

Seroma

Ventral hernia repair is associated with postoperative seroma in about 8–19% of cases [37, 38]. While seroma formation is a frequent occurrence after ventral herniorrhaphy, the rate of complicated seroma or seroma requiring intervention is as low as 1.4% [37]. Seroma complicating ventral hernia repair can be diagnosed clinically or radiologically with an ultrasound or a CT scan. On CT scan, seroma appears as a non-septated low attenuation fluid collection with or without a thin enhancing rim (Fig. 31.6), while on US it appears as simple hypoechoic noncomplex simple fluid collection (Fig. 31.7) [8].

Hematoma

Swelling and discomfort can be indicative of a postoperative hematoma complicating a ventral hernia repair. The rate of postoperative hematomas does not differ significantly between open and laparoscopic ventral hernia repairs [39]. In contrast to seromas, hematomas are characterized by higher fluid attenuation (30 and 80 Hounsfield unit (HU)). In addition, the hematoma content is often heterogeneous [40]. In some cases of active bleeding, an active blush or contrast extravasation can be seen with intravenous contrast-enhanced CT scan [8]. Hematoma management is dictated by the patient's symptoms such as pain and/or physical exam findings (for example, skin compromise).

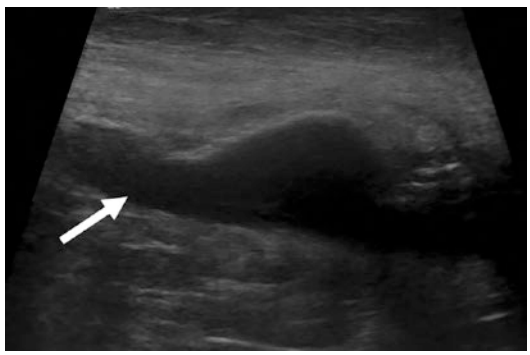

Fig. 31.6 A simple non-septated hypoechoic fluid collection after a laparoscopic umbilical hernia repair consistent with a seroma as seen on US

Fig. 31.7 A simple fluid collection seen on CT scan post laparoscopic recurrent incisional hernia (previous ileostomy site) compatible with an acute seroma

Pain

Postoperative acute pain after ventral hernia repair is expected to resolve within 4–6 weeks. Peripheral nerve injury or entrapment by mesh fixation can result in severe or persistent pain. The optimal mesh fixation method whether by tacks, sutures, or a combination of both is still debatable [41]. Nonabsorbable tacks are associated with a higher incidence of postoperative pain compared to absorbable ones. Furthermore, using more than 10 tacks can double the rate of acute postoperative pain [42]. While acute pain is diagnosed clinically, a CT scan or US can be obtained to rule out treatable causes of pain including seroma, hematoma, or recurrence.

Surgical Site Infection

Superficial site infections develop more frequently in open compared to laparoscopic ventral hernia (9% vs. <2%) [8]. The rate of deep surgical site infection which can be associated with mesh infection and/or abscess formation is much lower and estimated to occur in less than 0.7% [38, 43]. If mesh infection or abscess formation is suspected, a diagnostic confirmation with a CT scan is needed to rule out bowel injury and assess the need for drainage either surgically or percutaneously [41, 43]. Findings on CT scan suggesting an infection include a mix of fluid and air collection along with an irregular rim enhancement [8]. On US, it appears as an ill-defined heterogonous hypoechoic fluid collection [8].

Small Bowel Obstruction

While small bowel obstruction after ventral hernia repair is a rare complication that occurs in 1% of cases, it can lead to reoperation and increased morbidity [38, 44]. Early adhesion formation, trocar site hernia, or ventral hernia recurrence can all lead to early small bowel obstruction and requires rapid diagnosis and intervention [44, 45]. Once small bowel obstruction is suspected, an abdominal x-ray can be obtained first and it typically shows air-fluid levels with dilated loops of bowels (Fig. 31.8). However, a CT scan usually provides more detailed confirmation regarding the location of obstruction and possibly the underlying cause [45]. Findings on CT scan suggestive of small bowel obstruction include dilated loops of small bowel with intraluminal fluids along with decompressed loops and a transition point, or a hernia defect with herniated loops of bowel [8, 45].

Bowel Injury

Bowel injury during lysis of adhesions or trocar insertion occurs in 2% of ventral hernia repairs [46]. Despite its rare occurrence, enterotomy is considered one of the most serious complications associated with ventral hernia repair as it can increase the mortality rate to 8% if the injury is not recognized intraoperatively [46]. Missed small bowel injury is usually suspected on a postoperative day one or two and presents with sepsis [46]. A CT scan is the radiological imaging of choice when a leak or enterotomy is suspected as it can show free intraperitoneal air, free fluid, and inflammatory changes (Fig. 31.9).

Fig. 31.8 An abdominal X-Ray with obvious distended loops of bowel 3 days post laparoscopic ventral hernia repair due to bowel adhesions to an intraperitoneal mesh

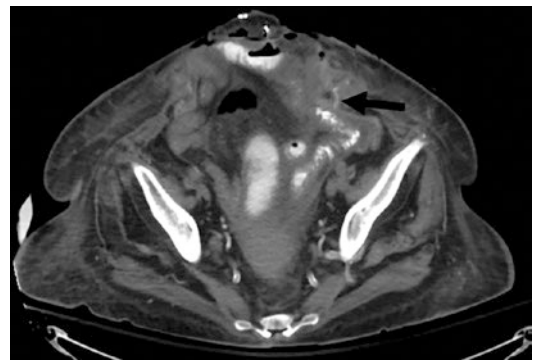

Fig. 31.9 A CT scan obtained on postoperative day 10 following emergent repair of an incarcerated ventral hernia with biologic mesh showing localized contrast extravasation from a non-healed serosal tear that was repaired during surgery

Chronic Ventral Hernia Complications

Chronic Pain

Chronic pain is present in around 17–28% of ventral hernia repair cases [47, 48]. Although the diagnosis of chronic pain is made clinically, radiological images including CT scan or US are usually obtained to rule out other complications. Like the case in acute pain, chronic pain can be related to tacks that are utilized for mesh fixation. Metallic tacks are seen on CT scan or plain X-ray (Fig. 31.10). A radio-opaque marker may be placed at the point of tenderness for correlation [49].

Seroma

While acute seroma formation is common after ventral hernia repair, the rate of seromas persisting beyond 90 days is between 0 and 20%. The rate of seromas requiring intervention is between 3 and 4% [41]. As discussed previously in chronic seroma following inguinal hernia repair, chronic seroma following ventral hernia appears as a fluid collection with a thick capsule on US or CT scan (Video 31.2) [40]. This thick capsule allows for complete excision of the seroma in symptomatic patients.

Mesh Infection and Erosion

The incidence of chronic mesh complications including chronic infection, erosion into bowel and fistulization is low [50]. On US, a hypoechoic fluid collection with a hyperechoic rim concerning for an abscess is noted. However, a CT provides further details, particularly in the setting of mesh erosion or fistula formation. CT scan findings suggesting chronic mesh infection include heterogeneous complex fluid collection around the mesh with adjacent edema and fat stranding [51]. Whereas, the existence of extraluminal air favors erosion or fistulization (Fig. 31.11) [52].

Small Bowel Obstruction

The rate of late small bowel obstruction occurring beyond 30 days after ventral hernia repair, is about 2–3% and differs in etiology compared to the acute postoperative period [47]. Similar to

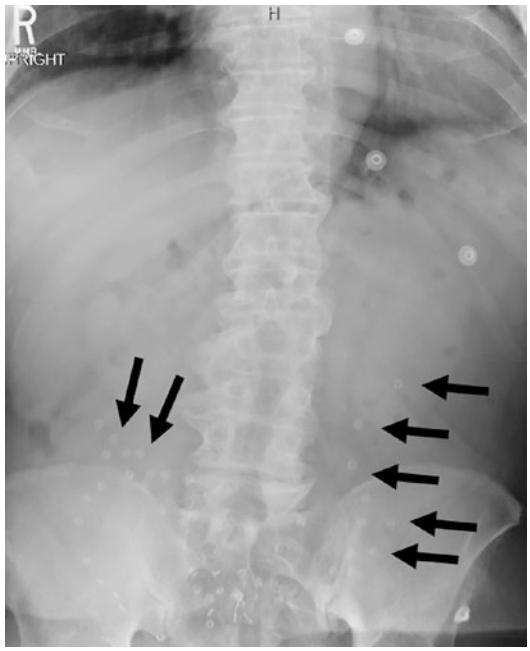

Fig. 31.10 Patient presenting with left lower quadrant focal point tenderness after a suprapubic hernia repair with mesh. Numerous metallic tacks are seen on plain X-Ray (black arrows) on the left and right side

Fig. 31.11 Colonic fistula tract (white arrow) noted on axial CT images obtained 3 months after emergenct hernia repair for bowel obstruction bridged with a Vicryl mesh. A fluid collection in the subcutaneous space is noted as well

early small bowel obstruction following ventral hernia, chronic obstruction can be diagnosed on plain X-ray or CT scan suggesting distended loops of bowel with air-fluid levels and a transition point to collapsed bowel [40].

Late Recurrence

Late ventral hernia recurrence is a known complication that occurs in up to 20% of cases [53]. Technical aspects related to recurrence include low mesh/defect size ratio or inadequate mesh-fascial edges overlap. Patient-related risk factors predisposing to a higher recurrence rate are poorly controlled diabetes, obesity, current smoking, and prior failed repairs [54]. While hernia recurrence can be seen on US, a CT scan is more helpful for operative planning as it can provide more information about the defect size, previous mesh location, and other anatomical features [41].

Acute Hiatal Hernia Complications

While hiatal hernia repair is a safe and effective procedure that is performed widely in the United States, it is estimated that 3% of patients will require reoperation [55]. In this section, the radiological features for the most common acute and chronic complications are highlighted.

Wrap Complications

Wrap complications can develop early after surgery and usually present with persistent or severe dysphagia, spitting, and vomiting. While these symptoms are common and often self-limited, diagnostic images may be needed to rule out wrap complications [49]. A contrast upper gastrointestinal tract study (UGI) is the study of choice to delineate the wrap anatomy and function [56, 57]. On UGI, a tight wrap appears as a luminal narrowing with proximal esophageal dilation and delayed passage of contrast. A gastric fundus pouching above the wrap indicates a slipped wrap [55]. An UGI study with an intact wrap above the diaphragm level implies a herniated wrap and recurrence (Fig. 31.12) [55].

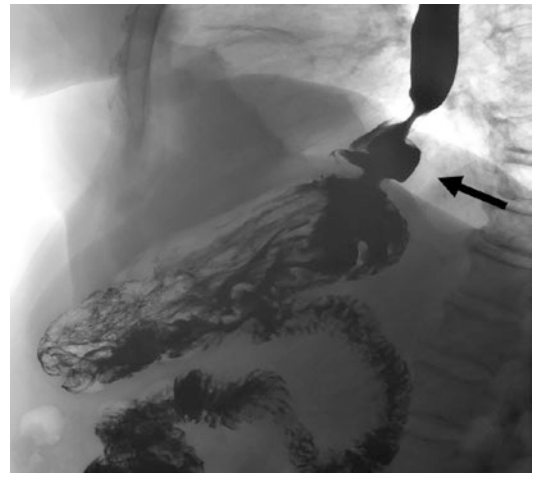

Fig. 31.12 Intact wrap (black arrow) migrating into the chest seen acutely post paraesophageal hernia repair on UGI

Early Recurrence

The incidence of early recurrence following hiatal hernia repair ranges between 12% and 45% and depends on the technique, mesh utilization, and anatomical features [58–60]. Most hiatal hernia recurrences are asymptomatic and diagnosed incidentally [61]. In contrast to clinical recurrences, radiologic recurrences do not require reoperations. UGI is usually the study of choice when recurrence is suspected as it can provide details about hernia size, anatomy, location of the gastroesophageal junction along with the stomach orientation in addition to delineating the wrap anatomy [25]. Findings on UGI that suggest recurrence include wrap disruption and gastric hernia at the hiatus level with the stomach or wrap above the level of the diaphragm (Fig. 31.13). This finding can also be seen on a CT scan with oral contrast [25]. If associated with symptoms, early recurrence usually requires reoperation.

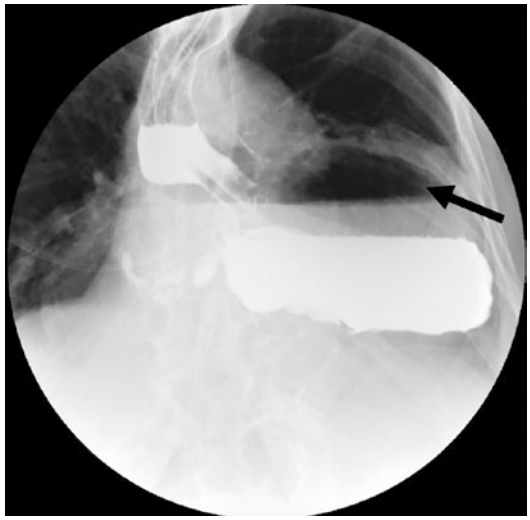

Fig. 31.13 Stomach herniation on postoperative day one after emergenct laparoscopic paraesophageal hernia repair (with no fundoplication) in a geriatric patient. A significant part of stomach is seen above the level of the diaphragm (black arrow)

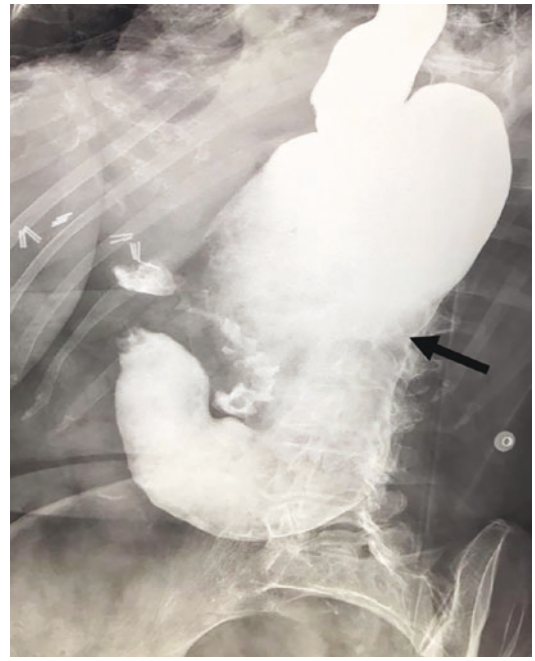

Fig. 31.14 Delayed gastric emptying on an UGI showing contrast pooling (black arrow) within the distended stomach (extending to the pelvis) 3 days after emergent paraesophageal hernia repair (without fundoplication). This was temporary and responded to motility agents

Delayed Gastric Emptying (DGE)

Paraesophageal hernias are accompanied by some degree of DGE. Some studies have shown that fundoplication can improve DGE by enhancing gastric emptying [62]. That said, DGE can complicate hiatal hernia repairs especially in cases with giant paraesophageal hernias (>50% of stomach in chest) or in the setting of intraoperative vagal nerve injury [63]. The diagnosis is established by delayed emptying of stomach contrast on UGI (Fig. 31.14). It is confirmed with a gastric emptying scintigraphy study suggesting retention of more than 10% of radiolabeled Technetium at 4 hours or more than 60% at 2 hours of standard low-fat meal [64].

Seroma and Hematoma

Acute seroma or hematoma can develop following hiatal hernia repair as serous or bloody fluids accumulate in the mediastinum [65]. Postoperative seroma/hematoma formation following hiatal hernia repair is diagnosed on CT scans showing fluid collections in the mediastinum. Hounsfield units can differentiate between simple serous collections and hematomas (Fig. 31.15). The absence of rim enhancement and air favor noninfected fluid collections and the absence of esophageal injury in the appropriate clinical setting.

Esophageal Perforation

While esophageal perforation is not common after hiatal hernia repair, it is associated with significant morbidity and mortality. The estimated rate is 0.9% after laparoscopic primary hiatal hernia repair and is increased to 6.5% reoperative cases [66]. Along with clinical signs and symptoms of an early leak, esophageal perforation can be diagnosed on CT scan or UGI study suggesting extraluminal contrast extravasation. Findings on CT scan that suggest esophageal perforation or leak include pneumomediastinum, contrast extravasation, attenuation of mediastinal fat,

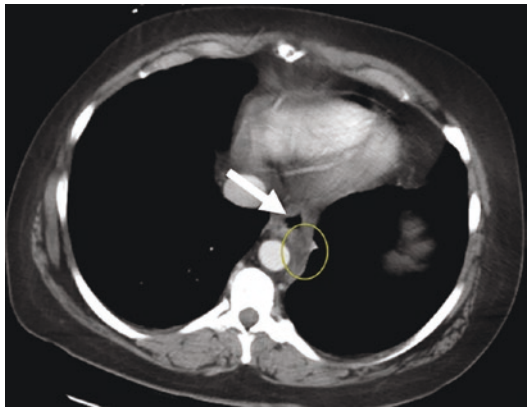

Fig. 31.15 CT scan showing esophagus (white arrow) with a surrounding small fluid collection in the mediastinum (encircled) after a paraesophageal hernia repair. The 3.1 × 1.4 cm low-density fluid collection is present posterior to the esophagus, without wall enhancement, wall thickening, or gas thus suggestive of a hematoma

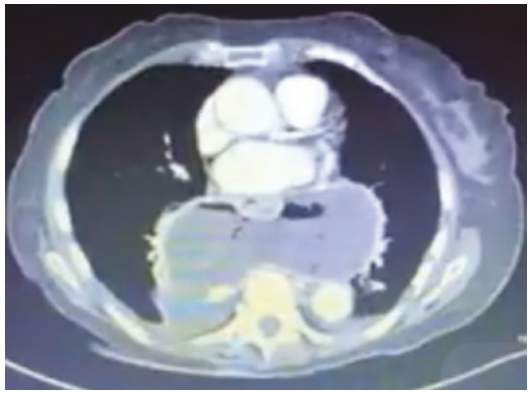

Fig. 31.16 CT scan of the chest showing a mediastinal collection containing air and fluid with rim enhancement suggestive of an esophageal leak after a giant paraesophageal hernia repair

localized mediastinal fluid with/without air, and pleural effusion (Fig. 31.16) [67, 68].

Chronic Hiatal Hernia Complication

Late hiatal hernia complications and changes include hernia recurrence and wrap complications. In images, these chronic changes appear similar to those in the acute setting described above.

References

1. Schmedt C, Sauerland S, Bittner R. Comparison of endoscopic procedures vs Lichtenstein and other open mesh techniques for inguinal hernia repair: a meta-analysis of randomized controlled trials. Surg Endosc Other Interv Tech. 2005;19(2):188–99.
2. Cihan A, Ozdemir H, Ucan B, Acun Z, Comert M, Tascilar O, et al. Fade or fate. Surg Endosc Other Interv Tech. 2006;20(2):325–8.
3. Tonolini M. Multidetector CT of expected findings and complications after contemporary inguinal hernia repair surgery. Diagn Interv Radiol. 2016;22(5):422.
4. Fitzgibbons RJ, Giobbie-Hurder A, Gibbs JO, Dunlop DD, Reda DJ, McCarthy M, et al. Watchful waiting vs repair of inguinal hernia in minimally symptomatic men: a randomized clinical trial. JAMA. 2006;295(3):285–92.
5. Smoot R, Oderich G, Taner C, Greenlee S, Larson D, Cragun E, et al. Postoperative hematoma following inguinal herniorrhaphy: patient characteristics leading to increased risk. Hernia. 2008;12(3):261–5.
6. Parra J, Revuelta S, Gallego T, Bueno J, Berrio J, Farinas M. Prosthetic mesh used for inguinal and ventral hernia repair: normal appearance and complications in ultrasound and CT. Br J Radiol. 2004;77(915):261–5.
7. Sanabria A, Domínguez LC, Valdivieso E, Gómez G. Prophylactic antibiotics for mesh inguinal hernioplasty: a meta-analysis. Ann Surg. 2007;245(3):392.
8. Tonolini M, Ippolito S. Multidetector CT of expected findings and early postoperative complications after current techniques for ventral hernia repair. Insights Imaging. 2016;7(4):541–51.
9. Eklund A, Rudberg C, Smedberg S, Enander L, Leijonmarck C, Österberg J, et al. Short-term results of a randomized clinical trial comparing Lichtenstein open repair with totally extraperitoneal laparoscopic inguinal hernia repair. Br J Surg. 2006;93(9):1060–8.
10. Wake BL, McCormack K, Fraser C, Vale L, Perez J, Grant A. Transabdominal pre-peritoneal (TAPP) vs totally extraperitoneal (TEP) laparoscopic techniques for inguinal hernia repair. Cochrane Database Syst Rev. 2005;2005(1):CD004703.
11. Vader V, Vogt D, Zucker K, Thilstead J, Curet M. Adhesion formation in laparoscopic inguinal hernia repair. Surg Endosc. 1997;11(8):825–9.
12. Andersson B, Hallén M, Leveau P, Bergenfelz A, Westerdahl J. Laparoscopic extraperitoneal inguinal hernia repair versus open mesh repair: a prospective randomized controlled trial. Surgery. 2003;133(5):464–72.
13. Simons M, Aufenacker T, Bay-Nielsen M, Bouillot J, Campanelli G, Conze J, et al. European hernia society guidelines on the treatment of inguinal hernia in adult patients. Springer; 2009.
14. Köhler G, Mayer F, Lechner M, Bittner R. Small bowel obstruction after TAPP repair caused by a self-

anchoring barbed suture device for peritoneal closure: case report and review of the literature. Hernia. 2015;19(3):389–94.
15. Dellabianca C, Bonardi M, Alessi S. Testicular ischemia after inguinal hernia repair. J Ultrasound. 2011;14(4):205–7.
16. Dilek ON. Hernioplasty and testicular perfusion. Springerplus. 2014;3(1):107.
17. Moore JB, Hasenboehler EA. Orchiectomy as a result of ischemic orchitis after laparoscopic inguinal hernia repair: case report of a rare complication. Patient Saf Surg. 2007;1(1):3.
18. Dedemadi G, Sgourakis G, Radtke A, Dounavis A, Gockel I, Fouzas I, et al. Laparoscopic versus open mesh repair for recurrent inguinal hernia: a meta-analysis of outcomes. Am J Surg. 2010;200(2):291–7.
19. Magnusson N, Nordin P, Hedberg M, Gunnarsson U, Sandblom G. The time profile of groin hernia recurrences. Hernia. 2010;14(4):341–4.
20. Miserez M, Peeters E, Aufenacker T, Bouillot J, Campanelli G, Conze J, et al. Update with level 1 studies of the European hernia society guidelines on the treatment of inguinal hernia in adult patients. Hernia. 2014;18(2):151–63.
21. Ramshaw B, Shuler FW, Jones HB, Duncan TD, White J, Wilson R, et al. Laparoscopic inguinal hernia repair. Surg Endosc. 2001;15(1):50–4.
22. Bittner R, Sauerland S, Schmedt C-G. Comparison of endoscopic techniques vs Shouldice and other open nonmesh techniques for inguinal hernia repair: a meta-analysis of randomized controlled trials. Surg Endosc Other Interv Tech. 2005;19(5):605–15.
23. Kocot A, Gerharz E, Riedmiller H. Urological complications of laparoscopic inguinal hernia repair: a case series. Hernia. 2011;15(5):583–6.
24. Chandler JG, Corson SL, Way LW. Three spectra of laparoscopic entry access injuries. J Am Coll Surg. 2001;192(4):478–90.
25. Agrawal A, Avill R. Mesh migration following repair of inguinal hernia: a case report and review of literature. Hernia. 2006;10(1):79–82.
26. Dalessandri KM, Bhoyrul S, Mulvihill SJ. Laparoscopic hernia repair and bladder injury. JSLS. 2001;5(2):175.
27. Kane NM, Francis IR, Ellis JH. The value of CT in the detection of bladder and posterior urethral injuries. Am J Roentgenol. 1989;153(6):1243–6.
28. Alfieri S, Amid PK, Campanelli G, Izard G, Kehlet H, Wijsmuller AR, et al. International guidelines for prevention and management of post-operative chronic pain following inguinal hernia surgery. Hernia. 2011;15(3):239–49.
29. Ducic I, Dellon AL. Testicular pain after inguinal hernia repair: an approach to resection of the genital branch of genitofemoral nerve. J Am Coll Surg. 2004;198(2):181–4.
30. Puri V, Felix E, Fitzgibbons RJ. Laparoscopic vs conventional tension free inguinal herniorrhaphy: 2005 Society of American Gastrointestinal Endoscopic Surgeons (SAGES) annual meeting debate. Surg Endosc Other Interv Tech. 2006;20(12):1809–16.
31. Delikoukos S, Tzovaras G, Liakou P, Mantzos F, Hatzitheofilou C. Late-onset deep mesh infection after inguinal hernia repair. Hernia. 2007;11(1):15–7.
32. Fawole A, Chaparala R, Ambrose N. Fate of the inguinal hernia following removal of infected prosthetic mesh. Hernia. 2006;10(1):58–61.
33. Rehman S, Khan S, Pervaiz A, Perry EP. Recurrence of inguinal herniae following removal of infected prosthetic meshes: a review of the literature. Hernia. 2012;16(2):123–6.
34. Osborn C, Fischer JE. How I do it: gastrointestinal cutaneous fistulas. J Gastrointest Surg. 2009;13(11):2068.
35. Hindman NM, Kang S, Parikh MS. Common postoperative findings unique to laparoscopic surgery. Radiographics. 2014;34(1):119–38.
36. Poulose BK, Shelton J, Phillips S, Moore D, Nealon W, Penson D, et al. Epidemiology and cost of ventral hernia repair: making the case for hernia research. Hernia. 2012;16(2):179–83.
37. Nguyen DH, Nguyen MT, Askenasy EP, Kao LS, Liang MK. Primary fascial closure with laparoscopic ventral hernia repair: systematic review. World J Surg. 2014;38(12):3097–104.
38. Bittner R, Bain K, Bansal VK, Berrevoet F, Bingener-Casey J, Chen D, et al. Update of guidelines for laparoscopic treatment of ventral and incisional abdominal wall hernias (international Endohernia society (IEHS))-part a. Surg Endosc. 2019;33(10):3069–139.
39. Zhang Y, Zhou H, Chai Y, Cao C, Jin K, Hu Z. Laparoscopic versus open incisional and ventral hernia repair: a systematic review and meta-analysis. World J Surg. 2014;38(9):2233–40.
40. Halligan S, Parker SG, Plumb AA, Windsor AC. Imaging complex ventral hernias, their surgical repair, and their complications. Eur Radiol. 2018;28(8):3560–9.
41. Earle D, Roth JS, Saber A, Haggerty S, Bradley JF, Fanelli R, et al. SAGES guidelines for laparoscopic ventral hernia repair. Surg Endosc. 2016;30(8):3163–83.
42. Belyansky I, Tsirline VB, Klima DA, Walters AL, Lincourt AE, Heniford TB. Prospective, comparative study of postoperative quality of life in TEP, TAPP, and modified Lichtenstein repairs. Ann Surg. 2011;254(5):709–15.
43. Heniford BT, Park A, Ramshaw BJ, Voeller G. Laparoscopic repair of ventral hernias: nine years' experience with 850 consecutive hernias. Ann Surg. 2003;238(3):391.
44. Jenkins ED, Yom V, Melman L, Brunt LM, Eagon JC, Frisella MM, et al. Prospective evaluation of adhesion characteristics to intraperitoneal mesh and adhesiolysis-related complications during laparoscopic re-exploration after prior ventral hernia repair. Surg Endosc. 2010;24(12):3002–7.

45. Boldo E, de Lucia GP, Aracil J, Martin F, Escrig J, Martinez D, et al. Trocar site hernia after laparoscopic ventral hernia repair. Surg Endosc. 2007;21(5):798–800.
46. LeBlanc KA, Elieson MJ, Corder JM III. Enterotomy and mortality rates of laparoscopic incisional and ventral hernia repair: a review of the literature. JSLS. 2007;11(4):408.
47. Liang MK, Clapp M, Li LT, Berger RL, Hicks SC, Awad S. Patient satisfaction, chronic pain, and functional status following laparoscopic ventral hernia repair. World J Surg. 2013;37(3):530–7.
48. Gronnier C, Wattier J-M, Favre H, Piessen G, Mariette C. Risk factors for chronic pain after open ventral hernia repair by underlay mesh placement. World J Surg. 2012;36(7):1548–54.
49. Malhi-Chowla N, Gorecki P, Bammer T, Achem SR, Hinder RA, DeVault KR. Dilation after fundoplication: timing, frequency, indications, and outcome. Gastrointest Endosc. 2002;55(2):219–23.
50. Basoglu M, Yildirgan M, Yilmaz I, Balik A, Celebi F, Atamanalp S, et al. Late complications of incisional hernias following prosthetic mesh repair. Acta Chir Belg. 2004;104(4):425–48.
51. Birolini C, De Miranda J, Utiyama E, Rasslan S. A retrospective review and observations over a 16-year clinical experience on the surgical treatment of chronic mesh infection. What about replacing a synthetic mesh on the infected surgical field? Hernia. 2015;19(2):239–46.
52. Pickhardt PJ, Bhalla S, Balfe DM. Acquired gastrointestinal fistulas: classification, etiologies, and imaging evaluation. Radiology. 2002;224(1):9–23.
53. Helgstrand F, Rosenberg J, Kehlet H, Strandfelt P, Bisgaard T. Reoperation versus clinical recurrence rate after ventral hernia repair. Ann Surg. 2012;256(6):955–8.
54. Huynh DT, Ghanem OM. Patient comorbidities complicating a hernia repair: the preoperative workup and postoperative planning. In: The SAGES manual of hernia surgery. Springer; 2019. p. 109–23.
55. Carbo AI, Kim RH, Gates T, D'Agostino HR. Imaging findings of successful and failed fundoplication. Radiographics. 2014;34(7):1873–84.
56. Granderath FA, Schweiger UM, Kamolz T, Asche KU, Pointner R. Laparoscopic Nissen fundoplication with prosthetic hiatal closure reduces postoperative intrathoracic wrap herniation: preliminary results of a prospective randomized functional and clinical study. Arch Surg. 2005;140(1):40–8.
57. Granderath FA, Schweiger UM, Kamolz T, Pointner R. Dysphagia after laparoscopic antireflux surgery: a problem of hiatal closure more than a problem of the wrap. Surg Endosc Other Interv Tech. 2005;19(11):1439–46.
58. Memon MA, Memon B, Yunus RM, Khan S. Suture cruroplasty versus prosthetic hiatal herniorrhaphy for large hiatal hernia. Ann Surg. 2016;263(2):258–66.
59. El Lakis MA, Kaplan SJ, Hubka M, Mohiuddin K, Low DE. The importance of age on short-term outcomes associated with repair of giant paraesophageal hernias. Ann Thorac Surg. 2017;103(6):1700–9.
60. Lidor AO, Steele KE, Stem M, Fleming RM, Schweitzer MA, Marohn MR. Long-term quality of life and risk factors for recurrence after laparoscopic repair of Paraesophageal hernia. JAMA Surg. 2015;150(5):424–31.
61. Müller-Stich B, Holzinger F, Kapp T, Klaiber C. Laparoscopic hiatal hernia repair. Surg Endosc Other Interv Tech. 2006;20(3):380–4.
62. Bais JE, Samsom M, Boudesteijn EA, van Rijk PP, Akkermans LM, Gooszen HG. Impact of delayed gastric emptying on the outcome of antireflux surgery. Ann Surg. 2001;234(2):139.
63. Tog C, Liu D, Lim H, Stiven P, Thompson S, Watson D, et al. Risk factors for delayed gastric emptying following laparoscopic repair of very large hiatus hernias. BJS open. 2017;1(3):75–83.
64. Tougas G, Eaker EY, Abell TL, Abrahamsson H, Boivin M, Chen J, et al. Assessment of gastric emptying using a low fat meal: establishment of international control values. Am J Gastroenterol. 2000;95(6):1456–62.
65. Willekes CL, Edoga JK, Frezza EE. Laparoscopic repair of paraesophageal hernia. Ann Surg. 1997;225(1):31.
66. Maret-Ouda J, Wahlin K, El-Serag HB, Lagergren J. Association between laparoscopic Antireflux surgery and recurrence of gastroesophageal reflux. JAMA. 2017;318(10):939–46.
67. Exarhos D, Malagari K, Tsatalou E, Benakis S, Peppas C, Kotanidou A, et al. Acute mediastinitis: spectrum of computed tomography findings. Eur Radiol. 2005;15(8):1569–74.
68. Backer CL, LoCicero J III, Hartz RS, Donaldson JS, Shields T. Computed tomography in patients with esophageal perforation. Chest. 1990;98(5):1078–80.

32 Preoperative Planning Utilizing Imaging

Desmond Huynh and Shirin Towfigh

Inguinal Hernia: Primary Inguinal Hernia

Recommended Imaging: Ultrasound, Sometimes MRI

In the setting of primary inguinal hernia, imaging serves as an adjunct to traditional history and physical exam. We do not recommend routinely ordering imaging prior to operation of primary inguinal hernias, as history and physical examination alone have been found to have sufficient sensitivity (74.5–92%) and specificity (93%) [1, 2]. The addition of imaging may improve these numbers by a few percentage points [1].

In situations where imaging has also been done despite an obvious examination confirming inguinal hernia, the additional information can help with operative planning. For example, a CT scan showing bilateral direct inguinal hernias, an unsuspected femoral hernia, or bladder involvement in the hernia, may change the discussion you have with the patient and the technique you offer (Fig. 32.1). The use of imaging is most important in situations where a definitive diagnosis for inguinal hernia cannot be made. For example, the clinical examination may be equivocal, such as in the case of small inguinal hernias or in obese patients. Also, a patient may have groin pain due to an occult hernia, i.e., a non-palpable hernia that is symptomatic.

We recommend ultrasound as the preferred first-line study. It is quick, relatively inexpensive, proposes no radiation to the patient, and is readily accessible in most centers and cities. That said, ultrasonography is not the most sensitive study. For inguinal hernias, meta-analysis of seven studies shows a wide range of accuracy for ultrasound [3] (Table 32.1). Most studies showing high accuracy for ultrasound in inguinal hernia are performed on clinically palpable inguinal hernias, where the need for adjunct imaging is questionable. Also, many studies are performed in centers with dedicated hernia radiologists.

In our experience with patients in the community seeking consultation for groin pain or with unclear diagnosis for inguinal hernia, we have reported much poorer results from ultrasound reports (56% sensitivity, 0% specificity) [4] (Table 32.2). Further, in the case of occult inguinal hernias, we have shown that ultrasound has 33% sensitivity and 0% specificity [4] (Table 32.3). This is because the positive predictive value of ultrasound was 100%, but the negative predictive value was nil in this subset of patients. Ultrasound has also been shown to be inaccurate in identifying hernia anatomy. For

D. Huynh
Department of Surgery, Cedars-Sinai Medical Center, Los Angeles, CA, USA

S. Towfigh (✉)
Beverly Hills Hernia Center, Beverly Hills, CA, USA
e-mail: drtowfigh@beverlyhillsherniacenter.com

S. Docimo Jr. et al. (eds.), *Fundamentals of Hernia Radiology*,
https://doi.org/10.1007/978-3-031-21336-6_32

Fig. 32.1 Ultrasound (**a**), non-contrast CT scan (**b**), and non-contrast MRI (**c**) pelvis showing inguinal hernias. With ultrasound, the use of Valsalva helps identify hernias. On CT scan, the "mickey mouse" sign shown is suggestive of bilateral direct inguinal hernias. MRI is much more sensitive and here shows occult bilateral direct and left femoral hernias, with fat content

Table 32.1 Diagnostic performance of ultrasonography for the detection of inguinal hernia. Occult hernias are non-palpable, symptomatic hernias. Modified from [3]

	n	TP	FP	TN	FN	PPV, %	nPV, %	Sensitivity, %	Specificity, %
Clinically obvious	190	188	0	2	0	100 (98–100)	100 (34–100)	100 (98–100)	100 (34–100)
Mixed	715	509	31	160	15	94.3 (92–95.9)	91.4 (86.3–94.7)	97.1 (95.3–98.3)	83.8 (77.9–88.3)
Occult	401	89	32	190	13	73.6 (651–80.6)	93.6 (89.3–96.2)	87.3 (79.4–92.4)	85.5 (80.3–89.6)
Total	1306	786	63	352	28	92.6 (90.6–94.2)	92.6 (89.5–94.8)	96.6 (95.1–97.6)	94.8 (81–87.9)

Numbers in parentheses are 95% confidence intervals. *FN* indicates false-negative; *FP* false-positive, *TN* true negative, and *TP* true positive

Table 32.2 Comparison of imaging modalities for detection of non-occult inguinal hernias. Modified from [4]

			Predictive value	
	Sensitivity	Specificity	Positive	Negative
Ultrasonography	0.56	0.00	1.00	0.00
Computed tomography	0.77	0.25	0.96	0.04
Magnetic resonance imaging	0.91	0.92	0.97	0.79

Table 32.3 Comparison of imaging modalities for detection of occult inguinal hernias. Modified from [4]

			Predictive value	
	Sensitivity	Specificity	Positive	Negative
Ultrasonography	0.33	0.00	1.00	0.00
Computed tomography	0.54	0.25	0.86	0.06
Magnetic resonance imaging	0.91	0.92	0.95	0.85

example, ultrasound can accurately differentiate between medial and lateral inguinal hernia in 62%, which is only slightly more accurate than physical examination (54%) [1].

Ultrasonographic results for inguinal hernia are very user-dependent. In the United States, most ultrasounds are performed by a technician and not by a radiologist. When ordering, the surgeon should clearly request a "hernia ultrasound," and not an abdominal ultrasound, groin ultrasound, or pelvic ultrasound, as each has its own standardized protocol and will not provide appropriate evaluation for inguinal hernias. The typical protocol for a hernia ultrasound includes, at the

least, a focus on the inguinal canal. Valsalva technique is recommended, but not mandated, in most protocols [5] (Fig. 32.1). Also recommended is that the patient is asked to stand, cough, move their leg around, etc., to optimize the ultrasound results. What we have noticed more commonly is that the technician has the patient supine only and asks them to perform a valsalva maneuver; this may not be adequate. An imperfectly performed hernia ultrasound, added to a disconnect between the technician who is performing the ultrasound and the radiologist who is interpreting it, maybe the reason why we see lower value and usage of hernia ultrasound in the United States than in other countries. Regardless, since ultrasound has a high positive predictive value, no further study is required if it confirms an inguinal hernia (Fig. 32.2).

For efficiency of care, surgeons can learn to use an in-office ultrasound, coupled with their clinical examination. Many offices and clinics have point-of-care ultrasounds used by various specialists that can be shared to reduce the cost of purchasing a dedicated ultrasound. Courses to learn how to perform ultrasonography are available through various outlets, including the American College of Surgeons (https://www.facs.org/education/accreditation/verification/ultrasound).

In the case where there is a clinical suspicion for inguinal hernia, and ultrasound is negative, we recommend MRI pelvis as the next step (Fig. 32.2). We do not recommend CT scans. That said, CT scan is likely ordered more commonly in the United States due to its accessibility. In many institutions, it is more efficient to order a CT scan than even an ultrasound. CT is also the imaging study that general surgeons are most comfortable reading themselves. However, CT scans are traditionally poor studies for the pelvis and for soft tissue anatomy, and hence its low value for evaluation of inguinal hernias that are not clinically notable [6]. Our study shows that CT scan of the pelvis poorly evaluates for inguinal hernias (77% specificity, 25% sensitivity, 96% PPV, 4% NPV) [4] (Table 32.2). CT is especially poor for occult

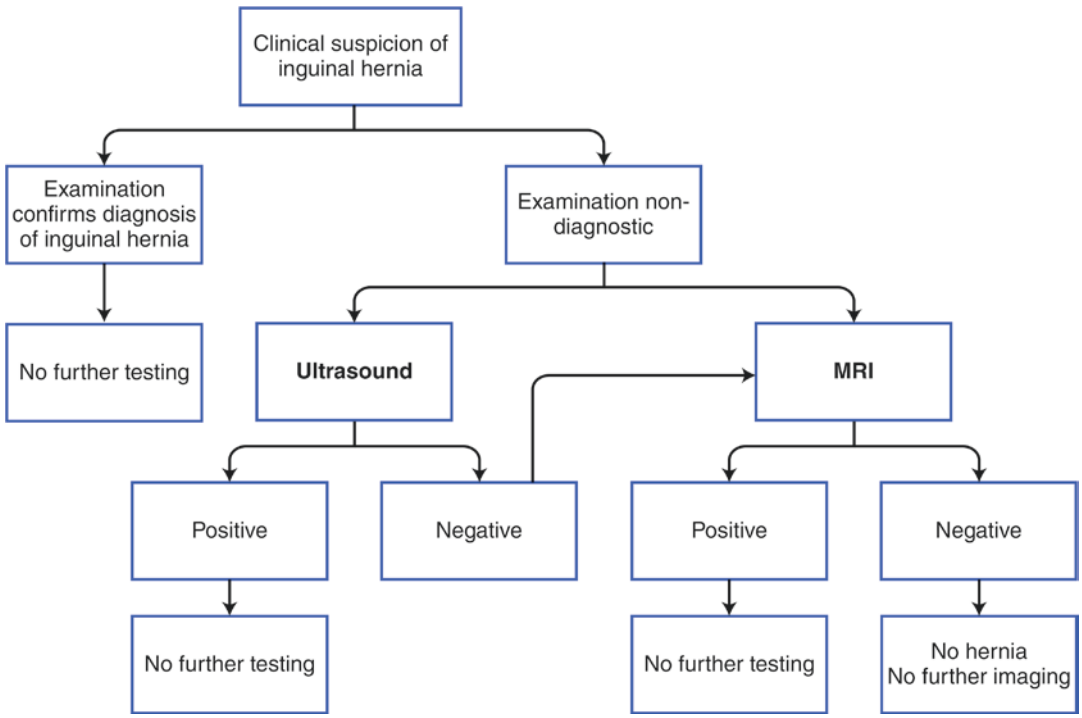

Fig. 32.2 Diagnostic algorithm for most efficient use of imaging when there is clinical suspicion of inguinal hernia

inguinal hernias, which are situations in which imaging is most valuable to confirm a clinical suspicion (54% specificity, 25% sensitivity, 85% PPV, 6% NPV) [4] (Table 32.3).

Based on our studies, we have shifted to MRI pelvis as the modality of choice for hard-to-evaluate groin pathology. MRI has been found to have diagnostic specificity of 96.3% and sensitivity of 94.5% [7]. For most clinical suspicions of inguinal hernias, our study shows MRI has 91% sensitivity, 92% specificity, with 97% PPV, and more importantly, the highest NPV, 79%, of all the imaging studies [4] (Table 32.2) For this reason, we skip CT scan and choose MRI pelvis as the next modality if ultrasound is "negative" and there remains a clinical suspicion for inguinal hernia, such as a convincing history or suggestive physical examination (Fig. 32.2).

The protocol we recommend to maximize the useful findings on MRI is provided to you here in "radiology speak" so that you can share it with your radiology team (Fig. 32.3). We recommend a non-contrast MRI of the pelvis, preferably 3 T, but 1.5 T is adequate. Both T1 and T2 images must be captured, and, importantly, all three views (coronal, axial, and sagittal) must be provided for the best evaluation. We find it is also important to add dynamic views, i.e., those with valsalva, in order to evaluate for small or occult hernias. This involves a bit more work for the technician, and more imaging for the radiologist to read, but is a valuable addition and capability of the MRI. For example, we have had multiple patients for whom the static MRI studies did not show a hernia, but the bear down views with valsalva were able to demonstrate a small inguinal hernia, which was clinically significant (Fig. 32.1). At some more advanced institutions, the bear down views of the MRI may also be provided as a video loop. These are fun and educational to view, but often not necessary if the pictures of the bear down views with valsalva without the video component can be provided.

Imaging findings alone should not be the sole indication for any surgical intervention.

Fig. 32.3 Beverly Hills Hernia Center dynamic MRI pelvis protocol

BEVERLY HILLS
hernia center

MRI PROTOCOL

for Non-Contract Dynamic MRI Pelvis
for Imaging of Occult Inguinal Hernias

1. For all of our groin pain MR studies, we have the patient place a fiducial marker on the site of pain.
2. We prefer 3Tesla MRIs, though 1.5T is acceptable. Open MRIs are not acceptable, as they lose resolution for the pelvis.
3. The following are then acquired:

- Axial, sagittal, and Coronal T2 HASTE with breath hold
- Axial, sagittal, and Coronal T2 HASTE with valsalva
- Single-slice sagittal plane dynamic valsalva acquisitions - typically about 5 individual acquisitions, both through and on either side of the fiducial marker
- Axial T1 gradient echo
- Axial T2 fat sat (either fast-spin echo or STIR depending on the machine)

The history is the most important part of the patient's evaluation. The examination is also very important, though in some situations, such as an occult inguinal hernia, the findings may be minimal, such as focal tenderness or fullness alone. There must be concordance between the history and the imaging findings, and hopefully an examination that further supports the imaging findings. This concept of double and triple concordance is seen throughout various specialties in surgery, and should also apply to hernia surgery. What we wish to minimize is operating on inguinal hernias that are asymptomatic, especially those that are not the primary cause for the patient's symptoms. This is a particular problem for inguinal hernias, as they are common and may be noted on imaging while they may be asymptomatic and not the primary cause for the patient's symptoms.

Patients with incidental imaging finding of inguinal hernia should not be automatically considered for hernia repair, as we know that watchful waiting is a safe option in male patients with asymptomatic or minimally symptomatic hernias [8]. The main exception is an asymptomatic but incidentally noted femoral hernia. It would be considered standard of care to electively repair asymptomatic femoral hernias, to protect against a relatively high rate of strangulation and death as compared to all other hernias [9] (Figs. 32.1 and 32.4). A detailed history and physical examination will help determine if the inguinal hernia noted on imaging requires surgical repair.

Inguinal Hernia: Complications, Post-inguinal Herniorrhaphy Pain, Chronic Pelvic Pain

Recommended Imaging: MRI, Sometimes CT or High-Resolution Ultrasound

Repair of an inguinal hernia may be complicated by seromas, hematomas, infection, recurrence, and chronic pain such as due to meshoma (i.e., balling of mesh), nerve entrapment. These may require another operation, and imaging plays an important role in preoperative planning.

Early Postoperative Complications

In the acute setting, most patients with pain will not require reoperation. Seromas may require aspiration, and ultrasound guidance may be helpful, especially in-office ultrasounds. Infections are fortunately uncommon and are typically superficial. A seroma will appear as a hypoechoic collection with a hyperechoic posterior margin secondary to posterior acoustic enhancement [7] (Fig. 32.5). On ultrasound, hematoma will have heterogeneity with dependent layering. This is helpful, as we typically do not aspirate or drain hematomas. It can be difficult to discriminate between a hematoma and an abscess on ultrasound sometimes, as they both demonstrate heterogeneity of fluid contents.

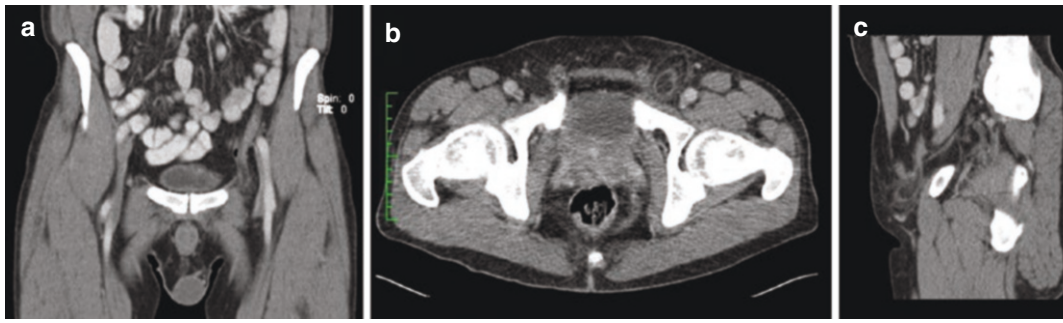

Fig. 32.4 Left femoral hernia on CT scan involving small intestine viewed in coronal (**a**), axial (**b**), and sagittal (**c**) views. Note anatomically how the bowel is under the iliopubic tract and medial to the femoral vessels

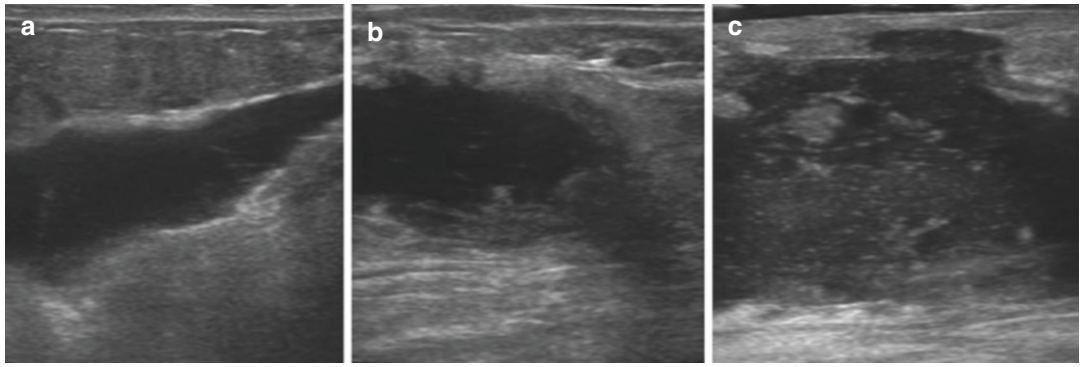

Fig. 32.5 Ultrasound findings of postoperative seroma (**a**), hematoma (**b**), and abscess (**c**) on ultrasound. Note the progression in heterogeneity in the fluid collection

If there is suspicion for a deep infection, 3D imaging is important to help rule out involvement of the mesh. CT of the pelvis can be used to help evaluate a collection, and MRI is our preferred study. Sophisticated ultrasonographers with high-resolution ultrasounds can gather good information, but that is not likely in most areas of the United States.

In the case of obvious abscesses, CT scan may be adequate for preoperative planning. Typical findings include heterogeneous collections exhibiting rim enhancement, and may contain gas or be associated with significant stranding.

Better than ultrasound and CT, MRI can provide a wider appreciation of the involvement of the repair, if any, with the infection, including any infection deep into the mesh implant. Structures deep into the mesh can be difficult to assess via ultrasound due to acoustic distortion. MRI can best visualize the mesh distinct from its surrounding soft tissue, whereas on CT scan, the mesh and surrounding tissues are similar. MRI can also better differentiate between a fluid collection, such as hematoma or seroma, versus an abscess or infected fluid collection (Fig. 32.6).

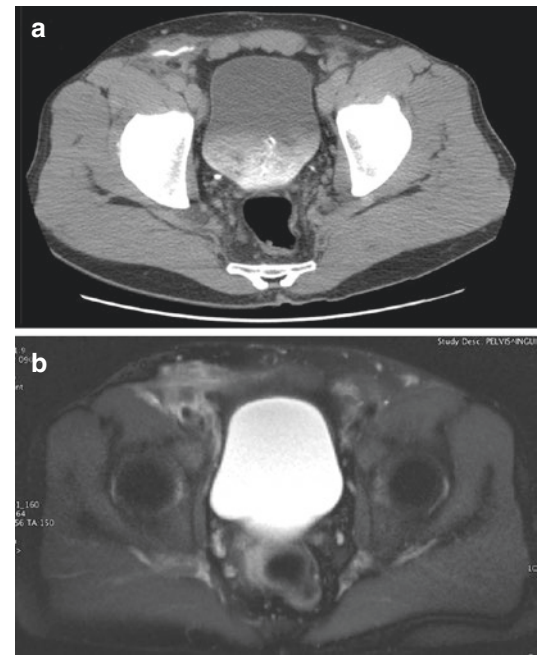

Fig. 32.6 CT (**a**) and MRI (**b**) pelvis of the same patient with infected right groin mesh. CT shows ePTFE mesh very distinctly bright. The surrounding soft tissue was interpreted on CT as "normal postoperative changes." MRI correctly identified the soft tissue as inflamed and thus diagnosed a mesh infection

Critical Situations: Mesh Infection, Intestinal Obstruction

CT scan is best used in acute settings and for critical situations, such as in management of a significant infection or pelvic abscess. If a mesh was implanted in the index repair, the location of the infection relative to the mesh will dictate the operative plan. If there is clearly normal tis-

sue separating the mesh from the abscess, then the abscess may be treated expectantly with antibiotics and drainage. If the abscess is abutting the mesh or the mesh is within the collection, then CT will help plan the extent of surgical debridement and mesh is almost always removed in this process. However, in more subtle low-grade infections, CT scan may be interpreted as normal postoperative changes, whereas MRI will show a distinct infection of the mesh with an associated fluid collection in the soft tissue (Fig. 32.6).

Also, CT scan is valuable in the evaluation of intestinal obstruction after inguinal hernia repair. This can occur as a result of adherence to or erosion of mesh, such as a retroperitoneally placed mesh. Intestinal obstruction, as a result of an internal hernia at the site of peritoneal rent after laparoscopic hernia repair, can occur with both the totally extraperitoneal (TEP) or, more commonly, transabdominal preperitoneal (TAPP) approaches. CT scan of the pelvis with or even without oral contrast will help in the rapid evaluation of a patient with intestinal obstruction after inguinal hernia repair. IV contrast is usually not necessary and does not add to the findings or operative planning.

Post-Inguinal Herniorrhaphy Chronic Pain

In the chronic setting, imaging is an important adjunct to clinically evaluating patients. In our practice, all patients undergo imaging as part of their evaluation of post-inguinal herniorrhaphy chronic pain. This is because there are a wide variety of causes of pelvic pain and groin pain, and meticulous evaluation is necessary before undergoing any operative planning. The algorithm for evaluation and treatment of post-inguinal herniorrhaphy chronic pain is complex and lengthy and outside the scope of this Chapter.

The role of imaging is multifold: First, it helps confirm what type of operation has already been performed. Sometimes operative reports may be missing, not informative, or inaccurate. We have seen situations where there was an operative report for a Lichtenstein anterior mesh placement, whereas a posterior Kugel-type mesh repair was performed. We have also seen operative reports for laparoscopic mesh repair where they failed to note that a keyhole technique mesh repair was performed. Lastly, we have read reports noting the use of "some tacks" for securing the mesh, and yet almost 20 tacks were found on imaging. All of these details can be gathered from good imaging and will significantly impact preoperative planning.

In general, for forensic imaging of inguinal hernia repairs, we prefer MRI. As noted above, MRI can best differentiate details and subtleties of the mesh anatomy from the rest of the soft tissue. CT scan, meanwhile, often shows mesh as a similar shade of grey as that of the surrounding structures, and lightweight meshes are nearly impossible to view on most CT scans. One notable exception is ePTFE; this mesh, though uncommonly used for inguinal hernias, shows as bright white on CT scan (Fig. 32.6). Ultrasound is often not useful, as the scar tissue from the hernia repair and the mesh implant can distort the acoustic signal and limit the amount of information one can gather. On the horizon is the use of high definition and 3D ultrasound in pelvic floor and pelvic mesh evaluation, and so in a few specialty centers this experience is being translated to evaluation of hernia mesh and chronic pelvic pain [10].

We recommend using the dynamic MRI pelvis hernia protocol in Fig. 32.3. MRI is capable of detecting the most common mesh materials, such as polypropylene and polyester, with surrounding fat density highlighting its location [11, 12]. Mesh is best evaluated on T1 and appear as dark linear strips slightly thicker than the surrounding fascial plane [7]. On T2 and other fluid-focused sequences, mesh is more difficult to identify. Review of imaging should rule out mesh-related problems, such as mesh folding or meshoma, and any inflammation associated with the mesh, as well as non-mesh problems, such as fluid collections and hernia recurrence. A meshoma may have a mass effect onto nearby structures, clinically presenting as pain with hip flexion (mass effect on psoas), neuropathic pain (impingement

of a nerve), and/or urinary frequency and urgency (mass effect on bladder) (Fig. 32.7).

Imaging of the mesh placement and integrity is one of the main reasons we image all patients we evaluate for post-inguinal herniorrhaphy pain. In some cases, for example, the patient may have a clinically obvious hernia recurrence, and perhaps the surgeon may not feel further evaluation by imaging is necessary. However, the recurrence may be as a result of mesh folding or meshoma, and the patient's symptoms may be related to the meshoma, not to the recurrence (Fig. 32.8). Imaging that shows both meshoma and recurrence may influence operative planning, as surgical mesh removal is the only cure for meshoma-related pain.

The dynamic nature of the MRI protocol will help identify small hernia recurrences or unstable repairs. We see this sometimes in patients undergoing laparoscopic patch repair of a large direct hernia. The patient's symptoms may recur, as the mesh billows into the direct defect. This is technically not a hernia recurrence, as the mesh repair is intact and bridges the defect. However, we consider this an unstable repair, as the mesh basically falls into the direct hernia weakness, reproducing symptoms. A dynamic image can help elucidate this problem. In general, smart use of imaging will help direct the surgeon as to the best plan of care. Again, the findings should be correlated with the clinical history.

Fig. 32.7 Left groin meshoma due to mesh plug with ipsilateral distortion of bladder as seen on axial view of CT scan with IV contrast

In addition to evaluating the mesh on imaging, it is important to take note of any fixation materials such as sutures or tacks, which may be contributing to the patient's symptoms. Either of these may be noted on MRI as circular artifacts. If the reason for chronic pain is excessive or unsafe placement of tacks (e.g., in the triangle of pain), we recommend a plain X-ray of the area (Fig. 32.9). Of course, this is only helpful if the tacks are metal. Absorbable tacks will not show on plain X-ray or on CT scan. They may be found on ultrasonography or MRI, as artifacts. Imaging can help guide surgical removal of the tacks. In the case of removing metal tacks, intraoperative fluoroscopy is helpful. Imaging can also help guide any diagnostic injections and nerve blocks if there is an associated neuropathy from the tack placement.

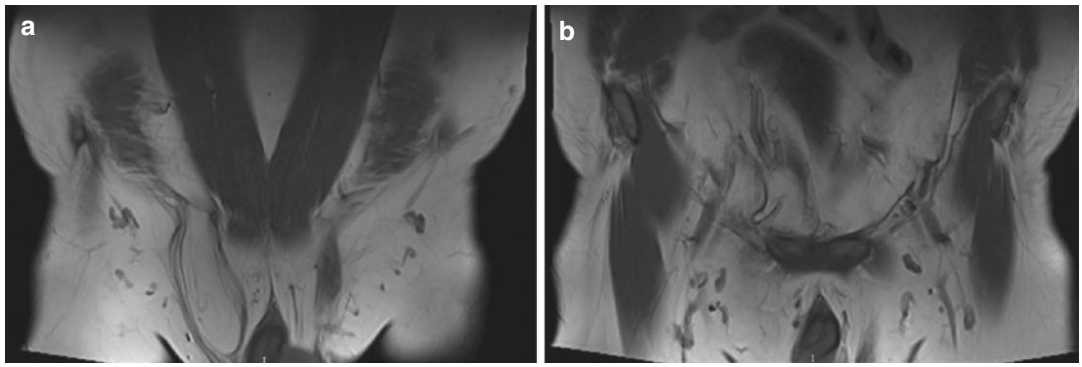

Fig. 32.8 MRI pelvis coronal view of right inguinal hernia recurrence with large preperitoneal fat extending into scrotum (**a**) due to folding of preperitoneal mesh (**b**) with possible meshoma as a cause of postoperative chronic pain

Fig. 32.9 Plain film AP pelvis radiograph following laparoscopic bilateral inguinal hernia repair demonstrating a large number of spiral metal tacks, many in the triangle of pain

Neuropathic Complications

During inguinal hernia repair, the vulnerable nerves are the iliohypogastric, ilioinguinal, genitofemoral, and lateral femoral cutaneous nerves. These may be injured or entrapped by mishandling, scar, mesh, suture, or other fixation types, leading to neuropathic pain. This can include dermatomal burning and/or hypersensitivity. Though challenging to perform and interpret, high definition, 3D ultrasound, and MR neurography can help evaluate these small peripheral nerves. On routine non-contrast MRI, the nerve entrapment, perineural fibrosis, and neuroma will appear as T2 hyperintensity within the nerve. This is more likely if there is a significantly large neuroma. If routine MRI findings are equivocal or require further interrogation, MR neurography may be helpful. These are highly specialized imaging modalities, use a 3 T magnet, and suffer from low signal-to-noise ratios[7].

In our practice, we have foregone the routine use of MR neurography. This is because clinical findings, and response to nerve blocks, are almost always diagnostic; we have noted no added value to imaging the nerves themselves. In situations where a hernia specialist is not able to evaluate the patient, then such imaging, with positive findings, may help lead the patient toward seeking treatment aimed at the nerves involved.

Chronic Pelvic Pain

In challenging cases of chronic pelvic pain, MRI not only serves as a highly effective means for detecting inguinal hernia but also provides imaging of the entire pelvis and thus other disorders that can cause pelvic pain. This includes an initial evaluation of the hip joints and the muscles of the hip girdle and pelvis. It will also show some intra-pelvic diseases, such as that of rectum, bladder, and gynecologic organs, and soft tissue disorders. MRI pelvis can also help identify disorders that can confound an evaluation of groin pain and hernia, such as hip labral tear, femoroacetabular impingement, iliopsoas tendonitis, hip bursitis, osteitis pubis, avascular necrosis of the femoral head, and various pelvic and hip girdle tendinopathies and strains, including that of the adductor and rectus muscles. With the dynamic imaging protocol, laxity of the pelvic floor may also be noted, such as with ligamentous laxity and pelvic floor organ prolapse (rectocele, cystocele, enterocele), all of which can cause groin and pelvic pain.

Ventral Hernia: Primary Ventral Hernia

Recommended Imaging: CT Scan, Sometimes Ultrasound

For evaluation of primary ventral hernias, our imaging modality of choice is CT scan. It can be ordered with or without oral contrast and often does not require IV contrast unless you are concerned about intestinal ischemia or an infectious

process. The CT scan can be ordered with or without valsalva. For ventral hernias, most are evident without valsalva and so valsalva should only be used in cases of occult hernias.

In general, imaging is helpful for most ventral hernias as an adjunct to the physical examination. The exception would be small simple umbilical or epigastric hernias, where the clinical decision-making is straightforward and imaging is almost never necessary. Information gathered from a CT can help guide operative planning. For example, it will help quantify the dimensions of the defect, the girth of the associated muscles, whether there is an associated rectus diastasis, and insight into sac content (e.g., intestine, omentum, preperitoneal fat).

In some situations, the surveillance of other abdominal pathology may also be helpful. For example, in the situation of a large or complex abdominal wall hernia, a significant finding of gallstones, a hiatal hernia, or massive intra-abdominal or retroperitoneal fat may prompt the surgeon to delay elective hernia repair. Perhaps in these situations, the surgeon should address other medical problems, such as biliary colic, acid reflux, and obesity, respectively, as examples.

In planning ventral hernia repair, the two major questions to be answered in the decision-making process include: a) what operative approach should I take, and b) do I need mesh, and if so, which one and what size? The first data point to help make these decisions is defect size. This is easily and accurately measurable on CT scan. The most important measurement is the maximum defect width, as most guidelines show defects up to 1 cm do not need mesh and defects 6 cm or greater require some sort of separation of abdominal wall components in order to close the defect. If the defect is wide, then CT scan evaluation of the girth of the abdominal muscles will help determine if the patient is a good candidate for a component separation, for example. In patients with thinned muscles, anterior component separation results in even further attenuation and weakness of the abdominal muscles, and a posterior transversus abdominis release may therefore be preferred. Similarly, if the CT scan shows the hernia to be within a wide rectus diastasis, that information may change the operative plan for a primary repair, as the risk of failure may be higher (Fig. 32.10). In this situation, perhaps the use of mesh, performing a plication of the diastasis, or even considering a concomitant abdominoplasty would be a better long-term option for the patient, with a lower risk of hernia recurrence at the thinned linea alba.

For some primary hernias, their characterization on CT scan may be diagnostic and thus will clarify the diagnosis. For example, evaluation of an enigmatic abdominal fullness may show on CT scan to be a Spigelian hernia, with intact external oblique muscle. Other rarer hernias, such as lumbar, perineal, and sciatic hernias, may be best characterized and diagnosed by CT scan (Figs. 32.11 and 32.12). The preoperative planning for these rare hernias is critical, as open vs. laparoscopic vs. robotic approaches are well described, and mesh choice and placement is critical to the best outcomes. Repair of these hernias involves knowledge of anatomy and critical structures nearby, and imaging is a useful guide for this.

Ultrasound is another option for imaging of a ventral hernia. This is an easily performed procedure in the office, if available. It can quickly quantify the dimensions of a small umbilical or epigastric hernia or the width of a suspected rectus diastasis. The benefit of ultrasonography is that it can be a dynamic study. In areas of unclear pathology, ultrasound can be useful to elicit valsalva maneuvers to identify an occult hernia.

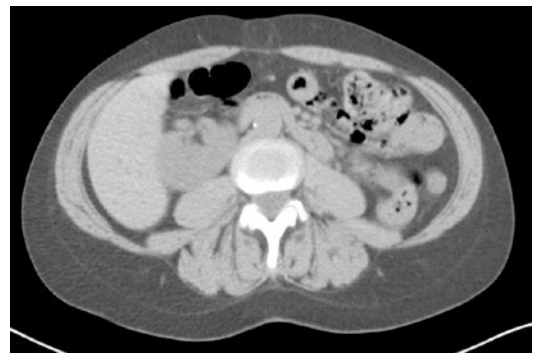

Fig. 32.10 Fat-containing epigastric hernia noted within a rectus diastasis on CT scan abdomen, non-contrast, axial view

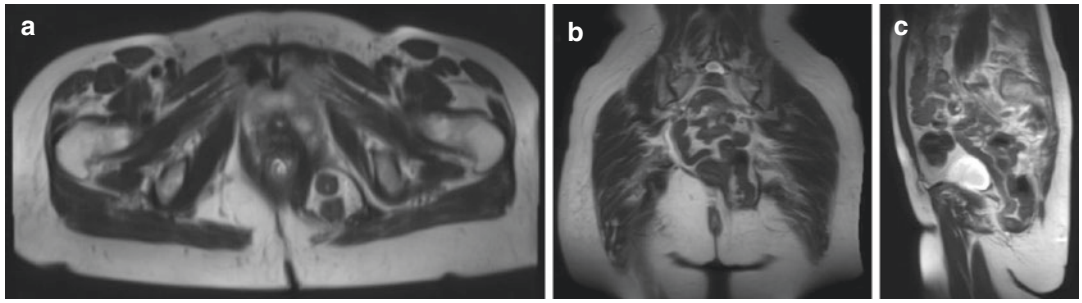

Fig. 32.11 Left perineal hernia with intestinal content as noted on MR pelvis scan axial (**a**), coronal (**b**), and sagittal (**c**) views. Dynamic studies with Valsalva can help accentuate pelvic hernias

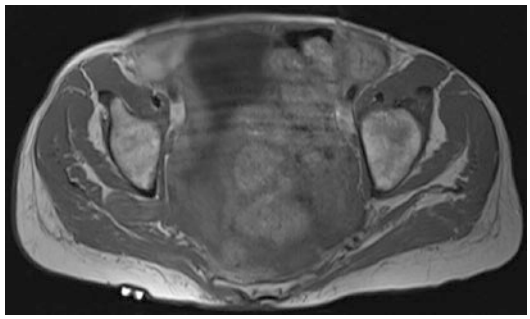

Fig. 32.12 Right sciatic notch hernia with small intestine content, noted in a patient with complaint of sciatic pain and fullness, MRI pelvis axial view. Note the radio-opaque marker over right upper buttock

Nevertheless, in larger or more complex hernias, the findings from a CT scan far outweigh those from ultrasonography.

MRI is an option for three-dimensional abdominal wall hernia surveillance without imposing the risk of radiation. However, most MRI protocols of the abdomen or pelvis are not performed to optimize abdominal wall pathology and thus are inadequate for ventral hernia assessment. For ventral hernia purposes, the MRI must be ordered as an anterior soft tissue study, and without contrast.

Ventral Hernia: Incisional Hernia

Recommended Imaging: CT Scan

For reoperative ventral hernias, i.e., incisional hernias, preoperative imaging plays an even more important role in preoperative planning. We recommend that all patients with incisional hernias undergo imaging prior to hernia repair. The data gathered is important for preoperative planning, mostly to optimize the decision-making toward the best surgical approach so that the patient has the lowest risk of yet another recurrence and of other complications.

CT scan will identify not only the dimensions of the hernia and the muscle girth, as described with primary ventral hernia evaluation, but it may also help assess why there was a hernia recurrence. This is valuable information when planning revisional surgery. Preoperative CT scanning will show the mesh, if present, and whether it pulled away, buckled, or is bellowing into the defect or a rectus diastasis (Figs. 32.13 and 32.14). It will also determine whether there are other hernias that are missed on physical examination, such as in Swiss cheese-type incisional hernias. Importantly, it will also help assess the intestines or other nearby organs. This is valuable information in revisional surgery, to reduce the risk of intestinal injury when approaching the hernia. It will also identify failures from a prior repair so that your technique can be modified to best address that (Fig. 32.13).

As with reoperative inguinal hernias, the first step in approaching a revisional ventral hernia repair is to completely understand the prior repair. Operative reports may not be available or may be inadequate or misleading in their reporting. In some situations, for example, operative reports may claim components separation, but imaging shows indeed no separation was per-

Fig. 32.13 Recurrent incisional hernia of the left flank with fat content, posterior to the left kidney, CT scan axial view. Note the failure of the intraperitoneal mesh at its most posterior extension and the multiple tacks that delineate the repair

Fig. 32.14 CT axial view of abdominal bulging. This is status post a mesh-based midline hernia repair. The midline mesh, barely visible, is billowing into the defect. Technically, there is no hernia recurrence, as the defect has been bridged, but the patient likely does not have a flat abdominal wall contour

formed. This is valuable information in order to plan the next operation.

Attempts have been made to objectively predict the surgical technique and the required size of mesh by using preoperative CT scan imaging. In 2018, Carbonell et al. showed that a Rives-Stoppa technique for ventral hernia repair would be sufficient if the sum of the widths of the patient's rectus abdomini at least equals twice the width of the defect, as measured on CT. In most patients, this means defects up to 10 cm wide can be repaired via retrorectus mesh repair [13]. However, some patients have retracted muscles and may require further lengthening, such as with preoperative chemodenervation (e.g., with botulinum toxin injections) or with a more extensive components separation operation (e.g., anterior Ramirez or posterior transversus abdominis release). This information, mostly gathered from imaging, can help with informed consent of the patient as well as operative timing and planning with the operating room team.

Patients with defects measured to be 10 cm or greater may present with concurrent loss of domain[11]. While there is some inconsistency in the literature, loss of domain is typically defined as hernia in which the sac contains 50% or more of the abdominal contents. This is best measured via CT scan axial views (Fig. 32.15). To provide the best chance of successful closure and repair in these patients, the surgeon may choose preoperative adjunctive therapies, such as progressive preoperative pneumoperitoneum and chemodenervation, (e.g., via botulinum toxin injections).

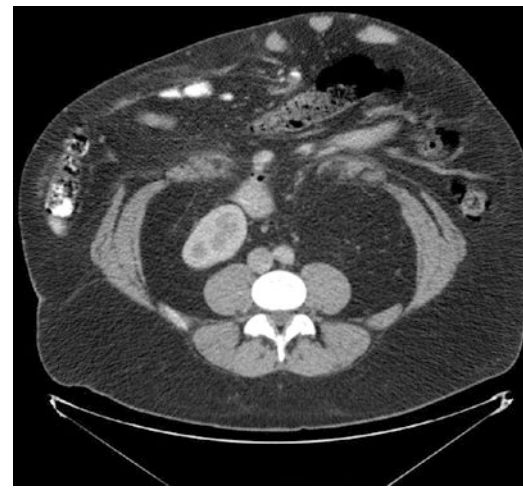

Fig. 32.15 CT axial view of a patient with incisional hernia and loss of domain. Note that more than 50% of the abdominal contents are extra-abdominal and there is a large amount of preperitoneal fat

The appearance of mesh on CT depends on the mesh material. In general, heavyweight mesh and ePTFE mesh are the most readily visible, whereas, lightweight mesh can be more difficult to see [11, 12, 14–16]. CT scan allows for the evaluation of the position of the mesh in relationship to hernia as well as to other internal organs, such as the intestines, bladder, and stomach. Most mesh will appear on CT scan as a thin body in distinct contrast to surrounding fat. The mesh may also be wrinkled or have a non-anatomic contour, which helps differentiate it from the surrounding structures.

Complications: Fluid Collections, Chronic Pain

In situations where there are complications, such as a seroma, mesh infection, intestinal obstruction, or intestinal fistula, CT scan is critical in the evaluation and planning of the patient. These CTs should be performed with IV and oral contrast, to get the most information about the clinical situation. Seromas are typically homogeneous fluid collections without enhanced walls (Fig. 32.16). Findings of stranding, enhancement of the fluid wall, and fluid with gas bubbles are concerning for an abscess and/or mesh infection. Identifying the repair, the mesh, any infection, and its relationship to nearby organs will help plan and follow the patient after treatment (Fig. 32.17).

To evaluate for modes of fixation, such as tacks, CT scan may be helpful (Fig. 32.18). Tacks may be a source of pain, especially if overused, and so imaging of the tacks is useful in preoperative planning of abdominal wall pain after hernia repair. X-ray is the best mode for evaluation of permanent tacks. Absorbable tacks are not visible on X-ray or CT scan, but may be visible as an artifact on some MRIs.

Fig. 32.17 Mesh is visible as a thin white line on this CT axial view. Note the fluid collections anterior and mostly posterior to the mesh. There are gas bubbles in the fluid, consistent with an infected fluid collection associated with the mesh, and thus also a mesh infection

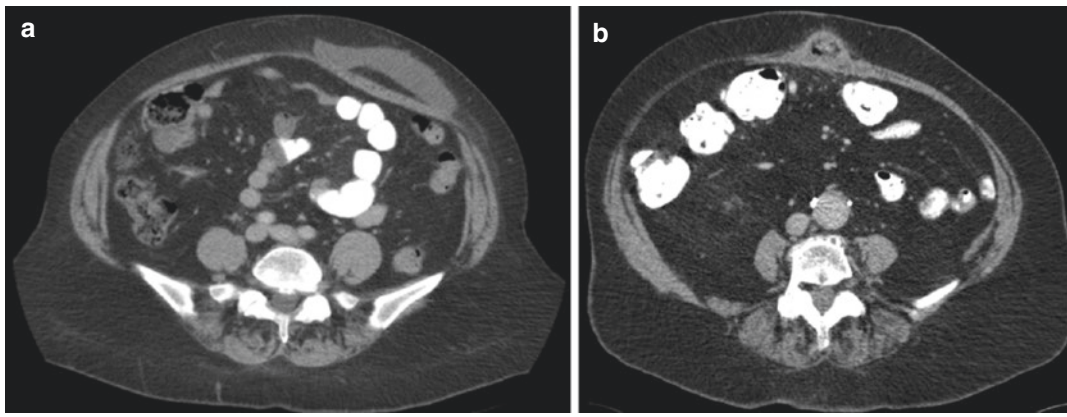

Fig. 32.16 CT with oral contrast axial views of postoperative seroma (**a**) and abscess (**b**) Note homogeneous fluid collection with the seroma (**a**) in comparison to the findings of gas, wall enhancement, and mesh involvement with the abscess (**b**)

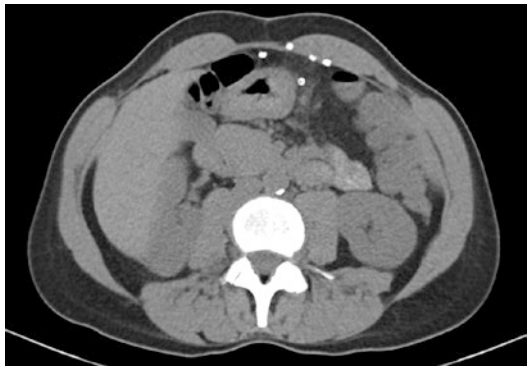

Fig. 32.18 Ventral hernia repair with mesh and tacks. Metal tacks are best noted on CT scan. Note also the diastasis, difficulty in identifying the intraperitoneal mesh on CT, and the one tack that has fallen away from the repair

Conclusion

Imaging is an important component of preoperative planning for hernia repairs. In straightforward situations, such as an obvious inguinal hernia or small primary umbilical hernia, a physical examination is often adequate. In most other situations, judicious use of imaging can help the surgeon plan for the best plan of care tailored to the needs, circumstances, and anatomy of the patient. Understanding the strengths and weaknesses of different imaging modalities (e.g., X-ray, US, CT, MRI) for inguinal and ventral hernias and how to order them to best answer a clinical question will allow the surgeon to devise an advanced plan of care.

References

1. Kraft BM, Kolb H, Kuckuk B, et al. Diagnosis and classification of inguinal hernias. Surg Endosc. 2003;17(12):2021–4. https://doi.org/10.1007/s00464-002-9283-y.
2. van den Berg JC, de Valois JC, Go PM, Rosenbusch G. Detection of groin hernia with physical examination, ultrasound, and MRI compared with laparoscopic findings. Invest Radiol. 1999;34(12):739–43. https://doi.org/10.1097/00004424-199912000-00002.
3. Robinson A, Light D, Nice C. Meta-analysis of sonography in the diagnosis of inguinal hernias. J Ultrasound Med. 2013;32(2):339–46. https://doi.org/10.7863/jum.2013.32.2.339.
4. Miller J, Cho J, Michael MJ, Saouaf R, Towfigh S. Role of imaging in the diagnosis of occult hernias. JAMA Surg. 2014;149(10):1077–80. https://doi.org/10.1001/jamasurg.2014.484.
5. Hashimoto BE, Abramson SJ, Coley BD, Harris RD, Hernanz-Schulman M, Newman B, Sinow RM, Sun MR, Diacon L, Estroff JA, Paushter DM. AIUM practice guideline for the performance of an ultrasound examination of the abdomen and/or retroperitoneum. J Ultrasound Med. 2012;31(8):1301–12. https://doi.org/10.7863/jum.2012.31.8.1301.
6. Laval-Jeantet M, Vadrot D, Arrive L, Buy JN. MRI of the pelvis in comparison with CT scan. Arch Int Physiol Biochim. 1985;93(5):61–6. https://doi.org/10.3109/13813458509080626.
7. Jacob BP, Springer International Publishing AG. The SAGES manual of groin pain. Springer; 2016.
8. Gong W, Li J. Operation versus watchful waiting in asymptomatic or minimally symptomatic inguinal hernias: the meta-analysis results of randomized controlled trials. Int J Surg. 2018;52:120–5. https://doi.org/10.1016/j.ijsu.2018.02.030.
9. Miserez M, Peeters E, Aufenacker T, et al. Update with level 1 studies of the European hernia society guidelines on the treatment of inguinal hernia in adult patients. Hernia. 2014;18(2):151–63. https://doi.org/10.1007/s10029-014-1236-6.
10. Ram R, Jambhekar K, Glanc P, et al. Meshy business: MRI and ultrasound evaluation of pelvic floor mesh and slings. Abdom Radiol. 2021;46(4):1414–42. https://doi.org/10.1007/s00261-020-02404-x.
11. Davis SS, Dakin G, Bates A, Society of American Gastrointestinal Endoscopic Surgeons. In: The SAGES manual of hernia surgery. 2019.
12. Rakic S, LeBlanc KA. The radiologic appearance of prosthetic materials used in hernia repair and a recommended classification. AJR Am J Roentgenol. 2013;201(6):1180–3. https://doi.org/10.2214/AJR.13.10703.
13. Blair LJ, Ross SW, Huntington CR, et al. Computed tomographic measurements predict component separation in ventral hernia repair. J Surg Res. 2015;199(2):420–7. https://doi.org/10.1016/j.jss.2015.06.033.
14. Tonolini M. Multidetector CT of expected findings and complications after contemporary inguinal hernia repair surgery. Diagn Interv Radiol. 2016;22(5):422–9. https://doi.org/10.5152/dir.2016.15578.
15. Parra JA, Revuelta S, Gallego T, Bueno J, Berrio JI, Fariñas MC. Prosthetic mesh used for inguinal and ventral hernia repair: normal appearance and complications in ultrasound and CT. Br J Radiol. 2004;77(915):261–5. https://doi.org/10.1259/bjr/63333975.
16. Fischer T, Ladurner R, Gangkofer A, Mussack T, Reiser M, Lienemann A. Functional cine MRI of the abdomen for the assessment of implanted synthetic mesh in patients after incisional hernia repair: initial results. Eur Radiol. 2007;17(12):3123–9. https://doi.org/10.1007/s00330-007-0678-y.

Iatrogenic Abdominal Wall Injuries

33

Vahagn C. Nikolian, Dina Podolsky, and Yuri W. Novitsky

Introduction

As the field of hernia surgery has expanded, the operations performed and the approaches used to restore abdominal wall anatomy have grown exponentially. These complex and diverse operations have changed the way that surgeons and radiologists interpret and evaluate imaging studies of the abdomen. In light of these significant changes, the peritoneum and abdominal wall must carefully be examined for the purposes of diagnostic accuracy and operative planning.

This text has reviewed many of the different hernias that may arise following thoracoabdominal operations. This chapter will focus on technical complications related to hernia repair and abdominal wall reconstruction. As abdominal wall reconstruction continues to evolve, it is imperative for surgeons and radiologists to recognize the potential limitations of operations as well as the common, and not so common, complications that may arise in the postoperative period.

V. C. Nikolian
Department of Surgery, Oregon Health & Science University, Portland, OR, USA
e-mail: nikolian@ohsu.edu

D. Podolsky (✉) · Y. W. Novitsky
Department of Surgery, Columbia University Medical Center, New York, NY, USA
e-mail: dp2957@cumc.columbia.edu; yn2339@cumc.columbia.edu

All members of the medical team should have a heightened awareness and index of suspicion for patients who deviate from the expected postoperative course following abdominal wall surgery. These deviations should prompt a broad differential of potential complications. Common postoperative events related to prolonged postoperative ileus, insufficient pain control, pulmonary embolus, and surgical site infections should be considered in the context of the operation. In addition, unique complications related to aspects of the operative approach, techniques in dissection, types of reconstruction, and mesh positioning should be considered. In all settings, developing an awareness of the operation performed and interacting directly with the operating surgeon can provide important information to better understand the operative field and develop more useful imaging reports [1].

Trocar Site Injuries

Minimally invasive surgery has become a routine element of surgical practice and has resulted in specific complications related to trocar access sites.

Trocar Site Bleeding

In the immediate postoperative period, the most common abdominal wall injury related to trocar

S. Docimo Jr. et al. (eds.), *Fundamentals of Hernia Radiology*,
https://doi.org/10.1007/978-3-031-21336-6_33

sites is abdominal wall bleeding related to vascular injury [2]. Following vascular injuries, anterior abdominal wall hematomas can develop because of injury to small perforating subcutaneous vessels, epigastric vessels, or injury to the well-vascularized muscle tissue itself. Diagnosis of an abdominal wall hematoma can be made by physical exam and confirmed with imaging studies. On ultrasound, a hematoma will appear as a hypoechoic area between fascial layers. If ultrasound findings are inconclusive, a CT scan can be obtained, which will show acute hematomas as high-attenuation (>30 HU) areas (Fig. 33.1). IV contrast can be given with the CT if there is a concern for ongoing extravasation, which will appear as bright areas within the collection.

Of particular concern, epigastric vascular injuries can manifest with significant blood loss. When identified, patients should be monitored with serial examinations and pressure dressings. In unstable patients, clinical focus should be turned to resuscitation and establishing control of bleeding via interventional radiology or surgical interventions, such as transfascial sutures or surgical clips.

Fig. 33.1 Acute intramuscular hematoma (solid arrow) from trocar site used for transabdominal preperitoneal inguinal hernia repair. No active extravasation from inferior epigastrics were identified

Trocar Site Dehiscence

Though rare in the immediate postoperative period, trocar site dehiscence will occur for general surgical populations in as many as 5.2% of cases [3]. Dehiscence will occur in the acute period, prior to sealing of the peritoneum. In these scenarios, the abdominal contents will protrude through a defect in the peritoneum and fascia, with overlying epidermis preserved. In contrast, port site evisceration can occur when both the fascia and the skin over the defect open. On imagining, this will present with either fat or viscera protruding through the trocar site. When the acute dehiscence involves incarcerated viscera, an immediate return to the operating room to repair the defect is required in order to prevent intestinal strangulation.

Trocar Site Hernia

Just as with all incisions, trocar sites are at risk to develop into incisional hernias. Of all series of cases, the extraction site for cholecystectomy is most often associated with trocar site hernias [4]. Different factors have been evaluated including pyramidal shape, larger trocar size (greater than 10 mm), patient age, obesity, and protracted operative times being associated with development of trocar site hernias [3, 5]. For patients presenting with abdominal pain at the site of trocar sites, careful evaluation for contents including fatty tissue and bowel can help to coordinate the urgency of any intervention. For patients with bowel involvement and symptoms, emergency surgery is necessary to prevent bowel compromise. In contrast, herniation of fatty tissue may not require an emergent operation.

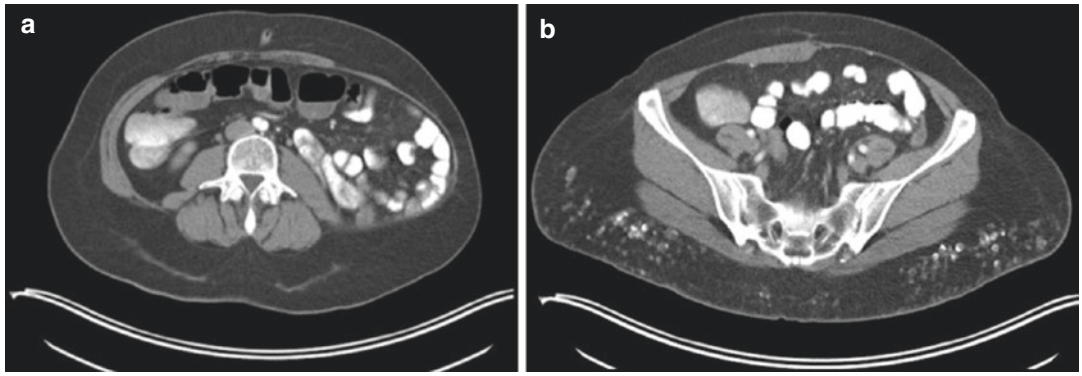

Fig. 33.2 Denervation injuries presenting for evaluation for suspected hernia. (**a**) Denervation injury of left lateral musculature, possibly related to spinal stenosis. (**b**) Denervation injury to left rectus muscle from prior flank incision related to urologic procedure

Denervation Injuries

The abdominal wall is innervated primarily from the ventral rami of T6/7 and L1. The nerve bundles run in the transversus abdominis plane, penetrating the posterior lamella of the internal oblique just medial to the semilunar line to innervate the rectus abdominis. So-called semilunar line injuries, caused primarily by surgeries that work in both the medial and lateral compartments of the abdominal wall, frequently lead to devastating denervation injuries via nerve transection. The muscle groups that are injured depend on the level of injury.

On imaging, the denervated muscle will appear atrophic and thin compared to non-injured muscle. Frequently there is significant laxity of the muscle. When the lateral muscle groups are denervated, this laxity can result in a "bowing out" of the abdominal wall, appearing like a hernia but without a clear fascial defect (Fig. 33.2). In other instances, there will be a clear defect in the semilunar space through which viscera protrude, developing into an iatrogenic semilunar line hernia.

Semilunar Line Injuries

Repair of semilunar line injuries can be difficult with variable success. While it is impossible to restore nerve function, there are different techniques to establish normal abdominal wall anatomy. The semilunar line can be reestablished via the anterior or posterior approach, and reinforced with mesh in either the intraperitoneal, preperitoneal, or onlay positions. Patients should be aware that while anatomy may be restored, function of the affected muscle groups will remain disabled (Fig. 33.3).

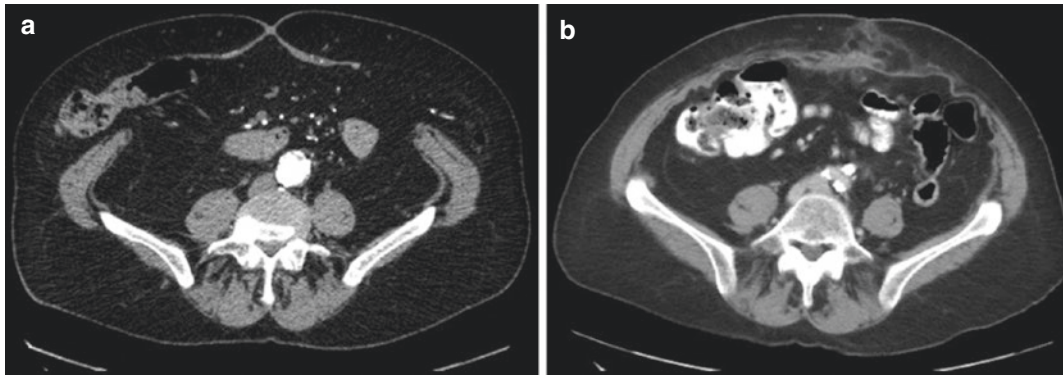

Fig. 33.3 Bilateral semilunar line injuries following attempted robotic posterior component separation via transversus abdominis release. (**a**) Free floating, denervated rectus abdominis muscles with retracted lateral abdominal musculature. (**b**) Imaging following complex abdominal wall reconstruction with retromuscular mesh and repair of bilateral semilunar lines

Mesh Complications

No discussion on hernia repair and abdominal wall reconstruction would be complete without a discussion of mesh complications. Studies have demonstrated that mesh reinforcement results in lower recurrence rates than suture-based repair [6]. When considering the optimal mesh, surgeons aim to reinforce hernia repairs with mesh that demonstrates good bacterial clearance, reduced foreign body reaction, and improved tissue ingrowth [6, 7]. Mesh reinforcement can be placed in a variety of planes within the abdominal wall. For those reviewing imaging and attempting to clinically correlate and communicate findings, the hernia community has recently developed a consensus classification system that attempts to establish standardized nomenclature related to planes of the abdominal wall [8] (Table 33.1). Adoption of these terms should help improve communication between clinicians.

Table 33.1 Anatomic descriptions of anterior abdominal wall planes [8]

Name of plane	Anatomic description
Onlay	Anterior: subcutaneous tissue Posterior: anterior rectus sheath and external oblique
Anterectus	Anterior: anterior rectus sheath Posterior: rectus abdominis muscle
Inlay	Mesh attached to edges of hernia defect with no overlap
Interoblique	Anterior: external oblique muscle Posterior: internal oblique muscle
Retro-oblique	Anterior: interior oblique muscle Posterior: transversus abdominis
Retrorectus	Anterior: rectus abdominis muscle Posterior: posterior rectus sheath
Retromuscular	Anterior: rectus abdominis (medial); transversus abdominis muscle (lateral) Posterior: posterior rectus sheath (medial); transversalis fascia (lateral)
Preperitoneal	Anterior: transversalis fascia Posterior: peritoneum
Intraperitoneal	Anterior: peritoneum Posterior: abdominal cavity

A variety of fluid collections can develop following the placement of reinforcing mesh. When assessing the fluid collections, it is important to understand the study modality and clinical presentation to make a radiographic diagnosis. It is common to encounter postoperative seromas, hematomas, abscesses, and inflammatory reactions in the vicinity of mesh. Seromas will often develop following the repair of abdominal wall hernias as a result of dissection of abdominal tissue planes. Seroma formation rates are proportionally related to the extent of dissection and the size of the original hernia. Seromas are comprised of blood and lymph fluid and are generally managed conservatively. The vast majority of these fluid collections will resolve without interventions. On imaging, seromas will demonstrate

a thin or imperceptible wall with minimal enhancement [9]. The fluid will be ill-defined and will be near the previously dissected hernia sac site or newly implanted mesh. If fat from the surgical dissection is left in the space, one may be able to identify floating locules within the serous fluid. Though it is tempting to aspirate these fluid collections, efforts should be made to avoid interventions unless the seroma is persistent, increasing in size, symptomatic, or there are concerns for infection. In contrast to a simple fluid collection, infected seromas will have a thickened, well-vascularized wall, surrounding inflammation, and the patient may demonstrate clinical signs of infection [10]. Infection following hernia repair is variable and dependent on multiple factors including wound classification, operative approach, complexity of repair, necessity for bowel resection, and type of mesh utilized during repair.

Hematomas will develop in the postoperative period and will often be associated with surgical technique. Hematomas are commonly encountered following retroumuscular dissection (e.g., transversus abdominis release) (Fig. 33.4). On imaging, these collections will be hyperdense on CT scan and heteroechoic on ultrasound. In the setting of inguinal hernia repairs, spermatic cord hematomas will often present and self-resolve over the course of weeks [10]. Hematomas with active extravasation of blood may need surgical evacuation to establish hemostasis.

Mesh-induced visceral complications are a recognized limitation of intraperitoneal mesh placement. Laparoscopic ventral hernia repair with Intraperitoneal onlay mesh has become one of the most common operations performed by general surgeons. This technically straightforward operation allows for the identification of abdominal wall anatomy, reduction of herniated contents, and subsequent placement and fixation of a large overlapping mesh circumferentially around hernia defects. Following positioning, the mesh is fixated to the abdominal wall with transfascial sutures or tracking devices. Surgeons have been encouraged to approach hernias in this manner due to the relatively low recurrence rate (<10%) [11] and in vivo data supporting the concept that implantable mesh is viscerally compatible [12]. In spite of these promising outcomes, mesh-related visceral reactions, adhesions, fistulae, and migrations are commonly reported outcomes following intraperitoneal mesh placement (Fig. 33.5) [13, 14]. To counteract some of these issues, approaches related to extraperitoneal mesh placement have been developed and are continuously being revised [15].

Mechanical mesh failure has emerged as an entity in hernia surgery over the course of the last decade. Often associated with lightweight mesh, mechanical mesh failure results when the tensile strength of the mesh is overcome by the stress and force exerted on the mesh by the abdominal wall

Fig. 33.4 Retromuscular hematoma following ventral hernia repair with posterior component separation. Given the size of hematoma and concern for tension on posterior fascial closure, percutaneous drain was placed to evacuate hematoma

Fig. 33.5 Recurrent incisional hernia with evidence of previous laparoscopically placed. Arrow identifying permanent tack on lateral aspect of mesh. Minimal mesh-intestinal interface in preoperative imaging. At time of surgery, evidence of mesh erosion into small intestine necessitating bowel resection

and underlying viscera [16]. Central mesh failure results in herniation of abdominal contents through defects in the mesh and has been reported in as much as 22% of open ventral hernia repairs [17] (Fig. 33.6). Mesh fractures and failures have also been associated with mesh bridges over unclosed hernia defects, sites of transfascial sutures, and surgical site infections [18].

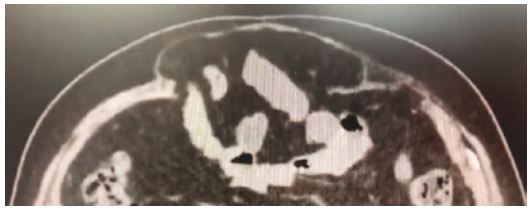

Fig. 33.6 Central mesh failure following ventral hernia repair with posterior component separation of placement of retromuscular polypropylene mesh

Interparietal Herniation

Given the potential issues related to intra-abdominal mesh, surgeons have developed alternative approaches to allow for extraperitoneal mesh placement. Ventral and inguinal hernia repairs using principles established by Rives [19] and Stoppa [20] allow for access into the retrorectus and preperitoneal space, respectively. The mesh is placed in an extraperitoneal position after reestablishing a visceral sac. Defects in the posterior layer must be identified and repaired to ensure that there is no opportunity for intra-abdominal viscera to herniate into the potential space between the mesh and the posterior closure (Fig. 33.7) [21]. Such interparietal hernias require a high index of suspicion to diagnose and treat. If identified, one must make a decision to either perform a laparoscopic repair (oftentimes with

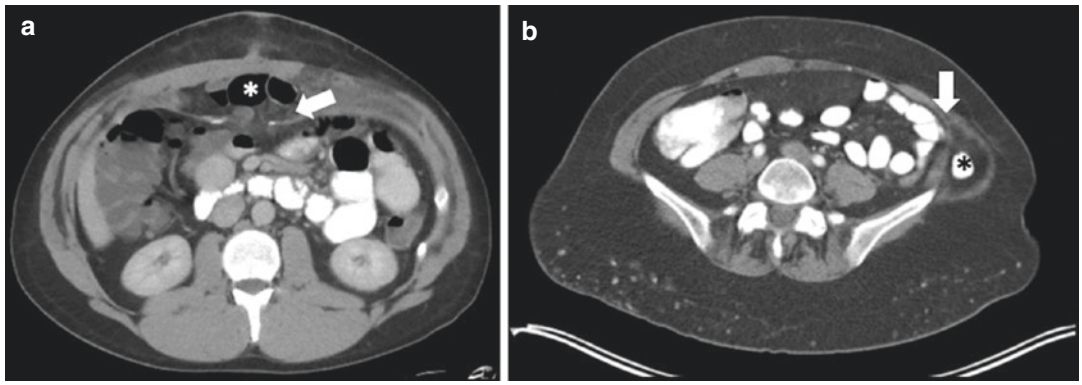

Fig. 33.7 Interparietal hernias. (**a**) Acute interparietal hernia following ventral hernia repair with retrorectus mesh placement. Patient was taken back emergently for revision of repair and further myofascial release via posterior component separation. Solid arrow demonstrating posterior fascial breakdown with incarcerated segment of small intestine. (**b**) Chronic interparietal hernia following open nephrectomy. Solid arrow defines fascial defect in the posterior lamella of internal abdominal oblique with herniated small intestine between transversus abdominis and internal abdominal oblique

intraperitoneal onlay mesh to reinforce the posterior defect) or to reexplore the wound via the original incision—which is a more involved operation and will require multilayered closure of the abdominal wall [22].

Conclusion

The last decade has seen significant advances in our understanding and appreciation of the abdominal wall. Hernia surgery incorporates a variety of operative approaches to treat hernia defects. Given these changes, iatrogenic injuries to the abdominal wall must be identified to allow for appropriate operative planning and patient care.

References

1. Patil AR, Nandikoor S, Mohanty HS, Godhi S, Bhat R. Mind the gap: imaging spectrum of abdominal ventral hernia repair complications. Insights Into Imaging. 2019;10(1):40.
2. Antoniou SA, Antoniou GA, Koch OO, Pointner R, Granderath FA. Blunt versus bladed trocars in laparoscopic surgery: a systematic review and meta-analysis of randomized trials. Surgical Endoscopy. 2013;27(7):2312–20.
3. Swank HA, Mulder IM, la Chapelle CF, Reitsma JB, Lange JF, Bemelman WA. Systematic review of trocar-site hernia. The British Journal of Surgery. 2012;99(3):315–23.
4. Uslu HY, Erkek AB, Cakmak A, et al. Trocar site hernia after laparoscopic cholecystectomy. Journal of Laparoendoscopic & Advanced Surgical Techniques. Part A. 2007;17(5):600–3.
5. Hindman NM, Kang S, Parikh MS. Common postoperative findings unique to laparoscopic surgery. Radiographics. 2014;34(1):119–38.
6. Burger JW, Luijendijk RW, Hop WC, Halm JA, Verdaasdonk EG, Jeekel J. Long-term follow-up of a randomized controlled trial of suture versus mesh repair of incisional hernia. Annals of Surgery. 2004;240(4):578–83; discussion 583–575
7. Orenstein SB, Saberski ER, Kreutzer DL, Novitsky YW. Comparative analysis of histopathologic effects of synthetic meshes based on material, weight, and pore size in mice. The Journal of Surgical Research. 2012;176(2):423–9.
8. Parker SG, Halligan S, Liang MK, et al. International classification of abdominal wall planes (ICAP) to describe mesh insertion for ventral hernia repair. The British Journal of Surgery. 2020;107(3):209–17.
9. Tonolini M. Multidetector CT of expected findings and complications after contemporary inguinal hernia repair surgery. Diagnostic and Interventional Radiology. 2016;22(5):422–9.
10. Tonolini M, Ippolito S. Multidetector CT of expected findings and early postoperative complications after current techniques for ventral hernia repair. Insights Into Imaging. 2016;7(4):541–51.
11. Barbaros U, Asoglu O, Seven R, et al. The comparison of laparoscopic and open ventral hernia repairs: a prospective randomized study. Hernia. 2007;11(1):51–6.
12. McGinty JJ, Hogle NJ, McCarthy H, Fowler DL. A comparative study of adhesion formation and abdominal wall ingrowth after laparoscopic ventral hernia repair in a porcine model using multiple types of mesh. Surgical Endoscopy. 2005;19(6):786–90.
13. Losanoff JE, Richman BW, Jones JW. Enterocolocutaneous fistula: a late consequence of polypropylene mesh abdominal wall repair: case report and review of the literature. Hernia. 2002;6(3):144–7.
14. Steinhagen E, Khaitov S, Steinhagen RM. Intraluminal migration of mesh following incisional hernia repair. Hernia. 2010;14(6):659–62.
15. Nikolian VC, Coleman NL, Podolsky D, Novitsky YW. Robotic-assisted transabdominal Preperitoneal ventral hernia repair. Surgical Technology International. 2020;36:95–7.
16. Warren JA, McGrath SP, Hale AL, Ewing JA, Carbonell AM. 2nd, Cobb WSt. Patterns of recurrence and mechanisms of failure after open ventral hernia repair with mesh. The American Surgeon. 2017;83(11):1275–82.
17. Petro CC, Nahabet EH, Criss CN, et al. Central failures of lightweight monofilament polyester mesh causing hernia recurrence: a cautionary note. Hernia. 2015;19(1):155–9.
18. Lintin LA, Kingsnorth AN. Mechanical failure of a lightweight polypropylene mesh. Hernia. 2014;18(1):131–3.
19. Rives J, Pire JC, Flament JB, Palot JP, Body C. Treatment of large eventrations. New therapeutic indications apropos of 322 cases. Chirurgie. 1985;111(3):215–25.
20. Stoppa RE. The treatment of complicated groin and incisional hernias. World Journal of Surgery. 1989;13(5):545–54.
21. Davis JR, Villarreal JE, Cobb WS, Carbonell AM, Warren JA. Interparietal hernia complicating retromuscular ventral hernia repair. The American Surgeon. 2016;82(7):658–9.
22. Carbonell AM. Interparietal hernias after open retromuscular hernia repair. Hernia. 2008;12(6):663–6.

End-Stage Hernia Disease

34

Joseph A. Mellia, Jaclyn T. Mauch, and John P. Fischer

Section 1: Introduction

An increasing number of patients have complex hernias requiring surgical management and repair. The central goal of hernia repair is to provide a stable, long-lasting closure of the abdominal wall defect that restores abdominal wall function and improves quality of life (QoL). In medicine, "terminal" or "end-stage" refers to a disease that cannot be adequately treated and is likely to progress without abatement. Despite there being well-established conceptual frameworks for end-stage diseases, such as heart failure and chronic kidney disease, no definition exists for end-stage hernia disease. In the author's opinion, end-stage hernia is a complex hernia in which repair is unlikely to improve abdominal wall function and QoL. Diagnosis of end-stage hernia is inherently a subjective assessment that depends on surgeon-specific skill sets, experience, and estimated likelihood of improvement, which is often based on surgeon intuition. Open dialogue with the patient is critical to guiding surgeon judgement. Questions such as "What would you do differently if this were repaired?" help understand the patient's goals and expectations. With these in consideration, the surgeon assesses the patient to determine whether the abdominal wall can or cannot be successfully reconstructed, the latter suggesting a terminal, end-stage condition.

Through careful review of prior operative reports, collection of patient history, and physical exam, surgeons assess risk within three domains to aid the decision-making process: patient characteristics (comorbidities, overall health), defect characteristics (size, number of defects, soft tissue stability), and abdominal wall function/QoL. From our experience, increased risk within one category is acceptable, usually resulting in a successful surgical repair. However, increased risk within two or more categories anecdotally increases the likelihood of an end-stage hernia, which is not amendable to surgical repair. Analysis of cross-sectional radiographic images

Supplementary Information The online version contains supplementary material available at https://doi.org/10.1007/978-3-031-21336-6_34.

J. A. Mellia
Division of Plastic Surgery, University of Pennsylvania Health System, Philadelphia, PA, USA

Division of Plastic Surgery, Mount Sinai Health System, New York, NY, USA
e-mail: Joseph.Mellia@mountsinai.org

J. T. Mauch
Division of Plastic Surgery, University of Pennsylvania Health System, Philadelphia, PA, USA

Division of Plastic Surgery, University of Michigan Health System, Ann Arbor, MI, USA
e-mail: Mauchja@med.umich.edu

J. P. Fischer (✉)
Division of Plastic Surgery, University of Pennsylvania Health System, Philadelphia, PA, USA
e-mail: John.Fischer2@pennmedicine.upenn.edu

S. Docimo Jr. et al. (eds.), *Fundamentals of Hernia Radiology*,
https://doi.org/10.1007/978-3-031-21336-6_34

greatly aids physical evaluation, promoting more accurate diagnosis, better goal-setting, and improved communication with patients. However, our current understanding of radiographic features predictive of key functional and QoL outcomes in hernia is limited. Notably, radiographic images are unable to capture dynamic aspects of the abdomen and abdominal wall compliance, a critical measure of the likelihood of successfully achieving a fascial defect closure. To date, surgeons have no proven, reliable method of identifying end-stage hernia patients until attempted surgical repair fails, in some cases worsening the patient's condition.

In Fig. 34.1, we present a patient whose complex hernia may be considered end-stage on the basis of both significantly impaired health condition and defect size. He was a 28-year-old male with a past medical history of multiple gunshot wounds to the abdomen. At the time of initial presentation, he underwent an emergent exploration of his abdomen with splenectomy and left nephrectomy, in addition to a small bowel resection with right ileocecectomy. The patient's initial presentation was profound for hemorrhagic shock, and he subsequently coded, requiring a left thoracotomy for control. His postoperative course was complicated by a small bowel obstruction, multiple episodes of sepsis, severe malnutrition, hypothyroidism, renal failure requiring dialysis, intra-abdominal abscesses, DVT, and the development of enterocutaneous fistula. Additionally, the patient had an open abdomen and underwent a split-thickness skin graft. He subsequently lost significant abdominal domain. On CT scan (Video 34.1 and Fig. 34.2), his abdominal wall was fibrosed with limited soft tissue and an enterocutaneous fistula. At presentation, the patient's chief complaint was severe, chronic hernia-related abdominal pain that made him unstable when standing and walking.

Fig. 34.1 Preoperative (left) and postoperative (middle, right) photo of a 28-year-old male with potential end-stage hernia

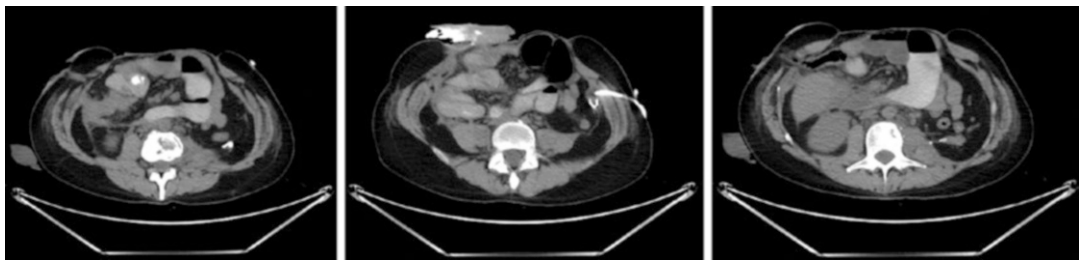

Fig. 34.2 Preoperative axial abdominal CT images of a 28-year-old male with potential end-stage hernia in Fig. 34.1

As a result of this complicated medical/surgical history and significant loss of domain, the patient in Fig. 34.1 required complex abdominal wall reconstruction to close his abdominal wall defect. Despite having significant risk within 2 of the 3 aforementioned domains, patient characteristics (impaired overall health status) and defect characteristics (loss of domain, fibrosed abdominal wall), the decision to operate was made based on the potential for improvement in abdominal wall function and QoL in the young man. Preoperatively, he underwent botulinum denervation of the lateral muscles. Intraoperatively, he required complete anterior component separation with onlay biosynthetic mesh. His postoperative recovery went smoothly, with only a small amount of delayed healing. Gastrointestinal continuity was established and at 12 months follow-up there was no evidence of a hernia recurrrence. The patient reported decreased chronic pain and was highly satisfied with his results. Overall, his repair was successful.

The patient presented in Fig. 34.1 represents an extremely complex, borderline end-stage hernia. There is no clear definition for "complex hernia," but it generally refers to increased risk within one of the following categories: patient medical history, hernia size and location, contamination and soft tissue, and clinical scenario [1]. Patient medical history includes risk factors for wound healing (i.e., obesity, diabetes mellitus, age), prior wound dehiscence, prior mesh infection, and increased intra-abdominal pressure [1]. In regard to size and location, defect width greater than or equal to 10 cm; parastomal, lumbar, lateral, and subcostal locations; and loss of domain greater than or equal to 20% make a hernia complex [1]. In regard to contamination and soft tissue, CDC class III or IV wounds, full-thickness abdominal wall defects, distorted anatomy, and denervation further increase complexity [1]. The patient in Fig. 34.1 had a complex hernia due to his complicated medical/surgical history, large defect with significant loss of domain, presence of contamination, and skin graft on bowel. Despite the favorable outcome of his repair, an alternative scenario in which the surgery failed, resulting in complications such as surgical site infection (SSI) and early hernia recurrence with no improvement in QoL would not have been surprising. Complex hernia is generally a multifactorial surgical problem in which surgical repair outcomes are variable and difficult to predict.

Achieving optimal outcomes in complex hernia repair has persisted as an elusive goal and a major challenge in the field of abdominal wall reconstruction (AWR). A set of techniques that have advanced the field for managing large, complex cases is the component separation technique. In the author's opinion, a component separation is a surgical maneuver that involves separation and or release of a muscle/fascial layer in the abdominal wall to medialize muscle/fascia and or access optimal planes for placement of mesh. Component separation techniques are generally categorized as anterior component separation (ACS) or posterior component separation (PCS) based on the anatomical location of the myofascial release. ACS techniques include multiple approaches that expose and divide the external oblique muscle and/or aponeurosis [2], while PCS exposes and divides the transversalis fascia and/or transversus abdominis muscle. In the setting of large, complex hernia defects, these techniques allow for restoration of structural and functional integrity of the abdominal wall, provision of stable soft tissue coverage, and optimization of esthetic appearance. Despite the potential advantages, component separation technique is associated with adverse outcomes and, in many patients, does not successfully repair the hernia. SSIs occur in up to 40% of patients [3–5] and recurrence occurs in 4–10% of component separations with mesh and 18.2% overall [4]. When a component separation technique is unsuccessful in providing a stable, long-lasting repair of the abdominal wall, the patient may be considered at or progressing toward end-stage.

Failure to prevent recurrence leads to a chronic, highly morbid disease state that progresses to end-stage hernia in a subset of patients. Flum et al. first called attention to this chronic disease cycle in 2003 with a publication detailing progressively higher 5-year cumulative frequencies of reoperation after each subsequent repair [6]. Specifically, Flum et al. found a 23.8%, 33.6%, and 38.7% reoperative frequency after the second, third, and fourth repairs, respectively [6]. Moreover, Flum et al. found that the length of reoperation-free time was progressively shorter

after each subsequent repair (Fig. 34.3) [6]. In 2015, Holihan et al. found that the previous number of ventral hernia repairs independently predicted recurrence and reoperation [7]. Furthermore, the authors described alarmingly high recurrence and repair rates. In their study, after 140 months, the recurrence rates for primary repair, secondary repair, tertiary repair, and quaternary repair were 37.5%, 66.4%, 67.5%, and 73.3%, respectively (Fig. 34.4) [7]. This progression toward the increased likelihood of surgical failure is likely where many end-stage hernias come from.

This sequence of repair, complications, reoperation, and increasingly complicated re-repairs has been conceptualized as a "vicious cycle" [7], often leading to end-stage hernia. This morbid health state has been shown to impair QoL and function [8–11]. The purpose of surgical repair with component separation technique is to minimize morbidity and prevent progression through this cycle. We propose a definition for "end-stage hernia," which has thus far been subjectively determined by surgeons on the basis of three key elements: patient characteristics (comorbidities, overall health), defect characteristics (size, num-

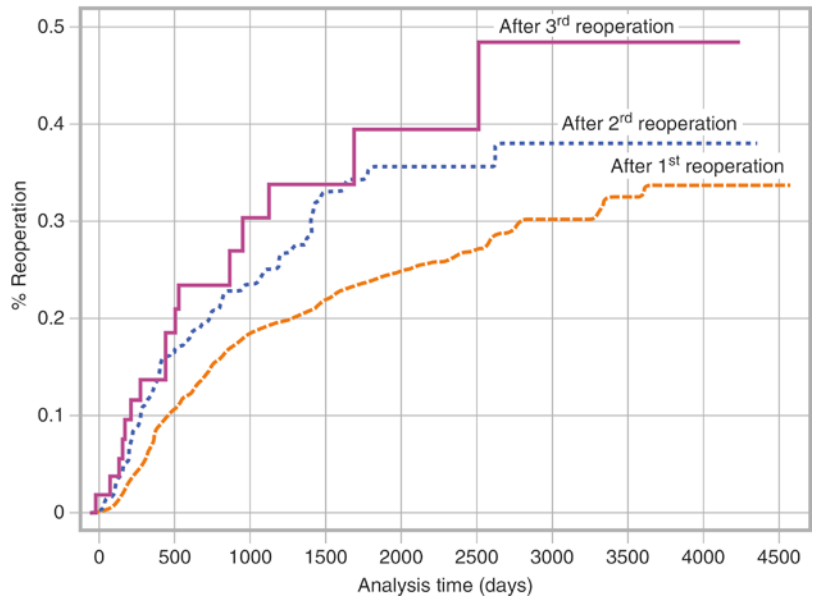

Fig. 34.3 Rate of reoperation after each subsequent repair, modified from Flum et al. [6]

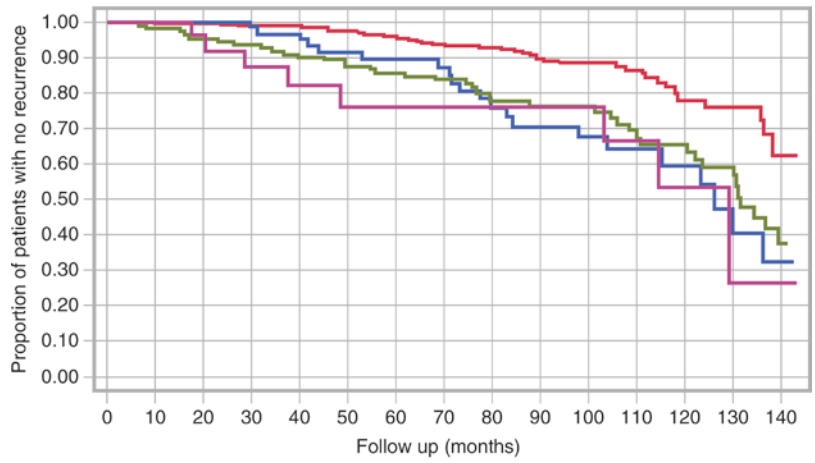

Fig. 34.4 Kaplan-Meier curve for hernia recurrence adapted from Holihan et al., $p < 0.001$ [7]. Red line, PVHR, primary ventral hernia repair; green line, IHR1, first time incisional hernia repair; blue line, IHR2, second time incisional hernia repair; purple line, IHR3, third time or greater incisional hernia repair

ber of defects, soft tissue), and abdominal wall function/QoL. We define end-stage hernia as a complex hernia with such a high degree of risk across these domains that even advanced techniques of surgical repair will fail, with no overall improvement in abdominal wall function/QoL. Currently, surgeons have no reliable method of determining whether or not a hernia is end-stage until an attempted repair fails.

In this chapter, we will explore the dynamic changes in both abdominal wall muscular function and QoL throughout the hernia disease process—from index abdominal operation to hernia formation, and through multiple repairs—in order to better understand this aspect of end-stage hernia disease. Additionally, will provide an overview of advanced analysis of radiographic abdominal wall images as a tool used in preoperative assessment, surgical planning, and outcome prediction, highlighting this technology's potential to inform a surgeon's judgment on whether a given abdominal wall defect is reconstructable or at end-stage.

Section 2: Anatomy and Function of the Abdominal Wall

To introduce the topic of abdominal wall muscular function in end-stage hernia, we present the case of a 62-year-old female with a past medical history significant for acid reflux, gout, hypertension, hypothyroidism, and fibromyalgia, who presented with a hernia recurrence following six repairs, including mesh placement (Fig. 34.5). Index surgery was a laparoscopic gastric banding complicated by bowel injury. In addition to chronic pain, the patient complained of impaired mobility, including difficulty rising from a supine position and instability when standing and walking. The patient had worked as a school crossing guard but has been home on disability for the past year. She reported a 50 lb. weight gain since the onset of her hernia, which she attributes to difficulty remaining physically active. Additionally, she had chronic irritation of her lower abdomen from hidradenitis suppurativa. Lastly, she had a prior transverse panniculectomy, with a residual

Fig. 34.5 Preoperative (left) and postoperative (right) photo of a 60-year-old male with potential end-stage hernia

Fig. 34.6 Preoperative axial abdominal CT images of a 62-year-old female with a potential end-stage hernia in Fig. 34.4

pannus and significant contour irregularity of the soft tissue of the abdominal wall.

On preoperative CT scan, there was concern that significant abdominal wall musculature atrophy and fibrosis would decrease abdominal wall compliance (Video 34.2 and Fig. 34.6), impeding successful primary closure thereby increasing the propensity for wound healing complications, recurrence, and further impairment of mobility. Ultimately, the patient's defect was repaired with an anterior component separation. In addition, she had a concurrent panniculectomy and an exploratory laparotomy to investigate her recurrent small bowel obstructions. It was found that she had extensive adhesions and mesh adherent to small bowel, requiring bowel resection and explantation of mesh. The patient's recovery was uneventful, without any postoperative complications and no recurrence at 1-year follow-up. She reported an improvement in mobility as evidenced by decreased difficulty rising from bed. However, her instability while standing/walking was not noticeably improved. Overall, the patient was satisfied with the outcome.

Normal Anatomy of the Abdominal Wall

In order to understand structural function of the abdominal wall in end-stage hernia, it is important to first understand normal functional anatomy of the abdominal wall. The abdominal wall is a complex unit of muscles that facilitates trunk movement and stability [12]. Normal function depends on the dynamic interplay among four muscles: the rectus abdominis (RA), external oblique (EO), internal oblique (IO), and the transversus abdominis (TA). The RA originates from the symphysis and inserts in the xiphoid process, ribs 5, 6, and 7. The RA mainly flexes the trunk. While the EO originates from the lower eight ribs and inserts in the iliac crest and the pubic bone, the IO originates from the anterior two-thirds of the iliac crest and the lateral two-thirds of the inguinal ligament and inserts on the three lower ribs. Together, EO and IO rotate the trunk and perform lateral flexion. The innermost muscle of the abdominal wall is the TA. It originates from the thoracolumbar fascia, the lower six costal cartilages, the anterior two-thirds of the iliac crest, and the lateral two-thirds of the inguinal ligament and inserts in the linea alba. Primarily, TA is responsible for retaining abdominal contents. It is also important for the generation of intra-abdominal pressure necessary for forced expiration. Structurally, all four muscles of the abdominal wall are held together via the rectus sheath. The rectus sheath is a fascial layer that surrounds the RA and is created by medial insertions of the EO, IO, and TA. The dorsal lamina of the rectus sheath runs from the costae to approximately 4 cm caudal to the umbilicus. Overall, muscle layers of the abdominal wall, connected via the rectus sheath, act synergistically to enable dynamic movement of the trunk [12].

Evaluation of Abdominal Wall Function

In patients with IH, strength of the abdominal wall is used to evaluate function. In studies that have quantitatively assessed strength, dynamometers have been used to measure the force of truncal flexion and/or extension [13]. For instance, in the *Biodex® isokinetic dynamometer (Biodex Corporation, Shirley, NY, USA)* system, the patient is strapped to a chair and performs dynamic truncal muscular flexion and/or extension at a predetermined constant angle speed. The measurable outcome of this movement is peak torque, which is the force generated around the axis, measured in Newton meters. In a comparison of truncal force differences between healthy volunteers and patients with IH defect measuring >10 cm, *Biodex®* showed significant validity and reliability [14]. Largely equivalent to the *Biodex®* system, *Cybex® dynamometer (Lumex Inc., Ronkonkoma, NY)* is another device used for mechanical measurement of truncal muscular flexion and/or extension force. However, it has not been validated in patients with IH and has not been used as extensively as *Biodex®* in this patient population [12].

In addition to dynamometers, clinical exams act as qualitative assessments, which are more cost-effective, accessible tools to assess abdominal wall function in patients with IH. Three different physical tests, double-leg lowering, trunk raising, and supine reaching, have been used to assess truncal strength in patients with IH [15]. Although pre- and postoperative tests were not compared, double-leg lowering and trunk raising were reproducible tests, suggesting that both may offer reliable, objective ways of determining changes in abdominal wall function following IH repair [15]. A 10-point abdominal wall function score has been created based on Parker et al.'s study, but it has yet to be validated.

Janda's test is a simiar clinical exam [16]. In this test, the patient is placed in the supine position with immobilized lower extremities. The patient is then asked to raise the trunk and keep a straight position. A perfect score of five indicates full trunk raise with hands touching the ears and elbows spread laterally. A score of zero indicates no trunk raise and no palpable muscle contraction. To our knowledge, this test has not been validated in patients with IH. While clinical exams are acceptable, cost-effective methods of assessing strength, they seem suboptimal to dynamometers, which provide objective, quantitative measures. The benefit of Janda's tests and similar clinical exams over dynamometers is their accessibility.

Herein, abdominal wall strength (AWS) will be used as a general term, meant to encompass all of the ways that force of the abdominal wall is measured. Furthermore, strength of specific muscles of the abdominal wall will not be discussed. This is because any measurement of AWS represents the composite effect of several muscle layers of the abdominal wall. For instance, dynamometry measures the combined truncal flexion strength that the abdominal wall muscles exert against the force sensor in a given direction, not the strength of RA alone, which is primarily responsible for this motion. Thus, in the case of truncal flexion weakness, the full scope of the compromise to the RA cannot be estimated. The true detriment is likely masked by the EO and IO, which act as synergists in this movement. As we explore the relationship between end-stage hernia and AWS, the inability to isolate abdominal wall muscles is a limitation.

Abdominal Wall Strength (AWS) and Incisional Hernia (IH)

AWS may play a role in hernia occurrence, the first step in the chronic, unrelenting disease process that leads to end-stage hernia. After midline laparotomy, the weakest point in the abdominal wall is usually the incisional scar, hence herniation at this location (i.e., incisional hernia). This was demonstrated when a vertical midline incision was associated with selective weakness of truncal flexion at 6 weeks following elective colorectal surgery [17]. Moreover, increased scar length was predictive of decreased truncal flexion strength [17]. Vertical midline incision through linea alba is not the only type of incision associ-

ated with decreased AWS. In fact, chevron incisions resulted in seven times more atrophy of the RA compared with midline incisions [18]. This is likely because chevron incisions involve greater manipulation and trauma to the RA. Similarly, in a study of patients undergoing infrarenal aortic repair, those with a paramedian incision demonstrated significantly more RA atrophy than those with a flank incision [19]. Altogether, these studies solidify an association between abdominal incision and muscular atrophy, which can be explained by two hypotheses. First, physical transection and manipulation of muscle fibers during surgery lead to muscle loss. Second, incising the abdominal wall musculature causes trauma to or transection of the intercostal nerves, leading to denervation and subsequent atrophy. RA atrophy measured by decreased cross-sectional area is associated with decreased AWS [20], but an association between RA atrophy and subsequent IH has not been proven in humans. In rats, however, musculature atrophy following midline laparotomy reduces abdominal wall compliance thereby transferring load forces to the midline wound [21]. This is a promising mechanism by which RA atrophy, a clear, well-studied consequence of abdominal incision, may contribute to IH pathogenesis in humans.

Once formed, IH may decrease AWS via anatomical disruption as opposed to histology changes. In patients with giant ventral hernias (> 10 cm wide), like the patient in Fig. 34.5, clinically measured hernia area was inversely correlated with AWS [22]. Jensen et al. compared RA tissue from patients with and without large midline IH and demonstrated comparable histology between groups. First, capillary density was the same in both groups. There were no significant differences in the number of capillaries per RA type I fiber or type II fiber, indicating no effect of IH on RA vascular supply. Normal vascularity is possibly a favorable condition for successful midline repair. Second, RA fiber-type distribution was similar between groups. A minor difference was that IH patients had a higher percentage of type I/IIa fibers compared with controls. This minor difference in fiber-type composition may be explained by previous surgical incision in the IH group, resulting in denervation of the skeletal muscle, which has been shown to increase the proportion of type I/IIa fibers [23]. The authors concluded that any potential clinical consequence of this change in fiber-type distribution was negligible. Since histology of the RA was comparable in patients with and without midline IH, decreased function of the RA may be primarily caused by mechanical dysfunction of the muscle, secondary to lateral displacement and loss of insertion point in the linea alba in IH. It is unknown whether decreased AWS (decreased RA function) increases the propensity for recurrence and ultimate progression to unfixable, end-stage hernia disease. Nonetheless, Jensen et al.'s findings highlight the importance of restoration of abdominal wall anatomy, specifically midline reconstruction, for optimal surgical repair [10, 12, 24].

Abdominal Wall Strength (AWS) Following Incisional Hernia (IH) Repair

Surgical restoration of the RA may improve AWS even in complex hernia patients with a history of multiple repairs. In comparison to normal, healthy controls, den Hartog et al. showed that IH patients have decreased AWS, even up to 6 years after operation. However, compared to baseline, patients with IH recuperate AWS following repair [10, 24]. The predominant theory is that medial repositioning of RA restores AWS. When necessary, component separation techniques are used to achieve medial approximation of the fascial edges, allowing for closure under tension. In patients undergoing posterior component separation (Rives-Stoppa technique complimented with TA release), restoration of the linea alba was associated with increased AWS measured at 6 months after operation. Similarly, a two-layered suture repair with medial approximation of the RA resulted in higher truncal AWS compared to the laparoscopic technique, in which the RA remains laterally displaced [25]. In the only prospective, case-control study in this area of research, patients with large IH demonstrated improved AWS at 1-year follow-up after IH repair with linea alba restoration [10], further signifying the importance of midline approxima-

tion. There were a couple of notable strengths of this study. First, since there was no change in hand strength or leg extension strength, the abdominal wall is responsible for the improvement in AWS, rather than an overall improvement in physical activity. More importantly, patients in the present study had large IHs (> 10 cm transverse diameter), likely including recurrent IHs, which indicates that reduction with midline approximation may improve AWS even after multiple repairs.

Improvement in AWS following linea alba restoration may stem from beneficial anatomical changes. In a rat model, disuse atrophy has been shown to reverse with IH repair [26]. By reconstructing the midline, reloaded muscles recovered to a near-normal state with regards to the size of the muscle and fiber-type distribution. These findings have been supported in humans using CT image analysis. Specifically, midline approximation with components separation resulted in expansion of the RA, atrophy of the EO, and presumed compensatory hypertrophy of the IO and TA [27]. Similar to anterior component separation, repair with TA release resulted in hypertrophy of the RA, EO, and IO [28]. On the other hand, bridging repair during laparoscopic repair did not result in any changes in the abdominal wall muscles. These findings suggest that recreation of the midline leads to improved anatomy of the abdominal wall, in addition to positive compensatory changes of the lateral abdominal wall musculature. Future studies are needed to determine the functional implications of these changes, especially their impact on AWS.

Restoration of the abdominal wall anatomy may even be more important than mesh placement in restoring AWS. At 1-year follow-up for giant IH repair using onlay, sublay, or intraperitoneal mesh placement, there was no difference in AWS among groups [29]. The authors highlighted several possible theories behind this finding. First, while sublay placement provides good postoperative comfort for the patient, it may naturally involve more denervation, subsequently weakening the abdominal wall. Second, although nerves are well preserved with onlay technique, patients experience a stiffer abdominal wall, making trunk movement difficult. Lastly, when intraperitoneal technique is used, multiple hernias are usually present, which possibly weakens the abdominal wall. The plane of mesh placement does not impact AWS. Whether or not mesh repair in general impacts AWS remains to be studied, especially in end-stage hernia patients undergoing multiple, complex repairs.

Conclusion

We define end-stage hernia disease as a hernia with such a high degree of complexity that repair with advanced techniques will fail. In regard to structural function of the abdominal wall, failure of repair means persistent or worsened hernia-related changes in the abdominal wall musculature, such that measurable AWS does not improve. In order to better understand this aspect of end-stage hernia disease, we explored the dynamic changes in abdominal wall structural function throughout the disease process from index abdominal operation to hernia formation, and through multiple repairs.

In summary, we demonstrate a compelling sequence of events, starting with an initial laparotomy that leads to RA atrophy and abdominal wall fibrosis, which reduces compliance of the abdominal wall and decreases AWS. Once IH forms, lateral displacement of the RA as opposed to histological changes are responsible for continued weakness. Midline approximation of the RA improves AWS following surgical repair, even in the setting of multiple previous repairs. This improvement is accompanied by significant pathological changes, including compensatory hypertrophy of several abdominal muscles, but the clinical relevance of this finding is unknown. If anything is like the heart muscle, the clinical outcome may resemble that of hypertrophic cardiomyopathy, in which the heart continuously remodels to temporarily maintain cardiac output, but ultimately fails [30]. Overall, these findings align with our definition of end-stage hernia by suggesting there is a point at which structural and functional damage to the abdominal wall musculature cannot be significantly restored with surgical repair.

The patient presented in Fig. 34.5 helps place this concept in proper context. The patient's complaint of impaired mobility (difficulty rising from bed) suggests impaired abdominal wall truncal flexion strength and stability. On preoperative CT, atrophy/fibrosis of abdominal wall musculature raised concern for noncompliance, which could have led to the transfer of load forces to the wound healing surface after surgical repair, increasing the propensity for a failed repair. Fortunately, this was not the case, and this seemingly end-stage hernia was successfully repaired without complications and an improvement in abdominal wall flexion, as evidenced by the patient's reported improvement in the ability to rise from bed. However, not all patients with similar complex hernia profiles have the same outcome. Identifying end-stage hernias in the preoperative phase will be crucial in providing better management of complex hernia patients in the future.

Section 4: Patient-Reported Quality of Life

To introduce our discussion of QoL as it pertains to end-stage hernia, we present a 48-year-old man with a large, recurrent incisional hernia (Fig. 34.7). At 18-years old, the patient had a Roux-en-Y gastric bypass, which was complicated by a bleeding ulcer requiring surgery. Approximately 10 years ago, the patient had a small ventral hernia repair with mesh. During that repair, an enterotomy occurred, leading to a prolonged ICU stay. Eventually, he underwent multiple other surgeries to try to repair this hernia, including multiple mesh implantations and excisions. During this course, he developed an enterocutaneous fistula and underwent bowel resections, a cholecystectomy, and a splenectomy. This complicated surgical course required wound vac placement and total parenteral nutrition for 2 years.

At presentation, the patient had multiple chronic open abdominal wounds and severe soft tissue attenuation in the setting of severe morbid obesity. Although not formally measured, the patient's quality of life was impaired, as determined by the continued need to constantly tend to his wound, unremitting abdominal discomfort and mild pain, and general dissatisfaction with his physical appearance. On CT scan, there was massive loss of abdominal wall domain (Video 34.3 and Fig. 34.8). The decision was made to repair his hernia using a posterior component separation technique with bridged biologic mesh. During the repair, the patient also underwent

Fig. 34.7 Preoperative (top) and postoperative (bottom) photo of a 60-year-old male with potential end-stage hernia

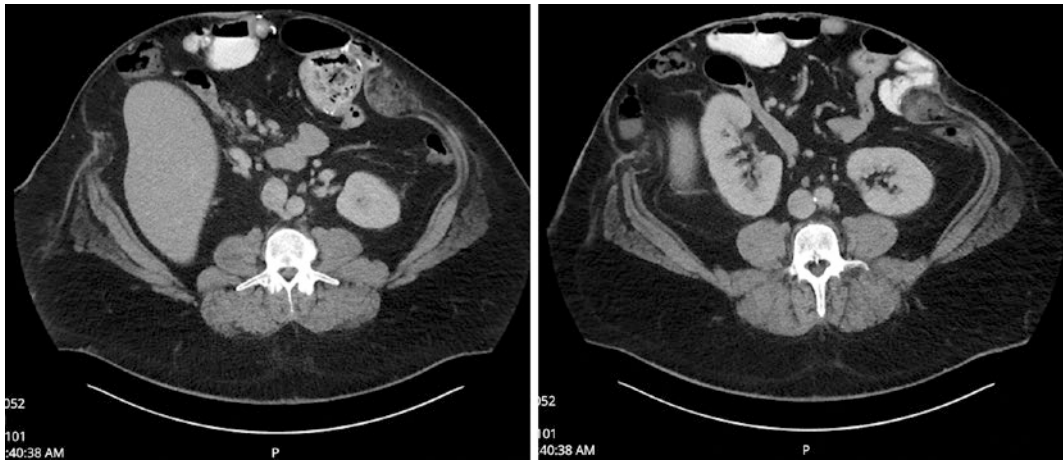

Fig. 34.8 Preoperative axial abdominal CT images of a 48-year-old male with potential end-stage hernia in Fig. 34.6

complex skin excision His postoperative course was complicated by wound dehiscence with exposed mesh, requiring washout, debridement, antibiotics, skin graft, and vac placement. At 6 months follow-up, the patient was free of recurrence, but he still had constant abdominal pain/discomfort and reported no significant improvement in satisfaction with appearance. The operation was not successful in improving his overall QoL.

Hernia-Related Quality of Life Tools

A growing body of research now details the impact that incisional hernia occurrence and repair have on patient QoL. Prior to the development of hernia-specific tools, the 12-item (SF-12) and 36-Item (SF-36) Short Form surveys were commonly used to elucidate ventral hernia-related QoL, but these forms fell short in capturing QoL domains specific to the hernia disease state [31, 32]. To address this flaw, several hernia-specific patient-reported outcomes measures were developed. These include the Hernia-Related Quality-of-Life Survey (HerQLes), Carolinas Comfort Scale (CCS), and the Abdominal Hernia-Q (AHQ) [31–33]. Each of these tools has various pros and cons. The CCS and HerQLes both focus on physical function and mesh sensation [31, 34–36], whereas the AHQ encompasses both the pre- and postoperative periods and captures a broad range of domains to include physical function, mood, body image, and preparedness for surgery [32]. Moreover, the AHQ was developed with extensive patient input, providing a valuable perspetive into the patient experience [32]. As the ventral hernia research field has yet to identify a standardized method for measuring patient QoL, the following discussion will be informed by the spectrum of tools described above [13].

Incisional Hernia (IH) Occurrence Quality of Life

Index IH occurrence post-abdominal surgery has been shown to impact many aspects of a patient's life. As the only patient-reported outcomes tool that was developed with extensive patient partnership, the AHQ's wide range of domains demonstrates that hernia occurrence impacts pain, sleep, daily routine, independence, anxiety levels, body image, self-confidence, mesh sensation in the abdomen, and clothing options [32]. Using the SF-36 and body image questionnaire, Van Ramshorst et al. showed that patients who developed an IH after abdominal surgery, compared to those who did not, reported lower physical functioning scores and lower body image scores [9]. Subsequently, patients who undergo hernia

repair experience improved QoL, decreased pain, and improved depression [37, 38]. Furthermore, studies have found that patients with an incisional hernia benefit from repair, independent of surgical technique [39]. Though, when surgical technique and hernia size were evaluated more closely, Sando et al. noted an improvement in QoL with mesh placement only in patients with a large-sized IH, reporting improvement in pain, physical impairment, and social involvement [40]. Interestingly, with the SF-36 and CCS, Jensen et al.'s study showed that while abdominal wall reconstruction improved overall QoL, the mental component score remained unchanged [10]. Unsurprisingly, Criss et al. demonstrated that when rectus muscles showed statistical improvement by isokinetic and isometric measurements using a dynamometer, QoL improved [24].

Cycle of Incisional Hernia (IH) Repair and Quality of Life

While repair of the initial IH clearly benefits patient QoL, the chronic, unremitting nature of hernia disease has a devastating and enduring impact. The recurrence rate for primary IH repair has been found to range from 23.1% to 37.5%, underscoring the large percentage of patients who undergo an oscillating experience in their hernia-related QoL [6, 7, 41]. To complicate this matter, recurrent incisional hernias are often more complex than the primary hernia and as articulated in the introduction have a much higher rate of recurrence [42].

The literature abounds with studies detailing the deleterious effect that hernia reoccurrence has on QoL. Langbach noted that after hernia repair satisfaction decreased with both chronic pain and hernia recurrence [43]. Once recurrence does occur, Colavita et al.'s prospective study demonstrated that it is associated with pain, activity limitation, mesh sensation, and lower QoL [44]. Moreover, recurrence often leads to chronic pain and reduced function, which further reduces QoL scores [8, 45]. This predictive change in QoL with recurrence, measured through returning pain, has been used by surgeons to predict recurrence after repair, highlighting the utility of tracking patient-reported outcomes [46].

End-Stage Hernia Disease Quality of Life

As we have established that IH and recurrence reduce QoL, it follows that patients who undergo re-repair do so with a decreased baseline QoL [34, 47, 48]. Given the high likeliness of an additional recurrence after a secondary repair, these patients experience a cycle of highs and lows in their QoL scores with each recurrence, repair, and complication. Nissen et al. found that after a ventral hernia repair, previous hernia repairs predicted negative affects on QoL, potentially initiating a decline with each subsequent repair and recurrence [48]. In this way, the decrease in QoL following recurrence and decreased baseline QoL for patients undergoing re-repairs underscores the importance of avoiding recurrence in order to optimize QoL outcomes.

Conclusion

An end-stage hernia is one with such a high degree of complexity that repair with an advanced component separation technique will fail. In regard to QoL, failure of repair manifests as minimal or no improvement, associated with limited physical function, chronic pain, low body image, and depression. In this section, we explored changes in QoL throughout the course of hernia progression from hernia repair, to recurrence, and to complications, in order to better understand QoL at end-stage. The current research makes clear that repairs improve QoL, but recurrences and subsequent re-repairs have deleterious effects on a wide range of patient QoL domains, including physical functioning, mesh sensation, pain, mental health, body image, and self-confidence. The patient presented in Fig. 34.7 is an example of a case where the QoL did not improve after repair, and, therefore, an argument can be made that the surgeon should not have operated. In

order to holistically address the complicated nature of end-stage hernia, surgeons should fully consider QoL when creating a plan for surgical care in the preoperative phase. Better surgeon judgment on whether a patient is end-stage, or unlikely to derive a benefit in QoL from repair, is important in optimizing care.

Section 2: Radiologic Imaging in IH

Complex hernia repair is used to provide a stable, long-lasting closure of an abdominal wall defect that restores structural function of the abdominal wall and improves QoL. In the previous two sections, we defined end-stage hernia as an unfixable condition in which surgical repair with advanced techniques is futile or even detrimental to the patient's condition. Aside from surgeon experience and instinct, there is no reliable, evidence-based method of identifying end-stage hernia until the repair is attempted and failed. We believe that this has led to the unnecessary use of healthcare resources and avoidable adverse outcomes for end-stage hernia patients. The preoperative phase is a crucial timepoint in hernia management where innovation may lead to better end-stage hernia identification and management.

Advanced radiologic image analysis has great potential to optimize preoperative assessment and surgical planning. Among radiologic techniques, CT imaging is already a standard of care that enhances physical examination of the hernia and surrounding anatomy. CT imaging offers an accurate panoramic view of the abdomen with exquisite anatomical detail, allowing for differentiation of hernias from other abdominal masses such as tumors, hematomas, and abscesses. Moreover, it allows for visualization of hernia sac contents and the abdominal muscle and fascial layers involved. With advancements in image processing software, surgeon-scientists have been able to measure new radiographic features that are potentially relevant to hernia management. In this section, we review current applications of advanced image analysis in hernia care. Our purpose is to demonstrate the potential role of advanced image analysis in optimizing management of end-stage hernia patients.

Obesity-Related Risk Assessment

Advanced imaging analysis may provide a better understanding of how obesity may increase the likelihood that a hernia is unfixable or end-stage. Obesity is arguably the most significant risk factor for IH [7, 49]. After IH repair, obese patients are more likely to develop adverse outcomes, particularly SSI and recurrence [50, 51]. Body mass index (BMI) has been used as the conventional marker for obesity. While BMI may partially predict obesity-related complications after surgery, this measure does not account for fat distribution within the abdominal cavity, which likely varies among patients with the same BMI. With the advancement in radiographic image analysis, surgeons have been able to identify and study patient-specific obesity measures [52]. Several studies have demonstrated the discrete influences that patient-specific obesity features have on outcomes. For example, visceral obesity was associated initial formation of IH in patients following colorectal surgery [53]. In patients undergoing IH repair via component separation, visceral fat volume was a significant predictor of recurrence [54]. Subcutaneous fat has been demonstrated as an independent risk factor for SSI in abdominal surgery, including IH repair [54, 55]. In fact, subcutaneous fat was a better predictor of SSI compared to BMI (Fig. 34.9) [56]. Although obesity has long been a proven risk factor for complications, we are only now beginning to understand how much risk increases with patient-specific obesity measures on radiologic images, such as subcutaneous fat. Identification of patient-specific obesity measures using advanced imaging analysis will enable more accurate and personalized risk assessment, which is especially valuable when assessing the likelihood of failed operation in complex, potentially end-stage hernia who are commonly obese.

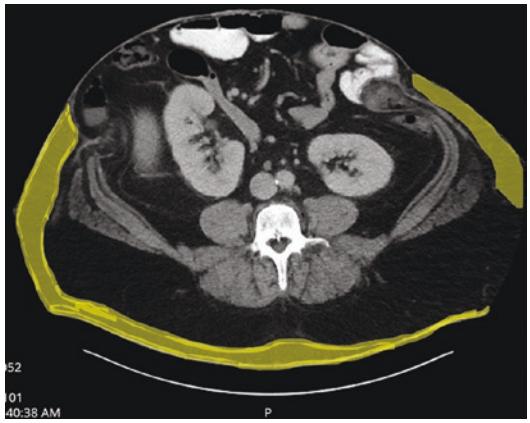

Fig. 34.9 Axial CT scan showing subcutaneous fat highlighted in yellow. Adapted from Levi et al. [56]

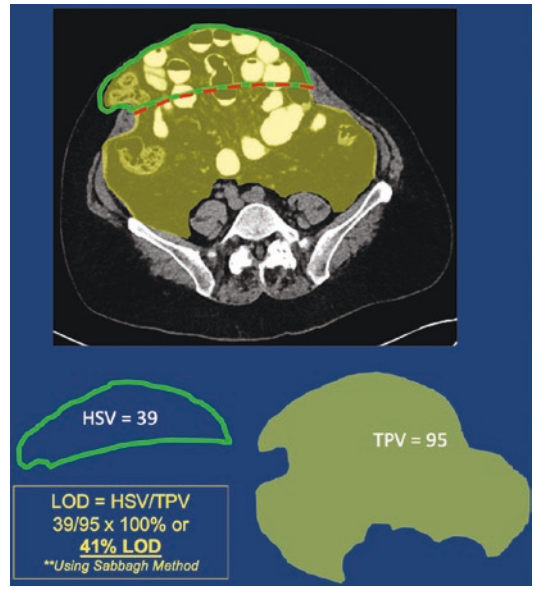

Fig. 34.10 Loss of domain (LOD) calculated using the hernia sac volume (HSV) and total peritoneal volume (TPV). Adapted from Sabbagh et al. [59]

Surgical Planning with Component Separation Techniques

In addition to risk assessment, radiologic imaging has great potential to enhance surgical planning in the setting of advanced component separation. It is important to preoperatively assess the ability to achieve fascial closure with a given surgical technique, especially in the case of large, complex hernias in which it is especially challenging. In Christy et al., the efficacy of a novel component separation index (CSI) in predicting the difficulty of achieving fascial closure was demonstrated [57]. Similarly, Love et al. showed that the rectus width to hernia width ratio (RDR) is a practical, reliable measure to predict the ability to close during Rives–Stoppa repair without abdominal muscle release [58]. In large IHs with loss of domain, IH sac volume to total peritoneal volume ratio (HSV:TPV) of less than 20% was predictive of tension-free fascial closure (Fig. 34.10) [59]. The software used to calculate volumes in this study was specialized with limited accessibility. However, Martre et al. presented a standardized volumetric analysis technique that any surgeon with basic computer skills and radiological knowledge can perform in the clinic in an autonomous and fast manner [60]. Preoperatively determining the likelihood of achieving fascial approximation with component separation is important because bridging biologic mesh for IH has been associated with poor outcomes [61]. The ability to predict whether a tension-free fascial closure before attempting the operation will add to the surgeon's armamentarium for identifying end-stage, surgically unamendable cases, which will help optimize the management of this subset of hernia patients.

Postoperative Outcome Prediction

Advanced image analysis has the potential to enhance outcomes prediction in patients with complex hernias. In our review of the literature, we found that hernia-specific radiographic features have been correlated with clinical outcomes, adding to our knowledge on hernia-related outcomes. For instance, hernia defect area and transverse defect size were associated with increased recurrence in patients undergoing component separation (Fig. 34.11) [62]. Similarly, DiCocco et al. found that recurrent hernias had

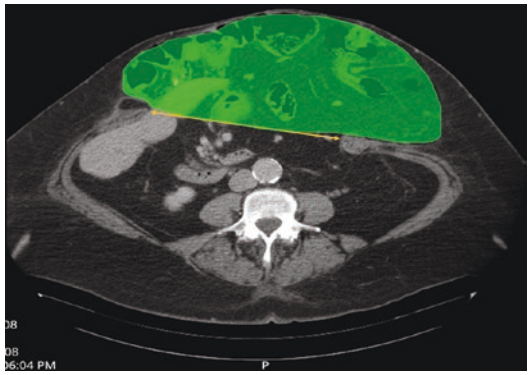

Fig. 34.11 Computed tomographic image showing axial measurements obtained using the TeraRecon, Inc., software. Defect size (transverse) is indicated by the yellow arrow and defect area highlighted in green. Adapted from Franklin et al. [62]

increased preoperative defect areas, but the difference was not statistically significant [63]. Contradicting these findings, recurrence did not correlate with any CT measurements of the abdominal wall, including hernia defect size, in another study [64]. In addition to recurrence prediction, for which the literature presents conflicting findings, other complications have been related to preoperative radiographic features. For instance, the ratio of the hernia sac to the hernia neck (hernia-neck ratio) is a simple, easily calculated parameter that, when >2.5, was associated with a 53-fold increased risk to develop complications [65]. Taller height and a hernia with smaller angle ("mushrooming hernia") had greater odds of incarceration [66]. Research in this area is still in its early stages, with few studies, conflicting findings, and no real-world impact. However, predicting outcomes is crucial in hernia management as it facilitates patient counseling, informed consent, and most importantly, determines the threshold for surgical intervention. We believe that more research in this area may lead to a definitive role for advanced image analysis in outcome prediction. This will be especially beneficial for the management of complex, end-stage hernias, in which outcomes are variable and often difficult to predict.

Shortcomings

Advanced image analysis in the preoperative phase has inherent limitations. CT-measured features may differ from clinically measured features and/or true dimensions determined intraoperatively. For instance, although hernia area determined by clinical evaluation correlated with AWS, CT-measured hernia area did not [22]. A possible explanation for this discrepancy is that while CT identifies all fibers, both functional and non-functional, clinical evaluation identifies only functional fibers with the capacity to contract on demand. Thus, CT-measured features may have less clinical relevance. This discrepancy is also seen in rectus abdominal diastasis, in which CT-measured width and clinically measured width have been shown to differ, the latter more closely representing the "truth" found intraoperatively [67]. An explanation is that laparotomy incision and paralysis under anesthesia likely alter anatomical dimensions. These limitations must be addressed as research in this area progresses.

Conclusion

To date, there is no reliable, evidence-based method of identifying end-stage hernia until the repair is attempted and failed, proving the hernia unfixable. There is a great opportunity for technological innovation in the preoperative assessment of complex hernias, specifically in judging the likelihood of a successful repair. Traditionally, CT imaging has been used primarily to confirm the presence of physical exam finding suspicious of hernia formation. However, with improved CT image resolution and the advent of image processing software in the last decade, advanced image analysis has emerged as a potential tool to guide clinical decision-making. In this section, we found that advanced image analysis has improved obesity-related risk assessment, surgical planning with components separation tech-

niques, and postoperative outcome prediction. Large-scale, multi-center prospective studies are needed to validate these hernia-related radiographic features before surgeons can use them to better manage complex hernias.

Section 5: Conclusion

In conclusion, end-stage hernia disease refers to a complex hernia that cannot be successfully repaired with component separation techniques, leaving the patient with no improvement in abdominal wall muscular function or QoL. In order to understand these aspects of end-stage hernia disease, we explored the dynamic changes in both abdominal wall function and QoL throughout the hernia disease process, from index abdominal operation, to hernia formation, and through attempted repairs. We demonstrate a degree of hernia complexity at which structural function of the abdominal wall and QoL is lost and not amenable to effective surgical repair, and we call this end-stage hernia. This is a condition in which any further surgical intervention would be associated with undue risk, significant healthcare resources, and detriment to the patient's health state. Currently, surgeons do not have an evidenced-based, reliable tool in their armamentarium for identifying end-stage hernia patients before surgery is attempted and failed. Innovation in radiographic image processing presents an opportunity for better management of complex hernias. We showed its ability to improve obesity-related risk assessment, surgical planning with components separation techniques, and postoperative outcome prediction. In summary, advanced radiographic image analysis is a promising tool that may be used to inform surgeon judgment of end-stage hernias, which will prevent unnecessary surgical intervention and optimizes outcomes for this subset of patients.

References

1. Slater N, Montgomery A, Berrevoet F, et al. Criteria for definition of a complex abdominal wall hernia. Hernia. 2014;18(1):7–17.
2. Ramirez OM, Ruas E, Dellon AL. " Components separation" method for closure of abdominal-wall defects: an anatomic and clinical study. Plast Reconstr Surg. 1990;86(3):519–26.
3. de Vries Reilingh TS, van Goor H, Charbon JA, et al. Repair of giant midline abdominal wall hernias: "components separation technique" versus prosthetic repair. World J Surg. 2007;31(4):756–63.
4. de Vries Reilingh T, Bodegom M, Van Goor H, et al. Autologous tissue repair of large abdominal wall defects. Br J Surg. 2007;94(7):791–803.
5. Lowe JB, Garza JR, Bowman JL, et al. Endoscopically assisted "components separation" for closure of abdominal wall defects. Plast Reconstr Surg. 2000;105(2):720–30.
6. Flum DR, Horvath K, Koepsell T. Have outcomes of incisional hernia repair improved with time?: a population-based analysis. Ann Surg. 2003;237(1):129.
7. Holihan JL, Alawadi Z, Martindale RG, et al. Adverse events after ventral hernia repair: the vicious cycle of complications. J Am Coll Surg. 2015;221(2):478–85.
8. Snyder CW, Graham LA, Vick CC, et al. Patient satisfaction, chronic pain, and quality of life after elective incisional hernia repair: effects of recurrence and repair technique. Hernia. 2011;15(2):123–9.
9. van Ramshorst GH, Eker HH, Hop WC, et al. Impact of incisional hernia on health-related quality of life and body image: a prospective cohort study. Am J Surg. 2012;204(2):144–50.
10. Jensen KK, Munim K, Kjaer M, et al. Abdominal Wall reconstruction for incisional hernia optimizes truncal function and quality of life: a prospective controlled study. Ann Surg. 2017;265(6):1235–40.
11. Carney MJ, Golden KE, Weissler JM, et al. Patient-reported outcomes following ventral hernia repair: designing a qualitative assessment tool. Patient. 2018;11(2):225–34.
12. Jensen K, Kjaer M, Jorgensen L. Abdominal muscle function and incisional hernia: a systematic review. Hernia. 2014;18(4):481–6.
13. Jensen KK, Henriksen NA, Harling H. Standardized measurement of quality of life after incisional hernia repair: a systematic review. Am J Surg. 2014;208(3):485–93.
14. Gunnarsson U, Johansson M, Strigård K. Assessment of abdominal muscle function using the Biodex

System-4. Validity and reliability in healthy volunteers and patients with giant ventral hernia. Hernia. 2011;15(4):417–21.
15. Parker M, Goldberg RF, Dinkins MM, et al. Pilot study on objective measurement of abdominal wall strength in patients with ventral incisional hernia. Surg Endosc. 2011;25(11):3503–8.
16. Janda V. Muscle function testing. Elsevier; 2013.
17. Paiuk I, Wasserman I, Dvir Z. Effects of abdominal surgery through a midline incision on postoperative trunk flexion strength in patients with colorectal cancer. Hernia. 2014;18(4):487–93.
18. Vigneswaran Y, Poli E, Talamonti M, et al. Rectus abdominis atrophy after ventral abdominal incisions: midline versus chevron. Hernia. 2017;21(4):619–22.
19. Yamada M, Maruta K, Shiojiri Y, et al. Atrophy of the abdominal wall muscles after extraperitoneal approach to the aorta. J Vasc Surg. 2003;38(2):346–53.
20. Jensen KK, Oma E, Kjaer M, et al. Histology and function of the rectus abdominis muscle in patients with incisional hernia. J Surg Res. 2020;253:245–51.
21. DuBay DA, Choi W, Urbanchek MG, et al. Incisional herniation induces decreased abdominal wall compliance via oblique muscle atrophy and fibrosis. Ann Surg. 2007;245(1):140.
22. Strigård K, Clay L, Stark B, et al. Giant ventral hernia—relationship between abdominal wall muscle strength and hernia area. BMC Surg. 2016;16(1):50.
23. Patterson MF, Stephenson G, Stephenson DG. Denervation produces different single fiber phenotypes in fast-and slow-twitch hindlimb muscles of the rat. Am J Phys Cell Phys. 2006;291(3):518–28.
24. Criss CN, Petro CC, Krpata DM, et al. Functional abdominal wall reconstruction improves core physiology and quality-of-life. Surgery. 2014;156(1):176–82.
25. den Hartog D, Eker H, Tuinebreijer W, et al. Isokinetic strength of the trunk flexor muscles after surgical repair for incisional hernia. Hernia. 2010;14(3):243–7.
26. Culbertson EJ, Xing L, Wen Y, et al. Reversibility of abdominal wall atrophy and fibrosis after primary or mesh herniorrhaphy. Ann Surg. 2013;257(1):142.
27. Hicks CW, Krpata DM, Blatnik JA, et al. Long-term effect on donor sites after components separation: a radiographic analysis. Plast Reconstr Surg. 2012;130(2):354–9.
28. De Silva GS, Krpata DM, Hicks CW, et al. Comparative radiographic analysis of changes in the abdominal wall musculature morphology after open posterior component separation or bridging laparoscopic ventral hernia repair. J Am Coll Surg. 2014;218(3):353–7.
29. Johansson M, Gunnarsson U, Strigård K. Different techniques for mesh application give the same abdominal muscle strength. Hernia. 2011;15(1):65–8.
30. Maron BJ, Bonow RO, Cannon RO III, et al. Hypertrophic cardiomyopathy. N Engl J Med. 1987;316(14):844–52.
31. Heniford BT, Walters AL, Lincourt AE, et al. Comparison of generic versus specific quality-of-life scales for mesh hernia repairs. J Am Coll Surg. 2008;206(4):638–44.
32. Mauch JT, Enriquez FA, Shea JA, et al. The abdominal hernia-Q: development, psychometric evaluation, and prospective testing. Ann Surg. 2020;271(5):949–57.
33. Krpata DM, Schmotzer BJ, Flocke S, et al. Design and initial implementation of HerQLes: a hernia-related quality-of-life survey to assess abdominal wall function. J Am Coll Surg. 2012;215(5):635–42.
34. Sosin M, Patel KM, Albino FP, et al. A patient-centered appraisal of outcomes following abdominal wall reconstruction: a systematic review of the current literature. Plast Reconstr Surg. 2014;133(2):408–18.
35. McCarthy M Jr, Jonasson O, Chang C-H, et al. Assessment of patient functional status after surgery. J Am Coll Surg. 2005;201(2):171–8.
36. Neumayer L, Jonasson O, Fitzgibbons R Jr, et al. Tension-free inguinal hernia repair: the design of a trial to compare open and laparoscopic surgical techniques. J Am Coll Surg. 2003;196(5):743–52.
37. Manoharan S, Liu G, Crump RT, et al. Incisional hernia repair surgery improves patient reported outcomes. Am J Surg. 2020;219(5):874–8.
38. Hope WW, Lincourt AE, Newcomb WL, et al. Comparing quality-of-life outcomes in symptomatic patients undergoing laparoscopic or open ventral hernia repair. J Laparoendosc Adv Surg Tech. 2008;18(4):567–71.
39. Rogmark P, Petersson U, Bringman S, et al. Quality of life and surgical outcome 1 year after open and laparoscopic incisional hernia repair. Ann Surg. 2016;263(2):244–50.
40. Sandø A, Rosen M, Heniford B, et al. Long-term patient-reported outcomes and quality of the evidence in ventral hernia mesh repair: a systematic review. Hernia. 2020;24(4):695–705.
41. Juvany M, Hoyuela C, Carvajal F, et al. Long-term follow-up (at 5 years) of midline incisional hernia repairs using a primary closure and prosthetic onlay technique: recurrence and quality of life. Hernia. 2018;22(2):319–24.
42. Hawn MT, Snyder CW, Graham LA, et al. Long-term follow-up of technical outcomes for incisional hernia repair. J Am Coll Surg. 2010;210(5):648–55.
43. Langbach O, Bukholm I, Benth JŠ, et al. Long term recurrence, pain and patient satisfaction after ventral hernia mesh repair. World J Gastrointest Surg. 2015;7(12):384.
44. Colavita PD, Tsirline VB, Belyansky I, et al. Prospective, long-term comparison of quality of life in laparoscopic versus open ventral hernia repair. Ann Surg. 2012;256(5):714–23.
45. Liang MK, Clapp M, Li LT, et al. Patient satisfaction, chronic pain, and functional status following laparoscopic ventral hernia repair. World J Surg. 2013;37(3):530–7.
46. Baucom RB, Ousley J, Feurer ID, et al. Patient reported outcomes after incisional hernia repair—establishing the ventral hernia recurrence inventory. Am J Surg. 2016;212(1):81–8.
47. Rogmark P, Smedberg S, Montgomery A. Long-term follow-up of retromuscular incisional hernia

repairs: recurrence and quality of life. World J Surg. 2018;42(4):974–80.
48. Nissen AT, Henn D, Moshrefi S, et al. Health-related quality of life after ventral hernia repair with biologic and synthetic mesh. Ann Plast Surg. 2019;82(5S):S332–8.
49. Lau B, Kim H, Haigh PI, et al. Obesity increases the odds of acquiring and incarcerating noninguinal abdominal wall hernias. Am Surg. 2012;78(10):1118–21.
50. Pearson DG, Carbonell AM. Obesity and abdominal wall reconstruction: outcomes, implications, and optimization. Plast Reconstr Surg. 2018;142(3S):30S–5S.
51. Heniford BT, Park A, Ramshaw BJ, et al. Laparoscopic repair of ventral hernias: nine years' experience with 850 consecutive hernias. Ann Surg. 2003;238(3):391.
52. Schlosser KA, Maloney SR, Prasad T, et al. Three-dimensional hernia analysis: the impact of size on surgical outcomes. Surg Endosc. 2020;34(4):1795–801.
53. Aquina CT, Rickles AS, Probst CP, et al. Visceral obesity, not elevated BMI, is strongly associated with incisional hernia after colorectal surgery. Dis Colon Rectum. 2015;58(2):220–7.
54. Winters H, Knaapen L, Buyne O, et al. Pre-operative CT scan measurements for predicting complications in patients undergoing complex ventral hernia repair using the component separation technique. Hernia. 2019;23(2):347–54.
55. Fujii T, Tsutsumi S, Matsumoto A, et al. Thickness of subcutaneous fat as a strong risk factor for wound infections in elective colorectal surgery: impact of prediction using preoperative CT. Dig Surg. 2010;27(4):331–5.
56. Levi B, Zhang P, Lisiecki J, et al. Use of morphometric assessment of body composition to quantify risk of surgical-site infection in patients undergoing component separation ventral hernia repair. Plast Reconstr Surg. 2014;133(4):559e–66e.
57. Christy MR, Apostolides J, Rodriguez ED, et al. The component separation index: a standardized biometric identity in abdominal wall reconstruction. Eplasty. 2012;12:e17.
58. Love M, Warren J, Davis S, et al. Computed tomography imaging in ventral hernia repair: can we predict the need for myofascial release? Hernia. 2021;5(2):471–7.
59. Sabbagh C, Dumont F, Robert B, et al. Peritoneal volume is predictive of tension-free fascia closure of large incisional hernias with loss of domain: a prospective study. Hernia. 2011;15(5):559–65.
60. Martre P, Sarsam M, Tuech J-J, et al. New, simple and reliable volumetric calculation technique in incisional hernias with loss of domain. Hernia. 2020;24(2):403–9.
61. Holihan JL, Askenasy EP, Greenberg JA, et al. Component separation vs. bridged repair for large ventral hernias: a multi-institutional risk-adjusted comparison, systematic review, and meta-analysis. Surg Infect. 2016;17(1):17–26.
62. Franklin BR, Patel KM, Nahabedian MY, et al. Predicting abdominal closure after component separation for complex ventral hernias: maximizing the use of preoperative computed tomography. Ann Plast Surg. 2013;71(3):261–5.
63. DiCocco JM, Magnotti LJ, Emmett KP, et al. Long-term follow-up of abdominal wall reconstruction after planned ventral hernia: a 15-year experience. J Am Coll Surg. 2010;210(5):686–95.
64. Blair LJ, Ross SW, Huntington CR, et al. Computed tomographic measurements predict component separation in ventral hernia repair. J Surg Res. 2015;199(2):420–7.
65. Fueter T, Schäfer M, Fournier P, et al. The hernia–neck-ratio (HNR), a novel predictive factor for complications of umbilical hernia. World J Surg. 2016;40(9):2084–90.
66. Mueck KM, Holihan JL, Mo J, et al. Computed tomography findings associated with the risk for emergency ventral hernia repair. Am J Surg. 2017;214(1):42–6.
67. Emanuelsson P, Dahlstrand U, Strömsten U, et al. Analysis of the abdominal musculo-aponeurotic anatomy in rectus diastasis: comparison of CT scanning and preoperative clinical assessment with direct measurement intraoperatively. Hernia. 2014;18(4):465–71.

Index

S. Docimo Jr. et al. (eds.), *Fundamentals of Hernia Radiology*,
https://doi.org/10.1007/978-3-031-21336-6